SOT

64TH ANNUAL MEETING
& ToxExpo • March 16–20, 2025
ORLANDO, FLORIDA

The Toxicologist: Late-Breaking Supplement

www.toxicology.org

Publication Date: March 7, 2025

Preface

This issue is devoted to the late-breaking abstracts of the 64th Annual Meeting of the Society of Toxicology, at the Orange County Convention Center, Orlando, Florida, March 16–20, 2025.

The abstracts are reproduced as accepted by the Scientific Program Committee of the Society of Toxicology and appear in numerical sequence. If a number is missing in the numerical sequence, the abstract assigned to the missing number was withdrawn by the author(s). Author names that are italicized in the author block indicate that the author is a member of the Society of Toxicology. For example, J. Smith. SOT members may sponsor abstracts that do not include an author with SOT membership. Authors who are members of designated organizations could serve as the sponsor of the abstract if an SOT member was not a co-author; these types of sponsorships are displayed with an organization name after the sponsor name (e.g., Sponsor: A. Smith, EUROTOX).

Access the Online Database of *The Toxicologist*

The SOT website features *The Toxicologist* and *The Toxicologist: Late-Breaking Supplement*. The publications can be accessed any time from the "Publications and Historical Documents" web page. All the abstracts in this edition of *The Toxicologist* also are available in the 2025 SOT Event App and SOT Online Planner.

To cite a 2025 SOT Annual Meeting Late-Breaking Abstract, please format as follows: *The Toxicologist: Late-Breaking Supplement*, a Supplement to *Toxicological Sciences 204*, Issue S2, Abstract #__ , 2025, Title, First Author.

Society of Toxicology
11190 Sunrise Valley Drive, Suite 300, Reston, VA 20191

www.toxicology.org

MONDAY POSTER SESSION MAP
Thursday, March 20, 2025—8:30 AM to 11:30 AM—W Hall A4
Poster Setup—8:00 AM to 8:30 AM
Late-Breaking Poster #s: LB101–LB360

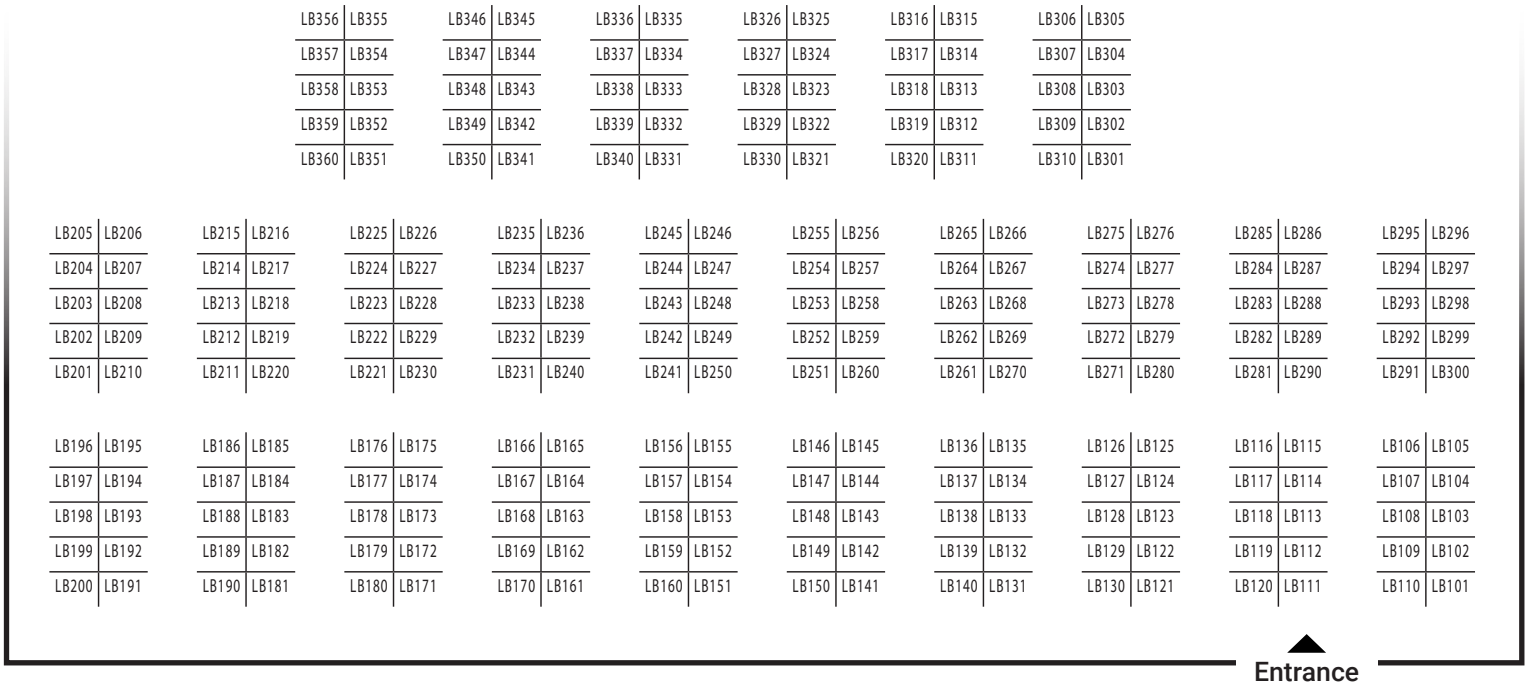

Thursday, March 20: Poster Session by Location

SESSION TITLE	ABSTRACT #s	POSTER BOARD #s
Late-Breaking 1: Air Pollution Toxicology; Cardiovascular Toxicology; Ecotoxicology; Education; Nanotoxicology; PFAS; Respiratory Toxicology	5000–5042	LB101–LB143
Late-Breaking 2: Carcinogenesis; Chemical Threats; Developmental and Reproductive Toxicology; Epidemiology; Food Safety; Medical Devices; Skin	5043–5095	LB144–LB196
Late-Breaking 3: Epigenetics; Immunotoxicity; Molecular Toxicology; Pesticides; Risk and Safety Assessment; Tobacco and ENDS	5096–5152	LB197–LB253
Late-Breaking 4: Animal Models; Kidney; Liver; New Approach Methods	5153–5187	LB254–LB288
Late-Breaking 5: ADME; Biomarkers; Computational Toxicology; Genotoxicity	5188–5220	LB289–LB321
Late-Breaking 6: Metals; Neurodegeneration; Neurotoxicity; Skin Sensitization	5221–5251	LB322–LB352

Photography or electronic capture of posters is prohibited without the consent of the poster presenter(s)/author(s). Please respect your colleagues' right to privacy.

Thursday, March 20: Poster Session by Topic

TOPIC	ABSTRACT #s	BOARD #s	SESSION TITLE
ADME/Toxicokinetics	5202–5207	LB303–LB308	Late-Breaking 5
Air Pollution Toxicology	5002–5005	LB103–LB106	Late-Breaking 1
Air Pollution: Particulate Matter	5006–5010	LB107–LB111	Late-Breaking 1
Animal Models	5161–5169	LB262–LB270	Late-Breaking 4
Bioinformatics	5208	LB309	Late-Breaking 5
Biomarkers	5193–5200	LB294–LB301	Late-Breaking 5
Carcinogenesis	5061–5064	LB162–LB165	Late-Breaking 2
Cardiovascular Toxicology/Hemodynamics	5030–5032	LB131–LB133	Late-Breaking 1
Chemical Threats and Bioterrorism	5085–5088	LB186–LB189	Late-Breaking 2
Clinical and Translational Toxicology	5201	LB302	Late-Breaking 5
Computational Toxicology and Data Integration	5209–5219	LB310–LB320	Late-Breaking 5
Developmental and Juvenile Toxicology	5043–5048	LB144–LB149	Late-Breaking 2
Ecotoxicology	5019–5029	LB120–LB130	Late-Breaking 1

TOPIC	ABSTRACT #s	BOARD #s	SESSION TITLE
Educating Future Toxicologists and Communicating with the Public	5000–5001	LB101–LB102	Late-Breaking 1
Endocrine Toxicology	5049	LB150	Late-Breaking 2
Epidemiology and Public Health	5075–5084	LB176–LB185	Late-Breaking 2
Epigenetics	5096–5101	LB197–LB202	Late-Breaking 3
Food Safety/Nutrition	5067–5069	LB168–LB170	Late-Breaking 2
Genotoxicity/DNA Repair	5188–5192	LB289–LB293	Late-Breaking 5
Human Exposure Assessment/Biomonitoring	5135–5137	LB236–LB238	Late-Breaking 3
Immunotoxicity	5125–5132	LB226–LB233	Late-Breaking 3
Inflammation	5133–5134	LB234–LB235	Late-Breaking 3
Kidney	5159–5160	LB260–LB261	Late-Breaking 4
Liver: *In Vitro*	5153–5155	LB254–LB256	Late-Breaking 4
Liver: *In Vivo*	5156–5158	LB257–LB259	Late-Breaking 4
Mathematical Modeling	5220	LB321	Late-Breaking 5

TOPIC	ABSTRACT #s	BOARD #s	SESSION TITLE
Medical Devices	5089–5091	LB190–LB192	Late-Breaking 2
Metals	5221–5230	LB322–LB331	Late-Breaking 6
Mixtures	5065–5066	LB166–LB167	Late-Breaking 2
Molecular Toxicology	5102–5104	LB203–LB205	Late-Breaking 3
Nanotoxicology: *In Vivo*	5012–5015	LB113–LB116	Late-Breaking 1
Natural Products	5070–5074	LB171–LB175	Late-Breaking 2
Neurodegenerative Disease: Parkinson's Disease	5233–5234	LB334–LB335	Late-Breaking 6
Neurotoxicity: Developmental	5240–5243	LB341–LB344	Late-Breaking 6
Neurotoxicity: General	5248–5250	LB349–LB351	Late-Breaking 6
Neurotoxicity: Metals	5244–5246	LB345–LB347	Late-Breaking 6
Neurotoxicity: Neurodegeneration	5235–5239	LB336–LB340	Late-Breaking 6
Neurotoxicity: Pesticides	5247	LB348	Late-Breaking 6
New Approach Methods: Computational	5170–5174	LB271–LB275	Late-Breaking 4

TOPIC	ABSTRACT #s	BOARD #s	SESSION TITLE
New Approach Methods: General	5175–5179	LB276–LB280	Late-Breaking 4
New Approach Methods: *In Vitro*	5180–5187	LB281–LB288	Late-Breaking 4
New Approach Methods: *In Vitro*	5251	LB352	Late-Breaking 6
Oxidative Injury and Redox Biology	5231–5232	LB332–LB333	Late-Breaking 6
Perfluorinated Alkyl Substances (PFAS)	5034–5042	LB135–LB143	Late-Breaking 1
Persistent Organic Pollutants (POPs)	5011	LB112	Late-Breaking 1
Pesticides	5122–5124	LB223–LB225	Late-Breaking 3
Reproductive Toxicology	5050–5056	LB151–LB157	Late-Breaking 2
Respiratory Toxicology	5016–5018	LB117–LB119	Late-Breaking 1
Respiratory Toxicology	5033	LB134	Late-Breaking 1
Risk Assessment	5113–5121	LB214–LB222	Late-Breaking 3
Safety Assessment: Pharmaceutical-Drug Development	5138–5148	LB239–LB249	Late-Breaking 3

TOPIC	ABSTRACT #s	BOARD #s	SESSION TITLE
Safety Assessment: Pharmaceutical-Drug Discovery	5149–5152	LB250–LB253	Late-Breaking 3
Skin	5092–5095	LB193–LB196	Late-Breaking 2
Stem Cell Biology and Toxicology	5057–5059	LB158–LB160	Late-Breaking 2
Systems Biology and Toxicology	5060	LB161	Late-Breaking 2
Tobacco and ENDS Toxicology	5105–5112	LB206–LB213	Late-Breaking 3

2025 Society of Toxicology Annual Meeting
Late-Breaking Abstracts

ABSTRACT NUMBER: 5000 **Poster Board Number:** LB101
TITLE: A transformative resource for human health risk assessment without new animal testing: an AFSA masterclass in animal-free safety assessment of cosmetics and ingredients

AUTHORS (FIRST INITIAL, LAST NAME) AND INSTITUTIONS: *C. Willett*. Humane Society International, Washington, DC.
KEYWORDS: Alternatives to Animal Testing; Education; Risk Assessment

ABSTRACT: Background and Purpose: An international consortium of toxicologists from industry and contract and non-governmental organizations created the first of its kind comprehensive, free, online resource demonstrating how to carryout human health safety assessments for cosmetics and cosmetic ingredients without the generation of new animal data. The purpose of this resource is to encourage a deep understanding about the processes, methods and data involved in performing a safety assessment without new animal testing and to increase the capacity to perform animal-free safety assessments. **Methods:** Partners of the Animal Free Safety Assessment (AFSA) Collaboration provided experts to contribute content and real-world case examples. Collaborators contributed through a series of teleconferences, e-mail communications and some in person meetings. Content was drafted in a shared Microsoft word document, then customized as learning content in a course format by staff and consultants from AFSA partner Humane Society International. Content was then recreated in an interactive format suing the Articulate 360 RISE platform and finally transferred for online dissemination and access via the Talent Learning Management System by consultant Cause Octopus. All content was reviewed and revised by contributors at each step of the process. The course involved nearly 60 individual contributors over the span of five years. **Results:** The human health risk assessment process for consumer products can be thought of as comprised of 8 overlapping but somewhat separable elements: Problem Formulation, Exposure estimation, Waiving approaches, the application of History of Safe Use, Predictive Chemistry (including (Quantitative) Structure Activity Relationships and Read-Across), In vitro Assay data synthesis (evaluation of bioactivity), Internal Exposure (dosimetry, including Physiologically Based Kinetic Modeling and In vitro to In Vivo Extrapolation) and finally, Integration of all information into a Risk Assessment Conclusion. Therefore, course content was organized into these 8 modules plus two additional modules, an introductory module covering the concepts behind animal-free or next-generation risk assessment, and a module covering the state of the global regulatory environment covering cosmetics and cosmetic ingredients (industrial chemicals). With the exception of the introductory module, which must be taken first, any module can be taken independently of any other. Each module is structured around learning objectives, quizzes are provided after each section and final exams at the end of each module. A passing score on the final exam will allow registrants to print a certificate of completion. Induvial modules have been made available as they were completed, but the entire course was finalized and launched in November 2024. As of Jan 2025, 1305 registrants from industry, contract research organizations, academia and regulatory bodies from 70 different countries have completed 1449 modules, with 883 modules in progress. **Conclusions:** To increase the application of non-test or non-animal human-relevant approaches to chemical safety assessment, it is important to enable capacity in using data generated from these newer approaches, including in silico, in vitro, and human-based data, to reach risk assessment conclusions. A first step to increasing capacity is to increase

familiarity and to provide examples in how these methods and data can be used to reach risk conclusions. The AFSA masterclass in Animal Free Risk Assessment of Cosmetics and Cosmetic Ingredients is the first of its kind comprehensive and freely available resource designed to do just that.

ABSTRACT NUMBER: 5001 **Poster Board Number:** LB102
TITLE: Integrating Toxicology into the One Health Paradigm: An Interdisciplinary Approach to Address Complex and Interconnected Environmental Challenges

AUTHORS (FIRST INITIAL, LAST NAME) AND INSTITUTIONS: *M. A. Ghorab*[1], *M. Urich*[2], K. Davis[3], and G. Waleko[3]. [1]US EPA, Washington, DC; [2]US EPA, Research Triangle Park, NC; and [3]US EPA, Cincinnati, OH.
KEYWORDS: Children's Health; Environmental Justice; One Health

ABSTRACT: Background and Purpose: Abstract In recent years, One Health - an integrative, interdisciplinary approach interconnecting human, animal, and environmental health - has emerged as an essential framework for addressing the complex and evolving landscape of toxicological challenges. In the context of escalating global phenomena such as climate change, biodiversity decline, urban expansion, industrial proliferation and legacy contamination, and the increased incidence of zoonotic diseases, there is a growing recognition that these crises extend beyond the capacity of singular scientific domains, necessitating robust, cross-disciplinary methodologies. Toxicology, as a discipline centered on elucidating the adverse effects of chemical exposure on biological and ecological systems within the context of biotic and abiotic factors, finds in the One Health approach a pivotal perspective that enhances its scope, relevance, and capacity to address these multifaceted challenges effectively. **Methods:** The presented poster underscores the essential role of systems-level thinking and a One Health approach in toxicology, with implications for risk assessment, and possible solutions or mitigation strategies. By bridging knowledge gaps and harmonizing disciplinary silos, One Health toxicology enables more precise identification of toxicological hazards and exposure pathways, facilitating informed decisions on chemical safety and public health and implementation of more efficient, and effective solutions. **Results:** Furthermore, the One Health paradigm facilitates inter-species comparison and extrapolation of adverse outcome pathways using advanced tools such as omics technologies and high-throughput screening, to address the intricate pathways of environmental stressors and toxicants. **Conclusions:** As these approaches continue to evolve within the One Health framework, they pave the way for policies that holistically protect human well-being and ecological resilience together. The integration of One Health principles into toxicology not only elevates the discipline and enhances scientific rigor, but also strengthens real-world applicability by promoting collaboration across scientific disciplines, solidifying the impact on global health initiatives, and ultimately ensuring a sustainable and healthier future for all interconnected systems.

ABSTRACT NUMBER: 5002 **Poster Board Number:** LB103
TITLE: Particulate matter 2.5 causes immunosuppressive environment by inhibiting antigen presentation of macrophages in lungs and exacerbates asthma by pulmonary infection

AUTHORS (FIRST INITIAL, LAST NAME) AND INSTITUTIONS: D. Kim[1], M. Song[1], J. Yuk[1], and K. Lee[1,2]. [1]Korea Institute of Toxicology, Jeongeup, Korea, Republic of; and [2]Department of Human and Environmental Toxicology, Daejeon, Korea, Republic of.
KEYWORDS: Macrophage; Infection; Particulates; asthma, immunosuppression

ABSTRACT: Background and Purpose: Particulate matter (PM) 2.5 and allergens in the air, causes lung diseases. PM2.5 is known to cause pulmonary immunosuppression and exacerbates allergen responses. However, the effect of co-exposure to allergens and PM2.5 on the initiation and development of allergies remains unclear. In this study, we aimed to investigate the effects of co-exposure to house dust mites (HDM) and PM2.5 and elucidate how the altered lung environment affects subsequent exposure to Spike protein (S1) infection. **Methods:** Mice were intratracheally co-exposed to HDM and diesel exhaust particulates (DEP). To investigate how the altered lung environment induced by co-exposure to HDM and DEP was affected by subsequent exposure to spike protein 1 (SI) infection and predicted potential mechanisms, mice co-exposed to HDM and DEP were challenged by S1 (0.4 mg/kg). **Results:** Compared to mice exposed only to HDMs, those co-exposed to HDM and DEP failed to induce typical asthma phenotypes, including T helper 2 (Th2), eosinophilic inflammation, and mucus cell hyperplasia in the lungs, and total immunoglobulin E (IgE) production in serum. Mechanistically, DEP induced an immunosuppressive state in the lungs by suppressing HDM-induced Th2 responses via reduction in macrophage phagocytosis and antigen presentation, accompanied by the presence of DEP-phagocytosed macrophages in the lungs. Remarkably, despite these phenotypes, the mice showed upregulation of total IgE production in the serum and pulmonary fibrosis accompanied by Th2 inflammation in the lungs after a single intratracheal administration of S1 (0.4 mg/kg) via mediating interleukin-17, nuclear factor-κB, and Janus kinase/signal transducers and activators of transcription signaling pathways. **Conclusions:** PM2.5 modulates the immune response to allergens and might exacerbate asthma by inducing pulmonary fibrosis upon subsequent pulmonary infection in the immunosuppressive environment of the lungs.

ABSTRACT NUMBER: 5003 **Poster Board Number:** LB104

TITLE: Diesel exhaust particles induces tissue specific inflammatory responses in juvenile mice

AUTHORS (FIRST INITIAL, LAST NAME) AND INSTITUTIONS: *A. G. Catala*[1], K. M. Casillas[2], H. J. Rosa[1], and *L. B. Mendez*[2]. [1]Universidad Ana G. Mendez, Cupey, PR; and [2]Universidad Ana G. Mendez, Carolina, PR.

KEYWORDS: Particulates; Juvenile Toxicity; Inflammation; neurotoxicity; diesel exhaust particles

ABSTRACT: Background and Purpose: Epidemiological studies have found associations between exposure to particle pollution and neurocognitive outcomes. The life stages of childhood and adolescence are particularly vulnerable to the effects of particle pollution, since their CNS is still in development, especially in regions related to executive functions. We have previously observed that exposure to diesel exhaust particles (DEP) induced a hyperactivity and executive dysfunction in juvenile mice. Since pro-inflammatory cytokines play an important role in cognitive function through their impact in synaptic plasticity and neurogenesis, we hypothesized that DEP exposure impaired executive function in juvenile mice by inducing tissue-specific inflammatory responses. **Methods:** To test this hypothesis, female and male C57BL6/J mice were exposed intranasally to either saline or increasing doses of DEP during postnatal days (PND) 25 to 33. Behavioral and cognitive outcomes were assessed on PND 36 to 38 and tissue was collected on PND 39. The infiltration of leukocytes in the respiratory tract was assessed by differential staining of cells collected in the bronchoalveolar lavage fluid (BALF) and the levels of 23 cytokines and chemokines were measured in lung and brain tissue with a multiplex bead-based immunoassay. **Results:** Six days after the last exposure, an increase in monocytes counts in the BALF was still present at all doses, while higher numbers of lymphocytes were observed in the lowest dose and for polymorphonuclear cells (PMNs) at the highest dose. However, the levels of cytokines and

chemokines in the lung of mice exposed to DEP were either similar to control or suppressed. Significant decreases in IL-1, IL-2, IL-6, IL-10, and IL-12 were observed at the lowest dose, suggesting that the resolution of the inflammatory response has already started in the lung. In contrast, significant increases in IL-9, IL-17, and IFN-gamma were still observed in the brain tissue six days postexposure, which suggest that neuroinflammatory response to DEP is persistent. **Conclusions:** Overall, results suggest that distinct inflammatory responses occur in the lung and brain of juvenile mice exposed to DEP, which can shed light on the vulnerability of the young brain to environmental toxicants.

ABSTRACT NUMBER: 5004 **Poster Board Number:** LB105

TITLE: Epigenomic predictors of Alzheimer's disease in olfactory mucosa of healthy women short-term exposed to high level of diesel emissions

AUTHORS (FIRST INITIAL, LAST NAME) AND INSTITUTIONS: T. Zavodna[1], K. Honkova[1], A. Afonin[2], Z. Krejcik[1], A. Mohamed[2], S. Avesani[3], T. Sandström[4], A. Muala[4], *J. Topinka*[1], T. Malm[2], R. Giugno[3], and K. Kanninen[2]. [1]Institute of Experimental Medicine of the Czech Academy of Sciences, Prague, Czech Republic; [2]University of Eastern Finland, Kuopio, Finland; [3]University of Verona, Verona, Italy; and [4]Umea University, Umea, Sweden.

KEYWORDS: Epigenetics; Gene Expression/Regulation; Neurotoxicology

ABSTRACT: Background and Purpose: Air pollution has been linked to various diseases, including neurodegenerative disorders such as Alzheimer's disease (AD). Ultrafine particles from traffic emissions can penetrate the respiratory system, cross the blood-brain barrier, and trigger neuroinflammation and oxidative stress. The olfactory mucosa (OM), a specialized tissue interfacing the external environment and the central nervous system, plays a crucial role in detecting airborne pollutants and may serve as an early marker of neurodegeneration. This study aims to investigate the effects of short-term exposure to diesel emissions on gene expression and DNA methylation in human OM cells using RNA sequencing (RNAseq) and microarray techniques. **Methods:** Nine healthy women aged 22-69 underwent two exposure sessions in a randomized double-blind study, at least three weeks apart: (1) control exposure to filtered air and (2) exposure to diluted diesel engine exhaust (PM_{10}, 300 µg/m^3) for one hour while exercising on a bicycle ergometer. Six hours after each exposure, olfactory mucosa biopsies were collected from one nostril per exposure session. RNA and DNA were isolated from the biopsies using AllPrep DNA/RNA/miRNA micro kit (Qiagen, USA). DNA treated with sodium bisulfite using the EZ DNA methylation Kit (Zymo Research, USA) was processed on the microarray platform Illumina Infinium MethylationEPICv2 BeadChip (Illumina, San Diego, USA). The methylation status at all of the 950,000 CpG sites, scanned by the iScan System (Illumina, USA), was estimated by measuring the intensity of the pair of methylated and unmethylated probes. cDNA libraries were prepared from ribosomal-depleted RNA (NEBNext® rRNA Depletion Kit v2 (Human/Mouse/Rat)) using the NEBNext® Ultra™ II Directional RNA Library Prep Kit for Illumina® (New England BioLabs). Libraries were sequenced on Illumina NovaSeq 6000 platform using NovaSeq 6000 S1 Reagent Kit v1.5 (200 cycles) (Illumina, San Diego, USA). All data were processed in R Studio using minfi package (DNA methylation) and standard pipeline for RNAseq (mRNA expression). Differential DNA methylation/gene expression was investigated using limma/DEseq2 packages. **Results:** RNAseq analysis of OM cells exposed to diesel engine exhaust identified a substantial number of differentially expressed genes (DEGs), with 3,777 genes being downregulated and 3,893 upregulated. Enrichment analyses highlighted affected pathways, including Reactome's Nervous System Development (OR=1.63) and BioPlanet's TGF-beta Regulation of the

Extracellular Matrix (OR=1.90), both relevant to AD pathophysiology. Evidence of air pollution-induced transcriptional regulation via DNA methylation was also observed, with age influencing susceptibility. One CpG site, cg25299214 (log2FC = 1.37, adj.p-val = 0.04), located in the *HDAC1* gene - a protein-coding gene linked to epilepsy - was identified after multiple corrections. Interestingly, members of the *HDAC* gene family were observed as predominantly downregulated in RNAseq data. Global methylation analysis revealed 4,603 hypomethylated and 5,212 hypermethylated CpG loci, with 20% located in gene promoters. A significant differentially methylated region (DMR) within the *GNAS* gene (chr20:58890068-58891082), containing 25 CpG sites, was also identified in RNAseq data (log2FC = 0.58, adj.p-val = 0.003). *GNAS*, a gene associated with transmembrane signal transduction, is highly relevant to AD progression and represents a promising biomarker for early diagnosis. Additionaly, a significant DMR annotated to RUNX3 (23 CpGs, min smooth fdr = 0.0004) was detected, corresponding to the RUNX3 gene upregulation (log2FC = 0.58, adj.p-value = 0.001) in RNAseq data. This transcription factor orchestrates complex gene expression programs controlling neuronal subtype specification and axonal connectivity. Upregulated RUNX3 expression is associated with brain disease. **Conclusions:** Short-term exposure to diesel engine exhaust induces significant changes in gene expression and DNA methylation in human OM, implicating critical pathways associated with neuronal development and AD. The interplay between transcriptional regulation and epigenetic modifications, such as those observed in *GNAS* and *HDAC* gene families and RUNX3 gene, underscores the potential of OM as an early indicator of neurodegenerative processes, and provide insights into the molecular mechanisms underlying air pollution's impact on neurodegeneration.

ABSTRACT NUMBER: 5005 **Poster Board Number:** LB106
TITLE: Rethinking Single Oxidant Air Pollution Exposure Metrics

AUTHORS (FIRST INITIAL, LAST NAME) AND INSTITUTIONS: E. Chan, S. McDow, K. Foley, T. Luben, and A. Wilkie. US EPA, Research Triangle Park, NC. Sponsor: *N. Sipes*
KEYWORDS: Respiratory; Oxidants

ABSTRACT: Background and Purpose: Short-term exposure to either ozone (O_3) or nitrogen dioxide (NO_2) alone is causally linked to respiratory effects and suggestive of a causal relationship for cardiovascular effects. While O_3 alone is currently used as an indicator of population exposure to total photochemical oxidants, we hypothesize that an alternative co-pollutant indicator of total oxidant exposure (the sum of O_3 and NO_2, termed Ox) would more comprehensively evaluate and address exposure disparities and health risks. **Methods:** We evaluate the use of Ox as an indicator of population exposure to total photochemical oxidants for the contiguous U.S. from 2004-2017 by comparing the Ox concentration metric to single pollutant NO_2 or O_3 concentrations, as well as exploring patterns related to geography, season, and urbanicity, starting at the county-level. **Results:** Seasonal trends of daily average O_3 and NO_2 concentrations are weakening. Also, although national levels of average NO_2 have decreased over time, there remains substantial county-level NO_2 in certain highly urbanized locations in all seasons. **Conclusions:** NO_2 concentrations made a negligible contribution to Ox in most locations across the contiguous U.S., making Ox a nearly equivalent indicator of population exposure to total photochemical oxidants as O_3 at the county level for most places. Evaluating Ox as an indicator of population exposure to total photochemical oxidants may require focusing in on specific urban areas as well as increasing the spatial resolution of analyses.

ABSTRACT NUMBER: 5006 **Poster Board Number:** LB107
TITLE: Effects of prolonged, repeated exposure to PM2.5 on the generation of inflammatory and senescent phenotype in lung fibroblasts

AUTHORS (FIRST INITIAL, LAST NAME) AND INSTITUTIONS: E. Jiang, J. J. Khater, A. M. Scruggs, and S. K. Huang. University of Michigan - Ann Arbor, Ann Arbor, MI. Sponsor: *T. Dvonch*
KEYWORDS: Particulates; Inflammation; Lung; Pulmonary or Respiratory System; Particulate Matter

ABSTRACT: Background and Purpose: When particulate matter is inhaled, it affects a variety of different cell types in the lung. Although its effects on bronchial epithelial cells are well-studied, its effects on other structural cells such as mesenchymal cells and fibroblasts are less appreciated. Fibroblasts are one cell type in the lung involved in extracellular matrix production and are responsible for repair after lung injury. Although these cells are most recognized for modulating matrix proteins, recent studies suggest that they also have critical roles in generating inflammatory mediators that are responsible for development of certain diseases. Particulate matter < 2.5μm diameter (PM2.5) is known to impact COPD, lung cancer, asthma, and IPF, though the mechanism isn't completely clear. Here, we sought to determine if exposure of lung fibroblasts to PM2.5 affects not just matrix production, but also the inflammatory and senescent phenotype of these cells. **Methods:** We exposed CCL-210 (a lung fibroblast cell line) to different concentrations (0 μg/cm² - 10 μg/cm²) of PM2.5 for different duration and frequency of treatments. This includes a single treatment over 5 days, 2 separate treatments every 3 days for a total of 6 days, or 5 separate treatments every 3 days for a total of 14 days. Afterwards, we harvested the RNA and protein, and ran real-time PCRs and western blots to visualize changes in RNA/protein. We looked at a variety of genes, including genes associated with myofibroblast differentiation, senescence, and inflammation. We used PM2.5 from the National Institute of Standards and Technology NIST (1649b) that was collected from air filters in Washington DC from 1976 and is traffic pollution. **Results:** Gene expression in myofibroblast differentiation, senescence, and inflammation did not change with the single or double exposures. However, when cells were treated repeatedly every 3 days for 14 days, markers of inflammatory phenotype, including interleukin (IL)-1β, IL-6, superoxide dismutase 2 and CXCL12 increased in a dose-dependent manner. CDKN2B, which is implicated in aging, senescence, and tumor suppression, also increased with repeated, but not single-treatment PM2.5. Repeated exposure, but not single exposure to PM2.5 also induced expression of CTHRC1, a marker of activated, fibrotic fibroblasts. **Conclusions:** Based on the current data, particulate matter dose-dependently increases the expression of certain markers of inflammatory and senescent genes over a 14-day exposure. This occurs with repeated treatments at low concentration of PM2.5 and not with single or double exposure, even at high doses of PM2.5. We conclude that PM2.5 exerts effects on fibroblasts that extend beyond mere modulation of matrix proteins and include generation of inflammatory genes that are recognized to drive lung disease. The data also emphasizes the importance of investigating repeated toxicologic exposures over prolonged periods compared to single exposure at high doses.

ABSTRACT NUMBER: 5007 **Poster Board Number:** LB108
TITLE: Alterations in Neuronal and Glymphatic Systems Induced by Black Carbon Exposure

AUTHORS (FIRST INITIAL, LAST NAME) AND INSTITUTIONS: *K. Lee*[1], D. Kim[2], and D. Kim[1]. [1]Korea Institute of Toxicology, Jeong-eup, Korea, Republic of; and [2]Korea Brain Research Institute, Dongu, Korea, Republic of.

KEYWORDS: Neurotoxicology; Inhalation Toxicology; In Vivo Models; Black Carbon; BBB

ABSTRACT: Background and Purpose: Black carbon, a major contributor to global warming, is emitted into the atmosphere through the combustion of fossil fuels. Upon inhalation, it poses significant health risks, inducing toxic effects in various human organs, including the respiratory system and the brain. While epidemiological studies have well-documented the relationship between black carbon exposure and its adverse effects on human respiratory and neurological systems, preclinical studies on its neurotoxic effects remain scarce. Comprehensive research is urgently needed to elucidate the toxic mechanisms of black carbon on the brain. In this study, we investigated the neurotoxic effects of black carbon following inhalation exposure in mice, with a focus on its impact on cerebral regions. **Methods:** Black carbon was generated by combusting propane gas and subsequently dispersed in an aqueous solution to prepare a black carbon suspension. The suspension was sprayed and dried to produce black carbon aerosols. Mice were exposed to these aerosols in a nose-only inhalation toxicity chamber at a concentration of 9.01 mg/m^3 for 6 hours per day over a period of two weeks. Brain tissues were collected post-exposure and subjected to immunohistochemical staining with NeuN, MAP2, NFL, Iba1, GFAP, AQP4, CD31, IgG, and Fibrinogen. These markers were used to evaluate changes in neuronal cells, microglial cells, astrocytes, cerebral vasculature, and blood-brain barrier integrity. **Results:** In the cerebral regions, a reduction in NeuN expression indicated neuronal loss. A decrease in MAP2 was observed, suggesting damage to neuronal dendrites. However, NFL levels remained unchanged, implying that axonal structures were not affected by black carbon exposure. Immunostaining for Iba1 revealed an increase in activated microglial cells, while no activation of astrocytes was detected. Around cerebral blood vessels, a significant reduction in AQP4, a key component of the glymphatic system, was observed. Despite this, CD31 and IgG staining did not show signs of vascular hemorrhage. However, the reduced fluorescence intensity of IgG staining suggests a potential decrease in cerebral blood flow. **Conclusions:** Two weeks of inhalation exposure to black carbon induced pathological changes in cerebral blood vessels and neuronal cells. These alterations are likely to affect various human activities, including cognitive functions. Further studies, such as behavioral assessments and mechanistic investigations, are required to comprehensively understand the impacts of black carbon on brain health.

ABSTRACT NUMBER: 5008 **Poster Board Number:** LB109

TITLE: Characterization of engineered stone dust reactive oxygen species generation and cytotoxicity *in vitro*

AUTHORS (FIRST INITIAL, LAST NAME) AND INSTITUTIONS: *W. Mandler*, A. K. Knepp, S. S. Leonard, W. McKinney, S. Keeley, and *Y. Qian*. National Institute of Occupational Safety and Health (NIOSH), Morgantown, WV.

KEYWORDS: Particulates; Safety Evaluation; Respiratory Toxicology; Reactive Oxygen Species; Silica

ABSTRACT: Background and Purpose: Engineered stone (ES), a composite material composed primarily of crushed quartz and a polymer binder, is widely used for countertops and flooring due to its durability and aesthetic appeal. However, the fabrication processes of cutting, grinding, and polishing generate respirable engineered stone dust (ESD), posing a significant occupational health hazard. ESD contains high concentrations of respirable crystalline silica (CS), a well-established causative agent of silicosis, lung cancer, and other respiratory diseases. Furthermore, these processes release volatile organic compounds (VOCs), potentially exacerbating toxicity. Recent global outbreaks of accelerated silicosis among ES workers, often affecting young individuals with relatively short exposure durations,

underscore the urgent need for comprehensive research and effective workplace safety regulations. The underlying mechanisms driving this accelerated form of silicosis remain incompletely understood. This study investigated ESD-induced cellular toxicity and the generation of reactive oxygen species (ROS) in vitro, comparing the effects of freshly generated and aged ESD particles. **Methods:** Particles were generated using a custom-built, automated system mimicking countertop fabrication. A circular saw with a stone-cutting disc cut ES slabs within a sealed stainless-steel chamber with HEPA-filtered air intake. Aerosols exited at 30 L/min, passing through a cyclone (5µm cut size) to select respirable dust, and collected on Teflon filters. Collected particles were stored under nitrogen gas at -80°C. A subset was aged in air at room temperature for two weeks. Three ES materials (A, B, C), natural granite, and Min-u-sil-5 (MS5, a CS positive control) were used. CS content varied: 60% (ES A), 20% (ES B), 0% (ES C), 30% (Granite), and 99.5% (MS5). Electron paramagnetic resonance (EPR) spin-trapping assessed free radical generation. Particles were exposed to hydrogen peroxide (H2O2) to evaluate hydroxyl radical (.OH) production via a Fenton-like reaction. RAW 264.7 macrophages were cultured and exposed to 10µg/well of fresh or aged ESD, or MS5, for 24 hours. Cell viability, apoptosis (Caspase 3/7), necrosis (Propidium Iodide), and ROS production (CellRox Deep Red) were measured using high-content imaging. The antioxidant N-acetyl cysteine (NAC) was used to assess the contribution of ROS to cytotoxicity. **Results:** Fresh materials exhibited significantly higher EPR peak intensities (indicating greater radical generation) than aged counterparts. All materials generated more radicals than background and MS5. In the presence of cells, fresh materials still showed higher EPR intensities, but aging significantly reduced this effect. Live cell counts were significantly reduced in wells treated with fresh ES materials and granite compared to controls, while aged materials and MS5 showed no significant difference. The percentage of apoptotic cells increased for all materials compared to controls, with no significant differences between fresh and aged materials. Necrotic cells increased in samples treated with fresh granite, fresh and aged ES A, and fresh ES B, with fresh materials showing significantly higher levels than aged counterparts. Oxidative stress increased in cells exposed to fresh and aged ES A and C, and aged granite. Despite decreased cell counts, total cell area increased in wells containing fresh and aged granite, fresh and aged ES A, fresh ES C, and MS5. Adding NAC did not attenuate the cytotoxic effects of ES exposure. **Conclusions:** Freshly-generated ES dusts exhibit different radical generating capacity compared to their aged counterparts. This capacity was only partially silica-content dependent. Cell viability, apoptosis, necrosis, and total cell area were all altered differently by aged vs fresh ES materials. The addition of antioxidant to the culture media did not attenuate any cytotoxic effects of ES exposure, indicating that ROS may not be the main factor contributing to the observed effects. Granite and ES A exposure tended to elicit the largest changes in toxicity and ROS production, while ES B produced fewer changes. ES C, which contains no measurable CS, was still capable of inducing ROS generation and cytotoxicity. These findings suggest that material silica content is an important, but not the sole factor contributing to cytotoxicity. Additionally, particle aging plays a significant role in ESD toxicity and should be a consideration in any future studies with these materials.

ABSTRACT NUMBER: 5009 **Poster Board Number:** LB110

TITLE: A study of ambient air monitoring of particulates and crystalline silica near aggregate production operations (APOs) in central Texas

AUTHORS (FIRST INITIAL, LAST NAME) AND INSTITUTIONS: L. Westbrook, *T. Phillips*, and *J. Petruska*. Texas Commission on Environmental Quality, Austin, TX.

KEYWORDS: Crystalline Silica, particulate matter

ABSTRACT: Background and Purpose: APOs remove or extract aggregates from the earth and often include rock crushing operations. Materials produced at APOs include crushed and broken limestone and sand. Workers exposed daily for several years up to a lifetime to high occupational levels of fine particles of crystalline silica may develop silicosis, an irreversible, progressive and fatal lung disease. Although silicosis is strictly an occupational disease, due to occasional close proximity of APOs to residential areas, Texas citizens are concerned about the impact of the emissions of particulate matter (PM) that may contain crystalline silica. To address this concern, the Texas Commission on Environmental Quality (TCEQ) conducted an air monitoring project to measure ambient air concentrations of PM and crystalline silica near APO facilities. **Methods:** The aim of this year-long monitoring project was to measure concentrations of crystalline silica PM and total PM at monitoring sites that were publicly accessible and downwind of APO facilities, as well as at a monitoring site that was publicly accessible but was not located near an APO facility (i.e., a background site). Three of the sampling sites chosen were located within 1 mile of an APO and were predominantly downwind of each facility. A fourth sampling site did not have any APOs nearby and was used as a background site. The goal was to determine what contribution, if any, the APO facilities had on ambient air concentrations of crystalline silica relative to that of background levels in the Central Texas area. At each location, a PM_4 crystalline silica sampler was deployed. The samplers used were Federal Reference Method (FRM) $PM_{2.5}$ samplers that had a modified flow rate to capture the PM_4 fraction. Each stationary site also had a total $PM_{2.5}$ sampler. Sample collection durations were 24-hours. The duration of this study was a year and the sampling frequencies reflected the annual sampling schedules common for ambient air monitoring. **Results:** Measured crystalline silica at the background site was similar to levels measured downwind of two of the three APOs; levels near a sand mine were consistently higher than background. All 24-hour PM_4 crystalline silica measurements were well below the TCEQ's health-based 24-hour air monitoring comparison value (AMCV, 24 $\mu g/m^3$). AMCVs are safe levels at which exposure is unlikely to result in adverse health effects. Long-term averages at all four sites exceeded the conservative cancer-based AMCV (0.27 $\mu g/m^3$) but were all below the more realistic silicosis-based AMCV (2 $\mu g/m^3$). The cancer-based AMCV assumes any exposure to crystalline silica causes an increased cancer risk. The silicosis AMCV is based on preventing silicosis and therefore protecting against developing lung cancer; silicosis co-occurs in workers who develop lung cancer. **Conclusions:** This study responded to citizens' concerns regarding exposure to fine particles of crystalline silica in ambient air in areas near and downwind of APO facilities. Overall, this study shows that ambient air exposure of residents to respirable crystalline silica concentrations due to APO operations are not expected to result in acute or chronic health effects.

ABSTRACT NUMBER: 5010 **Poster Board Number:** LB111

TITLE: Pm2.5 exposure and neurovascular damage: the role of blood-brain barrier integrity and mitochondrial dysfunction

AUTHORS (FIRST INITIAL, LAST NAME) AND INSTITUTIONS: *K. Kim*[1], *D. Kim*[2], *K. Lee*[2], and *D. Kim*[3].
[1]DGIST, Daegu, Korea, Republic of; [2]Korea Institute of Toxicology, Jeollabuk-do, Korea, Republic of; and [3]KBRI, Daegu, Korea, Republic of.

KEYWORDS: Neurotoxicology; In Vivo Models; Metabolism; Black Carbon; Blood-Brain barrier

ABSTRACT: Background and Purpose: Environmental pollution, particularly particulate matter 2.5 (PM2.5), has emerged as a significant public health threat, primarily affecting pulmonary and cardiovascular systems. However, growing evidence also links PM2.5 exposure to neurological

symptoms and neurodegenerative diseases, although the underlying mechanisms remain poorly understood. This study investigates the pathological changes and molecular mechanisms triggered by PM2.5 exposure, with a focus on cortical perivascular regions, blood-brain barrier (BBB) integrity, the glymphatic system, and mitochondrial dysfunction in brain endothelial cells. **Methods:** We employed an intratracheal instillation (ITI) model to simulate PM2.5 exposure and assessed pathological changes and molecular mechanisms in vivo. Transcriptomic analyses were conducted using in vitro models to elucidate molecular pathways. Co-culture systems of brain endothelial cells and astrocytes were utilized to examine the regulatory effects of Aquaporin 4 (AQP4) localization on glymphatic system function. Mitochondrial function assays were performed in brain endothelial cells to evaluate mitochondrial homeostasis. **Results:** PM2.5 exposure resulted in significant dendritic loss in cortical perivascular regions and heightened microglial activation, indicative of an enhanced pro-inflammatory response. BBB dysfunction was evident, with reduced perivascular matrix integrity and impaired glymphatic system regulation. Mitochondrial assessments revealed reduced mitochondrial membrane potential, elevated reactive oxygen species (ROS) production, and diminished ATP synthesis, indicating severe mitochondrial damage. Transcriptomic analysis identified activation of polycyclic aromatic hydrocarbon (PAH) receptors in brain endothelial cells, contributing to these pathological effects. **Conclusions:** This study provides critical insights into the molecular mechanisms underlying PM2.5-induced brain damage. Microglial activation, BBB disruption, and mitochondrial dysfunction emerge as key contributors to neurovascular injury. The findings highlight the essential role of mitochondrial health in maintaining BBB and glymphatic integrity. These insights offer potential targets for therapeutic strategies to mitigate the neurological risks associated with PM2.5 exposure, emphasizing the need for preventive measures to safeguard brain health in polluted environments.

ABSTRACT NUMBER: 5011 **Poster Board Number:** LB112

TITLE: Ecological risk of polycyclic aromatic hydrocarbons (PAHs), organochlorine (OCs) and organophosphorus pesticides (OPs) in the marine sediments of a protected Natural Park: *Parque Nacional Natural Los Corales del Rosario y de San Bernardo*, Colombia

AUTHORS (FIRST INITIAL, LAST NAME) AND INSTITUTIONS: B. E. Jaramillo-Colorado[1], M. Rosero-Moreano[2], and H. A. Henao-Castro[3]. [1]Universidad de Cartagena, Grupo de Investigaciones Agroquímicas, Cartagena, Colombia; [2]Universidad de Caldas, Manizales Caldas, Colombia; and [3]University of Cartagena, Cartagena, Colombia. Sponsor: B. Jaramillo-Colorado, Society of Environmental Toxicology and Chemistry

KEYWORDS: Pesticides; Sustainability; Exposure, Environmental; persistent organic pollutants

ABSTRACT: Background and Purpose: With exceptional landscapes and a variety of climates and environments, the National Natural Parks become ideal settings for sports activities that promote the close connection between nature and people, generating physical, mental, spiritual and social benefits. The *Corales del Rosario and San Bernardo* National Natural Park is in the Colombian Caribbean, between the coasts of the departments of Bolívar and Sucre, its extension is 120,000 hectares in the jurisdiction of the Tourist and Cultural District (D.T. and C.) of Cartagena de Indias. It has a valuable underwater set of ecosystems of the highest productivity and biodiversity; it has the largest coral shelf in the Colombian continental Caribbean (about 420 km2). It is being threatened by the intense urbanization, tourism, and anthropogenic activities that occur in the areas near this natural park. In recent decades, monitoring of persistent organic pollutants (POPs), such as Polycyclic Aromatic Hydrocarbons (PAHs), organochlorine

(OCs), and organophosphorus pesticide (OPs) have become necessary, as they outline serious threats to tropical aquatic ecosystems. Sediments act as important reservoirs of persistent toxic substances, especially PAHs and OCs known for their adverse effects on human health such as carcinogenicity and mutagenicity. Organophosphate pesticides have emerged as one of the most widely used pesticides in the world of agriculture as a substitute for organochlorine pesticides (OCPs) due to their low cost and high pest control efficiency However, as the extensive use of OPPs continues, their harmful effects are gradually becoming more evident. OPPs pose a threat not only to humans and aquatic organisms, but also a class of compounds that are difficult to degrade under natural environmental conditions. **Methods:** The contaminants were extracted from marine sediments using the microsoxhlet extraction method, and the separation and identification of the compounds was achieved by gas chromatography coupled to flame ionization (FID), electron microcapture (uECD), and nitrogen-phosphorus (NPD) detectors, using as a calibration method the addition of standard. **Results:** The results showed that the HAP's with the highest concentration was the chrysene in the marine sediments from *Isla del Rosario, Islote, Isla Tintipan, Isla Arena, Casa Agua, Isla Tesoro,* and *Barú*: 0.3, 0.6, 1.1, 0.7, 0.4, 0.2 and 0.8 µg/kg respectively; and fluoranthene in the sediments of *Isla Maravilla* 0.5 µg/kg. The study showed the presence of lindane and metallochlor being the pesticides with the highest incidence in the sampling areas. The islands where the highest residual content of OCPs was found in sediments were *Isla Grande, Isla Múcura, Isla Maravilla and Islote,* with concentrations ranging from $1.40x10^{-5}$, $2.60x10^{-6}$, $1.10x10^{-6}$, $4.24x10^{-8}$ µg/kg, respectively. About organophosphorus pesticides, the only one that could be detected was chlorpyrifos, in the sediments of *Isla del Rosario* at a concentration of 0.0006 µg/kg, and in those of *Isla Maravilla* 0.0014 µg/kg. **Conclusions:** The values obtained from the quantification do not exceed the limits established by the NOAA (National Oceanic and Atmospheric Administration), but the presence of these toxic pollutants in these ecosystems is taken in an alarming way, since it is known that they can be persistent, bioaccumulative and poorly degradable compounds, and can also be released into the water by both natural and anthropogenic processes. giving rise to possible adverse effects on the health of aquatic organisms, and can lead to consequences such as the overproduction of marine algae, producing the imminent death of several types of aquatic species. ACKNOWLEDGEMENTS. To the Vice-Rectory for Research of the University of Cartagena. Specially Thanks to the Corales del Rosario and San Bernardo National Natural Park, especially to Camilo Valcárcel for his support in the field trips.

ABSTRACT NUMBER: 5012 **Poster Board Number:** LB113

TITLE: Persisting neurobehavioral consequences of early developmental exposure to low level lead and fluoranthene in zebrafish

AUTHORS (FIRST INITIAL, LAST NAME) AND INSTITUTIONS: K. Nwachukwu, X. Cheng, E. Andonov, N. Pradeep, M. Dercole, N. Milev, B. Li, Y. Ge, J. Porter, A. Cho, Y. Saini, A. Patkar, O. Green, L. Kim, A. Hawkey, and *E. D. Levin*. Duke University, Durham, NC.

KEYWORDS: Polycyclic Aromatic Hydrocarbons; Neurotoxicity; Developmental; Neurotoxicity; Metals; Zebrafish

ABSTRACT: Background and Purpose: Developmental lead (Pb) exposure has long been known to cause persistent neurobehavioral toxicity in a variety of species. However, lead exposure never occurs alone. It always occurs in the context of other environmental toxicants. Too little is known about how lead interacts with other chemical exposures during development to produce neurobehavioral toxicity. **Methods:** In this project, we assessed in zebrafish the short and long-term neurobehavioral

consequences of early developmental exposure to lead (Pb) with a polycyclic aromatic hydrocarbon (PAH), fluoranthene (FA). Zebrafish were exposed to Pb (0, 3 and 10 µM), FA (0 and 1 µM) or binary Pb-FA mixture during the first five days post-fertilization (dpf). Behavioral effects were assessed during larval (6 dpf), juvenile (30 dpf), adolescent (2.5 months) and adult (7-8 months) ages. The behavioral test battery included assessment of swimming activity in light and dark conditions in larvae and juveniles, tap startle response and novel tanking diving in adolescents and adults, as well as social attraction to other zebrafish (shoaling) and retreat from a predator stimulus in adults. **Results:** Early developmental FA exposure significantly decreased swimming activity during the larval and juvenile life stages. In juvenile fish, the hypoactivity caused by early developmental FA exposure was attenuated by early developmental co-exposure to Pb. When tested in adulthood, the FA effect producing swimming hypoactivity continued to be exhibited in the novel tank, tap startle and predator escape tests and this continued to be reversed by concurrent early developmental Pb exposure. However, long-term neurobehavioral effects of early developmental FA exposure increasing anxiety-like response in the novel tank test and early developmental Pb exposure effect decreasing social attraction in the shoaling were not significantly diminished by co-exposure. **Conclusions:** These data indicate that zebrafish are sensitive models to persisting effects of early developmental exposure to FA or Pb which can cause long-term adverse neurobehavioral effects that extend into adulthood. Combined FA exposure with Pb can diminish the FA-induced locomotor hypoactivity. We have seen this previously with combined heavy metal and PAH exposures in zebrafish as well as rats. However, other neurobehavioral consequences of FA and Pb continue to be evident with combined exposure. This work was supported by the Duke University Superfund Research Center ES010356.

ABSTRACT NUMBER: 5013 **Poster Board Number:** LB114

TITLE: Exploring the impact of strobilurins on microglial functions and neuroinflammation: Insights into their neurotoxic potential

AUTHORS (FIRST INITIAL, LAST NAME) AND INSTITUTIONS: A. Mishra[1], A. Sriram[2], G. Harry[1], and *C. McPherson*[1]. [1]The National Institute of Environmental Health Sciences, Durham, NC; and [2]University of North Carolina at Chapel Hill, Chapel Hill, NC.

KEYWORDS: Neurotoxicity; Pesticides; Neurotoxicology; Azoxystrobin and Trifloxystrobin

ABSTRACT: Background and Purpose: Strobilurin fungicides function by inhibiting mitochondrial respiration at Complex III and energy production. Two forms, azoxystrobin and trifloxystrobin were recently reported to be present in house dust (Liu et al., 2022). Initial identification of neurotoxic effects of strobilurins showed a clustering of immune and synaptic-related genes in cultured rodent cortical neurons associated with neurological disorders (Pearson et al. 2016) and disruption of mitochondrial respiration (Nguyen et al. 2022). Early direct developmental exposure of the embryo showed altered cortical neuronal migration (2021). Further efforts of *in vitro* screening for neurotoxicity of azoxystrobin and trifloxystrobin were unable to provide data to support these observations. Based on the initial findings of a differential gene expression profile for neuroimmune-related genes (Pearson et al., 2016), the question arises as to the effect of strobilurins on brain immune cells, microglia. These cells perform functions that are critical for most aspects of brain development and maintaining homeostasis. A disruption in these processes has been linked to neurodevelopmental and neurodegenerative disorders. To examine effects of azoxystrobin and trifloxystrobin on microglia inflammatory and non-inflammatory functions as they may contribute to developmental neurotoxicity. **Methods:** BV2 microglia cells were

exposed to azoxystrobin (125nm , 250nm 500nm and 1um) or trifloxystrobin (125nm, 250nm, 500nm and 1um) for 24h. Mitochondrial function (Seahorse MitoStress test), phagocytic activity (image analysis of fluorescent bioparticles), induction of pro-inflammatory cytokines and disruption of inflammatory response to LPS (100 ng/mL, for 3h) were examined. **Results:** Decreased basal respiration and cell viability observed in the 1 um dose of azoxystrobin and trifloxystrobin that was not observed at doses (≤500 nm). Phagocytic capability (% phagocytic cells) and capacity (# of bioparticles/cell) were not affected by trifloxystrobin exposure. Trifloxystrobin slightly altered (≤3-fold change) IL-1β, TNF-α, SOCS3 or CCL3 mRNA expression. LPS-induced IL-1β mRNA expression was decreased in a dose-dependent manner and TNF-α, SOCS3 and CCL3 expression were not affected, **Conclusions:** This study reveals that azoxystrobin and trifloxystrobin do not alter mitochondrial energetics at non-cytotoxic doses. Trifloxystrobin selectively induces low-level proinflammatory cytokine expression at subthreshold concentrations and attenuates LPS-induced cytokine responses at higher doses. These results suggest strobilurins may induce mitochondrial toxicity at high doses while lower doses may significantly alter the immune response of microglial cells in the absence of mitochondrial functional changes

---

ABSTRACT NUMBER: 5014 **Poster Board Number:** LB115

TITLE: Plastic nanoparticle toxicity is accentuated in the immune-competent inflamed intestinal tri-culture cell model

AUTHORS (FIRST INITIAL, LAST NAME) AND INSTITUTIONS: C. St.Pierre[1], P. A. Caradonna[2], M. Steele[1], and *S. C. Sutton*[1]. [1]University of New England, Portland, ME; and [2]University of New England, Biddeford, ME.

KEYWORDS: Cell Culture; Gastrointestinal; Nanoparticles; inflammation; nanoplastics

ABSTRACT: Background and Purpose: Chronic oral exposure to nanoplastic has been reported to result in the added intestinal inflammation in a mouse model of irritable bowel disease. While important cell-based models of intestinal inflammation have been advanced in hopes of predicting the impact of nanoparticles on disease, none have successfully reflected that observed in the mouse. We sought to determine whether a high level and extended exposure of nanoplastic in an immune-competent tri-culture might result in the inflammation observed in the mouse. **Methods:** The cell models consist of a Transwell©-type insert with a filter membrane upon which lies a biculture monolayer of Caco-2 and HT29-MTX-E12 made up the barrier cells (apical compartment). This monolayer was exposed to digested 40 nm diameter polymethacrylate (PMA) with surface-functionalized COOH (PMA-) or NH_2 (PMA+) at a "low level" (143 µg/cm^2 monolayer surface area) or "high level" (571 µg/cm^2) for 24 or 48 h. Beyond the apical compartment in the well of the tissue culture plate, was a monolayer of macrophages, previously differentiated from THP-1 cells (basolateral compartment). Thus, the immune competent tri-cultures were examined as two models: healthy and inflamed. In the inflamed model, the barrier cell monolayer was activated with IFN-γ and the macrophages were activated with IFN-γ and LPS. The barrier cell integrity was measured by the transepithelial electrical resistance (TEER) assay, lucifer yellow permeability, confocal microscopy, and by a lactate dehydrogenase (LDH) assay. Proinflammatory cytokines secreted by the macrophages were also assayed. **Results:** A Sedimentation, Diffusion and Dosimetry model (ISDD) simulated that 8-12% of the PMA was deposited onto the barrier cell monolayer in 24 - 48-h. As reported previously, the inflamed model expressed a greater secretion of proinflammatory cytokines than the healthy model. Compared to controls (250 σ-cm^2), the TEER assay suggests that the structure of the barrier cells in the *inflamed* model was disorganized for both PMA,

high level, 48-h experiments (100 σ-cm^2). While neither the amount of PMA nor the exposure duration influenced the LDH secretion in the *healthy* model, only the high levels of both PMA- and PMA+ in 48-h exposure experiments resulted in a significantly increased LDH secreted by the barrier cells in the *inflamed* model, compared to inflamed control. This generalized disorganization was also reflected in the confocal microscopy. **Conclusions:** This study is the first to show an additive inflammation of nanoplastic in an inflamed intestinal model of the intestine. The requirement of a high level and longer exposure time may be attributed to the digestion-invoked agglomeration of the nanoplastic, the dosing volume, and/or some other factor(s) that contribute to the *in vivo* findings, but not *in vitro* models, such as: the relatively short *in vitro* exposure to nanoplastic, undifferentiated cells *in vivo* vs fully differentiated cells in vitro, the inclusion of a microbiome *in vivo*.

ABSTRACT NUMBER: 5015 **Poster Board Number:** LB116

TITLE: Proposal for a qualification system for New Approach Methodologies (NAMs) in the food and feed sector: example of implementation for nanomaterial risk assessment

AUTHORS (FIRST INITIAL, LAST NAME) AND INSTITUTIONS: *A. Haase*[1], J. Barroso[2], A. Bogni[2], S. Bremer-Hoffmann[2], V. Fessard[3], *A. Gutleb*[4], J. Mast[5], E. McVey[6], B. Mertens[5], A. G. Oomen[6], V. Ritz[1], T. Serchi[4], K. Siewert[1], D. Stanco[2], S. M. Usmani[1], E. Verleysen[5], O. Vincentini[7], M. van der Zanda[8], and F. Cubadda[7]. [1]German Federal Institute for Risk Assessment (BfR), Berlin, Germany; [2]European Commission, Joint Research Centre (JRC), Ispra, Italy; [3]French Agency for Food, Environmental and Occupational Health & Safety (ANSES), Maisons-Alfort, France; [4]Luxembourg Institute of Science and Technology (LIST), Luxembourg, Luxembourg; [5]Sciensano, Brussels, Belgium; [6]National Institute for Public Health and the Environment (RIVM), Bilthoven, Netherlands; [7]Istituto Superiore di Sanità - National Institute of Health (ISS), Rome, Italy; and [8]Wageningen Food Safety Research, part of Wageningen University and Research (WFSR), Wageningen, Netherlands.

KEYWORDS: Nanoparticles; In Vitro and Alternatives; Risk Assessment; Regulatory Implementation

ABSTRACT: Background and Purpose: Plenty of new approach methodologies (NAMs) for risk assessment have been developed but only some are included in OECD Test Guidelines (TGs) for regulatory implementation. Nevertheless, NAMs are increasingly applied, e.g. for nanomaterial (NM) risk assessments. The EFSA Guidance on NM risk assessment suggests that NAM-derived data concerning degradation/dissolution (in relevant biofluids), intestinal uptake/crossing, genotoxicity, cytotoxicity, oxidative stress, (pro-)inflammatory potential and barrier integrity, for many of which no OECD TGs exist, have to be evaluated first. Consequently, NM risk assessments involve data from non-guideline studies, requiring time-consuming and challenging case-by-case evaluations. Establishing an OECD TG is a formal process aiming for international use according to the Mutual Acceptance of Data (MAD). However, not every promising NAM can be prioritised for OECD TGs. A qualification, based on an expert opinion, may enable an efficient use of adequate NAMs for a specific context-of-use. Furthermore, it supports the optimisation of promising NAMs for regulatory applications. Existing qualification systems operate in the context of e.g., drug development tools (FDA) and research and development into pharmaceuticals (EMA). **Methods:** Firstly, existing qualification systems that operate in the context of drug development tools (FDA, 2020) and research and development into pharmaceuticals (EMA, 2008) served as examples to prototype a fit-for-purpose framework in the food and feed sector. OECD GD 211 was identified as a key publication for describing non-guideline methods to facilitate their regulatory application and we identified three key approaches for assessing method readiness to support method

validation, namely Bal-Price et al. (2018, https://doi.org/10.14573/altex.1712081) being established for developmental neurotoxicity (DNT), the Pepper framework (Crouzet et al., 2023, https://doi.org/10.1016/j.envint.2023.107910) being established for Endocrine Disruptors (ED) and the TRAAC framework (Shandilya et al., 2023, https://doi.org/10.1016/j.impact.2023.100461) being established for nano-specific methods. **Results:** We propose a generic framework for a NAMs qualification system in the food and feed sector (Haase et al., 2024, https://doi.org/10.2903/sp.efsa.2024.EN-9008). The qualification system itself can be regarded as a practical tool, which allows regulators to a) evaluate NAMs regarding their adequacy for a specific context-of-use, b) support the optimisation of submitted NAMs and c) ultimately facilitate their regulatory implementation for risk assessments of NMs in the food and feed sector. It covers all phases of the process, namely i) the submission phase, ii) the evaluation phase and iii) the outcome phase. We propose a clear structure for the process, the individual steps and we provide guidance for each of the phases. We propose to initially establish a qualification programme "NAMs for nano", covering NAMs for a) NM physicochemical characterisation, b) characterisation of NM in relevant biological fluids (e.g., to assess solubility, dissolution/degradation, other relevant particle transformations that have an impact on the assessments); c) toxicity screening (specifically involving intestinal uptake/crossing, genotoxicity, cytotoxicity, reactivity/ oxidative stress, (pro-)inflammatory responses and barrier impairment. The criteria to evaluate method readiness have been structured into three overarching sections, namely i) detailed test method description (preferably as SOPs) covering three parts (set-up of the NAM, its application and evaluation phase), ii) relevance and iii) reliability in the context of the regulatory application. Importantly, we have already initially tested the evaluation criteria for one selected example, the triculture system (Vincentini et al., 2022, https://doi.org/10.3390/cells11213357), which can be applied to investigate NM uptake/ transport across intestinal barrier and to evaluate NM effects on barrier integrity. **Conclusions:** We propose a fit-for-purpose qualification system to be applied for NAMs in the food and feed sector, which shall be initially established for NMs. We suggest to first establish three selected programmes and also propose some guidance through a criteria catalogue for evaluating these methods. We recommend to firstly test the system to evaluate selected NAMs in the context of NM risk assessment case studies such as those currently ongoing in our consortium. This will allow for a critical discussion of the proposed system, the suggested process and the proposed criteria. *Disclaimer: This communication reflects only the views of the authors and EFSA is not responsible for any use that may be made of the information it contains. The title and number of this grant is NAMS4NANO - Integration of New Approach Methodologies results in chemical risk assessments: Case studies addressing nanoscale considerations (GP/EFSA/MESE/2022/01)1.*

ABSTRACT NUMBER: 5016 **Poster Board Number:** LB117

TITLE: Alterations in Secreted Biomarkers Induced by Exposure of Air-Liquid Interface (ALI) Airway Tissues to 2,3-Pentanedione Vapor

AUTHORS (FIRST INITIAL, LAST NAME) AND INSTITUTIONS: *W. Gwinn*[1], G. Roberts[1], P. Yao[1], *M. Stout*[1], *K. Ryan*[1], A. Gupta[2], S. Pearson[2], J. Richey[2], *B. Moyer*[2], J. Shaw[2], S. Mukherjee[2], M. Snyder[2], and *D. Fallacara*[2]. [1]NIEHS, Research Triangle Park, NC; and [2]Battelle, Columbus, OH.

KEYWORDS: In Vitro and Alternatives; Biomarkers; Respiratory Toxicology; Air-Liquid Interface (ALI); 2,3-Pentanedione

ABSTRACT: Background and Purpose: 2,3-Pentanedione (PD) is a major and highly volatile component of artificial butter flavoring (ABF) used as a substitute for 2,3-Butanedione (BD) which has been associated with obliterative bronchiolitis (OB) in exposed-workers. PD and BD are structurally similar α-diketones that exhibit similar inhalation (airway) toxicity in vivo including adverse bronchial/bronchiolar effects in rats and mice and OB-like fibrotic lesions in rats. In a proof-of-concept study, PD was selected as a test article for the development and optimization of a VITROCELL 48 2.0 plus (VC) exposure system together with an Air-Liquid Interface (ALI) airway tissue model for the evaluation of PD vapor-induced airway toxicity in vitro. Although there are limited in vitro ALI airway data for PD, there are in vitro data for BD which were used as a guide for study design and anticipated findings since one would expect similar in vitro toxicological effects for PD based on the in vivo data in rodents. **Methods:** Organotypic ALI airway tissues (EpiAirway) derived from primary normal human (single donor), or rat (pooled) tracheobronchial epithelial (TBE) cells were exposed for 6 hours to PD vapor at seven concentrations (40, 70, 100, 130, 160, 200, or 240 ppm) or filtered clean air only (0 ppm) using the VC exposure system. The exposure concentrations and duration and rat strain (Wistar) selected were similar to those tested in previous in vivo inhalation studies with PD. Apical rinse and basolateral culture media samples and tissues were assessed for PD-induced toxicological effects at 0- and 18-hours post-exposure. The selected toxicity endpoints were airway injury/cytotoxicity (transepithelial electrical resistance (TEER), lactate dehydrogenase (LDH), and adenylate kinase (AK) assays), secreted protein biomarkers (Bio-Plex assay), and histopathology. These endpoints are relevant to previously reported in vivo rat and in vitro human ALI (BD) airway findings as well as key events in an Adverse Outcome Pathway (AOP 280: "α-diketone-induced bronchiolitis obliterans"). **Results:** Herein, the Bio-Plex data generated from PD-exposed human or rat ALI tissues using a 45- or 23-plex assay, respectively, and the different statistical approaches used to analyze the data are shown. Two methods were used to flag biomarkers as "active" (i.e., exhibiting a significant concentration-effect relationship) which were manual review and graphing of the data with statistical analysis (comparing the PD-exposed groups to each other and the 0-ppm control group using one-way ANOVA and Tukey's test) and a more systematic modeling (curve-fitting) approach based on ToxCast hit-call criteria (US EPA) using a single-dose (0 ppm) or two-dose (0 and 40 ppm) baseline. Analyses were conducted separately for each biomarker based on species, post-exposure timepoint, and sample type (apical or media). Of these, 28 biomarkers were flagged differently by the two approaches when considering only the positive concentration-effect relationships. This discordance was likely due to higher variability at baseline or across the range of exposure concentrations or the influence of outliers and out-of-range (OOR) values. For human, there were concentration-dependent alterations in a number of immunoregulatory and inflammatory cytokines/chemokines and growth factors which were concordant in apical and/or media samples (at 0- and/or 18-hours) using the two analytical approaches, including significantly increased levels of IL-1β, -1Ra, -2, -4, -5, -10, -13, -15, -21, -22, -23, -27, and -31; EGF, GM-CSF, GROα, and SCF; and IL-1α, -8, and -12p70 (single-dose baseline only). In previous studies, IL-1α, IL-1Ra, IL-8, and TGFα (an EGFR ligand) were shown to be increased after exposure of human ALI tissues to BD. For rat, there were far fewer upregulated biomarkers compared to human - only IL-2 and -10 and IP-10 (two-dose baseline only) were significantly increased. **Conclusions:** Based on the results of this proof-of-concept study with PD, this exposure system/ALI airway model has the potential to be used to investigate human-relevant inhalation (respiratory) toxicity in vitro, including the assessment of biomarker signatures induced by chemical exposure which may be linked to toxicity mechanism(s), and these signatures may vary depending on the type of analytical approach applied.

Rodent in vitro data also has the potential (together with in vivo data) to inform the extrapolation of human in vitro data for predicting human adverse health effects.

ABSTRACT NUMBER: 5017 **Poster Board Number:** LB118
TITLE: Development of an *In Vitro* Respiratory Toxicity Evaluation Protocol Using Artificial Bronchial Tissues

AUTHORS (FIRST INITIAL, LAST NAME) AND INSTITUTIONS: J. Choe[1], *G. Lee*[2], S. Lee[2], and *K. Lim*[1].
[1]College of Pharmacy, Ewha Womans University, Seoul, Korea, Republic of; and [2]R&D Institude, BioSolution Co., Ltd, Seoul, Korea, Republic of.
KEYWORDS: Respiratory Toxicology; In Vitro and Alternatives; Lung; Pulmonary or Respiratory System

ABSTRACT: Background and Purpose: Currently, the OECD Test Guidelines for evaluating acute inhalation toxicity rely on in vivo animal models. However, animal studies have limitations in predicting human toxicity and raise significant ethical concerns. Inhalational toxicity test can identify respiratory toxicants or systemic toxicants that can be absorbed through inhalation. This study aims to classify the respiratory toxicity of substances using the artificial airway tissue model, SoluAirway, with respect to OECD GHS categorization. **Methods:** 13 test substances were applied to SoluAirway using two treatment methods. In the Direct Application (DA) method, substances were directly applied to the tissue, followed by sealing with a vapor cap. In the Vapor Cap (VC) method, the vapor cap was soaked with the test substance and then placed over the insert. The substances were diluted in 3DW or corn oil, and after 4 hours of exposure, the tissues were washed by PBS. Toxicity classification was based on viability tests using the MTT assay, with additional measurements of Transepithelial Electrical Resistance (TEER) as supporting data. EC-25 (Estimated concentration to reduce cell viability to 25%) was estimated for the DA method and EC-50, for the VC method. **Results:** When classified into GHS Categories 1&2, 3&4, and 5&NC, the DA method showed a higher correlation with GHS classification. In the second experiment, 20 test substances were further tested, and the DA method was used to refine the evaluation criteria in an effort to improve the predictive capacity of the method. **Conclusions:** In this study, we classified test substances with VC method and the DA method to determine which test protocol is more consistent with the GHS hazard classification. The accuracy of VC based on EC-50 was 46.15% and the accuracy of DA based on EC-25 was 76.92%, confirming that DA is a more suitable treatment method for in vitro respiratory toxicity testing using SoluAirway. And TEER was proportional to viability, with the lower the viability of the tissue, the lower the value.EC-25 and EC-50 of DA method were evaluated through the viability results to find the most appropriate criteria to categorize the test substances. Based on the existing cut off and new suggested cut off, we evaluated the classification criteria that showed the highest accuracy. The highest accuracy of 90% was found when the new suggested 5 mg/tissue & 25 mg/tissue cut off applied on EC-25.

ABSTRACT NUMBER: 5018 **Poster Board Number:** LB119
TITLE: Investigating the Interactions between allergic stimuli and diacetyl in airway epithelial activation and barrier dysfunction

AUTHORS (FIRST INITIAL, LAST NAME) AND INSTITUTIONS: *T. Pressley*, K. Norton, and S. Georas.
University of Rochester, Rochester, NY.
KEYWORDS: Respiratory Toxicology; Diacetyl

ABSTRACT: Background and Purpose: Diacetyl (DA) is well known as a hazard in the manufacturing of butter flavored popcorn, and it has been found in a large percentage of flavored vaping products, despite its documented adverse effects. Diacetyl has been shown to activate airway epithelial cells and lead to fibrotic conditions such as bronchiolitis obliterans. We hypothesize that DA might also cause epithelial barrier dysfunction, similar to other inhaled toxicants, but this mechanism of damage is not well studied. The purpose of this project is to define the mechanism of DA-induced epithelial barrier dysfunction and examine whether this is affected by allergic inflammatory mediators. **Methods:** 16HBE cells, which are a human bronchial epithelial cell line known to form tight junctions (TJ) and adherens junction (AJ) in vitro, were used to study the effects of DA on epithelial barrier structure and function. Confluent monolayers grown on transwell plates with 0.4mm pore polyester membrane inserts were incubated with DA alone or in combination with the Th2 cytokine interleukin-4 (IL-4, 50 ng/ml) to model the effects of allergic airway inflammation. Dose finding and kinetic assays varying the concentration (0, 0.07, 0.14, 0.3, 0.6, 1.2, or 6 mM) and timing (2-48 hrs) of DA exposure were completed. The cytotoxicity of the treatments was examined using Lactate Dehydrogenase (LDH) cytotoxicity assay and a Water-Soluble Tetrazolium Salt (WST-8) cell viability assay. Macromolecular permeability to 4 kDa FITC-dextran and measured decreases in Transepithelial Electrical Resistance (TEER) were used to quantify epithelial barrier dysfunction. To study changes in epithelial barrier structure, whole cell lysates were measured via Western blot using a panel of antibodies directed against AJ and TJ proteins. The results from the western blots drove further exploration into changes in AJ and TJ protein localization using immunohistochemistry (IHC) staining targeting TJ proteins Occludin and ZO-1 and AJ protein E-Cadherin in preliminary experiments. Further Preliminary experiments utilizing primary Human bronchial Epithelial cells (Lonza), as well as lab-grown EpiAirway tissue (Mattek) treated with diacetyl, have shown results mirroring our findings in 16HBEs in both TEER and Permeability assay measurements. **Results:** When 16HBE cells (n=3) were treated with varying DA concentrations (0-6mM) for 24hrs, the measured TEER was significantly decreased in a dose dependent manner from 70.9% (+/-4.2) - 7.56%(+/-0.389) when compared to pre-treatment measured resistance. ($p<0.05$-0.01). The same cells showed no statistically significant increases in permeability for 0.07mM-0.6mM diacetyl treatments and significant increases in FITC-dextran leak from control cell leak of 9.25 ug/mL +/- 3.07 to 293 +/- 64.95, 329.2 +/- 10.25, and 285.5 +/- 28.06 ug/mL FITC-Dextran leak for 1.2mM, 2.4mM, and 6mM DA treatments respectively, all $p<0.0001$. Cyototoxicity assays revealed that DA concentrations >6mM were associated with loss of cell viability. When the cells were pre-exposed to IL-4, DA exposure caused a synergistic increase in permeability (e.g. 0.6mM DA alone causes a FITC leak of 43 +/- 1ug/mL whereas in combination with IL-4 FITC leak increased to 104+/- 14ug/mL, and IL-4 alone had negligible effects, $p<0.0001$ via 2-way ANOVA). Synergistic epithelial barrier disruption required longer than 1 hr DA exposure. When cells +/- IL4 pretreatment were challenged with 1 hour DA there were no significant changes in TEER or Permeability when comparing the combo exposures vs. DA alone. The analysis of protein expression via western blot showed no significant changes in the expression of tight and adherens junction proteins ZO-1, Occludin, E-Cadherin, or Claudin 1, 3 or 4 except at the highest dose of diacetyl alone. Preliminary experiments utilizing IHC to better understand the localization of TJ and AJ proteins are in progress. Ongoing studies are investigating the repeatability of our 16HBE findings in primary cell models. **Conclusions:** We conclude that DA acts in a dose dependent manner to cause epithelial barrier disruption using model epithelial monolayers in vitro. This disruption is independent of tight and adherens junctional protein expression changes in 16HBE cells. In combination with IL-4 pretreatment, diacetyl challenge synergistically decreases barrier function as determined by decreases in TEER and increases in permeability. Since IL-4 is produced during allergic inflammation, these results

support the hypothesis that allergic conditions such as asthma might exacerbate DA mediated epithelial damage in vivo.

ABSTRACT NUMBER: 5019 **Poster Board Number:** LB120
TITLE: Mercury monitoring in fish from collective territories impacted by mining activities in the colombian pacific

AUTHORS (FIRST INITIAL, LAST NAME) AND INSTITUTIONS: K. Martínez-Copetea[1], C. Palacios-Palacios[1], D. Perea-Ruíz[1], A. Romaña-Palacios[1], C. Vargas-Largacha[1], J. Mosquera-Murillo[1], Y. Palacios-Mosquera[1], V. Rentería-Ramos[1], M. Murillo-Nuñez[1], A. Palacios-Mena[1], E. Moreno-Mosquera[1], J. Gamboa-Orozco[2], D. Nieto-Lopez[2], and Y. Palacios-Torres[1]. [1]Environmental Toxicology and Natural Recourses Group, School of Naturals Sciences, Technological University of Choco-DLC, Quibdó, Colombia; and [2]WWF Colombia, Bogotá, Colombia.
KEYWORDS: Ecotoxicology; Metals; Biomonitoring; collective territories, Pacific; Mercury

ABSTRACT: Background and Purpose: Artisanal and Small-Scale Gold Mining is a threat to tropical forests and the livelihoods of community productive agroecosystems due to the release of mercury (Hg), which reaches aquatic and terrestrial ecosystems, where it becomes incorporated into the food chain. The objective of this research was to monitor mercury content in fish from collective territories affected by gold mining. **Methods:** Hg levels were quantified using a direct mercury analyzer (Lumex RA-915+, St. Petersburg, Russia). **Results:** The overall average Hg concentration was (0.15 ± 0.13 µg/g), with ranges from (0.02-0.67 µg/g). The highest Hg contents were found in *Astyanax atratoensis* (Lunareja Sardine) at 0.37 µg/g and *Andinoacara latifrons* (Coco) at 0.25 µg/g, while the lowest concentrations were reported for *Gilbertolus atratoensis* (Canoero) at 0.05 µg/g and *Hoplias malabaricus* (Quicharo) at (0.05 ± 0.02 µg/g). Ninety-six percent (96%) of the samples were below the limit set by the World Health Organization (WHO) (0.5 µg/g). **Conclusions:** the evaluated mining collective territories recorded low concentrations, suggesting the implementation of monitoring programs that allow for reducing toxicological effects on environmental and human health at early stages.

ABSTRACT NUMBER: 5020 **Poster Board Number:** LB121
TITLE: Gut toxicity and microbiome effects in zebrafish exposed to UV-weathered polypropylene microplastics

AUTHORS (FIRST INITIAL, LAST NAME) AND INSTITUTIONS: *J. Park*, J. Choi, and Y. Heo. Korea Institute of Toxicology, Jinju, Korea, Republic of.
KEYWORDS: Ecotoxicology; Microbiome

ABSTRACT: Background and Purpose: Weathered microplastics (MPs) have different physicochemical properties compared to virgin MPs, and therefore their effects on the environment and living organisms may be different. The present study aimed to evluated the potential gut toxicity and biokinetics of virgin polypropylene (PP) MPs and UV-weathered PP MPs (UV-PP) on intestinal permeability, oxidative stress, and immune function in adult zebrafish. **Methods:** The zebrafish were exposed to two types of PPs at a concentration of 50 mg/L each for 14 days. MP ingestion and excretion was verified using fluorescence microscpoe. Histopathological, biochemical, gene expression, and microbiome analysis were also performed. **Results:** After exposure, MPs accumulated mainly in the gastrointestinal tract, with UV-PP showing a higher accumulation than PP. Ingestion of PP and UV-PP induced intestinal damage in

zebrafish and increased gene expression and levels of enzymes related to oxidative stress and inflammation, with no significant differences between the two MPs. Microbial community analysis confirmed changes in the abundance and diversity of zebrafish gut microorganisms in the PP and UV-PP groups, with more pronounced changes in the PP-exposed group. Furthermore, Kyoto Encyclopedia of Genes and Genomes pathway analysis confirmed the association between changes in gut microbiota at the phylum and genus level with cellular responses such as oxidative stress, inflammation and tissue damage. **Conclusions:** This finding suggests that MPs residing in the environment for an extended period may vary on toxicity possibly due to the complex and diverse factors under environmental conditions as well as the inherent properties of the polymer.

ABSTRACT NUMBER: 5021 **Poster Board Number:** LB122

TITLE: Comparative biotransformation pathways of Legacy Pollutants in Gulf Killifish: Insights from waterborne and Intraperitoneal injection exposure

AUTHORS (FIRST INITIAL, LAST NAME) AND INSTITUTIONS: M. G. Rojo[1], *G. Collier*[1], *A. Janiga-MacNelly*[1], *R. Rifa*[1], P. Nirmani[1,2], A. Ramirez[3], C. Matson[1,2], and *R. Lavado*[1,2]. [1]Department of Environmental Science, Baylor University, Waco, TX; [2]Center for Reservoir and Aquatic Systems Research, Baylor University, Waco, TX; and [3]Mass Spectrometry Core Facility, Baylor University, Waco, TX.

KEYWORDS: Polycyclic Aromatic Hydrocarbons; Biotransformation; Ecotoxicology

ABSTRACT: Background and Purpose: Polycyclic aromatic hydrocarbons (PAHs) drive evolutionary adaptations. Gulf killifish (*Fundulus grandis*) from the Houston Ship Channel (HSC) have developed resistance to PAH-induced cardiovascular teratogenicity through chronic chemical exposure. Resistance is associated with a deletion in the aryl hydrocarbon receptor (AHR) gene. This study aims to characterize the biotransformation products of benzo[a]pyrene (BaP) in both PAH-adapted, HSC, and non-adapted, Galveston Bay, *F. grandis* populations, examining differences between populations and sexes, identifying biochemical pathways. **Methods:** Pollution-adapted *F. grandis* were collected from Vince Bayou (VB), HSC, while non-adapted reference fish came from Smith Point (SM), Galveston Bay. Both groups were maintained under controlled lab conditions and subjected to two BaP exposure experiments: a 15-day waterborne exposure (10, 40, 100 µg/L) and a 96-hour intraperitoneal (IP) injection (2.5 mg/kg and 5 mg/kg). Waterborne BaP was extracted using C-18 filters and MeOH, dried under nitrogen flow, and resuspended in 80% aqueous ACN for UPLC-FLD analysis. Bile metabolites were extracted using a sodium acetate buffer, and ethyl acetate: acetone (2:1) mix, followed by ethyl acetate. Free, “F”, metabolites were obtained by combining the organic fractions, followed by dryness, and resuspension in 40% ACN-60% 0.1% aqueous formic acid for LC-HRMS analysis. Aqueous fractions underwent enzymatic treatment with β-glucuronidase and aryl sulfatase to release glucuronide “G” and sulfate “S” conjugated metabolites, also analyzed by LC-HRMS. **Results:** The metabolic profiling of BaP in the waterborne exposure showed the presence of 1-OH-BaP, and 7,8-BaP-diol corresponding to 100µg/L treatment. In IP injections, BaP and their metabolites,7,8-Diol-BaP,1-OH-BaP, and 9-OH-BaP reported their presence in the dosing concentrations of 2.5mg/kg and 5mg/kg. Highest Log concentration (ng/µL bile) of 7,8-Diol-BaP “F” metabolites was detected in males of VB, 2.0, and SM, 1.67, of 100µg/L. In IP injections, highest mean concentrations were detected for 5mg/kg, in VB males, 0.28. As well, 7,8-Diol-BaP “G” metabolites showed the highest concentration in females of VB 100ug/L exposure, being 2.38, and 0.35-fold higher than males from the same population. Followed by 1.64 detected in males from SM and 1.58 in females from the same population. In 2.5 mg/kg IP injection treatments, the highest mean

concentration was reported for VB females, 0.47. 1-OH-BaP “F” metabolites demonstrated the highest mean concentrations in VB females, 2.57, of 100µg/L treatment and males from SM same treatment, 2.46. For IP injection, 5mg/kg, SM population reported the highest concentration among populations. In IP injections, highest mean concentrations were detected for 5mg/kg, in VB males, 0.28. As well, 7,8-Diol-BaP “G” metabolites showed the highest concentration in females of VB 100ug/L exposure, being 2.38, and 0.35-fold higher than males from the same population. Followed by 1.64 detected in males from SM and 1.58 in females from the same population. In 2.5 mg/kg IP injection treatments, the highest mean concentration was reported for VB females, 0.47. 1-OH-BaP “F” metabolites demonstrated the highest mean concentrations in VB females, 2.57, of 100µg/L treatment and males from SM same treatment, 2.46. For IP injection, 5mg/kg, SM population reported the highest concentration among populations with the same treatment, observing a 0.13-fold difference among males and females. “G” metabolites, showed the highest concentration in waterborne exposure, in SM males and females, 2.45, and 2.2, respectively. Followed by the VB population under the same treatment, which showed a concentration in males and females of 1.70, and 1.92, respectively. Mean concentration of IP injections, 5 mg/kg, showed a concentration of 0.35, in females, and 0.22 in males. “G” metabolites of 9-OH-BaP, were only reported for IP injections in females from SM and VB. 1.53 in SM 5mg/kg; 1.51 in VB and 1.49 in SM, both 2.5mg/kg. BaP was reported only in the female population of SM and VB, 2.5mg/kg treatment, showing a mean value of 1.80 in the SM and 1.13 in the VB population. **Conclusions:** The results showed a difference in the profile of metabolites generated, among waterborne exposure, 1-OH-BaP, and 7,8-BaP-diol, and IP injections, 7,8-Diol-BaP,1-OH-BaP, and 9-OH-BaP. The highest levels of concentrations of 1-OH-BaP, and 7,8-BaP-diol “F” metabolites were reported for VB populations exposed to 100µg/L. Differences among females and males were also observed. “G” metabolites of 7,8-BaP-diol,1-OH-BaP, and 9-OH-BaP, showed quantifiable results. Mean values of 7,8-BaP-diol reported the highest values for the VB females, 100µg/L and 2.5 mg/kg treatment. While for the other “G” metabolites, only the 1-OH-BaP, and 9-OH-BaP, were reported in SM females, 5mg/kg treatment. Differences in “G” released metabolites indicate glucuronidation as a significant route of phase II biotransformation for 7,8-BaP-diol, 1-OH-BaP, and 9-OH-BaP.BaP was reported in females from both populations (SM and VB), 2.5 mg/kg, treatment. Presence of the parent compound may result from direct partitioning into the gallbladder or transport across tissues. Future work will explore the impacts of AHR deletion genotype, on biotransformation and immune activation.

ABSTRACT NUMBER: 5022 **Poster Board Number:** LB123

TITLE: Evaluating the Protective Potential of Naringin Against Bisphenol S-Induced Oxidative Stress and Systemic Toxicity in Wistar Rats

AUTHORS (FIRST INITIAL, LAST NAME) AND INSTITUTIONS: O. Okeoghene, O. S. Taiwo, O. O. Igado, *A. A. Oyagbemi*, and *T. O. Omobowale*. University of Ibadan, Ibadan, Nigeria.

KEYWORDS: Oxidative Injury; Endocrine Disruptors; Bisphenol S (BPS), Naringin

ABSTRACT: Background and Purpose: Bisphenol S (BPS) is a widespread endocrine disruptor found in numerous industrial and consumer products. It disrupts hormonal balance and induces oxidative stress, leading to systemic injuries in various organs such as the heart, kidney, liver, and intestine. Naringin, a glycoside flavonoid commonly found in citrus fruits like grapefruit, is known for its antioxidant and anti-inflammatory properties. This study aimed to evaluate the potential of naringin to mitigate the toxic effects of BPS in key organs of male Wistar rats, focusing on oxidative stress, haematological

parameters, and serum chemistry profiles. **Methods:** Male Wistar rats were grouped into six treatment groups and dosed orally for 28 consecutive days: Group A (Control): Received corn oil alone. Group B (Naringin-only, low dose): 80 mg/kg/day of naringin dissolved in 280 ml of distilled water. Group C (Naringin-only, high dose): 160 mg/kg/day of naringin dissolved in 280 ml of distilled water. Group D (BPS-only): 50 mg/kg/day of BPS suspended in 160 ml of corn oil. Group E (BPS + Naringin, low dose): 50 mg/kg/day of BPS and 80 mg/kg/day of naringin. Group F (BPS + Naringin, high dose): 50 mg/kg/day of BPS and 160 mg/kg/day of naringin. Oxidative stress markers (H2O2 and MDA), antioxidant enzyme activities (GPx, GST, and GSH), haematological indices (WBC, NLR, PCV, Hb, and RBC), and serum chemistry parameters (TP, albumin, AST, and ALT) were measured to assess the effects of the treatments. **Results:** Oxidative Stress Markers: BPS significantly increased ($p<0.05$) H2O2 levels, with no significant change observed in MDA levels across the organs studied. Antioxidant Enzymes: BPS caused a significant ($p<0.05$) increase in GPx and GST activities but showed no significant difference in GSH levels. Haematological Parameters: BPS treatment led to a significant ($p<0.05$) increase in WBC and NLR, while PCV, Hb concentration, and RBC counts significantly decreased ($p<0.05$). Serum Chemistry Profiles: BPS-treated groups exhibited a significant ($p<0.05$) reduction in TP, albumin, AST, and ALT levels. Naringin Treatment: Neither 80 mg/kg/day nor 160 mg/kg/day of naringin significantly mitigated the toxic effects of BPS on oxidative stress markers, haematological indices, or serum chemistry parameters. **Conclusions:** This study demonstrates that BPS induces oxidative stress, alters haematological indices, and disrupts serum chemistry profiles in male Wistar rats, indicating its systemic toxicity. Although naringin is known for its antioxidant properties, the dosages and duration of treatment in this study failed to provide significant protection against BPS toxicity. Further research is necessary to explore optimal dosing strategies and treatment protocols for naringin to counteract endocrine disruptor-induced toxicities effectively.

ABSTRACT NUMBER: 5023 **Poster Board Number:** LB124

TITLE: Assessing the effects of brevetoxin exposure on zebrafish cognition through novel object recognition tests

AUTHORS (FIRST INITIAL, LAST NAME) AND INSTITUTIONS: H. Martin, M. Hammontree, *W. Hayes*, and A. Stafford. Florida College, Temple Terrace, FL.

KEYWORDS: Aquatic Toxicology; Behavioral; Neurotoxicology; Zebrafish; Brevetoxin

ABSTRACT: Background and Purpose: Brevetoxins are known to cause harmful effects on vertebrates, including humans. These effects manifest themselves most commonly as upper respiratory symptoms such as nasal congestion, throat irritation, cough, and eye irritation. However, brevetoxin's neurological and cognitive effects on humans have not been studied extensively. A standard measurement of a vertebrate's cognitive activity is the novel object recognition test (NORT). Zebrafish (*Danio rerio*) exhibit anxiolytic behavior when presented with a novel object, indicating the recognition of something new and potentially threatening in its environment. Reduction of this behavior when exposed to brevetoxin indicates alterations to fish cognitive functions, which could have further implications for humans living in areas such as the Gulf Coast of Florida, which experience large brevetoxin releasing algal blooms. **Methods:** A novel object recognition test (NORT) was used to explore the effects that brevetoxin (PbTx-2) may have on cognitive ability since these tests serve as a proxy for measuring memory capabilities. We exposed male and female adult zebrafish (Male-12, Female-13) to 10 nM PbTx-2 solution and then allowed them to explore a testing tank with a familiar and novel objects on opposite sides of the tank.

Results were recorded using EthovisionXT animal tracking and recording software. Mean time within a zone of proximity to each object, and latency to approach each object was recorded, and t-tests compared fish object preference before and after exposure to brevetoxin. Data on animal velocity, acceleration, and total distance moved were also collected. **Results:** There were trends in time around novel objects compared to familiar objects and the latency in which the fish approached the objects, but there were no statistical differences between control and intoxicated groups. Brevetoxin-exposed fish spend more time in proximity to both novel and familiar objects than nonexposed control fish. The data also revealed tangential trends of PbTx-2 on fish locomotion in that the intoxicated fish showed increased swimming velocity and total distance moved yet decreased acceleration compared to control fish. **Conclusions:** Overall, while none of the differences were statistically significant, trends indicate that brevetoxin exposure made the fish less anxious about the objects as they spent more time near novel and familiar objects after exposure to the toxin. Higher dose experiments must be conducted to elucidate whether PbTx-2 influences zebrafish's novel object recognition capabilities.

ABSTRACT NUMBER: 5024 **Poster Board Number:** LB125
TITLE: Influence of Coastal Urbanization and Feeding Ecology on Bioaccumulation in Elasmobranchs

AUTHORS (FIRST INITIAL, LAST NAME) AND INSTITUTIONS: *M. A. Walker*[1], *P. C. Powell*[1], *Z. J. Padgett*[1], K. Artosky[1], J. M. Schulte[2], M. M. Holst[3], T. K. Chapple[2], B. S. Frazier[4], and *K. D. Rock*[1]. [1]Clemson University, Department of Biological Sciences, Clemson, SC; [2]Oregon State University, Coastal Oregon Marine Science Experiment Station, Newport, OR; [3]University of California - Davis, Department of Anatomy, Physiology, and Cell Biology, Davis, CA; and [4]South Carolina Department of Natural Resources, Marine Resources Research Institute, Charleston, SC.
KEYWORDS: Aquatic Toxicology; Ecotoxicology; Bioaccumulation; Mercury, PFAS

ABSTRACT: Background and Purpose: Among the top drivers of biodiversity loss in marine ecosystems is pollution, which continues to increase concurrently with the human population. Sharks, a subset of elasmobranchs, are apex predators and are considered to be keystone species of marine ecosystems. As higher trophic organisms, they are particularly susceptible to pollutants that can bioaccumulate in their tissues, posing significant risks to their health and long-term viability. Coastal waters are critical elasmobranch feeding, breeding, and pupping grounds, bringing them near our urbanized and polluted coastlines, and highlighting the need to understand how occupancy of coastal marine waters contributes to contaminant exposure, data that can inform conservation efforts toward preserving shark populations. Several studies have demonstrated that differences in chemical bioaccumulation exist across species, age class, and trophic position; however additional factors such as occupancy of coastal ecosystems and species-specific differences in feeding ecology have yet to be extensively investigated. To address these knowledge gaps, we sought to (1) characterize differences in the bioaccumulation in sharks of the same species, focusing on the broadnose sevengill shark (*Notorynchus cepedianus*) residing in an urbanized estuary versus a non-urbanized estuary, and (2) compare contaminant body burden in sharks that utilize specialist (*Carcharhinus isodon*) or generalist (*Carcharhinus plumbeus)* feeding strategies. More specifically, we hypothesize that (1) sharks caught in an estuary with coastal urbanization will have higher concentrations of contaminants than sharks sampled from a non-urbanized estuary, and (2) the generalist feeders that consume a combination of primary and secondary consumers will have higher concentrations of contaminants than the specialist feeders whose diet is primarily (95%) Atlantic menhaden (*Brevoortia tyrannus*), a primary consumer. **Methods:** To test these

hypotheses, in situ environmental samples (water and sediment) and tissue samples (blood and muscle) from sharks were collected via catch and release procedural standards. Additionally for the second project, muscle tissue samples will be collected for prey species. For project 1 samples were collected from broadnose sevengill (*N. cepedianus*) sharks residing in San Francisco Bay, CA, a highly urbanized and polluted estuary, and Willapa, WA, a relatively pristine non-urbanized estuary. Project 2 samples were collected from finetooth (*C. isodon*) and sandbar (*C. plumbeus*) sharks residing in Bulls Bay and St. Helena Sound, SC. Measurements including PCL (precaudal length), FL (fork length), STL (stretch total length) and sex were recorded to evaluate physiological and ontogenetic variances. Mercury (Hg) concentrations were quantified using an MA-3000 thermal decomposition, amalgamation, and atomic absorption spectrophotometry mercury analyzer. A targeted list of 21 different per- and polyfluoroalkyl substances (PFAS) were measured using Triple Quadrupole Liquid Chromatography-Mass Spectrometry (LC-MS). **Results:** Project 1: No significant differences in Hg concentrations were observed across ontogeny or by sex in blood samples from broadnose sevengill sharks caught in San Francisco Bay. However, a significant difference in Hg concentrations was observed in the muscle of sevengill sharks, with subadults having higher concentrations compared to juveniles and neonates. Project 2: No significant differences in blood Hg concentration were observed in sandbar sharks across sex, however a suggestive trend was observed highlighting increasing Hg concentrations corresponding with increasing PCL. PFAS analysis of water and sediment samples from St. Helena Sound revealed 11 compounds detected in water samples and 8 PFAS detected in sediment. **Conclusions:** Both projects are ongoing as we continue to collect and analyze samples with the help of our collaborators at Oregon State University, UC Davis and the SC DNR. In addition to environmental samples and tissue samples from sharks, for project 2 we are also in the process of analyzing Hg and PFAS concentrations in finetooth and sandbar prey. Combined with stable isotope analysis (δ13C and δ15N) we hope to better understand trophic transfer of these ubiquitous contaminants in marine food webs. Addition analyses will include blood chemistry assays in order to evaluate associations between chemical body burden and health outcomes. These studies have the potential to provide information that can be used to protect marine biodiversity, ensure the health of marine ecosystems, safeguard human health, and advance scientific understanding of ecotoxicology in marine environments. Partnering with local community leaders and industries that rely upon a healthy ecosystem is an effective way forward and can help motivate stakeholders to make decisions with a more sustainable, long-term viewpoint.

ABSTRACT NUMBER: 5025 **Poster Board Number:** LB126
TITLE: Distribution of mercury contamination in fish in the Brazilian Amazon

AUTHORS (FIRST INITIAL, LAST NAME) AND INSTITUTIONS: *J. B. Freitas Júnior*. Universidade Federal do Pará - UFPA, Altamira, Brazil.
KEYWORDS: Ecotoxicology; Biomarkers; Metals; Fish; mercury

ABSTRACT: Background and Purpose: Methylmercury is found in the environment contaminating food, including fish and seafood. Dietary exposure is the most frequent form of exposure among indigenous and riverside dwellers in the Brazilian Amazon, posing risks mainly to the health of foetuses and children. The aim of this study was to analyze and disseminate the distribution of fish species most contaminated by mercury consumed by Amazonian population using an illustrative map. **Methods:** The construction of this product took place in two stages: the first consisted of a literature review on mercury contamination of fish in the Amazon, which was necessary for the construction of the second

stage, which consisted of drawing up the maps themselves, using georeferencing techniques. **Results:** The products produced are presented as Maps 1 and 2, which show the distribution of contamination of predatory and non-predatory fish respectively, by river basin in the Amazon region. Mercury concentrations in fish were above the limit set by the Brazilian Health Surveillance Agency (ANVISA) in 14 predatory species and three non-predatory species. **Conclusions:** The distribution of mercury contamination in the rivers of the Brazilian Amazon is shown in Maps 1 and 2, which can contribute to educational strategies aimed at preventing mercury exposure in vulnerable populations in the Amazon, especially pregnant women, who can benefit from this knowledge during prenatal consultations. As a health control measure, this product should be publicised in the health system and in schools in the regions involved.

ABSTRACT NUMBER: 5026 **Poster Board Number:** LB127

TITLE: Effects of Hg and Se on biomarkers for oxidative stress in stranded cetaceans in the Western Mediterranean Sea

AUTHORS (FIRST INITIAL, LAST NAME) AND INSTITUTIONS: S. Salcedo[1], L. Baños-Doménech[1], F. Sola[1], J. Peñalver[1,2], and *E. Martínez-López*[1]. [1]University of Murcia, Murcia, Spain; and [2]Autonomous Community of the Region of Murcia, Murcia, Spain.

KEYWORDS: Ecotoxicology; Environmental Toxicology; Metals; Biomarkers

ABSTRACT: Background and Purpose: Marine mammals, such as cetaceans, act as excellent indicators, reflecting changes in the marine ecosystem. They serve as sentinel species for public health and the health of our oceans, as they are apex consumers in the food chain and effectively accumulate pollutants. Mediterranean Sea is one of the regions studied due to its high levels of environmental pollutants, which result from its geographic and geomorphological characteristic. Throughout their evolution, marine mammals have developed adaptations to live in the aquatic environment, which may have modified their interaction with toxic substances. They have developed mechanisms to detoxify pollutants, but these contaminants, such as heavy metals, can disrupt redox cycles, affect antioxidant systems, and lead to the accumulation of dysfunctional proteins. Levels of antioxidant molecules, enzyme activity, and products of oxidative damage are useful biomarkers to assess exposure to pollutants, as they show the effects of toxins before organ functions are affected. **Methods:** We determinated the concentration of mercury (Hg) and selenium (Se) and the Se:Hg molar ratio, one of the indicators used to assess if Hg levels are producing any toxic effects, in liver, kidney and muscle of 148 striped dolphins (*Stenella coeruleoalba*), 23 bottlenose dolphin (*Tursiops truncatus*), and 5 common dolphins (Delphinus delphis) stranded along the Murcia coast, Southeast Spain (total 176 samples) in the period 2009-2023. Furthemore, we examined the response of stress biomarkers to the exposure to these metals in these species. In particular, glutathione-S-transferase (GST), catalase (CAT) and lipid peroxidation (TBARS) and biochemical biomarkers such as lactate dehydrogenase (LDH), alanine aminotransferase (ALT), aspartate aminotransferase (AST), alkaline phosphatase (ALP), acetylcholinesterase (AChE), and paraoxonase 1 (PON1). **Results:** Hg and Se were detected in all species cetaceans. The most detected compound was Hg in the muscle (52,27%), closely followed by Se in the muscle (46,02%) and Hg in liver (46,02%), while the lowest detected metal was Se in the kidney (29,54%). The highest concentrations of Hg (128,72 ug g-1w.w) and Se (30,65 ug g-1w.w) were detected in the liver, followed by kidney and muscle. In 29 % of the samples (6 juveniles and 24 adults) the hepatic concentration of Hg exceeds the toxic effects in cetacean (61 ug g-1w. w). In fact, Se mean levels

in liver (15,9%) exceed the limit of Se homeostatic control suggested for marine mammals (0.1-10 ug g-1w.w). In most cases evaluated the Se:Hg molar ratios were above 1, suggesting a Se molar excess which could become toxic at high leves. No significant differences in Hg or Se concentration were observed between species, sex and decomposition state. Although these differences were observed respect to age, being highest in adults. Besides, we found a positive correlation between Hg liver and AST and ALT (rho=0.403, p=0.03; rho=0.396, p=0.034, respectively) and Se liver and AST (rho=0.492; p=0.008). It appears that there could be an overload of the enzyme's capacity or an adaptive response induced by Hg and Se. **Conclusions:** Our results show Hg levels in liver of some individuals were within the range which provoke organ damage in cetacean, and also Se liver levels exceed the homeostatic control. Besides, these metals appear to alter the activity hepatic biomarkers such as AST and ALP. Therefore, it is essential to investigate the response of these biomarkers, not only for human health prevention but also for assessing the health of wildlife.

ABSTRACT NUMBER: 5027 **Poster Board Number:** LB128

TITLE: Evaluating the Interactions of PFAS and Marine Microbes in Sediment Samples in Two Estuaries with Varying Degree of Urbanization

AUTHORS (FIRST INITIAL, LAST NAME) AND INSTITUTIONS: *Z. J. Padgett*[1], *P. C. Powell*[1], M. C. Boland[1], *A. C. Elkins*[1], B. C. Campbell[1], *E. Friend*[2], A. Tweel[2], and *K. D. Rock*[1]. [1]Clemson University, Clemson, SC; and [2]South Carolina Department of Natural Resources, Charleston, SC.

KEYWORDS: None

ABSTRACT: Background and Purpose: Estuaries provide important habitats for an abundance of marine organisms and offer key ecosystem services, providing safe nursery grounds and supporting local fisheries. Despite their ecological and economic importance, estuaries are increasingly vulnerable to the negative impacts of coastal urbanization, including pollution where constant influx of chemical contaminants threaten the health of these ecosystems. Per- and polyfluoroalkyl substances (**PFAS**) have been detected in ocean waters at a global scale, with the highest concentrations observed in urban-influenced estuaries. Charleston Harbor, SC, a highly urbanized estuary, is known to be contaminated with PFAS, however more data is needed to ascertain how the presence of PFAS in SC's estuaries is impacting ecosystem health. Microbes play essential roles in estuaries, maintaining many biogeochemical processes such as nutrient cycling and even degradation of pollutants, including PFAS. PFAS have been shown to alter the abundance and diversity of microbiota in marine sediment, which is likely to impact ecological functions and have subsequent effects on higher trophic levels. Therefore, microbial communities may serve as important bioindicators of estuary health. The present study investigates PFAS concentrations and microbial composition in SC estuaries that differ in degree of urban influence, Charleston Harbor (**CH**, urbanized coastline) and St. Helena Sound (**SHS**, undeveloped coastline), to test the following hypotheses 1) PFAS concentrations in surface water and sediment samples from tidal creeks in SHS will be lower compared to CH, and 2) higher PFAS concentrations will be associated with increased prevalence of PFAS-degrading microorganisms and reduction or elimination of bacterial groups that are susceptible to PFAS toxicity. **Methods:** Sediment samples were collected using a Van Veen Grab, which retrieved material directly from the estuarine floor. The sediment was divided into two tubes: one for PFAS analysis and the other for microbial analysis. Water samples for PFAS analysis were collected by submerging a 1-liter high-density polyethylene (HPDE) bottle. PFAS concentrations in both sediment and water samples collected in June and October 2024

were measured using high-performance liquid chromatography tandem mass spectrometry (HPLC-MS/MS). Microbial composition and abundance in sediment samples collected in March and June 2024 were analyzed through Illumina 16s rRNA sequencing, with the data processed in QIIME 2. Alpha diversity metrics, including Shannon diversity and Pielou's evenness, were calculated, while beta diversity was assessed using Bray-Curtis visualization and Unweighted UniFrac analysis. **Results:** Our preliminary findings indicate differences in PFAS concentrations between CH and SHS, with PFOS levels generally higher in SHS compared to CH. For alpha diversity, Shannon diversity decreased from spring to summer, with March samples showing a higher diversity index than those collected in June. Beta diversity analysis revealed clear patterns: the Unweighted Unifrac plot demonstrated that microbial communities were more similar within the same site and season, while the Bray-Curtis plot highlighted distinct seasonal clustering, with March and June samples grouping together. **Conclusions:** Ongoing research is focused on understanding how microbial communities respond to PFAS at environmentally relevant concentrations, with an emphasis on their potential to break down these persistent compounds. Both aerobic and anaerobic culturing methods are being used to explore whether these microbes can utilize PFAS as an energy source or transform them through metabolic processes. By investigating these interactions, this study aims to address a critical knowledge gap in PFAS bioremediation. The findings could provide valuable insights into the role of microbes in mitigating the environmental impact of these hard to degrade contaminants and inform future strategies for managing PFAS pollution.

ABSTRACT NUMBER: 5028 **Poster Board Number:** LB129

TITLE: Scientific Initiative for Secondary School students to Promote School Research in Latin American Countries: empowering STEM talent

AUTHORS (FIRST INITIAL, LAST NAME) AND INSTITUTIONS: A. Botero Alvarez[1], Z. Alvarez Amaris[1], S. Mendoza Morales[1], A. Llorente Espinosa[1], *B. Arroyo Salgado*[2], L. Tejada Benitez[3], and L. Cervantes Ceballos[2]. [1]Liceo Campestre Jean Piaget, Chinu, Colombia; [2]University of Cartagena, School of Medicine, Department of Basic Sciences, Biomedical, Toxicological, and Environmental Sciences Research Group, Cartagena, Colombia; and [3]University of Cartagena, Chemistry Enginieer, Department of Basic Sciences, Biomedical, Toxicological, and Environmental Sciences Research Group, Cartagena, Colombia.
KEYWORDS: Ecotoxicology; Education; Environmental Toxicology; Young researchers, STEM

ABSTRACT: Background and Purpose: Research in toxicology among high school students in Latin American countries is essential to develop the critical and creative skills necessary to face modern challenges. In developing countries, this practice becomes more relevant by fostering local innovation, knowledge transfer and citizen participation, closing gaps and creating solutions to environmental health problems that drive sustainable human development. This project aimed to create spaces for citizen construction, participation and interaction in Science, Technology and Innovation (STI) through STEM tools in Colombian public and private educational institutions to encourage research in toxicology in young schoolchildren. The objective was to inspire, guide and create meaningful connections in the exciting world of knowledge between children and researchers. **Methods:** A participatory study was conducted with 10th grade students from Chinú (Colombia) and 9th grade students from Cartagena de Indias (Colombia). STEM education was used to expose them to scientific research and various scientific models in the area of toxicology in the laboratories of the Chemical Engineering program, and the Faculties of Medicine and Pharmaceutical Sciences and the Biotoxam Research Group of the University

of Cartagena, providing basic and specialized training in ecotoxicological tests, using the nematode Caenorhabditis elegans as a biological model for the study of environmental toxins and natural products. Additionally, a knowledge transfer program called "Science Explorers" was carried out through theoretical and practical sessions that covered topics such as the microscopic world of microorganisms, laboratory safety, and research procedures. **Results:** In collaboration with the University of Cartagena, laboratories were built within educational institutions and workshops were held to facilitate knowledge transfer through research practices led by researchers and graduate students (master's and doctoral levels) from the Biotoxam Research Group. Students demonstrated remarkable growth in scientific skills and obtained high scores on knowledge tests. In addition, there was a significant increase in admissions to advanced programs in biological sciences, medicine, and engineering, as well as enrollment in selective higher education institutions. **Conclusions:** Developing scientific activities from an early age strengthens analytical skills, problem-solving abilities, and teamwork. These skills are crucial to preparing students to compete in an increasingly demanding global market that requires creative professionals willing to contribute to knowledge economies. By prioritizing student research through strategic investments and partnerships, developing countries can position themselves as centers of innovation and progress, ensuring a promising future for new generations.

ABSTRACT NUMBER: 5029 **Poster Board Number:** LB130

TITLE: Zebrafish (*Danio rerio*), an *in vivo* predictive model for assessing acute toxic effects of anti-inflammatory drug exposure: ecotoxicity of emerging pollutants

AUTHORS (FIRST INITIAL, LAST NAME) AND INSTITUTIONS: *M. García-Espiñeira*[1], H. Gómez-Estrada[2], and *J. Florez-Cervantes*[3]. [1]Biomedical, Toxicological, and Environmental Sciences Research Group., University of Cartagena, Colombia; [2]Medicinal Organic Chemistry Research Group, University of Cartagena, Colombia; and [3]La Nueva Esperanza School. Ondas Minciencias Program, Turbaco, Colombia.

KEYWORDS: Aquatic Toxicology; Ecotoxicology; Pharmaceuticals; acetaminophen, diclofenac

ABSTRACT: Background and Purpose: Pharmaceutical contamination in aquatic ecosystems is considered an emerging problem, due to increase in the use of antibiotics, beta-adrenergic antagonists and non-steroidal anti-inflammatory drugs (NSAIDs) as the most prominent. In addition, there are few reports on the effects of these chemicals on organisms of the aquatic environment, especially when used in large quantities. We evaluated acute toxic effects of acetaminophen (CAS Number 103-90-2) and diclofenac (2-(2-(2,6-dichlorophenylamino) phenyl) acetic acid) purchased from Sigma Aldrich in zebrafish model. **Methods:** The animal procedures performed in our study met the principles established by the Institute of Immunology of the University of Cartagena protocol for animal experimentation. Adult individuals of *D. rerio* were donated by the Biodiversity and Applied Ecology Research Group Lab of The University of Magdalena. Animals were kept in aquaria with carbon-filtered dechlorinated water (4 females and 2 male/aquarium) at 26 °C - 28 °C with a photoperiod of 12 h light/12 h dark and water recirculation system at the Biotoxam Lab facility in Cartagena. Fish were subjected in duplicate in aquaria dissolved in dechlorinated water containing diclofenac and acetaminophen in the following concentrations: 0 (control/ untreated), 10 µg/mL, 50 µg/mL, 100 µg/mL and 500 µg/mL. Natural mating was observed for 8 days**.** Biological parameters of reproduction, mortality, and tissue damage of the gills and ovaries were assessed daily by histology to determine its presence or absence. **Results:** After 24 h of diclofenac exposure and 48 h of acetaminophen exposure at high concentrations of 100 and 500 µg/mL, 100% mortality was shown. At concentrations of 10 µg/mL

and 50 µg/mL, presence of unfertilized eggs was observed by stereomicroscopy. After 8 days of exposure, fish were anesthetized with eugenol oil and euthanized by transection of the cervical spine. The gills and ovaries were collected for histological analysis; samples were gradually dehydrated in ethanol, embedded in paraffin, sectioned at a thickness of 5 µm, and stained with hematoxylin and eosin**.** In females (n=8) and males (n=6), incident spots were quantified in the following elements: oogonia (Oo), cortical vesicular follicles (CV) and gills slight tissue alterations were evident. **Conclusions:** In conclusion, exposure to diclofenac and paracetamol induced histopathological lesions that may alter the functions regulated by the affected organs, which are related to important biological processes; subclinical changes originated from exposure at low concentrations. These histopathological lesions may become biomarkers of emerging contaminant effects on biological models. The experience of high school students assessing the toxicological effects of exposure to low-dose environmental chemicals from the pharmaceutical industry, may enhance their scientific awareness and adherence to policies of protection to the environment from emergent toxicants.

ABSTRACT NUMBER: 5030 **Poster Board Number:** LB131

TITLE: Chamber-specific impacts of lead exposure on calcium dynamics in human ipsc-derived cardiomyocytes

AUTHORS (FIRST INITIAL, LAST NAME) AND INSTITUTIONS: I. R. Melis[1], *C. W. Clark*[1], A. Monteiro da Rocha[2], H. Joo[1], *T. Ishikawa*[1], A. Siglin[1], *K. Sala-Hamrick*[1], T. J. Herron[2], and *L. K. Svoboda*[1]. [1]University of Michigan School of Public Health, Ann Arbor, MI; and [2]University of Michigan Medical School, Ann Arbor, MI.

KEYWORDS: Environmental Toxicology; Cardiovascular System; Stem Cells; Lead (Pb)

ABSTRACT: Background and Purpose: Lead (Pb) is a pervasive environmental toxicant linked to increased cardiovascular risk, yet its direct effects on cardiac function at the cellular level remain incompletely understood. Previous studies have shown that Pb disrupts calcium handling in cardiomyocytes, a key process for proper cardiac excitation-contraction coupling. This study aims to expand on these findings by investigating the chamber-specific effects of Pb exposure on calcium dynamics in human-induced pluripotent stem cell-derived atrial (aCMs) and ventricular cardiomyocytes (vCMs). Understanding these differential impacts provides insight into the mechanisms underlying Pb-induced cardiotoxicity. **Methods:** Atrial and ventricular cardiomyocytes were differentiated from human iPSCs using established cardiac-directed protocols that modulate the Wnt signaling pathway. Following differentiation, cardiomyocytes were purified using magnetic-activated cell sorting (MACS) to achieve over 98% purity. These purified aCMs and vCMs were used to investigate the effects of Pb exposure on calcium handling. Cells were exposed to environmentally relevant Pb concentrations in both acute and sub-chronic exposure models. Calcium dynamics, including beat frequency, calcium transient amplitude, and conduction velocity, were assessed using high-resolution optical mapping. Baseline functional differences between aCMs and vCMs were characterized prior to Pb exposure, and changes in calcium handling parameters were analyzed to evaluate dose- and time-dependent effects. This approach allowed for the identification of chamber-specific responses to Pb toxicity. **Results:** Baseline measurements revealed distinct chamber-specific profiles between aCMs and vCMs. Atrial cardiomyocytes exhibited significantly higher beat frequency ($p < 0.0001$) and conduction velocity ($p < 0.01$), while ventricular cardiomyocytes displayed greater calcium transient amplitude ($p < 0.0001$) and faster recovery times ($p < 0.0001$). Pb exposure induced dose-dependent effects: aCMs showed

significant increases in calcium transient amplitude ($p < 0.0001$) and upstroke slope ($p < 0.05$) at 500 µM Pb, while vCMs exhibited significant decreases in amplitude ($p < 0.0001$) and upstroke slope ($p < 0.0001$) at 500 µM Pb. Time-course analysis revealed dynamic changes based on Pb exposure duration. In aCMs, baseline fluorescence significantly decreased after 1 to 12 hours of exposure ($p < 0.0001$) but returned to baseline by 72 hours, while vCMs showed a significant increase after 1 to 3 hours ($p < 0.05$), normalizing by 6 hours. Calcium transient amplitude in aCMs peaked after 3 hours ($p < 0.0001$) and remained elevated at 72 hours ($p < 0.05$), while vCMs showed a significant decrease at 3 and 6 hours ($p < 0.01$), persisting at 72 hours ($p < 0.001$). These findings underscore chamber-specific differences in susceptibility to Pb toxicity and highlight distinct physiological responses to Pb exposure. **Conclusions:** This study highlights significant chamber-specific differences in the effects of Pb exposure on calcium dynamics in human iPSC-derived cardiomyocytes. Atrial and ventricular cardiomyocytes exhibited distinct responses to Pb, with aCMs showing increases in calcium transient amplitude and upstroke slope, while vCMs demonstrated reductions in these parameters at higher Pb doses. Time-course analysis revealed that Pb-induced disruptions were dynamic, with some effects, such as baseline fluorescence and calcium transient amplitude, partially normalizing over time, while others, such as amplitude reductions in vCMs, persisted. These findings emphasize the importance of considering chamber-specific physiology when assessing Pb-induced cardiotoxicity and provide critical insights into the mechanisms underlying Pb's impact on cardiac function. Ongoing studies are investigating the molecular pathways involved in these chamber-specific responses, aiming to identify potential therapeutic targets to mitigate the cardiovascular risks of Pb exposure.

ABSTRACT NUMBER: 5031 **Poster Board Number:** LB132

TITLE: Characterizing yolk-sac derived cardiac tissue resident macrophages for cardiovascular and developmental toxicity assessment

AUTHORS (FIRST INITIAL, LAST NAME) AND INSTITUTIONS: Y. Chen, N. Martin, C. Bortner, and G. Harry. National Institute of Environmental Health Sciences, Research Triangle Park, NC. Sponsor: *K. Ryan*

KEYWORDS: Macrophage; Cardiovascular System; Immunotoxicology

ABSTRACT: Background and Purpose: Tissue resident macrophages (TRMs) play key roles in innate immune responses and in sustaining critical tissue specific homeostatic functions. They mediate cell communication/interactions, participate in metabolic pathways, and secrete growth factors. In these functions, they integrate various environmental cues to support other tissue-resident cells function at steady state. As examples, brain TRMs, microglia, contribute to all aspects of brain development by influencing cell development and migration as well as cell plasticity. In the heart, TRMs support arterial elasticity control, electrical conduction, and tissue remodeling. A sub-population of TRMs can originate from embryonic yolk-sac progenitors, populating tissue from early stages of development and contributing to proper organogenesis. Yolk-sac derived TRMs are represented by microglia in the central nervous system (CNS) and in peripheral organs, they are one part of a diverse TRM community. The diversity but also similarity of TRM with blood borne macrophages in peripheral organs raises a difficulty in examining targeted effects *in vivo* using morphological methods. While unique cell populations can be identified by flow cytometry, experimental manipulation is limited. Cultures of microglia have been successfully used to examine functional inflammatory and non-inflammatory functions of yolk-sac derived TRMs, however, cells obtained from peripheral organs represent a more diverse origin and compromise the ability to study a unique cell population. For the brain yolk-sac derived macrophages in

rodents populate the tissue within the first few days after birth. A similar colonization age, within the first 2-4 days of life, is identified for yolk-sac derived TRMs in the heart. In both tissues, these cells are long-lived and display a low level of self-replication. Thus, not only do they represent a potentially vulnerable cell population during early development, but also a population of cells that may manifest alterations later in life due to earlier disruptions. We will present our data associated with the isolation of yolk-sac derived TRMs from the immature heart, characterization of that cell population, optimization of culture conditions, establishment of cell lines, and comparison of the immunophenotypes and inflammatory response. *Objective:* We hypothesized that yolk-sac derived TRMs are a potential target in developmental and chronic toxicant exposures that can contribute to adverse health effects if dysregulated. **Methods:** Heart yolk-sac derived TRMs were isolated from 2-day-old CD1 mice, digested and dissociated into a single cell suspension. Cardiomyocytes were separated by mass differences. The non-myocytes cardiac isolates were labelled with fluorophore-labeled surface marker antibodies and subjected to cell sorting by BD FACS Symphony S6. The target cardiac TRMs are defined as $CD45^+CD64^+F4/80^+CD11b^+Ly6G^-Ly6C^-CCR2^-TIMD4^+MHCII^{lo}$. The sorted cardiac resident macrophages were immortalized (iCRMs) and differential gene expression profiles in naïve and immune challenged (e.g. LPS) cells were compared using qRT-PCR to further characterize the immunophenotypes. **Results:** A total of six cell lines were generated. Four target cell lines: $CD45^+CD64^+F4/80^+CD11b^+Ly6G^-Ly6C^-CCR2^-TIMD4^+MHCII^{lo}$ macrophages (TIMD4+ iCRM); two alternative cell lines: $CD45^+CD64^+F4/80^+CD11b^+Ly6G^-Ly6C^-CCR2^-TIMD4^+MHCII^{hi}$ (DP iCRM), and $CD45^+CD64^+F4/80^+CD11b^+Ly6G^-Ly6C^-CCR2^-TIMD4^-MHCII^{hi}$ (MHCII iCRM) macrophages. The surface marker expression was verified with qRT-PCR. The four target TIMD4+ iCRM cell lines displayed various sensitivity to LPS stimulation as measured by qRT-PCR of pro-inflammatory cytokines. TIMD4+ iCRM.4 showed higher *Il1b* and *Il6* expression and as a comparison, *Il1b* expression in DP iCRM cell line was significantly lower than all four target TIMD4+iCRM cell lines. **Conclusions:** We have been successful in generating heart TRM cell lines representing differential immunophenotype profiles and responses. This will allow us to establish specific reporter cell lines to further explore the potential for environmental exposures to modulate the cell functions, interact with other tissue specific cells, contributing to adverse effects in the tissue.

ABSTRACT NUMBER: 5032 **Poster Board Number:** LB133

TITLE: Beyond redox: Effects of NH_4^+ and catecholaldehydes formed from MAO-mediated catecholamine metabolism in cardiomyocytes

AUTHORS (FIRST INITIAL, LAST NAME) AND INSTITUTIONS: *R. M. Crawford*, and E. J. Anderson. University of Iowa, Iowa City, IA.

KEYWORDS: Cardiovascular System; Mechanisms

ABSTRACT: Background and Purpose: Catecholamines are critical for regulating heart rate and rhythm but their intracellular metabolism via monoamine oxidase (MAO) in cardiomyocytes has emerged as a source of toxicity in recent years. Oxidative deamination of the catecholamine norepinephrine (NE) by MAO generates reactive metabolites including hydrogen peroxide (H_2O_2), ammonia (NH_4^+), and the catecholaldehyde 3,4-dihydroxyphenylglycolaldehyde (DOPEGAL), all of which could have consequential effects on mitochondrial metabolism and redox balance. Studies in experimental models have shown that MAO has a pathogenic role in the heart during ischemia/reperfusion, arrhythmogenesis, and pressure overload. Mechanisms underlying MAO's pathogenicity are not entirely understood but a majority of studies have focused on oxidative stress generated by MAO-mediated H_2O_2 production while

ignoring NH_4^+ and catecholaldehydes. These metabolites are particularly difficult to detect in biological systems owing to their high reactivity. Recently, our lab has shown that DOPEGAL readily forms stable conjugates with the dipeptide carnosine in cells, illustrating both the therapeutic potential of carnosine and use of these conjugates as a biomarker of MAO activity and toxicity. In this study we went 'beyond redox' to investigate NH_4^+ and DOPEGAL formation by MAO during NE metabolism, and the mechanisms underlying the biological effects of these metabolites in cardiomyocytes. **Methods:** Mitochondrial respiration (*J*O2) was measured in mitochondria isolated from left ventricle/septum of healthy, young adult (8-15 weeks) wild-type (WT) and cardiomyocyte-specific MAO-A deficient (cMAO-A^{def}) mice. Respiration was supported by a range of substrates (pyruvate, palmitoyl carnitine, glutamate) while clamped in phosphorylating state (0.1mM ADP) followed by NE or NH_4^+ administration. Detection of DOPEGAL was achieved with LC-MS/MS using primary adult cardiomyocytes isolated from WT mice and incubated with NE (100µM), in presence and absence of carnosine (1mM) and MAO inhibitors (MAOIs) for up to 24 hours. **Results:** Respiration analysis revealed that NE (5, 10µM) had no effect on JO_2 supported by pyruvate or palmitoyl-carnitine, but NE increased glutamate-supported JO_2 by 15%. This effect was abrogated in cMAO-A^{def} mice and with MAOIs. Importantly, the effect of NE was phenocopied with NH_4^+ and attenuated with an inhibitor of glutamic oxaloacetic transaminase-1 (iGOT1). MS analysis of conditioned media following cardiomyocyte incubation showed a peak at 1.64 retention time with same *m/z* and fragmentation pattern seen with the DOPEGAL-carnosine standard, and MAOIs completely blunted this peak formation. **Conclusions:** These findings provide greater insight into the mechanisms underlying MAO cardiotoxicity. Our data indicates that the NH_4^+ formed during MAO-mediated NE metabolism is linked to mitochondrial glutamate uptake and oxidation via GOT1, revealing a potential new pathway by which MAO impacts mitochondrial OxPHOS. Finally, our detection of DOPEGAL-carnosine adducts in conditioned media via LC-MS/MS validates the use of this biomarker as an index of MAO activity in cardiomyocytes, which can be exploited to develop novel pharmacotherapies which mitigate pathogenic effects of MAO.

ABSTRACT NUMBER: 5033 **Poster Board Number:** LB134

TITLE: Validation of Human Airway Organ Tissue Equivalents for Ammonia Gas Toxicity: Multi-Dose Characterization and Cross-Species Analysis

AUTHORS (FIRST INITIAL, LAST NAME) AND INSTITUTIONS: *J. Blackburn*, *T. Leach*, A. Pendino, L. Morris, A. Sharma, T. Young, K. Libby, K. Reeves, M. Rezapour, A. Atala, and *S. V. Murphy*. Wake Forest University, Winston-Salem, NC.

KEYWORDS: In Vitro and Alternatives; Inhalation Toxicology; Lung; Pulmonary or Respiratory System

ABSTRACT: Background and Purpose: Acute exposure to high concentrations of ammonia gas poses a significant threat to pulmonary health; however, its effects remain poorly understood due to the ethical and practical challenges associated with conducting research on human or animal subjects. Our lab has developed an airway Organ Tissue Equivalent (OTE) model, which is a 3D *in vitro*, micro physiological system to accurately represent the human airway biologically and functionally. The model incorporates native human cell types (epithelial, fibroblast, endothelial) and ECM on a high throughput 96-well Transwell format. The objective of this project is to leverage the airway OTE to characterize the response to acute ammonia gas exposure through chemical and biological measurements and transcriptomics. **Methods:** Using a high throughput approach, airway OTEs were developed and exposed to a range of ammonia gas concentrations (1500-3500ppm) and exposure times (15-30min). Chemical

assays and biological measurements were used to characterize viability, metabolism, toxicity, cilia active area, and TEER, and OTEs were further analyzed using RNA sequencing. All measurements were taken pre-exposure and at 0-, 6-, 12-, and 24-hours post-exposure. **Results:** The results of viability, metabolism, toxicity, cilia active area, and TEER showed worsening health with increased severity of exposure concentration or duration. From all assays and measurements, we identified a recoverable exposure condition of 1500ppm for 15min, a moderate condition of 1500ppm for 30min, and a non-recoverable condition of 3500ppm for 30min. Transcriptomics results supported findings with increased differentially expressed genes in more severe exposures. Additionally, genetic pathways involved with heat stress response, cilium assembly, and inflammation were significantly upregulated following exposure. Comparison to animal models found in literature showed agreement with the results of this study. **Conclusions:** The findings of this study provide critical insights into ammonia's toxicological effects, which are comparable to prior animal studies and to EPA human exposure guidelines. Additionally, the identified exposure conditions offer a valuable direction for evaluating medical countermeasures for lung injury, advancing the study of ammonia toxicity, and identifying broader impacts of *in vitro* toxicology.

ABSTRACT NUMBER: 5034 **Poster Board Number:** LB135
TITLE: Quantifying *In Vitro* Disposition of PFAS Using Human Breast Cancer (MCF7) and Osteosarcoma (U-2 OS) Cell Lines

AUTHORS (FIRST INITIAL, LAST NAME) AND INSTITUTIONS: C. Sumner, *J. Harrill*, and *B. Wetmore*. Environmental Protection Agency, RTP, NC.
KEYWORDS: Cell Culture; Perfluoronated Agents; In Vitro and Alternatives

ABSTRACT: Background and Purpose: The US EPA has recently started using *in vitro* new approach methods (NAMs) to efficiently screen and generate omics data on thousands of chemicals. Per- and poly- fluorinated alkyl substances (PFAS) are ubiquitous in the environment and are emerging contaminants of concern due to their extreme chemical stability and proposed toxicological effects. The research we are presenting is focused on generating experimental data on the disposition of PFAS in *in vitro* microplate test systems. This information can be used to inform in-vitro in-vivo extrapolation (IVIVE) of bioactivity data from NAMs used at US EPA. Prior research conducted by the US EPA investigated the difference between the free and nominal concentration of a chemical *in vitro*. Depending on the chemical's equilibrium partitioning, K_{ow}, or the presence of lipids and proteins in the media, the free concentration of the chemical will change leading to an uncertainty of the chemical concentration available to partition into the cells. The objective in this study is to determine what concentrations of PFAS bind to various percentages of fetal bovine serum (FBS), adsorb to the plastic of the cell culture vessel, or diffuse into the cells. Herein, data are presented on the disposition of PFAS after 24 hours of exposure in two cell lines with 10% FBS growth serum. **Methods:** Three 96 well polystyrene culture plates were used to assess the compartmental (plastic, media, or cells) distribution of 12 different PFAS compounds (short and long chain, sulfonated and carboxylated) after 24 hours of exposure. Each plate contained 10% FBS in Dulbecco's Modified Eagle Medium (DMEM) with two of the plates containing a human cell line (U-2 OS or MCF7). The design allows for each compartment to be analyzed separately; the media was transferred from two of the plates and tested for their PFAS concentration separate from the plastic. Therefore, the third plate containing cells was analyzed completely and served as a 100% representation of the PFAS concentration *in vitro* (identified as a

whole well crash). Each well in the culture plates was spiked to contain a final concentration of 10uM of PFAS. Acetonitrile was used to crash the biological material and extract the PFAS from the plastic. Quadruple replicate PFAS concentrations were analyzed from each plate using a Waters Xevo TQ-S micro-LC-MS/MS equipped with a T3 column. Cell growth (i.e. number of cells per well) and confluency 24 hours before and after dosing was quantified using an Opera Phenix Plus. Ionomycin served as a reference for cytotoxicity and DMSO as a vehicle control to confirm cell growth was not impacted by the PFAS and reduce uncertainty of PFAS diffusion into the cells. Additionally, the U-2 OS cell line expressed a trio of fluorescent markers for the nucleus (LaminB1), microtubules (alpha tubulin), and beta actin to confirm PFAS was not dramatically influencing cellular morphology which could potentially lead to a decrease of cellular concentration of PFAS. **Results:** Before dosing, the U-2 OS cells were about 50-60% confluent in the wells, and after 24 hours of dosing, the cells were about 75-85% confluent, indicating that cell growth was still occurring after exposure to PFAS. The concentration of PFAS in the media only compartment was statistically less than the whole well crash (p-value = 0.04). On average, the percentage of PFAS quantified in the plastic only compartment was about 13% of the total PFAS calculated in the whole well crash. Media extracted and analyzed separately from the plastic compartments in the culture plate containing cells consisted of similar concentrations of PFAS compared to the whole well crash (p-value = 0.9). However, lower concentrations of PFAS were extracted from the plastic and cells compartment, accounting for about 10% of the total PFAS. In contrast, the MCF7 cell line experiment did not yield any PFAS concentrations in the plastic compartments. The highest concentration of PFAS was identified in the media only plates. Compared to the whole well crash, the media only compartment contained 130% of the total PFAS. The media compartment extracted from the cells encompassed 95% of the total PFAS. It is possible that the plastic and cells compartment contained PFAS below the method detection limit (~0.1 uM). **Conclusions:** To improve interpretation of high throughput screening data, more research is needed on the distribution of chemicals *in vitro*. In our study, the behavior of PFAS differed across two human cell lines, highlighting the integral nature of experimental *in vitro* data collection. In the MCF7 experiment, the wells contained a greater volume of media than the U-2 OS cell line, which could indicate that the PFAS readily bind to the proteins and lipids in the FBS rather than adsorbed on to the plastic, leading to the higher percentage of PFAS in the media only compartment. In the U-2 OS cell line, the media extracted from the cells displayed similar concentrations to the whole well crash and lower percentages of PFAS in the plastic + cells compartment, which could be due to the lack of surface area for adsorbing to the plastic due to the monocellular layer occupying the bottom of the wells. Overall, there is a scientific knowledge gap on the kinetics of PFAS binding to the various components of a cell-based *in vitro* test system in microplate format. Further research needs to be conducted using different percentages of FBS to calculate partitioning kinetics and characterize the behavior of PFAS *in vitro*. Subclones of the U-2 OS cell line are being prepared in various percentages of FBS to evaluate these conditions. These studies provide empirical data that can be used to improve computational modeling of PFAS chemical distribution and IVIVE as applied to NAMs. *This abstract does not represent US EPA policy.*

ABSTRACT NUMBER: 5035 **Poster Board Number:** LB136

TITLE: Impact of per- and polyfluoroalkyl substances on human gut bacteria

AUTHORS (FIRST INITIAL, LAST NAME) AND INSTITUTIONS: Y. Tian, S. Koshkin, I. Koo, G. Ning, J. L. Gray, T. Cutler, A. Vijay, K. J. Oldro, B. D. Anderson, B. Swencki-Underwood, S. Tian, J. E. Bisanz, *J. M. Peters*, and A. D. Patterson. PSU, State College, PA.

KEYWORDS: Persistent Organic Chemicals; Metabolomics; Microbiome

ABSTRACT: Background and Purpose: Per- and polyfluoroalkyl substances (PFAS) are persistent environmental chemicals widely used in industrial and consumer products due to their unique chemical and physical properties. Human exposure to PFAS is nearly unavoidable, with these persistent chemicals accumulating in the body and potentially contributing to adverse health outcomes, including cancer and metabolic disorders. While much research has focused on the toxicity of PFAS to host tissues (e.g., liver), recent efforts indicate that environmental chemicals may also exert toxicity by directly or indirectly influencing the gut microbiome. However, the potential effects of PFAS on gut bacteria and their broader impact on human health remain unclear. **Methods:** This study employed a multidisciplinary approach to evaluate the effects of PFAS on gut microbiota. We utilized high-throughput bacterial growth assays, microbiome sequence-based community profiling, advanced microscopy techniques, RNA sequencing, and NMR- and mass spectrometry-based metabolomics to evaluate the impact of a diverse set of PFAS on human fecal bacteria and representative bacterial species. We also used crystal violet biofilm assays and microbial evolution experiments, combined with genomic analysis of PFAS-resistant strains, to explore the mechanisms underlying bacterial resistance to PFAS exposure. Microbial PFAS bioaccumulation and metabolism kinetics was analyzed using energy dispersive X-ray spectroscopy (EDS) and ultra-performance liquid chromatography-mass spectrometry (UPLC-MS/MS). **Results:** A diverse set of PFAS and 96 representative bacterial strains and human fecal microbial communities were screened revealing inter-species and interindividual variation in response. *Bacteroides* species were highly sensitive, while *Escherichia coli* (*E. coli*) and *Enterococcus faecalis* (*E. faecalis*) were resistant to a broad range of PFAS. We confirmed that carbon chain length and functional head groups significantly influence bacterial growth inhibition of PFAS. For example, PFOS showed stronger inhibitory effects compared to PFOA and PFHxS. PFAS-resistant strain *E. faecalis* exhibited tolerance under high PFAS exposure conditions. PFAS-resistant strains of *E. coli* and *E. faecalis* exposed to high levels of PFAS displayed demonstrated enhanced biofilm formation in response to PFAS increasing their resistance to antibiotics. PFAS uptake by bacteria occurred across a broad concentration range, from nanomolar to 400 µM, in both human fecal bacteria communities and specific gut bacterial species. **Conclusions:** These findings enhance our understanding of the potential health risks associated with PFAS exposure and offer insights into the intricate interactions between environmental chemicals and the human microbiome.

ABSTRACT NUMBER: 5036 **Poster Board Number:** LB137

TITLE: The non-linear toxicity of Perfluorohexane sulfonic acid in adult zebrafish: evidence of toxic effect response and modulation through microRNA expression

AUTHORS (FIRST INITIAL, LAST NAME) AND INSTITUTIONS: L. G. Garrett[1], D. M. Perone[2], *L. Truong*[2], *N. Garcia-Reyero*[3], E. Perkins[3], and G. D. Mayer[4]. [1]Univerisity of Colorado - Denver, Denver, CO; [2]Oregon State University, Corvallis, OR; [3]Environmental Laboratory, US Army Engineer Research & Development Center, Vicksburg, MS; and [4]Texas Tech University, Lubbock, TX.

KEYWORDS: Perfluoronated Agents; Environmental Toxicology; Gene Expression/Regulation; Molecular Toxicology; PFHxS

ABSTRACT: Background and Purpose: Toxic responses in organisms exposed to PFAS are found to have a non-monotonic relationship with dose, therefore making dose-response for this class of chemicals difficult to model and predict. Here we provide mechanistic evidence of a route via the downregulation

of microRNA expression which produces non-linear gene-expression under perfluorohexane sulfonic acid (PFHxS) exposure. **Methods:** Adult zebrafish were continuously exposed for 3 weeks to 6 concentrations of PFHxS. At the termination, total RNA was extracted and sequenced from the livers and gonads of the zebrafish (n=96; 50% male, 50% female) to determine the effect of PFHxS on gene expression. Pre-processing and alignment of sequenced reads was complete with nf-core rnaseq pipeline built under Nextflow. RNAseq analysis was performed using limma-voom approach to identify differentially expressed genes (DEGs, log2 fold change ≥ |1|, FDR ≤ 0.05) between control and 5 treatments across a concentration gradient (0.3uM, 1.5uM, 3uM, 15uM, 30uM). P-integration and visualization of was performed using MINT (mixomics) to determine statistical drivers between organs and sex. The top 1000 of differentially expressed genes by significance per sex-organ intersection (Male-Liver, Male-Gonad, Female-Liver, and Female-Gonad) were analyzed by DAVID and IPA software to determine functional gene ontology clusters and the dysregulation of pathways across concentration. **Results:** Our results show that concentrations with significant the downregulation of transcripts for microRNAs are not predicted to cause dysregulation of pathways. Interestingly, concentrations predicted to activate pathways in IPA did not show microRNAs at differentially expressed levels in DAVID. Therefore, we posited that concentrations with downregulation of microRNAs should show overexpression of their gene targets which may influence toxic outcome. Targets for differentially expressed microRNAs were determined for each affected concentration per sex-organ group using TargetScanFish6.2 by the family of microRNA. The expression levels (log2fold-change) of predicted targets with a context score less than -1 were extracted from the data for further analysis. Of the predicted targets, those found to be upregulated were selected as candidates for further analysis, which included genes involved in detoxification processes (*cyp2x12*) and xenobiotic response (*arnt*). **Conclusions:** We propose that the upregulation of detoxifying genes may provide a protective effect at concentrations where their silencers are under-expressed, connecting post-transcriptional regulation to toxicological response. Therefore, microRNAs' expression should be considered when analyzing PFAS class chemicals and modeling their non-monotonic dose relationships.

ABSTRACT NUMBER: 5037 **Poster Board Number:** LB138

TITLE: Perfluorononanoic acid (PFNA)-induced developmental toxicity in zebrafish embryos: eye and brain as targets

AUTHORS (FIRST INITIAL, LAST NAME) AND INSTITUTIONS: *S. Sharma*, *A. Rojas*, and *S. Dasgupta*. Clemson University, Clemson, SC.

KEYWORDS: None

ABSTRACT: Background and Purpose: Perfluorononanoic (PFNA) is a synthetic long chain (C ≥ 8) homologue of per and polyfluoroalkyl substances (PFAS) which is frequently detected in environment as an emerging contaminant with potential threats to living organisms. It has broad applications in industrial and consumer products including adhesives, water and paint repellent surfaces, non-sticky coatings and lubricants. PFNA is very stable and persistent in the environment due to high energy carbon-fluorine bonds and anti-degradation (photo and microbial) properties. Studies show that PFNA caused immune, cardiac, endocrine, reproductive and developmental toxicity. This study investigates the developmental toxicity of PFNA using behavioral assay and focuses on organ specific toxicity (brain and eye) via transcriptomic analysis. **Methods:** Tropical 5D zebrafish embryos were exposed to different concentrations of PFNA (0, 0.031, 0.31, 3.12, 6.25 and 12.5 µM) from 2-hour post fertilization (hpf) to

120 hpf under dark conditions in temperature-controlled incubator at 28 °C. Larval photomotor response (LPR) was conducted to assess change in behavioral patterns. For organic specific toxicity, embryos were exposed to 0 and 12.5 µM of PFNA till 120 hpf. Brain and eyes were dissected and extracted RNA was sequenced on an Illumina Platform. Gene Ontology (GO) and Kyoto Encyclopedia Genes and Genomes (KEGG) analysis were also conducted for pathway analyses. For statistical analysis, Kruskal-Wallis test followed by Dunn's test was opted for behavior data using GraphPad Prism, while R software was used for differential expression analysis. **Results:** PFNA exposure led to significant behavioral alterations in zebrafish larvae at 6.25 and 12.5 µM characterized by hyperactivity during light phases and distinct "O-bend" responses in the LPR assay. This hyperactivity is suggestive of neurotoxic and visual impairments which led us to focus on transcriptomic analysis of brain and eye. RNA sequencing showed 287 differentially expressed genes (DEGs) in brain while that of 683 in eye. GO and KEGG pathways analysis revealed that the common affected pathways in both organs were circadian rhythms, steroid biosynthesis, fatty acid metabolism and PPAR signaling. Additionally, disruptions in insulin and notch signaling were seen in brain, while P53 signaling and phototransduction pathways were affected in eye. **Conclusions:** This study demonstrates that PFNA exposure disrupts neurodevelopmental processes in zebrafish embryos by impairing circadian rhythm and vision. The findings underscore the neurotoxic potential of PFNA and its ability to interfere with both behavioral and molecular pathways in brain and eye. Collectively, this research highlights the need for environmental and regulatory evaluations of PFNA and other PFASs, focusing on their long-term impacts on neurodevelopment and circadian rhythm and potential health risks in contaminated ecosystems and populations.

ABSTRACT NUMBER: 5038 **Poster Board Number:** LB139
TITLE: Evaluating Racial Differences in PFAS Induced Toxicity and DNA Damage: The Role of Melanin

AUTHORS (FIRST INITIAL, LAST NAME) AND INSTITUTIONS: S. Sharma, *M. Meister*, and *C. Wright*. Chemical Insights Research Institute of UL Research Institutes, Marietta, GA.
KEYWORDS: Carcinogenesis; Cutaneous or Skin Toxicity; Environmental Toxicology; PFAS

ABSTRACT: Background and Purpose: Environmental factors, including per- and polyfluoroalkyl substances (PFAS), have been linked to melanoma, the most lethal form of skin cancer, which arises from the malignant transformation of melanocytes. While melanin content plays a role in the incidence of melanoma, the severity and lethality of the disease can vary significantly depending on other factors, including racial background. In Caucasian populations, early diagnosis contributes to better therapeutic outcomes; however, melanoma is often detected at later, more advanced stages in minority populations, leading to poorer prognoses. Therefore, this study aims to investigate whether racial differences contribute to the PFAS toxicity and DNA damage following PFAS exposure. **Methods:** Melanocyte cell lines from three different racial backgrounds Black, Caucasian, and Asian were treated with PFAS of varying carbon chain lengths (PFPeA Perfluoropentanoic acid; PFHxA Perfluorohexanoic acid; PFHpA Perfluoroheptanoic acid; PFOA Perfluorooctanoic acid; PFNA Perfluorononanoic acid; PFDA Perfluorodecanoic acid; and a mixture of all PFAS). These cells were exposed to 10nM and 10µM concentrations for 24 hours. After treatment, melanocytes were evaluated for melanin content, proliferation, reactive oxygen species (ROS) production (both cell ROS and lipid ROS), and DNA damage using CometChip and FlexMap3D assays to assess single- and double-strand DNA breaks, respectively. **Results:** Melanocytes from different racial backgrounds exhibit varying levels of responsiveness to PFAS,

with distinct differences in cellular and molecular pathways. Proliferation and ROS production varied significantly among the cell lines. Caucasian melanocytes, with relatively lower melanin levels compared to Black and Asian melanocytes, exhibited sustained proliferation in both the 10nM and 10µM PFAS treatment groups. However, ROS production in Caucasian cells showed an increasing trend with longer PFAS carbon chains. In contrast, Asian melanocytes, which have moderate melanin levels, displayed a significant reduction in both proliferation and ROS production as PFAS carbon chain length increased, across both (10nM and 10uM) treatment concentrations. Contrary to Caucasian and Asian cells, Black melanocytes, with higher melanin levels, showed minimal responses in terms of proliferation and ROS production following PFAS treatment. Further analysis of single- and double-strand DNA breaks revealed that single-strand DNA breaks played a key role in the observed functional outcomes. **Conclusions:** PFAS susceptibility in melanocytes is influenced by both the length of the PFAS carbon chain and melanin concentration, contributing to differential responses across racial groups. Higher melanin concentrations appear to offer protective effects, potentially scavenging free radicals and upregulating intrinsic antioxidant defenses, thus preventing PFAS-induced oxidative stress and uncontrolled proliferation. Caucasian melanocytes with lower melanin content exhibited increased sensitivity to PFAS exposure, characterized by significant increase in proliferation and disruption of Chk2-p53 axis, indicating an elevated risk for melanocyte dysregulation and melanoma initiation. In contrast, Asian melanocytes displayed impaired cellular metabolism and senescence through synergistic effect of p53 and p16. Collectively, these findings indicate that short-term PFAS exposure causes differential toxicity across racial groups. However, further research is necessary to unravel the molecular mechanisms underlying this toxicity and to assess the long-term effects of PFAS exposure in the context of melanoma.

ABSTRACT NUMBER: 5039 **Poster Board Number:** LB140
TITLE: Spatial Metabolomics Reveals Tissue Distribution of PFAS in the Kidney and Heart

AUTHORS (FIRST INITIAL, LAST NAME) AND INSTITUTIONS: J. A. Goodrich[1], J. W. Nelson[1], S. Maity[2], I. Tamayo[2], S. Sharma[3], L. Hejazi[3], N. Ragi[2], *S. Fenton*[4], P. Bjornstad[5], L. Pyle[5], M. Aung[1], S. Debnath[2], K. Margulies[6], J. Bopassa[2], and K. Sharma[2]. [1]University of Southern California, Los Angeles, CA; [2]University of Texas San Antonio, San Antonio, TX; [3]SygnaMap, Inc., San Antonio, TX; [4]North Carolina State University, Raleigh, NC; [5]University of Washington, Seattle, WA; and [6]University of Pennsylvania, Philadelphia, PA.
KEYWORDS: Perfluoronated Agents; Metabolomics; Kidney

ABSTRACT: Background and Purpose: Per- and polyfluoroalkyl substances (PFAS) are a widespread class of persistent pollutants that accumulate and induce toxicity in multiple organs, including the kidney and heart. Understanding the tissue and cellular targets of PFAS is critical to clarifying their underlying toxicity and informing potential intervention strategies to mitigate their detrimental effects. The purpose of this study was to (1) determine the spatial distribution of PFAS in human heart and kidneys using spatial metabolomics, and (2) validate the spatial distribution of PFAS in mice acutely exposed to these conditions. **Methods:** Spatial metabolomics profiling was conducted using matrix-assisted laser desorption ionization mass spectrometry imaging (MALDI-MSI) at 20 µm resolution. MALDI-MSI was performed on hearts from donors without diabetes (n=6) and patients with diabetes and left ventricular hypertrophy (LVH; n=5). MALDI-MSI data from a single human kidney biopsy from the Kidney Precision Medicine Project (KPMP) were obtained via METASPACE. For the human data, results were examined for perfluorooctanoic acid (PFOA), perfluorooctane sulfonate (PFOS), and perfluorodecanoic acid (PFDA).

Regulation of metabolites in response to PFAS was assessed by performing MALDI-MSI on heart and kidney tissues from Sv129 wildtype mice orally administered 10 mg/kg body weight of PFOS (n=3) or vehicle (n=3) daily for seven days. **Results:** Two of the five human heart samples from patients with diabetes and LVH revealed localization of PFOA in heart tissue. No PFAS were detected in hearts from patients without diabetes. Overlaying the MALDI-MSI data with pre-MALDI autofluorescence (AF) revealed that PFOA was localized next to blood vessels, likely in cardiomyocytes. In the human kidney, PFDA was identified. Overlaying the MALDI-MSI annotation of PFOA with SM(d18:1/16:0), a glomerular specific sphingomyelin, demonstrated that PFDA was distributed in the non-glomerular tubular region. In the mouse model, PFOS was detected in 100% of the heart and kidneys of treated mice and not detected in the vehicle treated mice (both FDR adjusted $p<0.05$). Using computational analysis with MSI-DeepPath, 15 metabolites exhibited significantly different levels in treated mice at an FDR threshold of 0.05; these included 50.0% lower levels of docosahexaenoic acid (DHA; FDR p-value: 0.03), an omega-3 essential fatty acid with reno- and cardio-protective effects. **Conclusions:** PFAS exhibit a distinct distribution fingerprint within heart and kidney tissue. Although the spatial distribution may vary between PFAS congeners and across species, these patterns closely align with previously recognized clinical manifestation of PFAS toxicity in the heart and kidney. These data underscore how spatial metabolomics can detect PFAS and provide insight on how PFAS regulate endogenous metabolites in human and animal tissues, offering a powerful platform for advancing the understanding of PFAS toxicity across organs.

ABSTRACT NUMBER: 5040 **Poster Board Number:** LB141

TITLE: Astrocyte Dysfunction as a Mechanism of PFAS-Induced Neurotoxicity: Implications for Neuroinflammation and Neurodegeneration

AUTHORS (FIRST INITIAL, LAST NAME) AND INSTITUTIONS: *J. Xie*, *J. L. Freeman*, and C. Yuan. Purdue University, West Lafayette, IN.

KEYWORDS: Astrocytes; Perfluoronated Agents; Neurotoxicology

ABSTRACT: Background and Purpose: Per- and polyfluoroalkyl substances (PFAS), including perfluorooctanoic acid (PFOA) and perfluorooctane sulfonate (PFOS), are persistent environmental contaminants with emerging evidence suggesting their potential neurotoxic effects. While their systemic toxicity on neurons has been extensively studied, the neurotoxic effects of PFAS, particularly on supporting glial cells such as astrocytes, remain poorly understood. Astrocytes play a critical role in maintaining neuronal homeostasis, including the regulation of glutamate uptake, the modulation of inflammatory responses, and the maintenance of mitochondrial function. **Methods:** To investigate the neurotoxic effects of PFAS on astrocytes, a combination of transcriptomic analysis and functional assays was employed. Cytokine expression profiles were analyzed to assess changes in neuroinflammatory responses, and ELISA was used to verify key findings. Functional assays were conducted to evaluate glutamate uptake capacity and astrocytic phagocytosis. Oxidative stress was assessed through measurements of lipid peroxidation, while mitochondrial function was analyzed using Seahorse assay. **Results:** PFAS exposure significantly altered cytokine expression profiles in astrocytes, with key pro-inflammatory cytokines upregulated as confirmed by ELISA, indicating dysregulation of astrocyte-mediated neuroinflammatory responses. Functional assays revealed suppressed glutamate uptake capacity, indicative of impaired excitatory neurotransmitter regulation, and a concomitant increase in astrocytic phagocytosis, potentially reflecting maladaptive responses to cellular stress. Enhanced lipid

peroxidation levels were observed, highlighting oxidative stress as a contributing factor to PFAS-induced neurotoxicity. Furthermore, mitochondrial function assays demonstrated significant impairments, indicating metabolic stress imposed by PFAS. **Conclusions:** These findings underscore the pivotal role of astrocytes in maintaining neural homeostasis and demonstrate that PFAS-induced dysfunction in these cells may drive the pathogenesis of neurodegenerative and neuroinflammatory diseases. This research highlights the need for further investigation into therapeutic interventions aimed at mitigating PFAS-induced neurological damage and emphasizes the importance of regulatory measures to reduce PFAS exposure.

ABSTRACT NUMBER: 5041 **Poster Board Number:** LB142

TITLE: Sex-dependent effects of PFOA on pancreatic islets from pro-diabetic mice with human islet amyloid polypeptide transgene

AUTHORS (FIRST INITIAL, LAST NAME) AND INSTITUTIONS: I. C. Cely, I. Ahn, N. Borkar, J. Franco, *G. Diamante*, G. Zhang, and *X. Yang*. University of California Los Angeles, Los Angeles, CA.

KEYWORDS: Perfluoronated Agents; Metabolism; Endocrine Toxicology

ABSTRACT: Background and Purpose: Perfluorooctanoic acid (PFOA) belongs to a class of toxic “forever” chemicals called poly-fluoroalkyl substances (PFAS) that are found in many consumer products such as nonstick products, food packaging and also firefighting foam and fire retardant. Regrettably, the ubiquitous exposure and robust stability of PFOA poses an alarming health risk to the public and in particular occupational workers such as firefighters, due to the association in prevalent and adverse health effects such as cardiovascular disease, metabolic dysfunction associated fatty liver disease, reproductive effects, cancer and more recently, diabetes. Diabetes is one of the most widespread metabolic disorders but the link to PFOA and the mechanism by which PFOA exposure can increase risk of diabetes is understudied and therefore warranted. In this study, we investigated whether PFOA exposure affects cultured pancreatic islets from pro-diabetic mice with human islet amyloid polypeptide (hIAPP) transgene. IAPP also known as amylin, is a protein co-secreted with insulin from pancreatic islet beta cells and when mutated, misfolds and aggregates to form islet amyloid, inducing diabetes as a result of IAPP toxicity. We hypothesize that PFOA exposure may affect islet function and accelerate diabetes development. **Methods:** Female and male hIAPP mice were assessed for changes in body weight, fat mass, muscle mass on a weekly basis starting from ages 3 weeks to 12 weeks of age. Mice were also assessed for changes in glucose metabolism by a 6-hour fasted intraperitoneal glucose tolerance test (IPGTT). Following this, pancreatic islets from 10-11 week old female and male hIAPP mice were isolated, cultured and exposed for 24 hours to 30uM PFOA, a concentration relevant to exposure levels of occupational workers. Islet function as well as PFOA target genes were assessed. **Results:** Both female and male hIAPP mice showed changes in body weight and body composition after the age of 3 weeks compared to their wild-type controls. In addition, we show that female and male hIAPP mice demonstrate impaired glucose tolerance by 9 weeks of age compared to the controls. Gene expression for Apoe, which encodes an apolipoprotein known to interact with IAPP to attenuate IAPP toxicity and linked to type 2 diabetes, along with candidate PFOA targets (Ppara, Pparg, Hmgcr), was assessed in PFOA and non-PFOA exposed pancreatic islets from female and male hIAPP mice. We found that PFOA exposure induced a significant decrease in Apoe expression in pancreatic islets from female hIAPP mice, and a similar nonsignificant trend was also observed in pancreatic islets from male hIAPP mice. Pancreatic islets from female and male hIAPP mice did not show changes in PFOA target genes in

response to PFOA exposure. **Conclusions:** PFOA treated pancreatic islets from female hIAPP mice demonstrate a significant decrease in Apoe, which may attenuate IAPP toxicity in islets and affect diabetes progression in a sex-dependent manner.

ABSTRACT NUMBER: 5042 **Poster Board Number:** LB143
TITLE: Evaluation of Cluster of differentiation 36 (CD36) as a critical factor in perfluorooctanesulfonic acid (PFOS)-induced adverse liver outcomes

AUTHORS (FIRST INITIAL, LAST NAME) AND INSTITUTIONS: J. Zeng, *J. Agudelo Areiza*, *O. Skende*, and *A. L. Slitt*. University of Rhode Island, Kingston, RI.
KEYWORDS: Perfluoronated Agents; Liver; Lipids

ABSTRACT: Background and Purpose: Perfluorooctanesulfonic acid (PFOS) is a synthetic perfluoroalkyl substance widely present in the environment and known to adversely affect human health. PFOS causes liver enlargement, induces steatosis, and causes cytotoxicity. CD36 is a membrane glycoprotein that facilitates the import of long-chain fatty acids into cells and contributes to lipid accumulation within the liver. The PFOS structure closely resembles a long-chain fatty acid, suggesting that CD36 may facilitate PFOS uptake into the liver. In vitro and modeling studies point to CD36 having PFOS binding sites. Therefore, it was hypothesized that CD36 is a critical factor for PFOS uptake and adverse liver effects. To investigate this, a Cd36-deficient mouse model was used to evaluate the role of CD36 in PFOS distribution and liver effects. **Methods:** Wild-type mice (WT, C57BL6/J) and mice with Cd36 globally deleted ($Cd36^{-/-}$, B6.129S1-$Cd36^{tm1Mfe}$/J) between the ages of 7-9 weeks were administered vehicle (0.5% Tween20 in PBS) or PFOS (10 mg/kg in 0.5% Tween20 in PBS) by oral garage for seven days. Liver, brain, kidneys, lungs, and plasma were collected during necropsy on the eighth day. Lipids extracted from the liver and plasma were assessed using triglyceride, cholesterol, and ALT reagent kits. Samples were read by a SpectraMax plate reader. **Results:** PFOS administration increased the liver-to-body weight ratio by 66% in WT mice and 72% in $Cd36^{-/-}$ mice. It also increased total liver lipids concentration similarly in WT and $Cd36^{-/-}$ mice by ~97%. Lastly, PFOS administration elevated liver triglyceride concentration by 83.7% in WT mice and 25% increase in $Cd36^{-/-}$ mice. **Conclusions:** Overall, these preliminary findings suggest that lack of Cd36 has a modest effect on PFOS-induced liver alterations. Ongoing studies will evaluate whether lack of Cd36 modified liver PFOS concentration.

ABSTRACT NUMBER: 5043 **Poster Board Number:** LB144
TITLE: The Morris Water Maze: An Assessment of Learning and Memory in Regulatory Developmental and Reproductive Toxicology (DART) Studies

AUTHORS (FIRST INITIAL, LAST NAME) AND INSTITUTIONS: S. A. Beck, D. P. Myers, D. Stannard, S. Edwards, A. Hedge, and S. Renaut. Lapcorp, Eye, United Kingdom. Sponsor: *D. Harischandra*
KEYWORDS: Neurotoxicity; Developmental; Behavior; Reproductive and Developmental Toxicology; Morris water maze

ABSTRACT: Background and Purpose: There are a number of water maze tasks that have been developed to evaluate learning and memory in regulatory developmental and reproductive toxicology (DART) studies. EPA OPPTS 870.6300 and OECD 426 test guidelines require an assessment of learning and memory on Developmental Neurotoxicity (DNT) studies for the testing of chemicals that may cause adverse neurodevelopmental outcomes. In addition, ICH Harmonized Tripartite Guideline S5 (R3) for the

testing of pharmaceuticals intended for human use also require an assessment of learning and memory to be evaluated in a complex learning task. The EPA OPPTS 870.6300 test guideline requires evidence of positive control data from the laboratory performing the test to demonstrate the sensitivity of the procedures being used. This is to demonstrate that the task is sensitive to detect learning impairments by using a chemical for which learning deficits have been established. The OECD Number 43 Guidance Document on Mammalian Reproductive Toxicity Testing and Assessment requires behavioral tests included in test batteries to be individually validated tests. **Methods:** Therefore, the purpose of this study was to validate and optimize the Morris water maze (MWM) to support preclinical safety studies utilizing the learning and memory assessment. The MWM is a test in which animals do not require strong motivating agents and rely on spatial cues to locate a hidden platform using allocentric learning. Allocentric learning relies on remembering, recalling and recognizing environmental stimuli (visual cues) called landmarks. As described by Morris (1984), accurate directionality requires continual monitoring of the animal's position in relation to the visual cues. The first objective of the study was to investigate the effect of water temperature on learning and memory. The second was to assess the effect of Scopolamine on the learning and memory of Sprague Dawley and Han Wistar rats on PND 63 ±1 days, using the ANY-maze video tracking tool. Four consecutive trials with a trial time of a maximum of 90 seconds, over four consecutive days, were performed to capture spatial learning. Data were reported as latency to the platform and path length. On the fifth day, 24 hours following the last learning trial, a memory probe trial was performed to assess reference memory. Data were reported as the number of platform zone crossings and time spent in the platform quadrant. In this study, we determine the optimum water temperature to use in the MWM assessment. In addition, using Scopolamine as a positive control, known to produce MWM spatial learning deficits, we demonstrate that the learning and memory assessment using the MWM can detect chemically induced changes. **Results:** Results showed that animals that were exposed to a water temperature of 23 ±3 °C exhibited a decreased latency to the platform across the four days of spatial learning and a decreased path length on Days 2 through to 4, compared with animals that were exposed to a water temperature of 29 ±3 °C. During the memory probe trial, animals that were exposed to a water temperature of 23 ±3 °C exhibited a 50% increase in the number of entries into the platform zone when the platform was absent and an increased amount of time spent in the platform quadrant, compared with animals that were exposed to a water temperature of 29 ±3 °C. During the assessment for the effect of Scopolamine on the learning and memory of Sprague Dawley and Han Wistar rats on PND 63 ±1 days, results showed that animals administered Scopolamine exhibited increased latency to platform and path length across the four days of spatial learning, compared with the Control group. During the memory probe trial, Sprague Dawley rats, administered with Scopolamine exhibited statistically significantly fewer entries into the platform zone and less time in the platform quadrant compared with Controls. Han Wistar rats administered with Scopolamine, also exhibited statistically significantly less time in the platform quadrant compared with Controls. However, in contrast to the Sprague Dawley rats, Han Wistar rats showed an increase in the number of entries into the platform zone, compared with Controls. The results demonstrate that animals exposed to a water temperature in the MWM that is the same as room temperature show a steeper learning curve indicating better learning ability, compared to animals exposed to a water temperature in the MWM that is warmer than room temperature. The results also demonstrate that animals administered Scopolamine were deficient in the spatial learning task. Deficiencies in reference memory were also observed; however, differences were noted between the strains. These differences may be due to the sensitivity to the inhibitory actions of Scopolamine on learning and memory. **Conclusions:** In conclusion, animals that learn in the MWM in water at room temperature showed a

superior swimming performance by reaching the platform quicker and remembering where the platform was, compared with animals that swam in the MWM in a warmer water temperature. This is important when performing regulatory DART studies to enable chemically or pharmaceutically induced changes to be detected effectively. The results from Sprague Dawley and Han Wistar rats administered with Scopolamine demonstrate the suitability of this learning and memory procedure, including the detection of Scopolamine related changes, providing the evidence required to support regulatory DART studies.

ABSTRACT NUMBER: 5044 **Poster Board Number:** LB145

TITLE: Transgenic zebrafish embryo models to evaluate chemical-induced developmental toxicity in craniofacial and cardiac anomalies

AUTHORS (FIRST INITIAL, LAST NAME) AND INSTITUTIONS: S. Liu[1], T. Kawanishi[2], A. Shimada[3], T. Takeshita[1], Y. Nukada[4], M. Miyazawa[5], K. Saito[1], Y. Ito[4], H. Takeda[6], and J. Tasaki[4]. [1]Kao Corporation, Kawasaki, Japan; [2]Department of Life Science and Technology, Institute of Science Tokyo, Yokohama, Japan; [3]University of Tokyo, Tokyo, Japan; [4]Kao Corporation, Tochigi, Japan; [5]Kao Corporation, Tokyo, Japan; and [6]Department of Live Sciences, Kyoto Sangyo University, Kyoto, Japan. Sponsor: S. Liu, Japanese Society of Toxicology

KEYWORDS: Developmental/Teratology; Chemical Hazard Assessment; Safety Evaluation; zebrafish embryo, NAMs

ABSTRACT: Background and Purpose: Craniofacial anomalies and heart defects are among the most common birth defects worldwide and are often attributed to a combination of genetic and environmental factors, including pharmaceuticals and chemical agents. While understanding conserved mechanisms behind these defects is crucial for assessing teratogenicity, specific mode of actions of teratogens that cause craniofacial anomalies and heart defects have yet to be fully determined. Recently, zebrafish have gained attention as an emerging model for evaluating developmental toxicity due to their high-throughput capabilities, conserved developmental process among vertebrates, and the availability of various tools for investigating teratogenic mechanisms. In this study, we established zebrafish reporter lines *sox10:EGFP*, *cmlc2:EGFP*, *kdrl:mRFP*, and *gata1*:mKate2 to visualize cranial neural crest cells (CNCCs), cardiomyocytes, vascular endothelial cells, and blood cells, respectively. Using these transgenic lines, we investigated the conserved mechanisms of chemical-induced craniofacial anomalies (Liu et al., Tox. Sci., 2023) and heart malformations (Liu et al., Tox Sci., under review). Additionally, we examined the critical periods for craniofacial anomalies and heart defects. These results are considered crucial for non-animal developmental toxicity evaluation. We also verified the accuracy of 40 chemicals to validate the utility of our transgenic assays for developmental toxicity evaluation. **Methods:** The zebrafish (*Danio rerio*) strain RIKEN WT (RW), *sox10:EGFP*, *sox10:Dendra2*, *cmlc2:EGFP*, *kdrl:mRFP* and *gata1:mKate2*, which are all on the RW background were utilized in the present study. Fertilized eggs were collected and incubated in E3 medium, and test compounds were administered at 4 hours post-fertilization (hpf). The exposure medium was replaced daily, and samples were collected from the 5-6 somite stage (ss, 11.5-12 hpf) until 96 hpf. Morphological observation was conducted through immunofluorescence staining or live and time-lapse imaging with fluorescence stereomicroscopy, confocal microscopy and light sheet microscopy. Additionally, Median malformation dose (EC_{50}) and Median lethal dose (LC_{50}) were calculated to derive the Teratogenic Index (TI), when this value is more than 2, the compound will be judged as positive for teratogenicity. **Results:** When we exposed the transgenic embryos to teratogens known to cause craniofacial anomalies and heart defects

in mammals, CNCC migration and subsequent morphogenesis of the first pharyngeal arch (PA1) were impaired at 24 hpf, leading to craniofacial anomalies. Heart defects were accompanied by functional defects, and thus heart morphology and blood flow were analyzed. Defects in cardiomyocytes and endocardial cells leading to heart looping defects were observed. Furthermore, cardiac progenitors were disrupted, leading to heart malformations and functional defects. These results showed that transgenic reporter lines were crucial for visualizing a series of developmental toxicity processes. Furthermore, the critical period for craniofacial anomalies and heart defects were determined as 12-24 hpf and 4-48 hpf, respectively. We next evaluated 40 compounds, including pharmaceuticals, general chemicals, and in-house materials, and obtained high concordance rates of 87% sensitivity, 88.2% specificity, and 87.5% accuracy. Three false negative substances were detected by the Tg zebrafish at high concentrations, similar to animal studies. Additionally, while the overall concordance rate improved by only 5% compared to the wild-type in terms of malformation endpoints, by analyzing conserved developmental and teratogenic mechanisms, a significant increase in detection rate was observed in tissues such as the craniofacial and cardiovascular systems. **Conclusions:** Given the conserved nature of developmental processes around the stage in both zebrafish and mammals, our results can be extrapolated to mammalian development and may contribute to predicting craniofacial anomalies and heart defects in humans. In addition, the predicted accuracy indicates that the transgenic zebrafish embryo is useful for evaluating teratogens, and the detection rates in the transgenic model are better than those in wild-type ones.

ABSTRACT NUMBER: 5045 **Poster Board Number:** LB146

TITLE: Evaluating Changes in Intestinal Mucosa Associated Microbiota, Permeability, and Cytokine Profiles in Gestational HIV Drug Exposed Adult Rat Offspring

AUTHORS (FIRST INITIAL, LAST NAME) AND INSTITUTIONS: Y. Yanamadala[1], *C. Muthumula*[1], G. Kuppan[1], *K. Karn*[1], *V. Sutherland*[2], *H. Cunny*[2], *J. H. Santos*[2], and S. Khare[1]. [1]National Center for Toxicological Research, Jefferson, AR; and [2]National Institute of Environmental Health Sciences, Durham, NC.

KEYWORDS: Microbiome; Developmental Toxicity; Post-Natal; Gastrointestinal; Abacavir, Dolutogravir, Lamivudine

ABSTRACT: Background and Purpose: The combination of antiretroviral therapy TC-ART (abacavir sulfate, dolutegravir, and lamivudine; ABC/3TC/DTG) has revolutionized HIV treatment by effectively targeting different stages of viral replication. While TC-ART was widely used during pregnancy, it is now only recommended after the first trimester to avoid potential cardiac or neurological impacts during organogenesis and early development. Independent studies have shown that (i) drugs in TC-ART can alter the intestinal microbiome and (ii) the intestinal microbiome can contribute to cardiac and neurological complications. In this study, we aimed to determine whether these microbial changes in mother effect the offspring and they persist into adulthood of the F1 generation. **Methods:** The effects of in utero and lactational exposure to TC-ART on the gut health of 12-month-old rat offspring were evaluated. Rat mothers were treated with either a low dose or high dose of TC-ART, with offspring indirectly exposed to the drug through the placental barrier and breast milk. At 12 months of age, the ileal tissue of the offspring was collected to assess changes in gut health. Ileal tissue from the adult offspring was analyzed for changes in mucosa-associated microbiome composition using 16S amplicon sequencing, mRNA expression of 84 key intestinal permeability-related genes using Qiagen custom kits,

and ileal mucosa-associated immune profiles using Bio-Rad multiplex kits. Tissue morphology and animal weights were also monitored. **Results:** Our findings revealed significant alterations in the gut microbiome, intestinal permeability, and cytokine profiles, with notable sex and dose dependent variations. Female offspring exposed to high-dose TC-ART exhibit microbial dysbiosis, characterized by an increased Firmicutes-to-Bacteroides ratio, expansion of several minor genera, disrupted expression of 45% of the cell junction genes studied, and pronounced blunt villi morphology. In contrast, male offspring displayed a higher prevalence of opportunistic bacterial genera, including *Pseudomonas*, *Enterococcus*, and *Escherichia*. Additionally, they experienced pronounced shifts in pro- and anti-inflammatory cytokine expression, with significant changes in IL-17, M-CSF, IL-5, IL-7, and IL-10 levels, among others. **Conclusions:** These findings suggest that early-life exposure to TC-ART can result in gut microbiome imbalances, compromised intestinal barriers, and altered immune profiles that persist into adulthood, indicating the necessity of evaluating the long-term safety of pregnancy drugs on offspring and highlighting the critical role of the microbiome in shaping overall health and developmental outcomes.

ABSTRACT NUMBER: 5046 **Poster Board Number:** LB147

TITLE: Social Interaction Assessment in Rodents: Positive Control Validation of Automated Three-Chambered Social Interaction Test in Rats

AUTHORS (FIRST INITIAL, LAST NAME) AND INSTITUTIONS: *D. S. Harischandra*[1], J. Proctor-Clarke[2], C. John[1], D. Schafer[1], M. Dray[1], B. Sparks-Smith[1], and P. Bushdid[1]. [1]Labcorp, Greenfield, IN; and [2]Labcorp, Harrogate, United Kingdom.

KEYWORDS: Neurotoxicity; Developmental; Behavior; Reproductive and Developmental Toxicology; Three-Chambered Social Interaction

ABSTRACT: Background and Purpose: Social interactions are fundamental and adaptive components of the biology of numerous species. The integrity of social interaction behavior is critical in maintaining social skills, interpersonal functioning, and effective social relationships that define societies. Deficits in social behavior and social recognition are well-recognized in several neuropsychiatric disorders, such as autism spectrum disorders, bipolar disorders, depression, obsessive-compulsive disorders and schizophrenia. Certain pharmaceuticals such as valproic acid, used to treat bipolar disorders and/or epilepsy, are shown to increase the risk of autism spectrum disorder (ASD) in children whose mothers were exposed to it during pregnancy. Additionally, certain anesthetics and sedatives such as propofol, administered during early postnatal development, are shown to increase the risk of neuropsychiatric disorders due to N-methyl-D-aspartate (NMDA) receptor antagonism or due to potentiation of the activity of gamma-aminobutyric acid (GABA) during the period of rapid brain growth or synaptogenesis. Therefore, when there are identified or anticipated effects due to the mode-of-action of new pharmaceuticals or chemicals, an assessment of social interaction assessment may be incorporated into Juvenile Toxicology, Pre and Postnatal Development (PPND) or Extended One-Generation Reproductive Toxicology (EOGRT) studies. Complex behavioral tests such as social interaction tests may vary greatly with the testing conditions and proficiency of the laboratory that conduct the tests. Therefore, as stated in OECD guidelines for testing of chemicals in neurotoxicity (OECD 424), development neurotoxicity (OECD 426), and guidance document of mammalian reproductive toxicity testing and assessment (OECD Guidance document number 43), the laboratory performing the study should present data demonstrating its capability to carry out the study and the sensitivity of the procedures used. Therefore,

it is imperative to conduct positive control validation studies with known phenotypic outcomes to validate equipment and optimize test procedures for a given behavior assay to get the most reliable and reproducible data in preclinical safety evaluation studies. **Methods:** The current study aimed to validate the three-chamber social test to assess social behavior in rats adhering to GLP regulations. Here, utilizing a valproic acid (VPA)- induced model of autism and a single or repeat-dose phencyclidine (PCP)- induced model of schizophrenia, we have evaluated the sensitivity of each model and validated procedures to reliably detect and measure social interaction deficits that underline known pervasive impairments in neuropsychiatric and ASDs. **Results:** Test conditions were optimized for the Three Chamber Sociability Test to use the ANY-maze automated video tracking tool to measure sociability (Sociability index) i.e., the propensity to spend time with another rat, as compared to time spent alone in an identical but empty chamber. In addition, the test animal's preference to interact with an unfamiliar animal versus a familiar animal was measured to evaluate the tendency to explore social novelty over a socially familiar target (Social Novelty Preference [SNP] index). Interestingly, while gestational exposure to VPA resulted in negatively affected natural delivery and litter data, increased observations of tail abnormalities and reduced brain weight without effect on body weight, recapitulating expected phenotypes of VPA-induced rodent model of autism, no discernible differences between VPA-exposed animals and concurrent controls were noted in sociability and SN assessments. In contrast, single-dose or repeat-dose PCP administration resulted in clinical observations that closely resemble psychosis-like symptoms and deficiencies in Sociability and SNP indices, mimicking the symptoms of schizophrenia. Data indicate that animals administered PCP observed 46.7 or 95.0% lower sociability indices upon single-dose or repeat-dose PCP administration than controls. Additionally, during the social novelty assessment, animals administered PCP were noted to have 4.3 or 50% lower SN preference indices upon single-dose or repeat-dose PCP administration regimen. **Conclusions:** Therefore, data indicate animals administered PCP, particularly upon repeat-dose PCP administration markedly diminish interactions with a familiar animal (Sociability index) or with a novel animal (SN preference index) successfully validating testing procedures to detect social interaction deficits in preclinical safety evaluation studies.

ABSTRACT NUMBER: 5047 **Poster Board Number:** LB148

TITLE: Early developmental toxicity of polycyclic aromatic hydrocarbons (PAHs) phenanthrene and fluoranthene: cytoskeleton as a target

AUTHORS (FIRST INITIAL, LAST NAME) AND INSTITUTIONS: A. A. Rojas, and *S. Dasgupta*. Clemson University, Clemson, SC.

KEYWORDS: Polycyclic Aromatic Hydrocarbons; Non-Mammalian Species

ABSTRACT: Background and Purpose: Polycyclic aromatic hydrocarbons (PAHs) are a class of organic compounds that are typically produced by incomplete combustion. Members of the PAH family can be further divided into low molecular weight and high molecular weight by the number of rings they contain. Higher ring PAHs have been shown to have higher toxicity than their lower ring counterparts. PAHs are known to be detoxified through aryl hydrocarbon receptor (AHR) activation, resulting in increase in levels of detoxification genes such as *cyp1a*. While much has been studied about the long-term effects of PAHs and their developmental toxicity through the AHR pathway, few studies have gone in depth on how they impact early developmental processes, prior to pluripotency. Using zebrafish as a model organism, our study investigates the impacts of PAHs during the pre-pluripotent stages of embryogenesis. **Methods:** Zebrafish embryos were collected and exposed to 0, 6.25, 12.5, 25, 50, and

100 µM concentrations of both phenanthrene and fluoranthene at 0.75 h post fertilization (hpf; ~2-4 cell stage), followed by phenotyping for mortality and morphological deficits hourly staring at 3hpf to 6hpf. To understand the genetic underpinnings of these effects, mRNA-seq was conducted on embryos exposed to 0 or 100uM of phenanthrene or fluoranthene; briefly, post-exposure, samples were pooled and RNA was extracted at 4 hpf (N=4 replicate pools). Sequencing was conducted on an Illumina platform and bioinformatics analyses were conducted using DeSeq2. To understand the role of cytoskeleton, embryos were exposed to 100 µM of phenanthrene and fluoranthene and fixed in 4% PFA at 4hpf. Embryos were then exposed to an Alexa Fluor 488-conjugated phalloidin probe (for F-actin) overnight, incubated in Hoescht 33342 for 15 minutes, and imaged within FITC and DAPI filters. Fluorescence and morphometric quantifications were conducted within Image J, using a 1-way ANOVA, followed by Dunnett's posthoc test ($p<0.05$). **Results:** Both fluoranthene and phenanthrene exposures showed concentration-dependent increase in mortality starting at 4.5 hpf, with 100% mortality in 100 µM exposure by 6hpf. Upon closer examination, the time of death for embryos exposed to PAHs began at 4hpf and progressed onward until 6hpf. Prior to mortality, embryos stained with phalloidin revealed substantial cytoskeleton disruption with ~38% and ~30% higher levels of phalloidin in the yolk sac, and ~14% and ~13% lower levels in the cell mass for phenanthrene and fluoranthene respectively. Surprisingly, mRNA sequencing data did not reveal large scale transcriptomic disruptions, with only 4 genes disrupted in the two PAHs. Specifically, our mRNA-seq data, combined with follow-up qPCR and immunohistochemistry, did not reveal any differential levels of *cyp1a* mRNA or protein- a common biomarker for PAHs- suggesting that at these stages, toxicity is *cyp1a*- or AHR2 independent. qPCR data showed nonsignificant changes in expression of *ahr1a* and *ahr1b*, further reinforcing the fact that the mortality we see is independent of AHR regulation. **Conclusions:** Our work revealed that both PAHs lead to early developmental mortality that is independent of AHR2-activation. Interestingly, both PAHs showed disrupted actin patterns, indicating that cytoskeletal network may be a target of PAHs at these stages. Future studies are going to investigate the PAH cytoskeleton interaction.

ABSTRACT NUMBER: 5048 **Poster Board Number:** LB149
TITLE: Tetrabromobisphenol S (TBBPS)-induced developmental toxicity in zebrafish embryos

AUTHORS (FIRST INITIAL, LAST NAME) AND INSTITUTIONS: *R. Serradimigni*, and *S. Dasgupta*. Clemson University, Clemson, SC.
KEYWORDS: Organophosphates; Non-Mammalian Species; Embryo; Tetrabromobisphenol S

ABSTRACT: Background and Purpose: Tetrabromobisphenol S (TBBPS) is a new brominated flame retardant (BFR) that serves as an alternative to tetrabromobisphenol A. Previous research has revealed that TBBPS can readily accumulate in environmental matrices and potentially pose risk to environmental and human health. However, being an emerging BFR, there is limited knowledge of its toxic effects. Additionally, there is a significant gap in investigating the impacts of BFRs in general on pre-pluripotent stages of development. The objective of this study is to use zebrafish as a model and determine the effects of TBBPS exposure on early embryogenesis. **Methods:** We initiated TBBPS exposures (0 and 40 µM) at 0.75 hours post fertilization (hpf) and monitored and phenotyped progression through early developmental processes including cleavage, blastula, and epiboly. To examine windows of sensitivity, we either -1) initiated exposure at various time points between 0.75-8 hpf (0.75, 2.5, 4, 5.5, and 7 hpf) or -2) initiated exposure at 0.75 hpf and moved the embryos to chemical free embryo media at 2.5, 4, 5.5, and 7 hpf. To examine the genetic basis of TBBPS-induced mortality, we then conducted mRNA

sequencing on embryos exposed to 0 or 40 µM TBBPS from 0.75-7 hpf (N=4 replicate pools), prior to embryonic mortality where embryos were still phenotypically normal. Sequencing was conducted on an Illumina platform and data analyses were conducted in DeSeq2 (padj<0.05). All statistical assessments for phenotypes were conducted using a one-way ANOVA, followed by a Dunnett's posthoc test (p<0.05). **Results:** Our data revealed that TBBPS treated embryos show normal development till ~7 hpf (shield stage); however, within the next 1 hour (by 75% epiboly), embryos show 100% mortality by 8 hpf. Interestingly, replacing the exposure medium with chemical-free media before 5.5 hpf prevents any mortality, suggesting that the chemical is rapidly detoxified. Initiating exposures at 0.75, 2.5, and 4 hpf result in 100% mortality, whereas 100% embryos exposed after 5.5 hpf show normal development at 8 hpf, further highlighting a potential sensitive window to be early gastrulation. DeSeq2 analysis showed 881 number of differentially expressed genes (293 increased and 588 decreased). Gene ontology assessments for differentially expressed genes revealed downregulation of cytoskeletal organization and tight junctions as a potential pathway for TBBPS-induced developmental arrest. **Conclusions:** Collectively, our genetic and phenotypic data shows that TBBPS exposure arrests embryonic development, with a proposed window of sensitivity lying between 4 and 5.5 hpf (early gastrulation). TBBPS exposure induces a suite of differentially expressed genes, many involved in cytoskeleton assembly pathways. Based on our results, we hypothesize the disruption of tight junctions and cell-cell interaction as a potential mechanism leading to developmental toxicity. Ongoing studies will include- 1) assessments of cytoskeletal organization and 2) evaluating the developmental impacts of environmentally relevant concentrations of TBBPS exposure.

ABSTRACT NUMBER: 5049 **Poster Board Number:** LB150

TITLE: Investigating Thyroid Hormone Disruption by Polybrominated Diphenyl Ethers (PBDEs) Through Interaction with Thyroxine-Binding Globulin (TBG)

AUTHORS (FIRST INITIAL, LAST NAME) AND INSTITUTIONS: *I. Sheikh*[1], T. Zughaibi[1], *A. Kadry*[2], *M. Ghorab*[3], M. Beg[1], and *S. Alharthy*[1]. [1]King Abdulaziz University, Jeddah, Saudi Arabia; [2]University of Maryland School of Public Health, College Park, MD; and [3]Michigan State University, East Lansing, MI.

KEYWORDS: Endocrine; Thyroid; Polybrominated Diphenyl Ethers; Bioinformatics

ABSTRACT: Background and Purpose: Polybrominated diphenyl ethers (PBDEs) are halogenated flame retardants widely used in consumer products to mitigate fire damage. Their environmental persistence and ability to leach out of products have raised concerns about their impact on human health. Structural similarities between PBDEs and thyroid hormones suggest their potential to mimic thyroid activity and disrupt thyroid function. Thyroxine-binding globulin (TBG) plays a critical role in thyroid hormone metabolism and distribution. This study aimed to explore the molecular interactions of frequently detected PBDE congeners—BDE-28, BDE-85, and BDE-154—with the TBG ligand-binding pocket. **Methods:** Molecular interactions between TBG and PBDEs were investigated using Schrödinger's induced fit docking (IFD). The structural binding analysis included the evaluation of molecular interactions and calculation of binding energy values. Comparative analysis was performed between PBDE ligands and thyroxine, the native ligand of TBG, to assess the potential for PBDE-induced interference with TBG function. **Results:** The docking analysis revealed that BDE-28, BDE-85, and BDE-154 were strongly bound within the TBG ligand-binding pocket. Key interacting residues showed significant overlap between the PBDE congeners and thyroxine. Binding energy calculations indicated that BDE-28 and BDE-85 had lower binding energies compared to thyroxine, while BDE-154 exhibited

binding energy values equivalent to thyroxine. These results suggest that BDE-154, a higher brominated congener, binds with comparable strength to thyroxine. **Conclusions:** This study provides preliminary evidence that higher brominated PBDE congeners, such as BDE-154, may effectively inhibit thyroid hormone binding to TBG. This inhibition could disrupt the circulatory transport and availability of thyroid hormones at target sites, potentially leading to thyroid dysregulation. Future studies are warranted to elucidate the in vivo implications of these findings and assess their broader impact on thyroid hormone homeostasis and human health.

ABSTRACT NUMBER: 5050 **Poster Board Number:** LB151

TITLE: Co-exposure to tributyltin and a high-refined carbohydrate diet leads to abnormal fertility, placenta, pregnancy outcomes, and offspring metabolic complications in female rats

AUTHORS (FIRST INITIAL, LAST NAME) AND INSTITUTIONS: J. B. Graceli[1,2], J. Zanol[2], M. Godoy Doro[2], and C. da Costa[2]. [1]SIU, Carbondale, IL; and [2]Federal University of Espirito Santo, Vitoria, Brazil.

KEYWORDS: Endocrine Disruptors; Endocrine Toxicology; Developmental Toxicity; Prenatal; Pregnancy; Tributyltin (TBT)

ABSTRACT: Background and Purpose: Tributyltin (TBT) is a persistent contaminant with adverse effects on reproductive health. Concurrently, the global surge in high-refined carbohydrate diet (HCD)-induced obesity raises concerns about metabolic and reproductive complications and their impact on pregnancy. While studies individually explore the consequences of TBT and HCD exposure, the combined effects on pregnancy, placental function, and fetal metabolism remain unexplored. Thus, this study aimed to test the hypothesis that co-exposure to TBT and HCD impair placenta morphophysiology and fetal metabolism. **Methods:** Female rats were divided into: 1) Control rats treated daily with a vehicle (0.4 % ethanol, via gavage) and fed with standard laboratory chow Socil (RD); 2) TBT rats treated daily with TBT (100 ng/kg/day, via gavage) and fed with RD; 3) HCD rats that were fed with HCD (~30 % refined sugars); 4) Rats that were treated daily with TBT and feed with HCD diet for 15 days. And then mated overnight by pairing with the control male. The mating confirmation was done in the morning by the presence of sperm in the vaginal smear (gestational day (GD) 0.5). On GD 19.5, females were anesthetized with ketamine and xylazine (90 mg/kg and 4.5 mg/kg, ip) and euthanized by cardiac puncture. The uterus was harvested, from which the fetuses and placentas were obtained. The sex, number and weight were recorded. Pregnant serum, liver, and fetuses were collected for metabolic evaluations. Placentas were separated by sex and collected for histology and molecular assessments. All the protocols were approved by the Animal Use Ethics Committee of the Federal University of Espírito Santo (Nº 01/2021). Comparisons between the groups were performed using one- or two-way ANOVA, followed by Tukey's multiple comparison test. All data are reported as the mean ± SEM. **Results:** HCD-TBT females increased body weight gain during exposure 9, 12 and 15 days ($p<0.05$). However, during the pregnancy, HCD-TBT female rats reduced gestational weight gain in the GD 6, 9 and 12 and showed an abnormal glucose tolerance compared to the control ($p<0.05$). Laparotomy evaluation allowed us to observe a reduced implantation efficiency and increased pre-implantation loss with an abnormal unilateral implantation pattern in HCD-TBT rats. Female HCD-TBT fetuses showed reduced liver weight and elevated liver cholesterol levels ($p<0.05$). Male HCD-TBT fetuses increased serum glucose levels, reduced HDL levels and reduced liver weight ($p<0.05$). In both sexes HCD-TBT fetuses, the placenta reduced diameter ($p<0.05$). Female placenta reduced total and basal layer thickness, increased glycogen cell clusters, and high GLUT1 protein expression ($p<0.05$). Male HCD-TBT placenta increased mTOR protein expression,

reduced labyrinth layer thickness, and increased glycogen cell clusters ($p<0.05$). Female placentas had elevated placenta macrophage activity, with no changes in the male placenta ($p<0.05$ and $p>0.05$). Male placentas presented increased glutathione levels, but not the females ($p<0.05$ and $p>0.05$). Female HCD-TBT placenta increased collagen deposition ($p<0.05$). **Conclusions:** Together, these data suggest that the co-exposure of TBT plus HCD induces pregnancy metabolic abnormalities. Moreover, fetal and placental morphology and metabolic changes were also observed, but with some related to sexual dimorphism features. Funding: FAPES (UNIVERSAL 03/2021 / PROFIX 15/2022)

ABSTRACT NUMBER: 5051 **Poster Board Number:** LB152
TITLE: Effect of maternal cadmium (Cd) exposure and high-fructose diet (HFrD) on essential metals in offspring mouse liver

AUTHORS (FIRST INITIAL, LAST NAME) AND INSTITUTIONS: J. Pancras[1], *C. Lau*[1], K. P. Das[1], L. S. Strader[1], *C. N. Miller*[1], and J. A. Sullivan[2]. [1]US EPA, Durham, NC; and [2]SEE Program, National Asian Pacific Center on Aging, Seattle, WA.
KEYWORDS: Liver; Metals; Developmental Toxicity; Post-Natal; Cadmium

ABSTRACT: Background and Purpose: Environmental exposure to pollutants combined with unhealthy diet can increase the risk of adverse health effects. Such effects can be more serious if the exposure scenario occurs during early life stages. This study evaluated the effects of maternal Cd exposure and consumption of a HFrD on essential metals in the offspring. **Methods:** Female CD-1 mice were given 0.5 or 5 ppm Cd in drinking water with or without a 60% HFrD for 2 weeks prior to pregnancy, during pregnancy, and lactation. Controls animals received deionized water and calorie-matching diet. Dams were maintained on the same diets until postnatal day (PND) 16. Offspring mice were sacrificed at gestational day (GD) 18, PND22, PND188, and PND360 timepoints. Essential metals (Ca, Cd, Cu, Fe, Mg, Mn, Mo, Na, Rb, Se, Sr, and Zn) were determined in the offspring liver using High Resolution - Inductively Coupled Plasma Mass Spectrometry (HR-ICPMS) after acid-digestion of the biospecimen. **Results:** Cd concentrations in maternal, fetal (GD18), and neonatal (PND22), and adult (PND188, 360) liver increased in a dose-dependent manner. Only a small fraction (0.023%) of the maternal Cd level was measured in the fetal liver, due to limited placental transfer. Approximately 0.065% of maternal Cd reached the offspring via lactation, totaling 0.08% of the maternal liver. About 45% of Cd was found in the liver of adult offspring, after reaching a peak level at weaning age, consistent with a biological half-life of 6 months. HFrD did not alter the hepatic bioaccumulation of Cd and other metal ions except for Rb which showed decreased level in fetal and neonatal liver. Offspring sex showed no effect in Cd bioaccumulation. Though neonatal liver showed sex specific differences in Fe, Mn, Mo, and Zn concentrations, there was not a consistent effect induced either by dose or diet. **Conclusions:** Study results did not support a change of hepatic metal homeostasis in mouse offspring after maternal exposure to Cd, in part due to low doses and brevity of exposure. Furthermore, HFrD did not impact absorption or burden of Cd in either the dam or their offspring.

ABSTRACT NUMBER: 5052 **Poster Board Number:** LB153
TITLE: Maternal exposure to biocide ingredient (PHMG-p) affect gene expression related to brain function in mice offspring

AUTHORS (FIRST INITIAL, LAST NAME) AND INSTITUTIONS: M. Song, J. Choi, J. Park, D. Kim, and K. Lee. Korea Institute of Toxicology, Jeongeup, Korea, Republic of.

KEYWORDS: Maternal exposure, Polyhexamethylene guanidine-pho

ABSTRACT: Background and Purpose: Maternal chemical exposure is increasingly linked with disrupted fetal and neonatal brain development and long-term neurobehavioral dysfunction in children and adults. Previous research suggested that prenatal period exposure to Polyhexamethylene guanidine phosphate (PHMG-p), previously utilized as an ingredient in humidifier disinfectants in South Korea, may lead to postnatal brain neurotoxicity in offspring, resulting in cognitive and developmental disorders, but evidence for clear proof is still insufficient. Therefore, the objective of this study was to investigate whether maternal lung damage caused by PHMG-p during pregnancy causes any toxicological effects on offspring brain development at the transcriptome level. **Methods:** PHMG-p (0 and 0.9 mg/kg) was intratracheally instilled in pregnant C57BL/6 mice on gestational day 8 (GD 8), and the brains of F1 offspring were collected at 3 and 5 weeks after birth, respectively for transcriptomic analysis. Differentially Expressed Genes (DEGs) with differences ≥ 1.5 fold ($p<0.05$) compared to the control group were selected, and Gene Ontology (GO) analysis were performed. **Results:** PHMG-p at a concentration of 0.9 mg/kg induced fibrotic damage in maternal lung tissue. Transcript expression was significantly altered in the brains of offspring from PHMG-p-exposed mothers, with changes in male offspring being greater than in females. GO analysis of DEGs also revealed that the largest biological process and pathway changes associated with brain injury were found in male offspring. Notably, several nervous system signalling pathways and neuronal cell functions were inhibited. Inhibitory changes in the BBSome Signalling pathway (involved in the regulation of mitochondrial function and neuronal development) were common in both males and females at week 3 and 5, predicting a possible impairment of normal mitochondrial function and neuronal development in the brain. **Conclusions:** In conclusion, we suggest that maternal exposure to a biocide component (PHMG-p) can affect offspring brain development and impair normal brain function.

ABSTRACT NUMBER: 5053 **Poster Board Number:** LB154
TITLE: Probing the Direct Effects of Phthalates on Vaginal and Cervical Cells

AUTHORS (FIRST INITIAL, LAST NAME) AND INSTITUTIONS: *P. C. Powell*[1], A. Petersen[2], H. C. Zierden[2], and *K. D. Rock*[1]. [1]Clemson University, Clemson, SC; and [2]University of Maryland, College Park, MD.
KEYWORDS: Endocrine Toxicology; Reproductive and Developmental Toxicology; In Vitro and Alternatives

ABSTRACT: Background and Purpose: The vaginal microenvironment is a complex system that has significant impacts on the reproductive well-being of the host. Under optimal conditions, bacteria, cells, and mucus all play a role in reducing inflammation and maintaining physical and biochemical barriers against infection and disease. Vaginal dysbiosis, characterized by the presence of pathogenic microbes, weakened mucosal and epithelial cell barrier properties, and inflammation affects 30% of women in the United States. Hormonal fluctuations, like those observed across the menstrual cycle, have been shown to impact an individual's susceptibility to vaginal dysbiosis and recent studies have identified a correlation between exposure to endocrine disrupting chemicals (EDCs) and bacterial vaginosis. Phthalates are a class of EDCs found in personal care and feminine hygiene products that have been linked to vaginal dysbiosis. The use of phthalate containing feminine hygiene products may lead to intravaginal exposure to phthalates, however, nothing is known about intravaginal exposure or its impacts on vaginal health. To address this knowledge gap, we sought to characterize the physiological consequences of direct phthalate exposure on human vaginal and cervical cells in vitro, testing the

hypothesis that direct phthalate exposure will induce an inflammatory response and weaken epithelial barrier properties in vaginal and cervical cells. **Methods:** Vaginal (VK2/E6E7), ectocervical (Ect1/E6E7), and endocervical (End1/E6E7) cell lines were purchased from ATCC and cultured per manufacturer instructions, in optimal media and antibiotics at 37°C in 5% CO2. Cells were seeded in six well plates at a density of 200,000 cells/well and allowed to grow for 24hr prior to treatment. Commercially available concentrated stocks (≤99% purity) of phthalates chosen based on their detection in menstrual products, specifically tampons (DEHP, DEP, DMP, DiBP, and DBP). Phthalates were diluted in dimethyl sulfoxide (DMSO) to achieve target phthalate concentrations based on their detection levels in tampons (0, .001, .01, 0.1, 1.0 µg/mL). Cells were dosed with a single compound or a mixture of all five phthalates for 24 hours. Each dose group was assigned a separate plate to avoid contamination via volatilization. After exposure, cells were detached from the wells using trypsin-EDTA solution and RNA was extracted using a hybrid TRIzol and QIAGEN RNeasy kit protocol. After quantifying RNA concentrations using a Qubit fluorometer, changes in gene expression were evaluated using digital PCR. **Results:** No significant changes in cell viability were observed as a result of phthalate exposure, however, significant changes in gene expression were observed as a result of cell type, phthalate congener(s), and concentration of phthalate. Target genes involved in inflammatory response, structural integrity, and growth were evaluated including IL-6, TGF-β1, and CK-8. **Conclusions:** Ongoing studies are evaluating VK2/E6E7, End1/E6E7, and Ect1/E6E7 protein expression for the genes that showed significant differences in expression and barrier integrity via TEER testing and immunohistochemistry. (e.g., claudin 1-4, and occludin). This research will help establish a preclinical foundation for future work evaluating the mechanisms by which phthalates contribute to vaginal dysbiosis. Furthermore, our work presents an opportunity to identify modifiable exposures to EDCs that could contribute to the betterment of female reproductive health.

ABSTRACT NUMBER: 5054 **Poster Board Number:** LB155
TITLE: Investigating Mechanisms of Phthalate Hepatotoxicity via the Hypothalamic-Liver-Ovarian-axis

AUTHORS (FIRST INITIAL, LAST NAME) AND INSTITUTIONS: *A. C. Elkins*, and *K. D. Rock*. Clemson University, Clemson, SC.
KEYWORDS: Endocrine Disruptors; Hepatic; Reproductive and Developmental Toxicology; Phthalates

ABSTRACT: Background and Purpose: The liver is a multifaceted organ involved in the metabolism and storage of nutrients, detoxification, and regulation of sex-steroid hormones estrogen (E_2), progesterone (P_4), and testosterone (T). Although the liver is responsible for metabolizing these hormones and regulating their bioavailability, it is also widely understood that sex hormones significantly influence hepatic functions and, when dysregulated, may contribute to liver disease. Endocrine-disrupting chemicals (EDCs), chemicals that interfere with hormone action in the body, have also been shown to alter hepatic function and compromise liver health. Phthalates are a class of EDCs that are well known for their reproductive toxicity and are of particular concern for women's reproductive health due to their prevalence in personal care, beauty, and feminine hygiene products. Numerous studies have demonstrated that phthalates can disrupt E_2 and P_4 signaling, and exposure has been linked to an increased risk of liver diseases, such as non-alcoholic fatty liver disease. However, the interacting mechanisms by which sex steroids and phthalates impact liver function are not well understood. To address this knowledge gap, we sought to characterize the impact of sex steroids, phthalates, and their combined exposure on the function of liver cells *in vitro*, testing the hypothesis that phthalates disrupt

liver functionality, including lipid metabolism and detoxification, by dysregulating the cross-interactions between the hepatocytes and sex-steroid hormones. **Methods:** The phthalates evaluated within this study (DEP, DBP, DiBP, BzBP, DEHP, and DiNP) were chosen based on their prevalence in the urine of pregnant women. Commercially available stocks (< 99% purity) were diluted in dimethyl sulfoxide (DMSO) to achieve human-relevant concentrations (0.1, 1, 10, 100 µg/ml). Estrogen, progesterone, luteinizing hormone, and follicle-stimulating hormone were purchased from Sigma Aldrich and diluted in ethanol to concentrations relevant to the hormonal fluctuations of the menstrual cycle. The HepG2 cell line was purchased from ATCC and cultured per the manufacturer's instructions at 37 in 5% CO_2. The cells were seeded in six-well plates at a density of 200,000 cells/well and allowed to reach 50% confluency before treatment. Cells were dosed with a single phthalate compound/hormone or a mixture of the phthalates for 24 hours. Each dose group was isolated to separate plates to avoid contamination via volatilization. Following the exposure, cells were detached from the wells using a trypsin-EDTA solution, and the RNA was extracted using a hybrid TRIzol and QIAGEN RNeasy kit protocol. Changes in gene expression were then evaluated using digital PCR. **Results:** Significant changes in gene expression were observed as a result of hormone exposure and phthalate exposure, varying by phthalate congener and concentration. Targeted genes involved in metabolism, hormone regulation, and xenobiotic detoxification, including SHBG, CYP1A1, and FGF21 were evaluated. Genes involved in detoxification (e.g., CYP1A1) and hormone bioavailability (e.g., SHBG) were significantly upregulated by phthalate exposure at the highest dose (100 µg/ml). **Conclusions:** Ongoing studies are evaluating the impact of hormone and phthalate co-exposures on gene and protein expression in HepG2 cells. This research will help identify overlapping and disparate mechanistic targets of female sex steroids and phthalates, providing novel insight into hepatic resilience and/or susceptibility to EDC exposure throughout a female's reproductive years.

ABSTRACT NUMBER: 5056 **Poster Board Number:** LB157
TITLE: Fertility assessment in regulatory safety studies: confoundng by undernourishment

AUTHORS (FIRST INITIAL, LAST NAME) AND INSTITUTIONS: M. McMahon, and H. Ketelslegers. Penman Consulting, Brussels, Belgium. Sponsor: H. Ketelslegers, EUROTOX
KEYWORDS: Reproductive and Developmental Toxicology; Regulatory/Policy; Nutrition; fertility

ABSTRACT: Background and Purpose: It is well-understood that the fertility of female rodents has evolved to rise and fall in synchrony with its nutritional status. It is less well-appreciated this relationship might lead to misinterpretation of fertility findings in regulatory toxicology studies assessing the safety of chemicals. Here, we provide a case study (taken from an ongoing regulatory assessment under EU REACH) exemplifying this problem and suggest further work to understand its implications. **Methods:** For each of a group of 13 chemically related substances, GLP-compliant OECD 422 test guideline (adopted 22nd March 1996) studies were conducted using Han-Wistar rats. The test substances were administered in the diet. Subsequently, as a result of these studies a bespoke OECD 421 study was conducted to assess reversibility of the mild effects observed in them. **Results:** In the OECD 422s, no effects on sexual function and fertility were observed except for a mild but statistically significant reduction in mean *Corpora Lutea* (*CL*) counts. The *CL* responses were sometimes dose-dependent and often the mean value in the High Dose (HD) group fell below the lower bound of the HCD range. In these studies, the test substances elicited aversive behaviour in rats, presumably due to unpalatability of the diet. Consequently, food consumption during the first week of the pre-mating period was transiently,

but severely, restricted and HD animal bodyweights at the point of mating were repressed compared to control, suggesting undernourishment. To test the hypothesis that undernourishment was related to fertility, correlation analyses were conducted to understand their relationship. Undernourishment was quantified as mean bodyweight gain during pre-mating in the HD group expressed as a percentage of concurrent control mean bodyweight gain; fertility was quantified as mean *CL* counts in HD group expressed as a percentage of concurrent control mean *CL* count. A statistically significant correlation coefficient was observed (Pearson's r = 0.615, $P < 0.05$). In the subsequent bespoke OECD 421, the effect on CL was found to be reversible. A pair-feeding study is underway to test definitively the hypothesis that undernourishment is the cause of the above-mentioned correlation. **Conclusions:** At the high doses used in regulatory safety studies, some test substances with no intrinsic effect on fertility might nevertheless appear to impair the parameter due to eliciting undernourishment of the dam as a secondary consequence of unpalatability. Additional feed-restriction studies in the specific context of the OECD 422 test guideline should be conducted to better understand the significance of this problem, as it may lead to incorrect conclusions in regulatory toxicology studies with significant implications for chemical safety assessments.

ABSTRACT NUMBER: 5057 **Poster Board Number:** LB158
TITLE: Arsenic-induced metabolic and epigenetic alterations in early mammalian germ cells

AUTHORS (FIRST INITIAL, LAST NAME) AND INSTITUTIONS: Y. Kang[1,2], S. Armstrong[1,2], and *P. Allard*[1,2].
[1]UCLA- Institute for Society and Genetics, Los Angeles, CA; and [2]UCLA - Molecular Biology Institute, Los Angeles, CA.
KEYWORDS: Embryonic Stem Cells; Environmental Toxicology; Epigenetics

ABSTRACT: Background and Purpose: Arsenic (As), a highly toxic and carcinogenic contaminant, is naturally present in the Earth's crust and widely distributed in the environment. Arsenic exposure induces epigenetic changes, including DNA and histone modifications, but the specific alterations in stem cells and their underlying mechanisms remain unclear. **Methods:** In this study, we conducted a comprehensive analysis of the DNA methylome, histone modifications, transcriptome, and metabolome in ESC and EpiLC models exposed to varying concentrations of sodium arsenite ($NaAsO_2$). **Results:** Compared to untreated cells, ESCs exposed to 1µM or 2µM sodium arsenite exhibited an upregulation of 12,448 and 22,074 DNA methylation regions, respectively. In contrast, EpiLCs treated with sodium arsenite showed a downregulation of 49,961 (1µM) and 61,785 (2µM) DNA methylation regions. Regarding histone modifications, significant reductions in H3K36me2 and H3K36me3 levels (~50-80% for 1µM and 60-90% for 2µM) were observed in both ESCs and EpiLCs exposed to sodium arsenite. Transcriptomic analysis revealed thousands of genes with differential expression changes in arsenite-treated ESCs and EpiLCs compared to untreated controls. Notably, differentially expressed ROS-related genes were identified. Metabolic disruptions also responded to sodium arsenite exposure in a stage-specific manner, particularly affecting S-adenosylmethionine (SAM) levels. **Conclusions:** Our findings demonstrate that Arsenic induces differentiation stage-specific epigenetic and metabolic disruptions, highlighting the need for further research into the mechanisms linking Arsenic exposure to developmental and environmental epigenetics.

ABSTRACT NUMBER: 5058 **Poster Board Number:** LB159

TITLE: Engineering a Midbrain Organoid Model with Integrated Microglia for Studying Developmental Neurotoxicity

AUTHORS (FIRST INITIAL, LAST NAME) AND INSTITUTIONS: *C. Murphy*[1], *X. Wu*[2], and *E. J. Tokar*[1]. [1]NIEHS, Durham, NC; and [2]East Carolina University, Greenville, NC.

KEYWORDS: Stem Cells; Neurotoxicity; Developmental; Methods/Mechanism

ABSTRACT: Background and Purpose: Environmental pollutants such as metals and perfluorooctane sulfonic acid (PFOS), a fluorinated organic compound widely used in industrial and consumer products, are known to induce neurotoxicity. The precise mechanism underlying the neurotoxic effects in humans remain poorly understood due to the lack of suitable human models. Stem cell derived midbrain organoids, contain key aspects of neuronal developmental and cellular interactions, and provide a platform to study environmental endotoxins. However, these models lack integrated microglia, which play a critical role in mediating neuroinflammatory response to toxins. To address these limitations, we are developing a model using human pluripotent stem cell- (PSC) based midbrain organoids integrated with microglia cells that will allow the study of effects of factors involved in neuronal development, microglial activation and neuroinflammatory pathways, and developmental neurotoxicity. This model will better mimic the cellular and molecular interactions of the developing brain under environmental toxicant exposures. **Methods:** Used midbrain organoids derived from human pluripotent stem cells (hPSCs) as previously described in our lab and microglia obtained from Bit.Bio LLC. Hybrid medium combinations were tested to determine optimal culture and maintenance conditions for both midbrain organoids and microglia. Utilized a transwell system to co-culture organoids with microglia; this system allows soluble factors to pass between the two compartments. Conducted ELISA Assays to examine markers of inflammatory activation and to test the hybrid media for compatibility. **Results:** Brightfield microscopy confirmed changes in cellular morphology, viability, and detachment as a sign of stress of the 2D microglia cultures following changes in the hybrid media compositions over a 20-day period. There was an approximate 1-fold increase of inflammatory cytokines, TNF-Alpha and IL-1Beta in the microglia-midbrain organoid co-culture model compared to 2D monocultures of microglia indicating an effect of the 3D organoid environment on microglial activation. Increased levels of cytokines in the co-culture model suggest that organoids with integrated microglia are a better model for studying inflammatory-associated factors in neurotoxicity than organoids lacking this important cell type. Changes in viability in response to different hybrid media combinations indicate that the media composition can influence the inflammatory response. Further optimization and testing are needed to determine the most suitable hybrid media ratio to be used via 2D and co-culture before creating the assembloid. **Conclusions:** Preliminary results described here highlight the influence of 3D microenvironments on microglial function, with implications for modeling neuroinflammation in vitro. To ensure the co-culture system is stable in the optimized hybrid media, we will continue to monitor baseline gene expression, synaptic function, and cellular morphology. Then, work to create an assembloid which integrates microglia directly into the organoids. Microglia integration and activation will be confirmed using immunostaining and specific microglia markers before testing neurotoxic factors. These assembloids would contain a key cell type in neural development and function and could be an optimal model for studying developmental neurotoxicity.

ABSTRACT NUMBER: 5059 **Poster Board Number:** LB160
TITLE: Heavy metal-laden particulate dust alters cell lineages in intestinal organoids

AUTHORS (FIRST INITIAL, LAST NAME) AND INSTITUTIONS: L. L. Appell, R. Atanga, and *J. In*. University of New Mexico, Albuquerque, NM.
KEYWORDS: Alternatives to Animal Testing; Bioinformatics; Gastrointestinal

ABSTRACT: Background and Purpose: Uranium is an under-recognized environmental toxicant, despite 2.1% of community water systems nationwide reporting uranium concentrations higher than the EPA maximum contamination levels. Uranium levels are particularly elevated in Hispanic, semi-urban communities. There are over 500 Abandoned Uranium Mines scattered across the Southwest, which co-occur with greater incidences of metabolic and digestive diseases in Indigenous and Hispanic populations. Thus, there is a need to understand the effects of particulate heavy metals on the digestive system. Previously, our group demonstrated human intestinal organoids to be a relevant model for investigating the physiological impact of environmental toxicants on the intestinal tract. **Objective and Hypothesis** Our objective is to understand the effects of non-fissile uranium bearing particulate dust (UBD) on the intestine, specifically looking at the function of proliferative and secretory cell types. We hypothesize that UBD exposure induces proliferative qualities in secretory cells rather than increasing proliferative cells. **Methods:** Human colonic organoids were exposed to UBD obtained from the Jackpile uranium mine, located on the Laguna Pueblo in New Mexico. Control and dust-exposed organoids (n=3 unique donors) were digested and processed for droplet-based single cell sequencing. **Results:** Upon exposure, secretory (goblet and enteroendocrine) cells expanded four-fold, while proliferative cell types decreased. Additionally, the number of cells undergoing replication decreased. Downstream analysis found that groups of microRNAs were more spread apart in the UBD-exposed condition, while the control showed more connections between cell groups. Several members of the microRNA let-7 family and its target HMGA1 were differentially expressed in the UBD condition. The let-7 family of non-coding RNAs may be suppressing replication and proliferation, thus increasing secretory cell numbers. **Conclusions:** These results suggest that acute uranium dust exposure induces changes in the ratio of proliferative and differentiated cell types, potentially affecting their primary functions. We would expand these findings by performing microRNA sequencing to compare UBD-exposed and control organoids. Our results also provide an improved understanding of uranium dust's impact on the gastrointestinal system, which may inform other physiological studies on the health of individuals exposed to heavy metals.

ABSTRACT NUMBER: 5060 **Poster Board Number:** LB161
TITLE: Inferring Transcription Factor Activity from TempO-Seq Gene Expression Profiling

AUTHORS (FIRST INITIAL, LAST NAME) AND INSTITUTIONS: *S. N. Martos*, C. Willis, *D. Haggard*, *J. A. Harrill*, and *B. N. Chorley*. US EPA, Research Triangle Park, NC.
KEYWORDS: Gene Expression/Regulation; Polycyclic Aromatic Hydrocarbons; Receptor; Aryl Hydrocarbon; Screening

ABSTRACT: Background and Purpose: Polycyclic aromatic hydrocarbons (PAHs), which are formed as byproducts of combustion, are ubiquitous in the environment. The activation of the aryl hydrocarbon receptor (AHR) and the subsequent induction of xenobiotic-metabolizing enzymes in response to PAH exposure has been well documented. In addition to AHR, some PAHs have also been demonstrated to

activate other nuclear receptors and transcription factors (TFs). Gene expression profiling studies have expanded our ability to evaluate transcriptional regulatory networks and infer nuclear receptor and transcription factor activity from xenobiotic exposures. As a result, it has become increasingly apparent that environmental contaminants can exert effects through multiple biological targets and differ in the degree to which they demonstrate target promiscuity. In this study, we set out to assess the extent to which PAHs affected AHR activity using transcriptional responses to infer TF activity. **Methods:** To assess transcription factor activity in response to chemical exposure in human bronchial epithelial cells, we exposed HBEC3-KT cells to eight concentrations of 86 test compounds in triplicate and measured transcriptional responses at 24 hours using a targeted RNA-sequencing method, TempO-Seq. Test chemicals include four of 13 PAHs with ongoing immunotoxicity studies being conducted by the National Institutes of Health Division of Translational Toxicology (NIH DTT); six chemicals classified as similar (Tanimoto coefficient > 0.8) to any of the 13 DTT PAHs by the CompTox Chemicals Dashboard; two chemicals identified as AHR agonists based on RefChemDB, a public database of reference chemical to target annotations; seven chemicals classified as similar (Tanimoto coefficient > 0.8) to RefChemDB-identified AHR agonists by the CompTox Chemicals Dashboard; and 67 chemicals from RefChemDB, that were not categorized as PAHs by the CompTox Chemicals Dashboard, where AHR agonism was not the target with highest support. For each chemical, limma (limma_3.60.6) was used to calculate moderated t-statistics for treatment versus DMSO (vehicle control), with model design accounting for plate-specific DMSO controls (gene expression ~ 0 + treatment group + plate). We then implemented the decoupleR (decoupleR_2.10.0) univariate linear model approach to infer TF activity scores (positive scores indicate activation and negative scores indicate inhibition) from moderated t-statistics using the CollecTRI gene regulatory network curated collection of TFs. We then ranked activation and inhibition scores for each chemical by dose level to evaluate the relative extent of TF activity. **Results:** The DTT PAHs tested showed varying degrees of AHR activity. AHR was the highest ranked activation score for benzo[k]fluoranthene at 100 nM, the second highest ranked activation score for benzo[a]pyrene at 10 µM, the tenth highest ranked activation score for phenanthrene at 3 µM, and the thirteenth highest ranked activation score for pyrene at 100 nM. AHR activation was ranked within the top ten activated TFs for at least one dose level of four of six chemicals (66.7 percent) identified as similar to DTT PAHs. In contrast, AHR inhibition was within the top ten inhibited TFs for at least one dose level of the other two PAH-similar chemicals tested. Of the two chemicals expected to be AHR agonists based on RefChemDB target annotations, AHR activation was within the top ten activated TFs for multiple dose levels of 3-methylcholanthrene and within the top 25 for 5,6-benzoflavone. One of seven (14.3 percent) the AHR agonist-similar chemicals had AHR within the top ten activated TFs; an additional three (42.9 percent) had AHR activation within the top 25; and one (14.3 percent) had AHR inhibition within the top ten. Of the chemicals not expected to have AHR as a primary target, seven (10.4 percent) had AHR activation within the top ten and an additional nine (13.4 percent) had AHR activation within the top 25 activated TFs. Seven (10.4 percent) had AHR inhibition within the top ten inhibited TFs. **Conclusions:** Overall, the use of TempO-Seq gene expression profiling to infer TF activation detected AHR activation by PAHs and AHR agonists, as expected. We also identified potential inhibition of AHR activity by compounds similar to PAHs and AHR agonists. From this analysis, it is unclear whether this represents direct inhibition of AHR or indirect inhibition through a more complex feedback loop. Finally, although not anticipated to be the primary target, additional chemicals appear to have potential to activate AHR responsive genes. Taken together, this demonstrates that this approach can uncover canonical TF activation and may identify additional TF targets that could contribute to chemical-specific effects. While this study focused on the association between PAHs and activation of AHR, this approach should be applied to additional

compounds and expanded in scope to examine more complex TF activation/inhibition network associations. *This abstract does not represent US EPA policy. Use of company and product names do not constitute endorsement by US EPA*

ABSTRACT NUMBER: 5061 **Poster Board Number:** LB162
TITLE: Treatment of isoliquiritigenin resulted in the toxicological induction of mitochondrial dysfunction and oxidative stress in cholangiocarcinoma cells

AUTHORS (FIRST INITIAL, LAST NAME) AND INSTITUTIONS: K. Choi, and S. Bae. Chungbuk National University, Cheongju, Korea, Republic of. Sponsor: *K. Kim*
KEYWORDS: Carcinogenesis; Oxidative Injury; Pharmaceuticals

ABSTRACT: Background and Purpose: Isoliquiritigenin (ISL), a bioactive phytochemical derived from the root of *Glycyrrhiza uralensis*, is known to exert anti-cancer effects by influencing cancer cell functions including proliferation, metastasis, angiogenesis, and autophagy. However, research on the anti-cancer effects of ISL on cholangiocarcinoma (CCA) is limited. **Methods:** In this study, we aimed to investigate the anti-cancer and toxicological effects of ISL on CCA cells, i.e., SNU-478 and HuCCT-1. Cell viability was measured using the Quanti-MAX water-soluble tetrazolium salt (WST)-8 cell viability kit. The clonogenic ability was evaluated by colony formation assay as described previously with slight modification and the types of cell death were evaluated using Alexa Fluor 488 Annexin V/Dead Cell Apoptosis Kit. In addition, mitochondrial membrane potential changes were analyzed using a JC-10 and mitochondrial ROS was detected by the superoxide indicator kit. Acridine orange staining was performed to detect lysosomal membrane permeability in these cells following treatments. Western blot analysis was performed to elucidate the mechanism of these changes. **Results:** In SNU-478 cells, ISL treatment resulted in a decrease in the expression of glucose-regulated protein 78 (GRP78). ISL treatment was also found to significantly reduce cell viability and colony area of both SNU-478 and HuCCT-1 cells. Further, the ISL treatment significantly increased the population of apoptotic cells, as observed through Annexin V/propidium iodide (PI) staining. PI staining showed that the ISL treatment induced significant cell cycle arrest in the growth phase 2 (G2)/M (mitosis) phase compared to the control group, indicating that ISL-induced reduction in cell viability is associated with cell cycle arrest as well as apoptosis. ISL treatment also resulted in a significant decrease in the mitochondrial membrane potential when observed through JC-10 staining. Mitochondrial Superoxide (MitoSOX™) staining revealed that ISL treatment significantly upregulated the generation of mitochondrial reactive oxygen species (ROS). Acridine orange staining indicated that the ISL treatment upregulated lysosomal membrane permeability, which could be related to autophagy. **Conclusions:** These results suggest that ISL affects the proliferation and apoptosis of CCA cells, which might be related to its regulatory role in various cellular functions, including mitochondrial dysfunction, ROS balance, and autophagy. This study provides empirical evidence that ISL could be a potential candidate for CCA therapy.

ABSTRACT NUMBER: 5062 **Poster Board Number:** LB163
TITLE: Pyruvate Kinase Activity Regulates Cystine Starvation Induced Ferroptosis in Pancreatic Cancer

AUTHORS (FIRST INITIAL, LAST NAME) AND INSTITUTIONS: T. Jordan, E. Ensink, H. Medeiros, and S. Lunt. Michigan State University, East Lansing, MI. Sponsor: S. Lunt, American Association for Cancer Research
KEYWORDS: Carcinogenesis; Metabolism; Antioxidants

ABSTRACT: Background and Purpose: Pancreatic ductal adenocarcinoma (PDAC) stands as one of the most lethal cancers in the United States, with treatments relying on cytotoxic therapies that cause severe side effects and promote chemoresistance. PDAC cells adapt to the nutrient-poor tumor microenvironment through metabolic reprogramming, including pyruvate kinase muscle isoform 2 (PKM2) expression, which influences antioxidant systems and ferroptosis—an iron-dependent, lipid peroxidation-driven form of regulated cell death. This study investigates the role of PKM2 in cystine metabolism and ferroptosis sensitivity to identify metabolic vulnerabilities for therapeutic targeting. **Methods:** PKM2 knockout (KO) human PDAC cells were generated using CRISPR and cultured under cystine replete (50 µM) or cystine starvation (0 µM) conditions. Ferroptosis was induced with 0.625 µM IKE and inhibited using 5 µM ferrostatin-1, 100 µM Trolox, and 100 µM deferoxamine. Apoptosis and necroptosis were inhibited with 50 µM Z-VAD-FMK and 10 µM necrostatin-1S, respectively. Cytotoxicity was assessed at 24 hours using alamarBlue and a Biotek plate reader. PKM2 activity was measured using a Promega kit, and PKM2 activation was induced with 12.5 µM TEPP-46. Malic enzyme 1 (ME1) inhibition was achieved using 50 µM ME1i. For *in vivo* studies, NSG mice were injected with human PDAC cells in the flank region and treated with either 50 mg/kg IKE, 30 mg/kg TEPP-46, or a combination of both. Tumor growth was monitored, and treatment efficacy was assessed by tumor weight and volume at the endpoint of the study. **Results:** PKM2-expressing PDAC cells are highly sensitive to cystine starvation-induced ferroptosis and this sensitivity can be rescued by pharmacological inhibitors of ferroptosis. In contrast, PKM2KO cells exhibit resistance to cystine starvation-induced ferroptosis. We found that the overall activity of PKM2 influences PDAC cell sensitivity to cystine starvation-induced ferroptosis both *in vitro* and *in vivo,* with the combination of PKM2 activation and cystine starvation significantly reducing cellular viability *in vitro* and tumor growth *in vivo.* PKM2KO resistance is also associated with metabolic reprogramming, including increased antioxidant production and elevated glutaminolysis, which enhances malate synthesis. The combination of increased antioxidant production, such as NADPH, and malate production led us to discover that PKM2KO cells have increased ME1 expression when compared to PKM2-expressing cells. Pharmacological inhibition of ME1 reduced cellular viability in both PKM2-expressing and PKM2KO cells to similar extents, leading us to believe that ME1 is a key metabolic enzyme responsible for PKM2KO PDAC cells resistance to ferroptosis. **Conclusions:** PKM2KO protects PDAC cells from cystine starvation-induced ferroptosis by altering metabolic antioxidant pathways, which we believe is due to an increased utilization of ME1. The combination of PKM2 activation and cystine starvation shows an additive effect on cellular viability and successfully shrunk tumors *in vivo*.

ABSTRACT NUMBER: 5063 **Poster Board Number:** LB164
TITLE: Studying the effect of p,p'-DDE exposure on major nuclear and cytoskeletal proteins in Non-Tumorigenic MCF10A cells

AUTHORS (FIRST INITIAL, LAST NAME) AND INSTITUTIONS: A. Tapaswi, J. L. Miller, and *J. A. Colacino*. University of Michigan, Ann Arbor, MI.
KEYWORDS: Pesticides

ABSTRACT: Background and Purpose: Breast cancer is the most commonly diagnosed cancer in women. An estimated 30% of breast cancers have been attributed to modifiable risk factors such as environmental chemical exposures. Exposure to common chemicals such as the pesticide DDT and its metabolite p,p'-DDE has been linked to increased breast cancer risk. We developed a method of

combining immunocytochemistry with high throughput imaging to identify major nuclear and cytoskeletal proteins that get affected by short term chemical exposure. We measured expression and localization β-catenin, a known canonical Wnt transcription factor, which provides insight into cell proliferation and cell cycle. We studied the expression pattern of Cytokeratin 8 (K8), a luminal cell marker, and Cytokeratin 14 (K14), a basal cell marker, to study hybrid basal-luminal populations, which is indicative of cellular plasticity, a new hallmark of cancer. We also quantified changes in expression of E-cadherin (Ecad) and Vimentin (Vim), indicative of the epithelial-to-mesenchymal transition, an established hallmark of cancer. Morphological and cell state perturbations could point towards potential mode-of-action for chemicals with undetermined mechanisms. **Methods:** MCF10A, a non-tumorigenic breast epithelial cell line, was cultured and plated in 384 well plates for chemical exposure and staining. Cells were treated with p,p' -DDE at 25nM to 25uM for 96 hours. Cells were also dosed with a known Wnt activator CHIR99021 at 10nM to 10uM dose range, as a positive control. We developed three high content imaging staining assays investigating Beta-Catenin, K8 - K14 and Vim - E-cad. Cells were also stained with Hoechst 33342, a nuclear stain and Cellmask, a cell body stain. The plates were imaged in the CellInsight CX5 microscope using automated imaging.Cellprofiler 4.2.1 was used to perform imaging quality control, illumination correction and analysis. A cell segmentation and feature extraction pipeline was setup which carried out illumination correction and image quality control. Multiple parameters were analyzed including Cell Size, Cell Shape, Object Intensity and Intensity Colocalization. Raw data was imported in R for further analysis. Mean intensity per well was averaged across 6 replicates, imaged with 9 fields per well, by treatment and concentration. The change in mean intensity was visualized using boxplots from the R package ggplot2 and a p value was determined by comparing mean intensity for control against the tested concentrations using the t-test. For cytokeratin8/14 and E-cadherin/Vimentin, 'high' and 'low' categories were created based on mean intensity to classify individual cells based on their expression patterns, with the goal of quantifying proportions of diverse cell populations in treated vs control wells. **Results:** Overall, as compared to control an increase in cell count was observed at all doses of DDE (p= 0.00011) and for 3 lower doses of CHIR (p=0.00011). A decrease in cell count was observed at CHIR 10uM (p=0.03). An overall increase in β-catenin nuclear intensity was observed for all doses of DDE (p=0.00011) and with CHIR at concentrations of 10uM (p=0.00011), 1uM (p=0.00011), 100nM (p=0.000750) and 10nM (p=0.04). An increase in β-catenin cytoplasm and β-catenin cell edge intensity was seen for all doses of DDE (p=0.00011) and for all 3 lower doses of CHIR (p=0.000110 and 10uM (p= 0.003). An increase in K8+/K14+ population was observed in 25uM (p=0.0003), 2.5uM (p=0.004), 250nM (p=0.006) and 25nM (p=0.004). For CHIR an increase was also observed in all doses but 10uM (p= 2.1e-09) had the highest increase. An overall increase in K8+ population was observed in all doses of DDE (p=0.005), although only 25uM DDE showed an increase in K14+ as well (p =0.01). Interestingly, CHIR at 10uM dose showed no significant change in K8+ population but showed an increase in K14+ (p=8e-05). We observed an overall decrease in Ecad+/Vim+ population in 25uM (p=0.0065) and 250nM (0.0030). For CHIR there was an overall decrease in Ecad+/Vim+ population in 100nM (p=0.01) and 10nM (p=0.002). Interestingly, a significant increase was observed in a Vim+/Ecad- population in the 25uM (p=0.0056) of DDE and 10uM (p=0.00019) CHIR. **Conclusions:** We observed increased cell count in treated samples, along with an increased expression of the canonical Wnt transcription factor B-catenin in both p,p'-DDE and CHIR99021 treated cells. Interestingly, an increase in beta-catenin expression observed in the cellular boundary, could potentially indicate an activation of Wnt pathway and cell proliferation. We also observed an increase in K8+/K14+ cells, a hybrid luminal-basal signature indicative of cellular plasticity potentially linked to the development of aggressive breast cancers. An increase was observed in Vim+/Ecad- cells reflecting an epithelial-mesenchymal transition

(EMT). With these high-content multi-panel assays, we summarized the changes occurring in the major nuclear and cytoskeletal proteins upon exposure, potentially indicating a mode of action of the toxicant related to alterations in cellular state. In-depth analysis of the data at a single cell level is currently ongoing. This would be key in defining modifiable risk factors leading to aggressive breast cancers and setting the stage for examination of additional common chemicals in the environment.

ABSTRACT NUMBER: 5064 **Poster Board Number:** LB165
TITLE: Benzene exposure is associated with clonal hematopoiesis

AUTHORS (FIRST INITIAL, LAST NAME) AND INSTITUTIONS: C. Xing[1], L. Zhang[2], J. He[1], B. Wu[1,3], J. Zhao[1,4], X. Cheng[1], J. Zhou[1], Y. Zhang[1], K. Jin[1], J. Shi[5], J. You[6], Q. Jia[7], and Q. Wang[8]. [1]National Institute for Occupational Health and Poison Control, Chinese Center for Disease Control and Prevention, Beijing, China; [2]Guangzhou National Laboratory, Guangzhou, China; [3]Science and Technology Research Center of China Customs, Beijing, China; [4]National Office for Maternal and Child Health Surveillance of China, West China Second University Hospital, Sichuan University, Chengdu, China; [5]Tianjin Occupational Diseases Precaution and Theraputic Hospital, Tianjin, China; [6]The Second Affiliated Hospital of Shandong University of Traditional Chinese Medicine, Jinan, China; [7]Shandong Academy of Occupational Health and Occupational Medicine, Shandong First Medical University & Shandong Academy of Medical Science, Jinan, China; and [8]Beijing Institute of Genomics, Chinese Academy of Sciences/China National Center for Bioinformation, Beijing, China. Sponsor: *B. Li*
KEYWORDS: Hematotoxicity; Mutation; Carcinogenesis

ABSTRACT: Background and Purpose: Clonal hematopoiesis (CH) is characterized by the clonal expansion of mutated hematopoietic stem cells (HSC). The most frequent CH mutations are found in DNMT3A, TET2 and ASXL1 genes. Individuals with CH are at an increased risk of developing hematologic cancers. Interestingly, CH is not driven by genetic mutation alone. Environmental factors such as aging, inflammation and chemotherapy play a critical role on the emergence of CH with genetic mutation. As an important industrial chemical and environmental contaminant, benzene is a well-known human leukemogen. However, the underlying mechanisms of benzene-induced carcinogenesis remain unclear. The objective of this study was to investigate whether occupational exposure to benzene caused an increase in clonal hematopoiesis. **Methods:** We analyzed for CH mutations in 157 benzene exposed individuals, comprising 103 benzene exposed workers and 54 benzene poisoning cases, as well as 44 unexposed controls in China. Whole exon sequencing was performed on DNA from peripheral blood lymphocyte of these individuals. Individual exposures were assessed using personal air monitoring. Air benzene concentrations were not detectable in unexposed control; in exposed workers, concentrations ranged from 0.157 to 48.72 mg/m^3 (median, 1.94 mg/m^3). **Results:** Among benzene poisoning cases, benzene exposed workers and controls, CH mutations were observed in 23.9 (14 of 54), 12.6% (13 of 103) and 4.5% (2 of 44), respectively. Statistically significant increase in the CH mutation were found to be dose-dependently associated with benzene exposure concentrations (P_{trend}=0.003). The CH mutation in the benzene poisoning group was significantly elevated (OR=7.206; 95% CI: 1.5-33.6, P=0.011) and showed a dose-dependent increase with the severity of poisoning (P_{trend}=0.0028). We also found that CH mutations, which are strongly associated with aging, such as DNMT3A, TET2, and ASXL1, were also present in individuals exposed to benzene. Notably, the most frequently mutated genes among benzene-exposed individuals were DNMT3A and KMT2C. **Conclusions:** Exposed to benzene increases

clonal hematopoiesis with somatic mutations linked to hematologic cancer. Benzene appeared to be a new environmental driver of clonal hematopoiesis.

ABSTRACT NUMBER: 5065 **Poster Board Number:** LB166
TITLE: The perinatal exposure to a low dose of glyphosate and a mixture of glyphosate, dicamba and 2,4-D induces oxidative stress in offsprings' liver and kidney: Implications for long-term health risks

AUTHORS (FIRST INITIAL, LAST NAME) AND INSTITUTIONS: P. Nechalioti, Z. Skaperda, F. Tekos, P. Vardakas, C. Nepka, and D. Kouretas. Department of Biochemistry & Biotechnology, University of Thessaly, Larissa, Greece. Sponsor: D. Kouretas, EUROTOX
KEYWORDS: Pesticides; Mixtures; Redox biomarkers; Oxidative stress; Glyphosate, 2,4-D, Dicamba

ABSTRACT: Background and Purpose: The increasing demands for food products have intensified the use of agrochemicals as effective weed management tools. Glyphosate, dicamba and 2,4-D are widely used herbicides, applied either alone or in combination to overcome weed resistance and enhance crop productivity. Despite their exponential application, the information about the toxicological profile of herbicide mixtures is scarce, raising serious health concerns, especially for the exposure during the early developmental stages of biological organisms. **Methods:** The study investigated the effects of perinatal exposure of Wistar rats to a low-dose of glyphosate and a mixture of glyphosate, dicamba and 2,4-D on liver and kidney redox homeostasis, the major organs of xenobiotic metabolism and detoxification. A total of 80 offsprings (40 males and 40 females), equally divided at 4 experimental groups, were exposed to the glyphosate either individually or in combination with dicamba and 2,4-D via drinking water. The dosing strategy was based on the recommendations of Organization of Economic Cooperation and Development (OECD) guideline TG 414 and started at gestational day 6 and continued throughout the gestation and lactation period up to 3 months post-weaning. The first group was administered the standard rodent diet and drinking water. The second group was administered glyphosate at the European Union (EU) Acceptable Daily Intake (ADI) (0.5 mg/kg bw/day) in drinking water. The third group was administered glyphosate at the EU No-Observed-Adverse Effect Level (NOAEL) (50 mg/kg bw/day) in drinking water. Finally, the fourth group was administered a mixture of glyphosate (0.5 mg/kg bw/day), dicamba (0.3 mg/kg bw/day), and 2,4-D (0.02 mg/kg bw/day) in drinking water, equivalent to their EU ADI doses. Following the exposure period, the animals were anesthetized, sacrificed by exsanguination, liver and kidney tissues were collected and a panel of redox biomarkers was evaluated, including reduced glutathione (GSH), decomposition rate of hydrogen peroxide (H_2O_2), total antioxidant capacity (TAC), thiobarbituric acid reactive substances (TBARS) and protein carbonyls (CARBS). The experiment was endorsed by the Ethical Committee of the University of Medicine and Pharmacy of Craiova. **Results:** The perinatal exposure to glyphosate at a NOAEL dose induced perturbations of redox homeostasis, as evidenced by the activation of adaptive antioxidant mechanisms in liver and the increased lipid peroxidation in kidney, resulting in oxidative stress. Furthermore, the perinatal exposure to the herbicide mixture at ADI dose caused oxidative stress in both liver and kidney, supported by the augmented lipid peroxidation levels. **Conclusions:** Exposure to low doses of glyphosate individually and in mixture form with dicamba and 2,4-D induces redox imbalance to offsprings' liver and kidney, signifying a negative impact on these vital organs, particularly during sensitive developmental stages. This research reinforces the long term, low-dose exposure regimen, providing useful insights into the detrimental effects of herbicide mixtures to antioxidant machinery. Ongoing studies that aim to

identify the mechanism of toxicity and the broader implications of exposure to glyphosate, dicamba and 2,4-D for adult physiology will contribute to the re-assessment of herbicides regulatory limits.

ABSTRACT NUMBER: 5066 **Poster Board Number:** LB167
TITLE: The effects of urinary metal mixtures on insulin resistance in Afro-Caribbean men and women

AUTHORS (FIRST INITIAL, LAST NAME) AND INSTITUTIONS: *N. Price*[1], R. Cvejkus[1], V. Wheeler[2], P. J. Parsons[3,4], C. Gennings[5], *A. Barchowsky*[6], *A. P. Sanders*[6], and I. Miljkovic[1]. [1]Department of Epidemiology, University of Pittsburgh School of Public Health, Pittsburgh, PA; [2]Scarborough General Hospital, Scarborough, Trinidad and Tobago; [3]Division of Environmental Health Sciences, Wadsworth Center, Albany, NY; [4]Department of Environmental Health Sciences, University at Albany, Albany, NY; [5]Department of Environmental Medicine and Climate Science, Icahn School of Medicine at Mount Sinai, New York City, NY; and [6]Department of Environmental and Occupational Health, University of Pittsburgh School of Public Health, Pittsburgh, PA.
KEYWORDS: Metals; Epidemiology; Exposure, Environmental; Diabetes

ABSTRACT: Background and Purpose: The global burden of type 2 diabetes (T2D) cannot be fully explained by genetics and lifestyle alone. Emerging evidence suggests environmental toxicants, including metal mixtures, may disrupt glucose metabolism and contribute to the development of T2D. Populations of African ancestry (PAA) have a high burden of T2D, exhibiting greater insulin resistance and reduced insulin clearance compared to populations of European ancestry. However, evidence that metal mixtures contribute to altered glucose metabolism in PAA is lacking, particularly among populations outside the U.S. and U.K. Given the unique genetic, cultural, and environmental contexts, studying the effects of metal mixture exposures among PAA is critical. This study examined associations between metal mixtures and insulin resistance in middle-aged and older Afro-Caribbean men and women without T2D. We hypothesized that a mixture of metals would have a joint positive effect on insulin resistance. **Methods:** The Tobago Health Study is a population-based study of middle-aged and older Afro-Caribbeans from Tobago. Urinary metals and metalloids (referred to hereafter as metals) were measured in men from 2014-2016 and in women from 2019-2020. Our study sample included 638 individuals. Individuals with T2D were excluded due to the effects of T2D on metal metabolism. A total of 253 women (mean age: 54 years) and 385 men (mean age: 60 years) with urinary metal measurements were included in the analysis. Insulin resistance was calculated using the Homeostatic Model Assessment for Insulin Resistance (HOMA-IR), derived from fasting insulin and glucose measurements. Urinary metal and metalloid (referred to hereafter as metal) concentrations (µg/L) were measured using an Inductively Coupled Plasma Tandem Mass Spectrometer (Agilent Model 8900 ICP-MS/MS). Metals were classified as highly detected if more than 60% of samples had values above the limit of detection. The 12 most highly detected metals included arsenic (As), barium (Ba), cadmium (Cd), cobalt (Co), cesium (Cs), copper (Cu), molybdenum (Mo), lead (Pb), tin (Sn), thallium (Tl), uranium (U), and zinc (Zn). Sex-stratified linear regression models were used to examine the relationships between log-transformed HOMA-IR and each of the 12 highly detected element concentrations individually. Additionally, weighted quantile sum regression (WQSR) was employed to assess the association of a mixture effect of metals with insulin resistance. Metal concentrations were binned into quintiles for both the individual metal and mixture models. To enable comparisons between men and women and between individual and mixture models, age, waist circumference, and urinary creatinine were included as covariates. These covariates were selected from demographic, lifestyle, and health behavior factors

because they were the most relevant confounders across all models. Holm's method was applied to adjust for multiple comparisons in the individual metal models. **Results:** In individual metal models for women, each quintile increase of Cu and Sn was associated with a 12.4% (95% CI: 1.4% - 24.6%) and 11.1% (95% CI: 1.8% - 21.3%) higher HOMA-IR, respectively. For men, each quintile increase of Mo was associated with a 4.7% (95% CI: 0.0% - 9.6%) higher HOMA-IR. However, after adjustment for multiple comparisons the effect estimates for Cu and Sn in women and Ba in men no longer met the criteria for significance. In WQSR models for women, each one unit increase in the metal mixture index was associated with 16.8% (95% CI: 1.0% - 34.6%) higher HOMA-IR. Sn, Cu and Ba were the main contributors to the mixture effect on insulin resistance in women. In mixture models for men the metal mixture was not significantly associated with HOMA-IR. **Conclusions:** Among women, the observed effect of the metal mixture on insulin resistance was greater than the effect of any individual metal alone which is evidence of a mixture effect. This finding highlights the importance of assessing metal mixtures in addition to individual metals to better understand combined effects on glucose metabolism. These findings also suggest potential sex differences in how metal exposures influence insulin resistance, underscoring the need for further research to confirm these associations and to investigate the potential biological mechanisms driving these differences.

ABSTRACT NUMBER: 5067 **Poster Board Number:** LB168

TITLE: Analysis of the Antimicrobial Effects of Orange Peel and Rosemary Oils as an Alternative to Chlorine in Mass Catering Environments

AUTHORS (FIRST INITIAL, LAST NAME) AND INSTITUTIONS: M. Altan[1], and F. Cakiroglu[2]. [1]Firat University, Elazığ, Turkey; and [2]Ankara University, Ankara, Turkey. Sponsor: *N. Basaran*

KEYWORDS: None

ABSTRACT: Background and Purpose: Ensuring safe food consumption is one of the greatest concerns for societies. In the rapidly expanding mass catering system, the most critical factor is food hygiene. Failure to maintain safe food in this sector leads to foodborne illnesses and poisonings. Various disinfectants are used for sanitizing foods in mass catering systems. Chlorine-based products are commonly recommended for sanitizing fresh vegetables to delay or eliminate microbiological growth. However, the formation of trihalomethanes, which are carcinogenic compounds due to the use of this disinfectant is a disadvantage. Some epidemiological studies on morbidity and mortality from cancer and on trihalomethane concentrations have shown positive correlations in certain carcinoma cases. Recently, the sector has been seeking to avoid chlorine by turning to non-chemical disinfectants and alternative, eco-friendly sanitation methods. **Methods:** In this study, we aimed to determine the effectiveness of orange peel and rosemary oil extracts compared to chlorine (calcium hypochlorite). For this purpose, garden cress and arugula were inoculated with Salmonella enteritidis (106 CFU/mL). Then, various concentrations of chlorine (calcium hypochlorite (Ca(OCl) at 50, 100, 200 mL/L), orange peel oil, and rosemary oil (0.1%, 0.3%, and 0.5% oil extracts) were applied to the samples for different durations (5 minutes, 15 minutes) for disinfection. **Results:** Rosemary and orange oils reduced Salmonella enteritidis levels. The concentration of essential oils used and the duration in the solution played a significant role in the degree of reduction. When comparing different disinfectants, it was determined that in both garden cress and arugula samples, 0.5% rosemary oil was more effective than both 0.5% orange peel oil and 200 mg/L chlorine concentration ($p < 0.05$). It was determined that in garden cress samples treated for 15 minutes, 0.5% rosemary oil concentration inhibited the growth of S. enteritidis (p

< 0.05). **Conclusions:** Disinfection of raw or minimally processed vegetables that are consumed without heat treatment is crucial for food safety and nutrition. Inspired by this study, further research may be conducted by commercial enterprises on different natural disinfectants to reduce costs and increase accessibility. This would help promote the widespread use of natural disinfectants in mass catering.

ABSTRACT NUMBER: 5068 **Poster Board Number:** LB169
TITLE: Pre-clinical safety assessment of Living Therapeutic Materials

AUTHORS (FIRST INITIAL, LAST NAME) AND INSTITUTIONS: *J. Mekontso Ngaffo*[1,2], and S. Trujillo Munoz[1]. [1]INM-Leibniz Institute for New Materials, Saarbrücken, Germany; and [2]Saarland University, Saarbrücken, Germany.
KEYWORDS: Biomaterial; Medical Device; Cytotoxicity; Biocompatibility

ABSTRACT: Background and Purpose: Living Therapeutic Materials (LTMs) enclose living biofactories within nonliving matrices, such as natural and synthetic polymers, and can produce and release drugs *in situ* and on demand. For therapeutic applications, LTMs are in direct contact with the host and thus their safety is to be guaranteed throughout the entire exposure time. Hence, the biocompatibility assessment of LTMs is a fundamental step during their development. **Methods:** We present a practical workflow for assessing the biocompatibility of LTMs *in vitro* that allows the parallel investigation of a higher number of application conditions. We tested the workflow for LTMs based on Pluronic hydrogels containing *ClearColi* as a model organism. We monitored bacteria growth, and quantified glucose consumption in the incubation medium, the cytotoxicity to mammalian cells and the release of pro-inflammatory cytokines. **Results:** The established workflow could assess 4 different conditions in parallel using various experiments over a period of a week. The Pluronic-based thin films were not cytotoxic to mammalian cells and did not induce the release of key pro-inflammatory cytokines. **Conclusions:** This marks a step towards establishing a roadmap for the biocompatibility assessment of LTMs in a standardized way.

ABSTRACT NUMBER: 5069 **Poster Board Number:** LB170
TITLE: An *in vitro* method for assessment of gastrointestinal toxicity of food additive and food contaminant nanoparticles

AUTHORS (FIRST INITIAL, LAST NAME) AND INSTITUTIONS: S. Ayehuni[1], *C. Pellevoisin*[1], J. Markus[2], M. Klausner[1], A. Helfrick[1], and A. Armento[1]. [1]MatTek Corporation, Ashland, MA; and [2]MatTek Europe, Bratislava, Slovakia.
KEYWORDS: Food Safety; Gastrointestinal; In Vitro and Alternatives; Nanoparticles

ABSTRACT: Background and Purpose: The expanding use of nanoparticles (NPs) in various applications has raised concerns about their potential health effects, particularly when ingested via food, water, drugs, or cosmetics. In the food industry, there is increasing use of NPs in the food processing, packaging and directly in food products for their antimicrobial, nutrient, coloring and texture-enhancing properties. However, the toxicological impacts of NPs on the human gastrointestinal tract remain incompletely understood. We have developed an in vitro method using the reconstructed human model of the small intestine, EpiIntestinal, to evaluate acute and chronic effects of various NPs, including some food additives such as titanium dioxide (E171), iron oxide (E172), silver (E174), and gold (E175). The evaluation was done through multiple endpoints: barrier integrity, tissue viability, oxidative stress and inflammatory response. In addition, a permeation study was conducted to assess applicability of the

EpiIntestinal to study systemic exposure to NPs from food industry. **Methods:** EpiIntestinal tissues were exposed to NPs (CuO, ZnO, SiO2, TiO2, Ag, Al, FeO, Au) at concentrations ranging from 5-900 µg/mL for 24 hours. Toxicity was assessed by measuring changes to barrier (TEER), tissue viability (MTT assay), histological analysis, cytokine release, oxidative stress (8-isoprostane release), and DNA damage (comet assay) The maximum tolerated dose (MTD), corresponding to concentrations with no acute toxicity (concentrations with less than 20% reduction in either TEER or MTT values), was estimated. In the second step, the EpiIntestinal model was exposed chronically to the MTD by repeated application every 48 hours for up to 18 days with TEER and MTT performed periodically. For the permeation study, 50 µL of polystyrene latex nanoparticles with red fluorophore were applied to the apical surface of the EpiIntestinal model and supernatants were collected from the basolateral compartment after 2hr, 4hr, 6hr, and 24hr. Permeated particles were quantified using a fluorescence spectrometer. **Results:** Following acute exposure, CuO, and ZnO, showed significant dose-dependent reductions in barrier integrity (TEER) and tissue viability (MTT). These NPs also induced histological damage and increased release of the pro-inflammatory cytokine IL-8. Analysis of culture supernatants showed a dose dependent increase of 8-isoprostane release following exposure to CuO and a slight increase by ZnO, and FeO but not to Ag nanoparticles. Taking these results together, TiO2, Ag, Al, and FeO showed minimal acute toxicity at the tested concentrations. After repeated application at the MTD dose which induced no acute toxicity, a progressive reduction of cell viability is observed with CuO and to a lesser extent for TiO2, Au, FeO and, only at longer exposure time, with Al. No significant changes were observed with ZnO, Ag and Si. The flux of polystyrene latex nanoparticles through EpiIntestinal was calculated from permeation study: 1.03 ug/cm2/hr. **Conclusions:** Our results demonstrate that the EpiIntestinal model provides a physiologically relevant platform for assessing the potential toxicity effects of NPs present in the food. The exposure conditions, acute and chronic, and the different endpoints evaluated showed specific activity profiles depending on the NPs considered. Beyond local effects, the permeation study also suggests utilization of the EpiIntestinal model to assess the risk of deposition of nanoparticles at distant organs and systemic exposure to nanoparticles in the food industry.

ABSTRACT NUMBER: 5070 **Poster Board Number:** LB171

TITLE: *In vitro* Evaluation of Antioxidant and Cytoprotective Potential of Four Hydroalcoholic Plant Extracts Against $CdCl_2$ Damage

AUTHORS (FIRST INITIAL, LAST NAME) AND INSTITUTIONS: *K. Caballero-Gallardo*[1,2], *J. Palomares-Bolaños*[1,2], D. García-Novoa[1], *J. Olivero-Verbel*[2], C. Valdelamar-Caballero[1], M. Carabalí-Carabalí[3], J. Guaza-Peña[3], E. Tegue-Amú[3], E. Banguero-García[3], and M. Carabali-Mera[3]. [1]Functional Toxicology Group, School of Pharmaceutical Sciences, Zaragocilla Campus, University of Cartagena, Cartagena, Colombia; [2]Environmental and Computational Chemistry Group, School of Pharmaceutical Sciences, Zaragocilla Campus, University of Cartagena, Cartagena, Colombia; and [3]Consejo Comunitario Aires de Garrapatero, Santander de Quilichao, Cauca, Colombia.

KEYWORDS: Natural Products; Cytotoxicity; Metals; Oxidative Stress

ABSTRACT: Background and Purpose: Colombia boasts vast biodiversity, encompassing numerous plants utilized in traditional medicine to address inflammatory, neuronal, and cardiovascular conditions. This study evaluates the chemical and biological properties of hydroalcoholic extracts from *Ageratum conyzoides* L., *Solanum americanum* Mill., *Zanthoxylum rhoifolium* Lam., and *Agave tequilana*,

traditional plants from the Colombian Pacific region, for their antioxidant and cytoprotective potential against heavy metal-induced damage. **Methods:** Plant selection was guided by ethnobotanical surveys with four keepers of traditional knowledge from the Aires de Garrapatero, an Afro-descendant community in the Colombian Pacific. Hydroalcoholic extracts were prepared from the bark, leaves, and roots of each species. Total phenolic and flavonoid contents were quantified using standard spectrophotometric methods. Cytotoxicity and cytoprotective effects were evaluated in SH-SY5Y cells exposed to $CdCl_2$, with oxidative stress assessed via reactive oxygen species (ROS) production using the H_2-DCFDA probe. Photoprotective capacity was analyzed by calculating the sun protection factor (SPF), critical wavelength (λc), and UVA/UVB ratio through spectrophotometry. Controls included gallic acid and vanillin. **Results:** The total phenolic content measured in the different species decreased in the following order: *A. tequilana* (240.9±5.5 mg GAE/g TS), *Z. rhoifolium* (87.7±0.1 mg GAE/g TS), *S. americanum* (41.7±1.5 mg GAE/g TS), and *A. conyzoides* (38.0±0.2 mg GAE/g TS). The total flavonoid content averaged 40.0±0.3, 69.4±4.2, 52.9±2.3, and 38.1±1.6 mg RE/g TS for *A. conyzoides*, *S. americanum*, *Z. rhoifolium*, and *A. tequilana*, respectively. The cytotoxicity of $CdCl_2$ was assessed, yielding an IC_{50} value of 38.4 µM in SH-SY5Y neuroblastoma cells. The IC_{50} values for *A. conyzoides* and *Z. rhoifolium* extracts exceeded 500 µg/mL, while lower IC_{50} values were observed for *S. americanum* (80.1 µg/mL) and *A. tequilana* (163.7 µg/mL). In the oxidative stress assay, only the extract of *A. tequilana* significantly increased ROS production compared to the control. The SPF range was classified as moderate for *A. conyzoides* (12.2±0.2) and *Z. rhoifolium* (17.5±0.4), and high for *A. tequilana* (38.4±0.4), with a spectral classification of 3 (λc: 354.5±4.8). The UVA/UVB ratio was consistently high (>0.8) across all extracts, while erythema transmission ranged from <1 to 6, and pigmentation transmission was optimal for all extracts, with values between 0.0 and 10.2. Finally, two species with the highest antioxidant content and increased ROS production at 24 hours were selected to evaluate their potential cytoprotective effect on SH-SY5Y neuroblastoma cells exposed to $CdCl_2$. A percentage recovery of cell viability with *A. conyzoides* extract was observed, ranging from 13% to 25% in cells treated with $CdCl_2$ (15.6-125 µM). **Conclusions:** These findings highlight the antioxidant and cytoprotective potential of these hydroalcoholic extracts, underscoring their relevance in phytotherapeutic applications. The study emphasizes the value of integrating ancestral knowledge with scientific research to discover natural agents for health improvement. Minciencias - University of Cartagena (Grant: 112721-416-2023).

ABSTRACT NUMBER: 5071 **Poster Board Number:** LB172

TITLE: Chemical composition and biological potential of Essential oil of Origanum heracleoticum L

AUTHORS (FIRST INITIAL, LAST NAME) AND INSTITUTIONS: S. Yazar[1], E. Beyzi[2], S. Stankov[3], M. Caglayan[4], M. Kulahcı[2], A. Stoyanova[5], and S. Yilmaz[6]. [1]Yeniyuzyil University, Istanbl, Turkey; [2]Gazi University, Ankara, Turkey; [3]Food Technology University of Plovdiv, Plovdiv, Bulgaria; [4]Biruni University, Istanbul, Turkey; [5]Food Technology University of Plovdiv, Plovdiv, Turkey; and [6]Ankara University, Ankara, Turkey. Sponsor: *N. Basaran*

KEYWORDS: None

ABSTRACT: Background and Purpose: Oregano is one of the most important aromatic spices consumed worldwide and is classified as a medicinal plant due to its biological and pharmaceutical properties. Essential oils (EO) exhibit remarkable biological activities attributable to their substantial concentration of volatile aromatic compounds. The objective of our research was to determine the chemical composition of Bulgarian white oregano (Origanum heracleoticum L.) essential oil (OEO) and its

biological activities including anticancer, antimicrobial, anti-biofilm and anti-quorum sensing properties. **Methods:** Agilent 7890A gas chromatograph (Agilent Technologies Inc., Santa Clara, USA) was used to analyze OEO. Additionally, GC/MS analysis was conducted using an Agilent 5975C mass spectrometer, utilizing the same column and temperature settings as in the GC analysis, with helium as the carrier gas. Human lung adenocarcinoma epithelial cells (A549), human hepatocellular carcinoma cells (HepG2), mouse fibroblast cells (L929), and human breast adenocarcinoma cells (MDA-MB-231) were used to evaluate the cytotoxic activity of oregano essential oil. **Results:** The main components of the OEO, comprising more than 3%, were carvacrol (76.90%) and p-cymene (12.84%). As a result of the MTT test, it was determined that all tested concentrations (3.9, 7.8, 15.62, 31.25, 62.50, 125, 250, 500, and 1000 µg/mL) of OEO significantly reduced cell survival of human lung adenocarcinoma epithelial cells (A549), human hepatocellular carcinoma cells (HepG2), and human breast adenocarcinoma cells (MDA-MB-231), while showing much less toxic effects on healthy mouse fibroblast cells (L929). Human lung adenocarcinoma epithelial cells (A549) were found to be more sensitive to the OEO than other cell lines. IC50 values clearly showed that OEO was more cytotoxic towards A549 and MDA-MB-231 cell lines at lower concentrations. Staphylococcus aureus ATCC 25923, Pseudomonas aeruginosa PA01, P. aeruginosa ATCC 27853, Candida albicans ATCC 10231, and Chromobacterium violaceum ATCC 12472 isolates were used to detect antimicrobial, anti-biofilm, anti-quorum sensing (anti-violacein) activity. **Conclusions:** In conclusion, our investigation revealed that the essential oil derived from Bulgarian oregano (O. heracleoticum L.) resulting in elevated biological activity as evidenced by the conducted assays. The OEO subjected to evaluation demonstrated notable anticancer efficacy across diverse cell lines and exhibited antimicrobial, anti-biofilm, and anti-quorum sensing properties against various microorganisms. The significance of our research lies in its illustration that the essential oil under examination holds potential applicability in pharmaceutical development owing to its inherent biological characteristics.

ABSTRACT NUMBER: 5072 **Poster Board Number:** LB173

TITLE: Microbial Activity and RNASeq Exploration of Cola Accuminata-Induced Gene Expression

AUTHORS (FIRST INITIAL, LAST NAME) AND INSTITUTIONS: *N. Tahniyat*, and *W. Gray*. Southern University and A&M College, Baton Rouge, LA.

KEYWORDS: None

ABSTRACT: Background and Purpose: The emergence of resistant bacterial strains necessitates the development of new antibiotics. Cola acuminata and Cola nitida, commonly consumed plant nuts, exhibit antimicrobial and antifungal activity against selective microorganisms. Previous studies indicated that the acetone extract of Cola acuminata (Biz-3w) possesses antimicrobial bioactivity against *Staphylococcus aureus*. This study aims to isolate the active components of Biz-3w, evaluate their sensitivity, and investigate their mechanisms of action. **Methods:** An analytical reverse-phase HPLC chromatographic method was employed to isolate Biz-3w_A1, an enriched antimicrobial fraction. The antimicrobial activity was evaluated using growth inhibitory turbidity and disc diffusion assays. A wavelength spectrum analysis identified individual compounds within the purified fraction. The bactericidal activity of Biz-3w_A1 was compared to vancomycin. Additionally, RNASeq gene expression profiling was conducted to examine *S. aureus* responses to two concentrations of Biz-3w_A1 (0.25× MIC and 2.5× MIC) after three hours of treatment. KEGG pathway analysis was used to identify the biochemical pathways affected. **Results:** Biz-3w_A1 was purified to 80% antimicrobial activity. Spectral

analysis revealed the presence of at least five individual compounds with maxima at 210-225 nm. Biz-3w_A1 demonstrated strong bactericidal activity against *S. aureus*, comparable to vancomycin, resulting in over 90% lysis of the bacteria within three hours. RNASeq analysis identified 102 genes that were differentially expressed following Biz-3w_A1 treatment, with 36 genes upregulated and 66 downregulated. KEGG pathway analysis revealed significant associations with the ABC transporter (19 genes), quorum sensing (11 genes), purine metabolism (10 genes), and *S. aureus* infection (11 genes) pathways. **Conclusions:** Cola acuminata represents a promising new source of antimicrobial agents. Biz-3w_A1 exhibits potent bactericidal activity against gram-positive bacteria and impacts multiple biochemical pathways in *S. aureus*. This highlights its potential as a candidate for further antimicrobial development.

ABSTRACT NUMBER: 5073 **Poster Board Number:** LB174

TITLE: *In vitro* approaches to predict botanical-induced human liver injury and drug interactions: Milk thistle, Yohimbe, and Kava as case studies

AUTHORS (FIRST INITIAL, LAST NAME) AND INSTITUTIONS: *S. S. Ferguson*[1], B. J. Gurley[2], *Y. Liu*[3], R. B. vanBreemen[4], A. I. Calderon[5], S. I. Khan[2], *A. P. Li*[6], and *A. L. Roe*[7]. [1]NIEHS, RTP, NC; [2]University of Mississippi, Oxford, MS; [3]FDA, Laurel, MD; [4]Oregon State University, Corvalis, OR; [5]Auburn University, Auburn, AL; [6]Washington State University, Spokane, WA; and [7]Procter & Gamble, Cincinnati, OH.

KEYWORDS: Botanicals; Natural Products; In Vitro and Alternatives; hepatotoxicity

ABSTRACT: Background and Purpose: Human liver injury and botanical-drug interactions (BDI) associated with consumption of dietary supplements and herbal medicines is a global concern. Understanding the potential for botanical-induced hepatotoxicity and BDI is challenging due to the complexity of botanical extract compositions and the idiosyncratic nature of many documented cases of liver injury. The Botanical Safety Consortium (BSC) is a public-private partnership formed by the US FDA, NIEHS, and HESI, and aims to improve overall botanical product safety by evaluating the suitability of *in silico* and *in vitro* tools to study complex botanical mixtures. The BSC hepatotoxicity and ADME working groups are exploring these tools for both safety screening and mechanistic studies. Results from multiple *in vitro* studies including cytotoxicity, CYP inhibition and induction, transcriptomics, and cell painting using a variety of assay systems (i.e., liver microsomes, and 2D and 3D hepatocyte tissue models) are presented in a series of case studies. The botanicals chosen for case studies include Milk Thistle (*Silybum marianum* L. Gaertn.), Yohimbe (*Pausinystalia johimbe* (K. Schum.) Pierre ex Beille), and Kava (*Piper methysticum* G. Forst.). **Methods:** Botanical test articles were provided in 100% DMSO stock solutions and then diluted in treatment medium to 0.25% DMSO. Hepatotoxicity was evaluated in both hepatocyte tissue models. Cryopreserved primary human hepatocytes from 3 donor preparations cultured in 2D configurations were exposed to botanical extracts alongside reference chemicals and assayed for ATP depletion as a marker of hepatocellular viability loss. Evaluations for the potential of botanical extracts to cause BDI focused on inhibition of CYP3A4 were evaluated with MetMax® human hepatocytes using luciferin IPA as substrate. Induction of CYP3A4 was evaluated with 2D cultures of primary human hepatocytes by changes in CYP3A4 mRNA expression, as per regulatory guidance (e.g., US-FDA). In addition to conventional 2D hepatocyte culture models, free-floating 3D microtissue cultures of primary human liver cells (10 donor pool, 5 male and 5 female donors) were plated in 384-well plates and exposed to botanical extracts alongside a number of reference drugs with a repeated exposure design over 96 hours. A range of assays was integrated with 3D microtissues and included

confocal fluorescent imaging (cell painting) of 3D microtissue cell morphology (nuclei, actin, endoplasmic reticulum, mitochondria), cytotoxicity assessments via liver enzyme leakage (i.e., lactate dehydrogenase (LDH) with the LDH-Glo® assay reagent), hepatocellular functionality via albumin production (Fortis ELISA), a novel method for CYP3A4 inhibition with 3D liver microtissues and the luciferin-IPA assay reagent, and broad-coverage high-throughput transcriptomics assays of ~3,000 gene targets using TempO-Seq™. Confocal images were generated using an Opera Phenix (Revvity), LDH, albumin, and CYP3A4 assays were measured with a CLARIOstar (BMG Labtech), and high-throughput transcriptomics using TempO-Seq was measured on a NovaSeq 6000 (Illumina). Data analysis included a range of concentration-response modeling, benchmark dose analysis), BDI liver injury classifications, and transcriptomic pathway analysis. To assess the potential for the formation of reactive metabolites, extracts were incubated with human liver microsomes, cytochrome P450 cofactor NADPH, and the biological nucleophile glutathione. Reactive metabolites trapped as glutathione conjugates were characterized using high resolution UHPLC-MS/MS. **Results:** Using the 2D human hepatocytes, the average cytotoxicity IC50 values based on ATP depletion for Milk thistle, Yohimbe, and Kava were 27.25, 53.7, and 10.8 ug/ml, respectively. Treatment with Milk thistle did not result in CYP3A4 inhibition or induction, but incubation with or without human liver microsomes resulted in formation of glutathione conjugates with the natural product taxifolin, a constituent of Milk thistle. Likewise, Yohimbe treatment did not result in CYP3A4 inhibition or reactive metabolite formation; however, a 3-fold induction in CYP3A4 mRNA was observed. Kava also did not result in CYP3A4 inhibition up to highest dose tested (15 ug/ml) or reactive metabolite formation. Treatment of 2D human hepatocytes with Kava extract did result in up to 15-fold induction in CYP3A4 mRNA. Multiple reactive metabolites of Kava's major constituent kavalactones were formed and trapped as glutathione conjugates. Cytotoxicity in 3D primary human hepatocytes was monitored using LDH leakage as a sensitive surrogate for ALT/AST liver enzymes after treatment with botanical extracts. The LOELs associated with Milk thistle, Yohimbe, and Kava were 418, >156, and >15 ug/ml, respectively. Albumin production, an oftentimes more sensitive measure of cytotoxicity than LDH leakage, resulted in identical LOELs for the three botanicals. Inhibition of CYP3A4 enzyme activity was modeled using an approach proficient for sub-chronic exposure studies. Milk thistle did not decrease CYP3A4 metabolism activity except when coincident with LDH leakage (cytotoxicity). Yohimbe and Kava extracts inhibited CYP3A4 metabolism at sub-cytotoxic concentrations consistent with scientific literature. Transcriptomic data revealed CYP1A1 and CYP1A2 mRNA content were markedly induced by Yohimbe (i.e., ~25- to 40-fold over vehicle control over 2 independent experiments) and comparable in magnitude to reference clinical drug agonist omeprazole (OMP). A similar but smaller increase in CYP3A4 mRNA content was observed with Yohimbe that was ~60% of the response observed with reference clinical drug inducer phenobarbital. These data suggest Yohimbe is proficient for activation of the aryl hydrocarbon receptor, pregnane X receptor, and constitutive androstane receptor at the exposure ranges evaluated, and indicates higher potential for botanical-drug interactions at sufficiently high exposure ranges. Kava also induced CYP3A4 mRNA content, though it only modestly increased CYP1A1/2 mRNA content relative to OMP. Transcriptomic data also revealed both Yohimbe and Kava altered a more than 100 gene expression targets in the exposure ranges evaluated, which is consistent with higher potential for liver injury. **Conclusions:** This is the first report of the potential for BDI (CYP3A4 and CYP1A2), and aryl hydrocarbon activation associated with Yohimbe. Kava resulted in massive induction of CYP3A4 mRNA in both hepatocyte models, which does not correlate with data from previous clinical studies. Metabolic activation data indicated that Kava forms multiple and abundant electrophilic metabolites with dose-dependent potential to be cytotoxic. In summary, these data highlight potential of non-clinical methods to address safety challenges of

botanicals. The *in vitro* tools and models presented in this work represent viable approaches to estimating the potencies for human liver injury, BDI, and hepatotoxicity mechanisms botanical extracts.

ABSTRACT NUMBER: 5074 **Poster Board Number:** LB175
TITLE: Protective role of brown seaweed Ericaria selaginoides extract against an induced oxidative stress in human Caco-2 cells

AUTHORS (FIRST INITIAL, LAST NAME) AND INSTITUTIONS: *A. Anadon*[1], M. Martínez[1], I. Ares[1], B. Lopez-Torres[1], J. Maximiliano[1], M. Martínez[1], M. Martínez-Larrañaga[1], C. Peteiro[2], A. Casal-Silva[3], M. Cueto[3], and T. Aymerich[4]. [1]Universidad Complutense de Madrid, Madrid, Spain; [2]Spanish Institute of Oceanography of the Spanish National Research Council, Santander, Spain; [3]Instituto de Productos Naturales y Agrobiología, Tenerife, Spain; and [4]Institut de Recerca i Tecnología Agroalimentaries, Monells, Spain.
KEYWORDS: None

ABSTRACT: Background and Purpose: The aim of this study was to assess the cytotoxicity and the antioxidant response of human colon adenocarcinoma Caco-2 cells to *Ericaria selaginoides* extract. **Methods:** Specimens of *Ericaria selaginoides* were collected from Cantabrian coasts (north of Spain). Freeze-dried samples of *Ericaria selaginoides*, were extracted with hexane-isopropanol-water. The phenolic content of algal extracts was determined. Cytotoxicity induced by *Ericaria selaginoides* extract was assessed determining cell viability by (3-[4,5-dimethylthiazol-2-yl]-2,5-diphenyl-tetrazolium bromide) MTT assays, and lactate dehydrogenase (LDH) leakage. Antioxidant activities of *Ericaria selaginoides* extract were assessed by determination of malondialdehyde (MDA) levels as a marker lipid peroxidation. Generation of ROS and nitric oxide (NO) production were also evaluated in human Caco-2 cells. *Ericaria selaginoides* extract effects against a cellular oxidative stress induced by t*ert*-butyl hydroperoxide (*tert*-BOOH) were also evaluated. **Results:** The phenolic content/mg extract was correlated to the antioxidant effect. The results of the biomarkers analyzed show that treatment of Caco-2 cells with *Ericaria selaginoides* extract enhance antioxidant defences, which imply an improved cell response to an oxidative challenge. Treatment of human Caco-2 cells with *Ericaria selaginoides* extract (1-100 µg/mL) evoked no changes in cell viability (MTT and LDH). We also examined whether cell death induced by 200 µM *tert*-BOOH after 3 h incubation period could be reverted with *Ericaria selaginoides* extract. *Ericaria selaginoides* extract (5-100 µg/mL) provided a significant increase of cell survival (37%-73%) compared to *tert*-BOOH. The treatment of Caco-2 cells with *Ericaria selaginoides* extract prevented the cytotoxicity induced by *tert*-BOOH. The dramatic increase in ROS generation induced in Caco-2 cells by *tert*-BOOH was significantly reduced when the cells were pretreated with *Ericaria selaginoides* extract. *Ericaria selaginoides* extract (5-100 µg/mL) significantly attenuated the ROS production induced by *tert*-BOOH. **Conclusions:** This research contributes to the knowledge of the potential of brown seaweed *Ericaria selaginoides* extract as a sustainable and affordable source of compounds with antioxidant properties. Acknowledgements: This work was supported by the Project Ref. PID 2020-15979RR-C33 from the Ministerio de Ciencia e Innovación, Spain (Project/AEI/10.13039/501100011033).

ABSTRACT NUMBER: 5075 **Poster Board Number:** LB176

TITLE: Derivation of Safety Limit for Respirable Talc using Carcinogenicity Inhalation Study in Rats and Linear Deterministic Method

AUTHORS (FIRST INITIAL, LAST NAME) AND INSTITUTIONS: *K. Blum*, M. Gawlik, and D. Harte. GSK, Environment Health and Safety, Munich, Germany.

KEYWORDS: Regulatory Science/Regulatory Toxicology; Chemical Hazard Assessment; Inhalation Toxicology; Occupational toxicology; Talc

ABSTRACT: Background and Purpose: Talc is widely used across various industries, leading to potential worker exposure. Numerous animal studies on carcinogenicity and chronic toxicity are available for talc and have been reviewed by the IARC (2010) and ECHA (2023). ECHA initiated a consultation on talc and proposed a re-classification of talc to a category 2 carcinogen under European Regulation (CLP) No. 1272/2008. This study aims to evaluate available data on talc's health implications and establish a health-based occupational exposure limit (OEL) for respirable fraction of talc based on the results of the GLP carcinogenicity inhalation study conducted under the National Toxicology Program (NTP 1993). **Methods:** An OEL represents the workplace concentration below which health risks are considered negligible. Using data from the carcinogenicity inhalation study, Benchmark Dose (BMD) modelling was used to identify a point of departure (POD), and adjustments were applied to calculate a safe dose for human health. In this study, F344 rats were exposed to respirable talc (concentrations: 0, 6, and 18 mg/m^3; MMAD 2.7 and 3.2 µm) via whole-body inhalation for 6 hours/day, 5 days/week, over a lifetime). Statistically significant increases in lung tumors were observed at the highest dose only in females. Other effects such as inflammation, reparative, and proliferative changes in lung tissues were observed in both sexes at all dosed groups. Using the multiple-path particle dosimetry model (MPPD2), a human equivalent deposited dose (HEDD) was derived, considering lung surface area differences between rats and humans. **Results:** A benchmark dose lower confidence limit (BMDL10) of 17.2 mg/m^3 was identified as the POD. After accounting for work-life exposure, and difference for particle deposition dynamics between rats vs. human modelled using MPPD, an OEL >100 $\mu g/m^3$ was derived using different deterministic methods. **Conclusions:** The mode of action for talc-induced lung tumors is not fully understood, but may involve inflammation, oxidative stress, and increased cell replication, with potential modulation by talc's physicochemical characteristics. Further research on talc's toxicological mechanisms and adjustments for human inhalation exposure (particles load and clearance) is needed given the limitations of the NTP GLP inhalation carcinogenicity study, such as: two dose groups, inconsistent concentration of talc during the study, lack of comparable human exposure concentrations, lack of no observed effect level for non-neoplastic (e.g. inflammation), possibly leading to overconservative estimation. Whilst it is important to approach occupational exposure with conservatism in relation to human health exposure, the ECHA position to re-classify talc as a category 2 carcinogen for all routes of exposure does not seem warranted or scientifically justified given the available data. Human epidemiological data demonstrated no association of occupational talc exposure with lung cancer. Based on this NTP data as a 'worst case scenario' an OEL for talc is proposed.

ABSTRACT NUMBER: 5076 **Poster Board Number:** LB177

TITLE: An Epidemiological Investigation of Reproductive Cancers Among Barbers, Cosmetologists, and Hairdressers

AUTHORS (FIRST INITIAL, LAST NAME) AND INSTITUTIONS: C. R. Langton, L. A. Wood, K. A. Keeton, and S. Benson. Valeo Sciences LLC, Ladera Ranch, CA. Sponsor: *A. Madl*

KEYWORDS: Epidemiology; Endocrine Disruptors; Reproductive Tract; Female

ABSTRACT: Background and Purpose: By way of occupation, individuals who work in barbershops or hair salons are frequently exposed to beauty products that contain some chemicals that have been classified as "possibly carcinogenic to humans" by IARC. Although inconsistent, past research has found barbers and hairdressers have higher risks for some cancers. Epidemiological cohort studies have found associations between personal use of certain haircare products and risk of hormone-related cancers, including breast and uterine cancer. Haircare products containing endocrine-disrupting chemicals are suspected to contribute to the association, yet studies are few and results are mixed depending on the study population and cancers investigated. Further elucidation is needed. Therefore, this investigation examined risk of reproductive cancers among female barbers, cosmetologists, and hairdressers. **Methods:** First, a systematic literature review was performed on the risk of breast, cervical, ovarian or uterine cancer among female barbers, cosmetologists, and hairdressers. Using a combination of *a priori* search terms, peer-reviewed publications were identified in PubMed, Embase, Web of Science, OVID, and Scopus through October 4, 2024. Reference lists from review articles and relevant studies were also searched to identify related research. Exclusion criteria included non-English, animal, and male-only studies, as well as meta-analyses, literature reviews, editorials, grey literature, incorrect exposure or outcome, and analyses that reported proportionate mortality ratios (PMRs) or hazard ratios. For populations investigated numerous times, only the study with the largest sample size and longest period of evaluation was included. Data were extracted and random effects meta-analyses were conducted to calculate meta-relative risks (meta-RRs) for each of the four cancer endpoints. To supplement the meta-analyses, standardized PMRs for the occupations and cancers included in the meta-analyses were calculated using three years of national mortality data (2020-2022) from the National Occupational Mortality Surveillance (NOMS) program and 36 years of mortality data (1974-2010) from the Washington State Occupational Mortality (WASOM) database. The NOMS estimates were adjusted for 5-year age groups and race. **Results:** The systematic literature search resulted in a total of 1,123 unique articles, of which 17 met the inclusion criteria. After removing overlapping study populations, eight studies with unique data from 10 countries were included in the meta-analyses. For the NOMS and WASOM data, 22,201 and 343,037 deaths were examined, respectively. Across the three datasets, occupation as a barber, cosmetologist, or hairdresser was not associated with risk of breast cancer (NOMS PMR=0.94, 95% Confidence Interval [CI]: 0.88, 1.01; WASOM PMR=0.96, 95% CI: 0.88, 1.05; meta-RR=1.03, 95% CI: 0.89, 1.20). For uterine cancer, a statistically significant decreased risk was observed in the NOMS data (PMR=0.75, 95% CI: 0.65, 0.86) and no association was observed in the WASOM data (PMR=1.01, 95% CI: 0.79, 1.28) nor in the meta-analysis (meta-RR=1.01, 95% CI: 0.83, 1.22). For cervical cancer, there was no association in the NOMS data (PMR=0.95, 95% CI: 0.79, 1.13), while there were slightly elevated, though statistically non-significant, risks in the WASOM data (PMR=1.27, 95% CI: 0.87, 1.78) and meta-analysis (meta-RR=1.15, 95% CI: 0.96, 1.38). For ovarian cancer, null associations were observed in the NOMS (PMR=0.93, 95% CI: 0.82, 1.05) and WASOM (PMR=0.95, 95% CI: 0.77, 1.15) data, but risk was slightly elevated, though statistically non-significant, in

the meta-analysis (meta-RR=1.18, 95% CI: 0.97, 1.45). **Conclusions:** Overall, the epidemiological evidence does not support an increased risk of reproductive cancers of the breast, cervix, ovary or uterus for female barbers, cosmetologists, or hairdressers. However, these analyses are not without limitation; most notably is the fact that many of the estimates were not adjusted for potential confounding factors, and the NOMS data were limited to three years. For the meta-analyses, the cancers were not always clearly defined, and some estimates may include cancers of surrounding organs. Despite these limitations, these data add important information to the potential occupational risks experienced by barbers, cosmetologists, and hairdressers.

ABSTRACT NUMBER: 5077 **Poster Board Number:** LB178

TITLE: Patterns and transitions of tobacco product use in the general adult population of Japan: A repeated cross-sectional survey (2021-2024)

AUTHORS (FIRST INITIAL, LAST NAME) AND INSTITUTIONS: D. Yuki, and N. Minami. Japan Tobacco Inc., Tokyo, Japan.

KEYWORDS: Behavioral; Tobacco Product; Postmarketing Surveillance

ABSTRACT: Background and Purpose: In Japan, heated tobacco products (HTPs) are increasingly being preferred and chosen by current adult tobacco product users. A growing body of scientific evidence indicates that HTPs have the potential to reduce the risks associated with smoking combustible cigarette (CC) by reducing the exposure to toxicants formed primarily during the burning of tobacco and inhaling the smoke. Post-marketing information, including patterns of use and transitions such as initiation/relapse is essential for assessing the population impact of HTPs. Our study provides the most recent trend data (2021-2024) on the use of tobacco products in an adult Japanese population. **Methods:** A nationwide, repeated, cross-sectional, internet-based, self-reported survey was conducted in accordance with relevant guidelines for marketing research. The internet survey was operated by a marketing research provider and conducted annually in April among approximately 300,000 adult research panel monitors (≥20 years). Participants were asked to complete a web-based questionnaire, which is designed to track their tobacco product use behavior (current product use status, product category used, and daily consumption for each product). All analyzes were weighted to obtain nationally representative estimates based on the latest official Japanese census statistics. **Results:** The data indicate slight decreases in the rate of exclusive CC smokers (defined as adults who reported smoking only CC); the rate of combined users (defined as adults who reported using both of CC and HTP); and an increase in the rate of exclusive HTP user (defined as adults who reported using only HTP). In terms of the 3-year transition probabilities from 2021 to 2024, adults who had never used or were not currently using any tobacco product exhibited a low rate of starting to use any product. Among combined users (CC + HTP), there was variation in product switching, with almost half changing their product use status over 3 years. **Conclusions:** The present survey results indicates that (i) HTP have increasingly replaced CC; (ii) a large number of HTP users choose to switch completely from CC to using only HTP; (iii) almost half of combined users (CC + HTP) changed their product use status over 3 years with combined use defining a transient behavior rather than a consistent pattern of use for some populations; and (iv) the introduction of HTP did not remarkably lead to initiation or relapse among adults who had never used or were not currently using any tobacco product. These findings demonstrate that HTP, which has been reported to have the potential to reduce the health risks associated with smoking, are an acceptable

product for adults who choose to switch away from smoking CC and, in turn, may reduce tobacco-related risk of harm at a population level.

ABSTRACT NUMBER: 5078 **Poster Board Number:** LB179
TITLE: Associations between urinary trace element concentrations with odds of uterine fibroid prevalence in African-Caribbean women

AUTHORS (FIRST INITIAL, LAST NAME) AND INSTITUTIONS: *A. Kiyanda*[1], *N. Price*[2], R. Cvejkus[2], J. Catov[2], V. Wheeler[3,2], P. J. Parsons[4,5], *A. Barchowsky*[1], *I. Miljkovic*[2], and *A. P. Sanders*[1]. [1]Department of Environmental and Occupational Health, University of Pittsburgh School of Public Health, Pittsburgh, PA; [2]Department of Epidemiology, University of Pittsburgh School of Public Health, Pittsburgh, PA; [3]Tobago Health Studies Office, Scarborough, Trinidad and Tobago; [4]Division of Environmental Health Sciences, Wadsworth Center, New York State Department of Health, Albany, NY; and [5]Department of Environmental Health Sciences, University of Albany School of Public Health, Albany, NY.
KEYWORDS: Reproductive System; Exposure, Environmental; Epidemiology; Uterine Fibroid; Cadmium

ABSTRACT: Background and Purpose: Uterine leiomyoma, or fibroids, are benign smooth muscle neoplasms of the uterine wall that can affect more than 70% of people with a uterus by the onset of menopause. While the cause(s) of uterine fibroids is still unknown, common risk factors include African Ancestry, family history, obesity, poor diet and early onset menstruation. Exposure to metals is a putative risk factor for uterine fibroids, and established metal-dysregulated pathways such as estrogen receptor signaling and epidermal growth factor receptor signaling likely play key roles in the promotion of uterine fibroid growth. Exposures to metals are relevant to populations residing in the Caribbean, who may have unique trace element exposure profiles due to their specific lifestyle factors and industrialization from mining, waste disposal sites and petrochemical plants. This study, nested in the Tobago Women's Health Study, offers a unique opportunity to observe these associations in a population of African Caribbean women. The objective of this study was to assess the cross-sectional associations between individual urinary concentrations of trace elements (e.g. non-essential or essential elements) with uterine fibroid prevalence. We hypothesized that non-essential elements of arsenic, cadmium, and lead would be associated with higher odds of uterine fibroids, while essential metals copper, manganese, and zinc would be associated with lower odds. **Methods:** The Tobago Women's Health Study, a population-based study in the Caribbean Island of Tobago, measured urinary trace elements and collected health history between 2019-2023. Four hundred sixty-six participants assigned female at birth had complete information on the history of uterine fibroid(s) reported by participants during their interview. In a sub-cohort of four hundred forty-four participants with complete data, we used logistic regression to estimate associations between log-transformed urinary concentrations of six prioritized elements (arsenic, cadmium, lead, copper, manganese, and zinc) with the odds of uterine fibroids. Arsenic concentrations were derived as the sum of inorganic arsenic metabolites. For each analyte, we performed a) a minimally adjusted regression where only urinary creatinine was adjusted as a covariate, and b) a model adjusted for covariates of urinary creatinine, age, BMI, and age of menarche. **Results:** In this cohort, the mean age was 55.7 +/- 8.8 years; the mean BMI was 31.02 +/- 5.66 kg/m2; and the mean age of menarche was 12.8 +/- 1.8 years. The prevalence of uterine fibroids was 48.4%. In minimally adjusted models, we observed that each ten-fold increase in urinary ng/mL concentration of cadmium (β:2.12; 95% CI: 1.00, 4.57) corresponded to higher odds of uterine fibroids. Associations with inorganic arsenic (β:1.73; 95% CI: 0.94, 3.25); copper (β:0.63; 95% CI: 0.22, 1.80); lead (β:2.26; 95% CI:

0.93, 5.57); manganese (β:1.14; 95% CI: 0.62, 2.12); and zinc (β:0.71; 95% CI: 0.37, 1.35) were not significantly associated with odds of uterine fibroids in the minimally adjusted models. In fully adjusted models, each ten-fold increase in urinary concentration of cadmium (β:2.25; 95% CI: 1.01, 5.08) was associated with significantly higher odds of uterine fibroids. Associations with inorganic arsenic (β:1.68; 95% CI: 0.89, 3.24); copper (β:0.61; 95% CI: 0.20, 1.85); lead (β:2.43; 95% CI: 0.97, 6.19); manganese (β:1.11; 95% CI: 0.60, 2.06); and zinc (β:0.68; 95% CI: 0.34, 1.32) while in the expected direction of effect, were consistent with unity and not associated with odds of uterine fibroids. **Conclusions:** Our findings support an association between non-essential elemental urinary cadmium concentrations with higher odds of uterine fibroids in this population of Tobagonian women. However, our findings do not support an association with exposures to the other selected urinary trace elements and odds of uterine fibroids. This is important to better understand the relationship between essential and non-essential trace elements and women's health in a cohort of African Caribbean women. Future analyses will assess the effects of metal mixtures on uterine fibroid prevalence in this population.

ABSTRACT NUMBER: 5079 **Poster Board Number:** LB180

TITLE: Chemical Inequities: Understanding the Health Risks in Beauty Products for Marginalized Communities

AUTHORS (FIRST INITIAL, LAST NAME) AND INSTITUTIONS: P. Y. Watkins, and *J. A. Colacino*. University of Michigan, Ann Arbor, MI.

KEYWORDS: Chemical of Concern; Cutaneous or Skin Toxicity; Environmental Toxicology

ABSTRACT: Background and Purpose: Personal care products and the chemicals they contain pose heightened risks to marginalized communities due to misleading marketing, spatial inaccessibility, and cost barriers. African American women are particularly vulnerable, reporting higher usage levels of personal care products than other ethnic groups. This increased use is influenced by cultural and societal pressures to conform to Western beauty standards, such as straightened hair, which necessitates frequent use of various beauty and hair care products. These factors contribute to disproportionate exposure to potentially harmful chemicals. This study aims to assess the prevalence of toxic chemicals in personal care products commonly used by African American women and evaluate their associated health risks. **Methods:** This study first employed a qualitative analysis to identify the 10-20 most popular products within the Hair, Cosmetics, and Fragrances categories, based on annual spending data among African American consumers. Popular products in each category were identified using online searches and Generative Artificial Intelligence tools (e.g., ChatGPT) and manual curation were used to map ingredients to unique chemical identifiers such as the CASRN. The ingredient lists of 47 selected products were compiled into a master dataset, documenting each chemical's CASRN, alternate CASRN, product function. We also assessed the availability of EPA ToxCast data or available data on the EPA's CompTox Dashboard through manual searching. This dataset was uploaded into R statistical software to identify the most frequently occurring chemicals across all products. The CompTox Chemical Dashboard was used to evaluate the toxicological profile of each chemical, including active ToxCast assays and data on reproductive/developmental toxicity, genotoxicity, and cancer, skin, and eye irritation potential. **Results:** Our analysis identified over 100 unique chemicals across the 47 selected products, with 50 chemicals appearing at least 10 times in the product list. Among these frequently occurring chemicals were linalool, dimethicone, titanium dioxide, yellow 5, and propylene glycol. In the Cosmetics and Hair Care categories, the most commonly identified chemicals were phenoxyethanol, linalool, and glycerin,

each appearing 17 times across the sample products. In the Fragrance category, denatured alcohol, parfum/fragrance, and limonene were the most frequently observed, each found in 8 or 9 of the 9 sampled fragrances. Of the 50 most frequently occurring chemicals, 16 lacked any existing ToxCast data in the CompTox Chemical Dashboard, while the remaining 34 had available ToxCast testing results. Of these chemicals that have available toxicity data, 68% flagged positive for genotoxicity, 30% for reproductive/developmental toxicity, 7% showed positive cancer data, and 65% were flagged skin/eye irritants. **Conclusions:** This study highlights the pervasive presence of harmful chemicals in personal care products frequently used by African American women, particularly in hair care. These findings also underscore the urgent need for stricter regulations on chemical disclosure and toxicity testing for beauty and personal care products. Culturally tailored education campaigns and increased availability of safer alternatives are critical to mitigating these risks. This research serves as a foundation for future studies and policy advocacy aimed at reducing health disparities linked to chemical exposure in marginalized communities.

ABSTRACT NUMBER: 5080 **Poster Board Number:** LB181

TITLE: Characterization of landfill leachate and removal of contaminants present in the leachate using constructed wetland

AUTHORS (FIRST INITIAL, LAST NAME) AND INSTITUTIONS: R. Ghaju Shrestha[1], A. Chapagain[2], S. Subedi[3], R. Maharjan[4], S. Tandukar[5], and J. Shakya[1]. [1]Institute for Research in Science and Technology, Lalitpur, Nepal; [2]Central Department of Environmental Science, Kathmandu, Nepal; [3]Central Deparment of Environmental Science, Kathmandu, Nepal; [4]Department of Civil Engineering, Kathmandu, Nepal; and [5]Organization for Public Health and Environment Management, Lalitpur, Nepal.

KEYWORDS: Chemical Characterization; Ecotoxicology; Sustainable Development

ABSTRACT: Background and Purpose: Leachate generated from landfill comprises of highly concentrated organic and inorganic compounds along with other hazardous contaminants. This study aims to characterize the components of leachate from landfill sites and investigate the effects of operational parameters of constructed wetland (CW) on the removal efficiencies of contaminants. **Methods:** In this study, leachate samples were collected from two landfill sites (Sisdol and Bancharedanda landfill sites) of Nepal. Physical and chemical parameters were tested in the leachate collected from landfill sites. In addition to this, the treatment of leachate containing contaminants was operated using a vertical lab-scale CWs without plant and CWs planted with *Phragmites australis* and *Chrysopogon zizanioides*. **Results:** The concentrations of phenol, copper, zinc, and iron were 0.9-96 and 8.0-108 mg/L, 0-45.0 and 595.0-1340.0 mg/L, 0.1-2.6 and 0.2-2.2 mg/L and 0.46-100.0 and 3.2-13.6 mg/L in leachate samples collected from Sisdol and Bancharedanda landfill sites, respectively. The CWs planted with *P. australis* removed phenol (32-95.4%), copper (0-46.6%), zinc (52.2-73.2) and iron (73.6-99.5%), whereas CWs planted with *C. zizanioides* removed phenol (5.5-94.1), copper (0-52.0%), zinc (6.82-86.0%), and iron (56.0-100%), effectively. **Conclusions:** This study indicates characterization of leachate is necessary to minimize the potential risks to human and ecosystem. It also showed the importance of CWs to remove the pollutant removal capability based on selection of plants.

ABSTRACT NUMBER: 5081 **Poster Board Number:** LB182
TITLE: Investigation of the effects of aflatoxins on infant health and development in developing countries

AUTHORS (FIRST INITIAL, LAST NAME) AND INSTITUTIONS: G. Kadan[1], N. Aral[2], and E. Aral[2]. [1]Cankiri Karatekin University, Cankiri, Turkey; and [2]Ankara University, Ankara, Turkey. Sponsor: *S. Yılmaz*
KEYWORDS: None

ABSTRACT: Background and Purpose: Fungi have important effects on development and growth. One of these fungi is aflatoxins. Due to their content, aflatoxins can disrupt DNA synthesis and lead to many negative results, especially cancer. This situation leads to important results in children as well as everyone else. Especially if aflatoxins are encountered during infancy, they can affect the developing systems of the baby and cause chronic diseases or negative results on growth and development. This situation can be even more critical, especially in developing countries. With these thoughts in mind, the aim of the study was to examine the effects of aflatoxins on infant health and development in developing countries. **Methods:** In the study, systematic compilation technique, one of the qualitative research methods, was used. In this context, a search was conducted in the Web of Science and Google Scholar databases with the keywords “Aflatoxin”, “Factors affecting infant health in developing countries”, “Effects of aflatoxins on infant health” and “Publications made after 2000”. 35 publications were reached in line with the criteria specified in the study. One of these publications was excluded from the scope of the study because it was a book chapter. Therefore, the research was completed with 34 articles. **Results:** It was determined that the publications included in the research were mostly made in 2021 (n=6). As a result of the research, it was determined that aflatoxins occur most in the environment where babies live, in the food they eat, in areas where cleanliness and hygiene are low, and that babies exposed to aflatoxins catch diseases more easily, and their head circumference and height remain below the expected percentile curves. **Conclusions:** Based on the results obtained as a result of the research, it can be recommended that families be trained, and the necessary work be carried out to make the living environment suitable, and that the necessary measures be taken by the states, especially in terms of ensuring food hygiene.

ABSTRACT NUMBER: 5082 **Poster Board Number:** LB183
TITLE: Circulating Levels of Per and Polyfluoroalkyl Substances (PFAS) are Related to Inflammation and Preterm Birth among Pregnant Black Women

AUTHORS (FIRST INITIAL, LAST NAME) AND INSTITUTIONS: *N. Saadat*[1], C. G. Engeland[2], R. Saeed[1], *V. Padmanabhan*[1], D. Misra[3], and C. Giurgescu[4]. [1]University of Michigan, Ann Arbor, MI; [2]Pennsylvania State University, University Park, PA; [3]Michigan State University, East Lansing, MI; and [4]University of Central Florida, Orlando, FL.
KEYWORDS: Inflammation; Perfluoronated Agents; Epidemiology

ABSTRACT: Background and Purpose: African American (Non-Hispanic Black) women have the highest rate of preterm (PTB; <37 weeks gestation) in the United States. Black women are more likely to live in disadvantaged neighborhoods with higher social and environmental exposures. Exposure of pregnant women to environmental toxicants including per- and polyfluoroalkyl substances (PFAS) has been linked to chronic inflammation and adverse birth outcomes including PTB. As Black women are reported to have high inflammation during pregnancy, we hypothesized that gestational exposure to PFAS chemicals

may be one source of increased inflammation during their pregnancy and thereby possibly increase the risk for PTB. **Methods:** Pregnant Black women (n=103) were recruited at prenatal clinics in the Midwest (Detroit, Michigan and Columbus, Ohio) and plasma samples were collected (at 8-18 weeks gestation). Nine PFAS chemicals were quantified in plasma by the LC-MS/ICPMS method and inflammatory markers were measured in plasma by multiplex assays. **Results:** Correlation analysis uncovered several positive associations between PFAS chemicals and proinflammatory markers: 1) perfluoroundecanoic acid (PFDeA) with interleukin(IL)-6, IL-8 and macrophage migration inhibitory factor (MIF) ($p<0.01$); 2) Perfluorononanoic acid (PFNA) with IL-6, MIF ($p<0.01$) and IL-8 ($p<0.05$); 3) Perfluorooctane sulfonic acid (PFOS) and Perfluorooctane sulfonamide (PFOSA) with IL-6 ($p<0.01$ and $p<0.05$ respectively); and 4) Perfluoroundecanoic acid(PFUA)with IL-6, MIF ($p<0.01$) and IL-8 ($p<0.05$). Preterm birth showed positive associations with PFUA ($p<0.05$) and proinflammatory markers IL-6 and MIF ($p<0.05$). **Conclusions:** These results suggest a pathway by which PFAS chemicals may lead to increased inflammation and ultimately to preterm birth. Coupled with our earlier findings of positive association of psychosocial stressors with inflammation, findings from this study highlight the importance of investigating the impact of maternal exposures on maternal inflammation and its contribution to adverse pregnancy outcomes in Black women.

ABSTRACT NUMBER: 5083 **Poster Board Number:** LB184

TITLE: Environmental chemical-wide associations with liver biomarkers among US adults in NHANES 1999 - 2018

AUTHORS (FIRST INITIAL, LAST NAME) AND INSTITUTIONS: *L. Y. M. Middleton*[1], V. K. Nguyen[2], X. Wang[1], *K. M. Bakulski*[1], and *J. A. Colacino*[1]. [1]University of Michigan, Ann Arbor, MI; and [2]Harvard University, Boston, MA.

KEYWORDS: Biomarkers; Environmental Toxicology; Liver

ABSTRACT: Background and Purpose: Liver disease is highly prevalent in the US. It is most commonly caused by alcohol use, diet, or viral infection, but livers are also highly susceptible to chemical damage due to their role in blood filtration and metabolism. Biomarkers of liver damage and dysfunction include the four enzymes aspartate transaminase (AST), alanine transaminase (ALT), gamma-glutamyl transferase (GGT), and alkaline phosphatase (ALP) as well as serum albumin and total protein. These enzymes elevate as a result of cellular damage. Hypoalbuminemia and changes in total protein are indications of liver dysfunction. Individual chemicals and chemical families including metals, phthalates, polychlorinated biphenyls (PCBs), and per- and polyfluoroalkyl substances (PFAS) have been associated with altered liver enzymes and liver function in the US population. However, there has not been a comprehensive evaluation of the effects of environmental chemical exposures. We evaluated the associations between 170 chemical exposures and the liver biomarkers AST, ALT, GGT, ALP, serum albumin, and total protein. **Methods:** Data were analyzed from the National Health and Nutrition Examination Survey (NHANES 1999-2018) for participants aged ≥20 years (n=36,175). NHANES is a continuous cross-sectional study which measures chemical biomarkers in blood and urine and administered questionnaires to participants. Chemical biomarkers with ≥50% of measurements above their lower limit of detection were included (n=170 chemicals). Chemicals were classified into 16 chemical families based on their function, structure, and/or chemical properties. Analysis was conducted using survey-weighted linear regressions of $\log_2$-transformed chemicals and liver biomarkers adjusted for age, sex, race/ethnicity, waist circumference, liver disease status, alcohol use, caloric

intake, Hepatitis A immunity, cotinine (a biomarker of tobacco smoke exposure), creatinine (for urinary biomarkers only), and survey cycle (for chemicals measured in more than one cycle. Multiple comparisons were accounted for using a false discovery rate (FDR). **Results:** Unweighted participants had a mean age of 48.4 years, 52.5% were female, and 46.0% were Non-Hispanic White. Twelve chemicals were detected in all participants and 73 chemicals were detected in 95% of participants. Fifty-three (31.2%) chemicals from 11 (68.8%) chemical families were associated with at least one liver biomarker (FDR<0.05). Serum cotinine was associated with all six liver biomarkers. Urinary cadmium was associated with five of six liver biomarkers and blood cadmium was associated with four. A doubling in the concentration of urinary cadmium was associated with a 2.9 unit/L (95% CI: 1.9, 3.8; FDR=$5.1*10^{-6}$) increase in GGT. **Conclusions:** Chemicals from a wide range of chemical families were associated with biomarkers of liver damage and dysfunction. These chemical exposures are potentially modifiable factors to decrease the burden of liver disease in the US.

ABSTRACT NUMBER: 5084 **Poster Board Number:** LB185

TITLE: When the Tide Turns Red: Using Real-World Health Data to Uncover the Impacts of Harmful Algae Blooms on Florida's Coastal Populations

AUTHORS (FIRST INITIAL, LAST NAME) AND INSTITUTIONS: *A. F. Manrique*, C. Wang, N. Chin, K. Rohlwing, D. Kaplan, M. Prosperi, and Y. Guo. University of Florida, Gainesville, FL.

KEYWORDS: Epidemiology; Environmental Toxicology; Lung; Pulmonary or Respiratory System; K. Brevis

ABSTRACT: Background and Purpose: Red tide algae blooms, caused by *K.brevis*, are naturally occurring phenomena along Florida's west coast. These blooms pose a significant public health threat as K. brevis produces potent neurotoxins known as brevetoxins. Observational studies from Florida have identified associations between red tide exposure and acute respiratory, gastrointestinal, and neurological diseases in coastal populations. Brevetoxin exposure occurs through multiple routes, including inhalation of aerosolized particles, ingestion of contaminated water and seafood, and dermal contact with affected waters. However, population-based studies on the health impacts of red tide are limited by small sample sizes, narrow geographic and temporal scopes, single health outcomes, and the lack of real-world health data. **Methods:** To address these limitations, we conducted a retrospective cohort study using real-world electronic health records (EHR) from the Patient-Centered Outcomes Research Institute (PCORI)-funded OneFlorida+ clinical research network. The study population included patients with at least one inpatient or outpatient encounter for acute respiratory, gastrointestinal, or neurological conditions between January 1, 2012, and December 31, 2019, residing in zip codes along Florida's west coast. Patients were observed for a minimum of six months, including three months prior to and three months following diagnosis, with extended follow-up for individuals receiving subsequent diagnoses during the initial three-month prospective period. Red tide exposure was assessed at the zip code level using centroid-based proximity (within 5 km of the coast) and cell count data from the Florida Fish and Wildlife Conservation Commission Fish and Wildlife Research Institute (FWC-FWRI) spanning January 1, 1994, to February 1, 2024. Descriptive statistics were used to characterize the cohort, and univariable and multivariable generalized estimating equation models estimated the effects of red tide exposure on health outcomes, accounting for environmental and social factors. **Results:** The study included 129,927 unique patients with 398,811 respiratory, 152,539 gastrointestinal, and 112,183 neurological diagnoses. Our population had an overall mean age of 32 years, was predominantly female (60%), and 50% identified as non-Hispanic White. Additionally, our models found the association

between red tide exposure and respiratory conditions to be significant, with a tenfold increase in red tide exposure leading to an additional 55 diagnoses of respiratory conditions per 100,000 people monthly. Unfortunately, our models did not find a significant association between acute gastrointestinal and neurological outcomes. **Conclusions:** Our study leverages robust, longitudinal EHR data to provide comprehensive insights into the health impacts of red tide exposure, addressing critical gaps in population-based research. We found that red tide algae blooms have a significant effect on the respiratory health of coastal communities in the state of Florida. This work underscores the importance of integrating environmental and clinical data to inform public health strategies and mitigate the adverse effects of harmful algal blooms.

ABSTRACT NUMBER: 5085 **Poster Board Number:** LB186
TITLE: A Novel *Ex Vivo* Human Fascio cutaneous Flap Perfusion Model to Investigate Radiation and/or Chemicals-Induced Injuries

AUTHORS (FIRST INITIAL, LAST NAME) AND INSTITUTIONS: A. Ejaz. University of Pittsburgh, Pittsburgh, PA. Sponsor: A. Ejaz, American Association for Cancer Research
KEYWORDS: Chemical and Biological Weapons; Chemical of Concern; Methods/Mechanism

ABSTRACT: Background and Purpose: Skin is the first line of defense against burns, chemicals, radiation, and trauma injuries. Recent research discovered a wide range of pathways and agents to treat skin injuries but still, there is a wide gap in the knowledge due to the complex nature of the injuries. Often, animal models are used for testing new agents, yet they lack anatomical feature resemblance to human tissue. Human tissue-based models are ideal; however, maintaining complex tissue ex vivo is challenging. Here we describe a novel, optimized, and well-characterized model of a full-thickness human skin perfusion system that utilizes surgical waste skin to cultivate flaps ex vivo. **Methods:** Abdominal panniculectomy samples were collected as surgical waste. Under sterile conditions, we isolated and cannulated perforators of the superficial and deep inferior epigastric systems. We perfused the cannulated tissue using a bioreactor system capable of real-time monitoring of pressure, flow rate, fluidic temperature, and tissue temperature. Albumin-supplemented culture media at 60mmHg pressure with 6ml/min inflow was perfused throughout the run time of approximately three weeks. Angiosome distribution was confirmed by fluorescein angiography and infrared imaging. Flow rate measurements, vascular reactivity, daily tissue biopsy samples for histology and electron microscopy, cell viability, lactate production, and gene expression levels were measured to assess the viability of the flap. Utilization of the skin perfusion model for chemical and radiation injuries was assessed by induction of chemical (Nitrogen Mustard) and radiation wounds. Samples were collected from the wounded and control tissue for histology, protein, and gene expression analysis. **Results:** Angiography verified that the SIEA to SIEV flap system successfully fed ~ 90% surface area of a large flap for two-three weeks. Flow rate, temperature, and pressure remained steady throughout ex vivo cultivation. The vascular reactivity test showed a physiological response of the vasculature upon application of a vasoconstrictor (epinephrine) and vasodilator (papaverine). H&E staining and TUNEL immunofluorescence staining revealed healthy and viable cells during the perfusion run. Isolated adipose stem cells and dermal fibroblasts at different time points during perfusion showed viability and proliferation dynamics compared to fresh tissue isolates. We observed a decrease in circulatory glucose levels and increased lactate levels upon insulin challenge. Nitrogen mustard wounds showed a gradual increase in the dead TUNEL-positive cells and ballooning of epithelial cells. Our gene analysis showed a significant decrease in

anti-apoptotic cells. Radiation injury is reflected as a loss of epidermal layer and cell death shown by TUNEL staining. Gene expression analysis reflected the upregulation of inflammation and anti-apoptotic genes. **Conclusions:** This system can be used to perfuse the tissue during and after pathology, allowing immediate and longitudinal data collection. This breakthrough system can help us understand the pathways and be used as a subclinical drug testing model.

ABSTRACT NUMBER: 5086 **Poster Board Number:** LB187
TITLE: Evaluation of Dried Blood Spot Sampling for the Verification of Exposure to Chemical Threat Agents via Liquid Chromatography-tandem Mass Spectrometry

AUTHORS (FIRST INITIAL, LAST NAME) AND INSTITUTIONS: *T. M. McClymont*, K. A. Walker, T. K. Rudd, K. Laitipaya, J. N. Vignola, *E. A. Johnson*, and R. C. diTargiani. USAMRICD, Gunpowder, MD.
KEYWORDS: Chemical and Biological Weapons; Agents

ABSTRACT: Background and Purpose: Exposure to chemical threat agents, such as nerve agents and opioids, pose a significant global safety concern. Identifying the specific exposure can be used to update the patient's medical records to verify exposure to chemical threats. Traditional analytical methods for verifying exposure require shipping refrigerated or frozen biomedical samples to reference laboratories, which presents logistical and financial burdens. Dried blood spot (DBS) sampling offers a promising alternative to streamline the collection, storage, and shipment of forensic samples. This study focuses on developing and validating DBS techniques using Mitra® 30 µL volumetric absorptive microsampling (VAMS®) devices and blood spot cards for exposure verification to various chemical threat agents in human whole blood. The use of DBS sampling would alleviate cold-chain storage burdens, reduces shipping size, simplifies international sample management, and allows for room-temperature storage of multiple samples. **Methods:** Human whole blood samples were exposed *ex vivo* to the metabolites pinacolyl methylphosphonic acid (PMPA), ethyl methylphosphonic acid (EMPA), norfentanyl, norcarfentanil, norsufentanil, and norlofentanil. The samples were loaded onto VAMS® devices or blood spot cards, dried, and extracted for analysis via liquid chromatography-tandem mass spectrometry (LC-MS/MS). Methods were validated for sensitivity, precision, accuracy, and recovery. **Results:** Results demonstrated sensitivity down to 0.5 ng/mL for PMPA, EMPA, and norfentanyl, 0.1 ng/mL for norlofentanil, and 0.05 ng/mL for norsufentanil and norcarfentanil. All methods met acceptable precision (≤15% coefficient of variation (CV), except for ≤20% at the lower limit of quantification (LLOQ)) and accuracy (≤15% error, except ≤20% at LLOQ) criteria with favorable recovery. Comparable performance was observed between VAMS® devices and blood spot cards. **Conclusions:** Comparable performance was observed between VAMS® devices and blood spot cards. These findings highlight the utility of DBS sampling in stabilizing whole blood samples and show promise as an improved collection method for verifying exposure to chemical threat agents in humans, thereby enhancing patient care and threat assessment capabilities.

ABSTRACT NUMBER: 5087 **Poster Board Number:** LB188
TITLE: Inhaled isoflurane as an adjunct to benzodiazepines prevents neuronal damage following nerve agent exposure in mice

AUTHORS (FIRST INITIAL, LAST NAME) AND INSTITUTIONS: *J. Leighton*, *M. Ellis*, *J. Janssen*, *A. Methvin*, and *E. Johnson*. United States Army Medical Research Institute for Chemical Defense, Edgewood, MD.
KEYWORDS: Chemical and Biological Weapons; Neurotoxicology; Neurotoxicity; Pesticides

ABSTRACT: Background and Purpose: Exposure to nerve agent is a contemporary threat to both warfighters and civilians. Nerve agents cause inhibition of acetylcholinesterase, resulting in a potentially fatal acetylcholine buildup in both the central and peripheral nervous system. Current treatments, namely atropine, 2-PAM, and benzodiazepines, work best when given promptly and repetitively. Delayed treatment may promote the development of benzodiazepine resistant seizure, which can continue indefinitely without additional management. For this reason, adjunct treatments to better control seizure are of particular interest. **Methods:** In this study, we tested the inhaled anesthetic isoflurane as an adjunct to midazolam for seizure control after nerve agent exposure. To do this, we utilized a unique human acetylcholinesterase knock-in/serum carboxylesterase knockout (C57BL/6-Ces1ctm1.1LocAChEtm1.1Loc/J; a.k.a KIKO) mouse model of nerve agent exposure that reliably produces sustained seizure. We administered inhaled isoflurane alongside midazolam at 40, 60, or 90 minutes after seizure onset. Mice were monitored for changes in EEG activity, behavior, and survival for 24hrs, after which brains were stained with Fluoro-Jade B and blindly scored for neuronal damage and degeneration. **Results:** Though mortality and behavior were not significantly different between isoflurane and midazolam-only controls, isoflurane treated mice showed a treatment time-dependent reduction of recurrent seizure activity, as well as reduced neuronal damage that was treatment time-dependent and brain region-specific. In mice that only showed peripheral symptoms of nerve agent exposure, isoflurane did not cause mortality and improved behavior in comparison to midazolam-only controls. **Conclusions:** The results of this study suggest that isoflurane or similar halogenated anesthetics approved for use in humans may be beneficial following nerve agent exposure in the control of seizure. The views expressed in this abstract are those of the author(s) and do not reflect the official policy of the Department of Army, Department of Defense, or the U.S. Government. The experimental protocol was approved by the Animal Care and Use Committee at the United States Army Medical Research Institute of Chemical Defense, and all procedures were conducted in accordance with the principles stated in the Guide for the Care and Use of Laboratory Animals and the Animal Welfare Act of 1966 (P.L. 89-544), as amended. This work was supported by the Countering Emerging Threats - Rapid Acquisition and Investigation of Drugs for Repurposing (CET RAIDR) program within the Joint Program Executive Office for Chemical, Biological, Radiological and Nuclear Defense (JPEO-CBRND) through interagency agreement A2305021021044866. J. Leighton, M. Ellis, & J. Janssen were supported in whole or in part by an appointment to the Research Participation Program for the U.S. Army Medical Research and Development Command administered by the Oak Ridge Institute for Science Education (ORISE) through an agreement between the U.S. Department of Energy and U.S. Army Medical Research and Development Command.

ABSTRACT NUMBER: 5088 **Poster Board Number:** LB189
TITLE: Neuropathological characterization of a juvenile rat model of acute organophosphate intoxication

AUTHORS (FIRST INITIAL, LAST NAME) AND INSTITUTIONS: *M. A. Muñoz*, P. M. Andrew, J. A. MacMahon, G. G. Gurkoff, *P. J. Lein*, and A. Izadi. University of California Davis, Davis, CA.
KEYWORDS: Chemical and Biological Weapons; Neurotoxicology

ABSTRACT: Background and Purpose: Organophosphates (OPs) that inhibit acetylcholinesterase (AChE) are a class of chemical compounds that include nerve agents and pesticides. Acute intoxication with these OPs can cause a cholinergic crisis that may progress to life-threatening *status epilepticus*. Survivors of OP poisoning often develop adverse neurological effects, such as persistent neuroinflammation and

neurodegeneration, cognitive impairment and spontaneous recurrent seizures. To date, most studies of acute OP intoxication have been done in adult models so relatively little is known about the response of the developing brain to OP-induced cholinergic crisis. A previous study using a juvenile rat model of acute intoxication with the OP diisopropylfluorophosphate (DFP) measured adverse neurological outcomes up to 28 days post exposure (DPE). This study identified persistent neurodegeneration up to 28 DPE in multiple brain regions, including the hippocampus, amygdala and piriform cortex. These animals also exhibited persistent microgliosis at 7 and 28 DPE; however, phagocytic microglia were not detected at either timepoint. Here, we extend these prior observations by quantifying neurodegeneration and microgliosis in multiple brain regions at 3 months post-exposure (MPE) in a juvenile model of acute DFP intoxication. **Methods:** Male Sprague Dawley rats at postnatal day 23 were randomly divided into two groups that were either surgerized to implant telemetric devices for electroencephalography (EEG) or not surgerized (naïve). Following a 5-d recovery, surgerized animals were administered DFP (3.75 mg/kg, s.c.) or an equal volume (300 µl) of vehicle (VEH, PBS, s.c.). One minute after DFP or VEH injection, animals were treated with atropine sulfate (0.1 mg/kg, i.m.) and 2-pralidoxime (25 mg/kg, i.m.). Naïve animals did not receive VEH or DFP. At 3 MPE, animals were anesthetized with isoflurane and perfused with PBS to collect brain tissue for histological analyses. Tissue sections were immunostained with antibodies specific for IBA1 or CD68, biomarkers of microglia and phagocytic cells, respectively, or stained with FluoroJade-C (FJC) to identify degenerating neurons. All slides were counterstained with DAPI to identify cell nuclei. Images were acquired at 20X magnification using a high-content ImageXpress XL imaging system and were analyzed using ImageJ (version 1.54h, National Institutes of Health, Bethesda, MD, USA). A one-way ANOVA was used to detect differences between the three groups: naïve, vehicle and DFP-intoxicated animals. **Results:** Animals administered DFP entered *status epilepticus* as confirmed electrographically. FJC staining revealed negligible neurodegeneration in hippocampal regions (CA1, CA3, dentate gyrus), piriform cortex, thalamus, amygdala or somatosensory cortex at 3 MPE, and there were no statistically significant differences in FJC staining between groups ($p < 0.05$; n=3-4 animals per group). We also observed no statistically significant group differences in the number of IBA-1 immunopositive cells or the % of IBA-1 cells that were immunopositive for CD68. Phagocytic microglia were largely absent post-intoxication, with the exception of one animal in the thalamus region. **Conclusions:** These preliminary data indicate that neurodegeneration and microgliosis do not persist at 3 MPE in DFP-intoxicated juvenile rats. While previous data have shown that neurodegeneration persists up to 28 DPE in juveniles, our results suggest that the juvenile brain may be recovered by 3 MPE, as indicated by the absence of FJC staining in any of the brain regions analyzed and the return of microglial numbers to control levels. However, results from this study are preliminary and larger sample sizes are required to derive more definitive conclusions.

ABSTRACT NUMBER: 5089 **Poster Board Number:** LB190

TITLE: 3-month dosed-feed toxicity study (including perinatal exposure) of g*arcinia cambogia* extract in sprague dawley rats

AUTHORS (FIRST INITIAL, LAST NAME) AND INSTITUTIONS: *Z. Henry*[1], G. Travlos[1], C. Willson[2], *E. Mutlu*[1], *S. Waidyanatha*[1], A. Zmarowski[3], J. Pierfelice[4], B. Sparrow[4], G. Roberts[1], and *C. Rider*[1]. [1]Division of Translational Toxicology, National Institute of Environmental Health Sciences, Durham, NC; [2]Inotiv-RTP, Morrisville, NC; [3]AmplifyBio, West Jefferson, OH; and [4]Battelle Memorial, West Jefferson, OH.

KEYWORDS: Botanicals; Natural Products; Reproductive and Developmental Toxicology

ABSTRACT: Background and Purpose: *Garcinia cambogia* extract (GCE), also known as *Garcinia gummi-gutta*, is a botanical weight loss supplement ingredient marketed with purported benefits such as appetite suppression, fat burning via thermogenesis, and inhibition of lipid synthesis. The active and predominant ingredient (30-70% by weight) found in the fruit's rind is hydroxycitric acid (HCA), a potent inhibitor of a fatty acid synthesis enzyme, ATP citrate lyase. The effects of GCE on weight loss are inconsistent and cases of liver toxicity have been reported. Adequate toxicological data is limited; therefore, the objective of this study was to evaluate the toxicity of GCE (65.1% HCA) using oral administration through dosed feed to mimic human exposure. **Methods:** Time-mated F_0 Hsd:Sprague Dawley® SD® dams were offered dosed feed *ad libitum* with 0, 300, 1000, 3000, 10000, 30000 ppm of GCE in feed (*ad libitum*) beginning on gestation day (GD) 6 and continuing through post-natal day (PND) 28. Pups received GCE via *in utero* exposure, followed by approximately 4 weeks of exposure via dam milk and/or dosed-feed consumption prior to weaning and randomization for the start of the 3-month exposure. Animals (F_1) selected to continue onto the 3-month exposure phase were provided the same GCE concentration received during the perinatal phase. The following endpoints were measured and/or assessed in the F_0 dams: HCA internal concentration, survival, clinical and maternal care observations, body weight, food consumption, and reproductive performance. The following endpoints were assessed in the F_1 offspring: HCA internal concentration, survival, clinical observations, body weights, food consumption, evaluation of sperm motility and counts, vaginal cytology for estrous cycling, clinical pathology, organ weights, and histopathology. **Results:** As expected, HCA internal concentrations increased with increasing exposure concentration. There were no GCE-related effects on dam survival, maternal care, or gestation length. Decreases in dam body weight and food consumption were observed at 30000 ppm. This exposure concentration also led to an increase in post-implantation loss (4.2% in controls and 28.5% in 30000 ppm group). The mean number of uterine implantation sites in F_0 females on PND 28 was similar across groups. GCE exposure decreased litter size, viability, and survival of offspring at 30000 ppm. Litter size at birth (PND 0) was significantly decreased with a mean of 9.4 compared to the control mean of 12.7. A decrease in viability at birth was manifested as a lower percent live birth (88.1% vs 93.6% controls) and a lower number of live pups per litter on PND 0 (mean of 8.4 vs 12.4 controls). The F_1 generation displayed transient decreases in body weight at doses ≥ 1000 ppm (pre and post weaning). Furthermore, 30000 ppm of GCE in feed led to decreases in food consumption in the males, lower sperm counts (with few to no motile cells in 4/10 males) and decreases in epididymis and testis relative and absolute weights. Histopathological findings in male rat reproductive tissue included testis germinal epithelium degeneration observed in males dose-fed 30000 ppm GCE, epididymis hypospermia and exfoliated germ cells, and chronic inflammation of the preputial gland (≥10000 ppm). In female rats, chronic inflammation of the clitoral gland was detected at 30000 ppm. Administration of GCE resulted in altered estrous cyclicity at 30000 ppm with greater incidence of acyclicity (4 of 10 females vs. 1 of 10 controls) and increase of days in diestrus followed by a decrease of days in estrus. Adult male and female F_1 rats exposed to ≥1000 ppm displayed lung inflammation, specifically histiocyte infiltration. There were no hematological or serum biochemical effects of GCE exposure observed. Also, no signs of liver toxicity were observed. Hormonal assessment of insulin, leptin, and adiponectin demonstrated dose-related decreases in insulin and leptin. No changes were seen in adiponectin. **Conclusions:** In summary, dietary exposure to GCE at concentrations up to 30000 ppm did not produce any overt toxicity. Histopathological changes in reproductive tissues were the predominant finding seen in both the male and female rats at 30000 ppm. Hormonal assessment of insulin and leptin suggests an

impact of GCE on metabolic homeostasis. The lack of liver toxicity observed in the rats does not reflect the adverse event reports of liver toxicity in humans.

ABSTRACT NUMBER: 5090 **Poster Board Number:** LB191
TITLE: Biocompatibility Assessment of an Elastomeric Material Formulation Change using Gamma Irradiation and Ethylene Oxide Sterilization

AUTHORS (FIRST INITIAL, LAST NAME) AND INSTITUTIONS: *S. Vijaykumar*[1], *Y. Zhou*[1], S. Roller[1], and *D. Malek*[2]. [1]Johnson & Johnson MedTech, Cincinnati, OH; and [2]Malek Toxicology Delaware, LLC, Delaware, DE.
KEYWORDS: Medical Device; Chemical Characterization; Safety Evaluation

ABSTRACT: Background and Purpose: The ISO-10993-1 standard provides requirements on the biocompatibility evaluation for medical devices when a material change occurs. For such a change, it recommends that the risk assessment should consider what is known about the additional material, the base material, and potential chemical interaction between the two. This case study describes the biocompatibility evaluation of a new elastomeric resin formulation and its behavior, when subjected to two different sterilization modes. The material was re-formulated as a 1:1 replacement of a single organic additive to meet regulatory (REACH) requirements, the base resin remaining the same. The new material would be used in marketed devices that are externally communicating components in contact with tissue, bone, or dentin for less than 24 hours, “Limited”, as defined in ISO 10993-1. Since the resin is used in devices sterilized by Gamma Irradiation or Ethylene Oxide, the evaluation considered the impact of both modalities. **Methods:** Test articles were production representative molded coupons with surface areas larger than any potential device component. Per the recommendations of the ISO standard, chemical characterization, including NVR/FTIR, GC-MS, LC-MS and ICP-MS was conducted, to assess toxicological information for the proposed formulation. This was followed by biological endpoint testing per ISO-10993-1 for a “Limited” medical device namely, cytotoxicity, acute systemic toxicity, irritation, sensitization and pyrogenicity. **Results:** Toxicological risk assessment focused on the extractables related to the new additive releasing from the base resin, as observed from the chemical characterization data. Margin of Safety <1 resulted with both sterilization modes, prompting further studies. Moreover, the extractables for the additive from ETO samples were nearly two and a half times higher than those obtained from Gamma irradiation. This difference in behavior with the two sterilization modes, likely results from the fact that gamma irradiation can cause crosslinking in elastomers which would lead to a lower tendency for swelling and extraction in solvents. This effect is subtle and may not necessarily be picked up in mechanical performance. However, chemical characterization provides a sensitive tool for probing the impact of sterilization on the material interaction between the new additive and the base resin. To mitigate the risk from the toxicological assessment a biological evaluation was proposed, per Section 5.10 in ISO-10993-18. To avoid redundant *in vivo* testing, in accordance with ISO-10993-2 the ETO sterilized sample was chosen as the representative, for it signified the worst-case. The test article comfortably met the biological endpoints per ISO-10993-1 for a “Limited” medical device. **Conclusions:** Based on the evaluation, the new formulation material was considered toxicologically equivalent to the current formulation for clinical application with both sterilization modalities. There were no new or increased biocompatibility concerns with this material formulation change.

ABSTRACT NUMBER: 5091 **Poster Board Number:** LB192

TITLE: Assessing the Sensitization Potential of Medical Devices from the Extractable & Leachable Profile: A Quantitative Risk Assessment Approach

AUTHORS (FIRST INITIAL, LAST NAME) AND INSTITUTIONS: P. Krishna[1], *W. Christian*[2], and *N. Goud*[3]. [1]Medtronic, Mumbai, India; [2]Medtronic plc, Jacksonville, FL; and [3]Medtronic plc, Indianapolis, IN.

KEYWORDS: Medical Device; Safety Evaluation; Risk Assessment; Sensitization

ABSTRACT: Background and Purpose: Medical devices are typically composed of a diverse group of materials, such as synthetic polymers, metals, adhesives, colorants, drugs, and compounds derived from plants and animals. Upon repeat exposure, some of these chemicals may induce hypersensitivity/allergic contact dermatitis in patients. Skin sensitization is one of the mandatory tests in the biocompatibility evaluation of medical devices and is being assessed primarily with animal test systems. However, recent advancements have led to the development of several *in vitro* models, though they have yet to be validated for use with medical devices. Currently, the concept of a tolerable contact limit, which is proposed for irritation in ISO 10993:17:2023, cannot be applied directly to sensitization as the methodology and uncertainty factors described do not fully address the complexities of extrapolating the experimental data to clinical scenarios for medical devices. To address this gap, an effort is being made to adapt the existing quantitative risk assessment approach for sensitization—widely used in the personal care industry for various chemicals (*e.g.*, cosmetics, fragrances, and preservatives)—to the context of medical devices. **Methods:** This approach was validated using chemicals extracted from a total of 40 devices, which contacted mucous membranes, tissue/bone, or blood for limited and long-term durations. The process follows a series of sequential steps analogous to the toxicological risk assessment approach used to evaluate the biocompatibility of medical devices. In the first step, all compounds identified via chemical characterization were screened for sensitization potential based on data within the scientific literature involving the Human Repeat Insult Patch Test, Local Lymph Node Assay, Guinea Pig Maximization Test (GPMT), or *in silico* tools used in conventional toxicological risk assessment. If a sensitization hazard existed, the No Expected Sensitization Induction Level, which may serve as a Point of Departure, was determined. The acceptable exposure level (AEL) was derived using sensitization assessment factors (SAFs), which account for differences between experimental conditions and real-life clinical situations. SAFs were modified specifically for medical devices, considering the complexity of construction and intended clinical use, as compared to consumer products. The chemical quantity released per unit surface area of the device was calculated and expressed as µg/cm² (EED_{max}), and the margin-of-safety (MOS) was determined by dividing the AEL by the EED_{max}, where a MOS ≥1 indicates the chemical exposure dose is unlikely to cause sensitization. Finally, the MOS results for each device were validated against *in vivo* testing using the conventional GPMT assay. **Results:** No potential sensitizers were identified in 14 out of 40 device extractable & leachable (E&L) profiles assessed. *In vivo* testing previously conducted on these 14 devices yielded negative results. Among the remaining 26 devices, potential sensitizers were detected in 21 E&L profiles, but all had favorable MOS values, while 5 device E&L profiles contained potential sensitizers with unfavorable MOS values (<1). Regardless of the MOS value, all devices previously generated negative results in the GPMT assay. **Conclusions:** This analysis demonstrated that the likelihood of potential sensitizers being present in the E&L profile of medical devices is relatively low, ranging from negligible to about 12.5%. The discrepancy between *in vivo* GPMT results and sensitization risk determined via toxicological risk assessment may be attributed to the exhaustive extraction conditions utilized during chemical analysis, which may generate a greater

chemical exposure than the extraction conditions used for *in vivo* testing. Although this approach aligns well with the principle of 3Rs—replacement, refinement, and reduction—in current safety assessment strategies for medical devices, the false positive rate suggests endpoint testing would be needed to completely address sensitization if risk characterization is unfavorable.

ABSTRACT NUMBER: 5093 **Poster Board Number:** LB194
TITLE: Immunological and oxidative stress responses of N/TERT-1 and N/TERT-2G keratinocyte cell lines

AUTHORS (FIRST INITIAL, LAST NAME) AND INSTITUTIONS: *J. de Oliveira Mallia*, R. Gatt, S. Griffin, G. Psakis, J. Attard, and M. Caruana. University of Malta, Msida, Malta.
KEYWORDS: Inflammation; Immunotoxicity; Keratinocytes

ABSTRACT: Background and Purpose: Reconstructed human epidermis (RHE) models play a crucial role in meeting regulatory and safety standards for products in the chemical, material, and medical device sectors. These models are typically constructed using primary human keratinocytes obtained from skin grafts of human donors. However, practical and economic limitations restrict the widespread application of RHE models. To address these constraints, researchers are actively exploring the use of immortalized keratinocytes to create models that closely mimic RHE. This approach offers improved feasibility for evaluating substances during the early phases of product development. This study reports the responses of N/TERT-1 and N/TERT-2G keratinocyte cell lines to oxidative stress and immune challenges to assess their suitability for dermatological testing. **Methods:** The cell lines were exposed to a range of concentrations of pathogen-associated molecular patterns; lipopolysaccharide (LPS), double-stranded genomic DNA (dsDNA), and phytohemagglutinin (PHA), and damage-associated molecular patterns; low molecular weight (LMW) polyinosine-polycytidylic acid (Poly I:C), high molecular weight (HMW) Poly I:C, hyaluronic acid (HA) for 24 h. Dose-responses were established by MTT cell viability assays, and cytokine and chemokine production using ELISA assays measuring interleukin (IL)-1α, IL-1β, IL-4, IL-6, IL-8, tumour necrosis factor-alpha (TNF-α), and transforming growth factor (TGF-β). Cells were also acutely exposed to 10-500 ppm H_2O_2 for 15 min and assessed by MTT and ELISA assays. Both cells lines were also exposed to 500 ppm H_2O_2 for 5 min or 10 µM menadione and assessed for oxidative stress markers superoxide dismutase (SOD) and glutathione (GSH), apoptosis induction through cleaved caspase-3 accumulation, and membrane integrity through JC-1 uptake and lipid peroxidation measuring thiobarbituric acid reactive substances (TBARS) activity. **Results:** The secretion of IL-1α, IL-6, IL-8, TNF-α and TGF-β significantly increased in N/TERT-1 cell following exposure to LPS, while that of N/TERT-2G cells remained unaffected. The production of IL-1α, IL-1β, TNF-α, IL-6, and IL-8 in response to dsDNA and LMW and HMW Poly I:C was increased in both cell lines. It was observed in N/TERT-1 cells that TGF-β was significantly decreased. Cytokine levels increased in a dose-dependent in response to H_2O_2 for N/TERT-2G cells. In contrast, a clear dose-dependent response was not observed for N/TERT-1 cells. The 500 ppm H_2O_2 exposure for 5 min was selected as cellular viability was not lower than 50%. Both cell lines displayed similar patterns for markers of oxidative stress, including SOD and GSH. A slightly higher sensitivity was observed for N/TERT-2G cells. Differences in lipid peroxidation and mitochondrial membrane potential were more pronounced, indicating that N/TERT-2G cells have a greater sensitivity to oxidative stress post-H_2O_2 exposure. The polysomy of chromosome 20, may have caused higher baseline levels for GSH in N/TERT-1 cells, increasing their oxidative stress resilience. Although MTT cell viability decreased following H_2O_2 exposure, apoptosis was not observed to be the primary cell death mechanism as significant changes in cleaved caspase-3 levels were not observed. **Conclusions:** These

findings emphasise the unique traits of N/TERT-1 and N/TERT-2G cells. N/TERT-1 demonstrates greater inherent resilience to oxidative stress, while N/TERT-2G exhibits heightened sensitivity, particularly to H_2O_2. Notably, N/TERT-2G may serve as a more suitable model for studying conditions such as psoriasis, characterised by heightened sensitivity to oxidative stress and immune dysregulation. In contrast, N/TERT-1 may better represent normal, resilient skin under baseline or less inflammatory conditions. These insights provide a foundation for more targeted and reliable approaches to investigating skin diseases, RHE construction, safety regulation and developing therapeutic interventions, underscoring the critical role of cell line selection in experimental design. This research was supported by the Malta Council for Science and Technology ACTIVE (R&I-2022-015L) project.

ABSTRACT NUMBER: 5094 **Poster Board Number:** LB195
TITLE: Role of the Pregnane X Receptor and Gender in Pressure Induced Wound Formation and Resolution

AUTHORS (FIRST INITIAL, LAST NAME) AND INSTITUTIONS: *G. E. Howell*, K. Burkett, A. Ismail, A. Thompson, E. Whitaker, and M. Sellers. Mississippi State University College of Veterinary Medicine, Mississippi State, MS.
KEYWORDS: Cutaneous or Skin Toxicity; Receptor; Knockouts

ABSTRACT: Background and Purpose: Delayed wound healing and chronic wounds are a common co-morbidity associated with both type 1 and type 2 diabetes mellitus. It is estimated that approximately 80% of patients with chronic wounds will lead to limb amputation and increased risk of death. There are well established risk factors for delayed wound healing such as compromised blood flow, tissue hypoxia, and hyperglycemia. However, the role of environmental exposures in delayed wound healing has not been previously examined. Therefore, the goal of the present study is to examine the role of the pregnane x receptor (PXR), a prominent xenobiotic receptor which binds a host of environmental contaminants as ligands, in wound healing using a pressure-induced wound model to recapitulate chronic wounds. **Methods:** Male and female wild type (C57BL6/J) and PXRKO mice were subjected to pressure-induced wound formation via two consecutive cycles of magnets placed on their backs for 12 hours and then off for 12 hours. Digital pictures of the wounds were taken on days 1, 4, 8, 10, 12, and 14 post wounding and wound areas calculated with ImageJ software. Data are expressed as both raw wound area and wound area normalized to the percentage of day 1 to negate differences in initial wound sizes. **Results:** Both male (n=8-13/day) and female (n=9-14/day) wild type mice had significantly larger pressure wounds on day 4 post wounding compared to male (n=8-13/day) and female (n=6-13/day) PXRKO mice. The wounds in male wild type mice were also significantly larger than male PXRKO mice on day 1 post wounding as well. Following normalization, male PXRKO mice appeared to have significantly delayed wound healing on days 8, 10, and 14 post wounding compared to corresponding male wild type mice. When examining gender specific effects within each strain, female wild type mice had significantly larger wounds at day 8 post wounding compared to male wild type mice. However, this trend did not appear to persist after day 8 post wounding. Conversely, male PXRKO mice appeared to have delayed wound healing on days 10 and 14 post wounding based on raw wound areas and day 14 based on normalized wound areas. **Conclusions:** The PXR appears to mediate initial pressure wound size in both male and female mice due to smaller wounds in PXRKO animals compared to wild type animals. However, absence of the PXR promotes wound healing delays in male mice compared to wild type mice and to PXRKO females indicating a critical role of this receptor in wound resolution in a sex dependent

manner. Thus, the present data indicate a pivotal role of the PXR in pressure wound formation and resolution which appears to be sex dependent.

ABSTRACT NUMBER: 5095 **Poster Board Number:** LB196
TITLE: Analytical method development and dermal absorption of steartrimoniumchloride (STC), a cosmetic ingredient

AUTHORS (FIRST INITIAL, LAST NAME) AND INSTITUTIONS: *K. Kim*, &. Kim, H. Kim, &. Chung, &. Lee, &. Kim, and &. Kim. Dankook University, Cheonan, Korea, Republic of.
KEYWORDS: Exposure Assessment; In Vitro and Alternatives; Risk Assessment; In vitro dermal absorption

ABSTRACT: Background and Purpose: Steartrimonium chloride (STC) is utilized in hair and hair dye products that are rinsed off at a maximum concentration of 2.5% and in leave-on products at a maximum concentration of 1.0% in both Korea and the European Union (EU). Additionally, STC is employed in leave-on face products at a maximum concentration of 0.5% within the EU. As no reports exist regarding the dermal absorption of STC in hair products, an **in vitro** dermal absorption study was conducted in compliance with the guideline according to the Ministry of Food and Drug Safety (MFDS) of Korea. **Methods:** Prior to conducting the dermal absorption study, analytical methods were established using liquid chromatography-mass spectrometry (LC-MS/MS) with a multiple reaction monitoring (MRM) technique for the quantification of STC in various matrices, including swabs, stratum corneum (SC), skin (dermis and epidermis), and receptor fluid (RF). To evaluate the skin absorption of STC in hair products, a Franz diffusion cell was utilized. A 2.5% gel formulation (wash-off) or a 1.0% cream formulation (leave-on) of STC was applied to mini pig skin at a dose of 10 µl/cm². Following a 30-minute application period, an interim wash-out step was performed to simulate typical hair dye conditions for the gel formulation. After 24 hours of application, the skin was wiped with a swab, and the stratum corneum (SC) was collected using tape stripping. Subsequently, the mini pig skin was sectioned into eight pieces, and receptor fluid (RF) samples were collected at 0, 1, 2, 4, 8, 12, and 24 hours. **Results:** The STC analytical method used in this study demonstrated excellent linearity (r^2 = 0.9945-0.9999), accuracy (84.9-113%), and precision (1.7-11.8%) in compliance with the validation guidelines. As a result, the total dermal absorption rate of STC was determined to be 5.32 ± 3.75 µg/cm² (1.25 ± 0.91%) and 0.22 ± 0.20 µg/cm² (0.10 ± 0.10%) for the gel and cream formulations, respectively. **Conclusions:** These results can be utilized for the exposure assessment of STC when used as a cosmetic ingredient.

ABSTRACT NUMBER: 5096 **Poster Board Number:** LB197
TITLE: Life cycle behavioral impacts and epigenetic changes following embryonic exposure to 6PPD

AUTHORS (FIRST INITIAL, LAST NAME) AND INSTITUTIONS: Y. Jung, J. Seo, and J. Park. Korea Institute of Toxicology, Jinju, Korea, Republic of. Sponsor: *S. Yoon*
KEYWORDS: Behavioral; Epigenetics; Developmental Toxicity; Post-Natal

ABSTRACT: Background and Purpose: N-(1,3-dimethylbutyl)-N’-phenyl-p-phenylenediamine (6PPD) is a globally used antioxidant and antiozonant used to protect rubber tires from cracking that caused by ozone reaction. 6PPD is of great concern as it can affect the health of ecosystem and is mainly discharged to the aquatic environment via tire wear particles in the ng/L to ug/L range. In this study, we analyzed behavioral effect of zebrafish after the embryonic to larval exposure to 6PPD. And

hypothesized that this effect is linked to epigenetic changes such as DNA methylation. **Methods:** Embryonic zebrafish (< 2hpf) were exposed to 6PPD for 7 days, and the behavioral effects of larval zebrafish were analyzed at the end of the exposure period. The fish were then collected and used to measure global methylation levels and the expression of methylation-related genes using qPCR method. **Results:** Exposure to a high concentration of 6PPD resulted in decreased mobility and a change in thigmotaxis in larval zebrafish. Global methylation levels were significantly increased after the exposure, which is in accordance with the *dnmt1* and *dnmt3* gene expression change pattern. As hypermethylation of DNA is generally associated with a decrease in the expression of associated genes, it is possible that the behavioral changes caused by exposure to 6PPD are related to DNA methylation. **Conclusions:** The present study demonstrated that exposure to 6PPD in early-life led to behavioral changes in zebrafish, which can be related to alteration of DNA methylation. The results of the present study lay the foundation for further research aimed at elucidating the underlying mechanisms through which 6PPD exposure leads to neurobehavioral effects and DNA methylation.

ABSTRACT NUMBER: 5097 **Poster Board Number:** LB198
TITLE: Arsenic Exposure and Its Impact on DNA Methylation Patterns

AUTHORS (FIRST INITIAL, LAST NAME) AND INSTITUTIONS: S. Lee[1], J. Kim[2], and Y. Hong[1]. [1]Dong-A University, Busan, Korea, Republic of; and [2]Chung-Ang University, Seoul, Korea, Republic of. Sponsor: Y. Hong, EUROTOX
KEYWORDS: Metals; Kidney; Epigenetics

ABSTRACT: Background and Purpose: Arsenic, ranked as the top-priority hazardous substance by the Agency for Toxic Substances and Disease Registry (ATSDR), is a naturally occurring element also released through human activities. In Korea, arsenic contamination has been identified in environmentally vulnerable areas, including abandoned mining sites, raising concerns about bioaccumulation and its potential health effects. Therefore, this study aimed to investigate the association between the concentration of urinary arsenic, and kidney function markers - NAG, β2-MG, eGFR. Additionally, we identified genes affected by epigenetic modifications induced by arsenic exposure. **Methods:** This study targeted residents living in environmentally vulnerable areas, including those near a smelter, a metal mine, and a reference area devoid of nearby pollution sources. A total of 450 participants were recruited between June 2021 and October 2022. Arsenic species were quantified using high-performance liquid chromatography coupled with an inductively coupled plasma-mass spectrometer. Genomic DNA was extracted from isolated PBMC using the QIAamp DNA Mini Kit and processed using reduced representation bisulfite sequencing method. Differentially methylated regions (DMRs) were detected using the callDMR function in DSS, with significant threshold of $p < 0.05$. Graphical representation of RRBS and RNA-seq results was performed using Python (v3.8.12) with matplotlib (v3.5.1) and seaborn (v0.11.2). **Results:** Among all study participants, 24 individuals reported having kidney disease, with 22 residing in the exposed areas and 2 in the reference areas. Total arsenic levels were higher in individuals of the vulnerable areas than in residents of the reference areas. The odds ratio of NAG exceeding its reference value increased by 96.5% for each unit increase in the logarithm of total arsenic concentration. β2-MG showed a significant association with blood Cd levels, however, no association was observed between eGFR and the heavy metals. To identify DMRs associated with specific functional genes by iAs exposure, we mapped DMRs in promoter-TSS regions to their corresponding differentially methylated genes. Hypo-methylated DMGs were significantly enriched in

terms of “DNA damage response” and “apoptotic signaling pathway”. In contrast, hyper-DMGs were associated with fewer terms and show relatively lower statistical significance. Taken together, these findings showed the relationship between iAs exposure and gene-specific DNA methylation. *NANOS3* (Nanos C2HC-Type Zinc Finger 3), *TNFRSF10B* (TNF receptor superfamily member 10b), *GADD45A* (Growth Arrest and DNA Damage-Inducible Protein GADD45 Alpha) are DNA methylation biomarkers for iAs exposure. **Conclusions:** In this study, we investigated the concentrations of arsenic species in residents of environmentally vulnerable areas, examined their associations with kidney dysfunction and their methylated pattern after exposed to arsenic. The findings of this studies may serve as a basis for establishing reference values for arsenic exposure to the end minimizing its impact on human health.

ABSTRACT NUMBER: 5098 **Poster Board Number:** LB199

TITLE: Lead (Pb) exposure is linked to increased placental weight and imprinted gene dysregulation during mouse development

AUTHORS (FIRST INITIAL, LAST NAME) AND INSTITUTIONS: *B. P. U. Perera*, *J. Pan*, A. Tapaswi, *J. M. Goodrich*, *D. C. Dolinoy*, and *J. A. Colacino*. University of Michigan, Ann Arbor, MI.

KEYWORDS: Epigenetics; Developmental Toxicity; Prenatal; Reproductive System; Genomic Imprinting; Lead (Pb)

ABSTRACT: Background and Purpose: Children and pregnant women are susceptible to lead (Pb), with gestational exposures linked to adverse pregnancy outcomes, delayed neurodevelopment, and growth defects. The epigenome regulates gene expression through DNA methylation, histone modifications, and non-coding RNA, and is susceptible to Pb exposure effects. Despite abundant literature on Pb-induced toxicity, the epigenetic regulatory mechanisms driving Pb-associated long-term health effects remain poorly understood. Eutherian mammals, which includes humans as well as all placental animals except marsupials and monotremes, undergo genomic imprinting, an epigenetically regulated process, to implement monoallelic gene expression based on parental origin. Imprinted genes (IGs) play critical roles in regulating complex biological and behavioral interactions between the mother and developing embryo. Perinatal Pb exposure in early development can disrupt genomic imprinting, which may increase disease risk later in life. Thus, further characterization of fetal sex-specific effects *in utero* is required to understand the impact of Pb exposure on genomic imprinting in the placenta. The goal of this study is to investigate *in utero* exposure to human-relevant Pb levels on placentas using an established mouse model. Specifically, the study aims to examine the impact on placental weight and IG expression at 13-15 days post-coitum (dpc). **Methods:** C57BL/6J female mice were exposed to control or Pb acetate (32 ppm) drinking water two weeks prior to time mating through sacrifice in mid-gestation, resulting in a mean maternal blood lead level of 9.7 ug/dL. Sires were removed to ensure the timing of the pregnancy and the final sample size was *n*=9 litters for control and *n*=10 litters for Pb. Upon sacrifice at 13-15 dpc, mouse placenta and embryo tissues were carefully dissected, cleaned, weighed, and snap frozen. Embryonic tissues (total *n*=147) were used to determine embryo sex. The exposure effect on placenta weight was analyzed using a linear mixed-effects model, accounting for litter as a random effect, followed by fetal-sex stratified assessment. A subset of placentas derived from 1 male and 1 female fetus per litter per group was used for RNA isolation and sequencing, resulting in a total of 36 placentas for control (*n*=8 for females and *n*=9 males) and Pb-exposed (*n*=9 for females and *n*=10 males) groups. A plexWell (SeqWell) approach was used for cDNA synthesis and library preparation. RNA-seq was conducted on the Illumina 10B Novaseq X Shared flow cell. Exposure group and fetal sex-specific

placental gene expression was analyzed using edgeR, and a list of 300 genes associated with genomic imprinting was used for IG-specific analysis. Control versus Pb-exposed groups were compared to determine differentially expressed genes (DEGs), with significance determined by false discovery rate<0.05. **Results:** Pb-exposed placentas had significantly higher weights (0.095g±0.0154g; *p*=0.012) compared to controls (0.086g±0.011g) for both sexes. RNA-seq identified a total of 14,287 genes, with 4,442 DEGs when comparing exposure groups including 2,159 upregulated and 2,283 downregulated by Pb. Among 151 IGs detected, 58 were differentially expressed by Pb exposure. In sex-stratified analyses, female placentas had 38 differentially expressed IGs (24 upregulated, 14 downregulated), while male placentas had 13 (11 upregulated, 2 downregulated). In total, 64 distinct IGs were differentially expressed across all mice, female, and/or male groups. Overlapping IGs were found between all mice and females (25 IGs), all mice and males (4 IGs), female-only (5 IGs), and male-only (1 IG). **Conclusions:** *In utero* exposure to Pb significantly increases placental weight in both male and female fetuses at 13-15 dpc. RNA-seq revealed substantial Pb-induced gene expression changes in the placenta, including 58 affected IGs. These findings suggest that Pb exposure disrupts placental function and fetal development through IG dysregulation, highlighting the importance of further research into the mechanisms and long-term consequences. Understanding the mechanistic links between Pb toxicity and epigenetic programming will lay the foundation for potential epigenetic interventions to alleviate long-term health effects that arise upon Pb exposure. Future studies will examine DNA methylation changes to elucidate Pb-induced gene expression alterations, informing potential interventions to mitigate the effects of early life Pb exposure.

ABSTRACT NUMBER: 5099 **Poster Board Number:** LB200

TITLE: Inflammatory cytokines and fibrogenic genes are epigenetically regulated by histone modifications in mice model of Folic Acid induced kidney fibrosis

AUTHORS (FIRST INITIAL, LAST NAME) AND INSTITUTIONS: *P. Roy*, *R. Kandel*, and *K. P Singh*.
Department of Environmental Toxicology, Texas Tech University, Lubbock, TX.

KEYWORDS: Epigenetics; Cytokines; Fibrosis

ABSTRACT: Background and Purpose: Repeated incidence of acute kidney injury leads to kidney fibrosis. The aberrant expression of inflammatory cytokines and fibrogenic genes are known to cause activation of resident fibroblast and excessive accumulation of extracellular matrix leading to fibrogenic changes in kidney. However, the underlying mechanism for aberrant regulation of genes in this process is not clear. Using mice model of folic acid-induced kidney fibrosis, our recently published data revealed the attenuation of fibrogenic changes by epigenetic therapeutics such as DNA methylation inhibitor 5 Aza 2-deoxycytidine and histone deacetylase inhibitor Trichostatin A**.** Changes in the levels of modified histone H3 with gene activating and repressing marks were also observed in this model. However, the precise role of these histone modifications in regulation of genes associated with fibrosis is not known. It is in this context that the objective of this study was to evaluate the role of histone modifications in regulation of inflammatory cytokines and other target genes associated with kidney fibrosis. **Methods:** The levels of modified Histone H3 with gene activating H3K9ac and suppressive H3K9me2 marks bound to the promoter regions of inflammatory cytokines and target genes associated with fibrosis were analyzed by ChIP-qPCR. **Results:** The result of this study revealed increased levels of H3K9ac whereas decreased levels of H3K9me2 are bound to the promoter of those genes that are activated in fibrosis.

Conclusions: Findings of this study suggest the regulation of inflammatory cytokines and other fibrogenic genes expression by epigenetic changes in histone marks.

ABSTRACT NUMBER: 5100 **Poster Board Number:** LB201
TITLE: Sex-stratified piRNA Expression Analysis Reveals Shared Functional Impacts of Perinatal Lead Exposure in Murine Hearts

AUTHORS (FIRST INITIAL, LAST NAME) AND INSTITUTIONS: *K. E. Sala-Hamrick*[1], *K. Wang*[2], *B. P. U. Perera*[1], *M. A. Sartor*[2], *D. C. Dolinoy*[1], and *L. K. Svoboda*[1]. [1]University of Michigan School of Public Health, Ann Arbor, MI; and [2]University of Michigan Medical School, Ann Arbor, MI.
KEYWORDS: Epigenetics; Metals; Cardiovascular System

ABSTRACT: Background and Purpose: Cardiovascular diseases (CVDs) are the leading cause of death worldwide, and developmental exposure to the metal lead (Pb) has been implicated in the incidence and progression of several CVDs. One potential mechanism underlying Pb-induced CVD is modification of DNA methylation. DNA methylation is the addition of a methyl group to cytosine bases in DNA, resulting in modulation of gene transcription without changing the underlying DNA sequence. Alterations in DNA methylation have been implicated in the development of coronary heart disease, heart failure, hypertension, and other CVDs. We have previously reported that developmental Pb exposure in mice alters DNA methylation in the heart in a sex-specific manner, but the underlying regulatory mechanisms are unclear. One potential mechanism by which Pb may modulate DNA methylation is dysregulation of PIWI-interacting RNA (piRNA) pathways. piRNA are a class of small non-coding RNA that canonically contribute to genomic stability by controlling DNA methylation of transposable elements in the germline. While piRNA were long thought to be exclusively expressed in the germline, work from our group and others has recently demonstrated somatic piRNA expression in mice and humans. Altered piRNA expression has been reported in the context of CVD, and we recently reported modulation of piRNA in the brain by Pb exposure. However, no studies thus far have linked Pb exposure and piRNA expression in the heart. Using an established mouse model of developmental exposures, the purpose of this project is to investigate the sex-specific effects of environmentally relevant Pb exposure during gestation and lactation on DNA methylation and piRNA expression in the heart. Our overall objectives are to provide a comprehensive analysis of baseline piRNA expression in the murine heart and to investigate sex-specific effects of human-relevant maternal Pb exposure on offspring cardiac piRNA expression. **Methods:** We utilized cryopreserved adult offspring hearts from a previous study conducted as part of the NIEHS Toxicant Exposures and Responses by Genomic and Epigenomic Regulators of Transcription (TaRGET II) Consortium. Experiments were performed using genetically invariant mice 93% identical to C57BL/6J. Two weeks prior to mating, dams were assigned to control or lead acetate water (32ppm, resulting in maternal blood Pb levels of 16-60 µg/dL). Exposure continued until offspring were weaned at 3 weeks of age, at which point they consumed Pb-free drinking water and standard chow *ad libitum*, until sacrifice at 5 months of age. Small RNA was extracted from whole heart tissue using standard protocols. To generate baseline maps of piRNA expression, we performed sodium periodate exclusion of the small RNA, which selects for 2'-O-methylation present in piRNA. Both sodium periodate treated and untreated samples were library prepped and sequenced. PePr peak calling software was used to determine relative enrichment of piRNA in periodate-treated versus untreated control samples, creating a baseline map of piRNA for comparison with Pb-exposed samples. EdgeR was used to determine differential expression of piRNAs from Pb-exposed versus control samples. These results

were filtered for significance by p-value < 0.05 (none were significant by FDR) and an absolute logFC > 1 and then were plotted using ggplot2 R package. Gene Ontology analysis was conducted for these filtered piRNAs using the Bioconductor package chipenrich. **Results:** In control mouse hearts, we found expression of 6,316 piRNA in our combined sex analysis, and from sex-stratified analyses, 9,231 piRNA in females and 5,972 piRNA in males. When these piRNA were mapped to the genome, 28-41% mapped to introns, including repetitive regions, and 12-28% of piRNAs mapped to exonic regions. When comparing Pb-exposed vs. control hearts, we found more potential Pb-induced cardiac piRNA changes in females (847) compared to males (187). These piRNAs mapped in both sexes to biological processes related to heart function and CVD development, including processes related to the mitochondria, energy metabolism, and heart muscle structure and function (FDR < 0.05). **Conclusions:** Overall, we characterized sex-stratified piRNA expression in both control and Pb-exposed murine hearts. In addition to providing a foundation for piRNA expression in the heart, these findings suggest a novel epigenetic mechanism by which developmental Pb exposure may impact CVD risk later in life. Future studies will link these molecular changes to Pb-induced alterations in cardiac function.

ABSTRACT NUMBER: 5101 **Poster Board Number:** LB202

TITLE: The Effects of Lead Exposure on piRNA Machinery (PIWIL) Expression: Implications for Epigenetic Regulation in Undifferentiated and Differentiated SH-SY5Y Cells

AUTHORS (FIRST INITIAL, LAST NAME) AND INSTITUTIONS: *J. S. Smith*, *R. K. Morgan*, *K. E. Sala-Hamrick*, *J. A. Colacino*, and *D. C. Dolinoy*. University of Michigan, Ann Arbor, MI.

KEYWORDS: Epigenetics; Neurotoxicity; Metals; Gene Expression/Regulation; Lead

ABSTRACT: Background and Purpose: Early life lead (Pb) exposure is a significant public health concern due to its long-term neurotoxic effects on cognitive health, potentially by altering epigenetic reprogramming in the brain. Pb exposure during neurodevelopment has also been shown to impair brain-derived neurotrophic factor (BDNF), a key regulator of neuronal survival, synaptic plasticity, and cognitive function. Dysregulation of BDNF and epigenetic pathways, including those involving piRNAs, may contribute to Pb's adverse effects on neurodevelopment. piRNAs, a class of non-coding RNAs, maintain genomic stability in the germline by promoting DNA methylation at transposable elements, and rely on their associated proteins, PIWILs, for functionality. However, their roles in somatic tissues, particularly the brain, are largely unexplored. This study investigates epigenetic mechanisms underlying gestational Pb exposure in vitro, comparing the gene expression of BDNF and PIWILs in SH-SY5Y (5Y) cells prior to and throughout differentiation in dopaminergic-like neurons. **Methods:** 5Y cells were stored in liquid nitrogen upon arrival and not used beyond P40, following manufacturer guidelines. Cells were cultured in EMEM, F-12, antibiotics, and 10% hiFBS until confluent, then exposed to Pb (0.16 µM, 1.26 µM, or 0 µM) for 72 hours. The 0.16 µM dose reflects a BLL of 3.5 µg/dL, the CDC's 2025 actionable level, while 1.26 µM reflects 1960s-70s blood lead levels (BLLs). RNA was extracted, reverse transcribed into cDNA, and PIWIL/BDNF expression was quantified via qRT-PCR with β-actin and GAPDH as reference genes. Reactions followed standard protocols, and Cq values were averaged from triplicates. ΔCq was calculated as (sample Cq - reference Cq), and fold differences in relative expression were determined using 2^(−ΔΔCq). Statistical significance ($p < 0.05$) was assessed via two-sided t-tests comparing each Pb treatment to the control. In a parallel study, 5Y cells were differentiated into dopaminergic-like neurons per published protocols adapted from Shipley et al., 2016 and exposed to 0.16 µM, 1.26 µM, 10 µM, or 0 µM Pb starting at differentiation day 5 (D5) through D18. The 10 µM dose was chosen to reflect an acute

exposure. Nucleic acid extractions and qRT-PCR for PIWIL expression were performed in the same manner as described above, with ACTG1 as the reference gene. **Results:** Undifferentiated cells, consistent with previous research, revealed expression of PIWIL1, 2, and 4 in all three conditions, with no expression of PIWIL3. PIWIL1 demonstrated significantly higher expression than both PIWIL2 and PIWIL4 in both exposure conditions and control ($p < 0.05$). BDNF was lowly expressed in both exposure conditions and control. Gene expression did not vary significantly between exposure conditions and control. Interestingly, during the first two weeks of 5Y differentiation, Pb exposure predominantly reduced PIWIL1 expression, with significant decreases observed on D9 and D12 in cells exposed to 0.16 µM ($p < 0.01$, D9), 1.26 µM ($p < 0.01$), and 10 µM ($p < 0.01$) Pb. By D15, PIWIL1 expression increased in the 0.16 µM and 10 µM Pb-treated cells ($p < 0.05$). Significant changes weren't detected on D18. In contrast, PIWIL4 expression remained largely unchanged, except for a significant increase on D12 in the 10 µM Pb group, relative to control cells. **Conclusions:** These findings offer novel insights into the effects of Pb exposure on PIWIL expression in both undifferentiated and differentiated SH-SY5Y cells. Specifically, this study underscores the dynamic nature of PIWIL1 prior to and throughout the cellular differentiation process, highlighting its potential role in the piRNA pathway and genomic stability maintenance following Pb exposure in neuronal cells. Future research will explore temporal changes to BDNF expression throughout the differentiation process and how PIWIL1 knockdown may affect DNA methylation. Additionally, future research will characterize the piRNA profile of 5Ys prior to and throughout differentiation following exposure to Pb.

ABSTRACT NUMBER: 5102 **Poster Board Number:** LB203

TITLE: Mitochondrial dysfunction causes aberrant expression of epigenetic regulatory genes in human kidney epithelial cells

AUTHORS (FIRST INITIAL, LAST NAME) AND INSTITUTIONS: J. L. Bockemehl, *P. Roy*, *R. Kandel*, and *K. P. Singh*. Texas Tech University, Lubbock, TX.

KEYWORDS: None

ABSTRACT: Background and Purpose: Mitochondrial dysfunction has been shown to be associated with adverse effects of nephrotoxicants in kidney. However, the mechanism underlying altered mitochondrial function-dependent renal pathophysiology is not clear. Mitochondrial ROS has been shown to alter the epigenome and expression of genes associated with critical cellular function. Whether mitochondrial dysfunction affects epigenetic regulatory genes is not known. **Methods:** Therefore, the object of this study is to evaluate the role of mitochondrial dysfunction on expression of epigenetic regulatory genes. Human kidney epithelial HK2 cell line was treated with rotenone that blocks mitochondrial complex I and its effect on cell viability, ROS production and expression of epigenetic regulatory genes were measured. **Results:** MTT assay for cell viability revealed significant reduction in the viability of HK2 cells after rotenone (10 nM) treatment for 72 hrs. DCF assay revealed a significant increased levels of reactive oxygen species in cells treated with rotenone. Gene expression analysis by quantitative real time PCR further revealed altered expression of epigenetic regulatory genes such as DNMT1, HDAC1, TET1, MBD4 and EZH2 in rotenone treated HK2 cells. **Conclusions:** These results suggest that mitochondrial dysfunction causes cytotoxicity, oxidative stress, and dysregulation of epigenetic regulatory genes. The findings of this study showing mitochondrial dysfunction triggered dysregulation of epigenetic regulatory genes may explain the epigenetic mechanism underlying aberrant expression of genes associated with kidney disease.

ABSTRACT NUMBER: 5103 **Poster Board Number:** LB204

TITLE: Investigating the toxicology of nitazenes and the efficacy of FDA approved antagonists on mu opioid binding, cardiac action potential, and cardiomyocyte contraction

AUTHORS (FIRST INITIAL, LAST NAME) AND INSTITUTIONS: M. Racine, J. Tressler, and *B. McCranor*. MRICD, Edgewood, MD.

KEYWORDS: Chemical and Biological Weapons; In Vitro and Alternatives; Toxicity; Acute

ABSTRACT: Background and Purpose: Synthetic opioids, have the potential to be used on the civilian population as a “non-lethal” chemical weapon, as was observed in the 2002 siege of the Moscow Dubrovka Theater. Wide scale availability of wholesale-level amounts (multiple kilograms) of synthetic opioids on online cryptomarkets, almost exclusively shipping from China, allow for both state and non-state actors to easily obtain opioid agents regardless of production capabilities. It has been noted, in animal models, that repeated use or exposure to opioids can produce toxic effects on organs, but the direct connection in human case reports is harder to discern due to the high incidence of polydrug use in causalities. Complicating the issue is the fact that the data on organ toxicity due to a single acute exposure to ultra-potent opioids is lacking. We propose to investigate the toxicology of potent synthetic opioids that are increasingly causing overdoes events in the United States. Project Objective: It has been noted, in animal models, that repeated use or exposure to opioids can produce toxic effects on organs, but the direct connection in human case reports is harder to discern due to the high incidence of polydrug use in causalities. Complicating the issue is the fact that the data on organ toxicity due to a single acute exposure to ultra-potent opioids is lacking. We propose to investigate the toxicology of potent synthetic opioids that are increasingly causing overdoes events in the United States.We will determine the affinity and EC50 of Acetyl fentanyl, etonitazene, metonitazene, and isonitazene for the μ, κ, and δ-opioid receptors. We will also assess the ability of the synthetic opioids to inhibit the human ether-a-go-go related gene (hERG) ion channels, which can be indicative of adverse cardiac events. **Methods:** Methods: in vitro μ opioid Receptor Binding AssayTango OPRM1-bla U2OS Cells Contain human μ Opioid Receptor with a beta-lactamase reporter systemWith receptor binding, beta-lactamase activity is activated, and cells will appear blue fluorescentWithout binding the cells appear green fluorescentFor our assayCells were dosed with scaled concentrations of acetylfentanyl, etonitazene, metonitazene, and isonitazeneIC50 concentrations were determinedMethods: hERG Fluoresence Polarization AssayAssess the ability of the synthetic opioids to inhibit the human ether-a-go-go related gene (hERG) ion channels - Indicative of adverse cardiac eventsUses a membrane fraction containing hERG channel protein and a high-affinity red fluorescent hERG channel ligand (tracer)Fluorescence polarization (FP) when fluorescent molecule (the tracer) is excited with plane-polarized light, the light is depolarizedIf the tracer is bound to a large molecule, then rotation is slowed and light remains more highly polarizedCompetitors displace the tracer from the hERG channel protein, lowering its fluorescence polarizationMethods: iCell xCELLigence demoxCELLigence RTCA CardioECR monitoring of cardiomyocytesEvaluates viability, contractility, and electrical activity involved in excitation-contraction (EC) coupling across the cardiomyocyte monolayerMeasurement of field potential signal using extracellular recording (ECR) electrodes Measurement of contractility and viability using impedance electrodesFor our assay50μM etotnitazene and isotonitazene Range of 1mM-1nM nalmefene Baseline recordings conducted for 30 minutes then viable wells were assigned to treatment groups. Control wells received 0.5% DMSOStably beating iCell Cardiomyocytes on RTCA systemMany parameters collected including beating rate, beating rhythm irregularity, beating period, and amplitudeAmplitude - the Cell

Index value difference from each positive peak to the following negative peak. **Results:** Preliminary results suggest an EC50 of 1.2 µM for acetyl fentanyl, 279 nM for etonitazene, 290 nM for metonitazene, & 18 nM for metonitazene. Higher than our calculated EC50 of 8.3 nM for fentanylConcentrations range from 200fM -200uM Only significant results are Acetylfentanyl and heroin vs control at the 3rd highest concentrationMoving forward with a different assay for mu, kappa, delta bindingConcentrations range from 800fM -800uM. **Conclusions:** Assay development nearly completeTango & hERG assayCardio AssayRevvity Mu, Kappa, Delta binding assayChoosing which Nitazene(s) to move forwardontinue evaluation of hERG Assay, development of new assays analyzing mu binding affinityMove into Aim 2: We will expose ferrets to a range of dosages of acetylfentanyl and the most potent nitazene compounds identified in Aim 1. We will measure respiratory parameters using a whole-body plethysmography chamber. We will assess organ toxicity at 24 hours and 7-days. The preliminary data is in agreement with the published data on relative potency.

ABSTRACT NUMBER: 5104 **Poster Board Number:** LB205

TITLE: Antimicrobial Agent Cetylpyridinium Chloride Causes Potent Mitochondrial Toxicity: Complex Effects on the Electron Transport Chain

AUTHORS (FIRST INITIAL, LAST NAME) AND INSTITUTIONS: N. E. Adelman, E. L. Ledue, S. R. Weller, J. E. Burnell, B. M. Aho, S. K. Trafton, E. Biro, *B. Obeng*, J. K. Shim, *S. T. Hess*, and *J. A. Gosse*. University of Maine, Orono, ME.

KEYWORDS: Chemical of Concern; cetylpyridinium chloride

ABSTRACT: Background and Purpose: Consumers are widely exposed to antibacterial agent cetylpyridinium chloride (CPC) via food and personal care products. Previous investigation demonstrated non-cytotoxic, low-micromolar CPC exposure causes mitochondrial toxicity in primary human keratinocytes, mouse NIH-3T3 fibroblasts, and rat RBL-2H3 mast (RBL) cells. In these mammalian cells, CPC suppresses both oxygen consumption rate (primary human keratinocyte EC_{50} 1.25 µM, RBL cell EC_{50} 1.75 µM) and ATP synthesis (RBL cell EC_{50} 1.7 µM, human keratinocyte EC_{50} 1.2 µM). To contextualize this severity, the canonical mitotoxicant carbonyl cyanide-3-chlorophenylhydrazone (CCCP) has an ATP synthesis inhibition EC_{50} of 1.2 µM in RBL cells. Super-resolution microscopy (fluorescence photoactivation localization) revealed CPC-induced damage to live cell mitochondrial nanostructure; mouse fibroblasts incubated with low micromolar CPC doses form mitochondrial “donuts,” a hallmark of mitotoxicity. Mitochondrial dysfunction and deformation are linked to several pathologies, including Alzheimer’s and Parkinson’s. Furthermore, the SARS-CoV-2 pandemic prompted the increased use of quaternary ammonium compounds, including CPC, due to their potential antiviral capabilities against enveloped viruses. This recent interest in new CPC applications, and continued CPC use in many over-the-counter products, highlights the need to fully understand CPC’s effects on eukaryotes at consumer-relevant concentrations. If CPC use is to be increased, so is the need to adequately and safely weigh the risks and benefits of using CPC-containing products, prompting investigation into the mechanism of CPC-mediated mitotoxicity. **Methods:** A Biolog electron flow assay was performed on intact and saponin-permeabilized RBL cells incubated with 0.5 and 1.0 µM CPC. The redox dye in the assay acts as a terminal electron acceptor of cellular respiration along the mitochondrial inner membrane. Electron flow rate from 31 substrates under each condition was calculated from dye reduction, detected colorimetrically via plate reader for ~1-3 hours. The electron flow rates were analyzed by One-way ANOVA and Tukey’s post-hoc. A mitochondrial malate dehydrogenase (MDH2) activity assay was used in

a plate reader to assess pure human recombinant MDH2 activity after incubation with and without CPC (0.5 and 1.0 µM). Coupled to the colorimetric redox reporter dye, NADH production rate was measured, representing MDH2 enzymatic activity. MDH2 activity initial rate, V_0, was analyzed over a range of substrate concentrations to determine Michaelis-Menten kinetics. All statistical analyses were done using Excel and GraphPad Prism. **Results:** Measurements of electron flow indicate that CPC targets Complex I, Complex II, and other electron transport chain (ETC) components, starting at concentrations as low as 0.5 µM CPC. In saponin-permeabilized RBL cells, CPC significantly inhibits electron flow from malate, α-ketoglutarate, and succinate beginning at 0.5 µM, and from α-glycerol phosphate beginning at 1.0 µM. For intact RBL cells, electron flow from succinate was not inhibited by CPC exposure. CPC significantly inhibited electron flow in intact cells from glucose-1-phosphate and gluconate-6-phosphate beginning at 0.5 and 1.0 µM, respectively. MDH2 Michaelis-Menten kinetics were not significantly affected by CPC exposure. **Conclusions:** These results indicate that CPC targets critical components of cellular respiration, diminishing both ATP production and OCR consumption, doing so at concentrations which are orders of magnitude lower (0.5 µM) than those previously reported in the literature (100+ µM). Typical CPC exposure is estimated to be in human blood at ~0.3 µM, which further contextualizes the effects we report here. Direct inhibition of malate dehydrogenase is not the cause of CPC's mitotoxicant effects, but the data suggest direct inhibition of ETC Complexes I and II. Typically unable to cross the plasma membrane (PM), succinate was observed causing strong electron flow in intact cells. The SUCNR1 receptor, found on the PM of RBL cells, may be the source of successful succinate-fed electron flow, and the abating of CPC mitotoxicity of Complex II. CPC's continued use, in spite of apparent potent mitotoxicity, warrants further research into the mechanism of action.

ABSTRACT NUMBER: 5105 **Poster Board Number:** LB206

TITLE: Construction of the blood-brain barrier biomimetic chip and its application in assessing the effects of e-cigarette additives on blood-brain barrier permeability

AUTHORS (FIRST INITIAL, LAST NAME) AND INSTITUTIONS: X. Li[1,2], F. Yu[1,2], S. Han[1,2], H. Chen[2,1], and H. Hou[2,1]. [1]China National Tobacco Quality Supervision & Test Center, Zhengzhou, China; and [2]Beijing Life Science Academy, Beijing, China. Sponsor: *S. Jia*

KEYWORDS: Tobacco Products; Alternatives to Animal Testing; Neurotoxicology

ABSTRACT: Background and Purpose: In recent years, e-cigarettes have become increasingly popular, and the health effects of e-cigarettes have attracted much attention. However, little is known about the damage that e-cigarettes may cause to the blood-brain barrier (BBB). Animal models usually exhibit species differences in terms of barrier tightness, transporter expression, and metabolic activity. Thus, the predictive results from the animal model are inaccurate to directly extrapolate to human beings. There is an urgent need to develop alternative models to better predict the BBB permeability of substances, and to explore effects of substances on the BBB. Here, we developed a constant-rate perfused array chip (cPAC) for establishing a BBB model and compared with the Transwell model to prove its advantages. cPAC is used to analyze the effect of e-cigarette additives on BBB permeability and BBB-related proteins. **Methods:** In this study, immortalized human brain microvascular endothelial cells (hCMEC/D3) were inoculated on transwell or cPAC to construct single-cell BBB models; SVG P12 cells and hCMEC/D3 cells were seeded on the upper and lower sides of the cPAC membrane to construct a co-culture BBB model of endothelial cells and astrocytes. We fully characterized the three established models by measuring transendothelial electrical resistance (TEER), the permeability of FITC-Na and FITC-

labeled dextrans of different molecular weights, the permeability changes of several efflux transporters substrates with or without specific inhibitors, and immunofluorescence characterization of tight junction proteins. We selected several e-cigarette additives that are commonly detected in actual samples: menthol, WS-23, lactic acid, benzoic acid, ethyl maltol, methylcyclopentenolone and ethanol. The additives were formulated into a series of concentration gradients with propylene glycol (PG), vegetable glycerin (VG) and a fixed concentration of nicotine to mimic e-liquid. The effect of various additives on the permeability of BBB was assessed by LC-MS/MS analysis of nicotine permeability in the presence of different concentrations of additives. We further verified whether the additives affected BBB permeability by regulating the expression of tight junction proteins. **Results:** The cPAC co-culture model showed the most superior blood-brain barrier function with the highest TEER values, the lowest transmittance of FITC-Na, FITC-4K/40K dextrans, and the robust expression of tight junction proteins. cPAC co-culture model was therefore selected for subsequent experiments. In the nicotine penetration experiment, 50 mg/g or higher doses of Menthol, 100 mg/g WS-23, 50 mg/g benzoic acid, 20 mg/g or higher doses of ethanol, 50mg/g ethyl maltol, and 20 mg/g or higher doses of methylcyclopentenolone significantly promoted nicotine penetration. However, Lactic acid did not show this effect in the 5-50 mg/g concentration range. It was further found that increased BBB permeability caused by additives was associated with decreased expression of tight junction proteins, such as ZO-1, Occludin and Claudin-5. **Conclusions:** We developed an *in vitro* blood-brain barrier model that is more in line with the physiological environment and used it to explore the effects of several e-cigarette additives on BBB permeability. We found that several selected additives increased blood-brain barrier permeability at certain concentrations and explained the reasons for the change in permeability from the perspective of gene expression. In conclusion, this study indicated that some e-cigarette additives have adverse effects on the BBB, and provided preliminary mechanistic insights into how e-cigarettes cause BBB dysfunction.

ABSTRACT NUMBER: 5106 **Poster Board Number:** LB207

TITLE: Construction of human lung organoid model and its application in toxicity evaluation of tobacco products

AUTHORS (FIRST INITIAL, LAST NAME) AND INSTITUTIONS: S. Han[1,2], X. Li[1,2], Y. Tian[1,2], Y. Jiang[1], Y. Wu[1], H. Wang[1,2], Y. Fu[2,3], H. Chen[2,3], and H. Hou[2,3]. [1]China National Tobacco Quality Supervision and Test Center, Zhengzhou, China; [2]Beijing Life Science Academy, Beijing, China; and [3]China National Tobacco Quality Supervision & Test Center, Zhengzhou, China. Sponsor: *S. Jia*

KEYWORDS: Tobacco Products; Alternatives to Animal Testing; Respiratory Toxicology

ABSTRACT: Background and Purpose: At present, the toxicity evaluation of tobacco products is mainly based on cell and animal models, which cannot authentically reflect the complex reaction and effects of aerosol exposure on human. Organoids which are defined as stem cell-derived 3D self-organizing micro-organs, have been proven to be more capable to recapitulate the key structural and functional features of *in vivo* organs than 2D cell cultures, and better reflect the complex cellular responses and interactions *in vivo*. In recent years, organoids have been increasingly used in toxicological studies. Given that the lung is the main target organ of smoke exposure, in order to more accurately assess the toxic effects of smoke exposure on human respiratory system, we constructed human embryonic stem cells (hESCs)-derived airway organoid model and verified its applicability in the toxicological evaluation of different tobacco products. **Methods:** hESCs were directed to differentiate into definitive endoderm (DE), anterior foregut endoderm (AFE), lung bud tip progenitor organoids (LPOs), and eventually airway

organoids (AOs) by sequentially adding specific growth factors and small molecule induction reagents *in vitro*. During the induction process, cultures of specific induction stages and final AOs were characterized. The successful culture of AOs was verified by immunofluorescence detection of markers of representative cell lineages in lung tissue, including basal cells (P63), ciliated cells (Ac-α-tubulin), goblet cells (MUC5AC), and lung epithelial cells (NKX2.1). Based on the constructed AOs model, we selected reference cigarettes and representative heated tobacco products (HTPs) and tested conventional toxicology indexes, such as cytotoxicity by LDH or CCK8 assay, genotoxicity by γ-H2AX detection, oxidative stress by ROS measurement, cell apoptosis by caspase 3/7 activity assessment and secretion of inflammatory factor by ELISA kits after AOs exposed to smoke aerosols. In addition, lung tissue-specific indexes were also tested, such as tissue structure and mucus secretion by H/E staining, and cell population change by gene expression analysis, to comprehensively evaluate the toxic effects of tobacco products on lung. **Results:** Immunofluorescence analysis of specific cell type markers validated the successful construction of AOs. Toxicity tests based on AOs showed that exposure of AOs to both cigarette and heated cigarette smoke aerosols induced cytotoxicity, genotoxicity, ROS production, cell apoptosis, and inflammatory responses, and also led to structural damage and variation in cell subgroups with increased goblet cells and decreased ciliated cells. This is consistent to some extent with results from animal inhalation exposure models, suggesting that lung organoids may be an alternative to animal experiments for the toxicity evaluation of tobacco products. **Conclusions:** In conclusion, we have constructed a more physiologically relevant lung model for the toxicological study of tobacco products, which can provide a more accurate and systematic means of evaluating the toxicological effects of tobacco products on the respiratory system.

ABSTRACT NUMBER: 5108 **Poster Board Number:** LB209

TITLE: Development of the *in vitro* micronucleus test in human-derived 3D EpiAirway tissues for exposure to whole aerosol from cigarettes, Heated Tobacco Products and Electronic Nicotine Delivery Systems

AUTHORS (FIRST INITIAL, LAST NAME) AND INSTITUTIONS: I. Crooks[1], M. Hollings[2], D. Breheny[1], and E. Bishop[1]. [1]B.A.T. (Investments) Ltd, Southampton, United Kingdom; and [2]Labcorp Early Development Laboratories, Harrogate, United Kingdom. Sponsor: *R. Leverette*

KEYWORDS: Alternatives to Animal Testing; Genetic Toxicology; Tobacco Products

ABSTRACT: Background and Purpose: In the genotoxic assessment of tobacco products, traditional approaches involve capturing the different phases of the aerosol (e.g. TPM or GVP) in solvents and applying these to non-human cell culture monolayers. Genotoxicity is typically measured by the *in vitro* micronucleus test (IVMN) and the use of trapped aerosols and cell cultures can be conducted to international test guidelines for the IVMN however, the use of organotypic airway models, such as the three-dimensional human EpiAirway tissue model represents physiological characteristics of the respiratory tract. As such, exposure to whole aerosol may be more relevant for this tissue model to increase the biological relevance of this assay system combined. This study was designed to develop the IVMN in 3D EpiAirway tissues and to optimise the assessment of genotoxic potential of cigarettes, Heated Tobacco Products (HTPs) and Electronic Nicotine Delivery Systems (ENDS). **Methods:** EpiAirway tissues were exposed to two positive controls, Mitomycin C (MMC) and vinblastine at two concentrations basolaterally under the Transwells. Three products were assessed - the 1R6F research cigarette, an HTP device with an internal reference consumable, eHTPB2 and an ENDS device with a

creamy tobacco flavouring containing 18 mg/mL nicotine. The aerosols from these products were generated on a Vitrocell VC 10 or VC 1/7 smoking robot, and these were diluted with humidified air at different flow rates to derive the dose. The diluted aerosols were subsequently delivered to the surface of the EpiAirway tissues under negative pressure, and three replicate tissues were exposed to the aerosol. 1R6F smoke was exposed to the surface of the tissues for up to 1 hour, and the HTP and ENDS aerosols exposed for up to 2 hours. Each exposure also included a dosimetry well to determine deposited nicotine and carbonyls. After exposure, tissues were allowed to recover for 48 hours, with the addition of EGF to enhance cell turnover. Micronuclei induction was determined using Litron MicroFlow kits. **Results:** Two positive controls, vinblastine and MMC, induced dose-related increases in micronuclei, demonstrating the feasibility to obtain a genotoxic response in this tissue model. 1R6F whole aerosol induced dose-related increases in micronuclei following a 1-hour exposure. The HTP aerosol also induced a weak micronuclei response, however a more concentrated aerosol and longer exposure period (2 hours) was required to induce this response relative to a cigarette. In addition, the micronuclei response from the HTP was significantly less than 1R6F. The ENDS did not induce micronuclei, despite testing with a more concentrated aerosol than 1R6F and increasing the exposure period to 2 hours. **Conclusions:** The genotoxic assessment of compounds is reasonably well established in 3D skin models, however the application of organotypic lung models for genotoxicity assessment is unfortunately lacking. Genotoxicity of inhaled substances has the potential to be investigated in organotypic 3D lung tissues, such as EpiAirway, adding a more biologically relevant exposure route and relevant tissue model, which will complement regulatory cell culture methods. Results indicate that it is feasible to obtain a genotoxic response from positive controls and reference cigarette aerosols under the conditions of this development phase.

ABSTRACT NUMBER: 5109 **Poster Board Number:** LB210

TITLE: Aerosol Chemistry and *in vitro* Evaluation of a Novel Herbal Heated Product Relative to Cigarette Smoke

AUTHORS (FIRST INITIAL, LAST NAME) AND INSTITUTIONS: I. Crooks, E. Marwick, A. Heath, E. Bishop, A. Baxter, I. M. Pinto, K. Pereira, S. Hadley, D. Breheny, and C. Garcia-Canton. B.A.T. (Investments) Ltd, Southampton, United Kingdom. Sponsor: *R. Leverette*

KEYWORDS: In Vitro and Alternatives; Genetic Toxicology; Tobacco Products

ABSTRACT: Background and Purpose: New products are emerging that support reduced risk profiles compared to cigarettes, such as products that heat but do not burn tobacco. These have been shown to produce reduced toxicant emissions and reduced *in vitro* toxicity as compared to conventional cigarettes. Here, we evaluate a novel herbal heated product (HHP) by assessing its chemical emissions and *in vitro* activity compared to a reference cigarette, 1R6F. **Methods:** The HHP and 1R6F reference cigarette were puffed under the HCI regime. The ventilation holes on the HHP were unblocked. The composition of emissions from the HHP were analysed using targeted GC-MS-SIM or HPLC-UV. Compounds identified in the HHP emissions were compared to those from 1R6F. All targeted analyte emissions measured in the HHP were significantly reduced compared to 1R6F. A battery of *in vitro* assays assessed the mutagenic, genotoxic and cytotoxic potential of the HHP and 1R6F. These comprised the Ames test (OECD 471), *in vitro* micronucleus (IVMN) assay (OECD 487) using V79 cells and a 3h± S9 and 24h -S9 treatment regime and the Neutral Red Uptake (NRU) assay using BALB/c 3T3 cells treated for 24h -S9. **Results:** 1R6F induced dose-dependent increases in revertants in strains TA98, TA100 and

TA1537 +S9, indicative of a mutagenic response. 1R6F was genotoxic in the IVMN in all treatment conditions and cytotoxicity was observed in the NRU and a mean IC_{50} value of 82.92 mg/mL was calculated. Contrary, the HHP did not induce increases in revertants in the Ames test that were considered to be mutagenic. Although the HHP also induced responses in the IVMN in all three treatment conditions, the responses were significantly less than 1R6F, despite testing at significantly higher concentrations. In the NRU, the HHP showed an indication of cytotoxicity, but no IC_{50} value could be calculated. These results show that the emissions from the HHP are less mutagenic, genotoxic, and cytotoxic than 1R6F cigarette smoke under the conditions of this study and the studied assays. **Conclusions:** The results of these studies suggest that the HHP has a potential role in tobacco harm reduction, however additional studies are needed to determine its practical utility for tobacco harm reduction.

ABSTRACT NUMBER: 5110 **Poster Board Number:** LB211

TITLE: Assessment of cancer and non-cancer risk estimates of selected constituents in heated tobacco aerosols in comparison to reference cigarette smoke

AUTHORS (FIRST INITIAL, LAST NAME) AND INSTITUTIONS: Y. Kanemaru, *L. Czekala*, T. Duarte, R. Bach, S. Larroque, *I. Baskerville-Abraham*, and J. Miller-Holt. JT International SA, Geneva, Switzerland.

KEYWORDS: Tobacco Products; Risk Assessment; Exposure Assessment

ABSTRACT: Background and Purpose: Quantitative Risk Assessment (QRA) is a systematic approach to estimate the potential impact of chemical exposures on human health by combining chemical and biological data. Such assessments are often used to support decision making to protect human health from environmental or industrial chemicals. QRA principles have been applied to estimate both cancer and non-cancer risks associated with constituents found in cigarette smoke. These studies have characterized the toxicological risks by using the yields of selected smoke constituents and their toxicity potency values, helping to prioritize toxicants in cigarette smoke for monitoring or reduction. QRA approaches also have been used as a theoretical metric to compare two different tobacco products. Recently, QRA approaches were applied to assess the impact of reduced emission of harmful constituents in non-combustible tobacco/nicotine products, such as e-cigarettes and heated tobacco products, relative to the risks posed by combustible cigarette smoke. In this study, a comparative QRA was conducted to evaluate both cancer and non-cancer risks associated with exposure to emissions from over 20 different Heated Tobacco Stick Products (HTSPs), with varying tobacco blends and flavors. The study aimed to provide a theoretical representation of the relative toxicological health risks between HTSPs and a reference combustible cigarette, to identify constituents that significantly influence risk estimates, and to determine the comparability among different HTSPs. Lastly, the magnitude of the relative reductions in risk estimates were compared to the reduced biological responses found in the *in vitro* mutagenicity, genotoxicity, and cytotoxicity assays. **Methods:** Aerosol/smoke generation, collection, and chemical analysis were performed at an ISO/IEC 17025:2017 accredited contract research organization. The test HTSPs and 1R6F cigarettes were conditioned according to the ISO 3402: 2023 standard. The aerosol/smoke generation was performed as specified in ISO 5501-1:2024 for HTSPs (55 mL puff volume, 30 s puff interval, 2 s puff duration, bell-shaped puff profile, unblocked ventilation holes), and in ISO 20778:2018 for 1R6F cigarettes (55 mL puff volume, 30 s puff interval, 2 s puff duration, bell-shaped puff profile, 100% blocked ventilation holes). Chemical analysis was performed on over 60 analytes, including priority compounds identified by public health

authorities such as the World Health Organization (WHO) and US Food and Drug Administration (FDA). At least three independent aerosol/smoke collections and measurements were performed according to the laboratory methods, along with concurrent air blank sample analysis. QRA of the emission analytes was performed using methodology and equations recommended by the US Environmental Protection Agency (EPA) for environmental site risk assessment, with minor adjustments for HTSP emission exposure (Marano et.al., 2018). Inhalation toxicity reference values for cancer endpoint, i.e., inhalation unit risk, and non-cancer end point, i.e., chronic reference concentration, were selected based on the three-tier hierarchy approach recommended by EPA. Exposure assumptions including daily product consumptions, exposure duration, life expectancy, inhalation rates, were made based on third-party databases, WHO health statistics, and US EPA's default assumption in risk assessment. To address the expected variability in the emission values and exposure parameters, a Monte Carlo method was applied to simulate distributions of cancer and non-cancer risk estimates. The simulation was computed with 10,000 iterations. The estimated cumulative cancer risk and non-cancer risk values were compared between individual HTSPs versus 1R6F cigarette to calculate relative reduction against cigarette smoke exposure. The Ames, *in vitro* micronucleus (ivMN), and neutral red uptake (NRU) assays were performed for aerosol collected matter and gas vapor phase in line with the corresponding OECD test guidelines and Health Canada Official Methods. **Results:** The chemical analysis of the emissions of the HTSPs, irrespective of the blend and flavor, demonstrated a significant reduction in all analytes compared to the reference combustible cigarette, with reductions ranging from 55 to 99%. To contextualize the reduction in emission values of individual analytes, a QRA was conducted to derive cumulative cancer and non-cancer risks estimates, including mean, median, 5^{th}, and 95^{th} percentiles using Monte Carlo simulation. The results indicated that the average percentage reduction in cumulative cancer risk estimates for HTSPs, relative to the 1R6F cigarette, ranged from 90% to 99%, while non-cancer risk estimates were reduced by approximately 90%. The constituents that significantly impacted cumulative cancer and non-cancer risk estimates of HTSP aerosols remained consistent across different HTSP variants. In contrast, the primary constituents driving the risk estimates differed between HTSPs and the reference cigarette. Additionally, biological responses in the *in vitro* toxicity assays, consistent with the QRA risk estimates reductions, were comparable across all tested HTSPs and significantly reduced relative to the reference cigarette. **Conclusions:** The QRA outcomes demonstrated significant reductions in both cancer and non-cancer risk estimates for HTSP aerosols compared to the reference cigarette smoke. The reduction in risk estimates was consistent across all HTSPs, irrespective of different blends and flavors. These findings are corroborated by the significant reduction in toxic emissions and *in vitro* toxicological responses observed for all HTSPs relative to the 1R6F reference cigarette. The directional consistency of these observations is in line with other independent studies using different commercial HTSPs, suggesting that by maintaining the principles of heating tobacco and not burning (i.e., where 350°C is the maximum tobacco consumable temperature) and ensuring HTSPs are manufactured to high quality and safety standards, products within the HTSP category may have comparable product risk reduction potential. Furthermore, these QRA data, in conjunction with offsetting adverse health outcomes approach and *in vitro* toxicological responses, facilitate the definition of acceptable comparability ranges, supporting the bridging of products and associated datasets, which will subsequently be linked to product-agnostic, categorical epidemiological data.

ABSTRACT NUMBER: 5111 **Poster Board Number:** LB212

TITLE: High Variability in Aldehyde and Metal Contents in Aerosols Emitted from Popular Pods and Disposable E-Cigarettes Purchased in Europe and in the US

AUTHORS (FIRST INITIAL, LAST NAME) AND INSTITUTIONS: A. Silva[1,2], V. Ilievski[1,3], K. N. Nguyen[3,4], K. Schilling[1,3], B. Yan[3,4], *A. Navas-Acien*[1,3], *D. Re*[1,3], and M. Hilpert[1,3]. [1]Department of Environmental Health Sciences, Columbia University, New York, NY; [2]Master of Science in Toxicology Program, Environmental Health Sciences, Mailman School of Public Health, Columbia University, New York, NY; [3]NIEHS Center for Environmental Health and Justice in Northern Manhattan, Columbia University, New York, NY; and [4]Lamont-Doherty Earth Observatory, Geochemistry Department, Palisades, NY.

KEYWORDS: None

ABSTRACT: Background and Purpose: The use of e-cigarettes, particularly among the youth, has raised public health concerns due to the potential exposure to harmful contaminants released in the aerosol. Notable contaminants include metals from hardware, such as the metallic heating coil, and aldehydes from the heating of e-liquids. The objective of this study is to investigate in aerosols produced from widely used Pods and disposable e-cigarettes, including one recently approved by the FDA, the influence of different parameters, including device type, e-liquid flavor, nicotine content, and country of purchase on the levels of released metals and aldehydes. **Methods:** Aerosols were produced for various e-cigarette, flavor, and nicotine combinations (n = 10) and collected using a converging and straight tubing section system before analysis. For metal analysis, samples were digested with a solution containing 2% HNO3, 1% methanol, and 0.02% Triton X-100 and nine metals (chromium, manganese, iron, nickel, strontium, copper, lead, vanadium, and zinc) were measured using Inductively Coupled Plasma Mass Spectrometry (ICP-MS). For aldehyde analysis, aerosol samples were derivatized using 2,4-dinitrophenyl-hydrazine (DNPH) and cleaned up using solid phase extraction (SPE) before analyzed for thirteen aldehydes (acrolein, acetone, acetaldehyde, formaldehyde, 2-Butanone, benzaldehyde, butyraldehyde, crotonaldehyde, hexaldehyde, methacrolein, pentanal, propionaldehyde, p-tolualdehyde) with Liquid Chromatography and Electrospray Ionization (ESI) Tandem Mass Spectrometry (LC-MS/MS). One-way analysis of variance (ANOVA) and Tukey's Honest Significant Difference (HSD) test were used to compare concentrations between groups. **Results:** Statistically significant disparities in aerosol metal concentrations were observed across e-cigarette devices and flavors for chromium ($p < 0.001$), nickel ($p < 0.001$), and lead ($p < 0.001$), all of which are known carcinogens and to have a wide range of toxic effects including to the brain. Concerningly, levels of these three metals were particularly high in the aerosol generated from an FDA-approved device containing a tobacco-flavored e-liquid and in the aerosols from a disposable device purchased in Europe (Spain and Germany) delivering sugary-flavored e-liquids (cotton candy ice and blue razz lemonade). For aldehydes, significant differences in aldehyde concentrations were also observed across devices and flavors; the possible carcinogen crotonaldehyde exhibited particularly high levels for cotton candy ice and tobacco flavors ($p < 0.001$). A disposable device with sugary-flavored e-liquids commonly exhibited higher levels of other aldehydes, including acetone ($p < 0.001$), butylaldehyde ($p < 0.001$), and hexaldehyde ($p < 0.001$), compared to Pods with tobacco-flavored e-liquids. Overall, most metal and to a lesser extent aldehyde concentrations of aerosols from tobacco-flavored Pods purchased in Europe (Spain and Germany) were generally lower than those from the Pods offered by the same manufacturer (with different nicotine contents) and approved by the FDA in the US ($p < 0.05$). Interestingly, e-liquid nicotine content often modified metal and aldehyde aerosol levels but in inconsistent directions that will require further investigations.

Conclusions: This study highlights the importance of evaluating the combined risk of exposure to metals and aldehydes, including carcinogenic compounds in e-cigarette aerosol. Analyses are underway to evaluate the potential exceedance of health limits and standards for inhalation exposure. The release of harmful contaminants, including crotonaldehyde, a possible carcinogen may be influenced by both sugary flavors and device type. Additionally, while some devices and flavors might exhibit low concentrations of aldehydes, they could also exhibit high concentrations of metals, which emphasize the complex relationship between device types, e-liquid flavor, nicotine content, and country of purchase.

ABSTRACT NUMBER: 5112 **Poster Board Number:** LB213
TITLE: Comparative Toxicological Assessment of Heated Tobacco Product Aerosol Versus Combustible Cigarette Smoke Using *In Vitro* Regulatory Cytotoxicity and Genotoxicity Assays

AUTHORS (FIRST INITIAL, LAST NAME) AND INSTITUTIONS: *U. Doshi*[1], D. J. Smart[2], and S. J. Harbo[2].
[1]Altria Client Services LLC, Richmond, VA; and [2]JTI SA, Geneva, Switzerland.
KEYWORDS: Tobacco Products; Genotoxicity; Cytotoxicity

ABSTRACT: Background and Purpose: The tested heated tobacco product (HTP) (Ploom® System) consists of heated tobacco sticks (HTS) and a battery-powered tobacco heating device. We conducted comprehensive testing to assess its reduced risk potential relative to combustible cigarettes. As part of the nonclinical toxicity evaluation, HTP-derived aerosol fractions from four HTS varieties (two menthol and two tobacco) as well as counterpart smoke fractions from the 1R6F reference cigarette, were assessed for cytotoxic and genotoxic potential in a 21 CFR Part 58-compliant in vitro study. **Methods:** HTP-derived aerosol fractions, namely aerosol collected mass (ACM) and gas-vapor phase (GVP), were generated via the modified ISO 20778 puffing regimen, and maximally concentrated in accordance with the technical constraints of the aerosol generation and Cambridge filter pad and impinger collection methodology. 1R6F smoke fractions, total particulate matter (TPM) and GVP, were generated via the ISO 20778 puffing regimen and concentrated based on historical experience with the reference product. Cytotoxic potential was assessed via the neutral red uptake (NRU) assay using Chinese hamster ovary (CHO) cells. Genotoxic potential was assessed via two OECD Guideline-governed tests, the non-cytokinesis-block in vitro micronucleus (MNvit) assay, also in CHO cells, and the bacterial reverse mutation (Ames) assay. The results from this study were also compared with published HTP in vitro studies. **Results:** Using optimized concentration ranges and employing a triplicate experiment testing approach, the HTP-derived aerosol fractions demonstrated markedly reduced (6-13-fold) cytotoxic potency versus the smoke fractions from 1R6F in the NRU assay (half maximal inhibitory dose (IC_{50}) of 90.3 µg TPM/mL and 258 µg TPM equivalent/mL for 1R6F TPM and GVP fraction, respectively, versus 856-1197 µg ACM/mL and 1446-2178 µg ACM equivalent/mL for HTP variants ACM and GVP, respectively). Similarly, although ACM/TPM and GVP from both product types induced genotoxic responses across all three treatment schedules of the MNvit assay, the genotoxic potency of HTP aerosol fractions was ≥6-fold lower compared to the cigarette smoke fractions. In the Ames assay, significant evidence of mutagenicity was observed in the combustible cigarette smoke-sensitive Salmonella strains in response to 1R6F-derived TPM when evaluated in the presence of a rat liver S9 metabolizing system. By contrast, the HTP aerosol fractions were non-mutagenic when assessed up to the limit of cytotoxicity or with the maximal feasible concentration (at least 10-fold higher than the mutagenic concentrations of TPM). **Conclusions:** The HTP aerosol fractions induced both cytotoxic and genotoxic responses in the mammalian in vitro assays; however, the potency at which these effects

manifested relative to 1R6F-derived smoke fractions was approximately an order of magnitude lower. Furthermore, under the test conditions, ACM and GVP aerosol fractions from the HTP were non-mutagenic in the Ames assay, whereas 1R6F-derived TPM was mutagenic. While these findings emanate from a specific in vitro toxicological context, they biologically corroborate the mainstream emissions characterization data of both product types, which demonstrate an overall 90% reduction in the levels of harmful and potentially harmful constituents in the HTP aerosol compared to 1R6F cigarette smoke. These results are also consistent with the published scientific literature on other HTPs documenting reduced in vitro cytotoxic and genotoxic potential relative to cigarette smoke.

ABSTRACT NUMBER: 5113 **Poster Board Number:** LB214

TITLE: Enhanced Ames Test: A Framework to Improve Sensitivity and Reliability through Selection of Appropriate Vehicle Control Volumes, Positive Control Concentrations and TA97a Tester Strain over TA1537

AUTHORS (FIRST INITIAL, LAST NAME) AND INSTITUTIONS: *G. Joshi*, Y. Soman, S. Sen, N. Benisur, and P. Pansare. Intox Pvt. Ltd, Pune, India.

KEYWORDS: None

ABSTRACT: Background and Purpose: The enhanced Ames test is a modified version of the classical Ames test designed to detect mutagenic potential of N-nitrosamines and Nitrosamine drug substance-related impurities. Enhanced Ames Test protocols focus on improved metabolic activation and alignment with human biology. However, lack of standardized conditions, positive control concentrations, and vehicle volumes reduces the sensitivity and reliability of the test. Objectives were to determine the optimal vehicle volumes, concentrations of N-Nitrosodimethylamine and 1-Cyclopentyl-4-nitrosopiperazine, and compare mutagenic response of TA97a over TA1537. **Methods:** We evaluated Enhanced Ames Test conditions using tester strains Salmonella typhimurium TA97a, TA98, TA100, TA1535, TA1537 and Escherichia coli WP2 uvrA pKM101, with the objective of validating four vehicles-analytical grade water, dimethyl sulfoxide (DMSO), ethanol, and acetone for optimal mutagenicity testing of various N-nitrosamines. Cytotoxic effects due to increased incubation period with each vehicle was tested across volumes of 100 µL, 50 µL, and 25 µL to identify the most suitable conditions for maintaining assay integrity. Concurrent strain-specific positive controls and different concentrations of N-Nitrosamines i.e., N-Nitrosodimethylamine and 1-Cyclopentyl-4-nitrosopiperazine were assessed to determine the highest mutagenic response. The assays were evaluated under three conditions: without a post-mitochondrial fraction (S9), with 30% rat liver S9, with 30% hamster liver S9; with 30 minutes preincubation. **Results:** Acetone and ethanol were cytotoxic at volume of 100 µL for tester strains TA98, TA100, TA1535, and TA1537, however, no cytotoxicity observed in TA97a and *E. coli* WP2 uvrA pKM101. No cytotoxicity observed at 50 µL volume for all the tester strains. In the absence of metabolic activation, 0.25 µg/plate 4-Nitroquinoline-N-oxide (4NQO) induced over 2-fold increase in the number of revertant colonies for tester strains TA98, TA100, and *E. coli* WP2 pKM101. 2 µg/plate sodium azide induced 3-fold increase in the number of revertant colonies for tester strain TA1535. For strains TA1537 and TA97a, 1 µg/plate ICR-191 produced over 3-fold increase in the number of revertant colonies. In the presence of 30% rat liver S9 and 30% hamster liver S9, 5 µg/plate 2-Aminoanthracene (2AA) induced more than 3-fold increase in number of revertant colonies across all tester strains. N-Nitrosodimethylamine at the concentration of 250 µg/plate and 1-Cyclopentyl-4-nitrosopiperazine at concentration of 125 µg/plate resulted more than 3-fold increase in revertant colonies in tester strains

TA100, TA1535, and *Escherichia coli* WP2 pKM101 and no significant increase (less than 2-fold) in revertant colonies was observed for tester strain TA98. Additionally, results revealed that tester strain TA97a showed more than 2-fold increase in revertant colonies with N-Nitrosodimethylamine and 1-Cyclopentyl-4-nitrosopiperazine when exposed to 30% hamster S9 mix, while TA1537 exhibited no significant response (less than 2-fold) under same conditions, demonstrating higher sensitivity of TA97a. **Conclusions:** Strain specific positive controls are validated, including 4-Nitroquinoline-N-oxide for TA98, TA100, and *E. coli* WP2 pKM101 without metabolic activation system; sodium azide for TA1535 without metabolic activation system; ICR-191 for TA1537 and TA97a without metabolic activation system; and 2-aminoanthracene for all the tester strains with 30% rat and hamster S9. With this, we determined optimal concentrations of 250 µg/plate for N-Nitrosodimethylamine and 125 µg/plate for 1-Cyclopentyl-4-nitrosopiperazine. Furthermore, TA97a is preferred over TA1537 for N-Nitrosodimethylamine, and 1-Cyclopentyl-4-nitrosopiperazine due to higher sensitivity and reliability. Based on sensitivity of assay, we endorse using TA97a as mandatory tester strain due to its enhanced plasmid-mediated repair system, which incorporates the R-factor plasmid pKM101, thereby providing increased sensitivity and reliability.Based on results presented, we recommend using a 50 µL volume of ethanol or acetone if vehicle is other than water or DMSO, tester strain TA97a along with TA1537 and inclusion of strain specific positive controls as described above for conducting reliable Enhanced Ames test for N-nitrosamines.

ABSTRACT NUMBER: 5114 **Poster Board Number:** LB215
TITLE: Lung injury of acetaldehyde exposure combined with alcohol in rats

AUTHORS (FIRST INITIAL, LAST NAME) AND INSTITUTIONS: Y. Tian[1,2], H. Wang[1,2], X. Li[1,2], Y. Fu[1,2], S. Ma[1], W. Wang[1], X. Li[1], F. Lu[1], S. Han[1,2], L. Cui[1,2], H. Chen[1,2], H. Hou[1,2], and Q. Hu[1,2]. [1]China National Tobacco Quality Supervision & Test Center, Zhengzhou, China; and [2]Beijing Life Science Academy, Beijing, China.
Sponsor: *S. Jia*
KEYWORDS: Risk Assessment; Lung; Pulmonary or Respiratory System; Oxidative Injury; inflammation; acetaldehyde; alcohol

ABSTRACT: Background and Purpose: A majority of people who abuse alcohol also associated with smoke. For smoker, acetaldehyde is one of important constituents in smoke, which may be associated with an increased risk of certain diseases. The study aimes to evaluate the potential influence of acetaldehyde exposure with alcohol consumption. **Methods:** Rats were randomly divided into four groups depending on exposure concentration of acetaldehyde in rats administrated with alcohol. The exposure groups were administrated with alcohol (6 g/kg) by gavage for 4 weeks combined with different concentrations of acetaldehyde aerosol (15 mg/m^3, 45 mg/m^3, 135 mg/m^3) by nose only inhalation exposure system for 2 weeks (4 h/day). During the exposure period, body weight and food intake were collected and analyzed. After exposure, blood samples and lung were obtained and inflammation and histopathology were examined. **Results:** The results showed that compared with Sham group, no obvious changes were observed for the rats in exposure groups. However, with the increase of acetaldehyde exposure, lung injury was induced significantly evidenced by thickened alveolar wall and aggravated infiltration of inflammatory cells in lung. In addition, inflammation factors such as TNF-α, IL-6 were obviously expressed in the lung and the activities of SOD and GSH were reduced and the content of MDA was obvious induced, which induced the redox imbalance and oxidative stress. **Conclusions:** In summary, the oral administration of alcohol combined with different doses of

acetaldehyde inhalation resulted in obviously inflammation, oxidative stress and subsequently lead to the lung injury.

ABSTRACT NUMBER: 5115 **Poster Board Number:** LB216
TITLE: *In vitro* toxicological evaluation and comparison of nicotineenantiomersin human lung and nerve cells

AUTHORS (FIRST INITIAL, LAST NAME) AND INSTITUTIONS: H. Wang, Y. Tian, S. Han, S. Li, X. Li, Y. Fu, H. Chen, H. Hou, and Q. Hu. China National Tobacco Quality Supervision & Test Center, Zhengzhou, China.
KEYWORDS: Apoptosis; Cytotoxicity; Genetic Toxicology; Synthetic nicotine; nicotine and synthetic nicotine

ABSTRACT: Background and Purpose: Synthetic nicotine (R-nicotine and (R,S)-nicotine) in e-liquids is gradually replacing natural nicotine (S-nicotine) and is expected to gain significant future market share. However, the toxicological risks of synthetic nicotine are still largely unknown. **Methods:** This study aims to reveal the toxicological profile of synthetic nicotine and synthetic nicotine based on human lung and neural cells, including cytotoxicity, genotoxicity, oxidative stress, mitochondrial damage and apoptosis. **Results:** The results showed that: (1) Cytotoxicity: the toxicity of all nicotine enantiomers to SH-SY5Y was greater than that of NCI-H292. The toxicity of R-nicotine was the highest in NCI-H292 cells, and S-nicotine was the highest in SH-SY5Y cells; (2)Genotoxicity: all nicotine enantiomers did not cause an increase in the risk of DNA damage and chromosome damage of the two cells; (3)Oxidative stress: all nicotine enantiomers did not increase ROS formation, but decrease GSH content in the two cells;(4) Mitochondrial damage: all nicotine enantiomers did not cause mitochondrial damage in the two cells; (5) Apoptosis: all nicotine enantiomers increased the level of caspase 3/7, but did not affect the permeability of cell membrane and phosphorylated C-jun level in the two cells. **Conclusions:** Overall, the differences in toxicological risks among different nicotine enantiomers do not appear to be significant.

ABSTRACT NUMBER: 5116 **Poster Board Number:** LB217
TITLE: The US EPA's IRIS toxicological review of inorganic arsenic: noncancer and cancer health outcomes and derived toxicity values

AUTHORS (FIRST INITIAL, LAST NAME) AND INSTITUTIONS: *J. S. Lee*[1], A. Davis[2], *I. Druwe*[1], J. Gift[1], E. Kirrane[1], A. Lee[1], T. Luben[1], M. Powers[2], R. M. Shaffer[2], and *K. Thayer*[1]. [1]US EPA, Research Triangle Park, NC; and [2]US EPA, Washington, DC.
KEYWORDS: Risk Assessment; Hazard Identification/Reduction; Dose-Response; Arsenic

ABSTRACT: Background and Purpose: Inorganic arsenic (iAs, CASRN 7440-38-2) is a naturally occurring compound that can be found in water, food, soil, and air. In addition, iAs can be released into the environment through industrial processes and emissions. Exposure to iAs is possible via ingestion of drinking water and food, inhalation of air, and dermal contact. In January 2025, US Environmental Protection Agency (EPA)’s IRIS program finalized a health assessment for iAs. This assessment was developed at the request of multiple EPA National and Regional Programs. **Methods:** The methods used in the assessment were summarized in the iAs Protocol and reviewed by the National Academies of Sciences, Engineering, and Medicine (NASEM; formerly the National Research Council). Skin, bladder, and lung cancer and skin lesions were considered accepted hazard outcomes for iAs based on previous assessments by EPA and other health agencies. EPA previously classified arsenic as carcinogenic to

humans based on epidemiological evidence, and that classification was retained in the current assessment. For these outcomes, the focus of this assessment was to update quantitative estimates of cancer risk. Additionally, new evidence synthesis conclusions were developed for noncancer effects of the circulatory system, fetal, newborn, and infant health outcomes, developmental neurocognitive effects, and diabetes based on the review of the available epidemiological evidence, as recommended, and supported by the NASEM. Traditional noncancer (i.e., the Reference Dose (RfD) and organ- or system specific RfDs (osRfDs)) and cancer (i.e., oral slope factors (OSF)) toxicity values were derived to meet the statutory requirements of stakeholders. In addition, probabilistic toxicity values (i.e., risk-at-a-dose values) were presented to allow users of the iAs assessment to estimate lifetime extra risk for individual endpoints at different iAs exposure levels (e.g., several-fold above the final RfD). A Bayesian dose-response meta-analysis was used to derive toxicity values for bladder cancer, lung cancer, diseases of the circulatory system (DCS), and diabetes. **Results:** On the basis of a robust epidemiological evidence base, the currently available evidence demonstrated that iAs causes DCS and diabetes in humans given sufficient exposure conditions. For DCS, the support for this hazard conclusion included evidence of increased ischemic heart disease (IHD) and hypertension, as well as related cardiovascular disease endpoints of atherosclerosis and repolarization abnormalities (e.g., QT prolongation). For diabetes, the supporting evidence included increased incidence of type 2 diabetes mellitus. An evidence synthesis judgment of moderate was reached for fetal, newborn, and infant health outcomes and developmental neurocognitive effects, and the currently available evidence indicated that iAs likely causes fetal, newborn, and infant health outcomes and developmental neurocognitive effects in humans given sufficient exposure conditions. For fetal, newborn, and infant health outcomes, the supporting evidence for this hazard conclusion included increased fetal and infant mortality, decreased fetal and post-natal growth, length of gestation, and birth weight. For developmental neurocognitive effects, the supporting evidence included cognitive and behavioral deficits in children and adolescents. **Conclusions:** For noncancer effects, candidate osRfDs of 0.058 µg/kg-day and 0.057 µg/kg-day were estimated for IHD and diabetes, respectively. For fetal, newborn, and infant health outcomes and developmental neurocognitive effects, candidate RfD toxicity values of 0.079 µg/kg-day and 0.105 µg/kg-day were estimated, respectively. Overall, an RfD of 0.06 µg/kg-day based on increased incidence of diabetes and IHD in humans was selected.Mean lifetime extra risks of 7.9 and 10.1 were estimated for bladder cancer and lung cancer, respectively, for a hypothetical U.S. cohort of 10,000 individuals exposed for a lifetime at the U.S. drinking water standard of 10 µg/L. A combined cancer slope factor of 3.17×10^{-2} $(\mu g/kg\text{-}day)^{-1}$ (valid for daily intakes less than 0.2 µg/kg-d) was also estimated. For the non-cancer endpoints, mean lifetime extra risks of 110 and 129 were estimated for IHD and diabetes, respectively, for a hypothetical U.S. cohort of 10,000 individuals exposed for a lifetime at the U.S. drinking water standard of 10 µg/L.

ABSTRACT NUMBER: 5117 **Poster Board Number:** LB218

TITLE: Component-based toxicological screening of black pepper fruit (*Piper nigrum*) essential oil and a safe-supported exposure limit for healthy adults

AUTHORS (FIRST INITIAL, LAST NAME) AND INSTITUTIONS: J. T. Dawson[1], D. T. Carter[1], D. I. Saavedra[1], S. A. Shah[1], A. Poudel[2], P. Satyal[2], and C. Bascoul[1]. [1]Product Safety, doTERRA, Pleasant Grove, UT; and [2]Essential Oil Science, doTERRA, Pleasant Grove, UT. Sponsor: *C. Mitchell*

KEYWORDS: Safety Evaluation; Risk Assessment; Natural Products; black pepper essential oil

ABSTRACT: Background and Purpose: Dose response assessment is an important application of toxicology used in translational medicine and human health risk assessment. While sufficient evidence for dose response assessment is available for many discrete compounds, the toxicology of most natural complex substances (NCS) is understudied. In cases where insufficient data is available on the whole NCS, risk assessment protocols instruct evaluation of the NCS on a component basis. Component based dose response assessments can be performed when the material composition of an NCS is sufficiently characterized and adequate toxicological endpoint data is available on the constituents. For this research, a component-based assessment of the systemic toxicity of black pepper (*Piper nigrum*) fruit essential oil was performed to determine oral and dermal exposure limits for use in human health risk assessment. **Methods:** Black pepper essential oil was characterized using gas chromatography mass spectrometry analysis of 41 authenticated material lots. Constituents were organized into toxicological groups and descriptive statistics were derived for each compound group by calculating the mean, median, minimum, maximum, and standard deviation. Toxicological data was evaluated for all constituents ≥1% in black pepper oil as well as many minor compounds <1% for which relevant toxicological data was available. Constituents for which there was insufficient data to determine a point of departure (POD) were considered not assessed for that endpoint. POD values were obtained from toxicological risk assessments and safety dossiers. Reference doses (RfD) for nongenotoxic compounds and derived minimal effect levels (DMEL) for genotoxic carcinogens were calculated using NOAEL and BMDL10 values, respectively. The normalized percentage of assessed compounds was calculated for each constituent. Risk-based exposure limits for the NCS were calculated for each constituent by dividing the constituent's RfD or DMEL value by its relative percentage in the whole material. From there, an adult safe-supported daily exposure value for the NCS was determined, as defined as the greatest exposure to the material from a discrete route of administration that does not exceed the risk-based exposure limit for any constituent. **Results:** Major constituents identified in black pepper essential oil from 10-25% include beta-caryophyllene, limonene, alpha-pinene, beta-pinene, and 3-carene. Other constituents from 1-10% include elemene, germacrene D, alpha-phellandrene, myrcene, selinene, and humulene. Overall, 73.9% and 85.2% of the constituents in black pepper essential oil had sufficient data to evaluate systemic toxicity and genotoxicity, respectively. No genotoxic compounds were identified. The primary exposure-limiting constituent for systemic toxicity was alpha-phellandrene. Assuming a dermal absorption value of 100% for alpha-phellandrene, the adult safe-supported exposure limit for black pepper oil was determined to be 317 mg/person/day for oral and dermal routes combined. **Conclusions:** Despite its widespread use as a food flavor, to our knowledge, a safe-supported limit for human exposure to black pepper essential oil has not been established. While Ames and in vivo micronucleus testing show negative genotoxicity results for black pepper oil, no repeated dose toxicity studies have been performed. This component-based assessment of black pepper essential oil supports a safe adult exposure limit of 317 mg/person/day (5.3 mg/kg bw/day) via oral and dermal routes combined restricted by the primary exposure limiting compound alpha-phellandrene. Note, that read-across data was not included in this analysis unless read-across was used to derive POD values in reputable toxicological risk assessments. Additionally, thresholds of toxicological concern and Cramer classifications were not considered. Further assessment is necessary to determine if the limit identified in this assessment is appropriate for sensitive populations. Given the GRAS status of black pepper oil, this research may be used to inform posology in pilot and exploratory clinical trials in healthy adult subjects and in human health risk assessments.

ABSTRACT NUMBER: 5118 **Poster Board Number:** LB219
TITLE: Chlorine dioxide as an effective agent for bioaerosol mitigation in critical facilities

AUTHORS (FIRST INITIAL, LAST NAME) AND INSTITUTIONS: S. Purohit, *M. Bourgeois*, G. Lukasik, and *R. Harbison*. College of Public Health University of South Florida, Tampa, FL.
KEYWORDS: Risk Assessment; Infection; Agents

ABSTRACT: Background and Purpose: Large-scale disinfection is essential in laboratories and operating rooms to ensure sterility during procedures. While ethylene oxide is widely used as a disinfectant, its application poses significant risks due to its flammability and carcinogenic properties. This study aimed to evaluate chlorine dioxide as an alternative disinfectant, emphasizing its non-carcinogenic nature and shorter disinfection cycle. Through comprehensive testing, the research focused on assessing the efficacy of chlorine dioxide in mitigating bioaerosols when integrated with air filtration systems. The findings contribute to understanding chlorine dioxide's potential as a safer and efficient disinfection method for critical indoor environments. **Methods:** This study evaluated the efficacy of chlorine dioxide in reducing bioaerosols under controlled laboratory conditions. A single jet atomizer operating at 35 PSI produced bioaerosols within a 742-cubic-foot chamber at 24-26°C and 40-50% relative humidity for 75 minutes. Air samples were collected at intervals of 0, 30, 60, 90, 120, and 180 minutes to assess natural decay and chlorine dioxide-mediated reductions. Aspergillus versicolor, Staphylococcus epidermidis, and Bacillus atrophaeus endospores were tested under identical conditions. A BioSampler Liquid Impinger (SKC Ltd) was used to collect 120 liters of chamber air in 20 milliliters of sterile Phosphate Buffered Saline (PBS). The results provided insights into the natural decay rates and the enhanced reduction of bioaerosols with chlorine dioxide-based filters. **Results:** In 30 minutes, the bioaerosol reduction for Aspergillus versicolor exceeded 98.95 percent and remained at 99.99%. Additionally, the filter's ability to reduce S. epidermidis bioaerosol was above 99.99 percent in 90 minutes and continued for 180 minutes. The reduction of Bacillus endospores was 99.3% in 180 minutes using the chlorine dioxide filters, and 99.99 percent in 180 minutes utilizing chlorine dioxide filters and HEPA filtration at the same time. **Conclusions:** The bioaerosol for Bacillus atrophaeus endospore, Staphylococcus epidermidis, and Aspergillus versicolor was significantly decreased by chlorine dioxide filters. At the end of 180 minutes, it had reached 99.9% for every microorganism tested. This research demonstrates that chlorine dioxide is a strong disinfecting agent for microorganisms and can be used for a large sterilization room, operation theatre and laboratory settings with added safety of being non carcinogenic and can be deployed in 90 to 180 minutes.

ABSTRACT NUMBER: 5119 **Poster Board Number:** LB220
TITLE: Evaluation of the Exposure of Various US Populations to Formaldehyde

AUTHORS (FIRST INITIAL, LAST NAME) AND INSTITUTIONS: R. Hyde, A. Hurtado Olson, N. An, C. Barlow, J. Ethan, C. Morton, A. Pulley, M. Thomas, J. Wiggins, and J. Wilkins. University of Maryland, College Park, MD. Sponsor: *A. Kadry*
KEYWORDS: Risk Assessment; Epidemiology; Carcinogenesis; Formaldehyde

ABSTRACT: Background and Purpose: Formaldehyde has both natural and anthropogenic sources, with composite wood products being the most common anthropogenic source of exposure. The primary route of formaldehyde exposure is inhalation. According to recent publications by the U.S. Environmental Protection Agency (EPA), inhaled formaldehyde can cause significant health effects in

humans, particularly respiratory effects. Children and individuals with preexisting respiratory conditions are especially vulnerable. Formaldehyde is classified as carcinogenic to humans via inhalation exposure. The noncancer reference concentration (RfC) for formaldehyde is 0.007 mg/m^3, with high confidence in this value. The cancer inhalation unit risk (IUR) is 1.1×10^{-5} per µg/m^3 (equivalent to 1.1×10^{-2} per mg/m^3), and the confidence in the IUR is medium. While inhalation is the predominant route of exposure, there is also a smaller but notable risk of dermal absorption. Formaldehyde exposure has been linked to increases in allergy and asthma symptoms, as well as adverse effects on reproductive health in both males and females. Developmental health impacts have also been observed in females. Furthermore, inhalation exposure has been associated with neurotoxic effects, including increased symptoms of amyotrophic lateral sclerosis (ALS), which may lead to severe outcomes, including death. This investigation aims to study the role of demographics and socioeconomic status in formaldehyde exposure across various populations in the United States. **Methods:** The National Health and Nutrition Examination Survey (NHANES), conducted by the Centers for Disease Control and Prevention (CDC), is a critical program that assesses the health and nutritional status of the U.S. population. By combining interviews, physical examinations, and laboratory tests, NHANES generates comprehensive data on various health issues, including chronic diseases, environmental exposures, and dietary patterns. In this study, we analyzed formaldehyde concentration data from two NHANES cycles (2013-2014 and 2015-2016) to investigate the potential influence of demographics and socioeconomic status on reported formaldehyde levels. Statistical analyses included measures of central tendency, analysis of variance (ANOVA), and t-tests. Additionally, a Tukey post-hoc test was conducted to adjust for multiple comparisons and ensure robust results. **Results:** This initial analysis of formaldehyde concentrations across various demographic groups revealed that age had a slight and statistically insignificant effect on formaldehyde levels. Similarly, gender did not significantly influence formaldehyde concentrations, suggesting that biological sex is not a key determinant in formaldehyde disposition. However, annual income was found to significantly impact formaldehyde exposure, highlighting the critical role of socioeconomic status in shaping exposure levels. Notably, significant differences were observed among racial groups, suggesting that race may also be an important determinant of formaldehyde exposure. These findings emphasize the complex interplay of socioeconomic and demographic factors in influencing environmental exposure levels, with socioeconomic variables, such as income, potentially exerting a more substantial influence than age or gender. **Conclusions:** This study highlights the multifaceted factors influencing formaldehyde exposure in the U.S. population, with data from NHANES cycles (2013-2014 and 2015-2016) providing critical insights. While age and gender were found to have statistically insignificant effects on formaldehyde concentrations, annual income emerged as a significant determinant, underscoring the role of socioeconomic status in shaping environmental exposures. Additionally, significant differences among racial groups suggest that race may also contribute to disparities in formaldehyde exposure. These findings reinforce the importance of addressing socioeconomic and demographic inequities in exposure assessments and public health interventions. A more thorough comparison of educational levels to racial and income groups is warranted as finding more specific demographics that have lower exposure to formaldehyde allows for additional shared characteristics and variables to be pursued between them. Further research is needed to lower formaldehyde exposure to prevent cancerous and non-cancerous effects.

ABSTRACT NUMBER: 5120 **Poster Board Number:** LB221
TITLE: Assessment of potential ecological risk for microplastics in freshwater ecosystems

AUTHORS (FIRST INITIAL, LAST NAME) AND INSTITUTIONS: *H. Moon*, S. Bae, and *J. Park*. Korea Institute of Toxicology, Jinju-si, Korea, Republic of.
KEYWORDS: Risk Assessment

ABSTRACT: Background and Purpose: From 1950 to 2018, plastic consumption has increased approximately 180 times. In particular, the increased demand for single-use plastics (e.g., disposable and protective products) during the COVID-19 pandemic has led to a significant increase in plastic waste. In general, engineered plastics have been developed using unrefined petroleum, combustible gases, and coal, mixed with organic compounds such as semi-synthetics (petrochemicals, partly natural) to form soft and flexible plastics. Urbanization, economic development, and population growth are the main causes of increased plastic waste, which - through their excessive use and inappropriate disposal - lead to serious environmental and health problems. However, their risk assessment to freshwater ecosystems has not been clearly investigated. Risk assessment has been constrained by the absence of microplastic (MP) concentration in some environment, the diverse types and shapes of MPs, and limitations of polystyrene (PS)-biased toxicity studies. This study examined exposure to MPs in rivers and lakes worldwide, located in: China (the Three Gorges Dam & Yangtze River; the lakes of Wuhan city), Vietnam (seven lakes of Da Nang city), Europe (the Rhine River); Finland (Kallavesi Lake), Argentina (nine lakes in the Patagonia region), Brazil (Guaiba Lake), and South Korea (Nakdong River, Han River, and Anyang Stream), and assessed the risks to aquatic ecosystems based on MP toxicity information and morphology. We also examine the limitations of the traditional risk quotient (RQ)-based risk assessment method for PS-biased toxicity studies. Potential ecological risks were assessed using pollution load index (PLI) and potential ecological risk index (PERI) considering the hazard scores of MP types. **Methods:** Toxicity data for PS-MPs in aquatic ecosystems were selected from Google Scholar and the Toxicity of Microplastics Explorer (ToMEx) database (https://microplastics.sccwrp.org/). Toxicity data were assigned according to standard testing guidelines recommended by the USEPA. Species sensitivity distribution (SSD) analysis was conducted for PS-MP using the SSD generator. Toxicity data for PS were available for nine aquatic species, which satisfied the recommendations of the European Union technical guidance document for the endpoint, study period, and taxa. The potential ecological risk of PS-MPs was assessed via the widely used RQ method. The level of MP pollution in surface waters was assessed using the PLI and PERI. To analyze the prevalence of MPs, we conducted PCA based on the PLI and PERI values for the morphology of MPs using MATLAB software as multivariate analysis tool. **Results:** RQ was approximately 10^{-6} to 10^{-4}, indicating negligible risk to aquatic organisms. In contrast, the calculated PLI (> 30: extreme danger) and PERI (> 1200: extreme danger) values suggest that MPs represent serious ecological threats at all the study locations. Furthermore, principal component analysis (PCA) indicated that MP fibers and fragments have a significant impact on the risks for freshwater systems. These MP morphologies derive from surrounding fishing and agricultural activities, and household and clothing industries. The areas surrounding these rivers and lakes are expected to become more densely populated, potentially leading to increased MP emissions and higher risks, suggesting a need to expand wastewater treatment facilities, reduce consumption of sigle-use plastics, and raise societal awareness of waste plastics. **Conclusions:** The results of this study show that: (i) Traditional RQ-based methods are of limited utility for assessing the risks associated with MPs (covering only a few types; PS); (ii) PLI and PERI values indicate that MPs in rivers and lakes of major cities worldwide pose serious ecological

threats to aquatic life; and (iii) PCA indicates that the greatest ecological threat results from MPs in the form of fibers and fragments, which originate from surrounding fishing and agricultural activities, and household and clothing industries. It should be noted that when assessing the risk of MPs, PLI should be evaluated together with PERI because the results differ according to the choice of MP background concentration (the lowest MP concentration). The areas surrounding these rivers and lakes (TGD & YR, WL, 7UL, RR, KL, 9LP, GL, NR, HR, and AS) are expected to experience higher population densities, potentially increasing MP emissions and risks. Therefore, the protection of aquatic biodiversity around these areas would require the construction of wastewater treatment plants capable of filtering MP emissions. In addition, there is a need to reduce consumption of single-use plastics and to raise societal awareness in order to reduce their disposal into freshwater ecosystems.

ABSTRACT NUMBER: 5121 **Poster Board Number:** LB222

TITLE: Re-examining the key characteristics of cancer for metallic elements: Lines of evidence to support mechanisms of action leading to a threshold model for carcinogenic response

AUTHORS (FIRST INITIAL, LAST NAME) AND INSTITUTIONS: *R. Sloboda*[1], and *K. Connor*[2]. [1]Nelson Labs, LLC, Salt Lake City, UT; and [2]Watertown, MA.

KEYWORDS: Carcinogenesis; Genotoxicity; Risk Assessment

ABSTRACT: Background and Purpose: Research into the carcinogenicity of metallic elements has identified a diverse array of putative mechanisms of action (MOA) leading to cancer, and for a select few, evidence for a MOA has provided support for a model of carcinogenicity that informs the human health risk assessment. Still, the involvement of multiple MOA and their possible interactions often obscures the identification of a single MOA that can be regarded as pivotal. As examples, some metals have well-established epigenetic mechanisms of action, but with concurrent reactive oxygen species (ROS) generation, impairment of DNA repair mechanisms, and/or immunological effects. The present analysis was undertaken to identify common factors and unifying themes in metal carcinogenicity that may help to improve the scientific basis for risk assessment. **Methods:** A literature review of mechanisms of genotoxicity and carcinogenicity for various metals has found that some elements are genotoxic, but not mutagenic, in vitro or in vivo only at high dose and in some cases, carcinogenicity has an exclusive association with a specific route of exposure, or a specific chemical species, or are characterized by a special human susceptibility (e.g., a certain genetic makeup). As exemplified by cobalt, selective carcinogenicity via inhalation may be related to cytotoxicity and chronic inflammation (threshold effects) which are necessary for inducing hyperplasia that may progress to cancer. Further, pathological processes leading to ROS damage have been more intensively studied in the lungs, where molecular oxygen, a precursor to ROS, is abundant. **Results:** Few, if any, metals appear to be direct-acting mutagens, but many operate through a hypothesized epigenetic mode of action, often based on the activity of a particular elemental species. Many also require biotransformation to gain entry to the site of target cells and at levels which overwhelm the binding capacity of specific blood proteins. Non-genotoxic carcinogens may act through mechanisms such as the activation of redox-sensitive transcription factors, production of reactive oxygen species (ROS), peroxisome proliferator-activated receptor (PPAR-α) activation, hormonal perturbation, immunosuppression, inhibition of DNA repair, or cytotoxicity-inducing mechanisms. Further, preneoplastic changes such as cell hypertrophy/hyperplasia, persistent tissue injury with chronic inflammation, and immunological signaling are often requisite changes preceding cancer and typically have a higher dose requirement. **Conclusions:** Metallic elements

with demonstrated genotoxic and carcinogenic potential include arsenic, antimony, beryllium, cadmium, chromium, cobalt, mercury, and nickel; however, most metals do not induce point mutations, and as such do not cause genetic alterations that are self-replicating. In addition, certain metals are not currently classified as carcinogenic, but display limited genotoxic potential, such as aluminum, vanadium, and tungsten. Based on the weight of evidence, US EPA has developed cancer slope factors for inhalation but not for the oral route of exposure for several metals, including cadmium, beryllium, cobalt, and certain compounds of nickel and vanadium. While metals were initially assumed to be non-threshold carcinogens, a closer look at recent literature suggests that several metals are likely to be associated with a threshold-based response, such as cobalt, nickel, and antimony. For these and other metals with a carcinogenic classification, there are key MOA which are associated with a threshold-based response. Importantly, because of significant differences in estimated cancer slope (potency) factors for non-threshold versus threshold carcinogens, it is important to examine the evidence for a MOA when estimating the carcinogenic potential for a metal of toxicological interest.

ABSTRACT NUMBER: 5122 **Poster Board Number:** LB223
TITLE: Development of a brodifacoum inhalation model in Norway rats

AUTHORS (FIRST INITIAL, LAST NAME) AND INSTITUTIONS: E. Johnson, A. Methvin, T. McClymont, *M. Ellis*, *J. Leighton*, J. Janssen, N. Benn, M. Chavez-Vazquez, and O. Altstadt. USAMRICD, Aberdeen Proving Ground, MD.
KEYWORDS: Toxicity; Acute; In Vivo Models; superwarfarin

ABSTRACT: Background and Purpose: Superwarfarins (SW), such as brodifacoum (BDF), are widely available rodenticides that can cause persistent anticoagulation via vitamin K cycle disruption in humans lasting weeks or longer. Exposure to SW is traditionally via oral ingestion and occurs as single cases. Recently, mass exposures by inhalation have become a major concern after hundreds of cases of varying severity, ranging from mild coagulopathy all the way to death, have been reported in individuals who inhaled BDF-laced synthetic cannabinoid products. This method of distribution is novel and there are currently no existing models for or toxicological data on inhalation exposure to BDF. To study these effects, an inhalation model was developed using the Norway rat as this strain is shown in the literature to produce the most perceptible and diffuse hemorrhaging, which is an expected toxic effect of BDF exposure and is small enough to use in standard inhalation chambers. This translates to higher clinical relevance with physical symptoms that more closely reflect a human casualty. **Methods:** Male Norway rats were exposed to various concentrations of aerosolized BDF dissolved in polyethylene glycol in a closed-loop inhalation device to determine the median lethal concentration (LCt_{50}) and median lethal dose (LD_{50}) of inhaled BDF. **Results:** Results thus far have shown mortality can occur at a 5-day timepoint with a dose higher than 1mg/kg, and 69% mortality by a 7-day timepoint in stepped doses from 0.5mg/kg to 2 mg/kg range. Our goal is to further refine the dosing until we achieve a four-day post-exposure timepoint of death to align more closely with extant oral dosing studies for comparison. Observations on weight, clinical manifestations, mortality (including both lethality frequency and latency to death), nesting status, posture, and any potential signs of hemorrhage were taken up to day 7 post exposure or when euthanasia criteria were met. **Conclusions:** A model of BDF inhalation exposure in Norway rats has been created to further study treatment options for SW exposures.

ABSTRACT NUMBER: 5123 **Poster Board Number:** LB224
TITLE: Behavior of the Pyrethroid Insecticide Cypermethrin in Lactating Goat using a Radiotracer Technology

AUTHORS (FIRST INITIAL, LAST NAME) AND INSTITUTIONS: K. Ahn, A. Bautista, and B. Osterman. Eurofins Agroscience Services, Hercules, CA.
KEYWORDS: Behavior; Biotransformation; Metabolism

ABSTRACT: Background and Purpose: Cypermethrin is a synthetic pyrethroid insecticide used in agriculture, public health, and animal husbandry. Radioactive [Cyclopropane (CY)-^{14}C] and [Phenoxy (PH)-^{14}C]cypermethrin (a mixture of *cis* and *trans* isomers) was orally dosed at 10 mg/kg feed to lactating goats daily for five days to characterize the cypermethrin-derived residues in goat tissues, milk, urine and feces. **Methods:** Urine, feces, and milk were daily collected during the dosing. Gastrointestinal (GI) tracts, liver, kidney, flank and loin muscle tissues, and omental, subcutaneous and renal fat tissues were obtained at sacrifice. Total radioactive residue (TRR, expressed as equivalent concentration) was determined using a liquid scintillation counter. HPLC with radiodetection was performed to provide a metabolic profile. **Results:** Average recovery of radiolabel in goats (excepting carcass) was 89.2% and 86.4% of the administered dose for the CY and PH labels, respectively. Most of the administered dose was recovered in the urine (52.9%), feces (21.1-22.6%) and the gastrointestinal tracts at sacrifice (12.4-13.3%). Other tissues including milk contained a total of ≤ 0.2% of the dose. TRR in liver and kidney was highest (> 0.05 mg/kg). TRR in fat tissues and milk fat was generally higher (0.01- 0.05 mg/kg) than that (0.01 - 0.02 mg/kg) in protein-related muscle tissues and skim milk. Cypermethrin was detected in milk fat and all fat tissues, but no cypermethrin was detected in muscle tissues. Examination of the isomeric composition of cypermethrin in tissue extracts showed an increase in the total cis isomer composition and a corresponding decrease in the total trans isomer composition. *Trans* isomer composition of cypermethrin was rapidly degraded. **Conclusions:** Initial cleavage of cypermethrin and oxidation of the cyano group on the phenoxy-benzyl moiety results in formation of cis/trans-DCVA acid and 3-phenoxybenzoic acid (3-PBA). DCVA acid forms glucuronide conjugates (both isomers). 3-PBA forms glycine and ethyl ester conjugates. Free residues were also observed in urine and feces. It suggests excretion of free acid and conjugated metabolites.

ABSTRACT NUMBER: 5124 **Poster Board Number:** LB225
TITLE: Cytotoxicity Assessment of Occupational Pesticide Exposure in Latina Farmworkers Through Personal Silicone Wristband Sampling

AUTHORS (FIRST INITIAL, LAST NAME) AND INSTITUTIONS: *L. C. Magaña*[1], *C. Abuede*[1], O. E. Cruz[2], A. Early[1], K. Soriano[1], C. Manabat[1], E. Hoh[1], and N. I. López-Gálvez[1]. [1]San Diego State University, San Diego, CA; and [2]Lideres Campesinas, Oxnard, CA.
KEYWORDS: Cell Culture; Toxicity; Acute; Cytotoxicity; Farmworkers

ABSTRACT: Background and Purpose: Occupational exposures and health-related outcomes in agricultural laborers, particularly Latina farmworkers, remain understudied. Latina farmworkers in the Imperial Valley are routinely exposed to multiple pesticides. These farmworkers are often unaware of the potential health risks associated with chemical exposures. This study aims to evaluate the cytotoxic effects of these agricultural and environmental exposures using an *in vitro* model to better understand the potential health risks posed to this vulnerable population. **Methods:** Silicone wristbands were used

as passive samplers to assess occupational chemical exposures among 80 Latinas (n=40 farmworkers, n=40 non-farmworkers) who were 40 years and older and residing in Imperial County, California. First, a chemical extraction method was optimized utilizing a blank silicone wristband. The wristband was cut into one-fourth segments (0.6-0.9 g) and extracted using a 1:1 hexane:acetone solvent mixture under three temperature and nitrogen flow conditions: (1) 40°C with nitrogen directed towards the glass container, (2) 55°C with nitrogen directed towards the glass container, and (3) 55°C with nitrogen directed away from the glass container. The extracts underwent sonication for 15 minutes, followed by solvent evaporation to dryness under a nitrogen stream. The dried extracts were reconstituted in 35 µL dimethyl sulfoxide (DMSO) and stored at -20°C for further analysis. The MCF-10A cell lines were exposed to five serial dilutions (1X, 3X, 10X, 30X, and 100X) of the extracts to assess cytotoxicity and cell viability. A Multi-Tox Glow Multiplex Assay was performed to evaluate cellular responses. Second, the 80 participant wristbands were extracted individually for *in vitro* culture. After optimizing the chemical extraction protocol, cells were exposed to the extracts for cytotoxicity and cell viability assessment. Extract cytotoxicity levels were benchmarked to ensure cell viability above 70% for downstream analysis. **Results:** The 55°C extraction condition with nitrogen directed towards the glass provided the most consistent analyte recovery with minimal degradation. Preliminary results demonstrated differential cytotoxic responses between participants, with extracts from farmworkers showing a significant difference in cytotoxicity than non-farmworkers. Cell viability levels met the threshold for further CALUX assay testing to evaluate thyroid hormone receptor β (TR) antagonism, androgen receptor (AR) antagonism, and estrogen receptor α (ER) agonism. **Conclusions:** This study provides critical insights into occupational pesticide exposure among Latina farmworkers and establishes a foundation for future bioassay applications using passive sampling with silicone wristbands for agricultural laborers. The findings support the need for targeted interventions to reduce agriculture-related occupational exposures and implement regulatory policies to mitigate exposure risks in this underserved population. Future research will identify common chemicals in extracts and further assess endocrine disruption potential using CALUX assays in both MCF-10A and MCF-7 cell lines to fill data gaps and evaluate links to adverse health outcomes, such as breast cancer, in Latina farmworkers.

ABSTRACT NUMBER: 5125 **Poster Board Number:** LB226

TITLE: Development of an *in vitro* lung-on-chip model and gene-expression signature for assessing immune-mediated changes to vascular permeability by cytokine drug candidates

AUTHORS (FIRST INITIAL, LAST NAME) AND INSTITUTIONS: *B. Bhatt*, K. Schmunk, G. Raggi, *L. Froment*, *A. Podtelezhnikov*, *K. Tanis*, *N. Hobi*, *N. Li*, and *R. Gonzalez*. Merck & Co, Rahway, NJ.

KEYWORDS: Immunotoxicology; In Vitro and Alternatives; Lung; Pulmonary or Respiratory System

ABSTRACT: Background and Purpose: Vascular Leakage Syndrome (VLS) is characterized by an increase in capillary permeability accompanied by a progressive extravasation of fluids and proteins which often result in edema and organ failure. Several cytokines and cytokine mutein therapy candidates, including tumor necrosis factor α (TNFα) and interleukin-2 (IL-2), have been reported to induce VLS in humans via primary or secondary immune-mediated effects on the endothelium. Historically, endothelial cell-based in vitro assays have been developed to inform on the potential for drug-induced vascular permeability changes. While showing some promise in detecting agents which directly impact endothelial functions (e.g., TNFα), most of these systems were known to be less sensitive to cytokine-induced endothelium damage through secondary immune activation mechanisms such as IL-2. In the present study, a ^{AX}Lung-

on-chip model was established using a trans-well based co-culture system comprising human primary pulmonary epithelial and endothelial cells alongside peripheral blood mononuclear cell (PBMC). The utility of the model was assessed for detecting primary and secondary immune-mediated changes in vascular permeability. Furthermore, cytokine production and gene-expression changes were analyzed to uncover potential mechanisms underlying the differential effects of cytokines. **Methods:** Human umbilical vein endothelial cells (HUVECs) were cultured on the AX-chip with or without the addition of epithelial cells to allow for the formation of a monolayer with tight junctions. These chips were treated with either cytokines directly, or co-cultured with PBMCs for up to 72 hours. Permeability changes were evaluated by TEER measurements and FITC-Dextran permeability assessment. Supernatant was collected at 24, 48 and 72 hours to measure cytokines and cells were harvested at 72 hours for gene expression analysis using standard genome-wide RNA-Seq protocols from total RNA extracted. **Results:** Results showed that treatment with TNFα (up to 0.3 ug/mL) in HUVEC cells with or without epithelial cells and IL-2 (up to 1 ug/mL in the presence of PBMCs) in HUVEC cells with epithelial cells induced a dose-dependent increase in permeability after a 24-hour incubation, demonstrated by a decrease in TEER measurements and an increase in fluorescently labeled dextran across the cell monolayer. HUVEC cells treated with IL-2 (up to 1 ug/mL in the presence of PBMCs) in the absence of epithelial cells did not induce permeability changes, suggesting that the addition of epithelial cells also play a role in the mechanism for indirect permeability changes induced by cytokines. There was an increase in interferon gamma (IFNγ) and IL-1β cytokines in cells treated with IL-2 in the presence of PBMCs. There was also an increase in IL-1β, IL-6, IL-10 and IL-13 in media from cells treated with TNFα in all conditions. In addition, gene expression changes to TNFα and IL-2 were also observed. **Conclusions:** Overall, our results showed the ^{AX}Lung-on-chip platform can detect effects of cytokine mediated vascular permeability changes in vitro. Importantly, we demonstrated that the complex in vitro platform not only detects the effects of TNFa which directly induces vascular permeability changes but is also sensitive to IL-2 mediated secondary vascular damage in the presence of PBMCs. Additionally, our data demonstrated various permeability parameters, cytokines, and gene expression changes to help identify potential vascular injury markers, further highlighting the value of the complex 3D model in identifying drug candidates carrying this hazard.

ABSTRACT NUMBER: 5126 **Poster Board Number:** LB227
TITLE: Incorporation of mast cells into organ-on-a-chip technology

AUTHORS (FIRST INITIAL, LAST NAME) AND INSTITUTIONS: *P. Lee*. U.S. Army DEVCOM Chemical Biological Center, Aberdeen Proving Ground, MD.
KEYWORDS: In Vitro and Alternatives; Immunotoxicology; Chemical and Biological Weapons; Sulfur Mustard

ABSTRACT: Background and Purpose: Organs-on-chips (OOCs) aims to recreate living tissues and/or organ microenvironments, however, commercial systems by in large lack an immune component. The absence of an immune component is a significant drawback to fully recapitulating the physiological human response following exposure to chemical and/or biological warfare agents. Within the innate immune system mast cells are pivotal effector cells contributing to a wide range of downstream immune responses. Mast cells are a prime choice to serve as a vital first step in developing OOC technology with an immune component, due to their ability to elicit a robust cytokine response. The integration of an immune component into OOC technology offers a more physiologically sound model of infection and/or

chemical exposure then what is commercially available, which will more closely simulate vertebrate infection with high fidelity, especially when compared to current alternatives. The development of an *in vitro* OOC system with mast cells has demonstrated to better match human sulfur mustard exposures. **Methods:** This work was the first proof-of-concept study at DEVCOM CBC aiming to incorporate innate immune cells into a commercially available OOC platform and show that an immune response could be elicited and quantified following chemical agent exposure. We were successful in integrating functional human mast cells into the endothelial channel of the Emulate lung-chips, and viable cocultures were established under microfluidic flow. **Results:** After exposure to HD and formaldehyde, cytokine and chemokine production was significantly increased in chips containing mast cells. Cytokines and chemokines corresponding to mast cells were detected in both the bottom and top channels of the chips, suggesting that a response elicited in the microvasculature can translate to the organ specific tissues to mitigate and address the effects of agent exposure. **Conclusions:** This work was the first proof-of-concept study at DEVCOM CBC aiming to incorporate innate immune cells into a commercially available OOC platform and show that an immune response could be elicited and quantified following chemical agent exposure. This study has allowed us to scratch the surface of understanding how immune cells may bolster the overall physiological accuracy of OOC systems.

ABSTRACT NUMBER: 5127 **Poster Board Number:** LB228

TITLE: *In vitro* de-risking approaches to improve the relevance of drug-induced mast cell activation evaluations and understand species differences for nonclinical drug safety assessment

AUTHORS (FIRST INITIAL, LAST NAME) AND INSTITUTIONS: *B. Vega*, F. Chen, *B. Bhatt*, *N. Li*, and *R. J. Gonzalez*. Merck & Co., Inc., West Point, PA.

KEYWORDS: Immunotoxicology; Immunotoxicity

ABSTRACT: Background and Purpose: Mast cells play critical roles in allergic response, anaphylaxis, and defense against pathogens and toxins. Mast cells secrete vasoactive and proinflammatory mediators including histamine, serotonin, and proteases stored in secretory granules to promote anti-pathogen immunity during infections. Uncontrolled mast cell degranulation (MCD) results in clinical signs of anaphylaxis consisting of flushing and/or more adverse events including changes in blood pressure, heart rate, respiratory rate, and in severe cases, mortality. Drug mediated pseudoanaphylaxis is an off-target effect often resulting in dose limiting toxicity including mortality or morbidity in animals encountered during development of peptide drugs. The underlying mechanism of drug-mediated pseudoanaphylaxis is typically through the activation of mast cells or basophils by substructures within many peptides such as basic residues and aromatic or aliphatic hydrophobic residues. **Methods:** We have previously established an ex vivo rat peritoneal MCD (rMCD) assay as a tool to assist in lead optimization and to elucidate the role of mast cells in the mechanism of toxicity for peptide drug candidates. The assay has demonstrated a strong *in vitro-in vivo* correlation and is highly valuable for lead optimization. **Results:** To understand the clinical translatability of these findings, we established an *in vitro* human MCD (hMCD) assay using a LAD2 mast cell line. LAD2 cells highly express Mas-related G protein-coupled receptor X2 (MrgX2), which is known to promiscuously bind diverse chemical structures causing MCD. The hMCD assay was qualified with over 60 chemically diverse benchmark compounds, including those reported to carry pseudoanaphylaxis risks in the clinic. We have evaluated over 1200 peptide drug candidates in both rMCD and hMCD and our results demonstrate good correlation (~80%) between the assays, suggesting peptide-mediated MCD effect is largely conserved between human and

rat. However, to better understand observed species differences in MCD responses, we evaluated a small set of representative peptides (~40) in MrgX2 reporter assay across species and further demonstrated correlation among human, nonhuman primates, and canine. Our results also showed some peptides demonstrated inconsistencies between LAD2 and human MrgX2 reporter assays, which may be attributable to nonspecific engagement of other key mast cell receptors expressed on LAD2 cells not captured in the reporter assay. **Conclusions:** Further work is ongoing to understand mechanisms of these discordant results between these two platforms to potentially better inform on human MCD risk assessment.

ABSTRACT NUMBER: 5128 **Poster Board Number:** LB229

TITLE: Establishing the Preclinical Immunotoxicity Reference Based on Immunophenotyping Data in Bama Minipigs

AUTHORS (FIRST INITIAL, LAST NAME) AND INSTITUTIONS: Q. Gu[1], M. Fu[1], X. Guo[1], L. Li[2], *J. Li*[1], and X. Jin[1]. [1]WuXi AppTec, Suzhou, China; and [2]WuXi AppTec, Shanghai, China.

KEYWORDS: Immunotoxicity; Preclinical Assessments; immunophenotyping

ABSTRACT: Background and Purpose: Therapeutics with immune-modulating effects may occasionally have unintended effects and cause collateral damage to normal tissues. During clinical trials of immunomodulatory therapeutics, instances with severe and even fatal adverse effects have been reported. These occurrences underscore the importance of immunotoxicity assessment in preclinical studies. One of the recommended parameters for preclinical immunotoxicity evaluation is immunophenotyping, which helps evaluate specific cell populations and supports the identification of potential biomarkers for clinical studies. Minipigs have emerged as a valuable alternative in regulated toxicology studies, particularly for their anatomical and physiological similarities to humans. As outlined in the ICH S11 guideline, they are a versatile model feasible for all administration routes, except inhalation, and are particularly popular in dermal studies. Although minipigs have a long history of domestication and utilization, their historical control data in immunotoxicology studies is relatively less well-established compared with other large animals, such as dogs and non-human primates. In this study, we surveyed one widely used Bama minipig breed for immune cell populations at baseline to establish a reliable reference range for lymphocyte immunophenotyping. **Methods:** Animals. The Bama Minipig used in this report originated from China. All animals were naïve and maintained in compliance with the Guide for the Care and Use of Laboratory Animals. All animal research was approved by the Institutional Animal Care and Use Committee. Immunophenotyping. Blood samples were collected with anti-coagulant potassium EDTA and washed with 2 mL of DPBS by centrifugation of 5 min at 400 g. Red blood cell was then lysed with BD Pharm Lyse lysing solution. Live/dead stain was stained with Fixable Viability Stain 510 for 10-15 minutes. An antibody cocktail was added which included: FITC anti-pig CD45, PE-Cy™7 anti-pig CD3ε, Alexa Fluor® 647 anti-pig CD16, and PE anti-pig CD79a. Cells were incubated with an antibody cocktail at room temperature for 30 minutes, protected from white light. Cells were then washed and re-suspended with DPBS and analyzed using BD LSRFortessaTM flow cytometer with FACS Diva software. **Results:** Lymphocyte immunophenotyping was conducted in peripheral blood collected from 46 untreated male and 45 untreated female Bama minipigs. The baseline percentage of lymphocyte subpopulations was reported as total T cell (CD45+CD3ε+), B cell (CD45+CD3- CD16-CD79a+), and natural killer (NK) cell (CD45+CD3-CD16+CD79a-). Various parameters were calculated to assess the data distribution, including the mean, standard deviation, minimum, 5th

percentile, 25th percentile, median, 75th percentile, 95th percentile, and maximum. In summary, the 90% reference range (from 5th to 95th percentile) for lymphocyte subset proportion was as follows: total T cells range from 79.4% to 94.1% in male and from 79.2% to 97.2% in female; B cells range from 2.4% to 11.5% in male and from 1.6% to 12.8% in female; NK cells range from 2.7% to 12.4% in male and from 1.0% to 9.4% in female. In addition, a difference between male and female minipigs was observed in the NK cell baseline percentage (p-value=0.0047), with a higher NK proportion in male minipigs. **Conclusions:** Based on lymphocyte immunophenotyping data from 93 individual animals, a reference range for total T, B, and NK cells in minipigs at a homeostatic immune state has been established. This database could serve as a reliable reference, aiding the interpretation of preclinical immunotoxicity findings.

ABSTRACT NUMBER: 5129 **Poster Board Number:** LB230

TITLE: Development of an *In Vitro* Natural Killer Cell Mediated Cytotoxicity Assay Using the NK-92 Cell Line

AUTHORS (FIRST INITIAL, LAST NAME) AND INSTITUTIONS: N. R. Barbo[1,2], M. Shabrang[3], *D. Phelps*[1,2], and K. Slentz-Kesler[2]. [1]Oak Ridge Institute for Science and Education, Oak Ridge, TN; [2]US EPA/CCTE, Research Triangle Park, NC; and [3]University of North Carolina Chapel Hill, Chapel Hill, NC.

KEYWORDS: Immunotoxicology; Immunotoxicity; In Vitro and Alternatives; Natural Killer Cells

ABSTRACT: Background and Purpose: Natural killer (NK) cells are effector lymphocytes and are an important part of the innate immune system. One key function of NK cells is their cytotoxic ability, which is essential for proper host defense. When a host cell is transformed (i.e., cancerous) or virally infected, major histocompatibility complex I is downregulated on the cell surface. NK cells recognize this and are then triggered to kill the target cell through the release of perforin and granzyme B. When exposed to immunosuppressive chemicals, NK cell mediated cytotoxicity may be inhibited, resulting in an increased susceptibility to infectious or neoplastic disease. Because of this, the United States Environmental Protection Agency includes an *in vivo* NK cell mediated cytotoxicity assay as a second-tier assay in their Health Effects Test Guidelines for immunotoxicity in rodent models. As part of our next-generation assay development, we are optimizing a new approach methodology (NAM) that can conduct high-throughput screening of chemicals for their ability to alter NK cell mediated cytotoxicity. Traditionally, *in vitro* NK cell mediated cytotoxicity assays involve the co-culturing of primary NK cells with a chromium-labeled target cell line. However, the use of primary cells in the traditional assay limits the overall screening efficiency due to the higher cost and inherent variability of primary cells that would need to be continually sourced from new donors. Additionally, chromium-release assays are often cost-prohibitive and hazardous, resulting in a movement towards using luciferase- or GFP-labeled target cell lines. In this assay, we co-culture the well-characterized NK-92 cell line with fluorescently labeled K-562-GFP target cells (from ATCC). NK cell mediated cytotoxicity is measured in the presence or absence of potential immunotoxic chemicals via high-throughput quantification of target cell death. Ultimately, our cell line-based assay will allow for the high-throughput quantification of NK cell mediated cytotoxicity following the exposure of immortalized NK cells to chemicals of interest. **Methods:** To optimize this assay, parameters for quantification of target cell death were explored. K-562-GFP cells were killed using three different protocols: heating cells at 65°C for 10 minutes, lysing cells using a detergent solution for 30 minutes, or exposing cells to the apoptosis-inducing chemical staurosporine (1 µM) for 24 hours. These cells were stained with 7-aminoactinomycin D (7-AAD), a

fluorescent dye that binds to the DNA of dead or damaged cells, and then analyzed on an Attune NxT flow cytometer. Separately, NK-92 and K-562-GFP cells were co-cultured, and a time course was run to determine the timepoint at which the greatest NK cell mediated cytotoxicity occurred. NK-92 cells were co-cultured with K-562-GFP cells at $1x10^6$ cells/mL and $3.2x10^4$ cells/mL respectively, resulting in an effector:target ratio of 25:1. Cytotoxicity was measured at 0-, 1-, 2-, 3-, and 4-hour timepoints. 7-AAD was added to the co-cultured cells which were then analyzed on an Attune NxT flow cytometer. Dead K-562-GFP cells were expected to be positive for both GFP and 7-AAD, distinguishing them from NK-92 cells (GFP-) and live cells (7-AAD+). Four chemicals were selected for initial testing of xenobiotic-induced changes of NK cell mediated cytotoxicity: prednisolone (100 µM, 10 µM, and 1 µM), prednisone (100 µM, 10 µM, and 1 µM), perfluorooctanoic acid (PFOA) (100 µM, 10 µM, and 1 µM), and dexamethasone (10 µM, 1 µM, and 0.1 µM). All concentrations of test chemicals were non-cytotoxic to NK-92 cells. Prednisolone, PFOA, and dexamethasone are suspected of inhibiting NK cell mediated cytotoxicity and prednisone should not affect NK cell mediated cytotoxicity. NK-92 cells were plated and treated with chemical for 24 hours. Chemical was then washed from the NK-92 cells and K-562-GFP cells were added at an effector:target ratio of 25:1 ($1x10^6$ NK-92 cells/mL; $3.2x10^4$ K-562-GFP cells/mL). Cells were co-cultured for 4 hours, followed by addition of 7-AAD and analysis on the Attune NxT flow cytometer. Dead K-562-GFP cells were defined as being positive for both GFP and 7-AAD. **Results:** Heat-killing was the most efficient protocol for killing K-562-GFP cells, resulting in 94.5% of cells labeled as 7-AAD+. Only 24.6% of lysis-killed and 2.7% of staurosporine-killed cells were 7-AAD+. Notably, GFP fluorescence across the target cell population decreased following cell killing, with 29.5% of heat-killed, 24.3% of lysis-killed, and 1.8% of staurosporine-killed cells being GFP-/7-AAD+. The lysis-killed and staurosporine-killed cells had a large percentage of GFP-/7-AAD- cells, with 74.6% of lysis-killed and 54.7% of staurosporine-killed cells being GFP-/7-AAD-, compared to only 3.3% of non-killed control cells being GFP-/7-AAD-. Lysis- and staurosporine-killed cells viewed under a microscope appeared small and shriveled, leading us to believe they were dead but did not pick up 7-AAD. In the co-culture time course study, it was found that the percentage of killed K-562-GFP cells increased over the 5 timepoints. The 0-hour timepoint had the lowest percentage of target cell death, with 6.0% of GFP+ K-562-GFP cells being 7-AAD+. At 1-, 2-, 3-, and 4- hour timepoints 14.9%, 23.8%, 22.0%, and 32.7% of GFP+ cells were 7-AAD+, respectively. Similar to the results found in the optimization of K-562-GFP cell killing control conditions, K-562-GFP cells appeared to lose GFP fluorescence over time. To quantify the decrease of GFP fluorescence, median fluorescent intensities of our GFP+ cells were calculated. From the 0-hour timepoint, there was a 5.2%, 15.3%, 16.7%, and 23.9% decrease after 1-, 2-, 3-, and 4-hours of co-culture, respectively. There was no change in NK cell mediated cytotoxicity observed in any concentration of prednisolone, prednisone, PFOA, or dexamethasone treatments when compared to the vehicle control ($p = 0.997$; one-way ANOVA). **Conclusions:** Heat-killing the K-562-GFP cells at 65°C for 10 minutes was most efficient according to 7-AAD staining and resulted in the least amount of GFP fluorescence loss. The discrepancy observed between the number of cells that were 7-AAD+ and the number of cells that lost their GFP fluorescence is suggestive of poor 7-AAD performance in this assay, as it does not reliably stain all dead cells. Further stains for the detection of dead cells will be tested, ensuring the staining of both apoptotic and necrotic cells. When assessing NK cell mediated cytotoxicity over time, the 4-hour co-culture resulted in the greatest amount of K-562-GFP cytotoxicity. Therefore, we chose to move forward with 4 hours of NK-92 and K-562-GFP cell co-culture to obtain the most dynamic range in this assay. However, when chemical exposures were integrated, there were no significant changes observed in NK cell mediated cytotoxicity, suggesting that there is more optimization that needs to be done to obtain data consistent with previous reports. NK cell mediated cytotoxicity is an important endpoint to assess when

determining if a chemical is an immunotoxicant and therefore potentially detrimental to human health. The development of this high throughput *in vitro* assay, using an NK cell line and fluorescently labeled target cells, would advance the application of NAMs in chemical screenings for immunotoxicity hazard. *This abstract does not reflect the official policy of the US EPA.*

ABSTRACT NUMBER: 5130 **Poster Board Number:** LB231

TITLE: Application of a high-content imaging strategy for developmental immunotoxicity in transgenic zebrafish larvae

AUTHORS (FIRST INITIAL, LAST NAME) AND INSTITUTIONS: S. Caty[1,2], *D. Phelps*[1,2], *J. Harrill*[1], S. Padilla[1], and K. Slentz-Kesler[1]. [1]US EPA/CCTE, Durham, NC; and [2]Oak Ridge Institute for Science and Education, Oak Ridge, TN.

KEYWORDS: Immunotoxicity; Transgenic Models; Reproductive and Developmental Toxicology; Zebrafish

ABSTRACT: Background and Purpose: The development of high-throughput new approach methods (NAMs) for assessment of chemically induced immunotoxicity is necessary for rapid identification of potential immunotoxicants in the environment. The developing immune system is of particular interest as exposure to toxicants during development can have long-lasting effects on immune system function. While immunotoxicity is an existing area of interest for chemical toxicity testing, most relevant assays utilize costly, low-throughput rodent models. Zebrafish (*Danio rerio*) are a common model for toxicity studies due to their rapid development and metabolic competency. In particular, they are useful for immunotoxicity studies because they possess the same major immune cell lineages as humans. However, many of the immunotoxicity studies with larval zebrafish rely on either a) microscopy techniques that require manual positioning and imaging of fish or b) flow cytometry, which requires pooling many individuals for adequate cell numbers for counting. Here, we sought to improve throughput by applying a high-content imaging strategy to a larval zebrafish developmental immunotoxicity assay. Specifically, transgenic zebrafish embryos were exposed to a test chemical for several days following fertilization, and high-content imaging was used to measure the resulting impact on the development of their neutrophils, a key cell type of the innate immune system. **Methods:** To enable the image-based counting of neutrophils in this assay, we utilized a transgenic zebrafish line with fluorescently labeled neutrophils (Tg(lyz:TagRFP) (Lam 2012, PMID: 22946052). Outbred, AB-based wild-type strain (US EPA) with no fluorescent labeling were used to determine background detection levels of the high content imaging assay. Neutrophils develop rapidly in the larval zebrafish and can begin to be detected in this transgenic line at approximately 48 hours post fertilization. Additionally, we tested the effect of phenanthrene, a polycyclic aromatic hydrocarbon, which has been previously demonstrated to have mixed effects on neutrophils. In one paper, phenanthrene exposure reduced neutrophil count (Ren 2025, PMID: 39481963), while in another, it reduced activity, but not count (Phelps 2020 PMID: 32407153). Transgenic zebrafish were raised in 10% Hanks buffered salt solution and exposed to a vehicle control (0.4% DMSO), 1, 3, or 10 µM phenanthrene (n=46-67 larvae per condition) beginning at 8 hours post fertilization. Wild-type zebrafish were reared in 10% Hank's buffered salt solution without added chemicals (n= 32). All zebrafish were reared at 26°C for four days post fertilization and then fixed with 4% paraformaldehyde for imaging. Chemical treatment was maintained until fixation without refreshing the chemical. Fixed zebrafish were imaged with the Opera Phenix Plus high-content imaging platform in ZF Plates (Diagnocine) using a 10x magnification lens in confocal mode. After imaging,

fluorescent neutrophils were identified and counted using spot detection in the Harmony software application. **Results:** High-content imaging with the Opera Phenix enabled rapid imaging and data analysis that can facilitate higher throughput zebrafish assays. Four 96 well plates of fish were imaged and analyzed within 3.5 hours. The assay was able to identify fluorescent neutrophils in transgenic fish (mean neutrophil count = 270, SD = 86) with minimal noise detected in the wild-type fish (mean neutrophil count = 16, SD = 14, wild-type vs vehicle control transgenic fish $p < 0.001$ from ANOVA Tukey HSD post hoc test). No significant differences in neutrophil counts were observed between vehicle control and any of the tested concentrations of phenanthrene ($p = 0.2$). We will continue to make improvements in experimental parameters, image acquisition, and image analysis to further reduce the incorrect detection of imaging artifacts in wild-type fish as fluorescent cells and to reduce the variation in neutrophil counts (vehicle control coefficient of variation = 31%). **Conclusions:** A high-content imaging strategy is a promising method to increase throughput for immunotoxicity assays in zebrafish. Future work will optimize these methods by evaluating whether zebrafish age and positioning (dorsal vs ventral) might reduce variability in neutrophil cell counts. Additionally, to establish a reliable positive control treatment, we will assess the effects of repeat chemical dosing and test additional reference chemicals, including inhibitors of *pu.1*, a key transcription factor involved in early immune system development. *This abstract does not reflect US EPA policy nor does mention of products or trade names constitute endorsement for use.*

ABSTRACT NUMBER: 5131 **Poster Board Number:** LB232

TITLE: Safety screening strategies to evaluate innate immune activation of therapeutic oligonucleotides

AUTHORS (FIRST INITIAL, LAST NAME) AND INSTITUTIONS: E. Malek Zadeh[1], G. Papadopoulos[1], A. Imanishi[2], M. Kimura[2], H. Komori[2], T. Sameshima[2], T. Shinozawa[2], T. Hickman[1], and M. Wagoner[1].
[1]Takeda Pharmaceutical Company Limited, Cambridge, MA; and [2]Takeda Pharmaceutical Company Limited, Fujisawa, Japan.

KEYWORDS: Therapeutic oligonucleotides, Immunostimulatory

ABSTRACT: Background and Purpose: Therapeutic oligonucleotides (ONs) are modified nucleic acid polymer chains which include anti-sense oligonucleotides (ASOs), DNA/RNA heteroduplex oligonucleotides (HDOs), small interfering RNA (siRNA), anti-miRNA (antagomirs) etc [1]. ONs represent a novel class of disease-modifying drugs with the potential to change the therapeutic landscape of many diseases [2]. These compounds bind to their target via Watson-Crick base pairing and modulate gene expression [3]. As of December 2024, the U.S. Food and Drug Administration (FDA) has approved at least 21 RNA-based therapeutics, including 4 approvals in 2023, showing the growing interest in this therapeutic area [4]. However, ONs are immunostimulatory molecules with the potential to induce harmful inflammatory responses. ONs can stimulate the innate immune system by binding to various pattern recognition receptors (PRRs), such as Toll-like receptors (TLRs), leading to the expression of genes involved in inflammation and host defense [5]. Screening oligonucleotides for immunogenicity will help select candidates with an improved safety profile in early preclinical development [6]. Peripheral blood mononuclear cell (PBMC) and whole blood assays (WBA) are commonly applied in vitro assays that assess cytokine induction by ONs, and aid in the selection of lead candidates with minimal pro-inflammatory properties [5]. Here, we propose a THP-1 cell-based assay as a high throughput screening assay that may supplement standard cytokine release assays for immunogenicity screening. THP-1 dual reporter cells are genetically engineered THP-1 cells that contain luciferase and secreted embryonic

alkaline phosphatase (SEAP) reporter genes, driven by promoters specific to Interferon Regulatory Factor (IRF) and Nuclear Factor-Kappa B (NF-kB) pathways [7]. The THP-1 dual cell line with cGAS knockout (KO) can further differentiate immune activation caused by cGAS-STING from Interferon-mediated responses. **Methods:** In this study, a lipid-based transfection method was used to investigate the ability of 12 ASOs to stimulate innate immune response in THP-1 dual reporter monocytes. The supernatant was harvested for analysis of SEAP and Lucia Luciferase activities using QUANTI-Blue and QUANTI-Luc detection reagents. The cGAS KO cells were tested in parallel to obtain mechanistic insight into the pathways involved in immune activation. In order to compare the activity in the THP-1 assay to the PBMC assay results, a standard PBMC cytokine release assay was conducted. Briefly, human PBMCs were incubated with ONs for approximately 24 hours. The supernatant was collected and 5 cytokines (TNF-a, IFN-a, IL-6, MCP-1 and IFN-g) were quantified using Cytometric Bead Array Kit (BD Biosciences). **Results:** For THP-1 dual reporter assay, oligos were ranked from least to most immunostimulatory. The oligos showed a concentration dependent increase in IRF induction. Transfected oligos activated the cytosolic DNA sensor cGAS and the IRF activity was abolished in cGAS KO cells suggesting the cGAS pathway mediated innate immune responses to cytosolic oligos. A modest dose-dependent increase in NF-kB activity was observed for all oligonucleotides and NF-kB activity was independent of cGAS pathway. THP-1 assay showed IRF activation for all ASOs. For the majority of the oligos, THP-1 assay results correlated with PBMC assay results. However, for some cases, positive IRF activity in THP-1 assay didn't induce potent cytokine release in PBMC assay. **Conclusions:** THP-1, as a high throughput assay, can differentiate between ONs with high and low response in PBMC cytokine release assay and can be implemented for mechanistic investigation of immune responses using the engineered cell lines. Screening of large libraries of oligos will help establish structure-function relationships and allow to create safety strategies for rational design of oligonucleotides with improved safety profiles. Therefore, the THP-1 reporter assay demonstrates value as a high throughput screening assay to evaluate immune activation and differentiate between pro-inflammatory and interferon-driven immune responses to identify immunostimulatory candidates early in drug development.

ABSTRACT NUMBER: 5132 **Poster Board Number:** LB233

TITLE: Understanding the Link Between Mast Cell Degranulation and Mitochondrial Function: The Impact of Household Chemical Cetylpyridinium Chloride

AUTHORS (FIRST INITIAL, LAST NAME) AND INSTITUTIONS: E. Biro, S. Plummer, J. Eom, B. Obeng, M. Tasker, D. Wagner, and *J. A. Gosse*. University of Maine, Orono, ME.

KEYWORDS: Immunotoxicology; Undergraduate Student; Signal Transduction; Cetylpyridinium Chloride

ABSTRACT: Background and Purpose: Consumers are exposed regularly to cetylpyridinium chloride (CPC) in personal care, cleaning, and food products. Mounting evidence suggests CPC breaches the blood-brain barrier, is bioavailable, and is toxic to eukaryotes at low doses, such as nanomolar toxicity to developing oligodendrocytes. Our lab previously showed that low-dose exposure to CPC causes mitochondrial toxicity on par with canonical mitotoxicant carbonyl cyanide-3-chlorophenylhydrazone (CCCP) in primary human keratinocytes, mouse NIH-3T3 fibroblasts, and RBL-2H3 mast cells. In addition, CPC limits function of the nervous and immune system cell type mast cells (MCs), by an unknown mechanism, yet the research to fully explore the toxicology of this drug is sparse. In response to various stimuli, MCs undergo a functional response, degranulation, in which bioactive substances like histamine and serotonin are exocytosed from pre-formed granules. Our investigation has suggested that CPC

inhibits IgE receptor crosslinker-stimulated tyrosine phosphorylation and thus degranulation in MCs at non-cytotoxic, exposure-relevant, low-micromolar doses, and specifically inhibits early signaling proteins in the MC activation pathway, but very little is known about later elements of the pathway. **Methods:** In order to fill this gap, calcium ionophore A23187 was utilized. The exposure of MCs to calcium ionophore enables for cytosolic calcium to be increased, a precondition required for degranulation, without crosslinking of the IgE receptor and the early tyrosine phosphorylation pathway. This allows for the classification of a target of CPC as upstream or downstream of the calcium influx step. An assay was performed to measure degranulation by treating RBL-2H3 MCs with CPC (0-10 µM) and 3.0×10^{-7} M ionophore as determined by preliminary dose-response testing to represent low antigen response (~7% degranulation). Degranulation was measured by quantifying the cleavage of fluorogenic substrate 4-methylumbelliferyl-*N*-acetyl-β-D-glucosaminide by β-hexosaminidase, which is released linearly with histamine during degranulation. The quantification was performed using a plate reader with fluorescence detection. A lactate dehydrogenase (LDH) based cytotoxicity assay was used to assess the cytotoxicity of experimental doses of CPC and ionophore. All statistical analyses were done using Excel and GraphPad Prism. **Results:** The data show that CPC highly stimulates ionophore-induced degranulation, in contrast to the potent CPC inhibition observed when tyrosine phosphorylation ensues by receptor crosslinking. Percent degranulation at doses of 1 µM CPC with ionophore increases by two-fold compared to ionophore only, and increases are also observed at 2.5 µM and 5 µM. At doses of 10 µM CPC, the percent degranulation returns to the control level of ~7%. No cytotoxicity is observed at any dose used in experimentation. **Conclusions:** These results demonstrate that the impact of CPC on late signaling elements is by a different mechanism than early element suppression. Our lab has shown through super-resolution microscopy (FPALM) that CPC causes damage to mitochondrial nanostructure in the form of fissioning, an effect known to be connected to toxicity and disease. Other labs have shown that a controlled amount of mitochondrial fissioning is required for immune cell function, allowing for mitochondria to pinch off from their normal healthy mitochondrial networks, in order to be rapidly deployed to the plasma membrane to aid in signaling including calcium influx and exocytosis. We hypothesize that CPC-induced mitochondrial fissioning is actually supporting and stimulating degranulation when CPC inhibition of early phosphorylation and other events is bypassed due to use of ionophore stimulation. Thus, ongoing experiments are assessing effects of CPC on mitochondrial translocation following crosslinking vs. ionophore stimulation. Despite this, human exposure continues to expand as CPC is increasingly used in response to SARS-CoV-2. This reinforces the need to fully describe the cellular and molecular mechanisms of CPC exposure to humans and wildlife such that regulators, companies, and consumers can make informed decisions about CPC usage.

ABSTRACT NUMBER: 5133 **Poster Board Number:** LB234
TITLE: Inflammation and neuronal damage following exposure to soman in mice

AUTHORS (FIRST INITIAL, LAST NAME) AND INSTITUTIONS: O. Altstadt, E. Johnson, A. Methvin, and *J. Janssen*. USAMRICD, APG, MD.
KEYWORDS: Inflammation

ABSTRACT: Background and Purpose: Chemical Warfare Agents, such as soman (GD) remain a significant threat. They are easily synthesized, can be deployed on the battlefield, or used as an agent of terror in a public setting. GD is a potent acetylcholinesterase inhibitor, and severe exposure causes a cholinergic crisis, often resulting in prolonged status epilepticus (SE). SE causes extensive cell death in

multiple brain structures, leading to the activation of multiple neuroinflammatory pathways. Both interleukin 1 (IL-1) and tumor necrosis factor α (TNFα) have pro-inflammatory roles in the brain, and they are involved in seizure development and maintenance. These dual inflammatory pathways can both exacerbate tissue injury or promote healing. This effect depends on not only the nature and extent of the injury, but also the interaction of multiple cells and other inflammatory factors as the injury progresses. This dual role of neuroinflammation has complicated the development of effective neuroprotective therapies for SE, so visualizing the roles of these pathways will aid in developing potential countermeasures. **Methods:** This study focused on inhibition of both IL-1 and TNFα signaling as an anticonvulsant and neuroprotective strategy. An IL-1R1/TNFR1A double knockout (KO) mouse model of GD exposure, seizure profiles, neuropathology, mortality, and various inflammatory markers were compared to a wild-type background mouse strain. Animals were exposed to a single dose of GD, then monitored for seizure and other behavioral signs. Following the end of the experiment, brains were processed for histological analysis. **Results:** Neural tissue stained with inflammatory markers for microglia (Iba-1) and astrocytes (GFAP) showed cells clustering in the hippocampus, piriform cortex, amygdala, and thalamus. The damage was far more substantial and widespread in wild type mice as compared to the double KO strain. In addition, Fluorojade B showed extensive neuronal death in hippocampus and thalamus. Additionally double KO mice were more resilient to the effects of GD exposure to include reduced seizure incidence, morbidity, and mortality. **Conclusions:** These data suggest that inhibition of specific pro-inflammatory pathways, such as IL-1 and TNFα, may be a viable addition to standard therapies to treat GD-induced SE. Disclaimer:The views expressed in this abstract are those of the author(s) and do not reflect the official views or policies of the Department of Army, Department of Defense, or the U.S. Government. The experimental protocol was approved by the Animal Care and Use Committee at the United States Army Medical Research Institute of Chemical Defense, and all procedures were conducted in accordance with the principles stated in the Guide for the Care and Use of Laboratory Animals and the Animal Welfare Act of 1966 (P.L. 89-544), as amended. These studies were funded by the Combat Casualty Care Reduction Program (CCCRP).

ABSTRACT NUMBER: 5134 **Poster Board Number:** LB235

TITLE: The Potential Protective Efficacy of Nicotine in Attenuating Inflammatory Lung Injury: Implications for COVID-19

AUTHORS (FIRST INITIAL, LAST NAME) AND INSTITUTIONS: M. Lin[1], S. Zefi[1], S. Shukla[1], W. Zhao[1], C. Ashby[1], and L. Mantell[1,2]. [1]St. John's University, Queens, NY; and [2]Feinstein Institute for Medical Research, Northwell Health, Manhasset, NY. Sponsor: L. Mantell, Society for Redox Biology and Medicine

KEYWORDS: None

ABSTRACT: Background and Purpose: The correlation between tobacco smoking and susceptibility to infection with SARS-CoV-2, which causes COVID-19 has remained controversial since the initial reports in early 2020. The inconsistent findings are likely due to the small sample sizes evaluated in early studies. Another key factor contributing to this ambiguity is the complex relationship between tobacco smoking, immune function and lung pathology during viral infections. Acute lung injury (ALI), which is characterized by stress and inflammation in the lungs, is one of the major health problems produced by COVID-19. Therefore, we determined the epidemiological correlation between tobacco smoking and susceptibility to COVID-19 and the potential protective effects of nicotine in the development of ALI.

This was accomplished by determining if tobacco smoking or nicotine exposure affects the risk and severity of COVID-19 and to determine if nicotine can decrease the inflammatory responses and oxidative stress that occurs in patients with COVID-19-induced ALI. **Methods:** We conducted a meta-analysis of 101,713 COVID-19 patients from 71 studies to determine the correlation between smoking and susceptibility to COVID-19. We also determined nicotine's potential protective effects by administering nicotine (400 μg/kg i.p., equivalent to 0.1% of one cigarette) to mice, 24 hours after hyperoxia exposure (>90% O_2). Also, we determined the *in vitro* effect of nicotine on mouse macrophage function and HMGB1 release under hyperoxic conditions. **Results:** Our meta-analysis indicated that 10.10% (10,270 out of 101,713) of COVID-19 patients were tobacco smokers, which was significantly lower than the global smoking prevalence of 21.90%. A comparative analysis of the prevalence of smoking among individual studies and their corresponding regional populations demonstrated a consistently lower percentage among COVID-19 patients (12.63 ± 11.34% vs. 19.26 ± 6.55%, $p < 0.001$). In a mouse model of hyperoxia-induced acute lung injury, nicotine administration significantly increased survival rates by 25% and 37.5%, after 120 and 132 hours of hyperoxic exposure, respectively. Nicotine also significantly attenuated hyperoxia-induced acute inflammatory lung injury, as it significantly decreased total protein content in bronchoalveolar lavage (BAL), neutrophil infiltration in the airways and the lung wet-to-dry weight ratio. Nicotine significantly decreased the accumulation of HMGB1, a key mediator of oxidative-induced stress, in the airways and plasma. In hyperoxic macrophages, nicotine (100 pM) induced a significant decrease in HMGB1 release, and this concentration of nicotine was 3,000-fold lower than the plasma nicotine concentration after smoking one cigarette. Nicotine significantly increased macrophage migration and phagocytic function, effects that may be partially mediated by α7 nicotinic acetylcholine receptor (nAChR), a critical component of the brain-lung inflammatory reflex response. Furthermore, nicotine significantly mitigated the hyperoxia-induced decrease in α7nAChR expression. **Conclusions:** These results suggest that nicotine may attenuate inflammatory lung injury by preserving the function of lung macrophages involved in the inflammatory reflex, potentially through affecting α7nAChR-mediated signaling pathways.

ABSTRACT NUMBER: 5135 **Poster Board Number:** LB236

TITLE: Assessment of mercury pollution in tropical forest impacted by gold mining in the Colombian Pacific

AUTHORS (FIRST INITIAL, LAST NAME) AND INSTITUTIONS: J. Palomeque-Blandon[1], A. Romaña-Palacios[1], E. Moreno-Mosquera[1], N. Nagles-Vergara[1], K. Martínez-Copetea[1], C. Palacios-Palacios[1], D. Perea-Ruíz[2], J. Gamboa-Orozco[2], and *Y. Palacios Torres*[1]. [1]Environmental Toxicology and Natural Recourses Group. School of Naturals Sciences, Technological University of Choco-DLC, Quibdó, Colombia; and [2]WWF Colombia, Bogotá, Colombia.

KEYWORDS: Aquatic Toxicology; Environmental Toxicology; Metals; Chocó; Mercury

ABSTRACT: Background and Purpose: Mercury is a toxic environmental pollutant found in muscle of fish from polluted sites, representing a human health risk. **Methods:** The aim of this study was to quantify Hg levels in muscle, gill and liver of most consumable fish species from mining district at Bebará River basin, as well as in human hair from people living on this area. Mercury was quantified using a total Hg (T-Hg) analyzer. **Results:** Average Hg concentration in all evaluated fish specimens was 0.16±0.02 μg/g, with values ranging between 0.01 and 0.96 μg/g. Maximum concentrations were observed in *Ctenolucius beani* (0.41 ±0.13 μg/g), *Pseudopimelodus schultzi* (0.38 ± 0.12 μg/g) and *Brycon henni* (0.25

± 0.0 µg/g). All species had mean T-Hg values below permissible concentrations set by USEPA (0.5 µg/g) but above maximum values to protect vulnerable people (0.2 µg/g). Mean T-Hg levels in liver were detected for *P. magdalenae* (0.07± 0.003 µg/g) and *P. schultzi* (2.85±1.55 µg/g). Mean T-Hg levels in gill was 0.09±0.01 µg/g (0.03-0.19µg/g). Mercury levels in human hair were 0.3 to 5.7 µg/g, with a mean concentration of 1.86±0.17 µg/g. Men had 1.5-fold greater values than women (2.1 vs. 1.7 µg/g), this may be the result of occupational exposure in gold mines. About 64% of the studied sample showed Hg values in hair above the WHO thresholds. **Conclusions:** the Hg-T values were closed to safety limits, suggesting some risks for public health, and the need to implement health and environmental education programs related to Hg exposure and its effects.

ABSTRACT NUMBER: 5136 **Poster Board Number:** LB237

TITLE: Estimation of Infant Exposures to Environmental Chemicals through Household Dust around the Tampa Bay region

AUTHORS (FIRST INITIAL, LAST NAME) AND INSTITUTIONS: *N. Vijayakumar*[1], L. Calcul[2], M. Bourgeois[2], F. Jaward[2], H. Alegria[2], and R. Kirby[2]. [1]Nova Southeastern University, Fort Lauderdale, FL; and [2]University of South Florida, Tampa, FL.

KEYWORDS: Children's Health; Environmental Toxicology; Polycyclic Aromatic Hydrocarbons; Phthalates, pesticides

ABSTRACT: Background and Purpose: Indoor environments have become a significant focus for environmental exposure research as people increasingly spend more time at home. Household dust serves as a reservoir for various chemicals, including polycyclic aromatic hydrocarbons (PAHs), pesticides, and phthalates. Young children, who tend to spend more time on the floor and exhibit mouthing behaviors, are particularly vulnerable to exposure to these chemicals as they come into contact with settled dust. This study aimed to quantify the levels of PAHs, pesticides, and phthalates in household dust and estimate the potential exposure to these chemicals. **Methods:** Dust samples (n=7) were obtained from homes around the Tampa Bay region. The dust samples were extracted for PAHs, pesticides, and phthalates and analyzed using gas chromatography and mass spectrometry (GC/MS). Probabilistic analysis was used to estimate infant exposures and cancer risk in specific age groups for both genders. **Results:** Among the polycyclic aromatic hydrocarbons (PAHs), fluoranthene exhibited the highest concentration in house dust, with a mean value of 754.04 ng/g, followed by benzo(b)fluoranthene. Diagnostic ratios further suggested that both petrogenic and pyrogenic sources contributed to the presence of these PAHs in the dust samples. Regarding phthalates, Di(2-ethylhexyl) phthalate (DEHP) was the most prevalent congener in household dust, with a mean concentration of 3.63 µg/g, followed by dibutyl phthalate (DBP) and Diisobutyl phthalate (DiBP). Among the pesticides, malathion was the most abundant, with a mean concentration of 3,082.61 ng/g, followed by carbaryl. In terms of exposure, higher Average Daily Doses (ADD) were observed in girls compared to boys for all the three chemicals studied. For PAHs, benzo(ghi)perylene had the highest ADD for girls aged 1 to 2 years, with a value of 2.13 ng/kg/day. For phthalates, DEHP had the highest ADD for girls in the same age group, reaching 10.70 ng/kg/day. Among pesticides, malathion showed the highest ADD in girls aged 1 to 2 years, with a value of 8.97 ng/kg/day. The Incremental Lifetime Cancer Risk (ILCR) analysis revealed that benzo(a)pyrene had the highest mean ILCR, with a value of 3.15E-06 for girls at birth to 1 month. The ILCR for other PAHs, including benzo(b)fluoranthene, dibenzo(ah)anthracene, benzo(a)anthracene, benzo(k)fluoranthene, and Indeno(123cd)pyrene, were also classified as presenting low carcinogenic

risks. **Conclusions:** The analysis of house dust revealed significant concentrations of polycyclic aromatic hydrocarbons, phthalates, and pesticides, with fluoranthene and DEHP being the most abundant contaminants. Gender-specific differences in exposure were evident, with girls, particularly those aged 1 to 2 years, exhibiting higher average daily doses for PAHs, phthalates, and pesticides compared to boys. This highlights a potential vulnerability in early childhood development. While the Incremental Lifetime Cancer Risk associated with PAH exposure was generally low, benzo(a)pyrene presented the highest ILCR, remaining within an acceptable risk threshold. These findings emphasize the importance of monitoring environmental contaminants in household dust, particularly for vulnerable populations, and suggest that while overall carcinogenic risks are low, continued vigilance and possible intervention measures are warranted to minimize potential long-term health impacts.

ABSTRACT NUMBER: 5137 **Poster Board Number:** LB238
TITLE: In the Line of Fire: Assessing Air Quality and Respiratory Impacts in Fire Stations

AUTHORS (FIRST INITIAL, LAST NAME) AND INSTITUTIONS: A. Castañeda[1], *L. C. Magaña*[1], M. Gault[1], D. Hunt[2], D. Picone[2], and N. López-Gálvez[1]. [1]San Diego State University, San Diego, CA; and [2]San Diego Fire Department Health and Safety Office, San Diego, CA.
KEYWORDS: Lung; Pulmonary or Respiratory System; Environmental Toxicology; Exposure Assessment

ABSTRACT: Background and Purpose: Firefighters are frequently exposed to high concentrations of particulate matter (PM) and volatile organic compounds (VOCs) due to firefighting activities, contaminated gear, and off-gassing. These contaminants accumulate from smoke, burning materials, and chemicals; which can cause long-term health risks including lung and cardiovascular disease. Firefighters' repeated exposure irritates the airway leading to chronic respiratory conditions such as obstructive and restrictive lung diseases. Prolonged heat exposure further stresses the respiratory system, increasing smoke inhalation further damaging the lungs. Despite "cancer-free" zones in fire stations, cross-contamination is common due to fast-paced environments, ventilation systems, and personal protective equipment (PPE), compromising air quality and worsening lung health. This research aims to identify harmful contaminants in San Diego County fire stations and assess their impact on respiratory health. By understanding these risks, we can better address the environmental hazards faced by firefighters and develop effective strategies to mitigate their long-term health effects. **Methods:** In collaboration with the San Diego Fire Department Health and Safety Office, a centrally located fire station in San Diego County was selected for an environmental assessment. Air quality was monitored in four areas: the apparatus bays (fire engine area), bullpens (lounging area), dormitories, and PPE storage areas. Two real-time air monitoring devices, the Zynect Air Quality Egg and the PurpleAir monitor were used to measure a range of environmental contaminants and conditions. These include carbon dioxide, sulfur dioxide, hydrogen sulfide, particulate matter (PM 1.0, 2.5, 10.0), volatile organic compounds, as well as ambient temperature (°C), pressure (kPa), and relative humidity (%). Data was collected on a consecutive seven-day trend analysis evaluating results against the United States Environmental Protection Agency (EPA) air quality thresholds to assess potential health risks. Spirometry testing was conducted using the New Diagnostics Design Medical EasyOne Air Spirometer to examine the correlation between exposure and respiratory health. Spirometry data was collected from participants (n= 15) at the start of their rotation and again after completing a 24-hour shift, three trials for spirometry were completed at both collection periods. Changes in lung function were assessed to find associations with exposure during their workday. The metrics analyzed were forced expiratory volume in

one second (FEV1) and forced vital capacity (FVC), with the FEV1/FVC ratio used to identify restrictive or obstructive lung patterns. **Results:** Based on the EPA's AirNow Index, the station is located in a community with moderate air quality, averaging in the 50th-100th percentile on the index scale. Station demographic assessments revealed worse health conditions attributed in part to outdated ventilation systems. Proximity to emergency vehicles and equipment contributes to the increased levels of contaminant levels due to off-gassing and increased exposure to diesel particulate matter. According to the California Healthy Places Index Map, this area ranks in the 70th percentile statewide, averaging 1.39 kg/day. Spirometry results for participants showed FEV1/FVC ratios ranging from -0.53 to 0.85 (Z-score range: -0.53 to 0.31) indicating outcomes that included normal lung function, possible restrictions, and mild to moderate obstructions. **Conclusions:** This study identifies the presence of harmful contaminants in key areas within fire stations which pose significant health risks to firefighters. The spirometry data collected from participants revealed varying degrees of lung function. These findings emphasize the need for further assessments of the relationship between environmental exposure and individual respiratory health. Future assessments should aim to identify additional areas with high pollutant concentrations and develop targeted interventions to improve air quality and reduce exposures. Incorporating spirometry assessments into future studies will be crucial for understanding how environmental conditions within fire stations directly impact lung function, enabling the development of strategies to protect firefighters' long-term health.

ABSTRACT NUMBER: 5138 **Poster Board Number:** LB239

TITLE: Use of a Transgenic Human PNPLA3I148M Knock-in Mouse for Nonclinical Safety Evaluations

AUTHORS (FIRST INITIAL, LAST NAME) AND INSTITUTIONS: *B. Brooks*[1], A. Shkumatov[1], *J. Kalanzi*[1], K. Henderson Park[1], J. Lade[1], D. Wong[1], I. Rulifson[1], J. Murray[1], H. Dou[1], L. Mihalcik[2], and *T. Harper*[1]. [1]Amgen Inc., Thousand Oaks, CA; and [2]Aclairo Pharmaceutical Development Group, Vienna, VA.

KEYWORDS: Preclinical Assessments; In Vivo Models; SiRNA; oligonucleotide therapeutics

ABSTRACT: Background and Purpose: The single nucleotide polymorphism (SNP) rs738409 of the patatin-like phospholipase domain containing 3 (PNPLA3^{I148M}) gene is associated with increased incidence of all stages of the non-alcoholic fatty liver disease (NAFLD) spectrum including non-alcoholic steatohepatitis (NASH), cirrhosis, and hepatocellular carcinoma. Hepatic targeting of *PNPLA3^{I148M}* mRNA with a GalNAc-siRNA is therefore an attractive strategy to inhibit *PNPLA3^{I148M}* expression and reduce the progression of NAFLD. The development of an siRNA that specifically targets the rs738409 SNP region of the *PNPLA3^{I148M}* transcript requires thoughtful species selection for nonclinical safety assessment since there are no standard nonclinical species that possess the rs738409 SNP. To address this challenge, we chose to generate a transgenic human PNPLA3^{I148M} knock-in mouse (hPNPLA3^{I148M}) for use during nonclinical safety evaluation of GalNAc-siRNAs specifically targeting the sequence encompassing the human rs738409 SNP. **Methods:** First, to develop a potential nonclinical model the transgenic hPNPLA3^{I148M} mouse line was created using gene-editing technology to remove the wild-type (WT) C57BL/6J mouse Pnpla3 gene and insert the full-length coding region of the hPNPLA3^{I148M} gene. Next, prior to use in toxicology studies, a phenotypic characterization study was performed comparing WT and homozygous hPNPLA3^{I148M} littermates. The results of this characterization study indicated no significant genotype-related phenotypic differences between the two sets of littermates. Lastly, to assess the utility of this model in nonclinical development, an exploratory WT and hPNPLA3^{I148M} mouse repeat-dose toxicology study was performed using a tool GalNAc-siRNA (siRNA-1) which specifically reduces

hPNPLA3^{I148M} and not WT variants. **Results:** Subcutaneous administration of siRNA-1 at 30 or 300 mg/kg once every two weeks for three doses (days 1, 15, and 29) demonstrated knock-down of *hPNPLA3^{I148M}* in the knock-in mice. Besides mRNA expression, siRNA-1-related findings were generally similar between WT and hPNPLA3^{I148M} mice; changes in enzyme levels (AST, ALP, ALT) and correlated microscopic liver findings (single cell necrosis with increased mitoses and hepatocellular vacuolation) were observed. The comparability of the findings between WT and hPNPLA3^{I148M} mice indicated the study findings were a result of siRNA-1 administration and not due to knockdown of the target gene (hPNPLA3^{I148M}). **Conclusions:** Here we demonstrated that the transgenic human knock-in mouse is a suitable model for repeat-dose toxicology studies during the safety assessment of GalNAc-siRNA targeting hPNPLA3^{I148M}, and similar models should be considered for other programs without a pharmacologically relevant nonclinical species. Furthermore, this approach could be applied to reduce reliance on the use of non-human primates during development of siRNAs and other oligonucleotide therapeutics.

ABSTRACT NUMBER: 5140 **Poster Board Number:** LB241

TITLE: Safety testing and biodistribution of viral vectors for *in vivo* cancer immunotherapy

AUTHORS (FIRST INITIAL, LAST NAME) AND INSTITUTIONS: H. Keller[1], D. Winterberg[1], S. Dehmel[1], S. Fricke[2], T. Schmid[2], J. Breuer[2], K. Teichert[3], A. German[4], U. Köhl[2], A. Schöbel[3], H. Zimmermann[4], N. Krug[1], and A. Braun[1]. [1]Fraunhofer Institute for Toxicology and Experimental Medicine ITEM, Hannover, Germany; [2]Fraunhofer Institute for Cell Therapy and Immunology IZI, Leipzig, Germany; [3]Fraunhofer Institute for Industrial Mathematics ITWM, Kaiserslautern, Germany; and [4]Fraunhofer Institute for Biomedical Engineering IBTM, Sulzbach, Germany. Sponsor: *A. Bitsch*

KEYWORDS: Safety Evaluation; Immunotoxicity; Toxicity; Acute; Biodistribution

ABSTRACT: Background and Purpose: Cell and gene therapeutics based on viral vectors have the potential to successfully combat previously incurable diseases such as cancer and hereditary diseases. However, technological hurdles severely restrict the pharmaceutical production of these novel drugs. The project 'GMP-AAV' focuses on developing technologies for an optimal manufacturing process of adeno-associated viral vectors (AAV) for use in in vivo cancer immunotherapy. This approach aims to enable direct genetic modification of T cells within the patient, offering a more accessible and cost-effective alternative to traditional ex vivo CAR-T therapies. The project specifically targets the evaluation of safety, tolerability, and biodistribution of the AAV6 anti-CD4 CAR system to support its future clinical application. **Methods:** The 'GMP-AAV' consortium investigates AAV-based in vivo generation using the example of anti-CD4 CAR T cells. This includes GMP-compliant AAV production, and a toxicological testing strategy based on regulatory guidelines (EMA/CAT/852602/2018, 2019) using pharmacologically relevant in-vitro, ex-vivo and in-vivo models. First, a biodistribution study will be conducted to analyze the distribution of the AAV in the organism, identify target cells in relevant organs and exclude potential off-target effects. For this purpose, a humanized mouse model is used that enables the activation of the T cell response by AAV6 anti-CD4 CAR. In addition, PBMCs will be used to study toxicological effects under near-human conditions. Moreover, inflammatory cytokine responses will be evaluated to ensure the clinical safety of the AAV6 anti-CD4 CAR system. **Results:** As a result of the project, a patented AAV construct for the generation of anti-CD4 CAR T cells, a process for the in vivo generation of anti-CD4 CAR T cells and key technologies for the efficient and safe GMP production of AAV-based gene therapeutics will be available. This will enable AAV cell and gene therapeutics to be made available to significantly more patients more cost-effectively and safely in the future. The results will be applicable for further

AAV-based cell and gene therapeutics beyond CAR-T cell therapy and for other advanced therapy medicinal products (ATMPs). **Conclusions:** With this approach, we are enabling safe testing of AAV constructs for the translation into clinical phase development.

ABSTRACT NUMBER: 5141 **Poster Board Number:** LB242
TITLE: Assessment of Embryo-Fetal Development in Nonhuman Primates Exposed to Teprotumumab, an Ocular Biotherapeutic for Thyroid Eye Disease

AUTHORS (FIRST INITIAL, LAST NAME) AND INSTITUTIONS: *A. D. Lake-O'Connell*, and *J. L. Bussiere*. Amgen, Thousand Oaks, CA.
KEYWORDS: Developmental/Teratology; Safety Evaluation; Bone; Biotherapeutics; Biologic

ABSTRACT: Background and Purpose: Tepezza® (teprotumumab-trbw) is a human IgG1 monoclonal antibody administered intravenously that antagonizes insulin-like growth factor receptor 1 (IGF-1R) signaling. IGF-1R plays a key role in fetal and juvenile skeletal development pathways thus a comprehensive nonhuman primate (NHP) embryo-fetal developmental (EFD) and juvenile toxicity study was conducted. Teprotumumab was originally developed as an oncology program with a nonclinical package based upon the ICH S6(R1) and S9 guidance prior to pivoting to thyroid eye disease (TED). It was approved in the United States (2020) and Japan (2024) for the treatment of adults with TED, a rare disease in adults characterized by inflammation and expansion of the peri- and retro-orbital fat and musculature surrounding the eyes. **Methods:** The toxicology program consisted of repeat dose toxicity studies in the only relevant species, the cynomolgus monkey, in addition to an NHP EFD study initiated in 2008 and a juvenile NHP study initiated in 2009. The EFD study was conducted prior to the ICH S6(R1) revised guidance from June 2011 with recommendations for enhanced pre- and postnatal (ePPND) study conduct. In the EFD study, offspring were evaluated from dams dosed with vehicle (n=6) or teprotumumab (n=7). Dams were dosed with teprotumumab at 75 mg/kg IV weekly after confirmation of pregnancy by ultrasound on GD20 through to delivery by C-section on GD142. In a 13-week juvenile study, NHPs ranged in age at initiation from 11-14 months old and were exposed to teprotumumab at three dose levels (3, 15 and 75 mg/kg/week) with incorporated radiography and bone densitometry evaluations. **Results:** Skeletal abnormalities were observed at GD142 in all offspring from the EFD study exposed to teprotumumab during gestation at an exposure margin of 2.8-fold the highest anticipated clinical exposure. The findings included rounding of the cranium, open fontanelles, micrognathia, narrowing of the nose, thinning of the cranial bones and decreased body weights compared to the control group. Slight, reversible and non-dose responsive decreases in serum alkaline phosphatase (ALP) featured in all adult NHPs (-41 to -49% of pre-study means) and juveniles (-17 to -30% of pre-study averages) in repeat dose studies. Skeletal effects in the juvenile NHP study manifested as decreased bone mass and narrower bones with thinner cortices in all dose groups (1.9-fold exposure margin at the highest dose). **Conclusions:** The NHP findings at clinically relevant exposures in the NHP EFD and juvenile tox studies confirmed that teprotumumab is teratogenic and impacts skeletal growth in the developing primate. These studies together with the literature of other IGF-1R inhibitors contributed to a waiver for conducting additional PPND studies as the hazard was well characterized. The study outcome contributed to the risk language for pregnancy and contraception in the U.S. and Japan labels. Ultimately teprotumumab was approved for adult TED patients with precautions based on the age and profile of this patient population.

ABSTRACT NUMBER: 5142 **Poster Board Number:** LB243

TITLE: Propylene glycol/propylene carbonate mixture: Feasibility as an oral dose vehicle to rat and dog toxicity studies

AUTHORS (FIRST INITIAL, LAST NAME) AND INSTITUTIONS: T. Masuyama, Y. Tanaka, Y. Yasui, K. Yamaguchi, K. Tada, and H. Ouchi. Central Pharmaceutical Research Institute, Japan Tobacco Inc., Yokohama, Kanagawa, Japan. Sponsor: *E. Spicer*

KEYWORDS: Preclinical Assessments; Safety Evaluation; Toxicity; Chronic

ABSTRACT: Background and Purpose: Propylene glycol (PG) and propylene carbonate (PC) are useful solvents for a poorly soluble compound and are often used together as a vehicle for test compounds in nonclinical toxicity studies. Although information on the toxicity of each solvent is widely known, that of the mixture is uncertain because the chemical properties may change. In fact, the solubility of a test compound is often greater in a mixture than in a single solvent. Further, the vehicle selection is limited due to tolerability and physiological effects of the solvents to appropriately evaluate the toxicity of the test compound. We therefore investigated the effects of the PG/PC mixture following multiple oral administration to rats and dogs and determined its maximum feasible dose. **Methods:** The PG/PC mixture at 1:1 volume ratio was administered orally once dairy for 2 or 4 weeks to rats (Crl:CD(SD), males, 6 weeks of age) and beagle dogs (both sexes, 7 to 12 kg body weights). Dose levels were set at 2.5, 5 and 10 mL/kg for the rats and 2 mL/kg for the dogs based on the preliminary data from single dose studies in rats and dogs. In the rat 4-week study, animals in the control group were administered a distilled water (10 mL/kg) in same manner. Clinical observations and measurements of body weights and food consumption were conducted routinely. Clinical pathology, necropsy and histopathological examinations were performed at the end of the dosing period. All experiments were approved by the Institutional Ethics Committee and conducted in accordance with the Guide for the Care and Use of Laboratory Animals (NIH, USA). **Results:** For rats, 4-week repeated oral doses of the PG/PC mixture were well-tolerated at 5 mL/kg whereas there were slight alterations in the clinical pathology parameters. 10 mL/kg of the PG/PC mixture induced increased water intake and urine volume and decreased food consumption with some alterations in some clinical parameters (including decreased blood glucose and increased albumin, bilirubin and calcium levels), suggesting that the dose level of 10 mL/kg would affect the evaluation of the toxicity of a test compound when used as the vehicle. For dogs, 2- or 4-week repeated oral doses at 2 mL/kg were also well-tolerated with no treatment-related findings/changes in the clinical observations, body weights or food consumption during the dosing period. With treatment for up to 2 weeks there were very slight treatment-related alterations in several clinical pathology parameters within the range of the physiological variation. With 4-week treatment, the erythrocyte-related parameters tended to decrease with increased plasma bilirubin levels. However, these effects were very slight and did not affect animals' physical condition. Histopathological examinations revealed no treatment-related findings in any organ/tissue in any of the treated rats and dogs. **Conclusions:** The PG/PC mixture was well-tolerated at up to 5 mL/kg in rats and 2 mL/kg in dogs for 4 weeks, indicating it was useful and feasible vehicle in oral dose toxicity studies using rats and dogs.

ABSTRACT NUMBER: 5143 **Poster Board Number:** LB244

TITLE: Reduced systemic toxicity and enhanced efficacy of CF10, a novel fluoropyrimidine, in colorectal cancer models

AUTHORS (FIRST INITIAL, LAST NAME) AND INSTITUTIONS: *N. Sah*[1], R. Young[1], C. Mani[1], G. Acharya[1], S. Kairamkonda[1], P. Luna[1], M. Reedy[1], W. Gmeiner[2], and *K. Palle*[1]. [1]Texas Tech University Health Sciences Center, Lubbock, TX; and [2]Wake Forest School of Medicine, Winston-Salem, NC.

KEYWORDS: Safety Evaluation; Clinical Toxicology; In Vivo Models; Colorectal Cancer; CF10

ABSTRACT: Background and Purpose: Colorectal cancer (CRC) is the 3rd leading cause of cancer-related deaths with over 53,000 fatalities in 2024 in the U.S. Despite the limited success of advanced targeted therapies, 5-fluorouracil (5-FU)-based chemotherapy regimens (e.g., FOLFOX and FOLFIRI) have remained the primary treatment options for most advanced-stage CRC. However, clinical utilities of 5FU are significantly limited by systemic toxicities and dose limitations. Notably, only ~5% of 5-FU is converted to its active form, limiting efficacy and increasing toxicity. These limitations contribute to the emergence of chemoresistant progressive disease, highlighting an urgent need to develop more potent and safer fluoropyrimidine (FP). We developed CF10, a nanoscale FP polymer with FdUMP repeats, which forms ternary complexes with thymidylate synthase (TS) and topoisomerase-1 (Top1), enhancing efficacy and reducing toxicity. **Methods:** CRC cell lines were treated with CF10 to evaluate the formation of TS-FdUMP ternary complexes and Top1-DNA cleavage complexes. Replication stress markers were analyzed via immunoblot assays. PARP and PARG activities were assessed to determine unresolved DNA damage. Cytotoxicity studies were performed to determine IC50 values for CF10 and 5-FU in CRC cell lines. Mouse flank xenograft models (HCT-116, HT-29, and CT-26) were used to evaluate the histological effects of CF10 and 5-FU on malignant and non-malignant tissues. Gastrointestinal toxicity was assessed through histological examination of intestinal tissues for signs of apoptosis and inflammation. Serum toxicity markers, including alanine aminotransferase (ALT), aspartate aminotransferase (AST), and blood urea nitrogen (BUN), were measured for systemic toxicity. Biodistribution studies were performed following intravenous administration of CF10 or 5-FU. Orthotopic HCT-116-luc CRC models were used to monitor tumor size and survival rates after CF10 and 5-FU treatment. A rat model was used to compare the toxicity profiles of CF10 and 5-FU. As primary patient-derived cell lines better represent the tumor heterogeneity, CF10 was tested on three primary patient-derived colon cancer cell lines to assess its effects on organoid growth in a concentration-dependent manner. Cell-derived xenograft (CDX) models were utilized to evaluate the therapeutic efficacy and toxicity profile of CF10. **Results:** CF10 induced TS-FdUMP and Top1-DNA complexes, increasing replication stress markers (FANCD2, CHK1, CHK2, and H2AX). Further, CF10 selectively inhibited poly(ADP-ribose) polymerase (PARP) and suppressed PARG activity, enhancing unresolved DNA damage in cancer cells while sparing normal cells. CF10 exhibited an IC50 value of 0.05 µM in colorectal cancer cell lines, significantly lower than 5-FU's IC50 of 5 µM, indicating over a 100-fold increase in potency. In HCT-116, HT-29, and CT-26 flank xenografts, histological analysis revealed that CF10 selectively targets malignant cells while sparing non-malignant cells and preserving intestinal villus integrity. In contrast, 5-FU induced significant apoptosis and inflammation in intestinal tissues. Unlike 5-FU, CF10 minimizes gastrointestinal toxicity by reducing RNA-mediated toxic effects, thereby offering a safer therapeutic profile. The ALT, AST, and BUN were within normal range, unlike the significant elevation seen with the 5-FU treatment. Furthermore, CF10 has better tumor localization which contributes to its robust anticancer effects. Improved tumor localization with CF10 reduced tumors and extended survival (84.5 vs 32 days; $P < 0.0001$) in the orthotopic HCT-

116-*luc* CRC mice model. Further in rat models, we tested the effects of the co-administration of ethynyl uracil (EU), an agent that inhibits the hepatic degradation of 5-FU with the dihydropyrimidine dehydrogenase (DPD) enzyme. At 50 mg/kg, CF10 caused no weight loss, unlike 5-FU, even with EU co-administration. The concentration-dependent inhibition of the growth of colon cancer organoids was seen. CF10 inhibited growth in patient-derived organoids and reduced tumor burden in CDX models, improving survival without toxicity. **Conclusions:** CF10 is over a thousand times more potent than 5-FU in killing CRC cells. Moreover, CF10 exhibits superior anticancer efficacy in both invitro and invivo models, along with a significantly improved toxicity profile, making it a promising candidate for treating metastatic CRC.

ABSTRACT NUMBER: 5144 **Poster Board Number:** LB245
TITLE: Retrospective Evaluation of Preclinical Safety Data of Monoclonal Antibodies from Two Charles River Laboratories Sites

AUTHORS (FIRST INITIAL, LAST NAME) AND INSTITUTIONS: C. Thirion-Delalande[1], J. Vein[1], I. Leconte[2], A. Gayot[2], C. Hennion[1], and *S. Bulera*[3]. [1]Charles River Laboratories, Evreux, France; [2]Charles River Laboratories, Lyon, France; and [3]Charles River Laboratories, Reno, NV.
KEYWORDS: Safety Evaluation; Histopathology; Immunotoxicology; Monoclonal antibodies (mAbs)

ABSTRACT: Background and Purpose: Monoclonal antibodies (mAbs) are highly target-specific and cover a wide range of therapeutic indications. We performed a retrospective analysis of toxicology studies of mAbs in Non-Human Primates (NHPs). **Methods:** We examined the data of 53 repeated-dose GLP toxicology studies in NHPs lasting from 2 to 26 weeks and conducted between 2014 and 2022 at two Charles River Laboratories France sites. To guarantee confidentiality with our sponsors, it is not possible to provide details of the identity or mode of action of the molecules tested. **Results:** The most common study design involved weekly administration to juvenile NHPs, with one control and three treated groups. Intravenous (IV) was the main route of administration, but 15 studies were performed by the subcutaneous (SC) route or by SC with an IV arm. Unscheduled mortality was reported in 18 studies, mostly in high-dose groups and sometimes related to exacerbation of mAb pharmacology. MAbs generally have a dose-proportional exposure profile, and 27 studies reported accumulation in plasma and a long elimination time. Clinical pathology analyses showed limited effects on hematology and clinical chemistry profiles. Anatomopathological examination evidenced a minimal list of target organs (mainly injection site, liver, and spleen) and, in a few studies, an immunological effect. **Conclusions:** This retrospective analysis indicates that mAbs have limited adverse effects, often related to their pharmacological mechanism of action, or to interactions with the NHP immune system. In 83% of the studies, the No Observed Adverse Effect Level was the highest dose evaluated, which highlights the opportunity to reduce animal use when mAb safety testing is conducted in non-clinical development.

ABSTRACT NUMBER: 5145 **Poster Board Number:** LB246
TITLE: Effectiveness of Droplet Digital PCR (ddPCR*)* and Hybridization Electrochemiluminescence Immunoassay (ECLIA) for Bioanalysis and Biodistribution of Gene Therapy Products

AUTHORS (FIRST INITIAL, LAST NAME) AND INSTITUTIONS: M. J. Thwaites, K. Gao, J. Leiva, Y. Han, T. Webster, J. Younan, *W. Lee*, and C. Giordano. ITR Laboratories Canada Inc, Baie D Urfe (Montreal), QC, Canada.

KEYWORDS: Pharmacokinetics; Bioavailability; Gene Therapy

ABSTRACT: Background and Purpose: As gene therapy continues to gain traction, the need for precise and accurate measurement of nucleotide-based test compounds *in vivo* is growing significantly. These molecules vary widely in size and chemistry, including but not limited to mRNA, short guide DNA, microRNA, and siRNA. Due to their inherent properties, even a minimal dose can result in substantial functional alterations by suppressing, modulating or restoring gene expression. Therefore, sensitive methodologies are essential to characterize the pharmacokinetics and biodistribution properties of gene therapy products for safety assessment purposes. In this study, we evaluated the effectiveness of Droplet Digital PCR (ddPCR) and Hybridization Electrochemiluminescence Immunoassay (ECLIA) for bioanalysis and biodistribution of nucleotide-based targets. We used genomic DNA as a representative of long and DNA-based molecules and microRNA as a representative of small RNA molecules, thus covering the complete spectrum of nucleotide-based molecules in both length and type (RNA vs DNA), as used in gene therapy. **Methods:** Genomic DNA (gDNA) was used as a surrogate for long DNA molecules and microRNA 122 (miR-122) as a representative short RNA molecule. Because ddPCR requires a minimum length of 70 bp, we extended the microRNA template using hybridization and ligation steps. The genomic DNA was directly quantified. Additionally, we used a hybridization Electrochemiluminescence Immunoassay (ECLIA) to detect miR-122, achieved through hybridizing to a dual-labeled probe followed by digestion and detection. Both gDNA and miR-122 were spiked and diluted into various matrices, including plasma and several homogenized organs, before analysis by ddPCR or Hybridization ECLIA. **Results:** Using gDNA, the ddPCR platform achieved remarkable sensitivity, with a lower limit of quantification (LLOQ) in the femtomolar (fM) range, coupled with impressive precision (%CV) and accuracy (%RE) in plasma. While ddPCR is ideally suited for quantifying target products longer than 70 bp, shorter molecules pose challenges. Therefore, to utilize this technology for smaller molecules such as microRNAs, the template must first be extended to accommodate the necessary elements for the amplification reaction. Using miR-122, we extended the template using the hybridization approach discussed above but the reproducibility of the ddPCR results were very poor. Given the proven robustness of ddPCR, we concluded that the hybridization and ligation step was likely responsible for the lack of reproducibility observed. Recognizing the prevalence of microRNAs as gene therapy tools, we aimed to develop a hybridization-based Electrochemiluminescence Immunoassay (ECLIA) method specifically designed to detect shorter oligonucleotides. Using this technique, we were able to achieve high precision and accuracy across various matrices including organs with acceptable inter-assay precision and accuracy. While not as sensitive as ddPCR, Hybridization ECLIA demonstrated sensitivity within the lower end of the nanomolar (nM) range. **Conclusions:** Our study demonstrates that ddPCR is a highly powerful platform for developing extremely sensitive bioanalytical and biodistribution assays for gene therapy products greater than 70 bp in length. For shorter oligonucleotides, such as microRNAs, siRNA molecules, or guide DNAs, Hybridization ECLIA provides an excellent alternative approach. Although not as sensitive as ddPCR, it still demonstrates acceptable lower limit of quantification (LLOQ) while maintaining a high level of precision and accuracy. Overall, our findings suggest that the length of gene therapy products is a critical factor in determining the optimal approach for bioanalysis and biodistribution in preclinical safety studies.

ABSTRACT NUMBER: 5146 **Poster Board Number:** LB247

TITLE: Validation Study and Focus on the Non-clinical Reproductive and Developmental Toxicity Evaluation System in Cynomolgus Monkeys

AUTHORS (FIRST INITIAL, LAST NAME) AND INSTITUTIONS: L. Zhou[1], Z. Sun[2], C. Pang[1], S. Mao[1], C. Wang[1], *L. Fu*[3], R. Hou[1], and Y. Tian[1]. [1]Hubei Topgene Biotechnology Co., Ltd., Wuhan, China; [2]Committee of Reproductive & Developmental Toxicology, CST, Shanghai, China; and [3]ATS, Breakthrough Pharmaceuticals, Inc., Shanghai, China.

KEYWORDS: Biotech Products; Safety Evaluation; Reproductive and Developmental Toxicology

ABSTRACT: Background and Purpose: In this study, cyclophosphamide and thalidomide were selected to conduct systematic verification tests of teratogenic positive drugs. The purpose was to establish a verification system for embryo - fetal developmental toxicity and perinatal developmental toxicity tests of cynomolgus monkeys in this laboratory, and to generate background data of this laboratory. **Methods:** 3 groups were designed in this study, namely the sodium chloride injection group, the cyclophosphamide group, and the thalidomide group. The number of pregnant animals in each group was 11, 20, and 16 respectively. Considering that the toxic effects of positive drugs had a certain teratogenic sensitive period, drugs were administered only during specific time periods. Specifically, cyclophosphamide at a dose of 20 mg/kg was administered subcutaneously (sc) on GD_{24}-GD_{28}, and thalidomide at a dose of 15 mg/kg was given via gavage administration (ig) on GD_{24}-GD_{30}. During the study, general condition observation, body weight, food consumption, and B - ultrasound examination were carried out, and TK test samples were collected regularly. On GD100, some pregnant monkeys were euthanized and the fetuses were taken out. The fetal weight (including the uterus), placental weight, fetal survival, fetal sex, appearance, weight, degree of development, internal organs, and bones were examined. The remaining pregnant monkeys gave natural birth, and then offspring physical development, functional tests, neurobehavioral tests, and offspring exposure (TK) tests were conducted. **Results:** 1: Sodium chloride injection group: In the EFD study, the overall abortion rate of pregnant monkeys during gestation was 18% (2/11), and the number of live births detected on GD_{100} was 6, and the abortion rate was 14% (1/7); In the PPND study, the number of live births in natural delivery was 3, and the abortion rate was 25% (1/4). No abnormalities were found in the observation of GD_{100} necropsy and natural delivery of the animals.2: Cyclophosphamide group: In the EFD study, the overall abortion rate of pregnant monkeys during gestation was 35% (7/20), and the number of live births detected on GD_{100} necropsy was 7, and the abortion rate was 30% (3/10); In the PPND study, the number of live births in natural delivery was 6, and the abortion rate was 40% (4/10). Compared with the sodium chloride injection group, the abortion rate of pregnancy in the cyclophosphamide group was significantly higher, and the maternal toxicity was obvious. F_1 exhibited facial deformity, developmental retardation or deformity of carpal bones, phalanx and ribs. Cyclophosphamide was considered to have significant embryo-fetal and young monkey toxicity.3: Thalidomide group: In the EFD study, the overall abortion rate of pregnant monkeys during gestation was 19% (3/16), and the number of live births detected at GD_{100} necropsy was 7, and the abortion rate was 13% (1/8); In the PPND study, the number of live births in natural delivery was 6, and the abortion rate was 25% (2/8). Compared with sodium chloride injection group, there was no increase in abortion rate and no maternal toxicity in thalidomide group. F_1 exhibited bone deformity of the four limbs (missing, undeveloped or shortened front/back limbs). Thalidomide was considered to have significant teratogenic effects. **Conclusions:** Under the conditions of this study, after cynomolgus monkeys were subcutaneously injected with 20 mg/kg cyclophosphamide on GD_{24}-

GD_{28}, and given 15 mg/kg thalidomide via gavage administration on GD_{24}-GD_{30}, teratogenic effects were found. The toxic characteristics and incidence were similar to those reported in the literature. The above results indicated that the embryo - fetal developmental toxicity and perinatal developmental toxicity tests of cynomolgus monkeys has been verified under the conditions of this laboratory, and some background data had been established. The continuous development of biological products has made the non - human primates (NHP) increasingly common, which was as the only relevant species for conducting developmental and reproductive toxicity (DART) studies. In the past decade, one - third of the BLAs (Biologics License Applications) approved by the FDA have involved DART tests using NHPs that could not be replaced with alternative molecules, transgenic animals, *in vitro* studies, etc. Research on reproductive and developmental toxicity of cynomolgus monkeys was crucial to promote the marketing of many drugs, and the establishment of reproductive and developmental toxicity evaluation system of cynomolgus monkeys were also encountered with many challenges.First of all, the basic knowledge and technology of raising monkeys were the basic conditions for carrying out experiments, and the laboratory personnel should have a full understanding of the reproductive physiological characteristics of non-human primate laboratory animals; Secondly, in order to ensure that the test complies with GLP standards, pregnant monkeys could not be purchased from feedlots for reproductive and developmental toxicity tests. Therefore, the mating and nursing of experimental monkeys were crucial; Thirdly, a proficient grasp of the knowledge of reproductive and developmental toxicology of drugs and its technology was required, along with highly skilled scientists and technically proficient personnel in this field; Fourthly, a monkey farm with sufficient population and a certain scale of GLP study site were sufficient guarantees to carry out experiments. Fifth, the GLP center for the evaluation of reproduction and development of cynomolgus monkeys should have a social living environment conforming to animal welfare, and a large mating cage with one male and multiple females in line with nature; Finally, conducting this study required extensive training and preparation, as much background data from the laboratory of the facility as possible, along with accurate judgment of positive results.To sum up, the establishment of non-clinical reproductive and developmental toxicity evaluation system for cynomolgus monkeys and its application in non-clinical assessment was a complex and meticulous process, which required the consideration of factors such as animal species specificity, animal age, physiological state, dose, administration route, cycle and frequency of test article according to ICH S5(R3), ICH S6, etc., as well as important factors such as the stability and toxicokinetics of the test article. Additionally, emphasis should be placed on the training of the experimental personnel and the guarantee of animal welfare, to ensure the scientific validity of the results and compliance with ethical standards.

ABSTRACT NUMBER: 5147 **Poster Board Number:** LB248

TITLE: Sydlab™ One: An automated microfluidic platform for scalable, high-content toxicological screening in *C. elegans*

AUTHORS (FIRST INITIAL, LAST NAME) AND INSTITUTIONS: M. Pierron, A. Vaudano, M. Bourgeois, L. Stojkovic, F. Tâche, M. Cornaglia, and L. Mouchiroud. Nagi Bioscience SA, EPFL Innovation Park, St-Sulpice, Switzerland.

KEYWORDS: Risk Assessment; Reproductive and Developmental Toxicology; Biotech Products

ABSTRACT: Background and Purpose: Conventional toxicological assays often face significant limitations: cellular models lack the complexity of whole organisms, while vertebrate testing is

expensive, ethically constrained, and has an inherent low throughput. *Caenorhabditis elegans*, a soil nematode and validated model organism, provides a promising middle ground. Performing assays with *C. elegans* allows testing on a whole organism at a scale similar to in vitro assays, with easier handling and in a cost-effective way compared to vertebrates. To reduce the experimental burden and improve scalability, we developed Sydlab™ One, an automated microfluidic platform capable of culturing multiple *C. elegans* populations in parallel and administering treatments throughout their entire lifecycle. **Methods:** Treated populations are monitored through hourly brightfield and fluorescence imaging, and our machine learning-based data analysis pipeline yields multi-phenotypic data for both parental worms and their progeny. We combine data science tools with our High-Content Screening (HCS) approach to provide early insights into the mode of action of test chemicals. In addition, the ability to perform fluorescence imaging enables the use of reporter strains, further broadening the scope of available phenotypic readouts and enabling mechanistic investigations. **Results:** To demonstrate Sydlab™ One's capabilities, we screened 21 benchmark chemicals at 5 concentrations each - including 16 with known toxicological profiles (e.g., methotrexate, thalidomide) and 5 considered safe (e.g., sodium chloride, ascorbic acid, progesterone) - by treating populations from the L4 stage (shortly before sexual maturity) into adulthood. Our platform achieved an 85.7% overall accuracy in correctly classifying the profile of the screened chemicals and a 93.3% positive predictive value for toxic effects. **Conclusions:** These results highlight the platform's potential for robust, scalable, and accurate toxicological and ecotoxicological testing, thus offering a novel medium for early dose calibration and hazard identification.

ABSTRACT NUMBER: 5148 **Poster Board Number:** LB249

TITLE: Nonclinical Safety Profile of an Antibody Oligonucleotide Conjugate, AOC 1044, for the Treatment of Duchenne Muscular Dystrophy

AUTHORS (FIRST INITIAL, LAST NAME) AND INSTITUTIONS: *T. S. Lahoti*, L. Leung, P. Kovach, A. Anderson, U. Etxaniz, M. Diaz, I. Marks, *E. Blasi*, A. Levin, and H. Younis. Avidity Biosciences Inc., San Diego, CA.

KEYWORDS: Pharmaceuticals; Regulatory Science/Regulatory Toxicology; Antibody oligonucleotide conjugates

ABSTRACT: Background and Purpose: Antibody oligonucleotide conjugates (AOCs) combine the tissue specificity of monoclonal antibodies with the precision and potency of oligonucleotides to enable the targeted delivery of oligonucleotides to previously untreatable tissues and cell types. Duchenne muscular dystrophy (DMD) is a debilitating genetic disease caused by mutations in the dystrophin gene, leading to reduced or absent functional dystrophin protein in muscle tissue. Antisense oligonucleotide-mediated exon skipping has been shown to be a promising therapeutic strategy, allowing restoration of an open reading frame and production of near-full-length dystrophin protein. AOC 1044 (delpacibart zotadirsen; *del-zota*) is comprised of an exon 44-targeting phosphorodiamidate morpholino oligomer (PMO44) conjugated to an antibody targeting human transferrin receptor 1 (TfR1), designed for delivery of PMO44 to skeletal muscle and heart tissue. **Methods:** The safety profiles of AOC 1044 and its components (antibody or oligonucleotide) were evaluated in vitro and in vivo in cynomolgus monkeys for up to 9 months of repeat dosing (IV, Q4W). **Results:** AOC 1044 was non-genotoxic and did not cause hybridization-dependent off-target activity. AOC 1044 was pharmacologically active in monkeys, as demonstrated by a dose-dependent increase in exon 44 skipping percentage in skeletal muscle and

cardiac tissue as assessed by droplet digital PCR. There were no adverse AOC 1044-related effects based on all examined endpoints (clinical pathology, pathology, safety pharmacology). The no-observed-adverse-effect level (NOAEL) was the highest AOC dose tested of 252 mg/kg (45 mg/kg PMO). Non-adverse minimal to mild findings included hematology changes consistent with the transient modulation of TfR1. Histopathology findings were limited to basophilic granularity of the renal tubular epithelium, presence of Kupffer cells in the liver, and mild vacuolation in the renal tubular epithelium. These changes are known class effects due to oligonucleotide accumulation in the endolysosome. Importantly, no safety concerns were associated with the dose-dependent increase in exon 44 skipping in skeletal muscle and heart of cynomolgus monkeys. **Conclusions:** The safety data from this study informed the selection of starting dose to test AOC 1044 in individuals with DMD amenable to exon 44 skipping.

ABSTRACT NUMBER: 5149 **Poster Board Number:** LB250
TITLE: Cardiotoxicity testing on CardioSpheres with a novel MEA technology

AUTHORS (FIRST INITIAL, LAST NAME) AND INSTITUTIONS: C. Hoebart, M. Lux, B. Baltov, S. Beyl, and *S. Hering*. Chanpharm, Vienna, Austria. Sponsor: S. Hering, Safety Pharmacology Society
KEYWORDS: Safety Pharmacology; Induced Pluripotent Stem Cells; Cardiovascular System

ABSTRACT: Background and Purpose: To date cardiotoxicity studies are predominantly carried out on two-dimensional (2D) monolayer cultures of human induced pluripotent stem cell (hiPSC)-derived cardiomyocytes, as described in Blinova *et al.* 2018 within the framework of the Comprehensive in vitro Proarrhythmia Assay (CiPA) initiative. However, cardiomyocytes that grow as a monolayer do not reflect physiological conditions, as in the heart multiple cell types interact in a three-dimensional (3D) environment, which can influence the response to pro-arrhythmic agents. The aim of this study was to investigate whether newly released 3D CardioSpheres from Fujifilm Cellular Dynamics are suitable for cardiotoxicity testing. To acquire multiple recordings of surface potentials from these CardioSpheres we made use of a novel proprietary perfusion chamber. In this study we also compared the sensitivity of 3D CardioSpheres to cardiotoxic substances with data obtained with standard monolayer hiPSC-cardiomyocyte culture using a voltage-sensing optical technique, calcium imaging and multi electrode arrays (MEA). **Methods:** CardioSpheres were generated as described by Fujifilm Cellular Dynamics by mixing hiPSC-derived cardiac fibroblasts, endothelial cells and cardiomyocytes[2] in ultra-low attachment plates and cultivating them for 7 to 30 days. These CardioSpheres were then either stained with the voltage sensing dye FluoVolt or with Calcium-6 for optical measurements or placed on MEAs for studies of the surface membrane potential. The novel FunnelChips fixed the CardioSpheres on the electrodes, thereby reducing motion artefacts throughout the experiment, including fluid exchange for compound application. Dofetilide and E4031 were then cumulatively applied in increasing concentrations from 10 up to 300 nM every 5 minutes. In order to compare results similar recordings were made with optical tools using the dye FluoVolt to measure action potentials and calcium 6 to record calcium transients. In these experiments dofetilide and E4031 were applied in a single concentration per well (10 up to 300 nM) with 5 minutes incubation time. **Results:** CardioSpheres were generated as stated by the supplier, with size and beating behavior corresponding to those described. The novel FunnelChip technology enabled stable electrical recording from the cardiac spheroid surfaces for up to 40 minutes. Compound induced prolongation of the field potential duration upon application of dofetilide and E4031 were detected. Corresponding dose-dependent increases in the action potential duration at 90% repolarization (APD90) and calcium transients were observed for the test compounds. The highest

applied concentration of dofetilide (300 nM) led to cessation of beating. Compared to hiPSC-derived cardiomyocyte monolayers the prolongation of the action potential by dofetilide was more pronounced in CardioSpheres. **Conclusions:** Our new FunnelChip MEA technology enables stable, long-lasting measurements of surface potentials on CardioSpheres. The sensitivity of CardioSpheres to gold standard hERG channel inhibitors dofetilide and E4031 were comparable or even higher than found in monolayer cultures. In addition, optical membrane potential or calcium transient recording revealed comparable effects regarding drug sensitivities. Future work will be focused on more extensively comparing 3D CardioSpheres to the well-established cardiomyocyte monolayer cultures using CiPA cardiac reference compounds of different risk categories (Blinova *et al.* 2018).

ABSTRACT NUMBER: 5150 **Poster Board Number:** LB251
TITLE: Generation of cardiac fibers for toxicity testing

AUTHORS (FIRST INITIAL, LAST NAME) AND INSTITUTIONS: M. Lux[1], C. Höbart[1], B. Baltov[1], S. Beyl[1], B. Richter[2], and S. Hering[1]. [1]Chanpharm, Vienna, Austria; and [2]Nanoscribe, Karlsruhe, Germany. Sponsor: S. Hering, Safety Pharmacology Society
KEYWORDS: Safety Pharmacology; Cardiovascular System; Induced Pluripotent Stem Cells

ABSTRACT: Background and Purpose: Cardiac safety pharmacology is currently based on patch clamp studies on mammalian cell lines overexpressing ion channels that are crucial for the cardiac action potential and studies on more complex cell models such as human induced pluripotent stem cell-derived cardiomyocytes (iPSC-CM). Two dimensional monolayers of iPSC-CM do not reflect the complex anatomy of the myocardium and toxicological studies on this model have limited significance. The aim of this study was therefore to develop MEAs with a three-dimensional surface enabling the formation of myocardial fibers. **Methods:** Groove structures for fiber growth were produced by means of 2-photon printing technology (Nanoscribe, Karlsruhe, Germany) on 60-electrode MEAs (Multi Channel Systems, Reutlingen, Germany). After coating with fibronectin, suspensions of iPSC-CM were applied to the grooved MEA surfaces. The cells were concentrated in the groove structures by centrifugation and the chip subsequently placed in a cell culture incubator (37°C, 5% CO_2). The formation of fibers was monitored by imaging. Drug-induced changes in cardiac surface potentials were measured with a MEA2100 Mini system (Multi Channel Systems) by cumulatively applying compounds in increasing concentrations from 10 up to 300 nM every 5 minutes. The time-delayed arrival of the excitation at the MEA electrodes along a fiber enabled the calculation of the speed of excitation propagation using a custom-made analysis software. **Results:** Myocardial fibers formed in the grooves (each containing up to 8 surface electrodes) within 5 to 7 days and remained in the grooves for up to 4 weeks. During an experiment this novel fiber technology enabled electrical recording for up to 40 minutes. The close contact between the MEA electrodes and fiber surfaces enabled measurements of surface potentials with a sufficient signal-to-noise ratio. The fibers appeared to be highly sensitive to the hERG channel inhibitors dofetilide and E4031 as evident from a dose-dependent prolongation of the field potential duration. By using customized software, it was possible to determine both the starting point of the excitation wave and the speed of the excitation in the fibers. **Conclusions:** Making use of 2-photon printing technology we developed novel MEAs that can not only estimate drug-induced changes in field potential duration but also simultaneously measure the speed of excitation propagation along myocardial fibers. Additionally, the signal-to-noise ratio was found to be improved in fibers compared to monolayers of iPSC-CM. In the future, the signal-to-noise ratio should be further improved by better

concentrating the cells in the groove structures, while also using less iPSC-CM. Further development of the technology will focus on developing a multiwell format, to enable studies on a larger scale.

ABSTRACT NUMBER: 5151 **Poster Board Number:** LB252
TITLE: A state-of-the-art method for high-throughput, automated locomotor activity testing in neuropharmacology, safety, and toxicology studies

AUTHORS (FIRST INITIAL, LAST NAME) AND INSTITUTIONS: G. Bell[1], T. Velie[1], K. Mendiola[1], H. Simenson[1], F. Mannara[2], K. Nichols[1], K. White[1], K. Swearington[1], A. Mehendale[1], M. Girand[1], C. Kolin[1], J. Alvarez[1], and E. Celerier[2]. [1]Harvard Bioscience, Holliston, MA; and [2]Panlab, Barcelona, Spain. Sponsor: M. Girand, Safety Pharmacology Society
KEYWORDS: Toxicity; Acute; Safety Pharmacology; In Vivo Models

ABSTRACT: Background and Purpose: Background: Quantifying spontaneous locomotor activity, stereotyped movements, anxiety-related behavior, and exploration parameters is pivotal in neuropharmacology, safety, and neurotoxicity studies to determine whether new chemical entities possess psychostimulant, sedative, or toxic effects. Such studies may involve large-scale assessments of locomotor activity in rodents under GLP compliance, which can be labor-intensive and timeconsuming. To address these challenges, we have developed the VivaMARS system for automated, high-throughput (up to 30 subjects by session) locomotor activity testing in rodents. Objective: This study aims to validate the VivaMARS platform with two reference compounds: caffeine (CAF), known to increase rodent locomotor activity, and chlorpromazine (CPZ), known to decrease rodent locomotor activit. **Methods:** All animal care and procedures were approved by the DSI IACUC. Experiments were performed using healthy adult CD1 male mice (4-5 weeks old, 25-35g, N=15) and adult Sprague Dawley rats (6-7 weeks old, 250-300g, N=25). Animals were procured from Charles River (Kingston, NY, USA). All animals were socially housed in an individually ventilated cage (Tecniplast; West Chester, PA, USA; GM500) inside a conventional facility with controlled temperature and humidity under a standardized 12-hour dark/light cycle. Food and water were provided ad libitum. Mice and rats were divided into five groups: Saline, CAF low-dose (4 mg/kg), CAF high-dose (16 mg/kg), CPZ low-dose (3 mg/kg), and CPZ high-dose (10 mg/kg). For the locomotor activity test, the animals are placed individually into the VivaMARS experimental arenas without previous habituation. Locomotor activity tests were conducted over a 60-minute period immediately after CAF administration and 30 minutes post-CPZ administration. Data was acquired and analyzed using the Ponemah software. Caffeine anhydrous was purchased from Sigma-Aldrich Inc.(Saint-Louis, US), and chlorpromazine hydrochloride from West-Ward Pharmaceuticals (Eatontown, US). CAF and CPZ were diluted and dissolved in saline (NaCl 0.9%). The solutions of the compounds were prepared fresh daily and injected intraperitoneally (IP) at a volume of 5 ml/kg. **Results:** The animal groups treated with CAF displayed an increase in the total distance traveled, the total number of rearing and mean speed during a 60-minute acute locomotor activity test. Conversely, the groups treated with CPZ exhibited a significant reduction in these measures. The increase in locomotor activity in the CAF-treated groups and the decrease in the CPZ-treated groups are consistent throughout the experiment. Values are represented as the mean ± SD of N=3 mice per group or N=5 rats per group. Statistical analyses were conducted using one-way ANOVA with Dunnett's post hoc test, Kruskal-Wallis ANOVA with Dunn's post hoc test, or two-way repeated measures ANOVA with Geisser-Greenhouse correction, according to the experimental conditions and distributional normality. ActiD = Activity with displacements, ActiND = Activity without displacement, Activ = Activity global (ActiD + ActiND). All the

parameters were increased in the CAF groups except ActiND, which was not significantly higher than the Saline group, and the immobility time, which decreased. Opposite effects are observed in the CPZ groups. Values are represented as the mean ± SD. Statistical analyses were conducted using one-way ANOVA. **Conclusions:** Our data demonstrates that the VivaMARS mobile activity rack system is a powerful and efficient platform for acute locomotor activity testing in rodents. Further experiments are needed for a more comprehensive validation of the instrument.

ABSTRACT NUMBER: 5152 **Poster Board Number:** LB253

TITLE: Temperature effect on hERG channel pharmacology measured using the Qube automated patch clamp system

AUTHORS (FIRST INITIAL, LAST NAME) AND INSTITUTIONS: D. Nagy[1], A. Lindqvist[2], M. Christensen[2], *R. Jacobsen*[2], and G. Mattson[2]. [1]Sophion Bioscience, Bedford, MA; and [2]Sophion Bioscience A/S, Ballerup, Denmark. Sponsor: D. Nagy, Safety Pharmacology Society

KEYWORDS: Cardiovascular System; In Vitro and Alternatives; Preclinical Assessments

ABSTRACT: Background and Purpose: The human ether-à-go-go related gene (hERG) function is crucial for cardiac repolarization. Inhibition of the hERG channel can prolong cardiac action potentials, increasing the risk of ventricular arrhythmias, including torsade de pointes (TdP). Therefore, in vitro evaluations of compound effects on the hERG channel are routinely conducted in drug development to detect potential arrhythmic side-effects. Traditionally, these evaluations are performed at ambient temperatures. However, previous studies have shown that potency for certain compounds is underestimated when compared to tests at near-physiological temperatures. This study aims to highlight the importance of a temperature-controlled measuring environment for accurate evaluation of hERG channel blockers and to demonstrate the capabilities of the Qube Automated Patch Clamp system in providing such an environment. **Methods:** We utilized the Qube 384 automated patch clamp system, equipped with a temperature control unit, to investigate the effects of temperature on concentration-response relationships for a panel of known hERG channel blockers, namely: verapamil, quinidine, erythromycin, sotalol, E-4031, and cisapride. The Qube system allows for up to 384 parallel recordings at controlled temperatures ranging from 8°C and above. Biophysical and pharmacological experiments were conducted to assess the impact of temperature on channel activation and inactivation kinetics, as well as compound potency. **Results:** Our experiments showed that temperature control significantly influences hERG channel pharmacology. We observed an increased rate of activation, a leftward shift in steady-state activation, and a rightward shift in steady-state inactivation with rising temperatures. Pharmacological responses varied with different compounds; for instance, verapamil and quinidine potencies remained unchanged with temperature variations, while erythromycin, sotalol, E-4031, and cisapride exhibited pronounced leftward shifts in potency when temperature increased from 18°C to 34°C. **Conclusions:** The findings underscore the importance of temperature control in hERG channel evaluations. The Qube 384 automated patch clamp system, with its ability to regulate and standardize temperature at the measurement site, proves to be a reliable tool for routine compound testing under controlled temperature conditions. This study confirms that accounting for temperature is critical in accurately assessing the pharmacology of hERG channel blockers, thereby enhancing the predictive power of in vitro assays in drug development.

ABSTRACT NUMBER: 5153 **Poster Board Number:** LB254
TITLE: Exploring Sex-Specific CAR-Driven Hepatocyte Proliferation in Murine *In Vitro* Models

AUTHORS (FIRST INITIAL, LAST NAME) AND INSTITUTIONS: A. Scheffschick[1,2], O. S. Talkhan[1,2], G. Schicht[1,2], V. Brandt[1,2], M. Goettel[3], E. Fabian[4], D. Seehofer[1,2], R. Landsiedel[4], and G. Damm[1,2]. [1]University Hospital of Leipzig, Leipzig, Germany; [2]Saxonian Incubator for Clinical Translation (SIKT), Leipzig, Germany; [3]BASF SE, Global Toxicology Agricultural Solutions, Limburgerhof, Germany; and [4]BASF SE, Experimental Toxicology and Ecology, Ludwigshafen am Rhein, Germany. Sponsor: G. Damm, EUROTOX
KEYWORDS: Hepatocytes; In Vitro and Alternatives; Carcinogenesis; Proliferation; Phenobarbital

ABSTRACT: Background and Purpose: The constitutive androstane receptor (CAR), a pivotal nuclear receptor, governs key hepatic responses to xenobiotics. Activation of CAR by compounds such as phenobarbital (PB), a recognized hepatocellular carcinoma (HCC) promoter in rodents, stimulates both xenobiotic-metabolizing enzymes and hepatocyte proliferation. While PB exhibits species-specific effects, promoting liver tumors in rodents but not in humans, CAR-driven hepatocyte proliferation also displays notable sex-specific variations. This study examines these differences in an *in vitro* murine model. **Methods:** Primary hepatocytes were isolated from C57BL/6J mice and cultured for five days. Cells were treated with low-dose (200 µM) and high-dose (1000 µM) PB, alongside HGF and EGF as controls for proliferation. Culture viability was assessed daily via protein content (BCA assay) and cellular activity (Alamar Blue assay). CYP enzyme activities (AROD assay) were measured on days 1 and 4, while proliferation was quantified using immunofluorescence staining (Ki67, BrdU) on days 3 and 4. **Results:** Cultures remained viable for five days, despite declining protein content and cell activity. No significant hepatotoxicity was observed across treatments. In male hepatocytes, PB induced dose-dependent increases in EROD (1.5x for LD, 1.8x for HD) and PROD (2.5x for LD, 3.2x for HD) activities. Female hepatocytes exhibited enhanced PROD activity only with LD PB (2x). Proliferation assays revealed robust responses in males, with LD PB increasing Ki67 by 5x after 72 hours. HD PB further amplified Ki67 by 8.3x and BrdU by 6.5x after 72 hours. Female hepatocytes demonstrated more variable responses, with LD PB significantly enhancing BrdU levels (3.8x) after 48 hours. **Conclusions:** These results underscore the sex-specific nature of CAR-mediated hepatocyte proliferation in mice, highlighting the necessity of integrating sex as a variable in toxicological research. Ongoing studies with primary human hepatocytes aim to delineate species-specific differences and mechanisms underlying these effects.

ABSTRACT NUMBER: 5154 **Poster Board Number:** LB255
TITLE: A 3D Bioprinted Vascularized Liver-on-a-Chip Platform for Human-Relevant Drug-Induced Liver Injury Assessment

AUTHORS (FIRST INITIAL, LAST NAME) AND INSTITUTIONS: S. Ng, C. Trinconi, C. Erice, H. Pham, D. Rodriguez, Q. Dasgupta, *J. Navarro-Yepes*, Y. Han, M. Doerfert, P. Crandell, W. Harley, A. Vieira Pigatto, A. Narkar, C. Mello, S. Datwani, and T. Pereira. Systemic Bio, Houston, TX. Sponsor: J. Navarro Yepes, American Association for Cancer Research
KEYWORDS: In Vitro and Alternatives; Hepatic; Metabolism

ABSTRACT: Background and Purpose: Drug development is a resource-intensive and high-risk endeavor, with 90% of clinical trials failing despite promising preclinical results. Traditional liver toxicity models face significant limitations, including species-specific differences, the rapid de-differentiation of primary human hepatocytes (PHHs), and the absence of a physiologically relevant microenvironment. These

challenges contribute to poor predictive power and high drug attrition rates in preclinical development. Liver microphysiological systems (MPS) offer a more human-relevant alternative, but existing models often lack structural complexity needed for meaningful translational insights. To address this, Systemic Bio's 3D bioprinted Human Vascularized Integrated Organ System (h-VIOS™) platform recapitulates native-like liver architectures and vascularization. This study validates h-VIOS™ for ADME-Tox applications by evaluating its response to small molecules, monoclonal antibodies, and antibody-drug conjugates, demonstrating its potential to enhance the relevance of preclinical insights and reduce late-stage drug failures. **Methods:** The h-VIOS™ liver platform integrates PHHs and non-parenchymal cells (NPCs) to replicate liver microtissue and vasculature. The interstitial architecture was optimized for lobular-inspired connectivity, cellular crosstalk, and permeability. Vasculature designs and flow parameters supported oxygen and nutrient transport, enabling functional liver sinusoidal endothelial cell (LSEC) linings. Baseline characterization included albumin production, urea synthesis and Phase I/II gene expression. Pharmacokinetics were validated by measuring elimination rates of compounds with known clearance via LC-MS. Hepatotoxicity studies utilized GO-ADC to model LSEC toxicity and Trovafloxacin or Urelumab (± PBMCs) to assess immune-mediated toxicity. Liver health was evaluated via biomarkers (albumin, ALT, cytokines), while immune recruitment was assessed with immunofluorescence, using machine learning-enabled algorithms, demonstrating robust liver function and drug toxicity modeling. **Results:** The h-VIOS™ platform demonstrated functional liver vasculature, as evidenced by robust coverage and preservation of key endothelial markers, including CD31, VCAM, ICAM, and PECAM. PHHs cultured in the h-VIOS platform showed significantly enhanced albumin and urea production compared to conventional 2D cultures and static conditions. Endpoint RT-qPCR analysis revealed that Phase I and II metabolic gene expression recovered to levels comparable to, or exceeding, those of freshly-thawed PHHs. For pharmacokinetic validation, intrinsic clearance rates for test compounds in the h-VIOS™ platform matched or outperformed legacy data from 2D and spheroid models, highlighting the preservation of Cytochrome P450 isoforms and Phase II enzyme activity. Upon treatment with GO-ADC, the platform showed dose-dependent hepatotoxicity, as evident by the reductions in hepatic cluster size, albumin production, associated with the elevated LDH and ALT levels. Notably, the vasculature compartment exhibited significant LSEC loss, accompanied by early toxicity markers, including elevated endothelial ICAM-1 and P-selectin levels and increased secretion of sPECAM and sICAM-1. These findings align with clinical manifestations of sinusoidal obstruction syndrome observed in patients and corroborated by non-human primate toxicology studies, reinforcing the platform's predictive accuracy for drug-induced liver toxicity. Furthermore, treatment with Trovafloxacin and Urelumab highlighted the functional roles of resident Kupffer cells (KCs) and their complex interplay with circulating immune cells and functional endothelium. Differential toxicity effects were observed in tri-culture systems (PHH+KC+/-LSEC) compared to mono-culture systems (PHHs). These effects were supported by elevated inflammatory cytokines (TNF-α, IFN-γ, and IL-6) and a dose-dependent decline in albumin production rates. These proof-of-concept studies underscore the h-VIOS™ platform's potential for evaluating drugs with complex mechanisms of toxicity, particularly advanced modality therapeutics, paving the way for more accurate preclinical drug assessment. **Conclusions:** Systemic Bio’s h-VIOS platform demonstrates physiologically relevant predictive capabilities for ADME and toxicology across diverse drug modalities and mechanisms of toxicity. By replicating a vascular and hepatic microenvironment inspired by native physiology, this system offers critical insights into the vascular effects of novel therapeutics, enabling more informed drug development, enhancing safety assessments, with the potential of minimizing the risk of clinical trial failures.

ABSTRACT NUMBER: 5155 **Poster Board Number:** LB256
TITLE: Hepatic AhR-mediated regulation of obesity

AUTHORS (FIRST INITIAL, LAST NAME) AND INSTITUTIONS: A. M. Olajuyin, *C. Elferink*, and *C. Wright*. UTMB, Galveston, TX.
KEYWORDS: Hepatic; Metabolism; Exposure, Environmental

ABSTRACT: Background and Purpose: The aryl hydrocarbon receptor (AhR) is a cytosolic, ligand-activated transcription factor that acts in concert with the AhR nuclear translocator (ARNT) to modulate target gene expression. We recently showed that female, but not male liver-specific AhR conditional knockout mice are protected from high fat diet-induced obesity and exhibited improved metabolic homeostasis. The sexually dimorphic phenotype was attributed to increased hepatic expression of fibroblast growth factor 21 (FGF21) in females. FGF21 is a circulating hepatokine that affects carbohydrate and lipid metabolism and induces thermogenesis in white and brown fat deposits. Additionally, hepatic *Fgf21* expression is under the control of several other physiological cues, including circadian rhythms. This observation is notable because both AhR and ARNT belong to the same Per-ARNT-Sim (PAS) protein family as several of the circadian rhythm proteins, including brain and muscle ARNT-like 1 (BMAL1). As the name implies, BMAL1 shares considerable sequence similarity to ARNT, and can interact with AhR, suggesting that *Fgf21* expression is regulated by interactions between circadian rhythmicity and AhR signaling. However, molecular mechanisms underlying these effects remain largely unknown. **Methods:** To examine whether *Ahr* and *Fgf21* expression follows circadian rhythmicity, and how the rhythmicity compares to expression of circadian rhythm proteins, Hepa 1c1c7 cells (mouse) and HepaRG cells (human) were synchronized by serum shock. In complementary experiments, liver samples were collected at Zeitgeber time (ZT) ZT0, ZT2, ZT4, ZT8, and ZT24 from female C57BL/6J mice and circadian expression profiles were generated for *Ahr*, *Fgf21*, *Bmal1*, *Per1*, and *Nr1d1*. Lastly, to probe whether AhR-ARNT binding to their cognate DNA site (xenobiotic response element, XRE) in the *Fgf21* promotor was a function of circadian rhythm, chromatin immunoprecipitation (ChIP) studies on whole liver from C57BL/6J mice was performed at ZT2, ZT8, and ZT24. **Results:** *Ahr* expression displays variation with a 24-hour periodicity in phase with *Fgf21* and *Bmal1* expression, in both mouse and human hepatic cell lines, and in mouse liver, suggestive of co-regulation of these proteins. Furthermore, ChIP studies revealed that AhR occupies all three XREs within the *Fgf21* promoter in phase with the expression pattern of *Fgf21*, peaking around ZT8, and exhibiting a diurnal rhythm suggestive of an oscillating endogenous AhR agonist. **Conclusions:** Hepatic *Fgf21* expression represents a nexus where AhR signaling and the molecular events underlying sexual dimorphism and circadian rhythmicity coalesce. Physiologically, AhR interactions with the clock machinery may be central to integration of cellular metabolism through regulation of *Fgf21* expression, among other genes (i.e., many of the same genes affected by AhR activation are controlled physiologically by the circadian clock). Accordingly, we are currently investigating the possibility that BMAL1 binding to the *Fgf21* promoter is AhR dependent

---

ABSTRACT NUMBER: 5156 **Poster Board Number:** LB257
TITLE: Differential impacts of single and repeated MCLR exposure on liver pathologies in healthy versus MASLD conditions

AUTHORS (FIRST INITIAL, LAST NAME) AND INSTITUTIONS: *V. O. Ikumawoyi*[1], T. Arman[1], J. Baron[1], K. D. Hart[1], D. T. Iverson[1], L. A. White[2], J. Aldan[1], and *J. D. Clarke*[1]. [1]Washington State University, Spokane, WA; and [2]Washington State University, Pullman, WA.

KEYWORDS: Environmental Toxicology; Hepatic; In Vivo Models; Microcystin-LR, Inflammation, MASLD, RNAseq

ABSTRACT: Background and Purpose: Microcystin-LR (MCLR) is a hepatotoxin produced by freshwater cyanobacteria. It is a risk factor for the development of hepatocellular carcinoma (HCC). Metabolic dysfunction-associated steatotic liver disease (MASLD), which is often caused by poor diet and lifestyle, is a prevalent disease that is characterized by steatosis, steatohepatitis, and fibrosis and contributes to the clinical burden of HCC. MCLR exposure alongside the consumption of a high-fat, high-cholesterol (HFHC) diet has been reported to lead to the pathological hallmarks of MASLD. However, there is a need to evaluate different exposure models and assess the risks of the progression of MASLD and the development of HCC. This study therefore investigated the effects of single versus repeated MCLR exposure on liver pathology and gene expression in control and HFHC diet-fed rats. **Methods:** Rats were fed either a control or HFHC diet for 8 weeks. For single exposure, rats were injected with vehicle (0.09% saline) or MCLR (30 ug/kg). For repeated exposure, rats received either vehicle or MCLR every 48 h for 2 weeks while maintained on their respective diets. Rats were euthanized 24 h after the last dose and blood and tissues were collected for subsequent analysis. Histological analysis, western blots, and RNA sequencing were performed on liver tissues. **Results:** Histological analysis of experimental rats revealed pathological features consistent with the development of MASLD. Necrosis was more prominent after a single MCLR exposure compared to repeated exposure regardless of diet, but the overall level of necrosis was lower in HFHC diet-fed rats. MCLR-elicited centrilobular inflammation was less severe in control diet rats after repeated exposure compared to a single MCLR exposure. However, in rats fed the HFHC diet, MCLR-elicited centrilobular inflammation increased to the same degree in both exposure scenarios. These data suggest that animals with pre-existing liver disease may be protected against certain aspects of MCLR toxicity (e.g., necrosis) but more susceptible to others (e.g., inflammation after repeated exposure). Single and repeated MCLR exposure significantly increased levels of alanine aminotransferase (ALT) in control rats and in those fed the HFHC diet. It was also observed that cholesterol had a greater magnitude of increase after repeated MCLR exposure in rats fed the HFHC diet demonstrating a dysregulated cholesterol metabolism. A greater number of genes were differentially expressed (DEGs) after single and repeated MCLR exposure in rats fed the control diet compared to the HFHC diet. Further analysis of the DEGs showed more genes were dysregulated after repeated MCLR exposure compared to a single exposure in both diets. KEGG pathways in cancer and phosphatidylinositol 3-kinase (PI3K)-Akt signaling kinases were upregulated in conjunction with increased c-Jun and cyclin-D1 protein levels in animals from both diet groups after repeated MCLR exposure. The expression of the oncogene, β-catenin increased after repeated MCLR exposure only in HFHC diet-fed rats, suggesting β-catenin may be important for MCLR-mediated carcinogenesis in pre-existing liver disease. **Conclusions:** This study highlights the potential for the involvement of β-catenin and dysregulated cholesterol metabolism in aggravating the impact of MCLR on pre-existing liver disease and portends that the presence of MASLD is an important factor that may determine the severity of liver pathologies after MCLR exposure.

ABSTRACT NUMBER: 5157 **Poster Board Number:** LB258

TITLE: Evaluation the effect of phosphodiesterase-4 enzyme inhibition with rolipram on acute liver injury induced by paracetamol toxicity

AUTHORS (FIRST INITIAL, LAST NAME) AND INSTITUTIONS: S. S. Palabiyik-Yucelik[1], N. Demirtas[2], N. Aydemir Celep[3], A. Bozkurt[4], Z. Halici[5], and E. Cadirci[5]. [1]Ondokuz Mayıs University Faculty of Pharmacy, Samsun, Turkey; [2]Atatürk University Faculty of Pharmacy, Erzurum, Turkey; [3]Atatürk University Faculty of Veterinary Medicine, Erzurum, Turkey; [4]Van Yüzüncü Yıl University Faculty of Pharmacy, Van, Turkey; and [5]Atatürk University Faculty of Medicine, Erzurum, Turkey. Sponsor: *N. Basaran*

KEYWORDS: Liver; Biomarkers; Paracetamol, Rolipram

ABSTRACT: Background and Purpose: When used in the proper therapeutic dosages, paracetamol (PARA) is a safe and effective primary medication for fever, pain, and inflammation. However, because it is an over-the-counter drug, patients are likely to abuse it. Overdose is the leading cause of acute liver injury in developed countries. Rolipram (ROL) is the first prototypical phosphodiesterase 4 (PDE4) enzyme inhibitor. However, although it is not used in clinical treatment due to its narrow therapeutic index and side effects, it is still used as an experimental drug to investigate the molecular mechanisms underlying PDE4-related pathologies. Endoplasmic reticulum stress (ERS) is a critical pathway in the cellular response to toxic substances and can trigger cell death pathways depending on its duration and severity. The role of the cAMP pathway and the ERS pathway in PARA toxicity has been evaluated in previous studies. However, to our knowledge there is no study in the literature evaluating the protective role of the PDE4 inhibitor ROL on this pathway and the relationship between this possible effect and ERS mediated by PDE4 enzyme inhibition. The aim of this study was to evaluate the possible protective role of the PDE4 enzyme inhibitor ROL in acute liver injury due to PARA toxicity and its possible mechanism via cAMP-mediated ERS. Thus, potential pathways for liver damage caused by drugs and other substances will be revealed. **Methods:** 56 Albino wistar rats were divided into 7 groups (n=8, per group). Toxicity was induced by administering 2 g/kg PARA orally following administration of 3 different doses of rolipram (1.25; 2.5 and 5 mg/kg, i.p.) and N-acetylcysteine (140 mg/kg, oral) to the animals that were fasted for 24 hours. Blood and liver tissues were collected from the animals that were sacrificed 24 hours after PARA administration. ALT, AST, PDE4D, cAMP levels in serum and GSH, PDE4D, and cAMP levels in tissue samples were measured by ELISA method. GRP78, IRE1, and CHOP mRNA expressions of liver tissue were measured by RT-PCR method. Liver tissue was evaluated histopathologically for necrosis, hemorrhage, and mononuclear cell infiltration. **Results:** First of all, when the biomarkers of liver damage were evaluated in our study, a significant increase in ALT and AST levels was observed in the PARA toxicity group compared to the healthy control group. Also, an increase in serum and liver PDE4D levels, a decrease in serum and liver cAMP, GSH levels were shown in PARA toxicity group. Molecular results also shown increased ERS with increased mRNA expression levels of GRP78, IRE1 and CHOP in the liver in toxicity group compared to the healthy control group. In support of biochemical and molecular findings, severe histopathological damage was also seen in the PARA toxicity group in histopathological evaluation. All of these changes caused by PARA toxicity were found to ameliorated with increased ROL dose. **Conclusions:** It has been shown biochemically, histopathologically and molecularly that PDE4 enzyme inhibition may be effective in the recovery of PARA-induced liver damage by increasing PDE4 activity and decreasing cAMP levels in rat liver tissue and probably by inhibiting the resulting ERS by this pathway. The changes in cAMP and PDE4 levels due to PARA toxicity are altered by ROL administration and it has been evaluated that the possible ER stress changes shown by the increase

in GRP78, IRE1 and CHOP mRNA expressions may be related to this. It has been shown mechanistically that ROL may play a role in inhibition of ER stress. These findings also revealed these pathways as potential targets for study in other liver injuries. Funding: This study was supported by Atatürk University Scientific Research Projects Coordination Office (project number: TYL-2024-13797).

ABSTRACT NUMBER: 5158 **Poster Board Number:** LB259
TITLE: Influence of alcohol and acetaldehyde on the function of liver in SD rats

AUTHORS (FIRST INITIAL, LAST NAME) AND INSTITUTIONS: H. Chen[1,2], Y. Tian[1,2], H. Wang[1,2], X. Li[1,2], Y. Fu[1,2], X. Li[1], F. Lu[1], S. Ma[1], W. Wang[1], S. Han[1,2], L. Cui[1,2], H. Hou[1,2], and Q. Hu[1,2]. [1]China National Tobacco Quality Supervision and Test Center, Zhengzhou, China; and [2]Beijing Life Science Academy, Beijing, China. Sponsor: *S. Jia*
KEYWORDS: Liver; Risk Assessment; Acetaldehyde, Inhalation; Ethanol

ABSTRACT: Background and Purpose: Smoking is the same common feature of social gatherings as drinking alcoholic. Acetaldehyde is one of the most abundant carcinogens in tobacco smoke and is also an important candidate toxin for alcohol abuse. Studies have shown that the metabolism of ethanol leads to the production of acetaldehyde and free radicals, which are the main factors that produce harmful effects. Therefore, our study aims to investigate the influence of alcohol and acetaldehyde on the function of liver. **Methods:** SD rats were randomly divided into a sham group and three treatment groups, which was exposure with acetaldehyde for 2 weeks and oral administrated with different concentrations of alcohol (2, 4 and 6 g/kg). After treatment, the blood and the liver were collected, the important indicators including AST and ALT revealed the function of liver were measured and inflammation and SOD activity were detected. **Results:** The results showed that the contents of AST and ALT in blood were increased obviously, indicating that the function of liver may be impaired. Moreover, the pathological showed disordered arrangement of liver cells and vacuolization, which suggested that liver damage was induced by alcohol and acetaldehyde treatment and with the increase of alcohol concentration, the liver damage was aggravated. **Conclusions:** In conclusion, these results indicated that ethanol and acetaldehyde treatment induced significant toxicity on liver.

ABSTRACT NUMBER: 5159 **Poster Board Number:** LB260
TITLE: Single Cell RNA Profiling of Mouse Kidney: Perinatal Pb Exposure is Associated with Cell Composition Differences at 3 Weeks and 10 Months of Age

AUTHORS (FIRST INITIAL, LAST NAME) AND INSTITUTIONS: J. Ciarelli, *J. Dou*, *R. Morgan*, *L. Middleton*, *A. Tapaswi*, *K. Sala-Hamrick*, *B. Perera*, *D. Dolinoy*, *J. Colacino*, and *K. Bakulski*. University of Michigan School of Public Health, Ann Arbor, MI.
KEYWORDS: Kidney; Metals; Lead

ABSTRACT: Background and Purpose: Lead (Pb) is a metal present in the environment and in various consumer and industrial products. Pb exposure is still ubiquitous in many areas of the world despite removal efforts. Exposure to Pb can result from ingestion, absorption, or inhalation. Pb accumulates in the kidneys, disrupts cellular functions, and can cause kidney damage, but the cell type-specific response requires further investigation. In this study we examine the effect of a human-relevant dose of Pb exposure during the perinatal period on kidney (3 weeks and 10 months of age) gene expression and cell composition using single cell RNA sequence analysis in a mouse model. **Methods:** Offspring of female

a/a non-agouti mice exposed to 32ppm of Pb-acetate in drinking water from 2 weeks before gestation through lactation and weaning were compared to offspring of control mice. All experimental mice were derived from separate litters, with one male and one female taken per liter. At either a 3-week or 10-month timepoint, offspring were euthanized, perfused with saline, and kidneys were collected and prepared for cell suspension. Kidney cells from control and Pb-exposed mice were processed using Chromium (10x Genomics). Single-cell RNA was sequenced, demultiplexed, and processed for cell cluster expression, with identification using scType and cell type annotation confirmed using the top 10 genes differentially expressed for each cluster. We assessed differences in cell composition by exposure group using beta regression, adjusting for all other cell types. All analyses were stratified by time point, and we performed sensitivity analyses additionally stratified by sex (3-week: 23 mice, 11 female, 12 male; 10-month: 23 mice, 12 female, 11 male). **Results:** After preprocessing, there were 14,280 kidney cells sequenced, mapping to 9 cell clusters (renal macrophages, T-cells, endothelial cells, proximal tubule cells, principal cells, alpha-intercalated cells, B-cells, loop of Henle cells, and immune cells). At 3 weeks, among controls, the most abundant cell types captured were principal cells (21.39%), proximal tubule cells (20.45%), and alpha-intercalated cells (18.17%). Pb was associated with reduced alpha intercalated cell proportions (18.17% controls versus 13.73% Pb; p-value = 0.02) and increased B-cell proportions (1.44% controls versus 2.52% Pb; p-value = 0.02). Among females at 3 weeks, Pb exposure was associated with reduced immune cells (0.7% controls versus 0.0% Pb; p-value = 0.04) and loop of Henle cells (3.85% controls versus 1.19% Pb; p-value = 0.05). At 10 months, among controls, the most abundant cell types captured were renal macrophages (29.84%), T-cells (22.45%), and endothelial cells (21.17%). Pb was associated with a reduction in endothelial cells (21.17% controls versus 17.26% Pb; p-value = 0.04). Among males at 10 months, Pb exposure was associated with decreased endothelial cells (22.08% controls versus 14.75% Pb; p-value = 0.003), increased T-cells (18.6% controls versus 27.29% Pb; p-value = 0.01), and increased alpha-intercalated cells (0.91% controls versus 2.13% Pb; p-value = 0.03). Future work will consider differential gene expression. **Conclusions:** Our study successfully identified cell types involved in kidney function using single cell RNA sequencing data. Perinatal Pb exposure results in differential cell composition in the mouse kidney, dependent on developmental time point and sex. Particular cell types of concern include endothelial cells, alpha-intercalated cells, T-cells, and B-cells, which have the potential to be affected by Pb exposure. Damage induced by Pb in these cell types may lead to decreased kidney function and result in poor health outcomes.

ABSTRACT NUMBER: 5160 **Poster Board Number:** LB261

TITLE: The Effects of Nephrotoxic Metal Mixtures on Vascularized Human Kidney Organoid Inflammatory Response and Cell Stress

AUTHORS (FIRST INITIAL, LAST NAME) AND INSTITUTIONS: D. R. Emlet[1], *Z. Zimmerman*[1], *I. Merutka*[2], *R. Turkington*[1], M. Eley[1], *N. F. Prince*[1], *C. Gennings*[3], *N. Jayasundara*[2], N. Hukriede[1], and *A. Sanders*[1].
[1]University of Pittsburgh, Pittsburgh, PA; [2]Duke University, Durham, NC; and [3]Mount Sinai, New York, NY.

KEYWORDS: Metals; Kidney; Nephrotoxicity

ABSTRACT: Background and Purpose: Environmental toxicants such as toxic metals can accumulate in multiple kidney tissues, including the nephrons (glomerulus, tubules and collecting duct), vascular tissue, and mesangial cells and may contribute to multiple etiologies of kidney disease. We assessed the effects of arsenic, cadmium and lead, as well as nephrotoxic metal mixtures (NMM) using a novel *in vitro*

engineered vascularized human kidney organoid system. Our objective was to quantify the effects of population-relevant individual and mixed metal exposures on genes involved in renal injury, inflammation, and cell stress. **Methods:** Human kidney organoids are a useful 3D model for studying kidney injury because they contain many cell types that reflect better injury response than 2D culture systems. Increasing the vascular density in human kidney organoids generates more mature organoids, and as such is critical for mechanistic studies in kidney health and disease. Here we employed a robust, reliable, and high-throughput engineered vascularized human kidney organoid system by mixing an inducible *ETS translocation variant 2* (*ETV2*) human induced pluripotent stem cell line (iETV2-hiPSC), which directs endothelial fate, with a non-transgenic naïve iPSC line, MANZ 2-2, in suspension organoid culture. Metal doses and mixing ratios were calculated using publicly available data from the National Health and Nutrition Examination Survey (NHANES) for years 2017-2020. Organoids were exposed to a range of population-relevant individual metals and NMM doses derived from urinary concentrations of arsenite, cadmium, and lead in a nationally-representative sample of U.S. women of reproductive age. The geometric means of urinary arsenite (0.17 µg/L), cadmium (0.15 µg/L) and lead (0.22 µg/L) were used to calculate molar concentrations for each metal, using 1xnM, 10xnM, and 1xuM as the tested concentration range. Mixing ratios were then calculated by summing the three molar concentrations to derive the relative proportion of arsenite, cadmium or lead to the total molar concentration. As such, the fixed-ratio mixture comprised 35% arsenite (NaAsO2), 36% cadmium (CdCl2), and 28% lead (PbCl2) by molar concentration. Mature organoids were transferred to culture media containing the appropriate concentration of individual and NMM combinations and cultured for an additional 48hr. Following exposure, organoids were collected, washed and lysed for total RNA isolation. Transcript levels of specific genes related to injury, inflammation, and cell stress were determined by RT-qPCR. **Results:** Over 5 organoid assays and 10 qPCR assays, similar results were obtained. The genes tested were markers of injury, inflammation, and cell stress, which included HAVCR, IL8, TNF alpha, CDKN1, IL6, CCL2, MMP9, GCLC, GCLM, GPX1, PCNA, BAX, SOD1, SOD2, and HO-1. While individual metal exposures did not result in changes in gene expression at the 10xnM concentration, the NMM-exposed organoids demonstrated dose-responsive increases in expression in a number of genes. Multiple genes demonstrated increased expression from 2-4 to 30-fold (including CDKN1, GCLC, GCLM, BAX, SOD1, and SOD2), and HO-1 expression increased 500-fold compared to controls. **Conclusions:** Using a novel *in vitro* vascularized human kidney organoid system, NMM exposures resulted in increased expression of genes involved in injury, inflammation, and cell stress. No individual metals demonstrated significant effects on gene expression. However, mixed metals at nM levels demonstrated notable increases in many genes in the panel of markers. These data suggest that levels of combined metals at population-relevant doses induce nephrotoxicity. The human organoid system model is ideally suited to study these effects and lays a foundation for a better understanding of mixed metals in nephrotoxicity.

ABSTRACT NUMBER: 5161 **Poster Board Number:** LB262

TITLE: Synergistic Neuroprotection Through Dual Inhibition of TNFα and IL-1 Signaling in Organophosphate-Induced Status Epilepticus

AUTHORS (FIRST INITIAL, LAST NAME) AND INSTITUTIONS: M. Chavez-Vazquez, and *E. Johnson*. U.S. Army Medical Reseach Institute of Chemical Defense, Gunpowder, MD.

KEYWORDS: Inflammation; Agents

ABSTRACT: Background and Purpose: Exposure of organophosphorus compounds such as soman (GD), a potent acetylcholinesterase inhibitor and chemical warfare nerve agent, can cause status epilepticus (SE), leading to severe neuropathology, behavioral impairments, and cognitive deficits. GD-induced SE results in widespread cell death in brain regions such as the hippocampus, thalamus, amygdala, and the piriform cortex, which triggers a robust neuroinflammatory response. This inflammatory cascade, involving multiple cells, cytokines, and receptors, can exacerbate tissue injury or promote healing, complicating the development of effective neuroprotective therapies. Neuroinflammation mediated by tumor necrosis factor-alpha (TNFα) and interleukin-1 receptor 1 (IL-1R1) signaling plays a significant role in seizure development, maintenance, and progression of brain injury. **Methods:** TNFα exerts its effects via two receptors, TNFR1A and TNFR1B, which mediate pro-inflammatory and anti-inflammatory responses, respectively, depending on the cell type and injury context. This study investigated the effects of inhibiting TNFα and IL-1 signaling pathways on acute neuropathology, mortality, and seizure profiles following GD exposure using wild-type and knockout (KO) mouse models. **Results:** Results from TNFR1A, TNFR1B, and IL-1R1 single KO strains, as well as IL-1R1/TNFR1A double KO strains, demonstrated that impairing TNFα and IL-1 signaling individually provided moderate neuroprotection. However, combined inhibition of these pathways in double KO mice showed significant synergistic effects, including reduced neuroinflammation, improved neuropathology, attenuated seizure activity, and decreased mortality. Morphological analyses using fluorescent immunohistochemistry revealed reduced activation of astrocytes and microglia in KO strains, indicating an attenuation of the inflammatory response. **Conclusions:** These findings suggest that a multi-pathway approach targeting both TNFα and IL-1 signaling provides superior neuroprotection compared to single-pathway inhibition. This strategy holds promise for extending the therapeutic window and improving outcomes for GD-induced SE. Further studies will explore the chronic neuroprotective and behavioral effects of this combined approach, paving the way for the development of novel, pathway-specific drugs to mitigate CNS injury.

ABSTRACT NUMBER: 5162 **Poster Board Number:** LB263

TITLE: Wound Decontamination Evaluation Pipeline (WDEP), Decontamination of wounds contaminated with chemical warfare agents

AUTHORS (FIRST INITIAL, LAST NAME) AND INSTITUTIONS: E. D. Clarkson. US Army Medical Research Institute of Chemical Defense, Aberdeen Proving Ground, MD.

KEYWORDS: Chemical and Biological Weapons; Organophosphates; In Vivo Models; Decontamination

ABSTRACT: Background and Purpose: Effective skin and wound decontamination are of significant military importance, as protective equipment designed to prevent exposure to chemical warfare agents may not be worn at the time of an attack or may become compromised during military activities. While normal, healthy skin may impede the ingress of many chemicals, it is not a perfect barrier. There is a time-critical window of opportunity to remove sufficient amounts of contaminant from the skin surface to prevent or limit local or systemic toxicity. Wounds afford chemical warfare agents a much more direct pathway into the blood stream. Concurrently, wounds also afford decontamination products a direct pathway into the blood stream. Accordingly, any decontamination product that will be used in wounds needs to be evaluated for potential systemic toxicity. The USA Medical Research Institute of Chemical Defense (USAMRICD) has many decades of experience testing decontamination products for intact skin and, more recently, in wounds. This project seeks to better define a standardized wound

decontamination pipeline at the USAMRICD to evaluate new or existing products. **Methods:** This pipeline will use both *in vitro* and *in vivo* assays to evaluate candidate decontamination products. In the first tier, an NMR-based *in vitro* assay will be used to measure the half-life of the decontamination product while an *in vitro* skin assay will be used to measure the penetration of the compound across the punctured epidermal and exposed dermal layers, as well as potential impacts to wound healing. The combined scores from both assays will determine if a compound continues through the pipeline. Any decontamination product continuing to the next tier will be subjected to an *in vivo* small animal screen utilizing anesthetized, guinea pigs. Both the median lethal dose (MLD) of compounds in wounds and the effectiveness of a decontamination product will be evaluated, and the compound's score will determine if it continues to the large animal assay. Any decontamination product continuing through to the final tier will be subjected to an *in vivo* large animal screen utilizing anesthetized pigs. **Results:** Any candidate that passes through all three tiers will be recommended as a possible wound decontamination product. **Conclusions:** The currently fielded decontamination product, Reactive Skin Decontamination Lotion (RSDL), is expensive and has a 5-year shelf life. We are working on providing a replacement product.

ABSTRACT NUMBER: 5163 **Poster Board Number:** LB264

TITLE: Primary cell-based and human iPCS-derived 3D models for toxicity test and disease modeling

AUTHORS (FIRST INITIAL, LAST NAME) AND INSTITUTIONS: B. Huang, N. Duan, X. Xie, X. Li, L. Zhou, and M. Qu. MileCell Bio, Shanghai, China.

KEYWORDS: None

ABSTRACT: Background and Purpose: Organ structure and function are difficult to study using traditional *in vitro* models such as monolayer cultures. Current *in-vitro* 3D models are promising but lack consistency between individual spheroids/organoids. Thus we have developed and improved 3D models for toxicity and disease modeling for both primary cell-based and human iPSC-derived models. Firstly, we model metabolic dysfunction-associated steatohepatitis (MASH) by rodent primary cells. After the primary hepatocytes formed normal spheroids, we induced liver spheroids by replacing the conventional culture medium with a nutrient-rich medium and evaluated the relevant factors. This led to the development of a 3D MASH spheroid model, which can be used for research on MASH and the development of related drugs. Secondly, we used an iPSC line to derive organs from three germ layers, including liver (endoderm), kidney (mesoderm) and the brain (ectoderm) and charaterize the organoids' structure and function. With improved the consistency of individual organoids, we applied them to model liver fibrosis, IgA nephropathy, and neurotoxicity. **Methods:** In C57 mouse primary cell-based 3D models, we first optimized the induction culture medium, and after constructing the spheroids, we further analyzed the relevant markers of 3D MASH spheroids through immunofluorescence and quantitative PCR. Finally, we evaluated the application of 3D MASH in drug screening.For iPSC-derived models, the same human iPSC line (ATCC-DYR0100) was differentiated into liver organoids, kideny organoids, and neural organoids, respectively. We applied different ways to control the sizes of the organoids in order to make inidvidual organoids consistent. We model liver fibrosis by detecting aSMA; IgA nephropathy by detecting nephrons and tubules (Nephrin/LTL); neurotoxcity by assessing the morphology and markers expression (SOX2/MAP2). **Results:** Compared to healthy cell spheroids, 3D MASH spheroids exhibit significantly higher levels of fibrosis. The relative expression of fibrosis markers, smooth muscle actin, and insulin resistance genes in the MASH group was higher than in the control group, with statistical significance. Additionally, compared to healthy controls, triglyceride and albumin

levels in 3D MASH spheroids were significantly increased. Treatment with Selonsertib or Obeticholic acid intervention reduced triglyceride and albumin levels in 3D MASH spheroids to the normal levels observed in healthy controls. After intervention, MASH-related factors showed significant changes, indicating that the developed 3D MASH spheroid model can be used for screening NASH inhibitors. For iPSC-derived models, each modified method improved the consistency of individual organoids and each type of organoids expressed their unique molecular markers. Improvements of human iPSC-derived models from the same cell line successfully mimic disease models or were applied to toxicity test. In liver fibrosis model, TGFb treated organoids increased the fibrosis marker protein expression(SMA). In IgA nephropathy model, IgA/IgG complex treated group decreased the nephrons and tubules (Nephrin/LTL) markers expression, and increased the stromal cell markers. In neurotoxcity test, Bisphenol A (20 µM, CAS 80-05-7), Bisphenol B (20 µM, CAS 77-40-7) or ethanol (100 mM, Cas 64-17-5) treated neural organoids show decreased size due to decreased cell proliferation(KI67 or SOX2); Doxorubicin (0.4 µM) disrupted the structure of the neural organoids and increased the cell apoptosis. **Conclusions:** Improvements of *in vitro* 3D models for both primary cell-based and human iPSC-derived models increased their potential for toxicity and disease modeling.

ABSTRACT NUMBER: 5164 **Poster Board Number:** LB265
TITLE: Histopathological and Physiological Characterization of Inflammatory and Neuronal Degenerative Markers in a Novel Traumatic Brain Injury and Organophosphate Exposure Polytrauma Mouse Model

AUTHORS (FIRST INITIAL, LAST NAME) AND INSTITUTIONS: *J. Janssen*, and *E. Johnson*. US Army Medical Research Insitute of Chemical Defense, Gunpowder, MD.
KEYWORDS: Histopathology; Toxicity; Acute; Inflammation

ABSTRACT: Background and Purpose: Treatment strategies are well established for traumatic brain injury (TBI) and organophosphate (OP) compound exposures alone. However, the resulting synergistic effects of a TBI/OP polytrauma and the effectiveness of standard medical treatments for both injury modalities in the polytrauma model are unknown. Understanding progressive central nervous system (CNS) injury dynamics are essential to improve care, particularly in cases of brain injuries, as it allows for a detailed examination of cellular changes and helps inform further treatment strategies. Thus, this study measured quantitative behavioral, EEG, and physiological observation (injury metrics) with a focus on the inflammatory responses and neuronal degeneration for TBI alone, OP exposure alone and the combined TBI/OP polytrauma. **Methods:** To investigate these aims, we used a novel TBI/OP polytrauma mouse model using human acetylcholinesterase knock-in/serum carboxylesterase knockout (C57BL/6-Ces1ctm1.1LocAChEtm1.1Loc/ J; KIKO) mice. For each experiment, mice received an open craniectomy for controlled cortical impact TBI and a subcutaneous wireless transponder for electroencephalographic (EEG) monitoring. Then, mice either received a TBI, were exposed to OP, or were given a TBI/OP polytrauma along with standard treatments. Mice were monitored for 72 hours post-exposure and injury metrics were quantified prior to euthanasia and brain extraction. Using immunohistochemistry, paraffin-embedded slides were labeled with glial cell markers to gauge the inflammatory response to individual and TBI/OP polytrauma injury. **Results:** Across all exposures, an inflammatory response was evident, although the intensity of this response varied depending on injury type and severity. Finally, degenerating neurons were labeled to visualize and quantify the extent of neuronal damage with differences again observed among the different injury groups. **Conclusions:** In sum, neuropathology and the inflammatory response to the TBI/OP polytrauma showed differences in outcomes compared to

individual injuries, suggesting that additional treatment strategies may need to be developed for polytrauma injuries. The views expressed in this abstract are those of the author(s) and do not reflect the official policy or views of the Department of Army, Department of Defense, or the U.S. Government. The experimental protocol was approved by the Animal Care and Use Committee at the United States Army Medical Research Institute of Chemical Defense, and all procedures were conducted in accordance with the principles stated in the Guide for the Care and Use of Laboratory Animals and the Animal Welfare Act of 1966 (P.L. 89-544), as amended. These studies were funded by the Combat Casualty Care Research Program (CCCRP). J. Janssen was supported in whole or in part by an appointment to the Research Participation Program for the U.S. Army Medical Research and Development Command administered by the Oak Ridge Institute for Science Education (ORISE) through an agreement between the U.S. Department of Energy and U.S. Army Medical Research and Development Command.

ABSTRACT NUMBER: 5165 **Poster Board Number:** LB266

TITLE: A single oral exposure to polyethylene terephthalate microplastics causes systemic and metabolic dysfunction in male and female rats

AUTHORS (FIRST INITIAL, LAST NAME) AND INSTITUTIONS: A. A. Lewis, and *A. Farraj*. US EPA, Durham, NC.

KEYWORDS: Environmental Toxicology; In Vivo Models; Toxicity; Acute; Microplastics

ABSTRACT: Background and Purpose: Microplastics, derived largely from degraded household and commercial plastics, have become a pervasive environmental concern, and may pose health risks resulting from ingestion and accumulation in living organisms. Polyethylene terephthalate (PET) microplastics, commonly found in consumer products such as plastic bottles and clothing, have been detected in human arteries and brains among other tissues, although their health impacts remain unknown. **Methods:** This study aims to evaluate the biological effects of a single oral gavage of PET microplastics in female and male rats. We hypothesized that oral administration of PET would cause dose-dependent changes in metabolic function and systemic markers of toxicity. Three-month old Sprague-Dawley rats were exposed once via oral gavage to sterile water vehicle or 5 or 50 mg/kg of PET microplastics, which were derived from cryomilling of plastic nurdles. Animals were monitored for 22 hours in an indirect calorimetry apparatus beginning immediately after gavage for changes in metabolic rate. Samples were collected approximately one day after gavage to measure systemic indicators of inflammation and injury, changes in gene expression in the liver and gastrointestinal tissue, and changes in hormones related to metabolic function. **Results:** Preliminary results indicate sex-specific differences in metabolism and systemic factors. While females exhibited a decrease in metabolic rate only with the high dose, males had similar decreases with both the low and high doses. Only males had significant decreases in insulin with low dose as well as dose dependent linear increases in blood platelets and plateletcrit, significant decreases in serum high-density lipoprotein (HDL) cholesterol, a trend towards increased serum glucose. Interestingly, both males and females had increases in low-density lipoprotein (LDL) cholesterol. **Conclusions:** These findings suggest that exposure to PET microplastics has the potential to elicit toxicity, highlighting the need for further research on the health impacts of exposure to microplastics and possible modifying factors (Abstract does not reflect U.S. EPA policy).

ABSTRACT NUMBER: 5166 **Poster Board Number:** LB267
TITLE: Development of injectable isoflurane for use in mice; structural and physiological considerations to avoid toxic symptoms

AUTHORS (FIRST INITIAL, LAST NAME) AND INSTITUTIONS: A. Methvin, *J. Leighton*, *M. Ellis*, *J. Janssen*, N. Benn, M. Chavez-Vazquez, T. Hamilton, and E. Johnson. U.S. Army Medical Research Institute of Chemical Defense, Aberdeen Proving Ground, MD.
KEYWORDS: Toxicity; Chronic; Necrosis; Isoflurane

ABSTRACT: Background and Purpose: Isoflurane (ISO) is a widely used volatile general anesthetic and has been FDA approved for over 40 years. It is safe and effective for human use, has a wide therapeutic index, and recovery after anesthesia is quick with few to no side effects (*Eger et al 1995*). ISO is also a particularly useful compound as it has been shown to provide anesthesia, analgesia, and muscle relaxation, which constitute the major requirements for surgical anesthesia. Additionally, ISO has been shown by our group and collaborators to be an anticonvulsant therapy for treatment-resistant seizures in organophosphate exposure models. This multi-targeting compound would allow for smooth procedures or emergency sedation with minimal additional drug use and potentially give additional benefits such as nervous system protection, rendering it particularly helpful for multimodal injuries. One logistical problem with fielding ISO in non-hospital settings is the requirement of an inhalation apparatus; injectable formulations may allow for use in more austere environments. **Methods:** Our collaborators have previously demonstrated ISO's solubility in intralipid and efficacy in a rat model. Our research group worked to develop viable injection formulations and routes of administration for a mouse model which would allow for lower costs and increased molecular tools for injury models and anticonvulsant evaluations. We found that transition to a mouse model presented several unexpected challenges. **Results:** Primary findings were that the emulsion itself can be easily disrupted by needle gauge size as shown with electron microscopy; intralipid has several unique characteristics which make it less suitable for far-periphery IV and can effectively enable creating a slow-release formula in the peritoneal cavity, and that physiological response is highly concentration dependent, with responses ranging from peripheral numbness to progressive necrosis and acute cardiac arrest. **Conclusions:** Through exploration of multiple routes, we have found one viable isoflurane concentration that can be injected IV for the target brief anesthetic dose, and are continuing to develop potential IP and IM injections.

ABSTRACT NUMBER: 5167 **Poster Board Number:** LB268
TITLE: Historical Control Data of Spontaneous Tumors in Transgenic CByB6F1-Tg(HRAS)2Jic (Tg.rasH2) Mice

AUTHORS (FIRST INITIAL, LAST NAME) AND INSTITUTIONS: J. A. Stanley. Labcorp, Greenfield, IN. Sponsor: *V. Marshall*
KEYWORDS: Transgenic Models; Carcinogenesis

ABSTRACT: Background and Purpose: Short-term (6-month) carcinogenicity studies using genetically engineered animals have been demonstrated to be a reliable alternative model to long-term conventional carcinogenicity studies. CByB6F1-Tg(HRAS)2Jic (rasH2) is a genetically engineered hemizygous transgenic mouse containing the human c-Ha-ras proto-oncogene (c-Ha-ras) and is approved by regulatory agencies for carcinogenicity assessment. Historical control data (HCD) are

important tools that can provide useful information on the evaluation of spontaneously occurring background findings in carcinogenicity studies. **Methods:** The present study provides a retrospective analysis of the mortality, body weights, and spontaneous tumor incidences in control article or vehicle control article (vehicle) administered rasH2 mice from 6-month carcinogenicity studies conducted at Labcorp from 2014 to 2023. **Results:** Mortality in the vehicle-administered Tg.rasH2 mouse was approximately 6% in both males and females. The most common spontaneous tumors observed in these studies were lung bronchiolo-alveolar adenomas (6.0% in males and 2.2% in females), hemangiosarcoma of the spleen (3.6% in males and 3.4% in females), Harderian gland adenoma (0.7% in males and 1.4% in females), and benign thymoma of thymus (0.6% in males and 2.1% in females). The incidence of all other neoplasms noted was generally low (less than 1%). The overall internal results obtained from Labcorp over a decade, including spontaneous tumors, were not significantly different from the available literature. **Conclusions:** Taken together, these data confirmed that the rasH2 mice had a low incidence of background tumors, high survival rate, and shorter required study duration than prevailing models, and can serve as a reliable model for 6-month rasH2 transgenic model carcinogenicity studies against the conventional 2-year rodent carcinogenicity studies.

ABSTRACT NUMBER: 5168 **Poster Board Number:** LB269

TITLE: A Refined Approach to Nausea and Emesis Assessment in Beagle Dogs Using a Cisplatin-Induced Emesis Model

AUTHORS (FIRST INITIAL, LAST NAME) AND INSTITUTIONS: *S. Wickwire*[1], J. Kamins[1], W. Gately[1], Z. McCarthy[1], L. Fletcher[1], D. Williams[1], S. Mathieu[2], M. Limoges[2], T. Martin[3], and *S. Jackman*[1]. [1]Charles River Laboratories, Shrewsbury, MA; [2]Charles River Laboratories Montreal, Senneville, QC, Canada; and [3]Intra-Cellular Therapies, Inc., New York, NY.

KEYWORDS: Behavior; In Vivo Models; nausea

ABSTRACT: Background and Purpose: Nausea is a physiologic and affective mechanism occurring independently of or as a precursor to emesis and is associated with illness, certain medications and medical treatments, and/or a symptom (clinical signs in animals) associated with a plethora of conditions, including pregnancy and emotional and conditioned responses. Assessment of nausea in humans is subjective and is inherently variable as it is based on individual perception (self-reported). In animals, nausea is typically evaluated by observing and rating the behaviors associated with nausea using a visual analog scale (VAS). The VAS consists of a 100 mm line on which observers place a mark to denote the severity of nausea-like behaviors, where 0 mm is defined as no nausea and 100 mm is the most severe nausea. The VAS is highly subjective and prone to inter-observer variability. Scoring individual nausea-like behaviors may aid in better understanding of severity of nausea-like behaviors in nonverbal species and mitigate subjectivity of the observation, subsequently reducing inter-observer variability. Additionally, assigning multiple scores allows for quantitation and/or visual representation of the severity of individual nausea-like behavior(s). The objective of the study was to establish a system to characterize nausea-like behaviors using a cisplatin-induced model of emesis in Beagle dogs. **Methods:** Eight Beagles (4/4 male/female) received intravenous infusions of 0.9% saline (25 mL/kg/hr for 3 hours), mannitol (150 mg/mL for 15 minutes), and cisplatin (0.9 mg/kg at 2 mL/min), and subsequent intravenous injections of saline. Temporary indwelling catheters were flushed with saline after each dose and prior to catheter removal to reduce the risk of skin lesion formation. Animals were singly housed on dosing days until completion of the 24-hour postdose interval. Food was available

throughout the 3-hour saline and mannitol administrations and was withdrawn prior to cisplatin administration. Treats were offered for inappetence assessment and food was offered the follow day after the completion of the 24-hour interval. Nausea-like behaviors and emetic events were observed for animals continuously for 7 hours following cisplatin dosing, and 24-hours postdose. Nausea-like behaviors were assessed according to 5 criteria: salivation, lip smacking, activity level, vocalization, and appetite. Salivation, lip smacking, activity level, and vocalization were assessed at 15-minute intervals to evaluate the onset and duration of effect. The frequency of lip smacking and vocalization were documented; salivation and activity level were scored once per interval as an overall assessment. Appetite was assessed no more than once per 60 minutes to prevent satiety. Emetic events included emesis and/or retching. Completion time of the observation period per 15-minute interval was recorded, regardless of when cessation of emetic events occurred. The time of completion for emetic events was recorded, regardless of when cessation of emetic events occurred, to capture the completion of the 7-hour observation period. Assessment of emetic events and nausea-like behaviors were made by a limited number of trained observers using clearly defined parameters in the Protocol. **Results:** The onset of cisplatin-induced inappetence mostly occurred at 2.75 hours into the observation period and persisted through 5 to 7 hours in males and through 7 hours in females. Appetite recovered for all animals at all 24-hour intervals assessed (Days 1 and 57, 85, or 113). Individual scores for each animal will be presented. **Conclusions:** This study established a system to characterize nausea-like behaviors using a cisplatin-induced model of emesis in Beagle dogs. Recording the frequency and/or assigning numerical values for individual nausea-like behaviors using clearly defined parameters and trained observers allows for an overall evaluation of response and differentiation of the severity of response even when the behaviors are variably expressed. In addition, the nausea-like behaviors are characterized by prevalence of specific clinical signs on a per animal basis, allowing for evaluation of individual response and any necessary veterinary treatments by clinical sign and severity. With an improved understanding of overall and individual behavior associated with nausea and emesis compared with the use of a visual analog scale, the efficacy of antiemetics can be more reliably characterized.

ABSTRACT NUMBER: 5169 **Poster Board Number:** LB270

TITLE: Folate supplementation in prairie voles prevents the neurobehavioral phenotype caused by developmental deltamethrin exposure

AUTHORS (FIRST INITIAL, LAST NAME) AND INSTITUTIONS: N. Saferin[1], I. Haseeb[2], A. M. Taha[3], S. E. Beecroft[3], S. Pillai[2], A. E. Neifer[1], R. Lakkuru[1], B. P. Kistler[1], C. N. Nawor[1], I. Malik[1], D. Hasan[1], J. A. Carlson[1], K. K. Zade[1], S. P. Dressel[3], E. M. Carney[3], R. Shah[2], S. Gautam[2], J. Vergis[1], K. L. Neifer[1], Z. V. Johnson[4], M. L. Gustison[5], F. S. Hall[3], and *J. P. Burkett*[1]. [1]University of Toledo College of Medicine, Toledo, OH; [2]University of Toledo College of Natural Sciences, Toledo, OH; [3]University of Toledo College of Pharmacy, Toledo, OH; [4]Emory University, Atlanta, GA; and [5]University of Western Ontario, London, ON, Canada.

KEYWORDS: Pesticides; Developmental/Teratology

ABSTRACT: Background and Purpose: Neurodevelopmental disorders (NDDs) have become a public health crisis, with the current prevalence estimated at 17% of the US population. There is an increased appreciation for the contribution of environmental exposures to NDD risk. Recent epidemiology has linked developmental pyrethroid pesticide exposure to risk for autism and developmental delay, and

mouse models of developmental pyrethroid exposure show neurobehavioral phenotypes relevant to NDDs. **Methods:** We performed a chronic low-dose exposure to vehicle or deltamethrin (3 mg/kg/3 days) with or without high-dose 5-MTHF (methylfolate) supplementation (5 mg/kg/3 days) in pregnant prairie voles, and tested the resulting offspring for behavioral and neurological phenotypes. **Results:** Developmentally exposed offspring showed wide-ranging behavioral deficits relevant to neurodevelopmental disorders, as well as direct disruptions to folate metabolism. 5-MTHF prevented the behavioral deficits, potentially via compensatory changes to folate metabolism. **Conclusions:** We conclude that developmental exposure to deltamethrin causes NDD-relevant behavioral deficits; DPE directly alters folate metabolism; and preventative 5-MTHF dramatically reduces the behavioral effects of DPE.

ABSTRACT NUMBER: 5170 **Poster Board Number:** LB271
TITLE: The Development of a Framework to Assess the Validity of quantitative Adverse Outcome Pathways (qAOPs) for Chemical Safety Assessment

AUTHORS (FIRST INITIAL, LAST NAME) AND INSTITUTIONS: M. Cronin[1], G. Chrysochoou[1], S. Enoch[1], J. Firman[1], A. Gomatam[1], *B. Hardy*[2], P. Marx-Stoelting[3], U. Sahlin[4], *S. Schaller*[5], A. Steinbach[3], K. Veltman[6], A. Verhoeven[7], and E. Zgheib[8]. [1]Liverpool John Moores University, Liverpool, United Kingdom; [2]Edelweiss Connect, Basel, Switzerland; [3]German Federal Institute for Risk Assessment, Berlin, Germany; [4]Lund University, Lund, Sweden; [5]esqLABS, Saterland, Germany; [6]National Institute for Public Health and the Environment, Bilthoven, Netherlands; [7]Vrije Universiteit Brussel, Brussels, Belgium; and [8]Certara UK Ltd, Sheffield, United Kingdom.
KEYWORDS: Computational Toxicology

ABSTRACT: Background and Purpose: Adverse Outcome Pathways (AOPs) are now accepted as fundamental approaches to organise toxicological and mechanistic information relating to adverse outcomes. AOPs have found particular use when applied to chemical stressors and assist in identifying relevant New Approach Methodologies (NAMs) for the molecular initiating and other key events (MIEs/ KEs). In order to make AOPs applicable for chemical safety assessment, quantitative AOPs (qAOPs) have been developed. qAOPs can be considered to be a "*mathematical representation of an AOP capturing quantitative relationships between elements of the AOP"*, specifically seeking to form quantitative relationships between MIEs and/or KEs. There are many potential uses of qAOPs, however, they will be fundamental for the extrapolation of *in vitro* (or other) NAM data to an adverse outcome or KE. This study has developed a framework to assist in the evaluation, verification and assessment of the validity of qAOPs in order to assist in the regulatory, or other, acceptance of NAMs. **Methods:** The framework to evaluate qAOPs builds on existing guidance around AOPs as well as other models in toxicology including quantitative structure-activity relationships (QSARs) and physiologically-based kinetic (PBK) models. It is informed by the relevant OECD guidance as well as the FAIR principles relating to the storage and sustainability of digital resources. The framework considers a qAOP to be made-up of three main components, namely i) the underlying AOP and specifically the KEs and key event relationships (KERs) to be quantified; ii) the data to be modelled; and iii) the model itself including considerations of its robustness, suitability and performance. The framework has enabled development of principles that demonstrate the validity of a qAOP and criteria, based on uncertainty, to support the assessment. **Results:** The assessment of current guidance showed that it is comprehensive for AOPs, and also includes some information on qAOPs. However, the current guidance is not currently fit-for-purpose to

allow for the validation of qAOPs in the same manner that is achieved for, e.g., QSARs. This investigation extended existing guidance, demonstrating that to be valid and fit-for-purpose, a qAOP should i) have a stated purpose through problem formulation; ii) quantify one, or more, KERs; iii) describe the uncertainties associated with the model to demonstrate confidence in causality, and/or mechanistic linkage, between KEs; iv) utilise relevant data for KEs of known quality; v) demonstrate appropriate statistical fit and predictive capabilities, including the definition of applicability domain; and vi) adhere to FAIR principles. A fundamental challenge to validating qAOPs is the broad variety of techniques that is encompassed, ranging from simple linear models for a KER, up to quantitative systems toxicology (QST) models. In order to address the complexity of validating this breadth of models, 17 criteria have been described which can be evaluated in terms of their uncertainty. The purpose of the uncertainty evaluation is to determine areas of high uncertainty (which may require refinement) and to determine if the overall level of uncertainty is acceptable for the stated purpose. **Conclusions:** A framework has been developed to allow for the evaluation, verification and demonstration of the validity of a qAOP for use in chemical safety assessment. The framework is based around 17 criteria for describing and defining the model. It also allows for the characterisation of uncertainties. It is intended that this framework will improve the acceptance of qAOPs and will facilitate their use in the application of NAM data. This project receives funding from the European Union's Horizon 2020 Research and Innovation programme under grant agreements No. 963845 (ONTOX) and No. 964537 (RISK-HUNT3R), which are part of the ASPIS cluster. The authors of this abstract acknowledge the contributions of many other researchers from the EU APSIS cluster which have enabled this study.

ABSTRACT NUMBER: 5171 **Poster Board Number:** LB272

TITLE: Deep Learning-Based Image Analysis Model for Detecting Unlearned Findings in Early Toxicity Screening Studies

AUTHORS (FIRST INITIAL, LAST NAME) AND INSTITUTIONS: T. Forest, *R. Wang*, T. Jenkins, K. Janardhan, G. Raipuria, and N. Singhal. Merck & Co, West Point, PA.

KEYWORDS: Histopathology; Machine Learning

ABSTRACT: Background and Purpose: Creating deep learning algorithms for identifying drug-induced changes in histology slides frequently involves training on prospectively identified histology findings. We previously created supervised learning models for image processing that accurately detect prospectively identified observations in rodent liver, kidney, and heart. While these supervised models are effective at detecting prospectively identified histology findings, our use-case in nonclinical toxicology study assessment requires sensitive detection of all potential histology findings. This study integrated an unsupervised learning methodology into the existing image analysis framework and evaluated its precision in detecting out of sample toxicity findings. **Methods:** Vehicle control liver whole slide images (WSI) from young Han Wistar rats were used to build an unsupervised learning model. WSI exhibiting both known and unknown features were scored, and the findings detected by the model were compared with histology diagnoses rendered by experienced toxicologic pathologists. **Results:** Compared to prior supervised learning models, the unsupervised model demonstrated improved detection of toxicity findings, including novel findings not included in training data. In the sample of WSI studied, the unsupervised model exhibited 100% sensitivity with respect to the pathologist diagnoses. Moreover, findings that were incompletely annotated by the supervised algorithms were more completely delimited by the unsupervised algorithm. Compared to the pathologist diagnoses, the

specificity of the unsupervised model was low and variable depending on the WSI evaluated. However, in these false positive detections the unsupervised model annotations highlighted genuine histology differences from the image patches used to train the model. **Conclusions:** Unsupervised deep learning algorithms sensitively detected and annotated various noteworthy histology findings that were not present in algorithm training data. Model specificity was impacted by detection of differences from the training data that were not considered noteworthy by a pathologist. Use of unsupervised models in nonclinical toxicology study assessment will require an approach that accommodates detection and adjudication of minor deviations from training data.

ABSTRACT NUMBER: 5173 **Poster Board Number:** LB274
TITLE: Exploration of New Approach Methods (NAMs) to Map Chemical Space of Acute Inhalation Toxicity

AUTHORS (FIRST INITIAL, LAST NAME) AND INSTITUTIONS: D. N. Williams[1], *J. Abedini*[2,1], *P. Ceger*[1], *D. Hines*[1], *A. J. Keebaugh*[3,4], *M. D. Nelms*[1], *T. R. Sterner*[3,5], and *R. A. Clewell*[3,6]. [1]RTI International, Research Triangle Park, NC; [2]EPA, Research Triangle Park, NC; [3]Air Force Research Laboratory, Wright-Patterson AFB, OH; [4]BlueHalo, Dayton, OH; [5]Henry M. Jackson Foundation for the Advancement of Military Medicine, Wright-Patterson AFB, OH; and [6]Eagle Integrated Services, Inc., Wright-Patterson AFB, OH.
KEYWORDS: Inhalation Toxicology; Toxicokinetics; Computational Toxicology

ABSTRACT: Background and Purpose: New Approach Methods (NAMs) seek to provide alternatives to toxicity testing and hazard screening to reduce dependence on animal studies and inform human health risk assessment. While in vitro and computational approaches provide drastically increased throughput over animal testing, testing all potential toxicants across all relevant test systems is not practical, and prioritization of substances and assay systems is necessary. Tools such Quantitative Structure-Activity Relationship (QSAR) modeling and read-across can help to screen potential chemical hazards, as well as identify test systems that could be used quickly to fill knowledge gaps for chemicals of interest. Previously, we demonstrated how a data-driven analysis workflow using chemical structure and bioactivity data could be used to recommend minimal assay sets to test for acute oral toxicity screening (Edwards et al., 2022). That work focused on chemical-assay combinations from the ToxCast/Tox21 (InVitroDB v.3.5) program and produced a model that includes approximately 2,100 chemical clusters that can be used to map novel chemicals to potential testing assays for acute systemic oral toxicity screening. In the present work, we expanded on previous efforts by investigating the feasibility of adapting this approach to screen for acute systemic inhalation toxicity. Specifically, our goals were to determine if sufficient data are present in existing literature and databases to develop a similar model to identify minimal assay sets for acute inhalation toxicity models, and to explore applications of read-across for acute inhalation toxicity screening. **Methods:** Our approach consisted of three phases: identification of inhalation data, data evaluation, and exploration of read-across for predicting acute inhalation toxicity. *Data identification.* A search was conducted for publicly available in vivo acute inhalation data (e.g., LC_{50} and/or Globally Harmonized System (GHS) classifications) and inhalation-relevant in vitro data. Sources of interest included the following: Integrated Chemical Environment (ICE), Risk Assessment Information System (RAIS), California Office of Environmental Health Hazard Assessment (OEHHA), and PubChem. *Data evaluation.* Data evaluation was comprised of three main elements: data availability, chemical coverage, and model needs. We considered several factors when evaluating data availability, including the volume, experimental conditions, and endpoints for which

data are available. Chemical coverage refers to the similarity of chemical structures relative to already established models. Model needs include evaluating how data quality and quantity affect model predictive capabilities. Chemical clusters were created to map each set of data, where the oral prediction model was used as a baseline. *Read-across exploration.* In vivo rat inhalation data from the curated database in ICE were used as the basis for inhalation toxicity activity; these data included chemicals spanning GHS categories 1 through 5. For each chemical, 16 physicochemical properties were predicted using the OPEn structure-activity Relationship App (OPERA, v2.9). To predict internal concentrations from exposures of 1 ppm by volume for 15 minutes, we used a generalized inhalation physiologically-based pharmacokinetic (PBPK) model from the httk R package (gas_pbpk), which was parameterized using physicochemical data available in ICE or QSAR predictions via OPERA. Model outputs included maximum concentrations of chemicals in plasma, liver, lungs, and mucus, and additionally, the area-under-the-curve of the concentration in plasma was tracked. We explored the effectiveness of physiochemical properties and model outputs for predicting inhalation-specific GHS classification categories. **Results:** ICE, RAIS, OEHHA, and PubChem in vivo inhalation toxicity data had differing conditions for exposure data, ranging from acute to chronic exposure lengths, species tested, and parameters measured. Data available within each of these sources included a range of exposure lengths (acute to chronic), single and repeat exposure conditions, a variety of species (e.g., human, rat, and mouse), and a variety of measured outcomes. We were unable to find a large source of publicly available in vitro inhalation data; as such, we used in vitro data from ToxCast/Tox21. We compared the chemical space of the available acute inhalation data to that of the oral acute toxicity assay recommendation model from previous work. The acute oral toxicity data consisted of 10,998 chemicals from the Interagency Coordinating Committee on the Validation of Alternative Methods (ICCVAM) Acute Toxicity Work Group, which had previously been grouped into 2,192 clusters and served as a baseline for describing the chemical space. The chemical space covered by inhalation-specific data was substantially reduced from the oral data. The ICE dataset contained the largest curated acute inhalation data (including 50% lethal concentration values, and GHS and Environmental Protection Agency classifications); in vivo rat inhalation studies were the most common type identified but included just 1,293 chemicals appearing in 31.3% of clusters. Of those 1,293 chemicals with in vivo rat data, only 356 chemicals in 13.1% of clusters also included in vitro assay data from ToxCast/Tox21. We then explored applications of read-across for acute inhalation toxicity screening to determine the utility of available data for predicting inhalation GHS category. The strongest positive associations with median LC_{50} were observed with the Henry's Law constant for the 356 chemicals that included both in vivo and in vitro data. Negative associations were observed between median LC_{50} and melting point, boiling point, and mucus maximum concentrations. After converting LC_{50}s to their respective GHS Categories, preliminary results indicate that these properties may be useful for indicating which chemicals are likely to be classified as non-toxic (GHS Category 5) for inhalation toxicity. For example, 95% of GHS Category 5 chemicals had mucus maximum concentration values under 50 µM. **Conclusions:** We identified and evaluated several publicly available sources of acute inhalation toxicity for suitability in model development to recommend assays to predict toxicity of novel chemicals. Due to the significantly lower amount of inhalation data available from these sources relative to our previous work with acute oral toxicity, it is unlikely that there is enough publicly available data to generate a model for a minimal assay set for inhalation toxicity predictions with comparable functionality to the acute oral model. Initial findings of read-across screening for inhalation toxicity do, however, suggest that there is potential to use available data for prediction of GHS category. Future steps may include a combination of these data streams and parameters to improve predictions. **Disclaimer:** The views expressed are those of the

authors and do not reflect the official guidance or position of the United States Government, the Department of Defense, the United States Air Force, or the United States Space Force. The authors are contractors working with Air Force Research Laboratory/711th Human Performance Wing. The views expressed do not reflect the official guidance or position of RTI International; UES, Inc. (a BlueHalo Company); Henry M. Jackson Foundation for the Advancement of Military Medicine, Inc.; or Eagle Integrated Services, LLC.

ABSTRACT NUMBER: 5174 **Poster Board Number:** LB275
TITLE: The Use of Linear Discriminant Analysis in Assessing Embryotoxicity in a Human-Induced Pluripotent Stem Cell Derived Organoid Model

AUTHORS (FIRST INITIAL, LAST NAME) AND INSTITUTIONS: J. S. Ghuge, Z. Ma, and B. L. Mush. Syracuse University, Syracuse, NY. Sponsor: B. Kmush, American Association for the Advancement of Science
KEYWORDS: Computational Toxicology; Induced Pluripotent Stem Cells; Developmental Toxicity; Prenatal

ABSTRACT: Background and Purpose: This study explores the use of human-induced pluripotent stem cell (iPSC)-derived cardiac organoids as a cutting-edge in vitro model for embryotoxicity screening of pharmaceutical compounds. While traditional animal-based methods such as Zebrafish Embryo Assays and Rodent Models face challenges such as high costs, lengthy timelines, and ethical issues, iPSC-derived organoids provide a physiologically relevant and efficient alternative. Preliminary experiments highlight the potential of the cardiac organoid model as a predictive tool for assessing the embryotoxic risk of chemicals. The study aims to develop and evaluate an embryotoxicity risk classification system based on this cardiac organoid model. **Methods:** Linear Discriminant Analysis (LDA) was employed to develop a predictive model for classifying pharmaceutical compounds into three embryotoxicity categories: Non-Embryotoxic, Weakly Embryotoxic, and Strongly Embryotoxic. We examined the functionality of 2600 cardiac organoids exposed to 20 therapeutic and antibiotic drugs at concentrations of 1 nM to 1 mM. One missing value was imputed with the mean for that drug and concentration. Zeros were added to address discrepancies in the number of organoids tested versus the number present in the dataset when high concentrations eliminated functionality. Values were normalized relative to the control group, expressing results as a percentage of baseline responses to reduce variability. Outliers were detected using scatter plots and box plots and those outside the 10th to 90th percentile range were excluded. Correlation analysis found that area ratio, corrected peak time, and contraction velocity were key features. Half-maximal inhibitory concentration (IC50) values from concentration response curves were utilized as model inputs. The model was trained on a dataset of nine compounds using stepwise variable selection. LDA's key assumptions, including normality and homogeneity of variance, were evaluated using the Shapiro-Wilk test for univariate normality, Mardia’s test for multivariate normality, and Box’s M test for covariance matrix homogeneity The model was validated using 11 drugs with known in vivo embryotoxicity data, and its performance was evaluated through 3x3 contingency tables. Analysis was completed using R version 4.4.2. **Results:** The initial LDA model based on the raw data failed Box’s M test ($p<0.001$), indicating significant differences in covariance matrices across groups. Therefore, the computation of the IC50 values and normalization to control was necessary. With outliers included, the model accuracy was 46.5%, therefore, the outliers were removed. The updated LDA model achieved an accuracy of 77.78% in classifying the compounds into embryotoxicity categories. It demonstrated strong class separation, with LD1 accounting for 72.86% of the variance and LD2 for 27.14%. The model

effectively distinguished between classes based on beat rate, T75, peak time, and area ratio. The Linear Discriminant scores for each class are calculated using the following equations:
$LD1 = (-1.158 \times 10^{-6}) x_1 + (5.510 \times 10^{-7}) x_2 + (2.695 \times 10^{-6}) x_3 - (6.765 \times 10^{-8}) x_4$
$LD2 = (6.582 \times 10^{-7}) x_1 - (2.967 \times 10^{-7}) x_2 - (2.307 \times 10^{-6}) x_3 - (9.182 \times 10^{-8}) x_4$
Where x_1, x_2, x_3, x_4 are beat rate, T75, peak time, and area ratio.
The strongly embryotoxic class exhibited the highest recall at 75%; the model was most effective at correctly identifying drugs in this category. However, the model showed varying levels of precision and recall for the other classes, highlighting differences in its predictive performance. **Conclusions:** Our LDA model demonstrated robust embryotoxicity classification capability. However, further refinements are necessary to improve precision, particularly for the weakly embryotoxic class. Misclassifications will be closely analyzed in conjunction with drug pharmacodynamics to gain deeper insights into drug-induced embryotoxicity mechanisms and enhance the model's reliability. The predictive performance of the model will be compared with established in vitro embryotoxicity models. This study highlights the potential of iPSC-derived organoids as an advanced tool to enhance pharmaceutical toxicology assessments. These findings highlight the potential of the LDA model in predictive toxicology, emphasizing the need for enhanced sensitivity and precision to improve its application in drug safety assessments.

ABSTRACT NUMBER: 5175 **Poster Board Number:** LB276
TITLE: Isolation of viable primary murine hepatocytes with a novel microfluidic-based cell sorting approach

AUTHORS (FIRST INITIAL, LAST NAME) AND INSTITUTIONS: C. Montoya[1], H. Johannsen[2], N. Chelius[2], C. Poggel[2], and T. Adams[2]. [1]Miltenyi Biotec, San Diego, CA; and [2]Miltenyi Biotec, Bergisch Gladbach, Germany. Sponsor: C. Montoya, American Association of Immunologists
KEYWORDS: Liver; Hepatocytes; Cell Culture; Ex vivo

ABSTRACT: Background and Purpose: Cancer, infectious diseases, and toxins can impair liver function, damage cells, trigger inflammation, and, in severe cases, cause liver failure. he isolation of primary hepatocytes is crucial for studying the mechanisms, detection, and prevention of liver toxicity. However, their significant size and elevated metabolic activity render them especially vulnerable to cell death and sorter-induced cellular stress during isolation. Traditional droplet cell sorters often cause significant cellular damage, leading to reduced viability. To address this, a newly developed microchip sorting cartridge, specifically designed for large cells, enables gentle sorting of hepatocytes using the low-pressure, sterile MACSQuant® Tyto® Cell Sorter. This workflow demonstrates the successful sorting and culturing primary mouse hepatocytes using gentleMACS™ Perfusion Technology and the MACSQuant Tyto Cartridge LC. **Methods:** Mouse hepatocytes were dissociated from the liver utilizing the Liver Perfusion Kit and gentleMACS Octo Dissociator with Heaters (Miltenyi Biotec). The primary hepatocytes were stained with APC-conjugated REAfinity® CD95 (FAS) Antibody and isolated utilizing the MACSQuant Tyto Cell Sorter and MACSQuant Tyto Cartridge LC. Hepatocytes were then cultured to confirm cell survivability. **Results:** CD95+ hepatocyte cells where enriched to 96.2% purity while maintaining cell viability comparable to non-sorted cells (over 77%). Following cell culture, hepatocyte survivability was confirmed through cell attachment, hexagonal morphology, and nuclei duplication. **Conclusions:** The isolated hepatocytes showed robust post-sorting plating capacity and exhibited typical morphological features, including a hexagonal shape and nuclei duplication. These results indicate that primary

hepatocytes were effectively sorted, with preservation of their viability and phenotypic properties in culture.

ABSTRACT NUMBER: 5176 **Poster Board Number:** LB277
TITLE: Utility of a Tiered Screening New Approach Method to Support Force Health Protection Decisions: A Case Study

AUTHORS (FIRST INITIAL, LAST NAME) AND INSTITUTIONS: *A. Keebaugh*[1,2], S. Grady[3], *M. Nelms*[4], *L. Sweeney*[1,2], T. Lalonde[5,2], *T. Sterner*[5,2], B. Cook[4], S. Hirway[1,2], and *R. Clewell*[6,2]. [1]BlueHalo, Dayton, OH; [2]Air Force Research Lab, Wright-Patterson Air Force Base, OH; [3]Johns Hopkins University APL, Laurel, MD; [4]RTI International, Research Triangle Park, NC; [5]Henry Jackson Foundation, WPAFB, OH; and [6]EIS, WPAFB, OH.
KEYWORDS: Alternatives to Animal Testing; Computational Toxicology; Organophosphates

ABSTRACT: Background and Purpose: Military personnel are potentially exposed to a variety of chemical substances, many of which have limited data regarding health risks. The Air Force Research Laboratory is developing a tiered screening strategy using new approach methods (NAMs) to reduce the time required to assess health risks of poorly characterized chemicals. Tier 0 employs an in silico model (Edwards et al., 2022) to identify a single or small set (< 5) of high-throughput (HT) in vitro assays to screen for acute toxicity (oral 50% lethal dose; LD_{50}<2000 mg/kg) using structural similarity to chemicals with both oral acute toxicity data and HT in vitro data. Tier 1 employs in vitro testing using the recommended HT assays and simple monoculture cell models. Finally, Tier 2 tests are performed in more complex three-dimensional microtissue assays. Theoretically, simple HT assays would be used to quickly screen for acutely toxic chemicals, and microtissue assays (using more biologically relevant organotypic models) would produce points of departure (PoD) for quantitative risk assessment that would be predictive of, or more conservative than, the in vivo PoD. To test this hypothesis, the tiered approach was implemented for prototype chemicals with evidence of neurotoxic or hepatotoxic effects, including: aldicarb, methomyl, 4-chlorobiphenyl (4-CBP), tris(1,3-dichloroisopropyl) phosphate (TDCPP), tris(2-chloroethyl)phosphate (TCEP), and chlorobenzene. NAM results were compared to existing in vivo data. **Methods:** Tier 0: The Edwards et al. model was employed to identify the minimum HT assays required to identify chemicals with acute oral toxicity. Tier 1: Each chemical was tested using the in vitro assays identified by the in silico model. Tier 1 also included testing of general markers of cell health (cell viability, inflammatory cytokines, and oxidative stress) in M059K (glial) and HepG2 (liver) monoculture cell models to capture conventional toxicological endpoints. Tier 2: Human liver microtissue (InSphero) and cerebral organoid models (AxoSim, Inc.) were used to evaluate similar endpoints to those identified by the in silico model, along with markers of cell health and assays to demonstrate functional decrements in the tissues. Benchmark dose (BMD) modeling was used to predict the concentration at 50% of maximal response (AC_{50}) and the 95% lower confidence limit of the concentration representing one standard deviation response difference from control (BMDL). The U.S. Environmental Protection Agency's HT toxicokinetic model adapted for the United States Air Force population was used for in vitro-to-in vivo extrapolation to establish oral human equivalent doses (HED) for the AC_{50} (HED_{AC50}), BMDL (HED_{BMDL}), or lowest observable effect level (HED_{LOEL}) if BMDL was not calculable. For each chemical, the HED_{AC50} for the model-identified assay was compared to acute oral toxicity (LD_{50}) data. Similarly, the lowest HED_{BMDL} or HED_{LOEL} for all assays were compared to the 95th lower percentile of in vivo points of departure ($POD_{Traditional,95}$) collected from various databases of primarily repeated-dose

studies. **Results:** In the Tier 1 HT assays, both aldicarb and methomyl were positive in the model-identified cell-free AChE inhibition assay. The in silico-identified assay for TDCPP and TCEP was human pregnane X receptor (PXR) receptor induction; both were positive in the PXR transactivation assay. PXR receptor induction was the most sensitive of all tested endpoints for TDCPP with a HED_{BMDL} of 0.08 mg/kg/day. The in silico-recommended assay for chlorobenzene and 4-CBP was retinoid X receptor α (RXRα) receptor induction; both chemicals were inactive in a commercial RXRα transactivation assay. In the Tier 1 cell health assays, increased IL-8 was the most sensitive effect for TCEP and chlorobenzene, with HED_{LOEL}s of 0.1 and 0.03 mg/kg/day, respectively. In the Tier 2 assays, HED_{BMDL} for human cerebral organoid AChE inhibition was 0.02 mg/kg/day for aldicarb and 0.001 mg/kg for methomyl; this was the most sensitive endpoint. In liver microtissues, TDCPP and TCEP exposure increased expression of the PXR-associated gene product CYP3A4, and chlorobenzene and 4-CBP exposure increased expression of RXRα-associated gene product CCL2. Reduction in cerebral organoid intracellular calcium oscillation peak amplitude was the most sensitive endpoint for 4-CBP, with a HED_{BMDL} of 0.006 mg/kg/day. Overall, HED_{AC50}s were generally protective compared to LD_{50} values, but they were not consistently predictive of LD_{50} concentrations. While 4-CBP did not have $POD_{Traditional,\ 95}$ for comparison, the most sensitive HED_{BMDL} and HED_{LOEL} values were more conservative than $POD_{Traditional,95}$ for all other chemicals except aldicarb, which was +0.3 logarithm less conservative than the $POD_{Traditional,95}$. HED_{AC50} values were consistently less conservative than $POD_{Traditional,95}$. **Conclusions:** The tiered assessment generally was able to derive HEDs that were at least as conservative as $POD_{Traditional,95}$ values when based on the most sensitive in vitro endpoint for each chemical, with half of the most sensitive results derived from Tier 1 assays and half derived from Tier 2 assays. HED_{AC50} concentrations from in silico-identified assays did not necessarily align with acute oral toxicity potency, however, they were generally more conservative than those values. Results for key assays identified by the in silico model were mostly consistent with analogous ToxCast data. The exception was the RXRα transactivation assay, which was negative in the current study for chlorobenzene, but positive in the ToxCast transactivation assay, which could be related to variability in gene reporters used between different laboratories. Ultimately, using this tiered approach allowed HEDs to be calculated that were conservative compared to traditional animal-based PODs for all but one chemical, and did so with fewer assays than would be expected in an untargeted approach. These results support the potential utility of this tiered approach for rapid testing of novel chemicals using a finite number of in vitro tests and provide a starting point for testing novel chemicals with unknown modes of action. However, additional work is needed to test the broader applicability, limitations, and recommended protocol for use of this NAM-based tiered approach for the diverse exposure scenarios encountered in military risk assessments. **Disclaimer:** No DoD endorsement implied.

ABSTRACT NUMBER: 5177 **Poster Board Number:** LB278

TITLE: Characterizing human common loss-of-function genes and their utility in functionally assessing population variability and chemical susceptibility

AUTHORS (FIRST INITIAL, LAST NAME) AND INSTITUTIONS: *C. Kim*, Z. Zhu, M. Tagmount, R. Bacher, B. Barbazuk, and *C. Vulpe*. University of Florida, Gainesville, FL.

KEYWORDS: Chemical Hazard Assessment; Systems and Integrative Toxicology; In Vitro and Alternatives; Population variability and chemical susceptibility

ABSTRACT: Background and Purpose: Toxicological risk assessment is a critical process designed to evaluate the potential adverse effects of chemical exposure on human health, playing a vital role in

public health decision-making and regulatory frameworks. A significant challenge in this assessment is the complexity of adverse outcomes arising from inter-individual variability. Differences in susceptibility to chemical exposure can stem from genetic factors, life stage, sex, and other determinants. Among these factors, understanding the genetic variability that contributes to differences in chemical susceptibility is key to more accurately assessing chemical risks, particularly for vulnerable populations. Advancements in human cell-based *in vitro* models have contributed to the development of new approach methodologies (NAMs), which facilitate the prediction of human-relevant toxicity without the need for additional *in vivo* data. **Methods:** By leveraging available human genomics resources and large-scale genetic screening tools such as CRISPR screens, we have introduced an innovative framework to address human population variability in chemical susceptibility, thus enhancing the evaluation of chemical safety. In our study, we examined the 1551 predicted loss-of-function (pLoF) genes cataloged in the human genome aggregation database (gnomAD), which represent genes most likely involved in modulating population-level responses to toxicants (PopVar genes). **Results:** Functional gene set enrichment analysis revealed that these PopVar genes are significantly enriched in various xenobiotic metabolism pathways, highlighting their critical evolutionary role in toxicity responses. Subsequently, we developed a PopVar sgRNA library and assessed the essentiality of these genes for cell survival using a CRISPR screening approach. This analysis identified 112 essential genes for cell survival, of which 89 had not been previously reported as essential in the DepMap database, further validating the importance of this gene set for evaluating toxicant responses. Furthermore, we examined publicly available GWAS and PheWAS databases to determine if the PopVar genes were associated with any phenotypes or traits relevant to toxicant responses. Our analysis revealed that traits associated with metabolism, including serum metabolite levels and liver enzyme activity, showed higher associations with PopVar genes compared to general genes, confirming the relevance of our gene set in assessing variability in toxicant responses. **Conclusions:** In summary, the creation of the PopVar sgRNA library, based on 1551 human pLoF genes selected from gnomAD, represents a novel and effective platform for large-scale evaluation of population variability and susceptibility to chemical exposure, advancing the *in vitro* NAM approach for toxicological risk assessment.

ABSTRACT NUMBER: 5178 **Poster Board Number:** LB279

TITLE: Rapid and predictive assessment of developmental and reproductive toxicity using ML-assisted high-throughput *C. elegans* image analysis

AUTHORS (FIRST INITIAL, LAST NAME) AND INSTITUTIONS: S. Mondal[1], A. Laing[1], A. Shen[1], A. Medewar[1], E. Hegarty[1], and A. Ben-Yakar[2,1]. [1]vivoVerse, LLC, Austin, TX; and [2]The University of Texas at Austin, Austin, TX. Sponsor: *M. Aschner*

KEYWORDS: Alternatives to Animal Testing; Reproductive and Developmental Toxicology; Pesticides; Screening technology; Machine-learning-based image analysis

ABSTRACT: Background and Purpose: Developmental Toxicity (DevTox) and Reproductive Toxicity (ReproTox) assessments are critical for evaluating the safety of chemical exposures on organisms' life cycles, reproduction, and development. Traditional assessments rely on vertebrate animal models, which are slow, resource-intensive and raise ethical concerns. The nematode *Caenorhabditis elegans* (*C. elegans*) has emerged as a promising alternative due to its genetic homology with humans, rapid life cycle, and cataloged wild-type genetic backgrounds. However, low-throughput and labor-intensive methods, coupled with limited endpoints, have hindered its adoption for high-throughput sub-lethal

toxicity studies. Our solution addresses these limitations by leveraging advanced microfluidic platforms and automated image analysis to establish *C. elegans* as a New Approach Methodology (NAM) for predictive toxicology. **Methods:** We developed a microfluidic imaging platform complemented by ML-driven image analysis to enhance throughput and resolution for DevTox and ReproTox assessments using *C. elegans*. The vivoChip device facilitates high-resolution 4D imaging of approximately 1,000 *C. elegans* from 24 populations. We integrate multiple endpoints for comprehensive toxicity evaluation. The analysis software (vivoAnalyzer) enables multiparametric analysis of *C. elegans* phenotypes including in utero embryonic development and embryo motility, and automated quantification of body volume, motility, and stress-induced autofluorescence using machine learning-assisted image analysis. Using a 2.5D U-Net architecture (vivoBodySeg), we achieved precise segmentation of *C. elegans* with an average Dice score of 97.80, enabling high-speed analysis of 36 GB datasets within 35 minutes on standard desktop hardware for DevTox endpoints. **Results:** Our assays show a rank correlation of 0.77 between *C. elegans*-based methods and reported rat data. Fully automated analyses of developmental and systemic toxicity yielded highly reproducible results (4-8% coefficient of variation) and enabled high statistical power. Combining multiple endpoints such as body volume, motility, stress-induced autofluorescence, and embryonic phenotypes, we improved the assay sensitivity and predictiveness. The *in-utero* imaging approach demonstrated a fourfold increase in sensitivity for detecting reproductive toxicity by quantifying embryonic development compared to total embryo counting. The vivoChip platform processed data up to 140 times faster than manual methods, offering rapid and scalable phenotyping. Validation studies using industrial and agricultural chemicals (e.g., propiconazole, chlorpyrifos, methylmercury) confirmed the platforms' robustness in environmental toxicology applications. **Conclusions:** The integration of microfluidic platforms and machine learning has established *C. elegans* as a robust model for DART and DevTox studies. These methodologies enable high-throughput, multiparametric analyses of sub-lethal toxicity phenotypes, providing repeatable and sensitive endpoints for chemical toxicity assessments. By addressing limitations in throughput and resolution associated with existing *C. elegans* methods, these approaches represent a significant advancement in the development of NAMs. The platform demonstrates potential for broad application in routine safety assessments of existing substances and predictive toxicology for new products, offering a viable alternative to vertebrate models and reducing the ethical and financial burdens associated with animal testing.

ABSTRACT NUMBER: 5179 **Poster Board Number:** LB280

TITLE: The application of new approach methodologies (NAMs) including transcriptomics and AI/ML modelling as an integrated safety strategy in drug discovery

AUTHORS (FIRST INITIAL, LAST NAME) AND INSTITUTIONS: P. Walker[1], M. Fernandes dos Reis[2], R. Rex[2], B. Park[1], S. Bevan[1], J. Eakins[1], A. Rosell-Hidalgo[1], C. Bruhn[2], T. Samatov[2], G. Aquino[2], D. Yuezak[2], R. Fritsch[2], *C. Strock*[3], and S. Madden[1]. [1]Cyprotex Discovery Ltd UK, Alderley Park, United Kingdom; [2]Evotec International GmbH, Göttingen, Germany; and [3]Cyprotex Discovery Ltd, Framingham, MA.

KEYWORDS: Bioinformatics

ABSTRACT: Background and Purpose: High drug failure rates in clinical development, primarily due to safety concerns and low efficacy, present a significant burden. As the major site for drug metabolism and bioactivation, drug-induced liver injury (DILI) remains a significant hurdle. Leveraging high-throughput, new approach methodologies (NAMs) such as 2D/3D human *in vitro* models and large data

approaches, such as RNA sequencing (RNA-seq)/transcriptomic (Tx) profiling is leading to valuable risk assessments, within early drug discovery. Artificial intelligence (AI), in particular machine learning (ML) predictive model generation, has become a powerful addition to the safety toolbox. ML algorithms can analyse large complex datasets including multiplexed NAM data, Tx data, and chemical structures to identify patterns associated with safety liabilities. This study evaluated a NAM based approach used as part of an early drug discovery safety cascade. **Methods:** A reference set of 130 compounds, classified as "no DILI" (n=58), "less DILI" (n=37), or "most DILI" (n=35) were analysed using a NAM based early drug discovery safety cascade. Each NAM uses a defined published risk assessment based on predicted human exposure threshold. The NAMs assessed from the safety cascade are BSEP inhibition, Glu/Gal, SeaHorse Stress Test, HepG2 and HepaRG liver microtissue high content imaging (HCI) and primary human hepatocytes (PHH) in combination with high-throughput RNA sequencing (transcriptomics). Either the number of safety alerts/flags from each NAM was used to assess overall DILI risk or a machine learning model-based prediction from the NAM input data. The PHH RNA-seq Tx was performed, utilizing both point of departure (PoD) and ML/AI prediction for DILI classification based on human exposure. The predictive values from the NAM based safety cascade were assessed as standalone assays or in combination. **Results:** The sensitivity (sens), specificity (spec), and accuracy (acc) were calculated for the NAMs used in the safety cascade. The NAM risk assessment using a ≥2 flag threshold yielded 69%(sens), 95%(spec) and 81%(acc). Whereas the ML model utilising the same NAM data demonstrated a risk assessment performance of 85%(sens), 88%(spec) and 86%(acc). An integrated approach combining the full safety cascade further increase confidence in the DILI risk assessment 85%(sens), 93%(spec), and 89%(acc). **Conclusions:** By combining NAMs in an early drug discovery safety cascade and modelling approaches dramatically increases the confidence in de-risking programs for DILI liability. Using ML modelling of NAM data outperformed traditional approaches such as weight of evidence approaches (e.g. ≥2 safety flags), improving sensitivity by identifying 11 additional true positive compounds (TP). Combining the full safety cascade produced the highest overall prediction accuracy (89%). This study illustrates the benefit of utilising NAMs and modelling in early safety liability screening cascade. This methodology supports early drug discovery and development and helps reduce late-stage drug attrition.

ABSTRACT NUMBER: 5180 **Poster Board Number:** LB281

TITLE: Leveraging Versatility of hiPSC-Derived 2D and 3D Cardiac Cell Models in Cardiac Safety Evaluation of Drugs

AUTHORS (FIRST INITIAL, LAST NAME) AND INSTITUTIONS: E. Kim, A. Kim, J. An, B. Kim, S. Kim, S. Lee, E. Kim, J. Lee, and D. Woo. NEXEL Co., Ltd., Gangseo-gu, Korea, Republic of. Sponsor: A. Kim, Japanese Society of Toxicology

KEYWORDS: Safety Evaluation; Safety Pharmacology; In Vitro and Alternatives; Induced Pluripotent Stem Cells

ABSTRACT: Background and Purpose: Human induced pluripotent stem cells (hiPSCs) enable the development of versatile models, including 2D monolayers and advanced 3D systems. These hiPSC-derived cell models support diverse applications, from basic research to drug screening. This study highlights the applications of hiPSC-derived 2D cardiomyocytes and 3D cardiac organoids (COs) in the cardiac safety evaluation of drugs and compares the advantages of each model. **Methods:** Differentiation into 2D cardiomyocytes and 3D COs was achieved using proprietary protocols. To assess

the feasibility of hiPSC-derived 2D and 3D cardiac models for drug screening, field potential duration (FPD) was measured in hiPSC-derived cardiomyocytes exposed to 28 CiPA drugs. Contractility was evaluated in 3D COs to compare drug responses between the 2D and 3D models. **Results:** The hiPSC-derived 2D cardiomyocytes demonstrated low batch-to-batch variation in basic electrophysiological characteristics and drug responses to representative reference drugs (E-4031, dofetilide, nifedipine, and mexiletine). Moreover, FPDcF variations following exposure to 28 CiPA drugs were categorized into distinct risk groups. Validation using the US FDA algorithm effectively distinguished high/intermediate and low-risk drugs with statistical significance. In contrast, COs exhibited superior functionality, with nearly two-fold improvements in contractility and calcium handling. Additionally, COs showed greater drug responses to isoproterenol when compared to the 2D models. **Conclusions:** This study underscores the potential of hiPSC-derived 2D and 3D models in the cardiac safety evaluation of drugs. Their high-throughput capability and physiological relevance make them valuable tools for drug evaluation and disease modeling. Furthermore, 3D models offer enhanced functional capabilities, such as evaluating contractility. These findings strongly suggest that hiPSC-derived models will provide the foundation for novel approaches in diverse applications.

ABSTRACT NUMBER: 5181 **Poster Board Number:** LB282

TITLE: Evaluation of the Safety and Efficacy of Bi-specific Antibodies using Organoids and Colorectal Cancer Spheroids

AUTHORS (FIRST INITIAL, LAST NAME) AND INSTITUTIONS: E. Heinzelmann[1], V. Anstett[1], F. Piraino[1], A. Roch[1], A. Chrisnandy[1], M. Norkin[2], V. Garnier[1], K. Homicsko[2], S. Hoehnel-Ka[1], and N. Brandenberg[1]. [1]Doppl SA, Lausanne, Switzerland; and [2]CHUV, Centre Hospitalier Universitaire Vaudois, Lausanne, Switzerland. Sponsor: S. Hoehnel-Ka, EUROTOX

KEYWORDS: Safety Evaluation; Alternatives to Animal Testing; In Vitro and Alternatives; Organoids

ABSTRACT: Background and Purpose: Developing ex vivo models that replicate immune-tumor interactions with high fidelity is essential for advancing immunotherapy research, as traditional two-dimensional *in vitro* systems often lack the complexity required to fully represent these interactions. **Methods:** In this study, we established a comprehensive 3D redirect lysis (3D-RDL) assay using colorectal cancer spheroids and adult stem cell-derived, healthy human organoids to evaluate the efficacy and safety profile of *Cibisatamab* - a bispecific antibody targeting carcinoembryonic antigen (CEA) on cancer cells and CD3 on T cells. This model allows to assess the cytotoxic activity and immune responses, capturing variations in therapeutic response not observable in simpler systems. Our model integrates live imaging and cytotoxicity analyses to enable precise, real-time tracking of antibody effects on CEA-expressing tumor cells compared to healthy cells. Additionally, by standardizing effector-to-target cell ratios in each co-culture, we established a reproducible workflow that enhances data accuracy and comparability across assays. Flow cytometry and Granzyme B release profiling further allowed us to characterize immune cell activation, revealing distinct T cell activation markers and Granzyme B release patterns tied to *Cibisatamab* treatment. **Results:** Our results show that *Cibisatamab* effectively induced cell death in cancer spheroids with high CEA expression while showing dose dependent on target, off-tumor binding and killing on non-cancerous cells of healthy organoids with intermediate CEA levels. This highlights our model's potential to predict clinical immunotherapy outcomes, capturing complex responses like immune activation, therapeutic selectivity, and potential resistance mechanisms.

Conclusions: Our findings underscore the utility of our model as a reliable, physiologically relevant tool for screening new immunotherapies and advancing our understanding of tumor-immune dynamics.

ABSTRACT NUMBER: 5182 **Poster Board Number:** LB283
TITLE: Inhalation exposure and toxic effects of e-cigarette: insights from a ventilated artificial lung exposure system

AUTHORS (FIRST INITIAL, LAST NAME) AND INSTITUTIONS: *H. Chen*, A. Harui, M. D. Roth, and Y. Zhu. University of California Los Angeles, Los Angeles, CA.
KEYWORDS: None

ABSTRACT: Background and Purpose: Electronic cigarettes (e-cigs) have gained immense popularity, particularly among younger generations. Prior studies have demonstrated that e-cig aerosols cause cytotoxicity in lung cells (*in vitro*) and lung injuries in animals (*in vivo*), raising concerns about the health risks associated with vaping. However, intrapulmonary exposures from vaping are dynamic and involve complex interactions between e-cig aerosols and human lungs, which traditional in vitro and in vivo methods often fail to replicate. Despite emerging evidence of potential toxicity, the lack of physiologically relevant models for studying vaping exposures limits our understanding of their actual health effects on human lungs. To address this gap, we developed a ventilated artificial lung system to study e-cig aerosol exposures as they would occur in human lungs. **Methods:** The artificial lung system features: (1) a lung chamber with anatomically precise 3D-printed airways spanning from the mouth to the 13th branching generation (G13); (2) integration of intermittent puffing with ongoing breathing to simulate various vaping patterns, including different vaping topographies and respiratory parameters; and (3) replication of the internal lung environment (37℃, 88±5% relative humidity, cyclical pressure changes <10 cmH2O and an alveolar gas mixture of 21% O_2, 5% CO_2, 74% N_2) to support the cultivation of primary human bronchial epithelial cells (HBECs). The system facilitates *in situ* characterization of inhaled e-cig aerosols within the lung chamber through a sampling port to assess intrapulmonary exposure. To evaluate and validate the artificial lung system in replicating key aspects of vaping exposure, we characterized e-cig aerosols during a simulated 4-puff vaping session. Furthermore, we exposed HBECs to e-cig aerosols through repetitive 4-puff sessions simulating vaping over two days and assessed the biological effects of exposure to different e-cig aerosols. **Results:** During a 4-puff vaping session, peak particle number concentrations within the lung chamber increased stepwise with each puff, followed by a gradual decrease in a first-order decay ($k = -0.52$, $r^2 = 0.99$) due to ongoing breathing. Inhaled e-cig aerosols were distributed through 3D-printed airways, with airflow fields transitioning from turbulence in the trachea-to-G4 region to laminar flow in the airways at G10 and higher. Consequently, inhaled e-cig particles deposited fractionally in the airways in a size-dependent pattern, aligning with predictions from lung deposition modeling. Our results also show significant hygroscopic growth of e-cig particles within the artificial lung, leading to a 19% greater deposition dose compared to data collected at room temperature and humidity. In this setting, HBECs in the artificial lung system were exposed only to the fraction of e-cig aerosols that would naturally reach the bronchus under region-specific laminar airflow conditions. Our study found that short-term exposure to e-cig aerosols from simulated vaping over two days did not cause acute toxic effects on HBECs in terms of cell viability, mitochondrial function, or histology, but did alter epithelial production of Fractalkine (CX3CL1), a chemokine involved in the pathogenesis of COPD, in a nicotine-dependent manner. When HBECs were exposed to e-cig aerosols generated from different e-liquid formulations, including propylene

glycol/vegetable glycerol (PG/VG) alone, PG/VG spiked with nicotine, or marketed JUUL pods, our preliminary RNA-Seq data identified unique transcriptome profiles associated with each exposure. Exposure to PG/VG alone exhibited modest differences in gene expression compared to the control group exposed to clean air. HBECs exposed to e-cig aerosols generated from JUUL pods, which contain a complete set of e-liquid constituents, exhibited more differentially expressed genes, with most changes also associated with exposure to PG/VG plus nicotine. **Conclusions:** This novel artificial lung system replicates key aspects of vaping exposure as it occurs in human lungs, capturing distinct aerosol characteristics associated with intermittent vaping, ongoing ventilation, and the warm and humid lung environment. It offers a more physiologically relevant *in vitro* model for studying inhaled exposures. Findings from the HBEC exposure study provide new insights into the subtle but potentially toxic effects associated with different e-liquid constituents, which may contribute to the development of human pathology.

ABSTRACT NUMBER: 5183 **Poster Board Number:** LB284

TITLE: 3D Primary Human Thyroid Microtissues: An *In Vitro* Model for Studying Thyroid Hormone Disruption

AUTHORS (FIRST INITIAL, LAST NAME) AND INSTITUTIONS: T. Nguyen-Jones[1], E. Rogers[1], *K. K. Wolf*[2], T. Stone[2], S. Presnell[1], *E. L. LeCluyse*[2], and J. Chen[1]. [1]LifeNet Health LifeSciences, Virginia Beach, VA; and [2]LifeNet Health LifeSciences, Research Triangle Park, NC.

KEYWORDS: Endocrine; Thyroid; In Vitro and Alternatives; Endocrine Disruptors; Thyroid Model

ABSTRACT: Background and Purpose: The rise of chemical production in the 21st century has come with increased human exposure to toxic substances which could lead to potential health hazards, such as disruption of thyroid hormone synthesis that might cause neurodevelopmental impairment and preterm birth. In recent years, different government agencies across the world have increased efforts to develop programs to identify, screen, and determine the potential effects of chemicals found in the environment on thyroid hormone synthesis. Currently, many of the *in vitro* models used for this purpose often utilize microsomes and cell lines which do not always accurately represent the human thyroid physiological conditions. Therefore, the development of more physiologically relevant human models has become an emergent need. The goal of this study was to evaluate the use of P1 cryopreserved human thyrocytes in the 3D thyroid microtissue assay for determining the response profiles of different thyroid-disrupting chemicals (TDCs). **Methods:** Our study used cryopreserved primary human thyroid cells (P1) from healthy male and female donors 18 - 52 years of age (n=3 individual lots). Cryopreserved thyrocytes were thawed and plated in a 3D cell culture format using Matrigel-coated 96-well plates. The cell cultures were stimulated with bovine thyroid stimulating hormone (bTSH) on day 2 and microtissues were allowed to form and mature until day 8. On day 8, cell cultures were dosed with either the known TPO inhibitor, methimazole, or NIS inhibitor, potassium hexafluorophosphate (KPF6) at 100 - 0.0001 µM, or anti-TSHR (thyroid-stimulating hormone receptor) recombinant human antibody K1-70 at 0.667 - 6.67 x 10^{-7} µM. Compound treatment was repeated on days 10 and 12, and media samples were collected on day 14 for analysis. H&E staining of formalin-fixed microtissues was used to confirm the presence of follicular structures. T4 ELISA was used to determine compound effects on T4 synthesis, while CellTiter-Glo was used for viability measurement. The half-maximal inhibitory concentration (IC_{50}) values for each compound were determined using GraphPad Prism. **Results:** Combined histology and ELISA results showed that the cryopreserved primary thyrocytes were able to form follicular structures as found in

the native thyroid and T4 average production ranged from 32.53 ± 1.06 ng/1 million cells/48hr to 196.28 ± 14.024 ng/1 million cells/48hr. When treated with reference compounds, T4 inhibition was accomplished, in a concentration-dependent manner, with both methimazole and potassium hexafluorophosphate. The average IC_{50} values for methimazole and potassium hexafluorophosphate were 0.214 ± 0.068 and 2.148 ± 0.692 µM, respectively, with >85% inhibition of T4 synthesis for both compounds. While complete inhibition curves were not obtained for the recombinant antibody K1-70, a decrease in T4 synthesis was still detected at the two highest concentrations, which resulted in 70% inhibition overall. A decrease in viability was observed for cells treated with higher doses of K1-70 antibody. **Conclusions:** In conclusion, we were able to reconstruct the follicular structure of the native thyroid for T4 synthesis and demonstrate T4 response to both small molecule and antibody-based reference compounds. Cryopreserved P1 human thyrocytes in the 3D microtissue assay not only offers a platform for environmental chemical screening, but also a promising approach for thyroid antibody-based therapeutic research.

ABSTRACT NUMBER: 5184 **Poster Board Number:** LB285

TITLE: *In vitro* pharmacologic profiling aids systemic toxicity assessment of chemicals, current status and future direction

AUTHORS (FIRST INITIAL, LAST NAME) AND INSTITUTIONS: M. Burbank[1], P. Kukic[2], *G. Ouedraogo*[1], J. Kenna[3], N. Hewitt[4], D. Armstrong[5], A. Otto-Bruc[6], J. Ebmeyer[7], M. Boettcher[7], I. Willox[6], D. Allen[8], A. Cuciureanu[8], and C. Mahony[9]. [1]L'Oréal Research & Innovation, Aulnay-Sous-Bois, France; [2]Unilever Safety and Environmental Assurance Centre, Bedfordshire, United Kingdom; [3]Independent consultant, Macclesfield, United Kingdom; [4]SWS, Erzhausen, Germany; [5]Armstrong Pharmacology Ltd, Macclesfield, United Kingdom; [6]Eurofins Cerep, Celle-Lévescault, France; [7]Beiersdorf AG, Hamburg, Germany; [8]International Collaboration on Cosmetics Safety (ICCS), New Jersey, NJ; and [9]Procter & Gamble Technical Centres Ltd, Reading, United Kingdom.

KEYWORDS: In Vitro and Alternatives

ABSTRACT: Background and Purpose: Evaluation of systemic toxicity based only on non-animal approaches is a challenging objective in cosmetic safety assessment. This requires a fundamental change from the current apical endpoint driven approach to a hypothesis driven, mode of action and exposure led framework. To achieve this, within the Cosmetics Europe Long Range Science Strategy (2016-2022) we developed a New Approach Methodology (NAM) toolbox, including an adapted *in vitro* pharmacology profiling panel (APPP), that enabled next generation risk assessment (NGRA) of cosmetic ingredients. The key insights provided by this approach have paved the way for continuing the project under the International Collaboration for Cosmetic Safety (ICCS), established in 2023. Experience with drugs indicates that human adverse reactions can arise via their interactions with defined tissue targets e.g. enzymes, receptors and channels. Screening for these interactions in vitro via use of the APPP can identify putative non-target modes of action (MoAs) and expand the coverage of biological space for NAM assessment of systemic toxicity. **Methods:** The APPP comprises 83 target assays: 80 are non-cellular and include 52 radioligand binding assays, 5 functional protein-protein interaction assays and 23 enzyme assays. It includes targets known to mediate adverse effects of pharmaceuticals in humans alongside additional targets whose biological activities are relevant for systemic adverse effects The target selection process followed a workflow based on Bowes et al. (2012) as well as other publications, which was complemented by consideration of: evidence from *in vivo* safety pharmacology studies;

mechanistic information; reported human clinical adverse effects; mechanism-based connections to established systemic toxicities (extracted from AOP-Wiki); protein and mRNA tissue expression data and pharmacological promiscuity rates observed in historical datasets. This was used to profile the activities of 129 cosmetic relevant chemicals. All chemicals were selected according to literature, legacy repeated dose toxicity data in rodents, critical effects, suitable biokinetic properties and availability of in vitro data. **Results:** First, chemicals were tested at a single concentration (10 µM) in the panel. Nearly half (63) of the 129 chemicals did not interact significantly with any targets (inhibition or stimulation <50 %). The remaining 66 chemicals interacted (≥50 % vehicle control activity) with one or more targets 7 of which interacted with more than 10 targets. To establish an estimate of potency, follow up concentration-response testing was undertaken for these 66 chemicals and the target assays where single concentration testing had identified ≥50 % effect. A 10 µM data point used in the initial test compound screen was included in the concentration-response testing of 212 assay-chemical pairs. The observed potencies ranged from 1 nM to 98 µM suggesting that these in vitro assays may detect target-specific biological activity to aid the human relevant cosmetic safety assessment. Internal data consistency was robust, as evidenced by the reproducibility between single concentration and concentration-response data and showed good concordance with data reported in the ToxCast and drug excipient datasets. **Conclusions:** Next steps will include considerations for expanding the biological coverage to other targets, as well as incorporating the impact of metabolism via test compound incubation with alginate-encapsulated immobilized human and rat liver S9 *in vitro.* Data resulting from these efforts can be analyzed alongside other new approach methodologies, to support multiple contexts of use for cosmetic chemical risk assessments that we can illustrate via case studies.

ABSTRACT NUMBER: 5185 **Poster Board Number:** LB286
TITLE: Assessing on-target cytotoxicity of CAR T cells co-culture model using gastrointestinal organoids

AUTHORS (FIRST INITIAL, LAST NAME) AND INSTITUTIONS: C. Ceroni, A. Roch, V. Garnier, F. Piraino, E. Heinzelmann, and S. Hoehnel-Ka. Doppl SA, Lausanne, Switzerland. Sponsor: S. Hoehnel-Ka, EUROTOX
KEYWORDS: Cytotoxicity; Immunotoxicity; Gastrointestinal; Immunotherapie

ABSTRACT: Background and Purpose: Developing investigational ex-vivo models that accurately replicate the intricate interactions between tissues and immune cells is crucial for advancing novel immunotherapeutic approaches. However, such co-culture systems are often challenging to establish and limited in their scope. Our study introduces a new method using healthy organoids to investigate the interactions between the gastrointestinal (GI) epithelium and Chimeric Antigen Receptor - T (CAR-T) cells. The primary aim is to assess any potential cytotoxic effects of CAR-T cells on the organoids, thereby evaluating the adverse effects CAR-T cell therapy may have on the healthy tissue. **Methods:** As CAR-T cell therapy relies on specific target interactions present in the native epithelium, it is crucial to maintain this specificity in the organoid model. The presence of the target of interest, as well as adherent and tight junction proteins, is assessed through immunohistochemistry (IHC) and immunofluorescence (IF) directly on the organoids. Our co-culture system uses microwells for the generation of GI organoids to which immune cells can be added. The interactions between the organoids and the immune cells are visualized using cell tracker dyes, allowing us to monitor the co-culture evolution over multiple days. Moreover, we utilize live imaging and image analysis techniques to quantify the cytotoxic effects and dose-limiting activity of CAR-T cells against organoids expressing the target of interest. **Results:** The high level of cultures' homogeneity ensured by our system allows us to

precisely control the effector-to-target ratio. Our findings demonstrated clear cytotoxic effects of CAR-T cells on organoids expressing the target of interest. Additionally, live imaging provided real-time insights into the dynamic interactions between CAR-T cells and the GI organoids. Quantitative analysis revealed dose-dependent cytotoxic activity, highlighting the potential for this system to evaluate both efficacy and toxicity of CAR-T cell therapies. **Conclusions:** This novel approach demonstrates the potential of organoid-based co-culture systems for assessing immunotherapeutic toxicity and efficacy. The ability to maintain specificity, monitor interactions over time, and analyze cytotoxic effects in a controlled environment represents a significant advancement in the development of improved immunotherapeutic strategies.

ABSTRACT NUMBER: 5186 **Poster Board Number:** LB287

TITLE: Innovative Microphysiological Model Using HepatoXcell Primary Human Hepatocytes and Locsense Artemis

AUTHORS (FIRST INITIAL, LAST NAME) AND INSTITUTIONS: E. K. Geervliet[1], M. Zuurveld[2], B. Shapiro[3], S. Sun[3], S. H. Roelofs[1], and *S. Lahiri*[3]. [1]Locsense B.V., Enschede, Netherlands; [2]Utrecht University, Utrecht, Netherlands; and [3]ATCC, Gaithersburg, MD.

KEYWORDS: Liver; Gastrointestinal; In Vitro and Alternatives; Gut-Liver Model, Intestinal Barrier; EGTA, Lipopolysaccharide

ABSTRACT: Background and Purpose: Lipotoxicity of the liver resulting in non-alcoholic steatohepatitis (NASH) can be caused by drugs such as amiodarone, perhexiline, and 4,4'-diethylaminoethoxyhexestrol (DH). Additionally, multiple environmental factors such as dioxin and Persistent Organic Pollutant (POP) exposure can contribute to the pathogenesis of this disease. Toxicologists assess for signs of liver damage that can result in liver diseases, such as NASH, in preclinical studies. Finally, there is a growing movement to identify how toxins can disrupt the gut microbiome and permeability and how this leakage can cause inflammation of the liver and hepatoxicity. To help reduce the burden of animal testing and to provide scientists with a model more representative of the in vivo situation, we generated an in-vitro gut liver model using intestinal epithelial cells and primary human hepatocytes. We then tested the effects of gut barrier integrity on the hepatocyte toxicity induced by lipopolysaccharide (LPS). **Methods:** Method: Caco-2 (ATCC® HTB-37™) cells were cultured on the transwell membranes for 21 days to form a mature intestinal barrier with tight junctions. HepatoXcell™ Pro (ATCC® PCS-450-011™) plateable cryopreserved primary human hepatocytes were cultured for 72 hours in the basolateral compartments with the transwells containing mature Caco-2 cell culture. The intestinal barrier was disrupted using EGTA. Intestinal barrier integrity was assessed by impedance and trans epithelial electrical resistance (TEER) measurements using the Locsense Artemis system. Cellular toxicity was induced by the addition of 2 µg/mL lipopolysaccharide (LPS) for 24 hours. Hepatotoxicity was measured by the WST-1 assay, along with measurement of hepcidin and iNOS expression. **Results:** Treatment with 5 mM EGTA caused damage to the barrier integrity of the Caco-2 cell culture as determined by the TEER measurement. When assessing hepatic toxicity induced by LPS, it was found that the hepatocytes cultured with Caco-2 cells that had damaged intestinal barrier integrity had significantly lower number of viable hepatocytes compared to the hepatic culture with undamaged intestinal barrier integrity. **Conclusions:** A damaged gut-liver model with disrupted intestinal barrier function was found to be more susceptible to hepatic toxicity induced by LPS. This gut-liver model system can be used to assess hepatotoxicity of different

compounds that may work through damaged intestinal barrier function as an alternative to in vivo animal models.

ABSTRACT NUMBER: 5187 **Poster Board Number:** LB288
TITLE: A 3D Bioprinted Vascularized Organ-on-a-Chip Platform for Human-Relevant Assessment of Drug-Induced Vascular Injury and Immune Toxicity from Biotherapeutics

AUTHORS (FIRST INITIAL, LAST NAME) AND INSTITUTIONS: Q. Dasgupta, K. Phan, C. Truong, *J. Navarro-Yepes*, P. Purkayastha, Y. Han, A. Antonio, T. Lin, M. Doerfert, C. Erice, A. R. Narkar, S. Datwani, S. Ng, and T. Pereira. Systemic Bio, Houston, TX.
KEYWORDS: Alternatives to Animal Testing; Preclinical Assessments; Immunotoxicity; Drug-induced vascular injury

ABSTRACT: Background and Purpose: Antibody-based therapeutics including monoclonal antibodies (mAbs), antibody-drug conjugates (ADCs), and bispecific antibodies can cause off-target toxicities such as drug-induced vascular injury (DIVI) and immune toxicity. The studies described here are part of ongoing efforts aimed at evaluating the predictive performance of Systemic Bio's h-VIOS™ (Human Vascularized Integrated Organ Systems) platform in assessing the effects of antibody-based therapeutics, specifically gemtuzumab ozogamicin (GO), sacituzumab govitecan (SG), and theralizumab (TZ). GO, SG, and TZ have distinct safety profiles, but all can cause vasculature-associated effects. GO was withdrawn from the market due to hepatotoxicity, SG shows thrombocytopenia but no toxicity, and TZ caused severe immune toxicity in human clinical trials but not in preclinical testing. By utilizing the h-VIOS™ platform to replicate the human vasculature, we aimed to provide a more relevant and dynamic representation of how these therapeutics interact with endothelial cells (ECs) and other vasculature components. **Methods:** The h-VIOS™ platform was used to assess the effects of GO, SG, and TZ on endothelialized liver and vascular scaffolds. GO was tested on 3D bioprinted liver scaffolds with liver spheroids and liver sinusoidal endothelial cells (LSECs) to evaluate toxicity on exposure to GO, IgG4 and free drug Calicheamicin. In the SG study, 3D bioprinted scaffolds seeded with HUVECs were treated with SG, control IgG1 and active drug SN-38. For TZ, an anti-CD28 mAb, we evaluated immune toxicity using scaffolds endothelialized with HUVECs and perfused with T cells. Scaffolds were tested for viability, proliferation, cytokine production, EC activation, and inflammation. **Results:** GO, SG, and TZ showed varying toxicity and endothelial dysfunction. GO treatment resulted in hepatotoxicity, including dose-dependent cell death, elevated LDH, and ALT levels. DIVI assessment revealed loss of endothelial coverage within three days, with GO causing cytotoxicity to LSECs and inflammation marked by increased PECAM and P-selectin. Soluble activation markers, such as sICAM-1 and sPECAM-1, were also upregulated. SG showed no vascular toxicity, reinforcing its reported safety profile. It caused minor EC activation and inflammation but did not lead to cell death or detachment. SG altered endothelial morphology, upregulating IL-6 and TNF-α, and increased soluble markers like sPECAM-1 transiently. sICAM-1, sVCAM-1 and sP-Selectin remained unaffected. SN-38, the free drug, caused significant endothelial damage. SG also induced immune recruitment without causing significant loss of endothelial coverage. TZ caused an inflammatory response as early as 24 h, with significant upregulation of IL-6, IFN-γ, and IL-8, typical of cytokine release syndrome (only in the presence of ECs). Flow cytometry revealed elevated IL-2 and IFN-γ in CD28+ T-cells, indicating TZ's specificity. T cells had an 86.5% CD28+ population initially. Post-theralizumab treatment, no significant change in the %CD28+ T cells across groups was observed at 24 h but was significantly lowered at 96 h across all three TZ concentrations.

The CD28+ T cell population revealed significantly higher Ki67 expression in all TZ-treated groups compared to the control (IgG4)-treated group. This hyper-proliferation seen in the T cell population could potentially cause T cell exhaustion and death. GO, SG and TZ were also tested on 2D model, an endothelial monolayer on well plates, but did not recapitulate similar toxicity profiles. **Conclusions:** The Systemic Bio h-VIOS™ model is a powerful predictive tool for testing vascular toxicity from antibody-based therapeutics, providing a more dynamic co-culture physiology and species specificity as compared to traditional 2D models or non-human primate studies. The findings underscore the importance of the endothelium in assessing the safety of biotherapeutics, especially those with vascular or immune-related toxicities. Systemic Bio's 3D vascularized disease model effectively recapitulates key hallmarks of GO, SG and TZ toxicity and can be utilized to assess dose-dependent safety and provide insights into the mechanistic aspects of DIVI for engineered therapeutic antibodies.

ABSTRACT NUMBER: 5188 **Poster Board Number:** LB289
TITLE: Integrating the Cell Painting and Micronucleus Assays for Genotoxicity Mode of Action Analyses

AUTHORS (FIRST INITIAL, LAST NAME) AND INSTITUTIONS: T. Takahashi, T. Oshiro, and T. Watanabe. Scientific Product Assessment Center, Japan Tobacco Inc., Yokohama, Japan. Sponsor: *S. Ito*
KEYWORDS: Mode-of-Action; Genotoxicity; Cell Painting

ABSTRACT: Background and Purpose: The *in vitro* micronucleus (MN) test assesses genotoxicity derived from multiple Mode of Actions (MoAs). To avoid misleading positive test results, analyzing the MoAs of MN induction by measuring additional endpoints supports conducting appropriate follow-up tests. The Cell Painting assay is a high-content imaging method that uses fluorescent dyes to label basic cellular components, enabling comprehensive profiling of thousands of morphological features, which can then be linked to cellular responses. Since both MN and Cell Painting assays are based on cellular morphology, we hypothesized that it is possible to perform them on the same images. To investigate this, we employed five genotoxic compounds with known MoAs to simultaneously analyze both MN induction and morphological responses in U-2 OS cells. **Methods:** U-2 OS cells were seeded into 96-well plates and pre-cultured for 24 hours before exposure to test chemicals (AF-2, ICR-191, Berberine Chloride, Menadione, and Taxol) for 24 hours. Plates were assigned to recovery or non-recovery culture conditions. The recovery group was incubated for an additional 24 hours in fresh medium at 37°C, while the non-recovery group was washed and stained immediately after chemical exposure. Cells were stained using the PhenoVue Cell Painting JUMP kit. In parallel, pre-cultured plates were prepared to calculate population-doubling (PD) counts during each experiment. Images were captured with Operetta CLS. Harmony 5.1 software was used to extract 1,300 morphological features and counting the numbers of cells and MN. Preprocessing of morphological features was performed using Python’s pandas and numpy packages. Benchmark concentrations (BMCs) for each feature and Phenotypic Altering Concentrations (PACs), a point of departure concentration for this assay, were calculated using the R tcplfit2 package. Statistical analyses were performed using JMP Pro 18. **Results:** After 24-hour exposure for test chemicals, MN induction was observed only for Taxol. Since the low PD was observed under this protocol, we added a 24-hour recovery culture step. Adding the step significantly increased PD and enabled significant MN induction for all the test chemicals. Regarding the 1,300 morphological features assessed, solvent control groups showed no significant differences between recovery and non-recovery conditions, except for three features related to Actin-Golgi-Plasma membrane channel features. When the test chemicals were exposed to the cells, recovery condition shifted the feature categories

representing PAC from cytoplasmic or cellular regions to nucleic ones for all the clastogenic chemicals but not for Taxol, a tubulin disrupting aneugen. These results suggested the recovery condition is beneficial as the morphological perturbations observed under this condition were consistent with the MN induction of the chemicals. To investigate whether diverse morphological changes under recovery culture conditions offer deeper insights into mechanisms of cell damage and genotoxicity, we conducted Principal Component Analysis (PCA) on 1,300 features for each dose of test chemicals. As MN ratio increased, dose-dependent separation from the solvent control in three directions was observed. Test chemicals in each group were identified as AF-2 and ICR-191 (direct-acting genotoxicants), Berberine Chloride and Menadione (mitochondrial damage-related), and Taxol (aneugen). PCA loadings revealed that features in nucleic regions of DNA and RNA channels aligned with Taxol, while features in ring regions of mitochondrial and endoplasmic reticulum channels contributed to the separation of Berberine Chloride and Menadione. **Conclusions:** This study established a protocol for observing significant MN induction and morphological perturbation, simultaneously. Adding recovery culture allowed to observe dose-dependent MN induction and obtain reasonable PAC feature categories. Morphological features contributing to plot separation in PCA were associated with channels and regions linked to MoAs of MN formation by test chemicals, such as mitochondrial stress for Berberine Chloride and Menadione, and chromosomal aberration for Taxol. Integrating Cell Painting assay into the MN test enhances the understanding of MoAs and strengthens the weight of evidence for *in vitro* genotoxicity evaluations.

ABSTRACT NUMBER: 5189 **Poster Board Number:** LB290

TITLE: Relationship between the mutation frequency and the GFP fluorescence intensity change in *in vitro* gene mutation tests using Hprt-EGFP knock-in CHO cells

AUTHORS (FIRST INITIAL, LAST NAME) AND INSTITUTIONS: Y. Kuroda[1,2], H. Asako[1], R. Akasaka[1], K. Kamiya[1], S. Hagio[1], S. Hayashi[1], K. Takeuchi[1], K. Ishida[2], D. Matsumaru[2], and T. Nakanishi[2]. [1]Biological Research Laboratories, Nissan Chemical Corporation, Shiraoka, Japan; and [2]Laboratory of Hygienic Chemistry and Molecular Toxicology, Gifu Pharmaceutical University, Gifu, Japan. Sponsor: Y. Kuroda, Japanese Society of Toxicology

KEYWORDS: None

ABSTRACT: Background and Purpose: *In vitro* mammalian cell gene mutation test (OECD test No. 476) is evaluation system detecting for genetic mutations induced by chemical substances. The cell lines used in this test measure forward mutations in reporter genes, specifically the endogeneous hypoxanthine-guanine phosphoribosyl transferase gene (referred to as the *Hprt* gene and HPRT test in this guideline). Mutant cells deficient in Hprt enzyme activity in the HPRT test are resistant to the cytostatic effects of the purine analogue 6-thioguanine (6-TG), and mutant frequency is calculated based on the number of mutant colonies in medium with 6-TG. We used CRISPR/Cas9 system to knock in 2A self-cleaving peptide (P2A) and enhanced green fluorescent protein (EGFP) genes just before the stop codon of the *Hprt* gene in CHO cells, and created Hprt-EGFP knock-in CHO cells. In these cells, the expression or function of the *Hprt* gene can be observed by detecting GFP fluorescence. In this study, we measured the GFP fluorescence intensity of Hprt-EGFP knock-in CHO cells after treatment with a mutagenic substance, compared the induction of mutations with changes in the fluorescence intensity, and examined the effectiveness of using this cell lines to evaluate mutations. **Methods:** The mutagenic substances used in the study were Methylmethansulfonate (MMS) and Mitomycin C (MMC). The study was conducted in

two patterns (Part 1 and 2). Part 1 was conducted using a protocol based on OECD test No. 476. Proliferating Hprt-EGFP knock-in CHO cells were treated with solvent, MMS (11, 33 or 100 µg/mL) or MMC (0.11, 0.33 or 1.0 µg/mL) for 4 hours. After the treatment period, the cells were cultured for 8 days (phenotypic expression), and then they were re-plated in medium with and without selective agent (6-TG) and cultured for 8 days for the determination of the number of mutants and cloning efficiency. In addition, the cells after phenotypic expression were analyzed by flow cytometer and the GFP fluorescence intensity of each cell was measured. In Part 2, proliferating Hprt-EGFP knock-in CHO cells were treated with solvent, MMS (1.2, 3.7, 11, 33 or 100 µg/mL), MMC (0.12, 0.37, 1.1, 3.3 or 10 µg/mL) or cycloheximide (3.7 11, 33, 100 or 300 µg/mL; non-mutagenic substance) for 4 hours. After the treatment period, the cells were cultured for 20 hours, and then the cells were analyzed by flow cytometer. **Results:** In Part 1, the mutation frequency of Hprt-EGFP knock-in CHO cells treated with MMS at 10 µg/mL or MMC at 0.33 and 1.0 µg/mL increased compared to the solvent control group. In addition, there was no significant change in the median GFP fluorescence intensity of the cells after phenotypic expression in the MMS and MMC treatment groups. In Part 2, the median GFP fluorescence intensity of the cells treated with MMS at 100 µg/mL or MMC at 0.12 µg/mL or more was higher than that of the solvent control group. On the other hand, no significant change was observed in the median GFP fluorescence intensity in the cycloheximide treatment groups. In addition, cytotoxicity was observed in the cells treated with cycloheximide at 100 and 300 µg/mL. **Conclusions:** In this study, a relationship was observed between the increase in the mutation frequency and the increase in GFP fluorescence intensity in Hprt-EGFP knock-in CHO cells treated with MMS or MMC. Since the expression of EGFP reflects the expression of Hprt enzyme, it was considered that there was a possibility that transcription and translation of the Hprt gene had increased in the mutant cells. In future research, we intend to evaluate EGFP-highly-expressing cells after treatment with mutagenic substances, clarify the cause of this phenomenon, and investigate whether it is possible to evaluate the mutagenicity of chemical substances simply by evaluating changes in GFP fluorescence intensity using Hprt-EGFP knock-in CHO cells.

ABSTRACT NUMBER: 5190 **Poster Board Number:** LB291
TITLE: Investigating a DNA repair nuclease's novel role in ferroptotic cell killing in cancer

AUTHORS (FIRST INITIAL, LAST NAME) AND INSTITUTIONS: *M. R. Flores*, D. Laverty, A. Berroyer, M. Palma, and M. Sabatier. Harvard T.H. Chan School of Public Health, Boston, MA.
KEYWORDS: Alkylating Agents; DNA Repair; Metabolism

ABSTRACT: Background and Purpose: In the past year, cisplatin was used in the treatment of an estimated 50-80% of patients with cancers, including osteosarcoma and lung cancers, however approximately 30-40% of these patients do not respond effectively to cisplatin-based therapies due to inherent or acquired resistance. Apoptotic resistance to cisplatin emphasizes the potential opportunity to induce alternative cell death mechanisms in cancer treatments. One such mode of cell death may be ferroptosis, a non-apoptotic form of cell death in which iron-mediated lipid peroxidation results in disruption of the cellular membrane. The key enzyme that protects against lipid peroxidation in cells is glutathione peroxidase 4 (GPX4), of which glutathione (GSH) is a co-factor. Notably, cisplatin is observed to have GSH-trapping capabilities that can induce ferroptosis, but the role of ferroptosis in cancer cells upon cisplatin treatment remains underexplored. **Methods:** To address this, I conducted an unbiased screen to evaluate the ferroptosis sensitivity of 17 cancer cell lines, including lines with DNA repair

deficiencies resulting from targeted protein knockouts that impaired specific repair pathways. My approach involved assessing the functionality of various DNA repair pathways—Nucleotide Excision Repair, Mismatch Repair, Non-Homologous End Joining, and Homologous Recombination—using the Fluorescence Multiplex-Host Cell Reactivation (FM-HCR) assay to measure DNA repair capacity in the different lines. I then conducted viability assays after treating the cells with ferroptosis inducers and inhibitors. Additionally, I performed luminescence-based glutathione assays and western blot analyses on selected cell lines identified as significant from the initial screen. **Results:** My data demonstrates that a DNA repair nuclease protects cells from pharmacological induction of ferroptosis in vitro. Notably, nuclease-deficient U2OS and H460 cells are up to 10-fold more sensitive to cell killing with ferroptosis inducers than WT, and have 4x lower basal GSH than WT. Additionally, the nuclease-deficient cells have significantly reduced GPX4 protein than WT. **Conclusions:** Thus, these nuclease-deficient cells could represent a specific vulnerability that can be targeted to enhance efficacy of cisplatin treatments, and nuclease expression levels may play a role in the normal tissue toxicity of therapies that kill cells via ferroptosis.

ABSTRACT NUMBER: 5191 **Poster Board Number:** LB292

TITLE: Perfluorooctanoic (PFOA) and perfluoropentanoic (PFPA) acids cause acute genotoxicity at parts per trillion levels *in vitro*

AUTHORS (FIRST INITIAL, LAST NAME) AND INSTITUTIONS: S. M. Matthews, B. J. Hinchcliff, C. Propper, and *M. C. Salanga*. Northern Arizona University, Flagstaff, AZ.

KEYWORDS: Ecotoxicology; Perfluoronated Agents; Genotoxicity; Polyfluoroalkyl substances

ABSTRACT: Background and Purpose: Polyfluoroalkyl substances (PFAS), like perfluorooctanoic acid (PFOA), are persistent environmental contaminants widely used in industrial and consumer applications. The eight-carbon PFAS, PFOA, is known for its strong bioaccumulation potential and extremely long half-life in environmental and biological systems. It has been linked to numerous toxic effects, including metabolic injury and genetic damage. Shorter-chain PFAS, like perfluoropentanoic acid (PFPA, five-carbon), are often perceived as less bioaccumulative and, therefore, safer alternatives. However, concerns remain about the environmental and health impacts of these shorter-chain alternatives. In Arizona, PFOA and PFPA have been detected in wastewater and biosolid waste streams, highlighting their environmental persistence and the significant need to understand the risks of legacy and short-chain PFAS species. **Methods:** In this study, we explored the impact of PFOA and PFPA on genomic integrity in human embryonic kidney cells (HEK 293T) exposed for 24 hours at environmentally relevant concentrations (0.02, 0.2, 2, and 20 parts per billion (ppb)). DNA damage was assessed using alkaline single-cell electrophoresis (comet assay). Olive Tail Moments (OTM) were calculated to quantify global DNA damage, incorporating comet tail length and DNA dispersion. The neutral comet assay is being conducted to further distinguish DNA damage types. OTMs in the neutral assay specifically indicate DNA double-strand breaks (DSBs), while alkaline OTMs reflect total DNA strand breaks, including single-strand breaks (SSBs) and alkali-labile sites converted to DSBs under alkaline conditions. **Results:** PFOA and PFPA exposure resulted in increased OTM across all concentrations compared to untreated controls. PFOA exposure caused an 8 to 12-fold increase in OTM, while PFPA resulted in a 7 to 13-fold increase, both statistically significant ($p < 0.05$, Kruskal-Wallis and Dunn's tests). Replicate experiments confirmed consistent response patterns. **Conclusions:** Environmentally relevant concentrations of PFOA or PFPA cause acute genotoxic effects *in vitro*, observable under alkaline comet conditions. These data support

the hypothesis that PFAS exposure potentiates DNA damage, and we will test our hypothesis in future experiments using the neutral comet assay. If DSB potentiation is a mechanism of toxicity, we anticipate reduced OTMs in the neutral assay, as SSBs and alkali-labile sites will not contribute to the comet tail under neutral conditions. Comparing alkaline and neutral assays will provide insight into the relative contributions of DSBs, SSBs, and alkali-labile sites, enhancing understanding of PFAS-induced genomic instability. These findings underscore the need for further molecular studies and regulatory consideration of PFAS exposure risks.

ABSTRACT NUMBER: 5192 **Poster Board Number:** LB293
TITLE: Investigation of Two Aneugenic Controls for CREST Micronucleus

AUTHORS (FIRST INITIAL, LAST NAME) AND INSTITUTIONS: S. W. Bruce[1], *S. Roy*[1], M. L. K. LaForce[1], S. D. Springer[1], K. S. K. Shore[1], W. Madraymootoo[1], T. Mortland[2], and C. Godin[2]. [1]Inotiv, Rockville, MD; and [2]Inotiv, Gaithersburg, MD.
KEYWORDS: Genetic Toxicology; Risk Assessment; Aneugen

ABSTRACT: Background and Purpose: As part of determining the mode of action for micronucleus induction in the *in vivo* micronucleus assay, there are a couple options for identifying the nature of micronuclei available per the testing guideline (TG474). The most used options include anti-kinetochore (CREST; Calcinosis, Raynaud's phenomenon, Esophageal motility abnormalities, Sclerodactyly and Telangiectasia) staining and fluorescence in situ hybridization (FISH) with pancentromeric probes. The FISH staining being used for studies with mice due to probe availability and anti-kinetochore (CREST) staining being used for studies with rats and mice due to ubiquitous nature. In this poster, we are investigating the use of two different aneugenic positive controls (Vincristine Sulfate and Colchicine) to determine the sensitivity and specificity of the detection for the purpose of creating a slide bank for use with anti-kinetochore (CREST) staining studies. **Methods:** Male Sprague Dawley rats (8-9 weeks old) were intraperitoneally administered Vincristine sulfate at 0.125 or 0.25 mg/kg or Colchicine at 2.0 or 3.0 mg/kg. The rats were administered the positive controls once. Bone marrow was collected 21 to 24 hours post administration. Smear slides were prepared for micronucleus evaluation prior to remaining bone marrow samples being enriched through a cellulose column for preparation of CREST micronucleus slides. The micronucleus slides were stained with acridine orange and scored using a fluorescence microscope. Each animal had 500 total erythrocytes evaluated for the proportion of polychromatic erythrocytes (PCEs) and 4000 polychromatic erythrocytes were evaluated for the incidence of micronuclei (MNPCE). Once the incidence of micronuclei was known, the CREST micronucleus slides for both aneugenic positive controls were stained using primary antibody (anti-nuclear antibody controls, centromere (ANA)), FITC-labelled secondary antibody (goat anti-human IgG), and propidium iodide/antifade and scored using a fluorescence microscope. At least 100 micronuclei were examined for anti-kinetochore staining for each dose group and at least 20 micronuclei per animal, when possible. **Results:** Significant increases in the incidence of micronuclei were observed with both doses of Vincristine sulfate in the micronucleus portion of the assay. A greater number of micronuclei were observed in the 0.25 mg/kg dose group than in the 0.125 mg/kg dose group. The incidence of kinetochore positive (K+) micronuclei was greater than 65% in the CREST micronucleus assay. Significant increases in the incidence of micronuclei were observed with both doses of Colchicine in the micronucleus portion of the assay. A greater number of micronuclei were observed in the 2.0 mg/kg dose group than in the 3.0 mg/kg dose group. The incidence of kinetochore positive (K+) micronuclei

was greater than 65% in the CREST micronucleus assay. **Conclusions:** Based on available literature, aneugens are geneally shows ≥65% MN with kinechore labeling (K+MN). In our study, both Vincristine sulfate and Colchicine induced micronuclei formation in the micronucleus assay and yielded an aneugenic signal in the anti-kinetochore (CREST) micronucleus assay in the line of available literature. This indicates the technique used in our laboratory was sensitive and specific to detect the micronucleus induced by aneugenic positive control evaluated in this study. Therefore, either positive control can be used for the creation of a positive control slide bank once a sufficiently titer dose level is obtained.

ABSTRACT NUMBER: 5193 **Poster Board Number:** LB294
TITLE: Development of an Automated High Throughput Comet Assay Device (AHTP-CAD)

AUTHORS (FIRST INITIAL, LAST NAME) AND INSTITUTIONS: *Y. Ji*[1], *N. Abdalla*[1], *J. Virzi*[1], A. D. Ramires Torres[1], C. Ross[2], and *M. S. Cooke*[1]. [1]University of South Florida, TAMPA, FL; and [2]Engineering Resources Group Inc, Pembroke Pines, FL.
KEYWORDS: Biomonitoring; Exposure Assessment; Genotoxicity; The comet assay

ABSTRACT: Background and Purpose: Single-cell gel electrophoresis (the comet assay) is one of the most widely used and highly sensitive methods to assess the genotoxicity in individual cells. However, the conventional comet assay has several limitations. It is labor-intensive and time-consuming, with the capacity to process only a limited number of samples per run. Additionally, the comet assay requires significant laboratory space to accommodate the necessary equipment, plus a skilled operator. To address these limitations, many high throughput comet methods, such as COMPAC-50 and CometChip, have been developed to minimize reagent use and assay duration with a concomitant higher number of samples. Even though there are many advantages to both methods, challenges persist. Issues such as potential operator variability, human errors, and other technical limitations remain, which can impact the accuracy and reproducibility of the results. These considerations highlight the need for continued development of the comet assay to improve the efficiency and reliability of the data. **Methods:** Our Automated High Throughput Comet Assay Device (AHTP-CAD) fully automates all stages from lysis to drying post-staining, complete with temperature control, together with a user-friendly design featuring functionality and performance. **Results:** Specifically, the platform possesses a digital screen enabling precise control of key parameters such as temperature, runtime, and overall assay workflow. This enhancement facilitates real-time monitoring and ensures reproducibility and reliability during comet assay process. Key innovations in AHTP-CAD include advanced temperature control systems within the electrophoresis process tank and buffer cooling tank. These systems significantly accelerate buffer cooling, ensuring efficient thermal management and process stability. These improvements enhanced ease of use, simplified workflow, increased efficiency, and offered more accurate assays, providing a more accessible and reliable comet assay processing. **Conclusions:** This automated device performs at least as well as our “manual” high throughput system, but with all the advantages of a fully “walkaway” device, such as a decreased need for human involvement and a decreased assay run time. Our automated device represents a valuable, high throughput approach for reliably assessing DNA damage with minimal operator involvement, particularly if combined with the automated analysis of comets.

ABSTRACT NUMBER: 5194 **Poster Board Number:** LB295
TITLE: Development of an optimized two-step SPE method for urinary nucleic acid adductomics

AUTHORS (FIRST INITIAL, LAST NAME) AND INSTITUTIONS: A. Keidel[1], *J. Virzi*[1], L. Deloso[1], C. Moller[1], D. Chaput[1], T. Evans-Nguyen[1], Y. Chang[2], *M. Chao*[2], *C. Hu*[2], and *M. S. Cooke*[1]. [1]University of South Florida, Tampa, FL; and [2]Taichung, Taiwan. Sponsor: M. Cooke, Society for Redox Biology and Medicine
KEYWORDS: DNA Adducts

ABSTRACT: Background and Purpose: The exposome represents the totality of endogenous and exogenous exposures across the lifespan. These exposures may result in DNA damage in the form of adducts, a key factor in the etiology of a variety of human diseases, including cancer. It is understood that adducts in the urine result from DNA repair and their subsequent excretion, making urine an ideal, non-invasive matrix in which to study the whole-body DNA adductome. **Methods:** However, measurement of adducts in urine presents challenges due to matrix interference, and the variety of the chemical nature across the spectrum of DNA adducts, which makes their "one-size-fits-all" extraction by solid phase extraction (SPE) challenging. Here, different types of SPE sorbents and their combination were evaluated for maximal recovery of DNA adducts in urine. **Results:** The SPE column combination of ENV+ in tandem with the PHE provided the best retention of a cocktail of 20 adduct standards. An untargeted high resolution mass spectrometry approach incorporating FeatureHunter software was used to demonstrate the ability of this SPE method to successfully recover endogenous urinary adducts beyond those represented in the standard cocktail. FeatureHunter identified an average of 500 adducts in mouse and human urine samples, of which isotopically labeled standards were used to identify a selection of the endogenous adducts and begin the characterization of the urinary adductome of mice and humans. **Conclusions:** We discovered that the number of DNA/RNA adducts recovered could be improved by using two SPE columns in tandem, allowing us to leverage different column adsorbent properties to retain the widest range of adducts. The combination of the ENV followed by the PHE cartridges provided the best adduct recoveries, resulting in a highly effective clean-up before urinary DNA adductomics.

ABSTRACT NUMBER: 5195 **Poster Board Number:** LB296
TITLE: Hemoglobin Adducts as Predictive Biomarkers for Nitro-PAH Exposure and Carcinogenic Risk

AUTHORS (FIRST INITIAL, LAST NAME) AND INSTITUTIONS: *C. F. Marques*[1], C. Mesaros[1], K. El Bayoumy[2], and *T. M. Penning*[1]. [1]Center of Excellence in Environmental Toxicology & Department of Systems Pharmacology and Translational Therapeutics, University of Pennsylvania Perelman School of Medicine, Philadelphia, PA; and [2]Department of Biochemistry & Molecular Biology, Penn State College of Medicine, Pennsylvania State University, Hershey, PA.
KEYWORDS: Biomarkers; Polycyclic Aromatic Hydrocarbons; Proteomics; Sulfonamide; 3-nitrobenzanthrone

ABSTRACT: Background and Purpose: Nitrated polycyclic aromatic hydrocarbons (NO_2–PAHs) are released in diesel engine exhaust (DEE), a major component of air pollution. DEE has been classified as a Group 1 carcinogen by the International Agency for Research on Cancer, and its levels in the environment are expected to rise due to climate change. Diesel fuel is widely used in trucks, trains, ships, mining, construction, and agriculture, which exposes workers to high levels of DEE and increases their risk of developing cancer and cardiovascular diseases. Among NO_2-PAHs, 1-nitropyrene (1-NP) and

3-nitrobenzanthrone (3-NBA) are classified as Group 2A or 2B carcinogens due to their mutagenic properties. To become mutagenic and tumorigenic, these compounds require metabolic activation through a 6-electron reduction of the nitro-group catalyzed by cytosolic nitroreductases (including aldo-keto reductases), producing a nitroso-intermediate. Nitroso moieties are highly reactive with cysteine residues and can form sulfinamide and sulfonamide adducts. The exposure to PAHs has been assessed using biomarkers. However, information about nitro-PAHs is scarce and based on urinary biomarkers, which are indirect measurements of non-carcinogenic metabolites. Our work intends to develop a new biomarker based on hemoglobin (HB) adducts with nitroso-PAHs intermediates. **Methods:** An initial in vitro approach was conducted to identify the formation of 3-nitrosobenzanthrone-HB adducts using bottom-up and top-down proteomics. These findings will be extended to other nitroarenes. A stable-isotope dilution methodology combined with liquid chromatography-mass spectrometry (SID-LC-MS) will be used to determine and quantify sulfinamide and sulfonamide adducts formed with HB in non-smokers exposed to varying levels of air pollution. **Results:** The top-down approach revealed the presence of a sulfinamide adduct (Δ259) on the HB alpha-chain, characterized by an increase in $[M+H]^+$ from *m/z* = 15126→15385. A sulfonamide adduct (Δ275) was also observed on the beta-chain with an increase in $[M+H]^+$ from *m/z* = 15865→16140. In the bottom-up approach, the analysis of tryptic peptides identified the presence of adducts in Cys93 and Cys112, with a mass shift in *m/z* =259.1 for the sulfinamide and *m/z* = 275.1 for the sulfonamide**. Conclusions:** The development of a direct biomarker for nitro-PAH exposure could serve as predictive tool for biomonitoring. This new biomarker may contribute to risk assessment and enhance early cancer screening and prevention efforts, particularly for individuals at high risk of exposure to nitroarenes.

ABSTRACT NUMBER: 5196 **Poster Board Number:** LB297
TITLE: Investigating DNA Repair Pathways and Substrates Using Urinary DNA Adductomics

AUTHORS (FIRST INITIAL, LAST NAME) AND INSTITUTIONS: *J. Virzi*[1], A. Keidel[1], *Y. Ji*[1], *Y. Chang*[2], *C. Hu*[2], *M. Chao*[2], and *M. Cooke*[1]. [1]University of South Florida, Tampa, FL; and [2]Chung Shan Medical University, Taichung City, Taiwan.
KEYWORDS: Biomarkers; DNA Adducts; DNA Repair

ABSTRACT: Background and Purpose: DNA damage is a seemingly inevitable consequence of both the internal cellular processes and the external environmental exposures that make up the human exposome. This damage is understood to contribute significantly to the risk of developing major diseases. Maintaining genomic integrity relies on DNA repair mechanisms, including base excision repair (BER), nucleotide excision repair (NER)—specifically global genome (GG-NER) and transcription-coupled (TC-NER), and the sanitization of dNTP pools. These pathways safeguard cellular function by preventing the accumulation of harmful lesions. After repair, DNA adducts are excreted in urine as the damaged nucleobases or 2'-deoxyribonucleosides, depending on the type of adduct and the specific repair pathway involved. To deepen our understanding of DNA adduct resolution, our study utilized a novel, non-invasive approach to assess total adduct burden, aiming to clarify substrates and repair pathways. **Methods:** We used five DNA repair-deficient mouse models to determine the pathways responsible for the presence of specific types of adducts in urine: C57 (repair proficient), $Aag^{-/-}$ (BER defect), $MTH1^{-/-}$ (defective dNTP pool sanitization), csb (TC-NER defect) and xpc (GG-NER defect). The mice were injected interpretationally with 750 mg/kg of a 1:1 molar solution of [$^{12}C_6$-]-benzene and [$^{13}C_6$]-benzene and then housed in metabolic cages to collect daily samples of urine. The mice were injected for seven days, and

observed for 14 days after until sacrifice. Urine samples were analyzed by LC-MS/MS for benzene metabolites, and by LC-HRMS for DNA adducts. **Results:** Our study showed that repair from benzene-associated damage and adducts appears 24 h after a one-time IP injection. Urinary concentrations of benzene metabolites, specifically trans, trans-muconic acid (tt-MA) and S-phenyl mercapturic acid (SPMA), increased significantly at day 1 and remained high until day 7, and then decreased to baseline on day 12, the same pattern was observed in Aag $^{-/-}$ mice. **Conclusions:** By using a mouse model exposed to benzene as an environmentally relevant toxin, our study showed that repair from benzene-associated adducts appear 24 h after a one-time IP injection. Through the comprehensive analysis of urinary biomarkers of benzene exposure (i.e., tt-MA and SPMA), and DNA adduct formation, we were able to successfully identify benzene specific adducts in urine along with kinetics of their formation and repair. These excretion patterns were linked to repair deficiencies in their respective mouse models, allowing for the determination of repair pathway substrates derived from benzene-induced damage. This approach will allow for identification of environmental stressors relevant to human populations.

ABSTRACT NUMBER: 5197 **Poster Board Number:** LB298

TITLE: Leveraging Biomarker Assessment for Target Prioritization for Success in Drug Programs

AUTHORS (FIRST INITIAL, LAST NAME) AND INSTITUTIONS: M. Mohsenin[1], D. Thomas[1], and S. Winter[2]. [1]Elsevier, NY, NY; and [2]Elsevier, Amsterdam, Netherlands. Sponsor: D. Thomas, International Society for the Study of Xenobiotics

KEYWORDS: Alternatives to Animal Testing; Biomarkers; Biological Modeling; Drug Discovery/Pharma/Risk Mitigation; binding, inhibition, positive regulation

ABSTRACT: Background and Purpose: Biomarkers play a critical role in providing invaluable insights into personalized medicine, early detection, and drug safety through exploring interactions in biological systems. Biomarker enabled drug discovery can help researchers identify relevant biological pathways linked to a disease, allowing optimization of drug programs by focusing on targets that are likely to lead to effective therapies. Additionally, biomarkers facilitate patient stratification, ensuring drug candidates are tested in suitable populations, which increases success rates in clinical trials. Researchers in discovery biology express concern about bias affecting literature searches. Elsevier's EmBiology provides deep biological evidence to support critical insights and decisions to enhance the efficiency of drug programs. Biological relationships can be explored to understand disease biology through targeted data supported by precedent data from publications and clinical trials. This tool is pivotal in determining the target focus for therapeutic intervention. **Methods:** EmBiology uses an AI-driven knowledge graph to map and visualize millions of biological relationships to help researchers uncover better pathways to discovery. EmBiology uses natural language processing (NLP) to extract content from millions of sources. This technology applies linguistics-based rules to identify and extract specific terms and interactions from literature, including *molecular entities or species* (genes, proteins, small molecules, multiple RNA species, and higher order structures like "complexes" and "functional classes"); *molecular interactions* ("binding," "inhibition," "positive regulation" and others. The entities are categorized by applying domain-specific ontologies created by life sciences experts. These extensive ontologies and dictionaries include comprehensive lists of synonyms for each entity, meaning researchers can search by the term you are most familiar with and retrieve a complete set of results for that term and all synonyms); and *contextual information* (used in experiment-organism, tissue/organ, or cell line). **Results:** The Machine Learning (ML) technology recognizes the structure of sentences and extracts relationship information in

raw form (subject-verb-object triples) and normalized form (domain-specific relations). This ensures the correct terms and relationships are harvested. These “semantic triplets” are then stored in the knowledge graph. A Sankey graph can be generated to view the exact location of the sentence describing the relationship, the number of article snippets in which the relationship was mentioned, as well as the other articles that include the relation before exporting the relevant data for further analysis on your bioinformatics tools. EmBiology data Is powered by over 150K+ clinical trials (clinicaltrials.gov), 36M+ abstracts, and over 9M+ full-text articles. **Conclusions:** Biomarkers are indispensable in drug discovery, bridging the gap between bench research and clinical application to fully illustrate the translational view of research and development. Understanding biological relationships via biomarkers can improve the precision, efficiency, and success rates of developing new therapies. By offering measurable indicators of biological processes, biomarkers help identify promising drug targets, guide preclinical and clinical studies, and predict therapeutic outcomes. EmBiology rapidly identifies biological relationships that may have otherwise been missed, clearing a path through vast amounts of research. The ability to search via relationships rather than keywords helps to avoid search and knowledge bias. Researchers can gain invaluable insight about cause-and-effect relationships in published experimental results, extracted from the full text of high-impact journals. This allows researchers to make more informed decisions in disease biology and bring effective and competitive therapies to the market faster.

ABSTRACT NUMBER: 5198 **Poster Board Number:** LB299

TITLE: Tissue-specific cfDNA methylation: A tool for detecting drug-induced testicular damage

AUTHORS (FIRST INITIAL, LAST NAME) AND INSTITUTIONS: N. Otani[1], D. Sasaki[1], *K. Omura*[2], A. Gore[3], J. Dang[3], Q. Liu[3], R. Liu[3], and H. Naraoka[1]. [1]Astellas Pharma Inc., Ibaraki, Japan; [2]Astellas Pharma Inc., South San Francisco, CA; and [3]Singlera Genomics Inc., La Jolla, CA.

KEYWORDS: Biomarkers; Testis; Toxicity; Acute; cell-free DNA, DNA methylation pattern analysis

ABSTRACT: Background and Purpose: DNA methylation patterns are known to exhibit tissue specificity. If tissue-specific methylation patterns can be detected as Cell-free DNA (cfDNA) in the blood, it has the potential to become highly specific biomarkers. In this study, we investigated the applicability of this methodology for detecting and assessing organ toxicity by exploring testicular toxicity biomarkers using Singlera's DNA methylation pattern analysis technology(1). **Methods:** Ethylene Glycol Monomethyl Ether (EGME), known to cause testicular damage, was administered to rats at four different doses (0, 50, 100, and 500 mg/day) for 3 different dosing periods (1, 5, and 10 days). The day after the final dose, bloods were obtained from rats for cfDNA collection, and the methylation score of plasma cell-free DNA was analyzed. Animals were euthanized at the same time as blood sampling and testes were collected for histopathology. **Results:** A single methylation score, which was calculated by integrating the analysis results of hundreds of testis specific methylation pattern regions, was used as a biomarker. As a result, methylation scores increased in the EGME treatment group compared to the control group in a treatment duration- and dose-dependent manner. Upon comparison with histopathological changes, the methylation score was able to sensitively detect organic changes of testicular toxicity. **Conclusions:** The above results suggest that DNA methylation pattern analysis technology for blood cfDNA may be able to detect testicular toxicity with high sensitivity. Reference: (1)Nature Genetics volume 49, pages635–642 (2017)

ABSTRACT NUMBER: 5199 **Poster Board Number:** LB300
TITLE: Preliminary Assessment on Agricultural Occupational Exposures in Relation to Acute Kidney Injury

AUTHORS (FIRST INITIAL, LAST NAME) AND INSTITUTIONS: C. E. Abuede, *L. C. Magaña*, O. E. Cruz, A. Early, and *N. López-Gálvez*. San Diego State University, San Diego, CA.
KEYWORDS: Biomarkers; Toxicity; Acute; Kidney; Agricultural Toxicity

ABSTRACT: Background and Purpose: Agricultural exposure studies often fail to include women over 40 and adverse health outcomes. Farmworkers are frequently exposed to pesticides, herbicides, and fungicides, which often lack disclosure of individual or highly toxic chemicals in their formulations. Combined exposure to pesticides, extreme heat, inadequate hydration, and prolonged exposure periods makes the kidneys vulnerable to acute injury, increasing the risk of chronic kidney disease. This study aims to assess the risk of acute kidney injury among Latina farmworkers by analyzing levels of several kidney injury biomarkers, including specific gravity and Lipocalin-2. **Methods:** Urine samples were collected from 80 participants—40 farmworkers and 40 non-farmworkers—all Latina women over 40 years old residing in Imperial County, California. The collection was facilitated by promotoras de la salud, or community health workers. A single urine sample was collected from each participant. Participants provided informed consent and answered several questionnaires, including a demographic survey, environmental exposures, and the PREPARE Screening Tool. Key urine analytes, including blood, specific gravity, and protein, were assessed using CLIA-approved dipsticks to identify potential kidney dysfunction. The kidney biomarker Lipocalin-2 expression was quantified using the Human Lipocalin-2/NGAL Enzyme-Linked Immunosorbent Assay (ELISA) Kit. **Results:** Farmworker women experienced more significant exposure to pesticides and extreme heat due to occupational factors than non-farmworker women. Initial findings indicate higher concentrations of specific gravity and protein in farmworkers than non-farmworkers. Elevated levels of Lipocalin-2 were measured, mostly among farmworkers. Elevated levels in non-farmworkers may suggest indirect pesticide exposure from the region's intensive agricultural activities. Lipocalin-2 levels can be elevated due to acute factors such as medication use, dehydration, and inflammation, all of which are indicative of acute kidney injury. **Conclusions:** The agricultural workforce is increasingly composed of women, predominantly Latinas. Substantiating evidence has shown differences in organ hormonal responses and metabolic panels based on sex. Female farmworkers face both acute and chronic exposure to occupational chemical hazards, often without awareness of the associated risks, which may contribute to adverse health outcomes such as dehydration and kidney damage. Since farming activities are continuously being linked to an increased risk of acute kidney injury, isolating by sex allows for necessary comparative risk analysis as well as contributing to the limited literature regarding Latina farmworker exposures. Future research should investigate additional urinary biomarkers of kidney function, such as IL-18 and KIM-1, to further elucidate exposure-related risks.

ABSTRACT NUMBER: 5200 **Poster Board Number:** LB301
TITLE: Lipid imbalance in brain extracellular vesicles after nitrogen mustard pulmonary exposure in rats

AUTHORS (FIRST INITIAL, LAST NAME) AND INSTITUTIONS: *S. M. Nicholson*, K. Patel, V. Sunil, *J. Laskin*, *A. Gow*, *A. Bernstein*, and *D. L. Laskin*. Rutgers University and Environmental and Occupational Health Sciences Institute, Piscataway, NJ.
KEYWORDS: Alkylating Agents; Biomarkers; Neurotoxicology; Nitrogen Mustard

ABSTRACT: Background and Purpose: Nitrogen mustard (NM) is an analog of the chemical warfare agent sulfur mustard; both are DNA alkylating agents capable of affecting the brain. NM targets neurons in vivo manifesting clinically as seizures, agitation, confusion, and long-term cognitive impairment, and structurally, as degeneration of neural cell nuclei, edema, and axonal degeneration. The etiology of neuropathological and neurobehavioral changes after NM exposure are unknown. We previously reported that NM causes lipid imbalance in the lung. Lipid imbalance is also a key feature of neurodegenerative diseases that affects behavior and cognition. Exosomes are small extracellular vesicles (EVs) arising from the endosomal-lysosomal pathway that participate in lipid transport. Defects in the endo-lysosomal pathway can contribute to neurological disorders. Tetraspanin protein CD63 or LAMP3 (lysosome-associated membrane protein 3) is an exosome-specific marker associated with the endosomal-lysosomal pathway that regulates cholesterol levels via sorting into exosomes as cargo. apolipoprotein E (APO)E colocalizes with CD63+ endosomes (precursors of exosomes) also playing a role in cholesterol transport. Acetylcholinesterase (AChE) is an exosome-specific marker that is altered by cholesterol. Herein, we investigated whether neurological impairment caused by NM is related to lipid imbalance as a consequence of disruption in lipid trafficking via the endosomal-lysosomal pathway. **Methods:** Male Wistar rats (~ 8 wk) were treated with NM (0.125 mg/kg) or PBS (n = 8 rats/group) via intratracheal instillation. Animals were euthanized 3, 7, 14, and 28 d after administration of (ketamine (80 mg/kg) and xylazine (8 mg/kg) via exsanguination. Intact brain tissue (cerebellum) was collected and brain EVs isolated following a method for spontaneous EVs-release involving 24 h incubation in serum-free suspension cultures in Neurobasal media supplemented with GlutaMAX and antibiotics/antimycotics. Brain EVs were enriched for small EVs by sequential centrifugation (removal of cellular debris and apoptotic bodies) and 0.2-mm syringe filtering. Brain EVs were purified by incubation (24 h) with precipitation solution, centrifugation, and column filtration. EV populations were characterized for expression of CD63 and AChE, total protein, cholesterol, and APOE. Nanoparticle tracking analysis (NTA) was used to assess EV size and concentration. **Results:** The average size of brain EVs after NM exposure was `53.0 (3 d), 134.8 (7 d), 147.6 (14 d), and 145.2 (28 d) nm which is within the range of small EVs (≤ 200 nm). NM had no effects on total protein levels or particle concentrations; purity analysis (particle concentration/total protein) showed EVs were of high purity. Increased CD63+ exosomes were observed at 3 d and 14 d post-NM, with no significant changes in APOE. A strong positive linear association ($p = 0.007$, $\beta = 4.360e\text{-}009$) between APOE and CD63+ exosomes was noted in PBS controls; this was not observed after NM ($p = 0.098$, $\beta = -2.594e\text{-}010$). Cholesterol concentrations increased at 3 d but decreased thereafter. At 14 d and 28 d post-NM, AChE+ exosomes were negatively associated with cholesterol ($p = 0.001$, $\beta = -1.36e\text{-}06$) in PBS controls, but positively associated ($p = 0.0003$, $\beta = 2.74e\text{-}06$) with cholesterol after NM; levels of AChE+ exosomes were also negatively associated ($p = 0.019$, $\beta = -34.28$) with CD63+ exosomes. **Conclusions:** NM respiratory exposure alters brain EVs, causing a loss in AChE activity and increases in CD63+ exosomes which transport cholesterol cargo. The secretion of CD63+ exosomes result in a compensatory increase in secretion of cholesterol, potentially to maintain cholesterol trafficking. Our AChE results affirm that cholesterol levels can alter AChE activity in the brain. These results suggest that NM induced neuropathology may be due to lipid imbalance through disruption of the endo-lysosomal pathway involving the generation of cholesterol carrying exosomes. Grant support: NIH AR055073, ES005022, Rutgers University Presidential Post-Doctoral Fellowship Program.

ABSTRACT NUMBER: 5201 **Poster Board Number:** LB302
TITLE: Nephrocardiac Effects of Chronic Microplastic and Arsenic Co-Exposure in a Rat Model

AUTHORS (FIRST INITIAL, LAST NAME) AND INSTITUTIONS: *R. M. Taylor*[1], *M. Garcia*[2], S. R. Gadam[1], L. V. Gonzalez Bosc[3], and J. T. Baca[1]. [1]Department of Emergency Medicine, The University of New Mexico, Albuquerque, NM; [2]Department of Pharmaceutical Sciences, University of New Mexico, Albuquerque, NM; and [3]Department of Cell Biology and Physiology, The University of New Mexico, Albuquerque, NM.
KEYWORDS: Environmental Toxicology; Exposure, Environmental; Exposure Assessment; Microplastic

ABSTRACT: Background and Purpose: Environmental exposure to microplastics (MPs) or arsenic (As) poses significant health risks, yet their combined toxicological effects remain poorly understood. MPs can act as vectors for toxicants like As, potentially exacerbating systemic and organ-specific damage. This study investigates the nephrocardiac effects of chronic co-exposure to MPs and As in rats, focusing on systemic retention, renal clearance, and organ function. **Methods:** Sprague-Dawley rats (n=6 per group; age and sex matched) were administered MPs (34-50 µm polyethylene microspheres: 500 µg/g and 1,000 µg/g dietary) and/or As (500 ppb in drinking water) over three months. Plasma and urine were collected at baseline (0 months), 1.5 months, and 3 months post-exposure. Dermal interstitial fluid (ISF) and organs were collected at the end. Renal function is being assessed via plasma creatinine to estimate glomerular filtration rate (eGFR). MPs in tissues are being quantified using Pyrolysis-Gas Chromatography Mass Spectrometry (Py-GCMS), while As levels and speciation will be measured using Inductively-coupled Plasma Mass Spectrometry (ICP-MS). **Results:** Although data analysis is ongoing, preliminary findings suggest that chronic MP and As exposure may result in systemic accumulation and organ-specific retention. Current assays focus on quantifying MPs in heart and kidney tissues, alongside plasma creatinine and As levels to establish foundational nephrocardiac function metrics. Expected outcomes include novel insights into how MP-As interactions influence renal clearance, inflammation, and cardiac health, providing a framework for interpreting systemic toxicity from environmental pollutants. **Conclusions:** This study employs innovative, minimally invasive techniques to investigate the systemic effects of chronic MP and As co-exposure. By integrating advanced analytical methods, we aim to establish a clearer understanding of nephrocardiac toxicological impacts. These findings will inform future studies on MP and As toxicity, advancing risk assessment models and mitigation strategies.

ABSTRACT NUMBER: 5202 **Poster Board Number:** LB303
TITLE: Metabolically Active Nuclear Receptor Reporter Assays: Enhancing Detection of Prodrug Activity with Hepatocyte Co-Cultures

AUTHORS (FIRST INITIAL, LAST NAME) AND INSTITUTIONS: S. Al Maalouf, N. Connolly, A. Woodman, and *J. P. Vanden Heuvel*. INDIGO Biosciences, State College, PA.
KEYWORDS: In Vitro and Alternatives; Receptor; Hepatocytes; Metabolites, prodrug, luciferase assays

ABSTRACT: Background and Purpose: Cell based reporter assay systems are valuable tools widely used to efficiently screen large numbers of candidate drugs, chemicals or environmental samples for biological activity such as toxicity and drug-drug interactions. However, when evaluating prodrugs which require metabolism for activation, additional assays, such as those using S9 liver microsomes, primary hepatocytes, or in vivo systems, are often utilized. Each of these methods presents its own challenges, and they can be cumbersome and cost-prohibitive during the in vitro screening stage. **Methods:** To address these limitations, we evaluated metabolically active nuclear receptor reporter cell systems that

offer better alignment with in vivo drug metabolism and activity. In this study, we assessed the performance of nuclear receptor luciferase reporter assays, such as PPARα and AhR, both alone and in co-culture with metabolically active liver cells. **Results:** Our results showed that PPARα reporter assays were unresponsive to fenofibrate when cultured alone; however, when co-cultured with metabolically active liver cells, fenofibrate metabolites successfully activated PPARα in the reporter co-culture cell system. Conversely, MeBio was metabolized in the AhR reporter cells co-cultured with liver cells, resulting in a less potent response in the presence of liver cells compared to the AhR reporter cells alone. **Conclusions:** These findings highlight the importance of evaluating metabolic activity in the in vitro drug screening process. The co-culture cell model used in this study provides direct evidence of metabolism without the challenges associated with S9 liver microsomes, or the availability of primary hepatocytes, offering a more efficient and cost-effective alternative for drug testing.

ABSTRACT NUMBER: 5203 **Poster Board Number:** LB304
TITLE: Enhanced insights into *in vitro* fenbendazole metabolism across species through feature-based molecular networking

AUTHORS (FIRST INITIAL, LAST NAME) AND INSTITUTIONS: J. Kim, Y. Jung, D. Lee, J. Cha, and H. Jo.
Yeungnam University, Gyeongsan, Korea, Republic of.
KEYWORDS: None

ABSTRACT: Background and Purpose: Fenbendazole (FBZ), an antiparasitic drug commonly used in veterinary medicine, has recently gained attention for its potential as an anti-cancer agent in humans. Despite its emerging applications, limited information exists on its metabolic pathways in humans, posing challenges to its safe and effective use. This study aims to comprehensively characterize FBZ-derived metabolites using feature-based molecular networking (FBMN), with a focus on cross-species metabolic comparisons. **Methods:** FBZ was incubated in liver microsomes from humans, dogs, and rats, as well as hepatocytes from humans, dogs, and monkeys, to investigate in vitro metabolism. Metabolic profiling was performed using liquid chromatography-high-resolution mass spectrometry in data-dependent MS^2 acquisition mode. FBMN was applied to optimally process spectral data, enabling systematic identification and visualization of FBZ metabolites across the tested species. **Results:** Nine FBZ metabolites were characterized, including seven oxidative metabolites (M1-M7) and two sulfate-conjugated metabolites (M2 sulfate and M7 sulfate). Species-specific differences in metabolic profiles were observed. In liver microsomes, oxidative metabolites (M1-M4) were relatively abundant in rats compared to humans and dogs. In hepatocytes, all metabolites except for hydrolyzed FBZ (M5) were more highly generated in monkeys than in other species. M5 was the predominant metabolite in both human liver microsome and hepatocyte incubates. Notably, integrative FBMN analysis enabled the identification of metabolites with high confidence, highlighting its utility for comparative metabolism studies. **Conclusions:** This study provides a comprehensive metabolic profile of FBZ and reveals significant interspecies differences in its biotransformation. By leveraging FBMN for enhanced metabolite characterization, the findings offer critical insights into the metabolism of FBZ, supporting its safe and rational therapeutic application in humans.

ABSTRACT NUMBER: 5204 **Poster Board Number:** LB305
TITLE: Application of physiology-based pharmacokinetics (PBPK) in predicting drug interactions between DMT and harmine in ayahuasca and synthetic drugs: evaluation of an overlooked risk

AUTHORS (FIRST INITIAL, LAST NAME) AND INSTITUTIONS: G. S. G. Ribeiro, B. A. B. Paranhos, F. Dörr, F. S. Martins, *P. Scharf*, and T. Marcourakis. University of São Paulo, São Paulo, Brazil.
KEYWORDS: Physiologically Based Pharmacokinetics; Pharmacokinetics; Neurotoxicology; Drug-drug-Interaction; Ayahuasca

ABSTRACT: Background and Purpose: Ayahuasca is a psychedelic beverage traditionally used in rituals and therapies by indigenous groups in the Amazon region. It contains N, N-dimethyltryptamine (DMT) and β-carbolines, such as harmine (HRM), which act as reversible inhibitors of monoamine oxidase A (MAO-A), allowing DMT absorption and distribution to the central nervous system. Fluoxetine (FL), widely prescribed for depression, is metabolized by CYP2D6 into its active metabolite norfluoxetine (NFL). Paroxetine (PR), another selective serotonin reuptake inhibitor commonly prescribed, also depends on CYP2D6 for its metabolism. The concomitant use of FL and PR with ayahuasca could theoretically cause serotonin syndrome, as both FL and PR are potent CYP2D6 inhibitors, an enzyme involved in the metabolism of HRM and DMT. This study aimed to develop PBPK models to analyze the pharmacokinetics (PK) of ayahuasca alkaloids in plasma and brain tissue to further investigate drug-drug interactions with FL and PR. **Methods:** The models were developed using PK-Sim® V11 based on *in vitro* parameters and clinical data observed in volunteers after oral and intravenous (IV) administration of ayahuasca, FL, and PR. Validation was performed using published PK data by visually inspecting plasma concentration-time graphs and comparing observed and predicted PK parameters. The mean fold error (MFE) was considered satisfactory when the predicted parameters were within twofold of the observed values. **Results:** MFE values for DMT ranged from 1.1 to 1.7 for AUC and from 0.84 to 1.1 for Cmax. For HRM, MFE values for AUC ranged from 1.18 to 1.5, and for Cmax from 0.79 to 1.1. FL showed MFE values ranging from 0.58 to 1.6 for AUC and from 0.72 to 1.7 for Cmax. Following oral administration of PR, MFE values ranged from 0.83 to 1.4 for AUC and from 0.69 to 0.8 for Cmax. After IV administration, PR's MFE values for AUC ranged from 0.83 to 1.62. Simulations of DMT plasma disposition before and after HRM inhibition indicated plasma AUC ratios of 1.67 and 2.92 for doses of 63 mg and 36.6 mg, respectively. For brain tissue, AUC ratios were 1.6 and 2.99 for the same doses. **Conclusions:** The PBPK models developed were effective in capturing the PK of all tested compounds, demonstrating their adequacy to predict DMT plasma and brain concentrations before and after MAO-A inhibition by HRM. Drug-drug interaction scenarios involving FL-HRM, FL-DMT, PR-HRM, and PR-DMT will be simulated to assess the extent of interactions caused by CYP2D6 inhibition, as HRM and DMT are substrates of this enzyme, while FL and PR have a high inhibitory capacity for the same enzyme.

ABSTRACT NUMBER: 5205 **Poster Board Number:** LB306
TITLE: Novel ABC and SLC transporter models for new drug testing

AUTHORS (FIRST INITIAL, LAST NAME) AND INSTITUTIONS: M. Ying, H. Liu, Y. Liu, and Q. Wang. IPHASE Bioscience, North Wales, PA. Sponsor: *W. Gao*
KEYWORDS: Metabolism; Xenobiotic Transporters; In Vitro and Alternatives

ABSTRACT: Background and Purpose: Studies using transporter models are essential for understanding the uptake and efflux of candidate compounds/drugs as well as detecting potential drug-drug

interactions (DDIs). Our research generates such models that encompass both ABC and SLC transporter family members, which can be utilized to identify substrates for specific transporters, and how candidate drugs influence the biosynthesis and function of transporters. **Methods:** The ABC transporters in this study adopted an “inside-out orientation” when expressed in either SF9 insect cells or 293T mammalian cells. Compared to the wild-type ABC transporters, the orientation change altered the direction of substrate movement, resulting the enrichment of substrates for subsequent detection. Then, the cells were fragmented into membrane bound vesicles with the transporter embedded. The uptake of substrates was measured via LC-MS after short periods of incubation. Regarding the SLC family members, the wild-type transporter allows substrates to accumulate inside the cells. In this study, the SLC transporters were transiently expressed in HEK293T cells, and substrate enrichment was tested as described above. **Results:** The generated ABC transporters included P-gp, BCRP, and BSEP. Those transporters on the membrane-bound vesicles were functional. Compared to the mock vesicles (vesicles without exogenous transporter), the enrichment of the substrates (probe) was increased significantly. Our data showed that after 5 minutes of incubation, vesicles containing P-gp transporter transported Talinolol at 7.5 times the rate of mock vesicles. Similarly, for BCRP, vesicles with this transporter increased the uptake rate of Dantrolene by 4.8 times. For the third member of the ABC family in our study, vesicles containing BSEP had an uptake ratio of 5 compared to control. The human SLC transporters expressed on 293T cells included OATP1B1, OATP1B3, OAT1, OAT3, OCT2, MATE1, and MATE2-K. Compared to mock-transfected cells, all SLC transporters exhibited significantly higher capability to transport probe substrates after short incubation (5mins). The functionality of OATP1B1, OATP1B3, or OAT3 transporters was tested using pravastatin and Estradiol-17β glucuronide. After the incubation, uptake of both drugs was 25 to 45 times the rate of cells with the mock. P-aminohippurate was used for OAT1 transporter test. Compared to mock, the level of P-aminohippurate in the cells was increased by 79 folds. When MATE1 and MATE2-K transporters were tested, the substrates TEA and metformin were taken up at a rate 15 to 35 times higher compared to the mock. Notably, the expression of transporters and substrate uptake did not compromise cell viability, with over 90% of cells surviving even after incubation with drugs. **Conclusions:** ABC transporters and SLC transporters generated in the study were fully functional. Our data demonstrated that transporters in the study efficiently moved the substrates after a short incubation period without compromising cell viability. The result indicates that our synthesized ABC and SLC transporters are suitable tools to identify transporter substrates and detect potential DDIs, especially those with low stability and high toxicity.

ABSTRACT NUMBER: 5206 **Poster Board Number:** LB307

TITLE: An Innovative *In Vitro* Approach to Cyanide Trapping of Reactive Metabolites While Controlling for Metabonate Formation

AUTHORS (FIRST INITIAL, LAST NAME) AND INSTITUTIONS: L. Albrecht, S. Roychowdhury, and K. Thomas. Eurofins Discovery Services North America, LLC., St. Charles, MO. Sponsor: *Y. Zhao*

KEYWORDS: Reactive Intermediate; Metabolism; Safety Evaluation

ABSTRACT: Background and Purpose: A leading cause of drug attrition, warnings and market withdrawals is drug mediated hepatotoxicity resulting from biotransformation. Biotransformation can result in covalent modification of DNA and cellular proteins causing drug-induced toxicities including mutagenicity, genotoxicity and idiosyncratic toxicity. Idiosyncratic toxicity may rely heavily on the formation of short-lived reactive metabolites which contain electrophilic groups that can covalently bind

to nucleophilic moieties in proteins to form toxic adducts. Drug conjugated proteins and peptides can lose functionality, accumulate or generate an active immune response. Reactive metabolite formation in drug candidates has potential for toxicity as well as adverse drug reactions including Drug-Drug Interactions (DDIs) and Drug Induced Liver Injury (DILI). Routine in-vitro metabolite identification has proven to be ineffective in capturing the entire spectrum of toxic metabolites as these metabolites may form quickly, have short half-life and covalently bind to protein or peptides. Given this scenario, a qualitative in-vitro cocktail method of various nucleophiles to evaluate broad formation of reactive metabolites was developed. The cocktail included glutathione, N-acetyl cysteine, semicarbazide and methoxyamine to assess soft electrophile formation as well as aldehyde reactives. Due to environmental, health and safety restrictions and company safety policies, potassium cyanide was not procured and included in the cocktail for evaluation of hard electrophile formation such as iminium ions. To ensure comprehensive coverage, an innovative solution, of which is the basis of this study, was developed to trap hard electrophiles. This was accomplished using hydrogen cyanide formation through CYP2E1 mediated metabolism of acetonitrile to cyanohydrin, which then spontaneously decomposes to hydrogen cyanide, formaldehyde and CO2. Furthermore, the method was developed to evaluate for false positive results and metabonate formation with inclusion of numerous control conditions, of which some are not previously reported in trapping protocols discussed in literature. Tris was incorporated to cross-link with formaldehyde and reduce possible methylations driven by Mannich reactions with formaldehyde and the drug molecule. These “Metabonates” are considered experimental artifacts and not true metabolites from enzymatic driven reactions. Taking into consideration that the preparation in human liver microsomes did not contain necessary cofactors for methylation to commence, detection of methylation reactions prior to cyanide adducting are non-enzymatically driven metabolites. **Methods:** Human liver microsomes are incubated with NADPH and a mixture of C13N15 labeled Acetonitrile and non-labeled acetonitrile for a total of 30 min to allow for Hydrogen Cyanide formation. Following initial incubation, liver microsomes in Tris buffer is added to the control conditions to aid in quenching the formaldehyde formation and replenish microsomal activity. Next, the test compounds at are added to the wells and NADPH is replenished. The entire solution is incubated for 60 minutes sampling timepoints at 0, 30 and 60 minutes to observe kinetics of formation and serve as a control. Clozapine and Ciprofloxacin, compounds known for clinical hepatoxicity and reactive metabolite formation, were used to demonstrate that the trapping of reactive metabolites is indeed through the metabolism of the labeled acetonitrile. Additionally, Ciprofloxacin is known for its ability to form metabonates in-vitro and was used to demonstrate the effectiveness of the control conditions including Tris. Additional control conditions included strategic combinations of no NADPH, DMSO, H2O, no Tris and no acetonitrile. Samples were acquired using ThermoFisher Orbitrap Exploris 120 and analyzed using FreeStyle and Compound Discoverer. **Results:** Analysis revealed successful incorporation of the labeled portion of acetonitrile adducted to expected reactive metabolites observed in literature for Clozapine and Ciprofloxacin. Ciprofloxacin samples with increasing concentrations of Tris revealed a dose response and successful reduction in metabonate formation of over 60% for some metabonates. This was accomplished while maintaining the same or similar detection signal for true enzymatic driven cyanide adducts or parent compound reactivity to cyanide. Optimal concentrations of Tris may further enhance this effect, especially in protocols utilizing KCN rather than the HCN generating system described here, this due to the constant generation of formaldehyde from the acetonitrile metabolism. The use of Tris may eliminate metabonate formation completely during standard trapping protocols using water as solvent, as the only formaldehyde present is endogenous levels remaining in the liver at time of collection. Ongoing experiments with other classes of compounds are in progress to optimize this

condition. **Conclusions:** This study demonstrated a simple, cost effective and safe way to perform cyanide trapping experiments without the use of potassium cyanide. Cyanide trapped reactive metabolites detected in early in drug development can alert to potential clinical toxicity and allow for these situations to be addressed early and often in drug discovery. This protocol also focuses on reducing false positives through incorporation of additional controls including Tris to evaluate for metabonate formation. In standard preparations, expert conclusions from reactive metabolite trapping experiments are needed to interpret results and decide whether the potential for toxicity exists based on possible mechanisms driving the detected metabolites. In the case of Ciprofloxacin, having no prior knowledge of human enzymatic driven drug metabolism could lead one to believe that the reported reactive metabolites could have meaningful implications, potentially moving to attrition or chemical manipulation. While early attrition is generally a goal in drug discovery, cases like this would call for unnecessary alerts to numerous reactive metabolites when only the parent reaction with cyanide is a true positive.

ABSTRACT NUMBER: 5207 **Poster Board Number:** LB308
TITLE: Insights into human toxicokinetics of data-poor bisphenol A analogs using physiologically based kinetic modeling

AUTHORS (FIRST INITIAL, LAST NAME) AND INSTITUTIONS: H. Bigonne, *S. J. Sturla*, and G. Aichinger. ETH Zürich, Zurich, Switzerland.
KEYWORDS: Alternatives to Animal Testing; Toxicokinetics; QSAR

ABSTRACT: Background and Purpose: Bisphenols (BP) AF, B, E, F, M, and S are increasingly used as BPA substitutes. Despite widespread exposure and potential adverse health outcomes, they are poorly understood in terms of toxicokinetics, i.e. their absorption, distribution, metabolism and excretion (ADME). **Methods:** We developed physiologically based kinetic (PBK) models for different human physiological standards to predict internal concentrations of prevalent bisphenols in organs of toxicological interest. To address the imbalances in available human data among these chemicals, we strictly refrained from read-across and used multimodal parameterization methods, including in vitro measurements of hepatic metabolism, computational prediction of gastrointestinal absorption and rat-human extrapolation of enterohepatic circulation (EHC). **Results:** The models were evaluated against available human toxicokinetic data for BPA and BPS, revealing that 83% of predicted Cmax, tmax and AUC values fell within a two-fold difference from in vivo measures. Using environmentally relevant exposure levels to compare internal levels of all tested bisphenols, we observed significant differences in toxicokinetic profiles. Concerning tissues of toxicological concern, BPS had the highest concentration in blood and testes, while BPM accumulated in the thyroid and BPAF in the breasts. **Conclusions:** Significant differences in toxicokinetics are a strong argument against the use of read-across for chemical risk assessment of data-poor bisphenols. The developed models are expected to facilitate a more precise evaluation of the hazard induced by BPA analogs, guiding their safer use.

ABSTRACT NUMBER: 5208 **Poster Board Number:** LB309
TITLE: Rodin: A Streamlined Metabolomics Data Analysis and Visualization Tool

AUTHORS (FIRST INITIAL, LAST NAME) AND INSTITUTIONS: B. Minasenko[1], D. Wang[1], P. Cirillo[2], N. Krigbaum[2], B. Cohn[2], J. Collins[1], *D. Jones*[1], and *X. Hu*[1]. [1]Emory University, Atlanta, GA; and [2]Public Health Institute, Berkeley, CA.

KEYWORDS: Bioinformatics; Metabolomics

ABSTRACT: Background and Purpose: Metabolomics is an emerging branch of omics aimed at studying metabolites in biological systems, with growing publications highlighting its value for diagnostics, biomarker discovery, and mechanistic insights. As data size and complexity expand, there is an urgent need for efficient, user-friendly tools that streamline big data analysis and accelerate discoveries. **Methods:** Rodin is implemented in Python using powerful libraries (NumPy, Pandas, SciPy, Statsmodels) for rapid processing and statistical modeling, while Django facilitates integration between the web interface and computational backend. A secure, AWS-hosted server environment handles session management and data storage, ensuring reliability and scalable performance. **Results:** When analyzing a dataset with 26,205 metabolomic features from mouse lung samples, Rodin completed the preprocessing, statistical testing, and pathway analysis in under two minutes. Compared to other software tools, it demonstrated superior speed, stability, and user-friendliness, largely due to minimal dependencies and its all-in-one design. Rodin allows downloading both significant and non-significant features, promoting comprehensive downstream analysis and reproducibility. The integrated pipeline for statistical testing, visualization, and pathway enrichment further reduces workflow fragmentation, enabling researchers of various computational skill levels to conduct advanced metabolomics studies efficiently. **Conclusions:** By consolidating multiple steps of metabolomics data analysis and visualization into a single platform, Rodin addresses the growing demand for accessible, high-throughput tools. Its streamlined, interactive interface accelerates discovery and enhances the reproducibility of results in metabolomics research.

ABSTRACT NUMBER: 5209 **Poster Board Number:** LB310

TITLE: Unsupervised Machine Learning-Based Read-Across Analysis Identifies Obesogenic Activity of the UV Filter Cinoxate

AUTHORS (FIRST INITIAL, LAST NAME) AND INSTITUTIONS: J. Gong, I. Park, S. An, S. Hwang, and M. Noh. Seoul National University, Seoul, Korea, Republic of. Sponsor: *D. Kim*

KEYWORDS: Computational Toxicology; Cinoxate

ABSTRACT: Background and Purpose: Environmental obesogens are exogenous substances that can disrupt metabolic processes and potentially lead to obesity. These effects are often mediated by nuclear hormone receptors (NRs), such as peroxisome proliferator-activated receptor γ (PPARγ). This study introduces a novel cheminformatics read-across approach, leveraging chemical fingerprinting and clustering methods to identify potential obesogenic compounds. **Methods:** A dataset of 8,435 Tox21 compounds was analyzed using principal component analysis (PCA) and t-distributed stochastic neighbor embedding (t-SNE) for dimensionality reduction of chemical fingerprints. Density-based spatial clustering and statistical tests were then applied to detect enriched clusters associated with specific NR activities. Experimental validation was performed through binding assays, adipogenesis experiments in human bone marrow-derived mesenchymal stem cells (hBM-MSCs), transcriptional analyses, and molecular docking. **Results:** Cheminformatics analysis identified a cluster selectively enriched for PPARγ agonist activity that prominently features methoxy cinnamate ultraviolet (UV) filters and obesogen-related compounds. Experimental validation demonstrated that cinoxate (CNX, 2-ethoxyethyl 4-methoxycinnamate) binds selectively to PPARγ (Ki = 18.0 μM) and induces an obesogenic phenotype in hBM-MSCs during adipogenic differentiation. Molecular docking and additional experiments confirmed that CNX acts as a potent PPARγ full agonist with a preference for recruiting the coactivator SRC3.

Conclusions: This study highlights the utility of cheminformatics read-across approaches for prioritizing potential obesogens. By employing this strategy, CNX, an organic UV filter, was identified as a PPARγ full agonist with significant obesogenic activity.

ABSTRACT NUMBER: 5210 **Poster Board Number:** LB311

TITLE: Use of Chemical Space Analysis to Advance Chemical Hazard Screening Relevant for United States Air Force Relevant Chemicals

AUTHORS (FIRST INITIAL, LAST NAME) AND INSTITUTIONS: *M. D. Nelms*[1], J. Abedini[1], B. Cook[1], *A. J. Keebaugh*[2,3], *T. R. Sterner*[2,4], and *R. A. Clewell*[2,5]. [1]RTI International, Durham, NC; [2]Air Force Research Laboratory, 711 HPW/RHBAF, Wright-Patterson AFB, OH; [3]BlueHalo, Dayton, OH; [4]Henry M. Jackson Foundation for the Advancement of Military Medicine, Wright-Patterson AFB, OH; and [5]Eagle Integrated Services, Inc., Wright-Patterson AFB, OH.

KEYWORDS: Computational Toxicology; Alternatives to Animal Testing

ABSTRACT: Background and Purpose: Regulatory agencies worldwide are increasingly committed to reducing and replacing the use of animals in chemical safety assessments through increased utilization of data from new approach methods (NAMs), including computational and in vitro models. This shift is motivated by the need for more human-relevant toxicological data and efficient chemical testing Adverse Outcome Pathways (AOPs) have emerged as a critical framework for integrating data from different NAMs and causally linking a molecular initiating event to adverse outcomes through a series of intermediate biological responses. AOPs offer insights essential for identifying informative non-animal testing methods, particularly when used alongside in vitro and computational approaches. The U.S. Air Force (USAF) is interested in leveraging NAMs, including quantitative structure-activity relationship (QSAR) models, to create a strategy for rapid toxicity screening. QSAR models predict the biological activity or toxicity of chemicals based on their molecular properties (e.g., structure), enabling rapid screening of large chemical libraries without the need for animal testing. We evaluated the utility of an existing QSAR model (Edwards et al., 2022) to identify the minimum set of in vitro tests needed to estimate acute oral toxicity of military-relevant chemicals. Chemical space mapping and ToxPrint descriptors were used to identify classes of chemicals that are either well or poorly addressed by the model. Eight case study chemicals with model-recommended assay endpoints tentatively linked to hepato- or neurotoxicity were further evaluated by comparing model-recommended endpoints to existing AOPs and published data. By integrating QSAR models, in vitro assays, and the AOP framework, the USAF aims to quickly identify novel chemicals that could pose health hazards/risks and recommend the most efficient test strategy for ensuring Force health protection and operational readiness.
Methods: Approximately 5,289 chemicals designated as USAF-relevant were collected from military exposure guidelines, emergency and occupational exposure guidelines, commonly used monitoring methods, compounds known to be present on USAF installations, and unpublished priority chemical lists. From this initial set of chemicals, we collected structure (QSAR-ready simplified molecular input line entry system [SMILES] strings) and physicochemical information, which were available for 5,289 chemicals. We used the structural information held within ToxPrint fingerprints to perform chemical space analyses comparing the chemical space of the USAF-relevant chemicals to those in the ATWG dataset. Subsequently, we used the QSAR model to assign a subset of these chemicals (n = 3,406) identified as being amenable to in vitro testing based on volatility and lipophilicity to one of 2,192 chemical clusters developed previously (Edwards et al., 2022) using ATWG chemicals. By mapping USAF-

relevant chemicals to these clusters, we could leverage the minimal ToxCast/Tox21 assay information associated with acute toxicity for each ATWG cluster to recommend high-throughput in vitro assay(s) in which to test the USAF chemical(s) described in the published analysis workflow. Eight chemicals were selected as case study compounds for further evaluation. Based on the model-recommended in vitro assays, these chemicals were assigned putative AOPs, which were then compared against existing in vivo and in vitro toxicity data. **Results:** We utilized several approaches, including the Uniform Manifold Approximation and Projection (UMAP) dimensionality reduction algorithm, to visually and quantitatively analyze the overlap between chemicals in the USAF and ATWG datasets. This enabled us to investigate the areas of chemical space where these datasets were similar and where they differed. Of 5,289 chemicals in the USAF-relevant dataset, 2,341 (~44%) were also present in the ATWG dataset. The Jaccard index overlap on the results from the UMAP algorithm also indicated a large overlap in the wider chemical space between the two datasets (Jaccard index overlap 52%). Whilst a large portion of the USAF-relevant chemical space is covered by the ATWG chemicals, we did identify several ToxPrint features that were unique or enriched in either the USAF-relevant or ATWG dataset. Of the ToxPrints present in at least three chemicals, 44 were either unique to or enriched in the USAF-relevant chemicals. These included features for several different polyaromatic hydrocarbons (e.g., anthracene), as well as aliphatic and aromatic azo-containing chemicals. Meanwhile, 86 ToxPrint features were either unique to or enriched in the ATWG chemicals; approximately half of these were different 4-, 5-, and 6-membered heterocyclic and heteroaromatic features. For the 8 case study chemicals, model-recommended assays were acetylcholinesterase (AChE; methomyl, aldicarb), adenosine 1 receptor (malathion), fatty acid binding protein (FABP1; diazinon), pregnane X receptor (PXR; tris(2chloroethyl) phosphate, tris(1,3-dichloro-2propyl) phosphate) and retinoid x receptor (RXR; chlorobenzene, 4-chlorobiphenyl). Existing AOPs link AChE with neurotoxicity and PXR and RXR with hepatotoxicity. No AOPs were found for adenosine 1 receptor or FABP1. In vivo chemical toxicity data available in the literature demonstrates organ toxicity consistent with each chemical's minimum assay-associated AOP for either hepato- or neurotoxicity. However, it should be noted that in vivo studies indicate that all the case study chemicals are both hepato- and neurotoxic. **Conclusions:** Our approach highlights the value of leveraging structural similarity to optimize testing strategies to facilitate the rapid toxicological assessment of novel chemicals. By using structural characteristics to group chemicals and integrating this with a previously developed bioactivity analysis workflow, this approach has potential to help limit the number of screening assays recommended for testing. Ongoing work is focused on testing the case study chemicals in AOP-relevant assays and evaluating the utility of the model across a broader chemical domain. The large overlap in chemical space observed between the USAF-relevant and ATWG datasets illustrates that, in general, the USAF-relevant chemicals are within the domain of applicability of the bioactivity analysis workflow. This enhances the confidence in assigning the USAF-relevant chemicals to the ATWG clusters. However, there were some local areas of USAF chemical space (represented by the unique/enriched ToxPrints) that were less well covered by the ATWG chemicals. These areas of structural space highlight gaps where targeted testing could be implemented to improve model coverage for USAF-relevant exposure and utility for novel chemicals. Case studies with specific chemicals also provide real-world examples of how in silico models can be used together with AOPs to support rapid assessment of chemical risk.-No DoD endorsement implied.

ABSTRACT NUMBER: 5211 **Poster Board Number:** LB312

TITLE: Two-step machine learning for automated quantification of zone-dependent hepatocellular hypertrophy in rat histology slides

AUTHORS (FIRST INITIAL, LAST NAME) AND INSTITUTIONS: *R. Wang*[1], C. Hendra[2], T. Jenkins[1], T. Forest[1], *R. J. Gonzalez*[1], and *F. Shah*[1]. [1]Merck & Co., Inc., West Point, PA; and [2]Merck & Co., Inc., Singapore, Singapore.

KEYWORDS: Computational Toxicology; Digital Pathology

ABSTRACT: Background and Purpose: Hepatocellular hypertrophy, the enlargement of hepatocytes often observed in rodent toxicity studies, is a critical finding with implications for adaptive responses, toxicity, and carcinogenicity. It is a common response to xenobiotics and has been associated with increased liver weight. However, accurate detection of hepatocellular hypertrophy, especially in mild cases, poses challenges for pathologists due to variations in hepatocyte sizes across different animal ages, sexes, and liver zones, complicating the identification and grading of its severity. Moreover, the subjectivity of pathological evaluation of hepatocellular hypertrophy introduces inconsistencies in assessments. Current commercial detectors for hypertrophy detection have struggled with accurately detecting hepatocellular hypertrophy in rats. The objective of this study is to develop a methodology for detecting rat hepatocellular hypertrophy with high sensitivity, thereby improving efficiency and reducing bias. **Methods:** We propose a two-step machine learning method, which includes automated liver vein segmentation and quantification of nuclei distance in rat liver histology images. This approach employs a U-Net model with a ResNet-50 backbone for vein segmentation, followed by an attention-based multi-instance learning model with a ResNet-18 backbone for classifying central veins and portal tracts. The methodology involves nuclei segmentation and distance calculations to quantify changes in hepatocyte size based on proximity to these veins in control versus treated rats in short-term toxicity studies. **Results:** 11 Whole Slide Images (WSIs) of male rat livers were used for the deep learning-based liver vein segmentation and classification to provide zonal information based on the location of central veins and portal tracts. Among these WSIs, 4 had non-remarkable findings, while 7 exhibited hypertrophy, necrosis, degeneration, and/or inflammation. In the first step, the vein segmentation method achieved over 70% overlap with the ground truth, and the classification method demonstrated high sensitivity and specificity in 5-fold cross-validation test sets. In the second step, the liver nuclei distance quantification demonstrated the capability to differentiate nuclei distances in control animals versus treated rats with liver hypertrophy findings. The difference in median hepatocyte nuclei distances in control animals was statistically significant between the two groups of animals. **Conclusions:** The two-step machine learning method, incorporating liver vein segmentation, enabled the quantification of hepatocyte size in relation to the distance from the portal tract and central vein, thereby enhancing the sensitivity of detecting hepatocyte hypertrophy. The nuclei distance quantification method facilitates direct comparison between control and treated animals, reducing bias and subjectivity in hypertrophy evaluation. This prototype algorithm sets the stage for exploring other lesion detection techniques within similar digital pathology workflows.

ABSTRACT NUMBER: 5212 **Poster Board Number:** LB313

TITLE: Extracting hepatotoxicity-related insights by expert-driven comprehensive analysis on animal toxicity data: Towards new approach methodologies-based risk assessment

AUTHORS (FIRST INITIAL, LAST NAME) AND INSTITUTIONS: *T. Yamada*[1], T. Maruyama-Komoda[1], K. Jojima[1], T. Kawamura[1], Y. Yamazoe[1,2], and K. Masumura[1]. [1]National Institute of Health Sciences Japan, Kawasaki, Japan; and [2]Tohoku University, Sendai, Japan.

KEYWORDS: Chemical Hazard Assessment; Computational Toxicology; Liver

ABSTRACT: Background and Purpose: While the regulatory risk assessment of chemical substances has largely relied on toxicity data from experimental animals, reducing animal testing is urgent due to the time, costs and animal welfare. We need robust methods to use data from cell-based or computational methods for improved risk assessment. New approach methodologies (NAMs) are promising, but selecting and combining appropriate NAMs for complex toxicity endpoints is challenging. The liver is a major target for xenobiotics. Hepatotoxicity is affected by liver distribution, reactive functional groups, and specific modes of action (MoA). Existing prediction tools for hepatotoxicity need accuracy improvement. This study aims to extract hepatotoxicity insights by analyzing physicochemical and ADME properties, structural features, MoA, and subchronic toxicity studies on food-related substances in rats to identify potential NAMs as screening indicators. **Methods:** We constructed a database with animal hepatotoxicity data from 90-day repeated dose toxicity studies of 213 substances, mainly pesticides, from the Food Safety Commission of Japan (FSCJ) reports. Physicochemical/ADME properties were calculated using ADMET predictor. Empirical ADME data were collected from FSCJ reports, FAO/WHO reports, and pesticide abstracts. Pesticide MoA data were collected using the Resistance Action Committee code and PubChem. Substances were classified into high-toxicity (H), low-toxicity (L), and intermediate groups based on LOEL values and hepatotoxicity severity. Criteria for LOEL were low (<30 mg/kg/d), medium (30-200 mg/kg/d), and high (>200 mg/kg/d). Severity criteria were severe (necrosis, bile duct findings, ALT elevation with histopathology), moderate (other histopathology), and mild (hematology, blood chemistry, liver weight changes). Substances with mild findings were excluded if the maximum dose was <100 mg/kg/day. 75 substances were classified as H and 68 as L. We explored factors related to hepatotoxicity, including liver exposure, chemical reactivity, and specific biomolecule interactions, using physicochemical properties, ADME, structural features, and MoA. A similar analysis was performed using 90-98-day subchronic toxicity data (250 substances) from ToxRef DB for validation. **Results:** We analyzed the relationship between physicochemical/ADME properties and hepatotoxicity. Hydrophobic substances need metabolism for excretion, while extremely hydrophobic substances accumulate in tissues. Substances with medium or greater MW need metabolism for excretion. Substances with logP 3-6 and MW>350 tended to be in the H group, likely retained in the liver. High logP and effective permeability (Peff) were associated with H group. Structural features related to hepatotoxicity included diphenyl ether, trihalogen-methyl group, and three or more halogens. Pesticides targeting molecules common to both target organisms and mammals, or important for liver function, were associated with hepatotoxicity. Mitochondrial and CYP inhibitors were significant. Using knowledge-based computational tools, Derek Nexus and VEGA, showed over half false-negative results, indicating difficulty in structural alert-based prediction. Our prediction model using logP/MW, logP/Peff, structural features, and MoA showed 69% sensitivity and 66% specificity. External validation with ToxRef data showed slightly different thresholds but relevant factors were extracted. **Conclusions:** We identified hepatotoxicity-associated properties: prolonged liver exposure (localization, accumulation,

metabolic persistence) and specific biomolecule interactions (targeting liver organelles/proteins). These findings will aid in selecting NAMs for improved hepatotoxicity assessment.

ABSTRACT NUMBER: 5213 **Poster Board Number:** LB314
TITLE: Development of an acyclic adverse outcome pathway (AOP) network based on the AOP-Wiki knowledgebase

AUTHORS (FIRST INITIAL, LAST NAME) AND INSTITUTIONS: S. Mukherjee[1], B. Gemler[1], P. Fullerton[1], J. Vasko[1], N. Winters[1], *S. Ito*[2], S. Hayashi[2], and K. Erami[2]. [1]Battelle, Columbus, OH; and [2]Japan Tobacco Inc., Yokohama, Japan.
KEYWORDS: Predictive Toxicology; Computational Toxicology; Adverse Outcome Pathway

ABSTRACT: Background and Purpose: The Adverse Outcome Pathway Wiki (AOP-Wiki) provides an open-source knowledgebase for researchers to share information on new AOP developments. These AOPs may then be networked together based on shared key events (KEs) and thus serve as a rich information source that may be utilized to make inferences about the effects of stressors across multiple AOPs. However, the open-source nature of AOP-Wiki makes it susceptible to inconsistencies such as duplicative key events, missing information, or errors making a straightforward rendering of an AOP network from the submitted AOPs extremely challenging. Additionally, unique KE IDs in AOP wiki are often associated with semantically-related KE descriptions. For example, both KE IDs 1364 and 1940 pertain to increase in reactive oxygen species. Furthermore, while AOPs are expected to be undirected, networking KEs across multiple AOPs may result in cycles which makes quantitation of the AOP network even more challenging. The purpose of this work was to (1) clean the KEs and associated metainformation in the AOP with a combination of manual annotation and semantic clustering and (2) construct a directed acyclic graph from the cleaned information by networking KE clusters across multiple AOPs, detecting cycles, and programmatically removing arcs to break the cycles without compromising the information content of the network. We believe that such a network will be useful in the future to assess quantitative risk across multiple stressors and multiple adverse events. **Methods:** Information on 1,341 KEs and their relationships across 460 AOPs was pulled from AOP-Wiki and filtered to retain AOPs with only mammalian and non-specified taxonomic applicability. Only KE relationships (KERs) that were annotated to be adjacent and of moderate or high confidence were kept. Missing or incorrect metadata, such as the KE action component or organ- or cell-level context was then corrected through both manual curation and machine learning methods. KE titles were then vectorized using scispaCy and embedded in a lower dimensional manifold using UMAP. These UMAP projections were then semantically clustered together within each level of biological organization (molecular, cellular, tissue, organ, individual, and population) using bisecting k-means clustering. To further refine the cluster composition, they were split based on curated metadata. Clusters were then stitched together to construct an AOP network based on the filtered KERs. The Eades, Lin, and Smyth algorithm was applied to the resulting feedback arc set to identify KERs responsible for cycles, which were then removed to produce a directed acyclic network. **Results:** Key event clusters ranged from one to six KEs in size. The resulting network was a directed acyclic graph that contained 649 KE clusters (nodes); 141 of which were molecular initiating events, 98 of which were adverse outcomes in at least one AOP, and 507 of which were simply key events, each connected by 852 KE relationships (edges). All cycles were eliminated by removal of only 35 unique KE relationships. The network thus obtained was then visualized using cytoscape. **Conclusions:** The above efforts organized KEs within AOP-Wiki into a

network of AOPs. For future applications, this graph can be synergistically integrated with data and knowledge bases and used for quantitative risk assessment via machine learning frameworks like the Bayesian Network analysis.

ABSTRACT NUMBER: 5214 **Poster Board Number:** LB315
TITLE: Multi-task Chemical Embeddings and Active Learning to Optimize Efficiency of Chemical Testing

AUTHORS (FIRST INITIAL, LAST NAME) AND INSTITUTIONS: N. J. Wichrowski[1], M. V. Clemens-Sewall[1], K. K. Rao[1], J. Y. Liu[1], C. L. Richardson[1], Y. Chushak[2,3], *T. R. Sterner*[2,3], and *R. A. Clewell*[2,4]. [1]The Johns Hopkins University Applied Physics Laboratory, Laurel, MD; [2]Air Force Research Laboratory (711HPW/RHBAF), Wright-Patterson AFB, OH; [3]Henry M. Jackson Foundation for the Advancement of Military Medicine, Wright-Patterson AFB, OH; and [4]Eagle Integrated Services, Wright-Patterson AFB, OH.
KEYWORDS: Computational Toxicology; QSAR; Chemical Hazard Assessment

ABSTRACT: Background and Purpose: The Air Force Research Laboratory (AFRL) is currently developing a suite of tools designed to rapidly and accurately predict health risks posed by acute chemical exposures to United States Air Force (USAF) personnel. The rise of machine learning (ML) methods powering quantitative structure-activity relationship (QSAR) models has enabled the data-driven development of predictive models for health effects screening. However, most QSAR-ML models described in published literature have limited utility for broad toxicological screening because they (i) are trained on a single endpoint, prioritizing marginal improvements in model accuracy for a specific task over generalizability to similar tasks, and (ii) rely on large, homogeneous training sets not readily available in toxicology. Thus, QSAR models are generally limited to only those endpoints where very large datasets exist, such as the Tox21 data. This current effort focuses on combining advanced ML in silico models with human cell in vitro methods to expand the utility of QSAR-ML to a broader number of toxicity endpoints, particularly those with suboptimal numbers of data points. Previously, we developed a novel ML pipeline based on a multi-task learning paradigm that improved prediction of endpoints with small-to-moderate datasets and allowed prediction of multiple disparate endpoints simultaneously. Here, we define and evaluate an optimization procedure for selecting small batches of untested chemicals to iteratively increase the predictive model's applicability domain based on new experimental results, while minimizing the number of necessary new in vitro tests—a process known as active learning. Ultimately, the goal of this work is to implement a practical strategy for toxicity screening of novel chemicals that maximizes the efficiency of chemical testing through model-informed data collection to support rapid risk assessment decisions for optimal force health protection. **Methods:** A novel ML pipeline was developed to produce a low-dimensional molecular representation scheme that preserves toxicological information useful for predicting multiple endpoints. The model is a directed message passing neural network (D-MPNN), trained on a curated subset of ToxCast (invitroDBv4.1 database) as stored in the EPA's CompTox Chemicals Dashboard. These data were generated from high-throughput assays run on large banks of chemicals, and the curated results include 2,098 assays and 6,388 unique chemicals. To ameliorate extensive and highly structured missingness in the available data, ML tasks were formed by aggregating assay results that correspond to the same biological target or subfamily of targets. Selection of which assays to include in an aggregated task was determined based on maximizing the total number of available data points while maintaining approximately equal numbers of active and inactive results. A multi-task D-MPNN was trained simultaneously on results for 12 such tasks and, as part of this process, learned a vector embedding (representation) for molecular

structures. This “chemical space” embedding was used as a starting point to train downstream models for tasks that lack sufficient data to develop a dedicated single-task model from scratch. For one such low-data task (representing solute carrier family 6A; SLC6A), an initial round of active learning was employed to improve model predictivity for chemicals of interest to the Air Force Research Laboratory (“military-relevant”). Given a list of military-relevant chemicals with no label available for SLC6A, a loss function was defined to quantify how useful a proposed batch of unlabeled chemicals would be if relevant experimental results were added to the downstream model’s training data. This loss function was optimized via the simulated annealing algorithm to produce a list of 10 chemicals that balance competing interests of expanding the model’s applicability domain, reducing model uncertainty on relevant compounds, and maintaining a relatively class-balanced dataset. These chemicals were then subjected to in vitro testing for the first step in an ongoing active learning approach to model development. **Results:** Model performance is quantified on the basis of test-set area under the curve (AUC) values for the receiver operating characteristic (ROC) curve. The multi-task D-MPNN used to define the molecular embedding scheme achieves a mean AUC across the 12 training tasks that is comparable to that of 12 analogous single-task models (0.72 vs 0.69, respectively). The embedding scheme itself more efficiently represents the relevant chemical space than other common molecular representations: the first 20 principal components capture 93% of the variance in representations computed via the chemical space embedding, compared to 33% for the same number of components based on an embedding defined by the Morgan fingerprint. Across 50 independently generated cross-validation splits of the available data, downstream models trained on the chemical space embedding statistically outperformed ($p < 0.0001$) models trained on single-task and fingerprint embeddings for at least 3 of 5 low-data tasks (tens to hundreds of available data points) not used for training the multi-task embedding. When selecting unlabeled chemicals for in vitro testing, the stochastic optimization procedure was repeated with 1000 random seeds to assess the stability of convergence. After 20,000 iterations for each seed, the median loss value was reduced from 1.507 to 0.744. After an additional 20,000 iterations, 665 of the 1000 optimizations had identified a (suspected) globally optimal list of chemicals with loss value 0.738, and all 1000 candidate lists yielded a loss value within 0.007 of this best observed value. A preliminary screen of the 10 proposed chemicals yielded negative (inactive) results, and confirmatory studies are in progress. **Conclusions:** The advantage of molecular representations from the proposed multi-task pipeline, over single-task models or fingerprint methods, is that the former combines information on multiple endpoints to provide a more generalizable model of chemical space. The proposed multi-task pipeline is robust against data scarcity, which often hinders high-quality single-task models, and offers a faster, lower-cost screening mechanism to precede in vitro testing in a tiered hazard identification capability. Combined with an active learning approach to strategically grow the available data for model training, this multi-task ML paradigm provides a promising path forward for extending the utility of computational methods to smaller datasets and less well-studied toxicological endpoints, and for expanding the range of hazards that can be identified early in a tiered screening effort, thereby improving the protection of occupational health and safety while minimizing the cost and time investment of toxicity testing. Disclaimer: No DoD endorsement implied.

ABSTRACT NUMBER: 5215 **Poster Board Number:** LB316
TITLE: A Machine Learning Approach for Predicting Inhalation Acute Toxicity (LC50) Values of Chemicals Using a Two-Stage Regression Model

AUTHORS (FIRST INITIAL, LAST NAME) AND INSTITUTIONS: *Y. Chen*[1], *K. Salazar*[1], *K. Mansouri*[2], and *N. Kleinstreuer*[2]. [1]U.S. Environmental Protection Agency, Washington, DC; and [2]National Institute of Environmental Health Sciences, Durham, NC.
KEYWORDS: Toxicity; Acute; Respiratory Toxicology; Computational Toxicology

ABSTRACT: Background and Purpose: Predicting the acute inhalation toxicity of chemicals, measured as median lethal concentration (LC_{50}) values, is key to assessing environmental and human health risks. Traditional *in vivo* methods are generally time-consuming or resource-intensive, thereby necessitating the development of predictive computational models to assess numerous chemicals. **Methods:** This study presents a machine learning-based two-stage regression model to predict acute inhalation LC_{50} values of chemicals in ppm and mg/L units. A database of 612 chemicals with experimentally measured 4-hr LC_{50} values served as the training set. Using the Python RDKit library, 210 molecular descriptors were calculated for each chemical, encompassing a wide range of physicochemical properties. In the first stage of model development, 15 machine learning algorithms were evaluated initially. With the Extra Trees algorithm yielding the best initial predictive performance, recursive feature elimination (RFE), data transformation optimization, and hyperparameter tuning were performed. A second-stage regression using a linear mode support vector regression (SVR) model was developed upon the first-stage model to enhance prediction accuracy further. **Results:** Two independent first-stage models were built to predict LC_{50} in ppm and mg/L units. The final models achieved an R^2 of 0.619 with a root-mean-square error (RMSE) of 0.873 for the ppm model and an R^2 of 0.538 with an RMSE of 0.904 for the mg/L model. A second stage model was built upon each first-stage model with a second data transformation. This two-stage approach improved the model's overall performance, achieving an R^2 of 0.902 with an RMSE of 0.377 for the ppm model and an R^2 of 0.917 with an RMSE of 0.332 for the mg/L model, significantly outperforming the single-stage model. **Conclusions:** The two-stage regression model demonstrates substantial improvements over traditional one-stage approaches, achieving both higher accuracy and efficiency in predicting LC_{50} values. This model offers a scalable and effective method with a suitable applicability domain for high-throughput toxicity screening. The integration of machine learning in predicting LC_{50} values has the potential to streamline toxicological assessments and reduce dependency on experimental testing, ultimately supporting regulatory and safety initiatives.

ABSTRACT NUMBER: 5216 **Poster Board Number:** LB317
TITLE: Integrating Machine Learning and Conformal Prediction: Quantitative Structure-Confidence-Activity Relationship (QSCAR) Framework for Refined *in vitro* Clastogenicity Predictions

AUTHORS (FIRST INITIAL, LAST NAME) AND INSTITUTIONS: *M. Shobair*, *E. Byrd*, *D. Onyango*, *S. Pfuhler*, L. Reinsalu, E. Rottinger, and *G. Daston*. Procter & Gamble, Mason, OH.
KEYWORDS: None

ABSTRACT: Background and Purpose: High-throughput screening (HTS) data in toxicology, while abundant, presents challenges for machine learning (ML) applications due to inherent experimental noise and biological complexity. The development of New Approach Methodologies (NAMs) for chemical hazard assessment requires not just predictions, but quantifiable measures of reliability and uncertainty.

Clastogenicity prediction remains particularly challenging, likely due to the variability of available *in vitro* clastogenicity data. **Methods:** We developed a Quantitative Structure-Confidence-Activity Relationship (QSCAR) framework that integrates conformal prediction with traditional machine learning approaches. This framework provides statistically rigorous uncertainty quantification and enhances prediction reliability through: 1) confidence-based prediction filtering, 2) probabilistic assessment of structural features' impact on prediction uncertainty, and 3) interpretable domain of applicability determination using SHapley Additive exPlanations (SHAP)-guided nearest neighbor analysis. The Vitic database was used for model building. 3108 and 11215 chemicals were used for modeling clastogenicity and mutagenicity, respectively. External validation was performed using a dataset curated by genotoxicity experts. **Results:** The QSCAR framework demonstrated significant precision enrichment across different confidence thresholds for both clastogenicity and mutagenicity predictions (p-value < 0.01). High-confidence predictions achieved 98% precision for mutagenicity predictions, compared to 57% for low-confidence predictions. Bayesian network analysis revealed carbon chain length as a key structural determinant of clastogenicity prediction reliability, with longer chains associated with more reliable non-clastogen predictions (probability = 0.85). The framework's interpretability module provided mechanistic insights through local chemical space analysis. **Conclusions:** The QSCAR framework advances NAMs development by providing a systematic approach to ML prediction uncertainty quantification and reliability assessment in computational toxicology. This work demonstrates how integrating modern ML techniques with confidence metrics improves the practical utility of in silico predictions for regulatory decision-making.

ABSTRACT NUMBER: 5217 **Poster Board Number:** LB318

TITLE: Machine learning analysis of hepatic and renal toxicity of nanoparticles in mice

AUTHORS (FIRST INITIAL, LAST NAME) AND INSTITUTIONS: *Q. Chen*[1,2], *K. Mi*[1,2], *W. Chou*[3], C. He[1,4], *N. A. Monteiro-Riviere*[5,6], *J. E. Riviere*[6,7], and *Z. Lin*[1,2]. [1]Department of Environmental and Global Health, University of Florida, Gainesville, FL; [2]Center for Environmental and Human Toxicology, University of Florida, Gainesville, FL; [3]Department of Environmental Sciences, University of California, Riverside, CA; [4]Department of Biostatistics, University of Florida, Gainesville, FL; [5]Nanotechnology Innovation Center of Kansas State, Kansas State University, Manhattan, KS; [6]Center for Chemical Toxicology Research and Pharmacokinetics, North Carolina State University, Raleigh, NC; and [7]1Data Consortium, Kansas State University, Olathe, KS.

KEYWORDS: Nanoparticles; Liver; Pharmacokinetics; Machine Learning, Kidney, Toxicity

ABSTRACT: Background and Purpose: A variety of nanoparticles (NPs) were designed as diagnostic agents to detect tumors or therapeutic agents to treat cancer. The *in vitro* cytotoxicity tests in target tumors or normal cells have been conducted to assess the biosafety of NPs. However, *in vivo* toxicity of NPs is less quantifiable, leading to uncertainty of NP biosafety. Existing studies suggest that liver and kidney are major target organs in NP biodistribution and toxicity. Therefore, this study was aimed to summarize the blood concentrations of biomarkers for liver and kidney toxicity in both tumor-bearing and healthy mice following NP treatments and develop a machine-learning model to predict the in vivo toxicity of NPs. **Methods:** We reviewed relevant studies between 2021-2024 and collected data on NP properties (e.g., materials, targeting strategy, and size), experimental designs (e.g., tumor model, cancer cell type, and dose), and toxicity biomarkers (alanine transaminase [ALT] and aspartate transaminase [AST] for hepatic toxicity; blood urea nitrogen [BUN] and creatinine [CREA] for renal toxicity). Subgroup

analyses were performed on toxicity biomarkers and machine-learning models were constructed to predict toxicity biomarker concentrations, including kernel ridge regression, random forest, light gradient-boosting machine, support vector machine, and deep neutral network models. **Results:** A total of 72 biochemistry studies were included in the analysis, yielding 417 toxicity datasets (157 for drug-loading NPs, 156 for the control groups, 84 for the groups of drugs alone, and 20 for others). Overall, the drug-loaded NPs increased the hepatic biomarker levels by 3.89% and 1.91% for ALT and AST, while reducing the kidney biomarker levels by 0.82% and 1.00% for BUN and CREA, respectively. In this database, 65 studies were conducted in tumor-bearing mice (378 datasets), while 7 were conducted in healthy mice (39 datasets). Compared with the biomarker changes in tumor-bearing mice, renal toxicity in healthy mice were greater (ALT: 3.87% *vs.* 6.82 %, $P = 0.78$; AST: 1.93% *vs.* 1.87%, $P = 0.85$; BUN: -1.74% *vs.* 6.45%, P = 0.07; CREA: -1.31 % *vs.* 5.31%, $P = 0.037$). In constructing the machine learning model, the results suggested that the kernel ridge model showed a better performance than other models ($R_{training}^2 = 0.98$, $RMSE_{training} = 1.57$, $R_{test}^2 = 0.33$, $RMSE_{test} = 0.31$). **Conclusions:** Most NP designs in our database slightly increased liver biomarker levels following drug-loaded NP treatment, while kidney biomarker levels remained minimally affected. Multiple physicochemical NP features and experimental settings significantly influenced NP toxicity. The developed machine-learning model provides a useful tool to predict liver and kidney toxicity.

ABSTRACT NUMBER: 5218 **Poster Board Number:** LB319
TITLE: Advancing QSAR Prediction Accuracy in Toxicology using Transfer Learning

AUTHORS (FIRST INITIAL, LAST NAME) AND INSTITUTIONS: *A. Hu*[1], *K. Q. Tanis*[2], R. Hao[2], *R. J. Gonzalez*[2], and *F. Shah*[2]. [1]Merck & Co., South San Francisco, CA; and [2]Merck & Co., West Point, PA.
KEYWORDS: None

ABSTRACT: Background and Purpose: Transfer learning (TL) is a widely applied technique in machine learning used across various datatypes. It enables the utilization of knowledge acquired from solving one problem to address distinct but related problems, and its significance is particularly evident in fields of toxicology where data availability is limited. The hierarchy of standardized preclinical toxicology processes is structured to generate progressively smaller datasets at each level, with each successive dataset generated in later stages of toxicity testing being considered more reliable. This creates a unique challenge for building QSAR models for *in vivo* toxicology albeit due to the limited availability of these data. We aim to demonstrate the applicability of transfer learning in the computational toxicology domain by leveraging different datasets from these varied stages of toxicity testing, allowing models trained on less expensive and more expansive *in vitro* data to enhance the prediction accuracy on more limited *in vivo* data. We hypothesize by pre-training a model on initial *in vitro* datasets and fine-tuning on the respective *in vivo* endpoints, the resulting model would outperform QSAR models built solely on *in vivo* data. **Methods:** We compiled data pairs from Merck *in vitro* and *in vivo* assays for nuclear receptor (NR) endpoints, including AhR, CAR, PXR, PPAR-alpha. These nuclear receptors play critical roles in toxicology as they mediate the body's response to xenobiotics. Rats and *in vitro rat* hepatocytes were exposed to diverse compounds, and transcriptional biomarkers of the activity of each nuclear receptor were measured. These in vivo and in vitro measurements were then used to classify compounds as "inducers" or "non-inducers" of each nuclear receptor. Transfer learning models were built using the *in vitro* transcriptional scores for these NRs and fine-tuned using *in vivo* NR data. Finally, TL models were benchmarked against commonly used QSAR ML models - Random Forest and XGBoost. Model

performance was assessed using R2 and Spearman's correlation, evaluated on a test set created through time-based splitting, with the most recently generated compounds included in the test set. **Results:** Our study shows that models pre-trained on in vitro transcriptional signature scores and fine-tuned on in vivo datasets can greatly outperform traditional QSAR approaches, including Random Forest and XGBoost, in predicting AHR, CAR and PXR activity, achieving an improvement in R2 exceeding 0.2. For PPAR-alpha, transfer learning and traditional machine learning models showed comparable performance. We believe this approach can be extended to other toxicological endpoints, even when working with relatively small datasets. **Conclusions:** We believe this approach can be extended to other toxicological endpoints, even when working with relatively small datasets.

ABSTRACT NUMBER: 5219 **Poster Board Number:** LB320

TITLE: A MultiFactor Approach for Early Risk Assessment of Innovative Advanced Materials: Safe-by-design Strategy for Multicomponent Nanomaterials

AUTHORS (FIRST INITIAL, LAST NAME) AND INSTITUTIONS: A. Mikolajczyk, D. Falkowski, and T. Puzyn. QSARLab/ University of Gdansk, Gdansk, Poland. Sponsor: A. Mikolajczyk, Society of Environmental Toxicology and Chemistry

KEYWORDS: Nanotechnology; Alternatives to Animal Testing; Computational Toxicology; Innovative Advanced Materials; nano-mixture metal oxides TiO2, ZnO and Ag + ions

ABSTRACT: Background and Purpose: Innovative Advanced Materials (IAMs), including nanomaterials, pose unique challenges in toxicity assessment due to their complexity and the interactive effects of their components. To date, no computational methodology has been capable of accurately predicting the joint effects of IAMs and nano-mixtures. This study introduces the MultiFactor Optimization Approach (MFOA), a groundbreaking computational framework specifically designed to fill this critical gap. Unlike existing methods, MFOA integrates dynamic experimental data and theoretical predictions, enabling the analysis of nonlinear interactions, including antagonism and synergy. By combining multiple toxicity indices—Sum of Toxic Units (STU), Additivity Index (AI), Mixture Toxicity Index (MTI), and Model Deviation Ratio (MDR)—with dose-response curve modeling, MFOA offers an unprecedented approach to joint effect prediction and comprehensive risk assessment. **Methods:** The MFOA methodology is innovative in its application of dose-response curve modeling and toxicity indexes, which directly compares model predictions with experimental data to reveal nonlinear interaction patterns often overlooked by traditional additivity models. The method is adaptable to various environmental and physiological conditions, ensuring its applicability across diverse IAM systems. Experimental validation, such as the observed synergistic effects between TiO2 and Ag+ ions linked to enhanced photocatalytic activity, underscores the model's capability to uncover complex interdependencies. This computational and empirical integration not only refines predictive accuracy but also elevates the robustness of safety evaluations for IAMs. **Results:** The application of MFOA to IAM nano-mixtures revealed groundbreaking insights. Antagonistic interactions were predominant, accounting for over 70% of observed joint effects. Synergistic effects were identified in approximately 15% of cases, most notably in mixtures containing TiO2 and Ag+ ions, where a 25% increase in toxicity was attributed to enhanced photocatalytic activity. The MDR index provided unique classifications in 10% of the mixtures, diverging from traditional indices and highlighting its capacity to detect nonlinear interactions. These findings validate MFOA as a robust and versatile framework for predicting joint toxicity, enabling more accurate risk assessments and refined regulatory evaluations. **Conclusions:** This study establishes MFOA as the first computational tool

capable of reliably predicting the joint effects of IAMs, marking a significant advancement in nanoinformatics. The findings demonstrate that antagonistic interactions dominate IAM nano-mixtures, with notable instances of synergy, providing novel insights into nanoparticle behavior and interaction mechanisms. By adhering to the principles of Safe and Sustainable by Design (SSbD), MFOA supports early-stage risk assessment and facilitates the development of safer nanomaterials. This methodology represents a transformative step in computational toxicology, bridging gaps in regulatory frameworks and fostering the sustainable design of environmentally friendly and biologically safe materials.

ABSTRACT NUMBER: 5220 **Poster Board Number:** LB321
TITLE: Large-scale machine learning analysis for nanoparticle-based antitumor therapy

AUTHORS (FIRST INITIAL, LAST NAME) AND INSTITUTIONS: *K. Mi*[1,2], *Q. Chen*[1,2], *W. Chou*[3], *C. He*[1,4], *N. A. Monteiro-Riviere*[5,6], *J. E. Riviere*[6,7], and *Z. Lin*[1,2]. [1]Department of Environmental and Global Health, University of Florida, Gainesville, FL; [2]Center for Environmental and Human Toxicology, University of Florida, Gainesville, FL; [3]Department of Environmental Sciences, University of California, Riverside, CA; [4]Department of Biostatistics, University of Florida, Gainesville, FL; [5]Nanotechnology Innovation Center of Kansas State, Kansas State University, Manhattan, KS; [6]Center for Chemical Toxicology Research and Pharmacokinetics, North Carolina State University, Raleigh, NC; and [7]1Data Consortium, Kansas State University, Olathe, KS.
KEYWORDS: Nanoparticles; QSAR; Pharmacokinetics; Antitumor therapy, Pharmacodynamics

ABSTRACT: Background and Purpose: Nanoparticle (NP)-based drug delivery systems hold great promise for cancer treatment by improving antitumor therapeutic effect and targeting release of drugs to tumors. However, designing efficient NP formulations for clinical usage remains a challenge due to the diverse properties of NPs coupled to variations across different cancer types. This study was designed to update the Nano-Tumor Database by incorporating data on NP-based anti-tumor therapy and apply it to machine learning (ML)/artificial intelligence (AI) to predict NP efficacy. **Methods:** The *in vivo* time-dependent tumor volume growth data for different NPs, along with NP physiochemical properties, tumor therapy strategies, and administration regimens, were collected from 369 studies published between 2021 and 2024. Various ML and AI algorithms, including classic models, kernel models, ensemble models, and neutral networks, were developed to predict the relative tumor growth inhibition (TGI, %) based on the collected features. Feature importance analysis was conducted to determine the contribution of each feature. **Results:** A total of 801 datasets, generating 6204 data points, were collected from the published papers. The median of TGI was 20.9% for drug-free NP formulations, 62.6% for single-drug loaded NPs, and 72.9% for combined-drug loaded NPs. The deep neural network (DNN) exhibited the best performance on TGI prediction, with a coefficient of determination (R^2) of 0.59 and a root mean squared error (RMSE) of 0.16 for the training set, and R^2 of 0.34 and RMSE of 0.22 for the test set. The use of assistive technologies, targeting strategy, and the type of drug-loading NP are the key features influencing TGI. **Conclusions:** This study significantly expands the Nano-Tumor Database, reports a new model to predict the anti-tumor efficacy of NPs, and provides a data source to build more advanced pharmacokinetic/pharmacodynamic models to facilitate clinical translation.

ABSTRACT NUMBER: 5221 **Poster Board Number:** LB322
TITLE: Inorganic arsenite represses human renal progenitor cell characteristics and induces neoplastic like transformation

AUTHORS (FIRST INITIAL, LAST NAME) AND INSTITUTIONS: *M. Haque*, S. Shrestha, *D. A. Sens*, and *S. H. Garrett*. University of North Dakota, Grand Forks, ND.
KEYWORDS: Kidney; Metals; Stem Cells

ABSTRACT: Background and Purpose: Arsenic, in the form of inorganic arsenite is toxic to the kidney and can cause acute kidney injury, manifesting as destruction of proximal tubule cells. Nephron repair is possible through the proliferation of resident tubular progenitor cells expressing CD133 and CD24 surface markers. **Methods:** We simulated regenerative repair in the continued presence of 4.5 µM i-As^{3+} using a cell culture model of a renal progenitor cell line expressing CD133 (PROM1) and CD24. Real-time quantitative PCR was used to determine gene expression changes and Western analysis was used to determine protein expression. **Results:** Continued exposure and sub-culturing of progenitor cells to arsenite led to a reduction in the expression of progenitor cell markers PROM1 and CD24 as well as a decrease in the ability of cells to differentiate into tubule-like structures. Cessation of arsenite exposure and recovery up to 3 passages resulted in continued repression of PROM1 expression and a reduction in the ability to differentiate. Chronically exposed cells exhibited an ability to form colonies in soft agar suggesting neoplastic transformation. They also exhibited an induction of CD44, a cell surface marker commonly found in renal cell carcinoma as well as in tubular repair in chronic renal injury such as in chronic kidney disease. **Conclusions:** These results demonstrate that long-term exposure to arsenite can affect the regenerative potential of renal progenitor cells as determined by the inability of the cells to differentiate and it can potentially induce neoplastic transformation of the cells.

ABSTRACT NUMBER: 5222 **Poster Board Number:** LB323
TITLE: Protein S-palmitoylation as key modulator of lung toxicity and inflammation in early RSV infection and cadmium exposure

AUTHORS (FIRST INITIAL, LAST NAME) AND INSTITUTIONS: *J. Jeon*, *C. Lee*, *Z. Jarrell*, *H. Lee*, *M. Orr*, *D. P. Jones*, and *Y. Go*. Emory University, Atlanta, GA.
KEYWORDS: Metals; Respiratory Toxicology; Metabolomics

ABSTRACT: Background and Purpose: Early-life exposure to respiratory pathogens and environmental toxicants significantly increases the risks of developing chronic respiratory diseases. Respiratory syncytial virus (RSV), a common respiratory pathogen that infects nearly all children by age two, is associated with higher susceptibility to chronic respiratory conditions later in life. Similarly, cadmium (Cd), a toxic metal commonly found in food and water, accumulates in the body over time and induces oxidative stress and inflammation. Our previous study showed a synergistic toxic effect of early-life RSV infection (eRSV) followed by cadmium (Cd) exposure on lung inflammation and fibrotic signaling, which is mediated by the involvement of protein S-palmitoylation (Pro-S-Pal), a lipid modification essential for regulating protein localization and stability. However, the specific molecular mechanisms and palmitoylated protein targets involved in inflammation are not fully understood. To address this gap in knowledge, we have focused on identifying the specific proteins undergoing palmitoylation and determining how these modifications influence key inflammatory processes. **Methods:** Female C57BL/6 mice (n=8 per group) were infected with RSV at postnatal day 14 to model early-life viral infection

(eRSV). After a 2-week recovery period, mice were exposed to Cd (3.3 mg $CdCl_2$/L) in drinking water for six weeks. A subset of these mice received 2-bromopalmitate (2-BP; 10 µM), an inhibitor of Pro-S-Pal to evaluate the mechanistic effect of palmitoylation. At the end of the experiment, lung tissues were collected and analyzed for Cd levels using inductively coupled plasma-mass spectrometry (ICP-MS), inflammatory cytokines and chemokines by ELISA, lung histopathology by H&E staining, metabolic profiling and pathways by liquid chromatography-high resolution mass spectrometry (HRM). HRM method relied on a dual platform: HILIC chromatography with positive electrospray ionization (HILIC-positive) and C18 reverse phase chromatography with negative electrospray ionization (C18-negative). Protein palmitoylation was profiled by using mass spectrometry-based palmitoylome proteomics. **Results:** Cd accumulation in lung tissue in both eRSV+Cd (0.014ng/mg) and eRSV+Cd+2-BP(0.011ng/mg) groups were significantly increased compared to controls (0.002 ng/mg, $p<0.05$).Inflammatory markers showed significantly elevated levels of IL-6 and TNF-alpha in eRSV+Cd group (IL-6: 45.54 pg/mL; TNF-α: 57.43 pg/mL; $p<0.05$), which were restored to control level by 2-BP treatment. Histopathological analysis aligned with these findings, as lung inflammation scores were significantly increased in eRSV+Cd but improved upon 2-BP treatment ($p<0.05$). Untargeted metabolomics identified a total of 9,495 and 4,317 features in HILIC-positive and C18-negative modes, of which 627 and 336 features, respectively, showing statistical significance ($p < 0.05$) among the control, eRSV+Cd, and eRSV+Cd+2-BP groups. Pathway enrichment analysis indicated significant disruptions in key metabolic pathways such as biopterin metabolism ($p = 0.0458$), glycolysis and gluconeogenesis ($p = 0.0020$), and purine metabolism ($p = 0.0364$), many of which were partially or fully restored upon 2-BP treatment. Palmitoylome proteomics showed that several proteins involved in inflammation and metabolic disruption were significantly palmitoylated by eRSV+Cd exposure while 2-BP treatment blocked palmitoylation of these proteins. Notably, palmitoylation of interleukin-17B (Il17b), xanthine oxidase, prostaglandin G/H synthase 1, carbonic anhydrase 3 and poly(A) polymerase gamma by eRSV+Cd, suggest important role for cytokines and lipid modification in driving lung inflammation, as well as purine metabolism, oxidative stress, and RNA processing. Collectively, these findings demonstrate that protein palmitoylation plays a key mechanistic role in the inflammatory and metabolic disturbances induced by eRSV+Cd, and that inhibiting this post-translational modification can mitigate pathological changes in the lung. **Conclusions:** This study shows that early-life RSV infection followed by Cd exposure induces significant lung inflammation and metabolic disruption through increased protein S-palmitoylation. Palmitoylome profiling identified palmitoylation targets, such as IL-17b, guanine deaminase, and xanthine oxidase, which may contribute to both inflammatory and metabolic regulation. Notably, 2-BP partially or fully restored normal cytokine levels, metabolite profiles, and improved lung pathology, highlighting the important mechanistic role for protein S-palmitoylation in RSV-Cd induced lung injury.

ABSTRACT NUMBER: 5223 **Poster Board Number:** LB324

TITLE: Quantifying the Metal Leachate Ratio in Tampons Under Simulated Physiological Conditions

AUTHORS (FIRST INITIAL, LAST NAME) AND INSTITUTIONS: H. McDavid, L. Gilster, D. Chen, and K. O'Malley. Georgetown University, Washington, DC. Sponsor: *A. Kadry*

KEYWORDS: Reproductive System; Metals; Toxicity; Chronic; Women's Health

ABSTRACT: Background and Purpose: Tampons, widely used menstrual products, remain underexplored regarding their metal content and leaching behavior under physiological conditions, raising potential health concerns due to intravaginal exposure. This study aimed to quantify total metal content in

tampons and assess the extent of metal leaching in simulated vaginal fluid (SVF), addressing critical knowledge gaps to inform consumer safety and regulatory policies. **Methods:** Eight tampon brands were analyzed for 27 metals using a two-phase approach. Total metal content was quantified through Microwave Acid Digestion (MAD) and Inductively Coupled Plasma Mass Spectrometry (ICP-MS). Leaching trials were conducted by incubating tampons in SVF at pH 4.2 and 4.57 for six hours at 37°C, with hourly sampling to evaluate metal release. Leachate ratios were calculated to assess bioavailability and potential exposure. **Results:** Detectable levels of metals, including lead (at 87.95 ng/g on average) and cadmium (at 183.1 ng/g on average), were observed across all samples. Most metals exhibited low leachate ratios (<0.01 for lead and cadmium), indicating limited mobility. However, calcium (with a 3.4 leachate ratio at pH 4.2) and vanadium (with a 1.76 leachate ratio at pH 4.2) demonstrated elevated leachate ratios, highlighting variability in leaching behavior. Significant differences were observed between brands, suggesting variability in material composition and manufacturing practices. **Conclusions:** This study reveals that tampons contain measurable levels of metals, some of which exhibit leaching potential under physiological conditions. While the low mobility of toxic metals like lead and cadmium is reassuring, the observed leaching of other metals raises concerns about cumulative exposure and bioavailability. This research provides a foundation for advancing understanding of menstrual product safety and developing policies prioritizing women's health.

ABSTRACT NUMBER: 5224 **Poster Board Number:** LB325

TITLE: Chronic Arsenic Exposure and hsa-miR-186 Overexpression Dysregulate Alternative Splicing in Human Keratinocytes, Promoting Carcinogenesis

AUTHORS (FIRST INITIAL, LAST NAME) AND INSTITUTIONS: *J. L. Scott*, *M. Banerjee*, A. Lykoudi, J. Y. Hwang, J. W. Park, and *J. C. States*. University of Louisville, Louisville, KY.

KEYWORDS: Metals; Carcinogenesis; Arsenic

ABSTRACT: Background and Purpose: Inorganic trivalent arsenic (iAs) is an established human carcinogen. Chronic environmental iAs exposure leads to several types of cancer, skin being one of the primary targets. Cutaneous squamous cell carcinoma (cSCC), an aggressive form of skin cancer, is often caused by environmental iAs exposure. iAs does not directly interact with DNA and thus causes cSCC without inducing characteristic point mutations. HaCaT cells are immortalized, benign, human keratinocytes used to model chronic iAs induced cSCC phenotype following 28-40 weeks of continuous exposure. We have used this model to demonstrate that chronic exposure to 100 nM iAs results in dysregulated mRNA and miRNA expression, alternative splicing, and protein degradation. hsa-miR-186 (mir-186) is induced in arsenic exposure associated cSCC tumors. The combination of miR-186 overexpression with chronic iAs exposure results in accelerated transformation of HaCaT cells. Dysregulated alternative splicing has recently been identified as a driver of carcinogenesis, but the impact of miR-186 overexpression individually and jointly with iAs exposure on alternative splicing is not well understood. **Methods:** HaCaT clones stably transfected with overexpressing miR-186 or scrambled control (SC) vectors were exposed to 0 or 100 nM iAs (up to 29 weeks) in independent triplicates, producing four experimental conditions: miR-186 + iAs, miR-186 - iAs, SC + iAs, SC - iAs. Short read RNA-seq was performed at 12 and 29-week time points. Differential alternative splicing events (FDR < 0.05 and $|\Delta\psi| \geq 5\%$) and differentially expressed genes ($p < 0.05$) were identified by replicate multivariate analysis of transcript splicing (rMATS) and unpaired t-test respectively. Gene ontology (GO) analysis was performed to identify overrepresented biological pathways populated by genes with differential

alternative splicing. We intersected the differential alternative splicing and the differential gene expression datasets to identify genes with simultaneous differential splicing and differential expression. Predicted dysregulated pathways were identified based on genes with concomitant differential splicing and differential expression, using ingenuity pathway analysis (IPA). **Results:** Over 1500 alternative splicing events were found in each of the six pairwise comparisons encompassing 5 major alternative splicing subtypes. miR-186 overexpression led to differential splicing of many splice regulators individually and jointly with iAs exposure. GO analysis showed that joint miR-186 overexpression and iAs exposure caused overrepresentation of many cancer-related biological pathways at each time point (regulation of DNA repair, DNA double strand break repair, sister chromatid segregation, cell division, cell death, and regulation of tRNA processing). More than 150 individual genes were both differentially expressed and differentially spliced for each pairwise comparison at each of the two timepoints. IPA analysis predicted dysregulation of several cancer related canonical pathways exclusively in the iAs exposed miR-186 overexpressing clones (extracellular matrix organization, actin cytoskeleton signaling, and integrin cell surface interactions). **Conclusions:** miR-186 overexpression and iAs exposure individually and jointly result in widespread dysregulation of alternative splicing and gene expression, impacting several pathways associated with carcinogenesis in a temporal manner. Many cancer-related pathways are enriched and functionally dysregulated exclusively by joint miR-186 overexpression and iAs exposure, explaining why the combination accelerates cSCC development. Long-term environmentally relevant arsenic exposure and mir-186 overexpression together and independently disrupt transcriptome wide alternative splicing modulating several cancer related pathways contributing to skin carcinogenesis. **Funding:** This research was funded by the National Institute of Environmental Health Sciences grants R01ES027778 (JCS) and P30ES030283 (JCS).

ABSTRACT NUMBER: 5225 **Poster Board Number:** LB326
TITLE: Potential Lead (Pb) Exposure in Preschool: A Public Health Concern

AUTHORS (FIRST INITIAL, LAST NAME) AND INSTITUTIONS: D. Dhakal[1,2], K. Shrestha[1], and S. Shakya[1]. [1]Tribhuvan University, Kathmandu, Nepal; and [2]National Society of Toxicology, Lalitpur, Nepal. Sponsor: *J. Manautou*
KEYWORDS: Acid digestion, lead exposure, school children; Pb - lead

ABSTRACT: Background and Purpose: Heavy metal - Lead (Pb) and its compounds are recognized as significant public health issues. Lead-loaded color paints remain one of the primary avenues through which children globally are exposed to lead. Even modest amounts of Pb exposure in young children can result in severe and irreversible neurological challenges, along with damage to vital organs. **Methods:** The research work was carried out at preschools in Kathmandu valley during 2016/017 and 2022/023, in which a stratified random sampling technique was used to collect the sample. The Pb was quantitatively analyzed using Flame Atomic Absorption Spectroscopy (FAAS) AA-7000, and then acid digestion using the EPA-3050B technique. **Results:** Despite the Government of Nepal setting a maximum lead limit of 90 ppm in paints in 2015, all samples (scraped from walls and furniture) collected from preschools in 2016/017 showed levels of lead exposure ranging from 112.6 ppm to 5053.4 ppm, with only a slight reduction observed between 109 ppm and 3406 ppm in 2022/023. Regarding lead-contaminated dust on school grounds (both indoor and outdoor), 60% of samples exhibited contamination levels between 40 ppm and 4010 ppm in 2017, while in 2022/023, all samples fell below 40 ppm. Additionally, 80% of the samples showed trace amounts of lead (15 ppm to 40 ppm), while 20% of the samples had levels

below 15 ppm in dust collected randomly from roadsides near the school locations. **Conclusions:** Overall, the weathering and chipping of lead-based paints can be identified as the main sources of lead exposure in school environments. It is widely acknowledged that there is no level of Pb exposure that can be considered safe for children. Therefore, it is advised that concerned authorities strengthen the existing rules and regulations regarding the use of lead-free paints in school premises.

ABSTRACT NUMBER: 5226 **Poster Board Number:** LB327
TITLE: *N*-acetyltransferase 2 phenotype impacts hexavalent chromium toxicity in human lung cells

AUTHORS (FIRST INITIAL, LAST NAME) AND INSTITUTIONS: A. Douglas[1], *I. Meaza*[2], Y. Qian[2], and *J. T. F. Wise*[1]. [1]Louisiana State University, Baton Rouge, LA; and [2]University of Louisville, Louisville, KY.
KEYWORDS: Metals; Cytotoxicity; Hexavalent Chromium; Hexavalent Chromium

ABSTRACT: Background and Purpose: Hexavalent chromium [Cr(VI)] is a well-established chemical carcinogen that is known to cause respiratory cancers, including lung cancer. It is well established that Cr(VI) is clastogenic and cytotoxic to human bronchial cells. However, the impact of genetic variability or single nucleotide polymorphisms (SNP) on the toxicity of Cr(VI) is unknown. *N*-acetyltransferase 2 (NAT2) is a polymorphic xenobiotic metabolism protein that is important for the genotoxicity and carcinogenicity of aromatic amines through its acetylation functionality. NAT2 is heavily impacted by SNP, resulting in slow, intermediate, and rapid acetylator phenotypes. NAT2 has been recently established to be functional in human bronchial epithelial and fibroblast cells. The objective of our study was to determine if NAT2 acetylator phenotypes impact the toxicity of Cr(VI) to primary human bronchial fibroblasts. **Methods:** We exposed primary human bronchial fibroblasts (with slow, intermediate, or rapid NAT2 alleles) to lead chromate or zinc chromate for 24 h (acute) or 120 h (prolonged) and measured the cytotoxicity of both chromate compounds using a colony formation assay and chemical ion uptake to normalize the data to total Cr inside the cells. **Results:** Both chromate compounds were cytotoxic to all three primary human bronchial fibroblasts at 24 h and 120 h. Interestingly, at 120 h of exposure, the bronchial fibroblasts expressing a rapid NAT2 acetylator were significantly more sensitive to chromate toxicity when compared to the bronchial fibroblasts expressing a slow NAT2 acetylator and cytotoxic impacts on the cells expressing an intermediate NAT2 acetylator were in between the rapid and slow in terms of cytotoxicity. **Conclusions:** Our results demonstrate NAT2 allelic variants (slow, intermediate, and rapid acetylator) are associated with a difference in Cr(VI) cytotoxicity. These data are important as they demonstrate how genetic variability in the population may impact Cr(VI) toxicity. Furthermore, these data indicate a need to understand how NAT2 is involved with Cr(VI) metabolism inside the cell. Future work is aimed at finishing the analysis of the clastogenicity of Cr(VI) with these NAT2 alleles and genotoxicity endpoints to determine if the impacts observed are limited to cytotoxicity or if these alleles are also associated with Cr(VI) genotoxicity and clastogenicity.
This work was supported by NIEHS grants R35ES032876 (John Pierce Wise Sr.) and USDA Hatch Projects (LAB94627 and LAB94629).

ABSTRACT NUMBER: 5227 **Poster Board Number:** LB328
TITLE: Inhibition of GLP-1 Receptor Signaling by Nickel

AUTHORS (FIRST INITIAL, LAST NAME) AND INSTITUTIONS: O. Chepurny, K. Dennehy, G. G. Holz, and *M. El Muayed*. SUNY Upstate Medical University, Syracuse, NY.
KEYWORDS: Metals; Endocrine Toxicology; Insulin, Diabetes Mellitus, Beta Cells; Nickel

ABSTRACT: Background and Purpose: Failure of insulin producing pancreatic islets in the setting of insulin resistance is the underlying cause for type 2 diabetes mellitus (T2DM). The cause of islet failure in T2DM is thought to be multifactorial, with genotype, lifestyle and environmental factors as main contributors. Insulin secreting β-cells within islets are unique in their high endowment of divalent metal transporters, necessary for achieving their exceptionally high content and turnover of zinc (Zn). We previously showed that nickel (Ni) is the non-essential metal with the highest concentration in human islets obtained from the general US population. The Glucagon-Like Peptide-1 Receptor (GLP-1R) is a G protein-coupled receptor (GPCR) that mediates enhanced insulin secretion from islets, promotes satiety as well as other actions in response to endogenously secreted GLP-1 following feeding and is therefore used as a therapeutic target for the treatment of T2DM and/or obesity. Previous work showed that divalent metals such as Zn and Ni can modulate the activation of G protein-coupled receptors (GPCRs) in either an inhibitory or enhancing fashion. We therefore examined the influence of Ni on activation of the GLP-1R. **Methods:** HEK293 cells stably expressing GLP-1R were infected with the cAMP FRET reporter H188 using an adenoviral vector. Cells were dissociated into a free-floating live cell suspension and transferred to 96 well plates. Cells were stimulated with the GLP-1 receptor agonist Exendin, Exendin + Ni (as $NiCl_2$), or negative control. H188 FRET signal was monitored using a 96 well plate reader for 300 seconds to record the intracellular cAMP increase in response to GLP-1. **Results:** The GLP-1R agonist exendin (0.1 nmol/L) resulted in a robust increase of cellular cAMP concentration -as previously reported. This response was inhibited in a dose dependent manner by Ni at concentrations of 10, 20, and 40 µmol/L, with the highest Ni concentration inhibiting exendin mediated GLP-1R stimulation by 80%. **Conclusions:** Ni from environmental exposure could potentially act as an inhibitor to GLP-1 signaling. Further research is needed to investigate environmental Ni exposure as a potential inhibitor of GLP-1R, which could have the potential to exacerbate the risk for T2DM.

ABSTRACT NUMBER: 5228 **Poster Board Number:** LB329
TITLE: Establishing a Guinea Pig Oropharyngeal Model for Particulate Hexavalent Chromium

AUTHORS (FIRST INITIAL, LAST NAME) AND INSTITUTIONS: *N. Butzke-Souza*[1,2], *I. Meaza*[1,2], *J. L. Wise*[1,2], *H. Lu*[1,2], *A. R. Williams*[1,2], *S. S. Wise*[1,2], *M. Delnicki*[1,2], J. Easley[1,2], *J. Kouokam*[1,2], *J. P. Wise, Jr.*[1,3], *S. T. Vielee*[1,3], *J. T. F. Wise*[1,4,5], *R. M. Wise*[1], and *J. P. Wise, Sr.*[1,2]. [1]Wise Laboratory of Environmental and Genetic Toxicology, Louisville, KY; [2]University of Louisville, Louisville, KY; [3]Pediatric Research Institute, Louisville, KY; [4]Wise Laboratory of Nutritional Toxicology and Metabolism, Baton Rouge, LA; and [5]School of Nutrition and Food Sciences, Baton Rouge, LA.
KEYWORDS: Guinea pigs; Hexavalent chromium

ABSTRACT: Background and Purpose: Hexavalent chromium [Cr(VI)] is an environmental chemical of concern due to its known carcinogenic potential in humans. Despite the serious health effects of Cr(VI) exposure, the mechanism of carcinogenesis is still unclear. To investigate the mechanism of Cr(VI) carcinogenesis, this study aimed to develop a more human relevant animal model. A major factor limiting translation of rodent Cr(VI) studies to human populations involves vitamin C, which can reduce carcinogenic Cr(VI) to noncarcinogenic Cr(III). Rats and mice, the commonly used rodent species for Cr(VI) studies, synthesize vitamin C in their liver. In contrast, humans cannot synthesize vitamin C and require it in their diet. Thus, rats and mice are likely more resistant to Cr(VI) than humans. Guinea pigs (*Cavia porcellus*), like humans, also do not produce vitamin C and require it through their diet. Further, mouse and rat lungs exhibit a monopodial branching pattern while human and guinea pig airways have a

dichotomous branching pattern. Given that particulate Cr(VI)-induced lung tumors occur at bifurcation sites, the branching pattern of the lung is another key consideration. Therefore, we developed an oropharyngeal aspiration model for particulate Cr(VI) in the guinea pig. **Methods:** Specifically, we exposed guinea pigs to particulate Cr(VI) for both subchronic (90 day) and acute (24 h) exposure. The representative particulate Cr(VI) compound used was zinc chromate, as it has been directly linked to lung cancer in exposed workers, and is a particulate, which is the most potent, carcinogenic form of Cr(VI). In total, 80 female and 80 male Hartley guinea pigs (10 of each per group per exposure time) were exposed via oropharyngeal aspiration to 0, 0.2, 0.4 and 0.8 mg/kg zinc chromate. Body weights were recorded weekly. At the end of the exposure time, animals were anesthetized with ketamine/xylazine, blood collected via the left ventricle, followed by perfusion with phosphate buffered saline through right ventricle. The organs were weighed and processed for metals analysis. To evaluate the concentrations of chromium and zinc in guinea pig lung, liver, and blood, tissue samples were digested with nitric acid and the metal levels measured using inductively coupled plasma mass spectrometry (ICP-MS). Chromium levels were measured to confirm that it reached the lung, and zinc levels measured to ensure no accumulation occurred. In the subchronic study, tibia lengths were measured and organ mass to tibia ratios were obtained by dividing the mass of each organ by the tibia length (which was measured with a digital Vernier caliper) to ensure the changes in the metal levels are not driven by organ weight changes. **Results:** Chromium concentrations increased in a dose-dependent manner in the lungs of guinea pigs in response to oropharyngeal exposure to zinc chromate. Liver and blood samples had comparatively less chromium. Zinc levels did not change in any of the tissues. Whole-body mass increased in exposed animals after the subchronic exposure; however, organ mass to tibia length ratios did not. **Conclusions:** Exposure to Cr(VI) is a human health concern due to its carcinogenic potential, yet the mechanism of carcinogenesis is unknown. We show oropharyngeal aspiration of particulate Cr(VI) results in chromium accumulation in the lung at levels higher than those detected in the liver and blood. Consistent with lung cell culture models indicating a lack of role for zinc, we also show zinc levels did not change in the lung despite using zinc chromate as our representative Cr(VI) compound. We also showed that organ weight to tibia ratios did not change. This study characterized a novel, more human-relevant animal model for Cr(VI) exposure that will allow future mechanistic studies to elucidate how Cr(VI) causes cancer. This work was supported by NIEHS grant R35ES032876 (JPWSr).

ABSTRACT NUMBER: 5229 **Poster Board Number:** LB330

TITLE: Indirect Oral Exposure as the Primary Determinant of Total Lead Exposure in a Proposition 65 Exposure Assessment of Kitchen Faucet Assembly Components

AUTHORS (FIRST INITIAL, LAST NAME) AND INSTITUTIONS: *J. Ator*. ToxServices LLC, Washington, DC.
KEYWORDS: Risk Assessment; Exposure Assessment; Metals; Lead

ABSTRACT: Background and Purpose: Analytical testing of residential-use kitchen faucet assembly components identified the presence of lead, which is included on California's Proposition 65 list of chemicals known to the State to cause cancer or reproductive toxicity. Lead is listed on Proposition 65 as a carcinogen, male and female reproductive toxicant, and developmental toxicant. We evaluated potential consumer exposure to lead measured in the faucet assembly components to determine if estimated exposure exceeds established Proposition 65 safe harbor levels and to assess health risks. **Methods:** ToxServices' exposure assessment was based on conservative laboratory measurements of total lead content utilizing acid/hot plate digestion of test samples followed by ICP-AES (ASTM E1479-

16). The exposure calculations followed risk assessment guidelines established in the California Code of Regulations (CCR), 27 CCR 25721 and 25821, and leveraged U.S. EPA and California Office of Environmental Health Hazard Assessment (OEHHA) methodologies for exposure assessment. For conservatism, ToxServices evaluated lead as a developmental toxicant, assuming exposure during pregnancy. We evaluated all relevant routes of exposure as required under CCR, including dermal exposure arising from direct contact with the evaluated components and arising from contact with water flowing through the evaluated components; indirect oral exposure arising from hand-to-mouth and hand-to-food-to-mouth transfer of lead following direct contact with the faucet components and also following contact with water flowing through the components; and ingestion of water flowing through the components. Route-specific exposure calculations were summed to obtain total daily exposure to lead, assuming only one faucet assembly is used in the home. **Results:** Total exposure to lead through use of the evaluated kitchen faucet components was less than California's developmental toxicity maximum allowable dose level (MADL) of 0.5 mcg/day. Unexpectedly, the primary determinant of total lead exposure was indirect oral exposure (hand-to-mouth transfer) following direct contact with the faucet components. This is likely due to the use of conservative default assumptions for parameters such as lead release rate, component-to-hand transfer efficiency, and hand-to-mouth transfer efficiency, in the absence of scenario-specific data for these variables. The other evaluated routes of exposure, dermal contact with the faucet components, dermal contact with water flowing through the components, and, in particular, ingestion of water flowing through the components, contributed minimally to total lead exposure. **Conclusions:** Based on ToxServices' exposure assessment, the evaluated faucet assembly components are exempted from Proposition 65 labeling for lead, and the lead present in the components does not pose a significant health concern for residential faucet users. This assessment highlights the importance of including all potential routes of exposure in an objective and comprehensive approach and not limiting an assessment to only those exposure routes assumed to be of greatest significance.

ABSTRACT NUMBER: 5230 **Poster Board Number:** LB331

TITLE: The Use of Single Cell Inductively Coupled Plasma Mass Spectrometry for the Characterization of Metal Uptake and Toxicity after Electronic Cigarette Exposure

AUTHORS (FIRST INITIAL, LAST NAME) AND INSTITUTIONS: *S. M. Alam El Din*, and A. Rule. Johns Hopkins Bloomberg School of Public Health, Baltimore, MD.

KEYWORDS: Metals; Inhalation Toxicology; Tobacco Products

ABSTRACT: Background and Purpose: The continued use of electronic cigarettes (e-cigs) among youth is a growing concern due to limited understanding of their potential health effects. Heavy metals, such as chromium (Cr), nickel (Ni), and lead (Pb), have been detected in e-cigarette aerosols. Studies have shown a positive correlation between Ni and Cr concentrations in e-cig aerosols and their levels in users' urine. However, the role of these metals in e-cig toxicity, as well as the mechanisms by which they transfer from aerosols to biofluids, remains poorly understood. This research aims to analyze and characterize metal uptake and toxicity following exposure to aerosols generated by popular e-cigarette devices. To accomplish this, a novel technique utilizing single-cell ICP-MS was employed. **Methods:** RAW and A549 cells were cultured in permeable cell culture inserts and exposed to e-cigarette aerosols using a VitroCell exposure chamber. Cells were exposed to 600, 300, 150, or 75 puffs of EBCREATE Blue Razz Ice. Each puff was defined as a 4-second inhalation followed by a 30-second rest. Media samples were

also collected post-exposure to confirm successful aerosol exposure. Following exposure, cells were fixed in 4% paraformaldehyde (PFA) for single-cell analysis or harvested and frozen for RT-qPCR and protein analysis.To validate the exposure, media samples were diluted 1:300 in 2% Optima HNO_3, metal content was analyzed using an Agilent 8900 ICP-MS, and data were processed using MassHunter 5.1. Cellular metal levels were quantified using an ESI MicroFast autosampler coupled with an Agilent 8900 ICP-MS operated in single-particle mode, with a dwell time of 0.1 seconds. Single-particle data were analyzed using SPCal. **Results:** Following exposure to 300 and 600 puffs, an increase in the number of A549 cells containing Zinc (Zn) was observed. Similarly, after 300 puffs, the number of RAW cells containing Ni increased. Furthermore, RAW cells exposed to 300 puffs exhibited a decrease in the expression of heme oxygenase (HO-1) and thioredoxin (TRX). In addition, levels of vascular endothelial growth factor (VEGF), glucose transporter type 1 (GLUT-1), and interleukin-1 beta (IL-1β) were also reduced after 300 puffs. **Conclusions:** These findings demonstrate that exposure to e-cigarette aerosols can lead to cellular uptake of metals such as Zn and Ni, with notable cell-type-specific differences. A549 cells exhibited increased Zn content after higher exposure levels, while RAW cells showed increased nickel content following only 300 puffs. These differences may be attributed to distinct mechanisms of metal uptake or variations in metal form (particulate versus ionic). Furthermore, the reduction in HO-1 and TRX expression in RAW cells, along with decreases in VEGF, GLUT-1, and IL-1β levels, suggests that e-cigarette aerosol exposure can disrupt critical cellular stress response pathways. Together, these results underscore the importance of further research to better understand the mechanism of uptake to better elucidate the toxicological effects of e-cigarette use and the role of metals in these processes.

ABSTRACT NUMBER: 5231 **Poster Board Number:** LB332

TITLE: Oxidative Biotransformation of 4-Alkoxyacetanilides by Peroxynitrite/CO_2: Formation of Ring Nitration Products Ortho to the Alkoxy Substituent(s)

AUTHORS (FIRST INITIAL, LAST NAME) AND INSTITUTIONS: *J. E. Hines*, C. J. Deere, O. A. Agu, and *R. M. Uppu*. Southern University and A&M College, Baton Rouge, LA.

KEYWORDS: Biotransformation; Mechanisms; Cytochrome P450; Cellular oxidants

ABSTRACT: Background and Purpose: 4-Alkoxyacetanilides (4-AAs), such as phenacetin [N-(4-ethoxyphenyl)acetamide], were among the first synthetic fever-reducing and non-opioid analgesics introduced in the early 1900s. While their phase I and II biotransformation pathways are well-documented, little is known about the nitrated or oxidized products formed through reactions with cellular oxidants like peroxynitrite (PN). Previous research has shown that 4-hydroxyacetanilide (commonly known as acetaminophen) produces nitrated and dimeric products under physiologically relevant conditions. We hypothesize that 4-AAs may undergo similar transformations, forming analogous or isomeric products. To explore these oxidative reactions and their potential molecular targets, we examined the reactions of PN with phenacetin, methacetin [N-(4-methoxyphenyl)acetamide], and 2-methylmethacetin [N-(4-methoxy-2-methylphenyl)acetamide] under physiologically relevant conditions. **Methods:** Peroxynitrite (PN) was synthesized by nitrosating hydroperoxide anion (HOO^-) with isoamyl nitrite (IAN) in a 50% (v/v) 2-propanol-water mixture (pH ≈12.5). Postprocessing removed unreacted H_2O_2, IAN, isoamyl alcohol, and 2-propanol, and the PN solutions were stored at -80 °C until use. Reactions of PN with methacetin, 2-methylmethacetin, and phenacetin were conducted at 25 ± 1 °C in 0.1 M phosphate buffer (pH 7.2) containing 0.2 mM diethylenetriaminepentaacetic acid and either 0 or 20 mM $NaHCO_3$. Products were analyzed using

reversed-phase HPLC (with or without solid-phase extraction), UV-Vis spectroscopy, and X-ray crystallography. Authentic samples of 2- and 3-nitromethacetin and 2- and 3-nitrophenacetin were synthesized by acetylation of 4-methoxy-2-nitroaniline, 4-methoxy-3-nitroaniline, 4-ethoxy-2-nitroaniline, and 4-ethoxy-3-nitroaniline. **Results:** Peroxynitrite (PN) was successfully synthesized using the IAN-alkaline H_2O_2 method. Initial yields were ≥90% (based on IAN), but postprocessing, which removed unreacted components (IAN, H_2O_2), 2-propanol, and isoamyl alcohol, reduced yields to 60-70%. PN synthesized has a broad absorption peak at 302 nm, lost upon decomposition along with redox properties. Reactions of PN, particularly in the presence of added carbonate, with methacetin, 2-methylmethacetin, and phenacetin produced low but significant oxidation yields (≤15 mol%), consistent with free radical-mediated mechanisms involving carbonate radicals ($CO_3^{\bullet -}$) and nitrogen dioxide ($^{\bullet}NO_2$). The primary product of these reactions was the 3-nitro isomer, formed via electrophilic aromatic nitration influenced by the electronic effects of methoxy (electron-donating) and acetamido (electron-withdrawing) groups on the phenyl ring. The 3-nitro isomers of methacetin and phenacetin exhibited identical UV-Vis spectra but distinct retention times on RP-HPLC, confirming structural differences. In contrast, the 2-nitro isomers, which were not produced in measurable yields during PN/CO_2 reactions but were synthesized for structural comparison, displayed distinctly different UV-Vis absorption spectra from the 3-nitro isomers formed in PN/CO_2 reactions. Structural confirmation of these isomers was achieved with high reliability using single-crystal X-ray diffraction. **Conclusions:** This study presents the first demonstration of the nitration of 4-alkoxyacetanilides by peroxynitrite under physiologically relevant conditions of pH and carbonate species. The low yields of oxidation and/or nitration are consistent with free radical-mediated mechanisms. The primary product of these reactions is 3-nitro isomer, formed preferentially over the 2-nitro isomer due to the electronic effects of the electron-donating methoxy group and the electron-withdrawing acetamido group on the phenyl ring. These findings align with the mechanism of electrophilic aromatic nitration.

ABSTRACT NUMBER: 5232 **Poster Board Number:** LB333
TITLE: Exploring the Internal Exposome: Oxidative Stress-Induced DNA and RNA Damage in Response to External Exposures

AUTHORS (FIRST INITIAL, LAST NAME) AND INSTITUTIONS: A. Bryant-Friedrich, N. V. Adiele, E. Asamoah, N. Yonis, and M. Bedi. Wayne State University, Detroit, MI. Sponsor: *H. Moustakas*
KEYWORDS: Oxidative Injury; Biomarkers; Chemical Characterization

ABSTRACT: Background and Purpose: The exposome is the totality of exposures an individual experiences throughout their lifetime, including environmental, socioeconomic, lifestyle, dietary, and genetic factors. It provides a framework for exploring exposure-disease links and understanding gene-environment interactions in developing, treating, and preventing complex diseases. The exposome can be divided into general, specific, and internal exposomes. Oxidative stress, an imbalance in reactive oxygen and nitrogen species, is an integral part of many deleterious internal processes and instigated by external exposures, contributing to oxidative damage to nucleic acids. Products of oxidative damage to nucleic acids include various DNA and RNA damage products. Previous studies from our lab identified some of these damage products and highlighted the potential roles of these compounds in oxidative stress. **Methods:** In this study, we aim to investigate the roles of DNA and RNA damage products in oxidative stress. Three damage products were synthesized and characterized using liquid chromatography-mass spectrometry (LC-MS) and nuclear magnetic resonance spectroscopy (NMR). The

synthesized damage products will be tested with nucleophilic amino acids and peptides, such as lysine, cysteine, and glutathione, to assess the formation of covalent adducts. These adducts will be identified using LC-MS and NMR. **Results:** NMR analysis confirmed the successful synthesis of the DNA and RNA damage products of interest, which was further validated using MS. Similarly, the formation of covalent adducts with our synthesized compounds will be confirmed using NMR and LC-MS. **Conclusions:** The successful synthesis of DNA and RNA damage products was confirmed, and ongoing analyses are underway to confirm their interactions with nucleophilic biological molecules, shedding light on their potential roles in oxidative stress and the internal exposome.

ABSTRACT NUMBER: 5233 **Poster Board Number:** LB334

TITLE: The *N*^{6}-methyladenosine mRNA Epitranscriptomic Pathway Drives Microglia-Induced Neuroinflammation in Neurotoxicity Models of Environmentally Linked Parkinsonism

AUTHORS (FIRST INITIAL, LAST NAME) AND INSTITUTIONS: *C. D. Miller*[1,2,3], A. Ealy[4], A. Gregory[1,3], W. Albers[1,5,3], H. Jin[1,3], G. Zenitsky[1,3], *A. Kanthasamy*[1,3], and *A. Kanthasamy*[1,3,2,5]. [1]University of Georgia, Athens, GA; [2]Department of Biochemistry and Molecular Biology, Athens, GA; [3]Isakson Center for Neurological Disease Research, Athens, GA; [4]Cleveland Clinic, Cleveland, OH; and [5]Department of Biology, Athens, GA.

KEYWORDS: Neurotoxicity; Metals; Aging; Glia; Epitranscriptomics; Manganese

ABSTRACT: Background and Purpose: Parkinson's disease (PD) and other mixed etiology dementias (MEDs) can be characterized by the accumulation of pathological α-synuclein (αSyn) in the basal ganglia (BG), including the substantia nigra (SN). The highest non-genetic risk factor for PD is aging, followed by exposure to certain environmental chemicals, including the heavy metal manganese (Mn) and the pesticide paraquat (PQ). These neurotoxicants directly affect glial cell populations, ensuing chronic neuroinflammation and progressive neurodegeneration. Emerging epitranscriptomic research reveals that N6-methyladenosine (m6A), the most abundant RNA modification in eukaryotic cells, plays a crucial role in regulating proinflammatory processes in many diseases. However, how m6A regulates microglial-driven neuroinflammation relates to PD and MEDs is completely unknown. To this end, we premise that dysregulation in the m6A pathway may promote neuroinflammatory processes observed in environmentally induced Parkinsonism and pathological αSyn-mediated synucleinopathies. **Methods:** In in vitro studies, we exposed C20 human microglial cells (HMGs) to LPS (1µg/mL), Mn (100µM), PQ (100µM), or αSyn fibrils (αSynf, 1µM). METTL3 knockdown (KD) was achieved utilizing siRNA against METTL3. For in vivo studies, mice were given saline or Mn (0.4 g/L)-containing drinking water for 30d. Alternatively, mice were injected with PBS or 5µg αSynf via stereotaxic surgery and aged for 60d. Human post-mortem PD and MED tissue was obtained from the University of California (UC) Davis Alzheimer's Disease Center and the Brain Endowment Bank at the Miller School of Medine, University of Miami. **Results:** Herein, we observed that Mn, PQ and αSynf but not LPS significantly upregulated the expression of the m6A writer METTL3 at 12 but not 6 or 24-h post exposure. The expression of the m6A reader protein YTHDF1 was significantly increased post 24-h LPS, Mn, and PQ exposure, whereas αSynf exposure led to a significant decrease in YTHDF1 expression at the same time point. Strikingly, METTL3 was significantly localized to cytoplasm at 12-h Mn but 12-h Pq and αSynf exposure induced nuclear localization. YTHDF1 was significantly nuclear in Mn exposure but was primarily cytoplasmic following αSynf exposure. Both Mn and αSynf exposure led to a significant increase in m6A mRNA modifications. qRT-PCR analysis of m6A modified proinflammatory cytokines revealed METTL3 Knockdown abolished

the increase in IL-1α, IL-6, and TNFα observed during Mn-mediated microglial activation and TNFα during αSynf-mediated activation. Corroborating in vitro results, striatal METTL3 was significantly increased and shifted to cytoplasmic in Mn-exposed mice compared to controls. On the contrary, METTL3 was significantly increased and localized to the nucleus, while YTHDF1 expression was significantly decreased and cytoplasmic in the STR of αSynf- compared to saline-injected mice. Finally, METTL3 was significantly increased while YTHDF1 was significantly decreased in AD and DLB post-mortem BG tissue samples and in the SN of PD post-mortem samples when compared to healthy controls. **Conclusions:** In conclusion, we demonstrate that METTL3 and YTHDF1 are dynamically dysregulated during Mn-, PQ- and αSynf-induced models of microglia activation. We also demonstrate METTL3 is potentially hyperactive in its methyltransferase activity, marked by a significant increase in m6A levels resulting in upregulation of proinflammatory cytokines, which were abolished upon METTL3 KD. Mn-specific induction of METTL3 cytoplasmic abundance suggests METTL3 plays a translational role in neurotoxicant-induced neuroinflammation. YTHDF1 demonstrated insult-specific localization patterns, suggesting context-specific functionality. Moreover, we confirm METTL3 and YTHDF1 dysregulation in both Mn- and αSynf-induced in vivo mouse models of neuroinflammation and dementia with lewy bodies (DLB) and PD post-mortem tissues. Collectively, our study being among the first to investigate m6A dynamics in PD models provides insight into how dynamic, spatiotemporal changes in m6A regulatory machinery in microglial cells may contribute to both genetically and environmentally induced neurodegenerative processes.

ABSTRACT NUMBER: 5234 **Poster Board Number:** LB335
TITLE: Effect of SV2C on dopamine neuron health in C. elegans

AUTHORS (FIRST INITIAL, LAST NAME) AND INSTITUTIONS: C. R. Depew, I. Lee, A. C. Knickerbocker, *G. W. Miller*, and *M. L. Bucher*. Mailman School of Public Health at Columbia University, New York, NY.
KEYWORDS: Neurotransmitter; Neurotoxicology

ABSTRACT: Background and Purpose: Dysregulation of dopamine homeostasis can jeopardize neuronal health due to the accumulation of excess cytosolic dopamine, which can undergo neurotoxic reactions that generate reactive oxygen species. Thus, factors that improve vesicular storage of dopamine may confer neuroprotection. We have recently shown that synaptic vesicle glycoprotein 2C (SV2C) improves vesicular storage of dopamine and protects against the toxic effects of MPTP exposure in in vitro and mouse models (Bucher et al. 2024). We now seek to characterize the potential of transgenic SV2C expression to protect against endogenous and exogenous dopamine toxicity in the model organism C. elegans. **Methods:** To model endogenous dopamine toxicity in C. elegans, we used strains that lack the protein responsible for vesicular dopamine sequestration (ok411; CAT-1null) and that overexpress an enzyme involved in dopamine synthesis (UA57; CAT-2OE). We generated a transgenic strain of C. elegans that expresses SV2C in dopamine neurons (JBRA; DATSV2C) and crossed this strain with the CAT-1null and CAT-2OE strains to generate additional models (DATSV2C::CAT-1null and DATSV2C::CAT-2OE). Exogenous dopamine toxicity was modeled using exposure to the neurotoxicant MPP+. All strains possess GFP expression within the dopamine neurons allowing for fluorescence-based analyses of neuronal health by microscopy. Additional analyses of body morphology and motor behaviors were performed using the COPAS large particle biosorter and WormLab, respectively. **Results:** Our previous research has demonstrated the impact of proper dopamine homeostasis on body length parameters in C. elegans (Lee and Knickerbocker et al. 2024). Preliminary analysis of the novel crossed strain

(DATSV2C::CAT-2OE) has shown the ability of transgenic SV2C to rescue body length in nematodes that overexpress endogenous dopamine. **Conclusions:** Our preliminary data suggest that introduction of transgenic SV2C can positively protect against dopamine toxicity in C. elegans nematodes. Further analyses of physiological markers mediated by the dopamine system and neuron health will allow us to establish a thorough understanding of how this protein may mitigate the adverse effects of dopamine neurotoxicity.

ABSTRACT NUMBER: 5235 **Poster Board Number:** LB336

TITLE: Intravenous Injectable Isoflurane Emulsion and an Antiseizure Treatment for Soman Exposure in a Mouse Model

AUTHORS (FIRST INITIAL, LAST NAME) AND INSTITUTIONS: N. Benn, M. Chavez-Vazquez, *M. Ellis*, *J. Leighton*, *J. Janssen*, T. McClymont, *A. Methvin*, and *E. Johnson*. USAMRICD, Gunpowder, MD.

KEYWORDS: Neurotoxicology

ABSTRACT: Background and Purpose: Isoflurane is an FDA-approved inhaled general anesthetic with a large therapeutic range, quick recovery following administration, and few side effects. Recently, there has been interest in using injectable formulations of volatile anesthetics for a variety of conditions. In this study, we investigated the role of intravenous isoflurane as an anticonvulsant for refractory status epilepticus following nerve agent exposure. Isoflurane has previously been shown to reduce seizure activity/recurrence and preserve brain tissue after exposure to other organophosphorus compounds. **Methods:** In the first part of the experiment, we searched for the optimal dose of isoflurane, which resulted in the fastest recovery and lowest mortality. Male C57BL/6J mice with an implanted jugular catheter were given intravenous isoflurane in Intralipid®, and their responses were recorded. The optimal dose found was 0.02ml of a 5% isoflurane emulsion, which resulted in a short period of sedation and slight respiration delay, with a return to normal respirations by one minute. This dose was then used to determine the potential of isoflurane as an anticonvulsant following nerve agent exposure. On exposure day, mice were given nerve agent, followed immediately by an oxime and atropine sulfate, then were observed for convulsive and seizure activity. After refractory seizure develops 40-50 minutes later, either midazolam alone or midazolam with emulsified isoflurane injection are given. For mice in both groups, EEG/seizure activity was collected for at least 40 minutes per day up to 72 hours post-exposure, followed by humane euthanasia. Histopathology analysis was conducted following perfusion and brain extraction. **Results:** Mice that received the isoflurane emulsion in addition to midazolam had improved seizure dynamics 24 hours after exposure compared to midazolam alone. Additionally, isoflurane injection appeared safe with a 100% survival rate in animals without developed seizure indicating that it can be used even without seizure confirmation, a likely scenario if deployed in austere environments without advanced medical care. Neuronal loss was determined using Fluro-Jade that showed differences between control and experimental group mice. **Conclusions:** Our results warrant future analysis into the role of isoflurane as an anticonvulsant agent following nerve agent exposure, further investigating seizure/EEG activity, histopathology, and cognitive health.

ABSTRACT NUMBER: 5236 **Poster Board Number:** LB337
TITLE: Imidacloprid unique and repeated treatment produces cholinergic transmission disruption and apoptotic cell death in SN56 cells

AUTHORS (FIRST INITIAL, LAST NAME) AND INSTITUTIONS: *P. Moyano*, A. Flores, J. San Juan, J. Garcia, J. C. Plaza, M. Fernandez, L. Abascal, O. Mateo, and *J. Del Pino*. Complutense University of Madrid, Madrid, Spain.
KEYWORDS: Apoptosis; Neurotoxicity; Pesticides; Cell Culture; basal forebrain cholinergic neurons; Imidaclorprid

ABSTRACT: Background and Purpose: Imidacloprid (IMI), the most widely used worldwide neonicotinoid biocide, produces cognitive disorders after repeated and single treatment. However, little was studied about the possible mechanisms that produce this effect. Cholinergic neurotransmission regulates cognitive function. Most cholinergic neuronal bodies are present in the basal forebrain (BF), regulating memory and learning process, and their dysfunction or loss produces cognition decline. **Methods:** BF SN56 cholinergic wild-type or acetylcholinesterase (AChE), β-amyloid-precursor-protein (βAPP), Tau, glycogen-synthase-kinase-3-beta (GSK3β), beta-site-amyloid-precursor-protein-cleaving enzyme 1 (BACE1), and/or nuclear-factor-erythroid-2-related-factor-2 (NRF2) silenced cells were treated for 1 and 14 days with IMI (1 µM to 800 µM) with or without recombinant heat-shock-protein-70 (rHSP70), recombinant proteasome 20S (rP20S) and with or without N-acetyl-cysteine (NAC) to determine the possible mechanisms that mediate this effect. **Results:** IMI treatment for 1 and 14 days altered cholinergic transmission through AChE inhibition, and triggered cell death partially through oxidative stress generation, AChE-S overexpression, HSP70 downregulation, P20S inhibition, and Aβ and Tau peptides accumulation. IMI produced oxidative stress through reactive oxygen species production and antioxidant NRF2 pathway downregulation, and induced Aβ and Tau accumulation through BACE1, GSK3β, HSP70, and P20S dysfunction. **Conclusions:** These results may assist in determining the mechanisms that produce cognitive dysfunction observed following IMI exposure and provide new therapeutic tools.

ABSTRACT NUMBER: 5237 **Poster Board Number:** LB338
TITLE: Investigating the Neurotoxicity of the Cyanobacterial Toxin N-(2-Aminoethyl)glycine (AEG) in Invertebrate Models

AUTHORS (FIRST INITIAL, LAST NAME) AND INSTITUTIONS: *L. Wang*, and R. Richer. Duke Kunshan University, Kunshan, China.
KEYWORDS: Environmental Toxicology; Neurotoxicology; Receptor; G-Protein Coupled; N-(2-Aminoethyl)glycine

ABSTRACT: Background and Purpose: As climate change progresses, increasing temperatures and eutrophication are driving harmful algal blooms, posing a threat to environmental health. These blooms are known for producing cyanobacterial toxins, including β-N-methylamino-L-alanine (L-BMAA), which are implicated in neurodegenerative diseases such as amyotrophic lateral sclerosis (ALS), Parkinson's disease (PD), and Alzheimer's disease (AD). Its newly identified isomer, N-(2-aminoethyl)glycine (AEG), remains less explored and showed even higher toxicity compared to BMAA in some studies. This study examines AEG's impact on invertebrate model organisms to elucidate potential toxicological pathways and implications, which could aid in developing preventive strategies or therapeutic interventions.

Methods: The study utilized *Drosophila melanogaster* and *Caenorhabditis elegans,* chosen for their well-characterized nervous systems and suitability for toxicology research. Developmental exposure of *Drosophila* embryos and larvae were conducted under varying concentrations of AEG. Both chronic exposure of *C. elegans* with lifespan assay by supplementing solid media with AEG were done and acute exposure using liquid media were performed. The presence of MGL-2, an ortholog of vertebrate group I metabotropic glutamate receptors implicated in AEG toxicity, is guiding further molecular and behavioral investigations in *C. elegans*. **Results:** Developmental exposure of *Drosophila* and lifespan assay for chronic exposure of *C. elegans* didn't show significant toxicity of AEG. The preliminary acute exposure experiment in *C. elegans* revealed a concentration-dependent toxicity of AEG under mM range. Concentrations of 200 mM and above resulted in a near-total incidence of paralysis or death immediately following treatment, with effects still being seen 36 hours post-exposure. Interestingly, a reduction in the paralysis and lethality rates was observed at these concentrations after 12-24 hours, suggesting a potential short-term recovery or adaptive response. Motor behavior like omega bends was observed under 100 mM AEG, which could be further investigated on a neuronal signaling level. Future experiments will focus on lower concentrations to see the chronic effects of the toxin on neurological functions. **Conclusions:** The results highlight the utility of both *C. elegans* and *D. melanogaster* for studying AEG's neurotoxicity in *vivo*. Future research will focus on motor behavior investigations and receptor-specific mechanisms to further characterize AEG's role in neurodegenerative processes.

ABSTRACT NUMBER: 5238 **Poster Board Number:** LB339
TITLE: Vmat2-interacting compounds mediate dopamine toxicity in *c. elegans*

AUTHORS (FIRST INITIAL, LAST NAME) AND INSTITUTIONS: A. C. Knickerbocker, C. R. Depew, I. Lee, *G. W. Miller*, and *M. L. Bucher*. Mailman School of Public Health, Columbia University, New York, NY.
KEYWORDS: Neurotransmitter; Neurotoxicology; Undergraduate Student

ABSTRACT: Background and Purpose: Dopamine (DA) has the potential to act as an endogenous neurotoxin when its sequestration into synaptic vesicles is impaired, resulting in accumulation of DA in the cytosol. Excess free cytosolic DA undergoes processes that generate neurotoxic reactive metabolites and reactive oxygen species, thus contributing to age-related neurodegenerative diseases like Parkinson's (PD). Vesicular monoamine transporter 2 (VMAT2) is responsible for the sequestration of DA out of the cytosol, thereby limiting endogenous neurotoxicity. Given significant evidence of dysfunctional VMAT2 expression and activity in PD, compounds that enhance VMAT2 expression, activity, maturation, etc. may be valid therapeutics for PD. The nematode, C. elegans has significant utility for modeling endogenous dopaminergic neurotoxicity due to its similar homology to humans and short lifespan with distinct stages. We have previously presented a comprehensive analysis of the effect of gene mutations in dopamine-related proteins on body size, development, and behavior in C. elegans. However, the neuron health of these DA mutants and the utility of these methods to model the effect of VMAT2-interacting compounds have yet to be identified. In this study, we demonstrate age-dependent neurodegeneration in DA mutant strains, and model the effect of various VMAT2-interacting compounds on neuron health. **Methods:** The following DA mutant strains were analyzed in this study: pdat (wild-type), pdat-cat1 (cat-1 - VMAT2 ortholog - null), UA57 (cat-2 overexpression causing DA overproduction), MBIA (cat-2 overexpression, cat-1 null). Analysis was performed from day one through day five adulthood to assess neuronal health by measuring GFP fluorescence as an indicator of neuronal integrity using high-throughput methods such as COPAS sampling or microscopy. To test for the rescue

of neurodegeneration, C. elegans were exposed to potential cat-1-enhancing compounds, including imipramine and 5-Aminoimidazole-4-carboxamide (AICA). **Results:** Overall trends indicated at later stages of adulthood (Days 3 - 5), C. elegans strains lacking cat-1 protein had significantly increased neurodegeneration evidenced by decreased GFP fluorescence. Exposure to 1µM imipramine significantly enhanced GFP fluorescence in pdats starting from day one adulthood, and UA57s from day two adulthood. Exposure to any dose of AICA and its solvent decreased GFP fluorescence in pdats and UA57s compared to NT controls. **Conclusions:** Our data suggest that the absence of cat-1 as a cytosolic DA sequestration mechanism contributes to age-dependent neurodegeneration in C. elegans, implicating DA as an endogenous neurotoxin. We also found that a 1µM dose of imipramine increases GFP fluorescence in pdat and UA57 mutants, suggesting a potential neuroprotective role for imipramine against DA toxicity. This study offers a novel way of measuring age-dependent neurodegeneration in C. elegans, allowing for a high-throughput screening of various compounds for their effect on neuron health.

ABSTRACT NUMBER: 5239 **Poster Board Number:** LB340
TITLE: The Overlapping and Differential Transcriptomic Roles of the TDP-43 Zebrafish Orthologs and their Implications for Future ALS Research

AUTHORS (FIRST INITIAL, LAST NAME) AND INSTITUTIONS: L. I. Montes, D. Jima, A. A. Nunnally, and *A. Planchart*. North Carolina State University, Raleigh, NC.
KEYWORDS: Gene Expression/Regulation; Neurotoxicology; In Vivo Models; Neurodegeneration, Zebrafish, ALS

ABSTRACT: Background and Purpose: Amyotrophic Lateral Sclerosis (ALS) is a devastating fatal neurodegenerative disease characterized by progressive motor deficits and ultimately paralysis due to motor neuron death. 5-10% of cases are attributed to genetic mutations (familial). 90-95% are of unknown etiology (sporadic), where toxicant exposures to lead, pesticides, and herbicides (within others) are suspected to be key contributors. The nuclear clearing and cytoplasmic aggregation of the TAR DNA Binding Protein of 43KDa (TDP-43) is a hallmark of ALS and bridges the gap between both subtypes, proving it to be an indispensable therapeutic target. TDP-43 plays an essential role in RNA metabolism, such as in transcription, splicing, and transport. However, the consequences at the transcriptomic level still remain poorly understood. The purpose of this study was to investigate the transcriptomic functional divergence and overlap between the TDP-43 zebrafish counterparts (tardbp and tardbpl) and understand their implications for future ALS research. **Methods:** In this study, we utilized the zebrafish as a powerful model system by leveraging CRISPR/Cas9 gene editing to knock out TDP-43 (TDP-43 KO). While in mammalian models TDP-43 KO is lethal, the unique genome duplication event of the zebrafish allowed us to examine the lowest level of TDP-43 function (tardbp(-/-); tardbpl(+/-)) and still obtain a viable model system. We employed RNA sequencing to investigate the functional divergence and overlap between both paralogs at the transcriptome level, as well as to identify the differentially expressed genes (DEGs) further promoting ALS pathogenesis. We compared the following groups: (+/+);(-/-), (-/-);(+/+), and (-/-);(+/-), using (+/+);(+/+) as the control. **Results:** We encountered 1156 of overlapped downregulated and 881 upregulated DEGs. We also found 238 downregulated and 350 upregulated DEGs exclusive to (-/-);(+/+), and 834 downregulated and 661 upregulated DEGs exclusive to (+/+);(-/-). Lastly, we found 965 downregulated and 911 upregulated DEGs exclusive to (-/-);(+/-). From these lists of genes some are consistent with the literature, while

others are novel targets for further investigation. **Conclusions:** Our findings highlight the utility of the zebrafish as a mechanistic model system to continue unraveling ALS pathogenesis; we identified plausible target DEGs augmenting ALS pathology; and provided a foundation of the divergence and overlap in transcriptomic roles of tardbp and its paralog tardbpl for future zebrafish ALS studies. For future studies, we will perform zebrafish exposures with toxicants suspected to contribute to ALS pathology and utilize the resulting DEGs as markers of tardbp and/or tardbpl dysfunction.

ABSTRACT NUMBER: 5240 **Poster Board Number:** LB341
TITLE: Assessing Developmental Cytotoxicity of Plasticizers, Pesticides, and Heavy Metals on Human Stem Cells Differentiating to Cortical Neurons

AUTHORS (FIRST INITIAL, LAST NAME) AND INSTITUTIONS: *A. M. Tukker*, M. L. Simmel, and *A. B. Bowman*. Purdue University, West Lafayette, IN.
KEYWORDS: None

ABSTRACT: Background and Purpose: Pregnant women face increasing exposures to environmental contaminants in their daily lives. Since many chemicals are known to cross the placental barrier, they may have harmful effects on the developing fetus and, thus, the developing nervous system. Notably, cells at the stem/progenitor stage show a heightened susceptibility to toxic substances, as demonstrated by the lasting impacts of in-utero methylmercury (MeHg) exposure on cortical function. Before exploring whether other toxicants induce similar vulnerabilities or result in long-term functional and homeostatic effects, it is crucial to establish appropriate exposure concentrations that reflect environmentally relevant levels found in cord blood and determine their acute cytotoxicity. This approach ensures that any observed phenotypic changes can be attributed to the sustained effects of the toxicants versus indirectly due to prior cell death. **Methods:** On the sixth day of cortical (CTX) differentiation of human induced pluripotent stem cells (iPSCs), neural progenitor cells (NPCs) were exposed to toxicants to simulate in vivo exposure of the developing central nervous system of embryos. Cultures were exposed to environmentally relevant cord blood concentrations of lead, MeHg, chlorpyrifos (CPF), and di(2-ethylhexyl) phthalate (DEHP). Cell viability was assessed 24 hours or 6 days after cessation of exposure using Alamar Blue (AB) and carboxyfluorescein diacetate (CFDA) cell viability assays. If a condition exhibited a statistically significant increase in cell death compared to the control, the concentration would be deemed too high for future chronic exposure studies. Hoechst/Propidium Iodide (PI) live cell staining and subsequent image analysis for 24-hour DEHP and CPF exposure were also performed. AB/CFDA data was obtained from 3 independent differentiations. **Results:** Our observations indicated that varying concentrations of different substances influenced the viability of NPCs. One Way ANOVA followed by post-hoc Dunnett's test were utilized for statistical analysis. Following a 24-hour exposure period (n = 8-24), the AB/CFDA assay noted a significant ($p<0.05$) decrease in NPC viability at (and above) 10 nM for DEHP (viability 67%; $p<0.05$, n = 8-24), and 1 µM for MeHg (viability 21%; $p<0.05$, n = 8-24). Following an extended exposure period of six days, our observations indicated a significant ($p<0.05$) decline in cell viability at (and above) a concentration of 1 nM of DEHP (viability 32%; $p<0.05$, n = 8-24). It is worth noting that some consistency has also been observed between Hoechst/PI live cell staining (n = 4-6) and the AB/CFDA results for DEHP and CPF. **Conclusions:** A significant decrease in viability observed during our acute exposures would suggest that certain concentrations should not be surpassed in the future experimental plan. Our findings will influence the toxicant concentrations chosen for future studies, which aim to replicate the involvement of the

placental barrier in the persistent effects on the central nervous system (CNS). Notably, apart from DEHP, only concentrations exceeding previously reported cord blood levels caused cytotoxicity. By comparing our results with literature values, we can better appreciate the context and implications of our findings. This research was supported by NIH [R01 AG080917 (ABB) and K99 ES036290 (AMT)].

ABSTRACT NUMBER: 5241 **Poster Board Number:** LB342

TITLE: Metal mixture elicits less than additive neuronal impairment in human brain microphysiological system

AUTHORS (FIRST INITIAL, LAST NAME) AND INSTITUTIONS: *B. J. Kincaid*, *J. Zhang*, A. Egert, *D. Alam-El Din*, *L. Smirnova*, and *T. Hartung*. Johns Hopkins Bloomberg School of Public Health, Baltimore, MD.

KEYWORDS: Neurotoxicity; Developmental; Neurotoxicity; Metals; In Vitro and Alternatives

ABSTRACT: Background and Purpose: Contaminants such as As, Cd, Cr and Pb are concerning developmental toxicants routinely found in comunities with a history of industrial manufacturing. Early life exposure to certain metal compounds are known to be associated with poor neurodevelopmental outcomes, with disruption to the balance of excitatory neuronal signaling as a possible mediator of such adverse effects. Exposure to these compounds does not occur in isolation, and the impact of complex mixtures of contaminants on developing brain networks remains unexplored. Our objective is to utilize a human brain microphysiological system (bMPS) to better characterize whether and how contaminant exposure elicits synaptic disruption through the assessment of structural and functional indicators of toxicity, and to assess whether metal neurotoxicity is additive at low doses reflective of current exposure levels. **Methods:** NIBSC8-derived neuroprogenitor cells (NPCs) are induced to form 3D aggregates by gyratory shaking (88 rpm, 8 cm radius) and allowed to mature while exposed to 100 nM As, 32 nM Cd, 100 nM Cr, or 320 nM Pb individually or in mixture over a 4-week window during early (weeks 0 to 4) or late (weeks 8 to 12) differentiation. Differentiation results in a coculture of maturing neurons, astrocytes, and oligodendrocytes. Non-cytotoxicity of doses and contaminant uptake and concentration was confirmed by ICP-MS. For neurite outgrowth, bMPS are pooled per condition and statically plated to allow for neurite projection for 48-72 hours. Samples are fixed, stained (TUBB3 / AF-568), and imaged at 4x magnification for use in Sholl analysis. For synaptogenesis assessment, bMPS are fixed and stained for excitatory pre-synaptic (SYP / AF488, VGLUT1 / AF647) and post-synaptic (PSD-95 / AF568, Homer1 / AF405) markers and imaged at 60x magnification. Colocalization was analyzed with SynapseJ. For electrophysiology assays, live bMPS are stained with Calbryte calcium indicator dye. Time series images were obtained with a FV3000RS Olympus confocal microscope at 12.5 frames/sec for 240 seconds. Whole organoid spike metrices were analyzed in python. For each assay, relative effect levels were summed for individual exposure groups to determine the theoretical additivity level. Mixture relative effect levels are scaled to theoretical additivity level. **Results:** The intensity density of synapses in all conditions was reduced in pre- and post- synaptic puncta, with Cd, Cr, and Mixture exposure maintaining this pattern in complete synaptic puncta. While the number of double positive pre-and postsynaptic puncta were unaffected by treatment, the number of quadruple-positive complete synapses was reduced by 29 -78 % in all conditions. This may indicate reduced homogeneity of protein distribution at the excitatory synapse resulting in the disrupted formation of complete synapses. Subchronic exposure to lead and a mixture of metals including lead yielded a minor, nonsignificant reduction in neurite density, indicating that impaired synaptogenesis is likely not due to impaired microtubule growth in extending axons or dendrites. Electrophysiological assessment of neuronal

activity shows an increase in the number and rate of spikes for Cd-exposed samples, with a trend toward dampening of these metrics for Cr-exposed samples, indicating altered excitability. In assessing deviation from theoretical additivity levels for mixture exposure, the majority of endpoints assessed exhibited a less than additive effect, with the exception of peak amplitude, which exhibited a slightly above-additive response. **Conclusions:** Taken together, this data provide evidence of a less-than-additive relationship between contaminants with confirmed synaptic toxicity when they are administered as a complex mixture.

ABSTRACT NUMBER: 5242 **Poster Board Number:** LB343

TITLE: The Search for Sensitive Anatomical Biomarkers Indicative of Altered Thyroid-Dependent Brain Development

AUTHORS (FIRST INITIAL, LAST NAME) AND INSTITUTIONS: M. G. Hawks[1,2], J. L. Ford[1], *R. C. Thomas*[1,2], and *M. E. Gilbert*[1]. [1]US EPA, Research Triangle Park, NC; and [2]ORISE, Oak Ridge, TN.

KEYWORDS: None

ABSTRACT: Background and Purpose: Thyroid hormones (TH) are crucial for proper brain development, disruption of which leads to neurodevelopmental impairments. For chemical regulation, there is a need for TH-sensitive readouts of developmental neurotoxicity. We examined a set of distinct neuroanatomical markers in rats exposed to varying levels of TH insufficiency: periventricular heterotopia (PVH) in corpus callosum, parvalbumin-expressing interneurons (Pvalb) in neocortex, and granule cells (GC) in cerebellum. PVH result from inappropriate migration of neurons, Pvalb is a calcium binding protein expressed in a subset of inhibitory neurons, and a delay in the migration of GC leads to the persistence of the external GC layer (EGL) in cerebellum. These TH-responsive structural deviations in neonatal rat brain were examined following maternal exposure to graded doses of the TH synthesis inhibitor propylthiouracil (PTU). **Methods:** Pregnant LE rats (5-9/dose) were exposed to PTU via drinking water (0, 0.5, 1, 3ppm) from gestational day 6 until postnatal day (PN) 23. Pups were euthanized at PN0, PN6, PN14, and PN22 and serum collected for TH analysis via LC-MS/MS. Brains collected on PN14 were immersion fixed for histological staining. Coronal sections (60µm) of the brains were stained for NeuN or Pvalb. PVH were analyzed in 25 NeuN-stained sections by measuring area of the PVH in each section to calculate volumes. Pvalb+ cells were enumerated in the somatosensory (SS) and cingulate (Cg) cortices using an automated cell counting algorithm (~8 sections/brain, 120-180µm apart in regions anterior to the hippocampus). Sagittal sections (40µm) of the cerebellum were stained with cresyl violet and EGL measured in the folia between lobes 3-4 and 7-8 of the vermis. Litter was the unit of analysis for statistical evaluations. **Results:** Significant dose-dependent reductions in serum T4 were seen in dams and pups at all ages tested. Dam T4 levels were significantly decreased by ~60% at 3ppm, with modest reduction of 8% at the 1ppm dose level. Reductions in pup serum T4 were greater than those observed in dam, and most pronounced on PN6 (80-90% reductions at 3ppm). Significant dose-dependent increases in PVH volume and incidence were observed, from a background mean of 0.00016mm^3 in controls, to 0.0008 at 0.5ppm, 0.004 at 1ppm and 0.0231mm^3 at the highest dose. The incidence of PVH increased above the background in control animals to 4/7 rats at 0.05ppm and in 6/6 at 1 and 3ppm. Pvalb+ cell number was significantly reduced by 40% in SS cortex at 1ppm, and by 75-80% in the SS and Cg cortex at 3ppm. The EGL areas in the folia between lobes 3-4 increased 12-24% above control means at all three dose levels but were highly variable and not statistically reliable. The area measures in the folia between lobes 7-8 were more consistent, trending towards statistical significance ($p<0.06$) with an

11-16% increase in EGL thickness at the two high dose groups. **Conclusions:** In the neonate, serum T4 levels were only modestly reduced at the lowest dose tested (5-35%) and did not differ from control in the PN22 pup or dam. Although small sample size may have obscured some effects at low doses, we confirmed the presence of PVH with moderate degrees of T4 insufficiency, reductions in Pvalb+ neurons in 2 cortical regions, and a potential delay in migration of the GC in the cerebellum. Errors in migration exemplified by PVH and persistence of the EGL in cerebellum can alter cytoarchitecture and connectivity in the developing brain. Pvalb+ neurons represent the largest source of GABAergic inhibitory tone - their loss can alter maturation and integration of developing neural circuitry. Efforts are ongoing to provide additional support and refinement to dose-response relationships of perturbations in brain associated with low level TH insufficiencies. *Does not necessarily reflect EPA policy.*

ABSTRACT NUMBER: 5243 **Poster Board Number:** LB344

TITLE: A data-driven approach to detect developmental neurotoxicity in the time-course of a microelectrode array neural network formation assay

AUTHORS (FIRST INITIAL, LAST NAME) AND INSTITUTIONS: M. Mayil Vahanan[1,2], *T. Shafer*[1], and *K. Carstens*[1]. [1]Environmental Protection Agency, Durham, NC; and [2]Oak Ridge Institute for Science and Education, Oak Ridge, TN.

KEYWORDS: Neurotoxicity; Developmental; Neurotoxicology

ABSTRACT: Background and Purpose: *In vitro* new approach methods have been developed to evaluate the developmental neurotoxicity (DNT) potential of environmental compounds. The neural network formation assay (NFA) uses a twelve-day chemical exposure model measuring changes in neuronal activity on days *in vitro* (DIV) 5, 7, 9, and 12 in primary rat cortical cells plated on microelectrode arrays. To date, NFA data over time have been reduced to a single value per concentration using an area under the curve (AUC) from concentration-response modeling of 17 different endpoints. The goal of this study was to further evaluate trends in bioactivity across development and identify potentially informative perturbations that may be masked by the AUC approach. It was hypothesized that developing neural networks may demonstrate transient responses or differences in sensitivity to chemical exposure during different time points that may not be detected by an AUC approach. A secondary goal of this study was to explore data-driven approaches for feature reduction in the NFA. **Methods:** Several approaches were taken to detect concentration-dependent changes in activity during the NFA. First, concentration-response modeling was performed on data collected from each individual recording day for the 17 previously established endpoints across 243 chemicals using the tcplfit2 R package (v 0.1.6), resulting in 4369 curves per dataset. Changes in activity (positive and negative hit calls) and potency estimates (concentration at 50% maximal activity) were determined. A chemical was considered active in a particular analysis method if it was active in at least 3/17 endpoints. Bioactivity metrics from each analysis method were compared and bioactivity profiles across development were identified using hierarchical clustering. Patterns of bioactivity were compared to those of the AUC data to determine added value. Next, a previously established toxicological tipping point approach was used to determine dose-dependent transitions in activity that followed a non-recovery trajectory. This approach computed a composite metric (total scalar perturbation) that reduced bioactivity to a single value. This approach was compared to bioactivity from individual DIVs and the AUC approach to evaluate potential differences in sensitivity of the responses. **Results:** Out of 243 chemicals, 53 were active in the individual DIV and AUC approaches, 28 chemicals were only active on DIV5, 17 chemicals were only active on DIV7,

zero chemicals were only active on DIV12, and one chemical was only active using the AUC approach. Of the 28 chemicals only active in the DIV5 analysis, five were putative DNT positive chemicals and five were putative DNT negatives, suggesting inclusion of DIV5 endpoints may increase the sensitivity of the assay, while also decreasing the specificity. Using hierarchical clustering across all endpoints and DIVs two distinct clusters of chemicals were identified that were only active on DIV5 that demonstrated perturbations in network synchrony endpoints or burst structure. A distinct subset of chemicals was identified with activity only on DIV7 that perturbed endpoints measuring changes in general activity. Moreover, a subset of chemicals identified to be active based on DIV-level analysis, were not detected in the tipping point analysis, i.e., no tipping point or recovery effect was detected. This suggests that the tipping point analysis may not detect some transient changes in activity occurring across development in the NFA. **Conclusions:** These results demonstrated that analysis of DIV5 and DIV7 resulted in different active chemicals than examining DIV12 and AUC alone, and these differences may be due to activity only occurring during early developmental days *in vitro*. Furthermore, reducing the 17 features to a total scalar perturbation value failed to detect some positive chemicals that were active when using a DIV-level analysis. Future work should focus on understanding the biological relevance of transient changes in bioactivity that are not currently detected by established analysis methods for the NFA. Lastly, exploration of other feature reduction methods may improve the sensitivity and specificity of the NFA for DNT assessment. *This abstract does not reflect U.S. EPA policy.*

ABSTRACT NUMBER: 5244 **Poster Board Number:** LB345

TITLE: Integrationof Large-Scale Clinical Data Mining and Experimental Approaches to UnravelProkineticin-2 Neuroprotective Signaling in the Olfactory System During Manganese Neurotoxic Stress

AUTHORS (FIRST INITIAL, LAST NAME) AND INSTITUTIONS: *G. R. Clabaugh*, H. Jin, V. Anantharam, *A. Kanthasamy*, and *A. G. Kanthasamy*. University of Georgia, Athens, GA.

KEYWORDS: Neurotoxicity; Metals; Chemokine, Signalling; Biomarkers

ABSTRACT: Background and Purpose: Chronic manganese (Mn) exposure affects the basal ganglia (BG) and has been implicated in the development of parkinsonism and Parkinson's disease (PD). Environmental Mn exposure has also been associated with olfactory deficits, but the underlying mechanism remains poorly understood. Prokineticin-2 (PK2) is a secretory peptide involved in olfactory bulb neurogenesis. Serendipitously, we discovered that PK2 mediates a novel neuroprotective compensatory response to early stages of neurotoxic stress in parkinsonian models by inducing mitochondrial biogenesis and anti-apoptotic pathways. Given the vital role of PK2 in olfaction and its protective functions in models of parkinsonism, we sought to exploit the large-scale clinical data set available in NIH Accelerating Medicines Partnership in PD (AMP-PD) database and integrate with experimental results using human iPSC and GenStat Transgenic mouse models to understand the role of PK2 in the metal induced olfactory dysfunction. Our overarching hypothesis is that PK2 serves as an early compensatory neuropeptide against neurotoxic stress. Comprehensive understanding of PK2 signaling may enable the development of novel drug discovery platforms targeting non-motor dysfunctions associated with neurodegenerative diseases. **Methods:** N27 rat dopaminergic cells were treated with 300 µM $MnCl_2$ for 3-12 h, and PK2 mRNA and protein levels were analyzed using RT-PCR and Western blot. Human induced pluripotent stem cells (iPSCs), differentiated into midbrain dopaminergic (mDA) neurons, were exposed to 200 µM $MnCl_2$ for 1-6 h, and PK2 immunoreactivity was

evaluated using ICC. Cell viability was assessed using both the MTS assay and flow cytometry. Transgenic Swiss Webster PK2-eGFP reporter mice were intranasally exposed to 300 µg of $MnCl_2$ for 5 or 30 days. Preclinical 7T MRI was used to visualize the Mn deposition in the brain following Mn exposure. CUBIC whole brain tissue clearing, immunohistochemistry (IHC), and Western blot analyses were used to characterize changes in PK2 signaling in the brain of H_2O or Mn-treated mice. To determine whether PK2 mRNA was changed in the blood of Parkinson's disease patients, we analyzed the AMP-PD whole blood transcriptomic data using DESeq2. **Results:** RT-PCR and Western blot analyses revealed that Mn-treated N27 cells had significantly higher PK2 mRNA and protein levels at the early 6-h timepoint. These findings were validated in human iPSC-derived mDA neurons treated with Mn, where ICC analysis revealed enhanced PK2 immunoreactivity in TH^+ neurons. To assess PK2's functional role, MN9D cells stably transfected with a PK2 expression vector demonstrated significantly resistant to Mn neurotoxicity compared to the empty-vector MN9D cells.PK2-eGFP reporter mice intranasally exposed to $MnCl_2$ showed increased MRI signal intensity in the olfactory bulb and anterior olfactory nucleus. To correlate our MRI findings with brain PK2 expression changes, we used CUBIC whole brain tissue clearing and light sheet microscopy. Interestingly, we found an increase in PK2+ neurons in the OB's subependymal layer (SEL), the region containing migratory neuroblasts. IHC and confocal microscopy further confirmed an increase in PK2+ cells in the SEL, accompanied by a correlated rise in DCX immunostaining, indicating an unexplored link between migrating neurons and PK2 during neurotoxic stress. Western blot analysis of OB lysates further validated increased PK2 protein expression in Mn-exposed mice. Finally, with the knowledge that PK2 is involved in the early stages of neurodegeneration, we investigated whether PK2 mRNA was differentially expressed in human PD patients. We utilized whole-blood RNA-sequencing data from the AMP-PD large-scale database. Comparison of the whole blood transcriptome of control (n = 1,097) and PD (n = 1,624) groups revealed a significant upregulation of PK2 mRNA while receptor expression (PKR1 and PKR2) remained unchanged. **Conclusions:** Collectively, these findings highlight PK2 as a promising therapeutic target and potential biomarker and for parkinsonism. PK2 appears to facilitate a novel compensatory signaling response during the early stages of Mn-induced neurotoxicity in the olfactory system. Additionally, the significant upregulation of PK2 mRNA in the whole blood of PD patients suggests its potential utility in stratifying PD patient populations to enhance predictive capabilities. Together, these results underscore PK2's potential as a promising therapeutic target for addressing environmentally linked neurodegenerative conditions (Supported by NIH/NIEHS R01 ES034196).

ABSTRACT NUMBER: 5245 **Poster Board Number:** LB346

TITLE: Developmental Pathophysiology of Childhood-Onset Manganese-Induced Dystonia-Parkinsonism in *Slc39a14*-KO mice

AUTHORS (FIRST INITIAL, LAST NAME) AND INSTITUTIONS: *R. Kapoor*, *A. N. Rodichkin*, *J. L. McGlothan*, and *T. R. Guilarte*. Florida International University Robert Stempel College of Public Health & Social Work, Miami, FL.

KEYWORDS: Neurotoxicity; Metals; Neurotoxicity; Developmental; Neurotoxicology; Manganese

ABSTRACT: Background and Purpose: In 2015, Tushl and colleagues reported several cases of childhood-onset manganese (Mn) induced dystonia-parkinsonism due to autosomal recessive mutations in the *SLC39A14* gene (Tushl et al., 2015). Mutation carriers have significantly elevated levels of blood Mn. Furthermore, MRI imaging demonstrated Mn accumulation in numerous brain regions and

progressive cerebellar (CB) atrophy, which may be responsible for some neurological symptoms observed in mutation carriers. We have previously characterized the *Slc39a14* knockout (KO) mouse model at postnatal (PN) day 60. At this age, *Slc39a14*-KO mice display phenotypic features similar to those described in mutation carriers (Rodichkin et al., 2021). Unpublished data from our lab also shows neuroinflammation and Purkinje cell death in the CB of *Slc39a14* KO mice at PN60 (see abstract # 2628). However, it is currently not known at what age the pathology observed in adult *Slc39a14*-KO mice begins. Here, we describe studies to characterize the behavioral and pathological phenotypes beginning at PN21in *Slc39a14*-KO mice relative to age-matched wildtype (WT) mice. **Methods:** We used *Slc39a14*-KO and WT male mice at PN21. Inductively Coupled Plasma Mass Spectrometry (IC-PMS) was used to determine Mn concentrations in the CB. Locomotor activity and tremors were assessed using activity cages and SDI tremor monitor system. Previous studies in developing mice with hereditary dystonia (Heijde et al., 2022; Horie et al., 2016) found deficits in a negative geotaxis test of sensory-motor reflex development and motor coordination. We used this test to compare the *Slc39a14*-KO mice to WT mice. Iba-1 immunohistochemistry (IHC) was used to assess neuroinflammation in the CB of the *Slc39a14* KO mice compared to age-matched WT littermates, and percent area coverage of activated microglia was analyzed using ImageJ software. **Results:** *Mn concentrations* - We found that Mn concentrations were significantly increased 10-20 fold ($p<0.0001$) in the CB of *Slc39a14*-KO mice relative to WT at PN21. *Behavioral Analyses* - *Slc39a14*-KO mice were significantly impaired in locomotor activity at PN21, which was assessed using negative geotaxis ($p=0.001$) and various parameters of activity cages like distance traveled ($p=0.006$), average speed ($p=0.002$), ambulatory time ($p=0.01$). Physiological tremors between 6-14 Hz were significantly reduced at PN21 in the *Slc39a14* KO mice ($p<0.0001$). *Immunohistochemistry* - Microglia activation was assessed using Iba-1 IHC in PN21 *Slc39a14* KO and WT mice. *Slc39a14* KO animals show a striking increase in microglia number and clustering in all the lobules of the CB. We found that there is a statistically significant increase in percent area covered by activated microglia in deep cortical tissue of the CB lobules Lobule 2 ($p=0.01$), Lobule 3 ($p=0.01$), Lobule 4&5 ($p=0.0007$), Lobule 6 ($p=0.0002$), Lobule 7 ($p=0.01$), Lobule 8 ($p=0.008$), Lobule 9 ($p=0.002$), Lobule 10 ($p=0.0001$) and Deep Cerebellar Nuclei (DCN) ($p=0.04$). **Conclusions:** These preliminary findings demonstrate that, similar to PN60 *Slc39a14*-KO mice exhibit significantly elevated Mn levels in the cerebellum (CB) at PN21, suggesting that Mn accumulation occurs prior to this age. Behavioral analyses show that, like PN60 *Slc39a14*-KO mice, at PN21 *Slc39a14*-KO mice perform significantly worse than WT littermates in all locomotor activity tests. The negative geotaxis test revealed marked deficits in *Slc39a14*-KO mice, indicating neurodevelopmental delays consistent with what is observed in human patients. Physiological tremors, critical for maintaining normal posture, were significantly reduced in *Slc39a14*-KO mice at both PN60 and PN21. Immunohistochemistry of microglia using Iba-1 showed increased microglial activation and clustering across all CB lobules especially the deep cortical layers, mirroring microglia activation patterns observed at PN60. Overall, these preliminary findings show that CB Mn accumulation, motor impairments, and microglia activation are evident as early as PN21 in *Slc39a14*-KO mice, suggesting pathology begins before this age. These results highlight the need for further investigations into earlier developmental time points to uncover mechanisms underlying SLC39A14 mutations associated with Mn-induced dystonia-parkinsonism.

ABSTRACT NUMBER: 5246 **Poster Board Number:** LB347
TITLE: Characterizing brain region-specific gene expression changes in the lead exposed mouse brain

AUTHORS (FIRST INITIAL, LAST NAME) AND INSTITUTIONS: *E. K. Matei*, *R. K. Morgan*, *A. Tapaswi*, J. Miller, *H. Wang*, X. Zhou, *K. Bakulski*, *D. C. Dolinoy*, and *J. Colacino*. University of Michigan School of Public Health, Ann Arbor, MI.
KEYWORDS: None

ABSTRACT: Background and Purpose: Lead (Pb) is a developmental neurotoxicant that is associated with childhood neurological disorders as well as impaired cognition later in life. Early-life Pb exposure contributes to gene expression changes in the brain, but brain-region specific changes caused by Pb exposure are still unknown. Furthermore, metals, such as Pb, have been implicated in Alzheimer's disease (AD)-related pathology in model systems. Since AD is also known to alter gene expression patterns in the brain, it is pertinent to assess whether early-life Pb exposure results in gene-expression changes consistent with AD pathology. Furthermore, throughout the AD clinical course, pathology occurs first in the hippocampus, followed by other brain regions, including the cortex and cerebellum. Therefore, measuring gene expression changes in distinct brain regions following Pb exposure will help elucidate whether Pb exhibits similar brain region specificity as AD. The purpose of this study is to assess immediate and long-term gene expression changes across brain regions in response to perinatal Pb exposure. **Methods:** *Sample Size, Exposure, and Tissue Collection* Mice used in this experiment were perinatally exposed to 32 ppm of Pb via drinking water provided to the dams. C57BL/6 females (F0 generation) between 6-8 weeks of age were randomly assigned to control or Pb water (32 ppm) exposure two weeks prior to mating with C57BL/6 males (8-10 weeks of age). Females were exposed to Pb via *ad libitum* drinking water mixed with Pb-acetate (pH adjusted to 4.5 with acetic acid). Exposure of the females to Pb water continued throughout gestation and lactation until weaning of the offspring (F1) at three weeks of age (PND21), at which time offspring were either sacrificed (PND21 group) or switched to control water and moved to long-term housing (until 18 months of age) (N ≥ 10 for each sex in each exposure group and time point). Three brain regions - hippocampus, cortex, and cerebellum - were collected from each mouse (N = 240 samples, 80 samples for each brain region). All tissues were immediately flash-frozen and stored at -80℃ prior to use. *RNA Isolation, Sequencing, and Processing* RNA was isolated from each brain region tissue type using the Qiagen Allprep Kit. For PND21 samples, RNA concentration and quality was assessed using the NanoDrop Spectrophotometer. For 18-month samples, RNA quantity and quality was assessed using the Qubit Flex Fluorometer. RNA samples were used for RNA library preparation and sequencing. Following quantification, total RNA samples from PND21 and 18-month-old mouse brain regions were converted to cDNA using the plexWell (SeqWell) plate-based method. Libraries were sequenced on the Illumina NovaSeq X Shared Flow Cell at the UM Advanced Genomics Core. Each run consisted of 96 samples with a sequencing depth of 2 billion reads total (20% of a 10 billion flow cell). Each individual cell was sequenced at a depth of 20 million reads. Reads were deconvoluted using the unique i7-i5 barcode index for each sample. RNA-sequencing reads were transferred to the University of Michigan Great Lakes computational cluster for pseudo-alignment to the mouse genome (Gencode version M35) using Salmon v1.9.0. This generated a counts-per-sample matrix. Counts matrices were filtered to remove genes with low counts using the edgeR filterByExpr() function with default settings. Normalization factors and dispersion parameters were then calculated prior to generating a log2-transformed counts per million (cpm) matrix for analysis. *Statistical Analysis* Differential gene expression analysis (FDR < 0.05) of PND21 and 18-month RNA transcript count data

was performed using the edgeR package in R statistical software. A linear mixed model of exposure was used which adjusted for sex. Results were stratified by brain region and time point. We reported the magnitude of the gene expression difference between Pb treatment and controls using log2 of the fold change (logFC). We used false discovery rate (FDR) adjusted p-values to account for multiple comparisons. **Results:** Analysis of RNA-sequencing data from PND21 mouse brain regions (cerebellum, hippocampus, and cortex) identified 9 genes (cerebellum), 55 genes (hippocampus), and 6 genes (cortex) that differed in expression between Pb-exposed and control samples (FDR < 0.05). In the PND21 cerebellum, 4 genes showed increased expression in Pb-exposed mice and 5 genes showed decreased expression in Pb-exposed mice. In the PND21 hippocampus, 2 genes showed increased expression in Pb-exposed mice and 53 genes showed decreased expression in Pb-exposed mice. In the PND21 cortex, 3 genes showed increased expression in Pb-exposed mice and 3 genes showed decreased expression in Pb-exposed mice. Example genes of interest that were found to be differentially expressed include *Apob* (logFC = -5.74, FDR = 0.0007) and *Apoa1* (logFC = -4.81, FDR = 0.0006) (both in the hippocampus). Analysis of RNA-sequencing data from 18-month mouse brain regions (cerebellum, hippocampus, and cortex) identified 0 genes (cerebellum), 1 gene (hippocampus), and 2 genes (cortex) that differed in expression between Pb-exposed and control samples (FDR < 0.05). The genes differentially expressed in the hippocampus and cortex showed increased expression in Pb-exposed samples versus control. Differentially expressed genes included *Slenbp2* (hippocampus; logFC = 2.31, FDR = 0.016), *Muc5b* (cortex; logFC = 4.86, FDR = 0.032), and *Krt13* (cortex; logFC = 5.78, FDR = 0.032). **Conclusions:** PND21 and 18-month-old mice exposed to Pb during gestation showed differential gene expression changes. Pb-exposed mice exhibiting differential expression of genes associated with AD, such as *Apob* and *Apoa1* in the hippocampus, suggests a potential mechanism by which perinatal Pb exposure contributes to AD via gene expression alterations. Further analysis of gene expression overlap between the studied timepoints will assess genes that exhibit altered expression in both early- and late-life. Gene expression analysis stratified by sex will also be performed to observe whether male and female mice are differentially affected by Pb exposure. Future analysis will include pathway analysis using fgsea to identify biological pathways in which differentially expressed genes are enriched and Multisubject Single Cell (MuSiC) cell deconvolution of the bulk gene expression data with a single-cell mouse brain reference dataset to determine whether cell proportions in each brain region are altered in exposed versus control states. Identification of the impacts of perinatal Pb exposure on the brain will allow for greater understanding of the role that Pb plays in neuroinflammation, neurotoxicity, and AD pathology, as well as provide potential routes for disease intervention.

ABSTRACT NUMBER: 5247 **Poster Board Number:** LB348

TITLE: Glial Scar Formation and Neuroinflammatory Responses in the Temporal Lobe Following Acute DFP Intoxication in Rats

AUTHORS (FIRST INITIAL, LAST NAME) AND INSTITUTIONS: *T. Teodoro*, *P. Bernadino*, M. Lou, A. Gelli, and *P. Lein*. University of California, Davis, CA.

KEYWORDS: Inflammation; Neurotoxicity; Pesticides; Neurotoxicology

ABSTRACT: Background and Purpose: Acute organophosphate (OP) intoxication remains a significant global health concern, affecting millions annually. Cholinergic crisis triggered by acute OP intoxication often progresses to life-threatening status epilepticus (SE). While standard-of-care (SOC) improves survival rate, it falls short in preventing adverse neurological sequelae, including spontaneous recurrent

seizures (SRS) and cognitive impairment. OP-induced SE activates numerous pathological processes, including neuroinflammation, oxidative stress, and neurodegeneration. A common response to central nervous system injury is the formation of glial scars, a physicochemical protective barrier that isolates damaged from healthy tissue; however, these formations can be detrimental to neuronal plasticity, axonal growth, and general healing of functional nervous tissue. A growing body of evidence also suggests a role for glial scars in OP-induced brain injury. In the context of acute OP poisoning, glial scar formation potentially contributes to impaired neuronal regeneration, chronic neuroinflammation, and the development of SRS. A more comprehensive understanding of the formation and persistence of glial scars following acute OP intoxication is pivotal for understanding and possibly addressing neuropathologies derived from acute OP intoxication. **Methods:** Adult male and female Sprague-Dawley rats (n=138; 97 male, 41 female) were administered diisopropylfluorophosphate (DFP; 4 mg/kg, s.c.), while vehicle control animals (VEH; n=66; 41 male, 25 female) received an equal volume (300 µL) of phosphate-buffered saline (PBS, s.c.). One minute after DFP or PBS injection, animals were given atropine sulfate (2 mg/kg, i.m.) and 2-PAM (25 mg/kg, i.m.), followed by two sequential injections of midazolam (0.65 mg/kg, i.m.) 40- and 50-min post-exposure, simulating current SOC. The rats were euthanized at 1, 3, 7, 14, and 28 d post-exposure (DPE) and their brains were collected for immunohistological (IHC) analyses. The presence of glial scars was evaluated in the piriform cortex and amygdala. A glial scar was defined as a region devoid of immunoreactivity for the astrocytic markers GFAP and aquaporin-4 surrounded by increased expression of both these astrocytic markers. Quantitative IHC was performed only on animals with glial scars to measure expression of IBA1, NeuN, and laminin as biomarkers of microgliosis, neurons and extracellular matrix, respectively. Expression of these biomarkers in the core of the lesion (scar core or SC) vs. the periphery of the scar (SP) was analyzed at varying times post-exposure. A Chi-square or Fisher's exact test was used to compare the incidence of glial scars in DFP vs. VEH. One-way analysis of variance (ANOVA) was used to compare the scar core vs. periphery, while repeated measures ANOVA was used to compare qIHC findings between time points. **Results:** Of the 138 DFP-intoxicated rats, 54 animals did not develop glial scars, while the remaining 82 animals developed lesions that met our criteria for identifying them as glial scars. DFP rats showed a higher incidence ($P < 0.05$) of glial scar formation compared to VEH, which had no scar formation in any animal. Additionally, there was a tendency for an increased incidence of glial scar formation on 3 DPE and 7 DPE ($P < 0.05$). The qIHC of NeuN showed a notable decrease of NeuN+ cells in the SC compared to the SP, which was statistically significant at 7, 14, and 28 DPE ($P < 0.05$), but not at 1 and 3 DPE ($P > 0.05$). Expression of the microglial marker IBA1 was significantly increased in the SC at all time points ($P < 0.05$), with higher values in the SC at 3, 7, 14, and 28 DPE compared to 1 DPE. At 1 DPE, there was no statistical difference in laminin expression between the SC and SP, but there was significantly increased expression of laminin on 14 and 28 DPE in the SC relative to 3 and 7 DPE ($P < 0.05$). **Conclusions:** Our findings demonstrate that DFP-intoxicated animals exhibited a significantly higher incidence of glial scar formation compared to VEH. Immunohistochemical analysis revealed notable changes in cell populations within the glial scar, characterized by a reduction in NeuN+ cells at later time points in the SC compared to the SP. Furthermore, microglial recruitment, as indicated by increased IBA1+ cell count, was significantly increased in the scar core at all time points. Lastly, extracellular matrix organization was disrupted in these pathological formations, evidenced by increased laminin in the SC compared to the SP. These results suggest that DFP intoxication induced the formation of glial scars, which in turn contributed to sustained neuroinflammation and neurodegeneration. These results define the temporal dynamics of glial scar formation following acute OP intoxication and inform

future studies for assessing glial scarring as a contributing factor to long-term adverse neurological consequences of acute OP intoxication.

ABSTRACT NUMBER: 5248 **Poster Board Number:** LB349

TITLE: Investigation of the Effects of Quercetin and Hesperidin on Oxidative Stress and Brain Damage on Cyclophosphamide-Induced Neurotoxicity in Rats

AUTHORS (FIRST INITIAL, LAST NAME) AND INSTITUTIONS: C. Adiguzel[1], S. Yimaz[2], F. Apaydın[1], A. Ucar[3], and *S. Yılmaz*[3]. [1]Gazi University, Ankara, Turkey; [2]Karamanoglu Mehmet Bey University, Karaman, Turkey; and [3]Ankara University, Ankara, Turkey.

KEYWORDS: None

ABSTRACT: Background and Purpose: Cyclophosphamide (CP) is a potent agent that is widely used in chemotherapy. It is thought that flavonoids may have positive effects on toxicity, one of the serious side effects of CP. In this study, it was aimed at investigating the possible protective effects of quercetin (QUE) and hesperidin (HSP) against oxidative stress and brain damage in CP-induced neurotoxicity in rats. **Methods:** QUE (100 mg/kg/day) and HSP (100 mg/kg/day) intragastrically administered to 36 Wistar male rats for 15 days. On the 15th day, a single dosage (i.p.) of CP (200 mg/kg/day) was administered, followed by sacrifice. Throughout the application, the amount of feed consumed was recorded daily, and body weights and fasting blood glucose levels were measured three times. When the experiment was completed, brain tissue sections were examined with a light microscope in terms of histopathological changes, and superoxide dismutase (SOD), catalase (CAT), glutathione peroxidase (GPx), glutathione S-transferase (GST) enzyme activities and malondialdehyde (MDA) levels in this tissue were examined. SPSS program has been used in the statistical assessment of the findings collected as a result of the research. Kruskal-Wallis test was used for intra-group evaluations and Mann-Whitney U test was used for pairwise comparisons (significance was based on Bonferroni test). A p value of 0.05 was accepted for statistical significance. **Results:** It has been determined that CP injection decreases the activities of antioxidant enzymes (SOD, CAT, GPx and GST) establishing the enzymatic defensive line($p<0.05$). CAT, GPx and GST enzymes were highest in the QUE group, while SOD enzyme was highest in the HSP group and MDA was highest in the CPE group. It has been found that CP exposure induces notable pathological findings on brain tissue, hence it is a neurotoxic agent and also raises the level of MDA, which is a product of lipid peroxidation ($p=0.001$). It has been found that QUE and HSP supplements improve SOD, CAT, GPx and GST activities ($p=0.05$), and reduce neurotoxicity by improving pathological findings in brain tissue. When the pairwise comparisons were analyzed, it was concluded that there were strong significant differences between the groups in terms of all antioxidant enzymes and MDA levels. **Conclusions:** As a consequence of considering the effects of CP on oxidative stress and brain tissue damage, it is thought that it may be useful to establish dietary habits that are high in antioxidants, especially QUE and HSP, against oxidative stress and organs toxicities such as neurotoxicity in patients using drugs containing this active substance, and dietary supplements under the control of a medical professional when required.

ABSTRACT NUMBER: 5249 **Poster Board Number:** LB350

TITLE: Potential neuroprotective effect of harmine in SH-SY5Y cells differentiated into dopaminergic neurons exposed to cocaine

AUTHORS (FIRST INITIAL, LAST NAME) AND INSTITUTIONS: J. L. F. Ribeiro[1], M. L. Pereira[1], L. A. G. Terra[1], F. Dörr[1], P. P. Borges[1], *P. Scharf*[1], R. C. T. Garcia[2], and T. Marcourakis[1]. [1]University of Sao Paulo, Sao Paulo, Brazil; and [2]Federal University of Sao Paulo, Sao Paulo, Brazil.

KEYWORDS: Neurotoxicology; Cell Culture; Cytotoxicity; Neuroprotection; Harmine

ABSTRACT: Background and Purpose: Harmine is one of the primary β-carbolines found in Ayahuasca, a psychoactive beverage traditionally used by indigenous peoples of the Amazon region. Numerous studies have investigated the pharmacological properties of harmine, including its role in promoting neurogenesis. Cocaine is widely used in South America, known to cause significant neuronal damage through mechanisms such as oxidative stress, mitochondrial dysfunction, and neurotrophic modulation, all of which contribute to the development of mental disorders. SH-SY5Y cells is a robust model for simulating neurotoxic conditions; however, their differentiation into mature dopaminergic neurons provides a more stable culture and enables a more precise analysis of cocaine-induced toxicity and harmine's neuroprotective effects. Thus, the present study aims to investigate the potential neuroprotective effects of harmine against cocaine-induced neurotoxicity, using human neuroblastoma SH-SY5Y cells differentiated into dopaminergic neurons. **Methods:** SH-SY5Y cells were differentiated into dopaminergic neurons through a two-step protocol involving sequential treatment with retinoic acid (10 µM) for five days, followed by brain-derived neurotrophic factor (BDNF, 50 ng/mL) for another five days. The acquisition of a dopaminergic phenotype and neuronal maturity was confirmed via flow cytometry and confocal immunofluorescence, analyzing the expression of tyrosine hydroxylase and NeuN. To evaluate the neurotoxicity profile, the differentiated cells were exposed to a range of cocaine concentrations (1-10 mM) and harmine concentrations (1-1000 µM). Concentration-response curves were constructed using the MTT assay to determine the lethal concentration 50 (LC50) of cocaine and the no-observed-adverse-effect level (NOAEL) of harmine after 24 and 48h of incubation. These results were further validated through complementary viability assays, including flow cytometry and acridine orange staining. Lastly, cell viability was assessed following co-exposure to cocaine and harmine at the established concentrations. **Results:** The cell differentiation protocol resulted in a homogeneous and stable culture of dopaminergic neurons, as evidenced by increased fluorescence intensity and marked expression of tyrosine hydroxylase and NeuN by flow cytometry. Cocaine exposure for 48 h induced a significant reduction in cell viability starting at a concentration of 4 mM, predominantly by necrosis. For harmine exposure for 48 h, viability was reduced starting at 100 µM, thus establishing the NOAEL at 10 µM. Co-incubation with harmine attenuated the neurotoxic effects of cocaine. **Conclusions:** Differentiation of SH-SY5Y cells provides a valuable model for investigating cocaine-induced neurotoxicity. This model mimics mature dopaminergic neurons, enabling more accurate assessment of cocaine's effects and the potential neuroprotective properties of compounds like harmine. Our findings demonstrate that harmine can mitigate cocaine-induced damage, exhibiting neuroprotective effects. These results underscore the significance of this model for neurotoxicology research and contribute to the development of novel therapeutic approaches for cocaine-related disorders.

ABSTRACT NUMBER: 5250 **Poster Board Number:** LB351

TITLE: N,n-dimethyltryptamine on cocaine-induced modulation of the kynurenine metabolic pathway in sh-sy5y cells differentiated into dopaminergic neurons

AUTHORS (FIRST INITIAL, LAST NAME) AND INSTITUTIONS: M. L. Pereira[1], J. L. F. Ribeiro[1], F. Dörr[1], P. P. Borges[1], *P. Scharf*[1], L. Torres[2], D. Chagas-Paula[2], R. C. T. Garcia[3], and T. Marcourakis[1]. [1]University of São Paulo, São Paulo, Brazil; [2]Federal University of Alfenas, Minas Gerais, Brazil; and [3]Federal University of São Paulo, São Paulo, Brazil.

KEYWORDS: Neurotoxicology

ABSTRACT: Background and Purpose: Cocaine use disorder (CUD) is a global public health issue. Despite the severity of the problem, therapeutic options available for CUD treatment are limited. Ayahuasca, a psychoactive brew used in religious contexts, has been gaining interest due to its therapeutic potential. Its main components, β-carbolines and DMT, exhibit neuroplastic properties that have proven relevant in the treatment of psychiatric disorders, including CUD. Tryptophan is metabolized into several products, including kynurenine (KYN), serotonin, melatonin, tryptamine, and DMT. In the brain, KYN is synthesized by the enzyme indoleamine 2,3-dioxygenase (IDO). The KYN metabolic pathway splits into two branches: a neurotoxic branch, forming quinolinic acid (QA), and a neuroprotective branch, forming kynurenic acid (KYNA). There is evidence suggesting that abnormalities in the kynurenine pathway may be implicated in depression, CUD, and neurodegeneration, and that drugs such as ethanol and cocaine dysregulate this pathway by inducing IDO, increasing the production of neurotoxic metabolites like QA. Furthermore, it has been shown that DMT inhibits this enzyme in human glioma cells. Our aim is to identify the alterations in the KYN pathway induced by cocaine and evaluate the ability of DMT to reverse these changes in differentiated human neuroblastoma SH-SY5Y cells into dopaminergic neurons. **Methods:** SH-SY5Y cells were differentiated into dopaminergic neurons through treatment with retinoic acid (10 µM) for five days, followed by BDNF (50 ng/mL) for another five days. The differentiation characterization was performed using immunofluorescence and flow cytometry for NeuN and tyrosine hydroxylase. To determine the LC_{50} of cocaine and the NOAEL of DMT, concentration-response curves for cocaine (1 to 10 mM) and DMT (0.1 to 2 mM) were constructed over 24 and 48 hours using MTT bromide reduction assays and flow cytometry for cell viability analysis. Standardization of tryptophan and its metabolites quantification: after inhibiting the metabolism of the differentiated cells, the analytes of interest were extracted using an extraction solution (40% acetonitrile, 40% methanol, and 20% water). The quantification of tryptophan and its metabolites was performed via LC-MS/MS using a Shimadzu Prominence chromatographic system coupled to an AmaZon Speed ion trap mass spectrometer. Chromatographic separation was conducted on a Luna® 3 µm C18(2) 100 Å reverse-phase column with a pre-column of the same stationary phase, maintained at 32°C. **Results:** The neuronal differentiation protocol resulted in a homogeneous and stable culture of dopaminergic neurons, as evidenced by increased fluorescence intensity of tyrosine hydroxylase and NeuN. Cocaine exposure for 24 and 48 hours reduced cell viability at concentrations starting from 4 mM, while the NOAEL of DMT was determined to be 1 mM. Co-exposure with DMT attenuated the neurotoxic effects of cocaine. The standardized method demonstrated sensitivity for detecting tryptophan, kynurenine, serotonin, and the acids kynurenic, quinolinic, nicotinic, and picolinic, with retention times of 12.1 min, 9.6 min, 7.6 min, 16.0 min, 6.8 min, 4.5 min, and 3.9 min, respectively. This method will be used to investigate the effects of cocaine and the modulation by DMT on the kynurenine pathway. **Conclusions:** Differentiated SH-SY5Y cells enable the investigation of the impacts of cocaine, particularly on dopaminergic cells, and the

protective effect of DMT on the central nervous system. Furthermore, our work explores the impact of cocaine and DMT on the kynurenine pathway and the involvement of this pathway in cocaine-induced neurotoxicity.

ABSTRACT NUMBER: 5251 **Poster Board Number:** LB352

TITLE: Assessing skin sensitizing hazard of Drug Products and Active Pharmaceutical Ingredients using GARD: New Approach Methodology in Occupational Health and Safety

AUTHORS (FIRST INITIAL, LAST NAME) AND INSTITUTIONS: A. Chérouvrier Hansson[1], T. Lindberg[1], *A. Forreryd*[1], R. Gradin[1], H. Johansson[1], and C. Taxvig[2]. [1]SenzaGen AB, Lund, Sweden; and [2]H. Lundbeck A/S, Copenhagen, Denmark.

KEYWORDS: In Vitro and Alternatives; Chemical Allergy; Safety Evaluation; GARDskin Dose-Response

ABSTRACT: Background and Purpose: Skin sensitizers are chemicals capable of inducing hypersensitivity reactions, such as Allergic Contact Dermatitis (ACD). Identifying and characterizing these chemicals' skin sensitizing potential is essential for limiting hazardous exposure. Significant efforts have been made in the scientific community to develop New Approach Methodologies (NAMs) to replace animal testing for skin sensitization. Internationally recognized test guidelines as well as integrated strategies have been developed, combining *in vitro*, *in chemico*, and *in silico* approaches for predicting skin sensitization potential. While widely accepted in cosmetics and personal care, NAMs' application in the pharmaceutical sector for product development and Occupational Health and Safety (OHS) is less prominent. The aim of this study is to demonstrate how NAMs, including the *in vitro* GARD® assay, combined with *in silico* data, can be used by the pharmaceutical industry to assess the skin sensitization potential of drug products and Active Pharmaceutical Ingredients (APIs) to take protective measures and improve occupational safety in production environments. In this study, the drug product is an oral medicine used to treat mental health problems, and the two APIs are compounds that affects how dopamine works in the brain, helping with symptoms like hallucinations or delusions, and helps boost certain chemicals in the brain to improve mood and reduce feelings of depression, respectively.
Methods: Following reports of allergic reactions in production and quality control, a drug product and two APIs A and B were assessed. The drug product contained approximately 0.5% of API A and 9.4% of API B. *In silico* predictions using Nexus Derek software identified all compounds as potential sensitizers. The *in vitro* assay GARDskin Dose-Response (GARDskin DR) was conducted to confirm these predictions. The GARDskin method (OECD 442E) is an *in vitro* assay for assessment of chemical skin sensitizers. The method provides binary hazard identification of skin sensitizers by evaluation of transcriptional patterns of an endpoint-specific genomic biomarker signature, comprising 196 genes, referred to as the GARDskin Genomic Prediction Signature (GPS), in the SenzaCell cell line. Final classifications are provided by a machine-learning prediction algorithm in the form of Decision Values (DV), the sign of which is evaluated by the prediction model. Any test chemical with a positive mean DV is classified as a skin sensitizer. Conversely, any test chemical with a negative mean DV is classified as non-skin sensitizer. GARDskin DR is an adaptation of the conventional GARDskin method, in which test chemicals are evaluated by the GARDskin prediction algorithm in an extended range of concentrations, to investigate the dose-response relationship between GARDskin DVs and test chemical concentration. It provides a quantitative estimation of sensitizing potency, referred to as cDV_0, which corresponds to the lowest required dose able to generate a positive mean DV. The readouts can predict correlating LLNA EC3 values, which are traditionally used to measure the skin sensitizing potency of chemicals. Furthermore,

it can predict human skin sensitizing potency NOEL and GHS/CLP classification (1A or 1B), all with high statistical significance. **Results:** All test items were identified as sensitizers by GARDskin DR with the following results:

- Drug product: cDV_0 = 12.8 µg/ml. Predictions: LLNA EC3 = 7.63%, NOEL = 3108 µg/cm², GHS/CLP 1B.
- API A: cDV_0 = 1.51 µg/ml. Predictions: LLNA EC3 = 1.08%, NOEL = 254 µg/cm², GHS/CLP 1A.
- API B: cDV_0 = 1.77 µg/ml. Predictions: LLNA EC3 = 1.19%, NOEL = 315 µg/cm², GHS/CLP 1A.

Conclusions: Both APIs were classified as strong sensitizers, while the drug product was classified as a weak sensitizer, reflecting the dilution effect of excipients. The GARDskin DR assay demonstrated a clear dose-dependent increase in DVs for all three test items, confirming their classification as skin sensitizers, with varying potencies. Based on the test outcomes, recommendations were made to improve occupational safety in handling these sensitizers:

- Avoiding dust inhalation and skin/eye contact.
- Minimizing prolonged and/or repeated exposure.
- Using appropriate personal protective equipment (PPE).
- Removing contaminated clothing and washing it before reuse.
- Ensuring thorough hand washing after handling, during breaks, and at the end of each shift.
- Handling substances in closed systems with proper ventilation.

These findings highlight NAMs like GARDskin DR as useful tools for enhancing OHS and safety protocols in pharmaceutical manufacturing.